



Pravat Kumar Shit
Gouri Sankar Bhunia
Partha Pratim Adhikary
Ch. Jyotiprava Dash
Editors

Groundwater and Society

Applications of Geospatial Technology

 Springer

Groundwater and Society

Pravat Kumar Shit • Gouri Sankar Bhunia
Partha Pratim Adhikary • Ch. Jyotiprava Dash
Editors

Groundwater and Society

Applications of Geospatial Technology



Springer

Editors

Pravat Kumar Shit
PG Department of Geography
Raja N.L. Khan Women's College,
Autonomous
Midnapore, West Bengal, India

Partha Pratim Adhikary
ICAR Indian Institute of Water
Management
Bhubaneswar, Odisha, India

Gouri Sankar Bhunia
RANDSTAD India Pvt Ltd.
New Delhi, Delhi, India

Ch. Jyotiprava Dash
ICAR Indian Institute of Soil and Water
Conservation, Research Centre
Koraput, Odisha, India

ISBN 978-3-030-64135-1 ISBN 978-3-030-64136-8 (eBook)
<https://doi.org/10.1007/978-3-030-64136-8>

© The Editor(s) (if applicable) and The Author(s), under exclusive license to Springer Nature Switzerland AG 2021

This work is subject to copyright. All rights are solely and exclusively licensed by the Publisher, whether the whole or part of the material is concerned, specifically the rights of translation, reprinting, reuse of illustrations, recitation, broadcasting, reproduction on microfilms or in any other physical way, and transmission or information storage and retrieval, electronic adaptation, computer software, or by similar or dissimilar methodology now known or hereafter developed.

The use of general descriptive names, registered names, trademarks, service marks, etc. in this publication does not imply, even in the absence of a specific statement, that such names are exempt from the relevant protective laws and regulations and therefore free for general use.

The publisher, the authors, and the editors are safe to assume that the advice and information in this book are believed to be true and accurate at the date of publication. Neither the publisher nor the authors or the editors give a warranty, expressed or implied, with respect to the material contained herein or for any errors or omissions that may have been made. The publisher remains neutral with regard to jurisdictional claims in published maps and institutional affiliations.

This Springer imprint is published by the registered company Springer Nature Switzerland AG
The registered company address is: Gewerbestrasse 11, 6330 Cham, Switzerland

*Dedicated to
The Millions of Farmers of India*

Foreword



I am happy to learn that Springer is bringing out a book entitled *Groundwater and Society: Applications of Geospatial Technology*. The book is edited by Pravat Kumar Shit, Gouri Sankar Bhunia, Partha Pratim Adhikary, and Ch. Jyotiprava Dash, who are eminent scholars and researchers in the field of groundwater resources and application of geospatial technology.

Demand for fresh water has become crucial in the last few decades and the problem will intensify in the future. Therefore, the issues and concerns regarding fresh water are experiencing growing recognition among academicians throughout the world. Groundwater in this context is one of the formidable solutions, but its availability, reckless use, and also misuse are yet to be investigated with deeper introspection. Considering the need of the hour, research on judicious use and management of groundwater is gaining importance in India.

In the twenty-first century, groundwater is an essential key for societal growth and development. Due to population growth, rapid urbanization, industrialization, and associated groundwater contaminants, serious health risks are evident and they pose a challenge to our society. The contribution of groundwater is immense in improving agriculture development, food security and many other aspects. So, our human society needs to establish an action plan that will considerably reduce contaminants and pollution of groundwater resources and allow development of the potential of groundwater resources and management of these resources using geospatial modeling and indigenous low-cost technologies through eco-friendly approaches.

This book presents an overview of recent advances in geospatial knowledge for the assessment and management of groundwater resources, giving special attention to how to use the local level of groundwater resources for societal development. The present volume also deals with various aspects of hydrogeological characteristics, groundwater quality, groundwater vulnerability, groundwater resources management, as well as social and economic considerations.

It is hoped that the contents of this book will contribute to an improved understanding of the impacts of human activity on groundwater resources and will provide useful guidance for policy makers and planners to include groundwater in crop adaptation schemes and strategies. I do believe that this book will be very beneficial for undergraduate and postgraduate students, researchers, social workers, and scientists working in the field of environmental sciences, hydrogeology, soil sciences, and agricultural sciences.

I extend my warm greetings to all those associated with the publication and congratulate Springer for launching this book.

Professor, Department of Geography,
University of Burdwan, Bardhaman,
West Bengal, India

Sanat Kumar Guchhait

Acknowledgments

The preparation of this book has been guided by several hydrologic pioneers. We are obliged to these experts for providing their time to evaluate the chapters published in this book. We thank the anonymous reviewers for their constructive comments that led to substantial improvement of the quality of this book. Because this book was a long time in the making, we want to thank our family and friends for their continued support. Dr. Pravat Kumar Shit thanks Dr. Jayasree Laha, principal, Raja N.L. Khan Women's College (Autonomous), Midnapore, for her administrative support to carry on this project. Dr. Partha Pratim Adhikary thanks ICAR-Indian Institute of Soil and Water Conservation, Research Centre, Koraput, Odisha, for its support to edit this book. This work would not have been possible without constant inspiration from our students, knowledge from our teachers, enthusiasm from our colleagues and collaborators, and support from our family. Finally, we also thank our publisher and its publishing editor, Springer, for their continuous support in the publication of this book.

Contents

Part I Groundwater Resources and Societal Development

- 1 Introduction to Groundwater and Society: Applications of Geospatial Technology 3**
Pravat Kumar Shit, Gouri Sankar Bhunia, Partha Pratim Adhikary, and Ch. Jyotiprava Dash
- 2 Groundwater and Society in India: Challenging Issues and Adaptive Strategies 11**
Subrata Jana
- 3 Groundwater Research and Societal Development: Integration with Remote Sensing and Geographical Information System 29**
Gouri Sankar Bhunia, Pravat Kumar Shit, Partha Pratim Adhikary, and Debashish Sengupta
- 4 Geospatial and Geophysical Approaches for Assessment of Groundwater Resources in an Alluvial Aquifer of India 53**
Partha Pratim Adhikary, S. K. Dubey, Debashish Chakraborty, and Ch. Jyotiprava Dash
- 5 Groundwater and Space Technology: Issues and Challenges 83**
Gouri Sankar Bhunia, Pravat Kumar Shit, Harsha Das Gupta, and Partha Pratim Adhikary

Part II Groundwater Availability, Quality and Pollution

- 6 Groundwater Quality Through Multi-Criteria-Based GIS Analysis: Village Level Assessment 105**
Baisakhi Chakraborty, Sambhunath Roy, Gouri Sankar Bhunia, Debashish Sengupta, and Pravat Kumar Shit

7	Analysis of Groundwater Potentiality Zones of Siliguri Urban Agglomeration Using GIS-Based Fuzzy-AHP Approach	141
	Suraj Kumar Mallick and Somnath Rudra	
8	Assessing the Groundwater Potentiality of the Gumari River Basin, India, using Geoinformatics and Analytical Hierarchy Process	161
	Sadik Mahammad and Aznarul Islam	
9	Application of AHP for Groundwater Potential Zones Mapping in Plateau Fringe Terrain: Study from Western Province of West Bengal	189
	Manas Karmakar, Monali Banerjee, Mrinal Mandal, and Debasis Ghosh	
10	Performance of Frequency Ratio Approach for Mapping of Groundwater Prospect Areas in an Area of Mixed Topography	221
	Subhas Garai and Pulakesh Das	
11	Artificial Neural Network for Identification of Groundwater Potential Zones in Part of Hugli District, West Bengal, India	247
	Shashank Yadav and Chalanika Laha Salui	
12	Multi-criteria Analysis for Groundwater Quality Assessment: A Study in Paschim Bardhaman District of West Bengal, India	259
	Payel Das and Niladri Das	
13	Performance of WQI and HPI for Groundwater Quality Assessment: Study from Sangramgarh Colliery of West Burdwan District, West Bengal, India	289
	Tanushree Paul and Manas Nath	
14	Assessment of Groundwater Quality Interaction Using One-Decade Data: A Case Study from a Hard Rock Area	305
	S. Satheeshkumar, S. Venkateswaran, and R. Suresh	
15	Fluoride Dynamics in Precambrian Hard Rock Terrain of North Singhbhum Craton and Effect of Fluorosis on Human Health and Society	319
	Biswajit Bera, Sumana Bhattacharjee, Meelan Chamling, Arijit Ghosh, Nairita Sengupta, and Supriya Ghosh	
16	Coastal Aquifer Vulnerability for Saltwater Intrusion: A Case Study of Chennai Coast Using GALDIT Model and Geoinformatics	349
	Debabrata Ghorai, Gouri Sankar Bhunia, and Pravat Kumar Shit	

Part III Sustainable Groundwater Resources Management

17 Watershed Development Impact on Natural Resources: Groundwater and Surface Water Utilization 365
 Partha Pratim Adhikary, M. Madhu, P. Jakhar, B. S. Naik, H. C. Hombegowda, D. Barman, G. B. Naik, and Ch. J. Dash

18 Long-Term Groundwater Behaviour Over an Agriculturally Developed State of North-West India: Trend and Impact on Agriculture 381
 Omvir Singh, Amrita Kasana, and Pankaj Bhardwaj

19 Spatial Appraisals of Groundwater Recharge Potential Zone Identification Using Remote Sensing and GIS 407
 Gouri Sankar Bhunia, Pranab Kumar Maity, and Pravat Kumar Shit

20 Spatial Mapping of Groundwater Depth to Prioritize the Areas Under Water Stress in Rayalaseema Region of Andhra Pradesh, India 429
 Ch. Jyotiprava Dash, Partha Pratim Adhikary, and Uday Mandal

21 Exploring Vulnerability of Groundwater Using AHP and GIS Techniques: A Study in Cooch Behar District, West Bengal, India 445
 Dipankar Saha, Debasish Talukdar, Ujjal Senapati, and Tapan Kumar Das

22 Applicability of Geospatial Technology, Weight of Evidence, and Multilayer Perceptron Methods for Groundwater Management: A Geoscientific Study on Birbhum District, West Bengal, India 473
 Niladri Das, Subhasish Sutradhar, Ranajit Ghosh, and Prolay Mondal

23 Water Resource Management in Semi-arid Purulia District of West Bengal, in the Context of Sustainable Development Goals 501
 Amit Bera and Shubhamita Das

Index 521

About the Editors



Pravat Kumar Shit is an assistant professor in the PG Department of Geography, Raja N. L. Khan Women's College (Autonomous), West Bengal, India. He received his M.Sc. and Ph.D. degrees in geography from Vidyasagar University and PG diploma in remote sensing and GIS from Sambalpur University. His research interests include applied geomorphology, soil erosion, groundwater, forest resources, wetland ecosystem, environmental contaminants and pollution, and natural resources mapping and modeling. He has published 8 books (6 books for Springer) and more than 60 papers in peer-reviewed journals. Dr. Shit is currently the editor of the GIScience and Geo-environmental Modelling (GGM) Book Series, Springer Nature.



Gouri Sankar Bhunia received his Ph.D. from the University of Calcutta, India, in 2015. His Ph.D. dissertation work focused on environmental control measures of infectious disease using geospatial technology. His research interests include environmental modeling, risk assessment, natural resources mapping and modeling, data mining, and information retrieval using geospatial technology. Dr. Bhunia is associate editor and on the editorial boards of three international journals on health GIS and geosciences. Dr. Bhunia has published more than 60 articles in various Scopus-indexed journals.



Partha Pratim Adhikary is a senior scientist at ICAR–Indian Institute of Water Management, Bhubaneswar, India. He obtained his Ph.D. in agricultural physics from ICAR–Indian Agricultural Research Institute, New Delhi, India. His research interests include solute transport, soil and water conservation and management, pedotransfer functions, and geospatial modeling of natural resources. Dr. Adhikary has published more than 60 research papers in peer-reviewed journals and three books. His other publications include book chapters, popular articles, technology brochures, technical bulletins, and scientific reports. He is the associate editor of *Indian Journal of Soil Conservation*. Currently, he is the editor of Springer Nature book series GIScience and Geo-environmental Modelling.



Ch. Jyotiprava Dash is presently working as scientist (soil and water conservation engineering) at ICAR–Indian Institute of Soil and Water Conservation (IISWC), Research Centre, Sunabeda, Koraput, Odisha. She obtained her bachelors’ degree in agricultural engineering from OUAT, Bhubaneswar, and master’s and Ph.D. degrees in agricultural engineering with specialization in soil and water conservation engineering from ICAR–Indian Agricultural Research Institute (IARI), New Delhi, India. Dr. Dash has an experience of more than 10 years of research, training, and extension in the field of soil and water conservation, watershed management, geostatistics, surface and groundwater modeling, remote sensing, and GIS. She is recipient of IASWC Young Scientist Award. Dr. Dash has more than 50 publications to her credit, which include research papers in journals of national and international repute, book chapters, technical and extension bulletins, popular articles, and e-publications.

Part I
Groundwater Resources and Societal
Development

Chapter 1

Introduction to Groundwater and Society: Applications of Geospatial Technology



Pravat Kumar Shit, Gouri Sankar Bhunia, Partha Pratim Adhikary ,
and Ch. Jyotiprava Dash

Abstract Water is the basic requirement for the development of civilization. The primitive civilizations were developed along the surface water bodies to meet the demand of water for the society. With the progress of time, the population-led demand for water was increased in those civilizations and which ultimately led to conflicts. The Indus valley civilization was destroyed mainly because of issues related to water management. In the recent times with the advent of modern tools and gadgets, the issues related to water have increased manifold. The demand from drinking, domestic, agriculture and industry has also increased alarmingly. To meet these demands, use of groundwater has increased tremendously all over the world. With the higher demand, the problems also became higher. In this context, modern tools and techniques like remote sensing, geographical information system, geostatistics and modelling have the potentiality to manage the groundwater-related problems and play a vital role for societal development. In this book we intended to offer novel advances and applications of remote sensing, geographical information system and geostatistical techniques in a precise and clear manner to the research community to achieve in-depth knowledge in the field. The scientific understanding, development and application of geospatial technologies related to water resource management have been advanced. Geostatistics and geospatial techniques for groundwater science assemble the most up-to-date techniques in GIS and geostatistics as they relate to groundwater. Therefore, this book will help the readers

P. K. Shit

PG Department of Geography, Raja N.L. Khan Women's College (Autonomous), Midnapore,
West Bengal, India

G. S. Bhunia

RANDSTAD India Pvt Ltd., New Delhi, Delhi, India

P. P. Adhikary (✉)

ICAR-Indian Institute of Water Management, Bhubaneswar, India

e-mail: partha.adhikary@icar.gov.in

Ch. J. Dash

ICAR-Indian Institute of Soil and Water Conservation, Research Centre, Koraput, India

e-mail: jyoti.dash@icar.gov.in

to find the recent advancement of the geospatial techniques and its application in the groundwater resources in a single volume.

Keywords Societal development · Remote sensing · GIS · Groundwater Quality and Pollution Assessment · Precision agriculture · Resource management

1.1 Introduction

Groundwater is the water found below the earth surface and accounts for 30% of available freshwater of the earth. It is a very important natural resource and has a significant role in the economy of any nation. People from all over the world are using sub-surface water to meet their various needs like drinking, washing, etc. for a long period of time (WWAP-UNESCO 2009). The increase in population increases the demand, and thus the exploitation of groundwater is gradually increasing. The contribution of groundwater to irrigation and food industry is highly significant and slowly leads to its over-exploitation (Smith et al. 2016). Globally, we use nearly 70% surface and sub-surface water as irrigation. India is the largest user of groundwater in the world followed by China and the USA, using an estimated 250 km³ of groundwater per annum. The developing countries are using groundwater at a faster rate. For example, in India, the contribution of groundwater is 62% in agriculture sector, 85% in rural water supply and 45% in urban water consumption. All over the world, groundwater is being used for industrial development, and it triggered unprecedented changes in the state of groundwater level. The groundwater is pumped out faster than it can replenish itself through underground recharge. This imbalance of input and output in groundwater extract creates a lot of problem (Chenini and Mammou 2010).

The groundwater crisis is an issue which can be solved at local level but has a global concern. The issue of groundwater management needs to be addressed in a global scale to ensure sustainable use of groundwater resources and to reverse the depletion of reserved groundwater. If this valuable resource cannot be managed properly, it will be a threat to the existence of living beings in the near future. Despite the increasing pressure placed on water resources by population growth and economic development, the laws governing groundwater rights have not changed accordingly, even in developed nations. Nor is groundwater depletion limited to dry climates: pollution and mismanagement of surface waters can cause over-reliance on groundwater in regions where annual rainfall is abundant.

Availability of good quality water in abundant quantity is the prime concern for the establishment of human settlement. The early settlers were totally dependent on surface water (Maisels 2001), and with the advent of civilization this demand enhanced considerably. This leads to the competition for faster development among the people (Taylor et al. 2013) which leads to the gradual increasing of water demand as well as scarcity. The earlier settlers were also exposed to climate change and other monsoonal aberrations (Pereira et al. 2009), although water

pollution was not so much important. To get rid of this crisis, people started the groundwater extraction to overcome the water scarcity problem. The regulating water demands are also dramatically increased, promoting the deficit of groundwater storage, depletion of the water table (Qureshi et al. 2010) and reduction of recharge rate. The humans are in dire need to find out the adaptive strategies and restrain water demands alongside the increase of rainwater recharging capacity, groundwater storage and efficiency in water utilization.

Therefore, for the optimal utilization and preservation of this treasure, systematic planning and management using modern tools and techniques are essential. For the greater interest, a measurement of groundwater resource is really significant for the sustainable management, and with the advent of powerful and high-speed personal computers, efficient techniques for water management have evolved, of which RS (remote sensing), GIS (geographic information system) and GPS (Global Positioning System) and geostatistical techniques are of great significance (Magesh et al. 2012; Kumar et al. 2014; Adhikary et al. 2011, 2015; Thapa et al. 2017; Nasir et al. 2018).

1.2 Key Aims of the Book

Groundwater is inarguably the world's single most important natural resource. It is the foundation of the livelihood security of millions of farmers and the main source of drinking water for a vast majority of people residing in rural as well as urban areas. The prospects of continued high rates of growth of the world's economy will depend critically on how judiciously we are able to manage groundwater in the years to come.

Over the years the world is consuming huge amount of groundwater for its growth and development. The contribution of groundwater is immense to make our world better in food security and many other aspects. Even as groundwater has made us self-sufficient in food, we are now facing the crisis of depleting water tables and water quality. The deep drilling by tube wells that was once part of the solution to the problem of water shortage now threatens to become a part of the problem itself. We, therefore, need to pay urgent attention to the sustainable and equitable management of groundwater.

Our intention in editing this book is to offer novel advances and applications of RS-GIS and geostatistical techniques in a precise and clear manner to the research community to achieve in-depth knowledge in the field. It will help those researchers who have interest in this field to keep insight into different concepts and their importance for applications in real life. This has been done to make the edited book more flexible and to stimulate further interest in topics. All these motivated us towards novel advances and applications of geospatial technologies and geostatistics.

This book advances the scientific understanding, development and application of geospatial technologies related to water resource management. Geostatistics and

geospatial techniques for groundwater science assemble the most up-to-date techniques in GIS and geostatistics as they relate to groundwater, one of the most important natural resources. Therefore, this book will help the readers to find the recent advancement of the geospatial techniques and its application in the groundwater resources in a single volume.

1.3 Sections of the Book

The book is organized into three parts: (I) Groundwater Resources and Societal Development; (II) Groundwater Availability, Quality and Pollution; and (III) Sustainable Groundwater Resources Management.

1.3.1 Section I: Groundwater Resources and Societal Development

This section concerns itself with the specific uses and management of groundwater as a component of integrated water management for societal development. Modern geospatial and geostatistical technologies have been described and used to address the issue of groundwater-related conflicts generally arising in the society. Overall, these fundamentals are tried to capture in five chapters of the section. These chapters are essential either to understand the spatial process of groundwater variation or to quantify these variations through the lens of society. The second chapter talks about how societal development has been started with the availability of freshwater in the world and how the conflicts have arisen because of water scarcity and pollution. In this context how the integrated approach of remote sensing and geographic information system has the potentiality to address the issue of groundwater scarcity and quality on a spatial scale through the involvement of the society has been described in Chap. 3. Chapter 4 deals with geospatial and geophysical approaches for assessment of groundwater resources in alluvial aquifers. This has been described through a case study from India. There are many issues related to groundwater management using space technology. Chapter 5 deals with those issues and suggested comprehensive solution to deal with those issues. The village level assessment of groundwater quality has the most importance to solve the problem comprehensively. Thus Chap. 6 documented the village level assessment of groundwater quality through multi-criteria-based GIS analysis. Overall, this section talks about how geospatial techniques will be useful to address the groundwater-related societal conflicts and how modern tools can play a greater role for societal development.

1.3.2 Section II: Groundwater Availability, Quality and Pollution

The second section deals with the regularity and monitoring of groundwater resources. This section discusses about the groundwater potential zone identification, the amount of water available in the aquifer, recharge and discharge characteristics of groundwater resources. Here remote sensing and GIS techniques have been extensively used. In this section, the threats of over-extraction and subsequent groundwater pollution emerging out because of high dependency led to high exploitation of groundwater resources by societal, economic and environmental development. The evolution of effective management systems to address these threats has been discussed. Ten chapters have been dedicated in this section. Delineation of groundwater potential zones is a very important issue which serves as the first point for groundwater management. Chapters 6, 7, 8, 9, 10 and 11 discuss about the delineation and mapping of groundwater potential zones using modern tools, techniques and modelling. The applicability of GIS-based Fuzzy Analytical Hierarchy Process approach has been highlighted in these chapters. The performance of Frequency Ratio Approach and Artificial Neural Network has also been discussed with case studies in this section. The appraisal of groundwater quality is the topic of present-day research. Chapters 12, 13 and 14 deal with this aspect. Multi-criteria-based GIS approach, use of groundwater quality indices and HPI were used to understand managing groundwater pollution through case studies. Chapter 15 deals with fluoride dynamics in Precambrian hard rock terrain of North Singhbhum Craton and effect of fluorosis on human health and society. Thereby the problem of fluoride has been dealt with in this section. Salt water intrusion in the coastal aquifer is a problem. Therefore Chap. 16 assesses the coastal aquifer vulnerability for saltwater intrusion using GALDIT model and geo-informatics. This thing has been explained through a case study of Chennai coast.

1.3.3 Section III: Sustainable Groundwater Resources Management

The third section deals with the application of geospatial techniques to tackle man-induced changes in groundwater conditions. The environmental and socio-economic impacts on groundwater resources have been dealt with in detail. How different approaches like watershed management and agro-forestry can remediate the twin problem of groundwater quantity and quality deterioration and the role of RS and GIS to support in this aspect has been addressed. The role of stakeholder's participation to tackle the groundwater-related problems for long-term basis through which viable national, regional and local systems can be evolved has also been addressed. Altogether there are seven chapters to cover these aspects. Chapter 17 discussed about the impact of watershed development models on water resources

especially on groundwater utilization. This has been illustrated with a live case study from a tribal watershed of India. Chapter 18 deals with the impact of long-term groundwater behaviour on agricultural development. This has been discussed with a case study from an agriculturally developed state of north-west India. Chapter 19 deals with the spatial appraisals of groundwater recharge potential zone identification using remote sensing and GIS. Water stress is an important aspect which controls the agricultural activity through the world. In this aspect Chap. 20 deals with spatial mapping of groundwater depth to prioritize the areas under water stress in the Rayalaseema region of Andhra Pradesh, India. Groundwater vulnerability was explored using AHP and GIS techniques in Chap. 21 with the help of a case study from India. A geoscientific study on Birbhum District, West Bengal, India, was presented in Chap. 22 where the applicability of geospatial technology, weight of evidence and multilayer perceptron was used for groundwater management. This study critically examined the modern tools and techniques for efficient management of groundwater resources. The last chapter deals with water resources management in the context of sustainable development goals of the United Nations. This is addressed with the help of a good case study from India. Overall, this section has given comprehensive idea about the importance of RS, GIS, modelling and other modern tools and techniques for sustainable water resources management.

References

- Adhikary, P.P., Dash, C.J., Bej, R., Chandrasekharan, H. (2011). Indicator and probability kriging methods for delineating Cu, Fe, and Mn contamination in groundwater of Najafgarh Block, Delhi, India, *Environmental Monitoring and Assessment* 176 (1-4), 663-676.
- Adhikary, P.P., Chandrasekharan, H., Dubey, S.K., Trivedi, S.M., Dash, C.J. (2015). Electrical resistivity tomography for assessment of groundwater salinity in west Delhi, India, *Arabian Journal of Geosciences* 8 (5), 2687-2698.
- Chenini, I., & Mammou, A. B. (2010). Groundwaters recharge study in arid region: an approach using GIS techniques and numerical modeling. *Computers & Geosciences*, 36(6), 801-817.
- Kumar, T., Gautam, A. K., & Kumar, T. (2014). Appraising the accuracy of GIS-based multi-criteria decision making technique for delineation of groundwater potential zones. *Water resources management*, 28(13), 4449-4466.
- Magesh, N. S., Chandrasekar, N., & Soundranayagam, J. P. (2012). Delineation of groundwater potential zones in Theni district, Tamil Nadu, using remote sensing, GIS and MIF techniques. *Geoscience Frontiers*, 3(2), 189-196.
- Maisels, C. K. (2001). *Early civilizations of the old world: the formative histories of Egypt, the Levant, Mesopotamia, India and China*. Psychology Press.
- Nasir, M. J., Khan, S., Zahid, H., & Khan, A. (2018). Delineation of groundwater potential zones using GIS and multi influence factor (MIF) techniques: a study of district Swat, Khyber Pakhtunkhwa, Pakistan. *Environmental Earth Sciences*, 77(10), 367.
- Pereira, L. S., Cordery, I., & Iacovides, I. (2009). *Coping with water scarcity: Addressing the challenges*. Springer Science & Business Media.
- Qureshi, A. S., McCormick, P. G., Sarwar, A., & Sharma, B. R. (2010). Challenges and prospects of sustainable groundwater management in the Indus Basin, Pakistan. *Water resources management*, 24(8), 1551-1569.

- Smith, P., House, J. I., Bustamante, M., Sobocká, J., Harper, R., Pan, G., ... West, P.C., Clark, J.M., Adhya, T., Rumpel, C. and Paustian, K. (2016). Global change pressures on soils from land use and management. *Global Change Biology*, 22(3), 1008-1028.
- Taylor, R. G., Scanlon, B., Döll, P., Rodell, M., Van Beek, R., Wada, Y., ... & Konikow, L. (2013). Ground water and climate change. *Nature climate change*, 3(4), 322-329.
- Thapa, R., Gupta, S., Guin, S., & Kaur, H. (2017). Assessment of groundwater potential zones using multi-influencing factor (MIF) and GIS: a case study from Birbhum district, West Bengal. *Applied Water Science*, 7(7), 4117-4131.
- World Water Assessment Programme (United Nations), & UN-Water. (2009). *Water in a changing world* (Vol. 1). Earthscan.

Chapter 2

Groundwater and Society in India: Challenging Issues and Adaptive Strategies



Subrata Jana

Abstract The scarcity of freshwater is escalating higher than the predicted level in India alongside the other countries in the world. The surface, subsurface and groundwater resources are gradually reducing in quantity and quality concern. The states and union territories of the western, southern and central India are already severely suffering from the scarcity of freshwater. Rate of groundwater extraction accelerated after the implementation of the green revolution and urban-industrial development. The river's natural flow has been diverted and protected for socio-economic development. Therefore, the lower riparian states are deadly affected by ecological and hydro-geomorphological perspectives. The fisheries have been widely adopted in those areas as an alternative to traditional crop cultivation, which extract more groundwater for freshwater supply and enhance the rate of groundwater depletion. Moreover, the rainwater recharge into the soil layer as well as in the groundwater table has been gradually reducing due to concretized urban infrastructural development. The surface runoff becomes accelerated, enhancing the soil erosion rate. In India, about 75% of total water bodies have been polluted from domestic wastes. Besides, about 80% of rural people are compelled to use unsafe water, which resulted in the death of more than 700 children per year from diarrhoea. In this situation, India achieves the third place in the world in terms of water export. In such juxtaposition condition, about 60% and 85% of irrigation water and drinking water supply came from the groundwater, respectively. Recently, over 60% of tube wells are malfunctioning due to excessive rate of groundwater depletion. The suffering of the people is tremendously increasing concerning the availability of drinking water and irrigation water. People are extracting groundwater from the far depth to overcome the crop failure and drinking water problem. But, the severity of water scarcity becomes enhancing year after year in conjunction with global warming and climate change. In this concern, the government has taken different water scarcity preventive measures in individual household level to the regional level. Now, the main motto is to execute the 3-R concept (recycle, reuse and recharge) in association with the other various techniques of water storage (like

S. Jana (✉)

Department of Geography, Belda College, Belda, Paschim Medinipur, India

rainwater harvesting) and groundwater recharge (like percolation tank, recharge tube well). In addition, awareness programmes are being campaigned from the grass-root level to increase the efficiency in water utilization among the people.

Keywords 3-R concept · Climate change · Crop failure · Groundwater depletion · Rainwater harvesting · Urban-industrial development · Water scarcity

2.1 Introduction

Availability and supply of freshwater is the primitive aspect to the establishment of human settlement, not only for their drinking water but also for their livelihood practices. The early civilizations were entirely dependent on the surface water supply (Enzel et al. 1999; Maisels 2001). Afterwards, increasing population density immensely enhanced the demand for freshwater. People were running across the earth's surface to find out the suitable place for constructing settlement on the basin of surface water sources. Therefore, almost the entire freshwater source areas in the earth were occupied by human beings. The fresh surface water storage becomes reducing with the promotion of competition for faster development among the people (Shah 2009; Taylor et al. 2013). People planned to bifurcate the rivers and natural water sources with their innovative ideas, which emphasizes the gradual increasing of water demand as well as scarcity. People started groundwater extraction to overcome the water scarcity problem. Water demands also dramatically increased, promoting the deficit of groundwater storage and depletion of the water table (Kulkarni et al. 2004; Qureshi et al. 2010). Moreover, the societal development leads to the concretization of the earth's surface, which promotes the deficiency in the ability of water recharge into the soil layer as well as in the groundwater table.

India is the largest user and third largest exporter of groundwater; it extracts about 230 km³ groundwater per year that is about 25% (more than the combined use of China and the United States) of the global total (Maheshwari et al. 2014; Murtugudde 2017; India Today 2019). In India, over 60% of irrigated water and 85% of drinking water supply depend on groundwater (World Bank 2011, 2012; Grönwall and Danert 2020). The freshwater demand is gradually increasing with the prolonged socio-economic development and associated livelihood practices. The primitive nature of agricultural practices has converted into modern trends with the implementation of technological innovations. The green revolution has emphasized enhancing crop production using more fertilizers and irrigational water supply (Singh 2000; Pingali 2012). Recently, the traditional agricultural land has been converted into fisheries concerning more profit, particularly in the coastal and floodplain areas (Gowing et al. 2006). The effect of industrialization is also enhancing the scarcity of water (Lal 2000). In every case, groundwater has been extensively extracted in support of the available supply and scarcity of surface water. Besides, the water quality has deteriorated with the encroachment of harmful pollutants. The inconsistent nature of monsoonal rainfall also enhanced the episodic scarcity of

groundwater (Sinha et al. 2015). Therefore, the gross availability of freshwater storage and supply shrinks dramatically with the ever-increasing demands. In India, about 60% of aquifers will be in a critical situation in 20 years if the recent trends continue (Gandhi and Namboodir 2009; World Bank 2012).

The earlier human civilizations had tremendously suffered from global warming and associated climate change and inconsistency of monsoon rainfall pattern in India among the other regions of the world (Pereira et al. 2009), although water pollution was not an issue at all for abolished or shifting of civilization in that period, which is the most threatening issue in the recent perspective. The excessive rate of glacial retreats also becomes a threat to the future society regarding the availability of freshwater supply in most of the rivers in northern India (Richardson and Reynolds 2000). The people are at the terminating stage to survive, and there have been urgent needs to find out the adaptive strategies and restrain water demands alongside the increase of rainwater recharging capacity, groundwater storage and efficiency in water utilization. So, the present study emphasizes the efficient utilization of freshwater concerning the sustainability of human civilization incompetent from earlier societies.

2.2 Water Source and Civilization: A Changing Spectrum

2.2.1 Water Source and Establishment of Settlements

There has been a reciprocal relationship between the water source and establishment of the settlement, as water is the backbone of a society. The people can only survive within this earth because of water. People use water for drinking as well as for irrigation. The ancient people established their settlements in the wider floodplain areas of the major river valleys depending on the river courses as a water source (Postel and Richter 2012; Singh et al. 2017). The Indus civilization is the best example of ancient civilization, which was formed based on the Indus River in northwestern India (Possehl 2002; Dixit et al. 2018). However, the well-established civilization was entirely ruined due to the reducing water supply and prolonging drought phase (Sangomla 2019). Remaining people moved mainly towards the east and north ensuring water availability. In the later phase, people have distributed over the major river valley regions of India. Moreover, the monotonic and inconsistent nature of Indian summer monsoon (ISM) emphasized the water scarcity on a regional basis (Basu et al. 2020). People are fighting against such water scarcity through the utilization of groundwater. Therefore, the modern civilizations not only preferred and formed their settlement just in the riverside location, nearer to the floodplains and in the coastal areas but also selected places for their settlement based on the availability of groundwater. The population density and water demand have reciprocally increased in the well-established settlement areas. The water quality also deteriorates with the increasing demand for societal development (Adhikary et al. 2015). The physicochemical compounds have been released from the industrial

effluents and also from the extensive agricultural sectors. People have been compelled to extract water from the subsurface and groundwater storage. In the modern perspective of the settlement construction, the availability and source of surface water is not the mandatory aspect. People can construct far away from surface water source points based on the availability of groundwater.

2.2.2 Water Source and Livelihood Practices

People have adopted agricultural practices to survive their livelihood. The fertile floodplain areas have been utilized depending on the river water source and direct rainwater in this purpose. Initially, life-supporting food grain cultivation was the prime aspect of earlier people. However, the other cash crops were also cultivated in the following periods due to more profit issue, which required more water for irrigation (Singh and Jyoti 2019). People were distributed in the different landscape areas of the hills, plateaus and plains in finding their way of livelihood. Despite the harsh terrain condition, the unfavourable undulated lands of hilly and plateau regions have been modified for their agricultural land. The crop failure was the familiar issue in the dry regions and the fringe areas of the plateau and hills (Glantz 2019; Singh et al. 2019). Therefore, people constructed the check dams in the different parts of the tributaries to provide irrigation water in their agricultural land. The large dams and barriers have been also constructed to solve multiple problems. In this consequence, the lower courses of the river valley become water fed during the dry seasons, creating the ecological imbalances with the extinction of local aquatic species (Choudhury et al. 2019; Sarkar and Islam 2020). The dam and reservoir water did not fulfil the excessive demand for irrigation water in the ever-increasing areas of agricultural land. In this concern, the groundwater is to be the only alternative option to the farmers. Recently, about 90% (228.3 billion m³) of the total available groundwater (253 billion m³) was used for irrigation purpose (DownToEarth 2019a). Moreover, fisheries become intensively emerging in the areas of floodplain, delta plain and coastal zone for better profit in the fishery sector. Voluminous groundwater has been extracted every year to fulfil the demand for freshwater in the fisheries (Colvin et al. 2019).

2.2.3 Modern Civilization and Deterioration of Groundwater Quality

The industrial revolution brings new thinking and better aspects of development. Uneven competition creates an unbalanced development among different societies. Water is the most important aspect for industrial setup in any area. The natural river flow has been diverted to fulfil the demands of water for urban-industrial

development (Arfanuzzaman and Syed 2018; Kumar and Verma 2020). The groundwater is also extracted for the other activities in the industry-based towns. Industrial effluents are mostly discharged into the natural water flows of rivers without any significant level of treatment (Gurjar and Tare 2019; Mohanakavitha et al. 2019; Mishra et al. 2020). The pollutant materials have penetrated the soil layer and mixed with the subsurface water table. After the green revolution in India, chemical fertilizers and pesticides have been massively utilized in the agricultural fields. The excessive level of pesticides and chemicals has been washed out from the agricultural fields and ultimately mixed up with the subsurface and surface water. The groundwater tables are also contaminated with the pollutants of subsurface water due to the seasonal fluctuation of water table caused by the monsoonal rainfall. The untreated urban waste and pathogens are also accelerating the degradation level of water quality. Therefore, the water quality of the surface, subsurface and groundwater has continually deteriorated every year.

2.2.4 Water Quality and Human Health

Even in the twenty-first century, most of the people both in the rural and urban areas have compelled to take the untreated drinking water. Especially, the miseries of the rural people are exceptionally in worst conditions regarding the supply and availability of safe drinking water. The shallow depth tube wells and dug wells, even the surface water, are the most important source of drinking water. The poor people never think about the quality of water; they only think about the availability of it. Mainly, water from the riverbed and underground has been supplied in the urban areas. In India, the drinking water from the surface, subsurface and groundwater has been contaminated with harmful pollutants and metals in most of the areas. About 75% of total water bodies remain polluted in the country (Saha 2019); among those about 75–80% of water bodies are polluted from the domestic sewage (Mallapur 2016). Therefore, people of the rural as well as urban areas are continuously suffering from drinking water problems.

In India, 816 municipalities adopted the sewage treatment plants among which only 64% is in the operational stage and the rest are in non-operational and under construction stage (Table 2.1). The operational plants are only treated 81% waste out of the total treatment capacity of 23277.36 million litres per day (Table 2.1). Moreover, water pollution is enhancing with the poor sanitation facilities in rural areas and even in the urban areas and slum areas (Table 2.2). In India, about 12.6% and 18.9% of households, respectively, in the urban and slum areas don't have any sanitation facilities (Table 2.2). Therefore, the miseries of the common people are accelerated during the rainy seasons due to contamination of water bodies with the harmful physicochemical components coming from wastes. Moreover, the peoples of the coastal areas have been suffering from the saline water encroachment into the groundwater table (Behera et al. 2019). Concerning the water quality index, India remains in the 120th place among 122 countries, and about one billion people are

Table 2.1 Status of sewage treatment plants in India (based on CPCB 2015; Mallapur 2016)

States	Punjab	Maharashtra	Tamil Nadu	Uttar Pradesh	Himachal Pradesh	All India
Capacity of municipal STPs (MLD)	1245.45	5160.36	1799.72	2646.84	114.72	23277.36
Total number of municipal STPs	86	76	73	73	66	816
Operational capacity (MLD)	921.45	4683.9	1140.83	2372.25	79.51	18883.20
Number of operational STPs	38	60	33	62	36	522
Number of non-operational STPs	4	10	1	7	30	79
Number of under construction STPs	31	6	28	3	–	145
Number of proposed STPs	13	–	11	1	–	70

Note: STPs stand for sewage treatment plants, and MLD is the million litres per day

Table 2.2 Status of sanitation facilities in India (after Mallapur 2016)

Type of latrine	Urban households (%)	Slum households (%)
Latrine within the premises	81.4	66.0
Water closet	72.6	57.7
Pit latrine	7.1	6.2
Other latrine	1.7	2.2
No latrine within the premises	18.6	34.0
Public latrine	6.0	15.1
Open field	12.6	18.9

suffering from unsafe drinking water (The Economic Times 2018; India Today 2019). Also, in India, about 80% of rural people are compelled to use water from unsafe sources, and every day more than 700 children (under 5 years of age) die in diarrhoea connected with the unsafe water and poor sanitization (India Today 2019).

2.3 Groundwater Depletion and Society

2.3.1 Climate Change and Groundwater Depletion

Climate change or climatic oscillations have also remained in the different periods of human civilizations, and people made their adjustment and adapt to the harsh condition in those periods. But, human civilization is now in trouble and tremendously affected in the recent context of global warming and climate change. The water scarcity has been prolonging with the gradual depletion of the groundwater

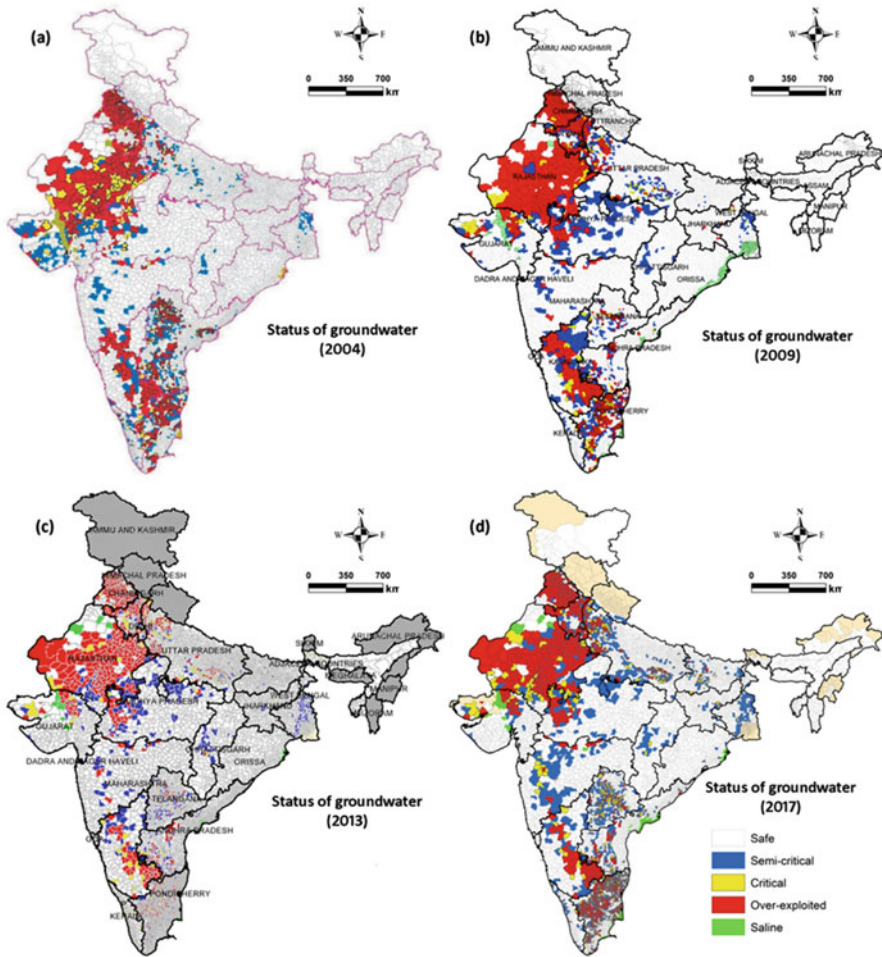


Fig. 2.1 Categorical safety status of Indian groundwater in the year of (a) 2004, (b) 2009, (c) 2013 and (d) 2017. (Based on CGWB 2020)

table and scarcity of surface water in association with seasonal drought events. As per the Intergovernmental Panel on Climate Change (IPCC) special report (2018), the ratio of population rendering to water stress owing to climate change would be reduced by 50% if the global warming can be limited to 1.5 °C instead of 2 °C as approved in the Paris Agreement (Hoegh-Guldberg et al. 2018; DownToEarth 2020b). The regional inconsistent nature of monsoonal rainfall creates a harsh impact over the Indian society, mainly in central, western and southern India (Fig. 2.1). The people suffering in those regions have been panic-stricken day by day, particularly during the summer months (Fig. 2.2). Indeed, groundwater plays a crucial defensive role against the water scarcity on a regional basis. For instance, crop productivity declined by 20% due to deficit rainfall during 1963–1964. But it

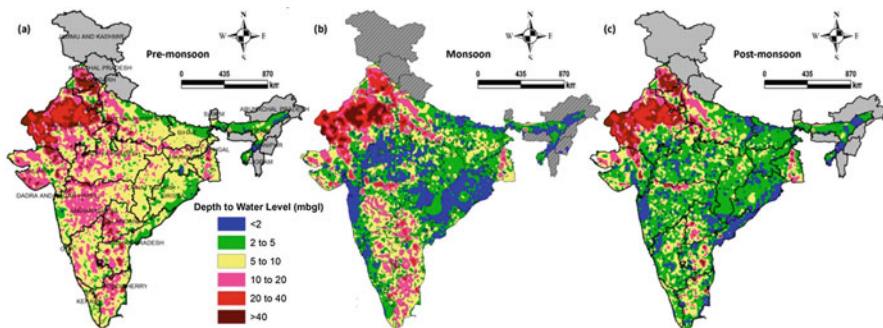


Fig. 2.2 Spatio-temporal fluctuation of groundwater level in India during (a) pre-monsoon, (b) monsoon and (c) post-monsoon seasons of 2019. (Based on CGWB 2020)

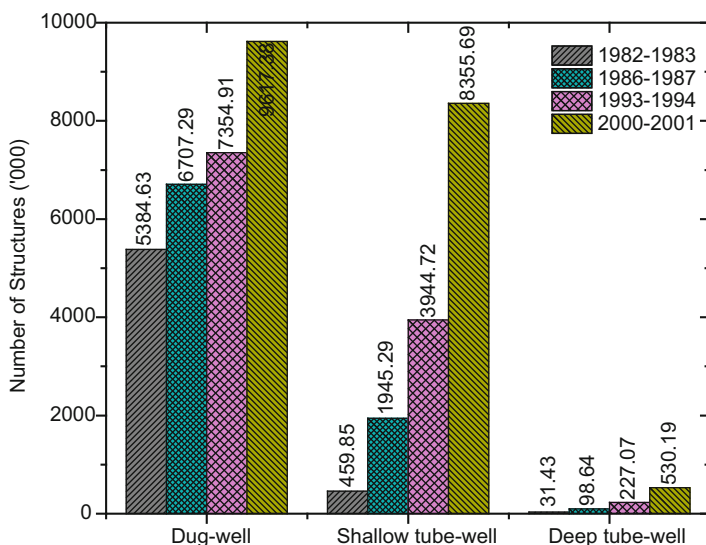


Fig. 2.3 Escalating number of groundwater extraction structures in India during 1982–2001. (Based on CGWB 2007)

had a very negligible impact on crop productivity at similar drought effects during 1987–1988 (Gornall et al. 2010; World Bank 2012), which was only possible due to use of groundwater in extensive areas. However, the groundwater table is constantly declining, and sometimes the tube wells are not able to supply the required water and failed to pull out waters, which invite crop failure in drought-prone areas (Kala 2017; Singh et al. 2019, 2020).

The number of dug wells and tube wells (shallow and deep) has constantly increased (Fig. 2.3), which might dig out up to the deeper part depending on the local and regional level variation of the water table to extract groundwater and minimize the sufferings of the people. The naturally recharged water during the

rainy season also moved up to the deeper part due to the degradation of subsurface impermeable layer by boreholes of tube wells. Therefore, the local dug wells also shrank during the dry season. This condition has been intensified after the construction of the deep tube wells, while the dug wells are naturally able to supply the required drinking water to the villagers in the rain-fed drought-prone areas. Therefore, the number of tube wells (both the shallow and deep) is dramatically increased compared to the dug wells (Fig. 2.3). Over 60% of wells are unable to extract water due to depletion of groundwater table in Indian states (like Delhi, Punjab, Haryana, Himachal Pradesh, Uttar Pradesh, Tamil Nadu, Andhra Pradesh, Karnataka, Kerala and Meghalaya) and union territories (like Chandigarh, Dadra and Nagar Haveli and Puducherry) (World Bank 2012; CGWB 2018). Consequently, people are suffering to survive their livelihood and compelled to leave those areas. As per the CGWB (2018), among India's total administrative blocks, 253 have been categorized as 'critical', 681 as 'semi-critical' and 1034 as 'over-exploited', meanwhile 4520 administrative blocks still remained under 'safe' category in terms of rate of groundwater depletion (World Bank 2012; CGWB 2018). This situation is more awfully visible in the highly populated and economically developed areas. The severity level of the groundwater status has continuously increased year after year in the numerous administrative blocks (Fig. 2.1). The affected coastal areas from the saline water encroachment into the groundwater aquifers have been tremendously increasing alongside the increasing salinity level in the western parts of the Indian territories (Fig. 2.1), whereas the areas having over-exploited, critical and semi-critical level are also increasing, particularly in the western and southern India (Fig. 2.1). According to the CGWB (2018), during the pre-monsoon period, the water level declined in about 61% of wells out of 14,465 monitored wells in India within a decade (2007–2016). Among those wells having groundwater at more than 40 m below ground level, the number increased by 49 wells in terms of groundwater depletion in 2017–2018 compared to 2016–2017 (World Bank 2012; CGWB 2018). Moreover, the seasonal water fluctuation level (Fig. 2.2) associated with the depth to water level is increasing in terms of spatial extents in the western and southern Indian territories. Although central India has been buffering its groundwater deficit with a sufficient volume of groundwater recharge during monsoon season, it becomes eradicated during crop cultivation in the post-monsoon and pre-monsoon seasons (Fig. 2.2).

2.3.2 Urbanization and Groundwater Depletion

Urbanization initiates the concretization of the earth's surface, which minimizes the penetration level of rainwater into the subsurface layers. Therefore, the surface runoff and soil erosion rate have maximized in most of the areas. The volume of groundwater is gradually decreasing in conjunction with the minimum level of recharge facilities. Moreover, urban society needs more facilities, and most of these are related to water utilization. In most of the urban centres, groundwater is

the only option for completing people's livelihood. The number of people is also increasing with the expansion of urban areas. Therefore, more water is required for the individual urban sites, which is entirely collected from the groundwater. The juxtaposition effects of climatic inconsistency and associated reducing rainfall, concretization and associated reducing groundwater recharge, and extrapolated groundwater extraction due to urbanization and societal development intensify the gradual depletion of groundwater table mostly in the urban areas among the other parts of the country. During 2000–2010, the increasing rate of groundwater depletion is higher (23%) in India than the global rate of 22% (India Today 2019). The drinking water supposed to be supplied in the major cities which will come far away from their existing locations. In this regard, the proposed planning is to supply water in Delhi from the Tehri dam (more than 300 km away), Hyderabad from Nagarjuna Sagar Dam (105 km away) and Bengaluru from the Cauvery River (100 km away) to fight against water scarcity (Narain 2006; DownToEarth 2019b). But, long-term sustainability and cost-effectiveness are the main issues of these mega-projects. A similar type of project is adopted for Udaipur, Rajasthan, which draws water from Jaisamand Lake (60 km away), but the lake is drying up, and the city is dreadfully looking for a new way to overcome the upcoming thirst.

2.4 Groundwater and Future Society

The availability of surface water is reducing dramatically, and in most areas, it becomes polluted. In the context of global climate change, the inconsistency of monsoon rainfall and rapid rate of glacial melting will create suffering for the future generation in water availability concern (Pritchard 2019). The per-capita water demand is also swiftly increasing, in contrast with the reducing per-capita water availability (Fig. 2.4). The sustainability of the present and future human society is under a threatening condition concerning water stress and scarcity (Fig. 2.4). Therefore, groundwater is the key option for the future society to survive the human civilization and the only way of adaptation in the scenario of climate change. But, the unscientific human activities and rigorous development bring a threat to maintaining the quality and quantity of groundwater in addition to surface water. The population density, landholding size, water intensity of planted crops, the behaviour of water user, power subsidies for pumping irrigation water, government policies towards groundwater and overall economic policies of the country are playing a critical interacting influence on groundwater extraction and sustainability (Kumar 2018). Every year, people are obliterating law and order and encroaching into wetland and other water bodies after landfilling process, which leads to reducing water availability as well as degrading the water quality (Banerjee 2012; Bindra 2017). Therefore, there is an urgent need to take best suitable adaptive strategies through the 3-R concept (*Recycle, Reuse and Recharge*) to survive on earth. Concerning the sustainability, about 0.25 million stations have been set up to monitor the groundwater

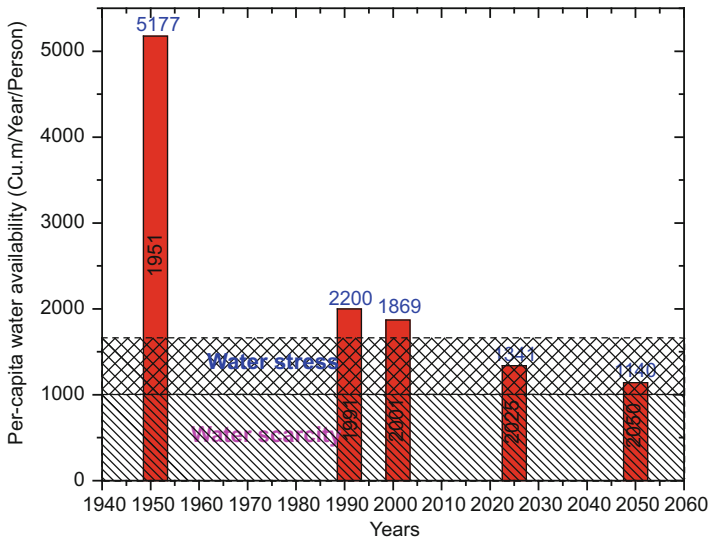


Fig. 2.4 Past and future of water availability status in India under water stress and scarcity condition. (Modified after CGWB 2007)

status for the restoration of groundwater in the impending 50 years through the application of scientific and artificial intelligence (DownToEarth 2019c).

2.4.1 Efficiency in Water Utilization

The convenient and limited utilization of water is the prior aspect to adaptation with the future threats of water scarcity. A maximum percentage of freshwater is utilized as irrigation water. Wheat and rice are the two extensively cultivated and highest water-guzzling crops in India. An average of 1654 litres and 2800 litres of water is required to produce 1 kg of wheat and rice, respectively (India Today 2019). In this regard, a four-member family consumes about 84,600 litres of water per month. Moreover, in the economic year 2014–2015, India virtually exported 10 trillion litres of water through exporting 3.72 million tonnes of basmati rice (India Today 2019). Therefore, the actual water export from our country is not only the highest in terms of drinking water supply, but also it becomes the highest position in terms of virtual water export through exporting food grains. In the socio-economic perspective, the irrigational water supply can't stop, but water utilization can be minimized through the selection of suitable crop in the region and seasonal perspectives. The dry-crop farming (like maize, millets and sorghum), crop diversification and crop rotation methods are the best options to minimize the water use, and it can also minimize the loss of water through evapotranspiration (Rana and Rana 2011). After the elapsed period (over 50 years) of commencement of the green revolution, the government

authorities also encourage the farmers to plant other crops instead of rice cultivation. Bamboo trees plantation in the drought-prone areas will be most effective as it helps in recharging groundwater, minimizing soil erosion and even syncing carbons (DownToEarth 2020a). A large volume of water can be restored through the adaptation of zero-tillage cultivation method (Honsdorf et al. 2020; Singh et al. 2018). The areas' specific cropping pattern and crop selection can be useful to minimize the water uses. The bio-fertilizers should be introduced, instead of the chemical fertilizer, through which the moisture-holding capacity will increase (Mahdi et al. 2010). The irrigation water needs to be supplied through the pipelines instead of the open canal, and the evaporation loss should be minimized. In this connection, the farm-specific sprinkler irrigation method can be easily applied. The use of groundwater should not be permissible in the fisheries sector from where the maximum volume of water is evaporated. In our every day's life, we waste plenty of water without realization. For example, a single person can exploit up to 37 litres in 5 minutes showering, 570 litres per week for washing, 15 litres every day for mouth washing, 18 litres for every toilet visit and 25 litres for cleaning kitchen utensils and vegetables (India Today 2019). All these activities are necessary in our daily life, but we waste water without stopping the irrelevant water flow from a tap in most of the cases. The waste of safe drinking water is commonly observed in the restaurants by using only half of a bottle or glass during food intake. Besides, the water can be reused in different ways like irrigation, fisheries, horticulture, gardening, car washing, toilet use and washing of kitchen utensils at the first stage; also it can be injected directly into the subsurface layer. The government should take necessary steps like any kind of treated or untreated water should not be permitted to mix with a river and random and unlimited withdrawal of water from any sources without any prior concern.

2.4.2 Water Storage

The rainwater storage in the individual household level as well as in regional level is required to solve the water scarcity up to a certain level. The rainwater can naturally be stored into the soil layer, which also provides the water supply in the following fields depending on the elevation, terrain condition and soil characteristics. The tanks and ponds in the different terrain and landscape units can be constructed to store the excessive rainwater during the rainy season, which can be utilized in the rest of the season. In this concern, the Mahatma Gandhi National Rural Employment Guarantee Act (MGNREGA) plays a vital role in association with creating the employment opportunities among the rural dwellers (Esteves et al. 2013; Chakraborty and Das 2014). The stored water can also maintain the soil moisture level in the surrounding areas (Tiwari et al. 2011). The construction of micro-level check dams at the upper catchment areas is a fruitful method to supply irrigation water in the surrounding agricultural lands. Although the large dams and reservoirs store voluminous water, in ecological and hydro-geomorphological aspect it creates

a harsh impact in the downstream section (Bhattacharyya 2011; Singh 2016). The ecological flow must be reduced, which can't able to maintain the ecological balance in the lower riparian stretches (Choudhury et al. 2019; Sarkar and Islam 2020). Rainwater harvesting plan is the most appropriate method of rainwater storage, and it can be stored in various ways like roof-top harvesting and underground harvesting (Sivanappan 2006). Most of the urban areas can utilize the rainwater at least for 3 months during the rainy season with the acceptance of this method. For instance, according to the Centre for Science and Environment (Delhi), the daily water demand in Delhi is about 2765 million litres for 18.8 million populations (as per the 2011 census). As per the IMD, during 13–19 August 2020, about 118.4 mm rainfall was received in Delhi (1483 km² area), which can produce 87 million litres of water (Sengupta 2020). But, the rainwater runoff co-efficient was about 13% of the total rainfall (during 13–19 August 2020), estimated by the Centre for Science and Environment.

2.4.3 Groundwater Recharge

The natural groundwater recharge capacity is reducing gradually due to the unscientific land management, forest degradation and dramatic rate of urban infrastructural development on different parts of the earth's surface (Chennamaneni and Rao 2007). As a result, the surface runoff as well as the soil erosion rate is increasing tremendously, which reciprocally triggers both events. The groundwater and subsurface water recharge capacity is reducing with due effects from increasing the surface runoff (Harbor 1994; Misra 2011). The thickness of the soil layer is also decreasing continuously, which promotes a minimum level of water holding capacity into the soil layer. The exposed permeable layers are also degrading due to the infrastructural development, and it leads to minimum rainwater recharge into the groundwater table. In this regard, artificial water recharge techniques (like check dam, percolation tank, spreading channel, recharge tube well, underground dam, subsurface dykes) are more effective and need to be implemented for the survival of the human civilization (CGWB 2007; Bhattacharya 2010). In the rural areas, the damaged tube wells mostly remain unused, and the upper part of the hollow is filled up with earthen material. However, the rainwater can easily be injected through such degraded tube wells. The paddy has been cultivated thrice per year in many places of the intensive subsistence cultivation systems. As a result, the agricultural fields remained saturated throughout the year. The permeability capacity has gradually reduced, and no such water can recharge into the soil layer and even into the subsurface layer. If the agricultural fields remain vacant or can be utilized for dry crops instead of rice paddy, the topsoil and the upper layer can be cracked during the dry season. Therefore, a certain volume of rainwater can easily enter into the subsurface and even into the groundwater table. In the urban areas, some part of the surface areas should remain vacant and require the water recharge facilities, through which the rainwater can also easily recharge into the groundwater.

2.5 Conclusion

In the history of human evolution, there is enough evidence of ruined human civilizations in the different historical periods. But, in the recent context of global warming, climate change and associated hydro-meteorological hazards, the existing human beings are facing a harsh experience regarding their persistence in the future earth. The volume of required freshwater resource is reducing with the gradual increase in demand. In this contradictory situation, sustainability is being the prime issue in the era of globalization and overturning socio-economic perspective. People are now a little bit concerned and might be scared about their existence and sustainability in this earth. People are now thinking and finding out the way to survive, and fighting not only to minimize the use of freshwater but also to preserve it. The urban-industrial and socio-economic development is also promoting water quality degradation. In overall perspectives, the quantity and quality of freshwater resources are diminishing from the earth. In India, the water scarcity is severely persisting mainly in the western, southern and central parts, along with the entire Indian territories. About 90% of total groundwater is used for irrigation purpose, while 75% of the total surface water bodies have been polluted in India. Most of these water bodies are being polluted from the domestic wastes. To tackle this situation, the government has taken many plans to prevent misuses of water and promote the awareness about the recycle, reuse and recharge of water. The adaptive strategies have been taken in the agricultural sector by implementing the dry crops and advanced cultivation techniques, which can prevent excessive use of irrigation water. However, all these adaptive strategies are not sufficient to overcome the existing severity of water scarcity. People should be more responsible about the existing deadly condition and hopefully, change their daily lifestyle concerning wastage of freshwater.

Acknowledgement The author would like to express his gratitude to Dr. Pravat Kumar Shit, Department of Geography, Raja N. L. Khan Women's College, for his suggestions in the completion of this book.

References

- Adhikary, P.P., Chandrasekharan, H., Trivedi, S.M., Dash, C.J. (2015). GIS applicability to assess spatio-temporal variation of groundwater quality and sustainable use for irrigation, *Arabian Journal of Geosciences* 8 (5), 2699-2711.
- Arfanuzzaman, M., & Syed, M. A. (2018). Water demand and ecosystem nexus in the transboundary river basin: a zero-sum game. *Environment, Development and Sustainability*, 20(2), 963-974.
- Banerjee, S. (2012). The march of the mega-city: Governance in West Bengal and the wetlands to the east of Kolkata. *South Asia Chronicle*, 2, 93-118.

- Basu, S., Mohanty, S., & Sanyal, P. (2020). Possible role of warming on Indian summer monsoon precipitation over the north-central Indian subcontinent. *Hydrological Sciences Journal*, 65(4), 660-670.
- Behera, A. K., Chakrapani, G. J., Kumar, S., & Rai, N. (2019). Identification of seawater intrusion signatures through geochemical evolution of groundwater: a case study based on coastal region of the Mahanadi delta, Bay of Bengal, India. *Natural Hazards*, 97(3), 1209-1230.
- Bhattacharya, A. K. (2010). Artificial ground water recharge with a special reference to India. *International Journal of Recent Research and Applied Studies*, 4(2), 214-221.
- Bhattacharyya, K. (2011). *The Lower Damodar River, India: understanding the human role in changing fluvial environment*. Springer Science & Business Media.
- Bindra, P. S. (2017). *The Vanishing: India's Wildlife Crisis*. Penguin Random House India.
- CGWB (2007). *Manual on artificial recharge of groundwater*. Central Ground Water Board, Ministry of Water Resources, Government of India, p. 198.
- CGWB (2018). *Ground Water Year Book - India 2017-2018*. Central Ground Water Board Ministry of Water Resources, River Development and Ganga Rejuvenation, Government of India, Faridabad, p. 104.
- CGWB (2020). 'Dynamic Ground Water Resources of India'. Central Ground Water Board Ministry of Jal Shakti, Department of Water Resources, River Development and Ganga Rejuvenation, Government of India. <http://cgwb.gov.in/Dynamic-GW-Resources.html> [Accessed on 15 September 2020].
- Chakraborty, B., & Das, S. (2014). MGNREGA and water management: sustainability issues of built forms in Rural India. *Journal of Construction in Developing Countries*, 19(2), 33.
- Chennamaneni, R., & Rao, S. (2007). Assessment of Urban Carrying Capacity. A Case Study of Environmental and Institutional Implications for Water Resource Management in Hyderabad. Dept. of Resource Economics Faculty of Agriculture and Horticulture, Humboldt- University of Berlin, Germany. Research Report 8, p. 45.
- Choudhury, N. B., Mazumder, M. K., Chakravarty, H., Choudhury, A. S., Boro, F., & Choudhury, I. B. (2019). The endangered Ganges river dolphin heads towards local extinction in the Barak river system of Assam, India: A plea for conservation. *Mammalian Biology*, 95(1), 102-111.
- Colvin, S. A., Sullivan, S. M. P., Shirey, P. D., Colvin, R. W., Winemiller, K. O., Hughes, R. M., ... & Danehy, R. J. (2019). Headwater streams and wetlands are critical for sustaining fish, fisheries, and ecosystem services. *Fisheries*, 44(2), 73-91.
- CPCB (2015). *Inventorization of sewage treatment plants*. Central Pollution Control Board, Ministry of Environment and Forests, Govt. of India Parivesh Bhawan, East Arjun Nagar, Delhi.
- Dixit, Y., Hodell, D. A., Giesche, A., Tandon, S. K., Gázquez, F., Saini, H. S., ... & Petrie, C. A. (2018). Intensified summer monsoon and the urbanization of Indus Civilization in northwest India. *Scientific reports*, 8(1), 1-8.
- DownToEarth (2019a). 'Environment ministry's 50-year plan to tackle water crisis'. DownToEarth, 08 August 2019. <https://www.downtoearth.org.in/video/water/environment-ministry-s-50-year-plan-to-tackle-water-crisis-66095> [Accessed on 16 September 2020].
- DownToEarth (2019b). 'Rainwater harvesting: Catch water where it fall'. DownToEarth, 01 July 2019. <https://www.downtoearth.org.in/video/water/catch-where-it-falls-to-fight-drought-and-to-create-employment-65368> [Accessed on 10 September 2020].
- DownToEarth (2019c). 'Environment ministry's 50-year plan to tackle water crisis'. DownToEarth, 08 August 2019. <https://www.downtoearth.org.in/video/water/environment-ministry-s-50-year-plan-to-tackle-water-crisis-66095> [Accessed on 10 September 2020].
- DownToEarth (2020a). 'Growing a cooperative forest can lead to water conservation and generate livelihood'. DownToEarth, 10 February 2020. <https://www.downtoearth.org.in/video/water/every-drop-counts-how-a-cooperative-turned-250-acres-of-dharmapuri-green-69222> [Accessed on 10 September 2020].
- DownToEarth (2020b). 'Water & climate emergency: A fluid future'. DownToEarth, 28 May 2020. <https://www.downtoearth.org.in/news/water/water-climate-emergency-a-fluid-future-69827> [Accessed on 15 September 2020].

- Enzel, Y., Ely, L. L., Mishra, S., Ramesh, R., Amit, R., Lazar, B., ... & Sandler, A. (1999). High-resolution Holocene environmental changes in the Thar Desert, northwestern India. *Science*, 284(5411), 125-128.
- Esteves, T., Rao, K. V., Sinha, B., Roy, S. S., Rao, B., Jha, S., ... & IK, M. (2013). Agricultural and livelihood vulnerability reduction through the MGNREGA. *Economic and Political Weekly*, 48 (52), 94-103.
- Gandhi, V.P. & Namboodir, N.V. (2009). Groundwater irrigation in India: gains, costs and risks. *Indian Institute of Management, Ahmedabad*, No. 2009-03-08, p. 38.
- Glantz, M. H. (2019). *Desertification: environmental degradation in and around arid lands*. CRC Press.
- Gornall, J., Betts, R., Burke, E., Clark, R., Camp, J., Willett, K., & Wiltshire, A. (2010). Implications of climate change for agricultural productivity in the early twenty-first century. *Philosophical Transactions of the Royal Society B: Biological Sciences*, 365(1554), 2973-2989.
- Gowing, J. W., Tuong, T. P., & Hoanh, C. T. (2006). Land and water management in coastal zones: dealing with agriculture-aquaculture-fishery conflicts. In C. T. Hoanh, T. P. Tuong, J. W. Gowing, & B. Hardy (Eds.), *Environment and livelihoods in tropical coastal zones: Managing agriculture-fishery-aquaculture conflicts* (pp. 1-65). Wallingford: CAB International.
- Grönwall, J., & Danert, K. (2020). Regarding Groundwater and Drinking Water Access through A Human Rights Lens: Self-Supply as A Norm. *Water*, 12(2), 419.
- Gurjar, S. K., & Tare, V. (2019). Spatial-temporal assessment of water quality and assimilative capacity of river Ramganga, a tributary of Ganga using multivariate analysis and QUEL2K. *Journal of Cleaner Production*, 222, 550-564.
- Harbor, J. M. (1994). A practical method for estimating the impact of land-use change on surface runoff, groundwater recharge and wetland hydrology. *Journal of the American Planning Association*, 60(1), 95-108.
- Hoegh-Guldberg, O., Jacob, D., Bindi, M., Brown, S., Camilloni, I., Diedhiou, A., ... & Hijioka, Y. (2018). Impacts of 1.5 C global warming on natural and human systems. *Global warming of 1.5°C*. In: Masson-Delmotte, V., P. Zhai, H.-O. Pörtner, D. Roberts, J. Skea, P.R. Shukla, . . . & T. Waterfield (eds.) *Global Warming of 1.5°C. An IPCC Special Report on the impacts of global warming of 1.5°C above pre-industrial levels and related global greenhouse gas emission pathways, in the context of strengthening the global response to the threat of climate change, sustainable development, and efforts to eradicate poverty*, pp. 175-311.
- Honsdorf, N., Verhulst, N., Crossa, J., Vargas, M., Govaerts, B., & Ammar, K. (2020). Durum wheat selection under zero tillage increases early vigor and is neutral to yield. *Field Crops Research*, 248, <https://doi.org/10.1016/j.fcr.2019.107675>
- India Today (2019). 'World Water Day: 21 Indian cities, including Delhi, will run out of groundwater by 2020, affecting 100 million people'. *India Today (Web Desk)*, New Delhi, 22 March 2019. <https://www.indiatoday.in/science/story/world-water-day-2019-water-crisis-india-1483777-2019-03-22> [Accessed on 15 September 2020].
- Kala, C. P. (2017). Environmental and socioeconomic impacts of drought in India: lessons for drought management. *Applied Ecology and Environmental Sciences*, 5(2), 43-48.
- Kulkarni, H., Shankar, P. V., Deolankar, S. B., & Shah, M. (2004). Groundwater demand management at local scale in rural areas of India: a strategy to ensure water well sustainability based on aquifer diffusivity and community participation. *Hydrogeology Journal*, 12(2), 184-196.
- Kumar, M. D. (2018). *Water Policy Science and Politics: An Indian Perspective*. Elsevier.
- Kumar, N., & Verma, A. (2020). Inter-basin Water Transfer and Policies of Water Resource Management. In *Environmental Concerns and Sustainable Development* (pp. 257-274). Springer, Singapore.
- Lal, M. (2000). Climatic change-implications for India's water resources. *Journal of Social and Economic Development*, 3, 57-87.
- Mahdi, S. S., Hassan, G. I., Samoon, S. A., Rather, H. A., Dar, S. A., & Zehra, B. (2010). Bio-fertilizers in organic agriculture. *Journal of phytology*. 2(10): 42-54.

- Maheshwari, B., Varua, M., Ward, J., Packham, R., Chinnasamy, P., Dashora, Y., ... & Shah, T. (2014). The role of transdisciplinary approach and community participation in village scale groundwater management: insights from Gujarat and Rajasthan, India. *Water*, 6(11), 3386-3408.
- Maisels, C. K. (2001). *Early civilizations of the old world: the formative histories of Egypt, the Levant, Mesopotamia, India and China*. Psychology Press.
- Mallapur, C. (2016). '70% Of Urban India's Sewage Is Untreated'. *The Wire*, 27 January 2016. <https://archive.indiaspend.com/cover-story/70-of-urban-indias-sewage-is-untreated-54844> [Accessed on 16 September 2020].
- Mishra, S., Kumar, A., Mishra, S., & Kumar, A. (2020). Estimation of physicochemical characteristics and associated metal contamination risk in the Narmada River, India. *Environmental Engineering Research*, 26(1).
- Misra, A. K. (2011). Impact of urbanization on the hydrology of Ganga Basin (India). *Water resources management*, 25(2), 705-719.
- Mohanakavitha, T., Shankar, K., Divahar, R., Meenambal, T., & Saravanan, R. (2019). Impact of industrial wastewater disposal on surface water bodies in Kalingarayan canal, Erode district, Tamil Nadu, India. *Archives of Agriculture and Environmental Science*, 4(4), 379-387.
- Murtugudde, R. (2017). 'Pakistan World's Top Groundwater Exporter, India Ranks Third'. *The Wire*, 3 May 2017. <https://thewire.in/agriculture/pakistan-worlds-top-groundwater-exporter-india-third> [Accessed on 15 September 2020].
- Narain, S. (2006). Community-led alternatives to water management: India case study (No. HDOCPA-2006-10). Human Development Report Office (HDRO), United Nations Development Programme (UNDP), p. 33.
- Pereira, L. S., Cordery, I., & Iacovides, I. (2009). *Coping with water scarcity: Addressing the challenges*. Springer Science & Business Media.
- Pingali, P. L. (2012). Green revolution: impacts, limits, and the path ahead. *Proceedings of the National Academy of Sciences*, 109(31), 12302-12308.
- Possehl, G. L. (2002). *The Indus civilization: a contemporary perspective*. Rowman Altamira.
- Postel, S., & Richter, B. (2012). *Rivers for life: managing water for people and nature*. Island Press, London.
- Pritchard, H. D. (2019). Asia's shrinking glaciers protect large populations from drought stress. *Nature*, 569(7758), 649-654.
- Qureshi, A. S., McCornick, P. G., Sarwar, A., & Sharma, B. R. (2010). Challenges and prospects of sustainable groundwater management in the Indus Basin, Pakistan. *Water resources management*, 24(8), 1551-1569.
- Rana, S. S., & Rana, M. C. (2011). *Cropping system*. Department of Agronomy, College of Agriculture, CSK Himachal Pradesh Krishi Vishvavidyalaya, Palampur, p. 80.
- Richardson, S. D., & Reynolds, J. M. (2000). An overview of glacial hazards in the Himalayas. *Quaternary International*, 65, 31-47.
- Saha, D. (2019). 'Government must prioritise on conserving water'. *DownToEarth*, 24 May 2019. <https://www.downtoearth.org.in/blog/water/government-must-prioritise-on-conserving-water-64737> [Accessed on 16 September 2020].
- Sangomla, A. (2019). 'Climate change pushed Indus Valley migrants west to east: Study'. *DownToEarth*, 21 November 2019. <https://www.downtoearth.org.in/news/climate-change/climate-change-pushed-indus-valley-migrants-west-to-east-study-67862> [Accessed on 15 September 2020].
- Sarkar, B., & Islam, A. (2020). Drivers of water pollution and evaluating its ecological stress with special reference to macrovertebrates (fish community structure): a case of Churni River, India. *Environmental Monitoring and Assessment*, 192(1), 45.
- Sengupta, S. (2020). 'It rained hard in Delhi; what if all that water did not go waste'. *DownToEarth*, 21 August 2020. <https://www.downtoearth.org.in/news/water/it-rained-hard-in-delhi-what-if-all-that-water-did-not-go-waste-72959> [Accessed on 10 September 2020].

- Shah, T. (2009). Climate change and groundwater: India's opportunities for mitigation and adaptation. *Environmental Research Letters*, 4(3), 035005.
- Singh, A. (2016). Managing the water resources problems of irrigated agriculture through geospatial techniques: An overview. *Agricultural Water Management*, 174, 2-10.
- Singh, A. K., & Jyoti, B. (2019). Measuring the Climate Variability Impact on Cash Crops Farming in India: An Empirical Investigation. *Agriculture and Food Sciences Research*, 6(2), 155-165.
- Singh, A. K., Das, B., Mali, S. S., Bhavana, P., Shinde, R., & Bhatt, B. P. (2019). Intensification of rice-fallow cropping systems in the Eastern Plateau region of India: diversifying cropping systems and climate risk mitigation. *Climate and Development*, 1-10.
- Singh, A., Thomsen, K. J., Sinha, R., Buylaert, J. P., Carter, A., Mark, D. F., ... & Paul, D. (2017). Counter-intuitive influence of Himalayan river morphodynamics on Indus Civilisation urban settlements. *Nature Communications*, 8(1), 1-14.
- Singh, G., Bhattacharyya, R., Das, T. K., Sharma, A. R., Ghosh, A., Das, S., & Jha, P. (2018). Crop rotation and residue management effects on soil enzyme activities, glomalin and aggregate stability under zero tillage in the Indo-Gangetic Plains. *Soil and Tillage Research*, 184, 291-300.
- Singh, R. B. (2000). Environmental consequences of agricultural development: a case study from the Green Revolution state of Haryana, India. *Agriculture, ecosystems & environment*, 82(1-3), 97-103.
- Singh, R. K., Singh, A., Kumar, S., Sheoran, P., Sharma, D. K., Stringer, L. C., ... & Singh, D. (2020). Perceived Climate Variability and Compounding Stressors: Implications for Risks to Livelihoods of Smallholder Indian Farmers. *Environmental Management*, 1-19.
- Sinha, A., Kathayat, G., Cheng, H., Breitenbach, S. F., Berkelhammer, M., Mudelsee, M., ... & Edwards, R. L. (2015). Trends and oscillations in the Indian summer monsoon rainfall over the last two millennia. *Nature communications*, 6(1), 1-8.
- Sivanappan, R. K. (2006). Rain Water Harvesting, Conservation and Management Strategies for Urban and Rural Sectors. In *National Seminar on Rainwater Harvesting and Water Management* 11-12 Nov. 2006, Nagpur, pp. 1-9.
- Taylor, R. G., Scanlon, B., Döll, P., Rodell, M., Van Beek, R., Wada, Y., ... & Konikow, L. (2013). Ground water and climate change. *Nature climate change*, 3(4), 322-329.
- The Economic Times (2018). 'India suffering worst water crisis in history, says Niti report'. *The Economic Times*, 14 June 2018. <https://economictimes.indiatimes.com/news/politics-and-nation/india-suffering-worst-water-crisis-in-history-says-niti-report/articleshow/64591891.cms?from=mdr> [Accessed on 15 September 2020].
- Tiwari, R., Somashekhar, H. I., Parama, V. R., Murthy, I. K., Kumar, M. M., Kumar, B. M., ... & Sengupta, A. (2011). MGNREGA for environmental service enhancement and vulnerability reduction: rapid appraisal in Chitradurga district, Karnataka. *Economic and political weekly*, 46(20), 39-47.
- World Bank (2011). 'Water Sector in India'. The World Bank, 29 September 2011. <https://www.worldbank.org/en/news/feature/2011/09/29/india-water> [Accessed on 14 September 2020].
- World Bank (2012). 'India Groundwater: a Valuable but Diminishing Resource'. The World Bank, 06 March 2012. <https://www.worldbank.org/en/news/feature/2012/03/06/india-groundwater-critical-diminishing> [Accessed on 14 September 2020].

Chapter 3

Groundwater Research and Societal Development: Integration with Remote Sensing and Geographical Information System



Gouri Sankar Bhunia, Pravat Kumar Shit, Partha Pratim Adhikary, and Debashish Sengupta

Abstract Although the global freshwater supply available is more than sufficient to satisfy all existing and consistent water demands, its spatial and temporal concentrations are not. In doing so, we face several challenges, particularly considering a changing and volatile future climate and an increasingly increasing population driving accelerated social and economic growth, globalization and urbanization. The remote sensing and geographic information system (GIS) have been used to reduce the time and financial costs of rapid groundwater resource assessment. Open-source geospatial technology helps in visualizing groundwater data over time and automatically measuring changes in the amount of aquifer storage to help management determine the viability of aquifers. The present chapter discusses the challenges that groundwater management faces today, and a future study is needed to help educate those who aspire to build a more secure and prosperous future.

Keywords Groundwater management · Modelling · Societal development · Soft computing · Spatial variation

G. S. Bhunia
RANDSTAD India Pvt Ltd., New Delhi, Delhi, India

P. K. Shit
PG Department of Geography, Raja N.L. Khan Women's College (Autonomous), Midnapore, West Bengal, USA

P. P. Adhikary
ICAR-Indian Institute of Water Management, Bhubaneswar, India
e-mail: partha.adhikary@icar.gov.in

D. Sengupta (✉)
Department of Geology & Geophysics, IIT Kharagpur, Kharagpur, West Bengal, India
e-mail: dsgg@gg.iitkgp.ac.in

3.1 Introduction

The main concept for social researchers is that “extreme issues” can better be dealt with through the engagement and development of human and social resources, by actors in processes which require dialog, learning and intervention (Curtis et al. 2016). Groundwater is a vital resource for humans and natural habitats and a significant natural resource in the world. In order to improve groundwater management, the value of drawing on theory and social research approaches is increasingly being recognized. This trend partially reflects the growing maturity and accepts that all environments have been modified by human activity and function as social-ecological systems (SES). In terms of groundwater, the “change in access to water supplies” reforms included reduction in the access to groundwater and annual quotas, implementation of groundwater exchange and improvements to regulations to allow for the subsequent recovery and use “banking” of excess water in aquifers (Contor 2009; Thompson et al. 2009).

In many parts of Asia, and in particular, in populous South Asian regions and the North China plain, groundwater has become the main source of irrigated agriculture. More than 50% of the world’s total annual usage comprises India, Pakistan, Bangladesh and Northern China, which use 380–400 km³ of groundwater per year. However, the trends of Asian groundwater use differ widely. Many scientists believe that groundwater production is self-regulating in the long term, with people unable to pump more water than the aquifers. It says that the economics of extracting water from profound aquifers will be the same long before the hydrogeology of aquifers puts a constraint on further growth. In comparison, two-thirds of India (almost half of the Indian sub-continent) is twice disadvantaged: semiarid temperate with minimal precipitation for water supply and heavy basalt aquifers with low storm values. Therefore, India is one of the worst contenders for extreme groundwater irrigation, and yet the Indo-Gangetic plain accounted for two-thirds of the tubewell irrigation of the country. For example, in the eastern Gangetic basin, the production of groundwater is linked to (geogenic) arsenic movement. Coastal areas are usually moist and have good alluvial aquifers; but in some cases, even in early phases of groundwater production, salinity or water entering the coastal aquifers is generally a concern. The dominance of basalt and crystalline rock formation in peninsular India is demonstrated in Table 3.1, with a map of major Indian aquifers by the Central Ground Water Board.

Governance includes relations between institutional systems, procedures and practices to decide how control influences the way decision-making is made and how roles are performed (Lockwood et al. 2010). The prospect for collective self-regulation of groundwater is being discussed with increasing intensity, as obligations are being shifted away from central authorities. The “Collective Groundwater Management by Users of Water” definition is often called local, group and/or participatory management (Yamamoto 2008). For example, in Gujarat, India, government agencies have supported the establishment of farmers’ cooperatives, as well as other reputable local organizations, in collaboration with local non-governmental

Table 3.1 Resource management challenges of intensive groundwater use in Asian agriculture (Shah 2007)

Hydro-geological Settings		Socio-economic challenges			
		Aquifer recharge and storativity	Surface and groundwater availability	Unavailability of fresh groundwater	Natural groundwater quality concern
Major alluvial plain	Arid	■ ■	■ □	■ ■ ■	■
	Humid	■	■ ■ ■		■ ■
Coastal plain		■ ■ ■	■	■ ■ □	■
Intermontane valley		■	■ ■	□	■
Hard-rock areas		■ ■	□	■	■ ■ ■

organizations (Tewari and Khanna 2005). “Groundwater management” implies for Mukherji and Shah (2005) a change from the expert-led processes that are derivative from the hydrologists’ “mathematical model building exercises” and the water managers’ “speaking and implementing the legislation concerning groundwater. However, groundwater administration has its own challenges, such as those related to the incomplete rights of ownership, respect for rules when the resource is largely invisible, insufficient knowledge of surface and groundwater connection and the impact of the use of groundwater in considerable distances from where it is extracted (Bolin et al. 2008). Rural landowners are important players in the field of groundwater governance in developing and under-developed economies. Groundwater availability and water quality are also a major factor that influences human well-being (e.g. food security, employment, work and health). It is complicated and challenging that rural farmers experience realistic transition, not least because of the possible effect of a broad variety of variables (personal and social) on their decisions (Mazur et al. 2013).

3.2 Significance of Remote Sensing and Geographic Information System in Groundwater Research

The basic water cycle has inputs with more or less storage changes equal to outputs. While researching a hydrology, hydrologists use the hydrological budget. The hydrological budgets include rainfall, surface flow and groundwater flow. The consequences are evapotranspiration, erosion, soil runoff and movements of groundwater and air. Both such quantities can be measured or calculated using environmental data and can be displayed graphically using GIS. One of the most advanced remote sensing and geographic information systems leading hydrogeological science methods that aid in the evaluation is groundwater management and restoration. The prevalence and orientation of primary and secondary porosity influences greatly the quality of groundwater in any terrain. Exploring groundwater requires

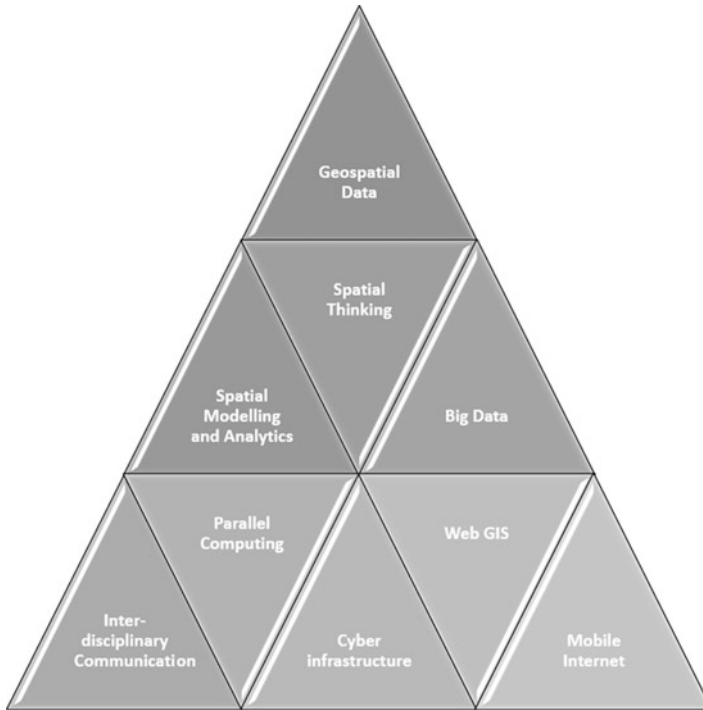


Fig. 3.1 Sustainable groundwater management pyramid with GIS applicability

identifying and mapping different lithological, structural and geomorphological units. Satellite-based remote sensing data allow the preparation of maps, particularly at regional level, for lithological, structural and geomorphological purposes. These differences make it possible to identify different rock minerals on earth surface features by analysing their spectral signatures. In a variety of researches, the use of spectral mirroring in order to enhance the understanding of rock formations in an image is common (Elbeih 2015). GIS is highly flexible, especially in the field of spatial analysis, modelling, visualization, data processing and management. The assessment in remote sensing of the groundwater potential is determined by the relationship between groundwater and surface water, vegetation, soil moisture and surface temperatures. Furthermore, the incorporation of the Geographical Information System offers a broader opportunity to observe and systematically measure geomorphic units and lineament features in order to demarcate potential groundwater zones. Figure 3.1 explains the linkages and the issues for sustainable management of groundwater resources, and the importance of GIS is also explained.

The approach for evaluating the groundwater potential in remote sensing currently consists primarily of an assessment of a single factor model and an assessment of a multi-source hydrological framework. If groundwater is heavily saturated or the depth of the groundwater

is poor, capillary water supplies a high moisture content of the soil. When the groundwater density deepens or increases groundwater, the soil moisture content reduces, so that the soil humidity cannot sustain the plant and induce soil drought. Today, soil moisture methods and hypotheses for use of remote sensing are very advanced, and various studies have been conducted. Li (2010) used Moderate Resolution Imaging Spectroradiometer (MODIS) data to gather soil moisture data in the Maowusu Desert and developed a groundwater vulnerability model for remote sensing knowledge assessment. The thermal infrared remote sensing system can be used to infer the groundwater potentials using the thermal infrared band ($10.4 \sim 12.5 \mu\text{m}$) since the temperature of the surface of the water is irregular. The capacity of groundwater can be traced to the irregular temperature variations in the arid and semi-arid regions. By using Landsat-TM thermal infrared remote sensing data, Fu et al. (1999) quantitatively recovered the Shiyang River Basin's surface temperature. The area with an irregular surface temperature indicates the groundwater field enrichment and the irregular zone temperature is less than the average soil temperature 7 K. However, numerous factors, for example, the difference in emissivity, topography, wind speed, atmosphere and local conditions, can affect surface temperature. Groundwater has a significant impact on vegetation, and vegetation represents groundwater potential. The study of changes in vegetation through remote sensing may indirectly infer the change in groundwater information. Tweed et al. (2007) studied the effect on the groundwater recharge of the changes in the surface vegetation cover. They combined the related groundwater profile for growth through the use of remote sensing technology data. The results show that conditions in vegetation are well-related when they are 2 ~ 8 m in depth with groundwater. Thompson and Moore (1996) extracted Digital Elevation Model (DEM) topography and found that the groundwater depth is closely related to the water storage region of the unit long contour line and pitch in the measurement of groundwater in a small mountain basin.

For the study of paleo-drainage patterns, large depressions, playas and catchment areas, Kwarteng (2002) used aerial photos, Landsat Thematic Mapper (TM) images and DEM. Both parameters absorb significant amounts of water during flash floods and fresh water lenses. Jaiswal et al. (2003) intended to leverage the groundwater by integrating a series of maps of themes into a GIS environment to reflect village-wise groundwater prospective areas in Madhya Pradesh's Gorna sub-basin. A probabilistic approach was proposed by Oh et al. (2011) which used satellite imagery and GIS to estimate potential groundwater supplies in a specific region. The technique adopted involves the collection of the 15 key variables that influence the capacity of soil water. The groundwater potential was then mapped by a frequency ratio model that shows the relation between the hydrological data, the actual capacity and the variables (derived from a pumping test). The latest results of the Gravity Recovery and Climate Experiment (GRACE) satellite for the assessment of terrestrial water change over large regions were described by Swenson et al. (2003). GRACE is a twin-satellite project used to detect mass changes in water storage and assist in evaluating groundwater depletion, evaporation residual basin scale or validation of hydrological models (Swenson et al., 2003). The earth's field of gravity induces

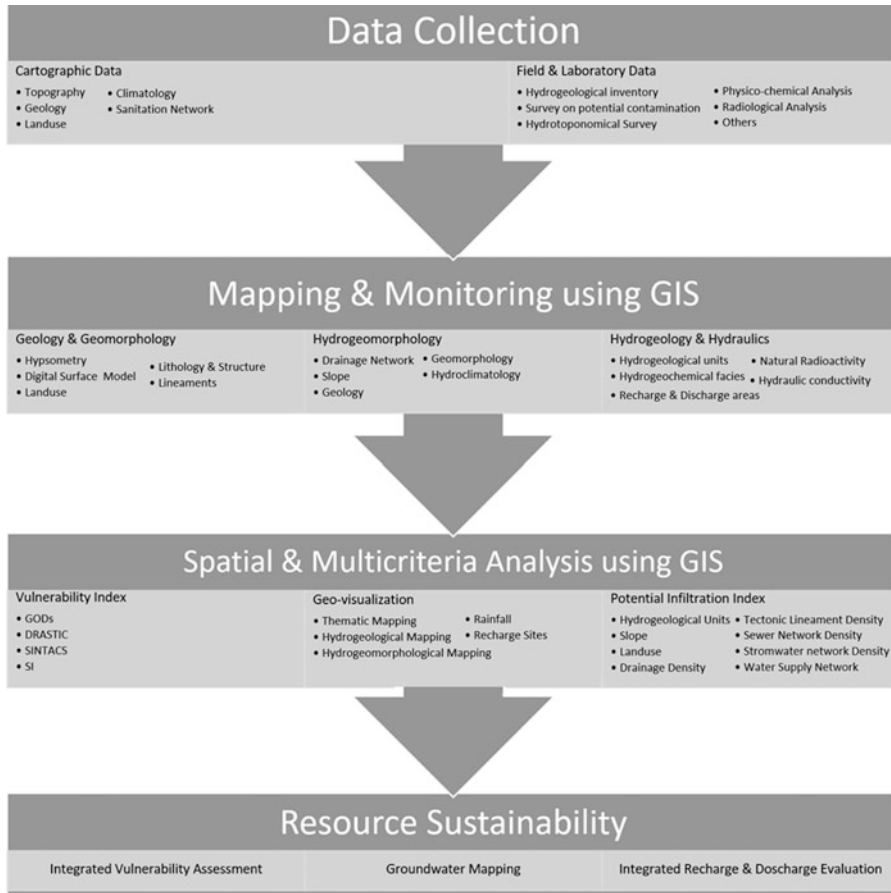


Fig. 3.2 Role of GIS in groundwater research

satellite accelerations, where they reach a relatively high concentration of mass and deceleration until they are removed. According to Meijerink (2007), microwaves and radar images are used in numerous applications in the field of hydrogeology, geological formations and lineaments and large-sized pits (with radar images related to the groundwater). For the groundwater heads and flow studies around the lakes, radar altimetry is critical for the detection of lake levels. Furthermore, radar data are available for reliable DEM's and land subsidy calculation. Therefore, GIS plays a significant role for groundwater research nowadays. Figure 3.2 illustrates the role of GIS in groundwater research and step-by-step analysis of the potentiality of GIS to enrich the research on groundwater.

Numerical models are used to analyse problems in hydrology and hydrogeology, but these models are less usage-friendly and lack the diffusion of information in

concept understanding, leading to a large divide between developers and practitioners. A variety of genetic algorithm methods, such as groundwater remediation, reservoir operating, groundwater level projections and water quality, were used in the past to resolve hydrological challenges. Machine learning methods have been used in the past few years for the forecasts of Hydrological Research fields (e.g. Artificial Neural Networks (ANNs), Support Vector Machine (SVM) (LeCun et al. 2015; Vapnik 2013)). Guio Blanco et al. (2018) used random forest algorithms to spatially estimate soil water retention and performed well for predicting water content in a volumetric way. Kenda et al. (2018) have proposed work to forecast shifts in the groundwater level with satisfactory results based on data obtained in the Ljubljana Aquifer using methods of simulation (regression trees and random forests and gradient boosting). The integration of Extreme Learning Machine and Quantum-Behaved Particle Swarm Optimization and regular Xinfengjiang Reservoir run data in China have been proposed by Niu et al. (2018). Taormina et al. (2012) addressed studies on the use of Fuzzy Neural Networks (FNNs) as an alternative to computational models of long-term groundwater-level modelling in coastal unconfined aquifers. Backpropagation neural networks (BP-NN) have been used in Sirat (2013) for the prediction of contamination of groundwater with pesticides by 1302 domestic and rural hydraulic wells in the Middle Continent of the United States, including Illinois, Iowa and 12 other states. The progression in artificial intelligence over the last two decades helps these developments to be incorporated into computational computing systems to resolve the limitations in their development (Chau 2006).

3.3 Application of Geospatial Technology for Groundwater

Through the advancement of space technology, remote sensing techniques are now possible in broad areas to measure the surface and subsurface water. Such techniques are very useful to rapidly map wide and inaccessible areas of groundwater. The need for remote sensing groundwater research is to demarcate and delineate all possible characteristics associated with groundwater localization. Such features are taken from the respective items for satellite data and inserted into the thematic information collected from the desired topographical sheets. The use of traditional methods for groundwater management, such as geophysics, statistics, geostatistics, numerical modelling, etc., is often severely restricted by the dearth of appropriate data. Regular and long-term surveillance by these traditional methods of groundwater and vadose zone systems is costly, time consuming and disruptive (Jha and Chowdary 2007). Groundwater is the toughest to track by satellite sensors although the GRACE has effectively seemed to assess the decline of groundwater and the swelling of the Three Gorges Reservoir (Wang et al. 2011).

3.3.1 Groundwater Exploration

All of the liquid freshwater supplies were contained in the underground (99%). Furthermore, the geographic earth composition varies and primarily depends on atmospheric factors as well as the sub-surface geology, topography, hard rock outcrops, landforms, recharge-discharge zone, etc. Groundwater exploration is an investigation into the hydrological cycle, the condition of groundwater and identification of the size, amount and form of aquifers. Groundwater can be explored in various ways. The four key methods of groundwater exploration are the areal system, the sub-surface system, the surface method and experimental methods. Groundwater exploration in hard rock terrain is a very demanding and tedious activity if fractured and fractured media are mixed in the promising groundwater areas.

In general, different types of aquifers need specific methods for analysis and appropriate level of details; regardless of hydrogeological field surveys or remote sensing, procedures are used to understand the movement of soil and locate possible boring sites for potable water management. Any sub-surface map created by remote sensing should be interpreted rather than an accurate illustration of real bodies and structures until they are tested in the field as an approximation of image characteristics (Fig. 3.3). This is especially important in areas where the detection of subsurface anomalies from satellite data is extremely difficult for diverse geologies and

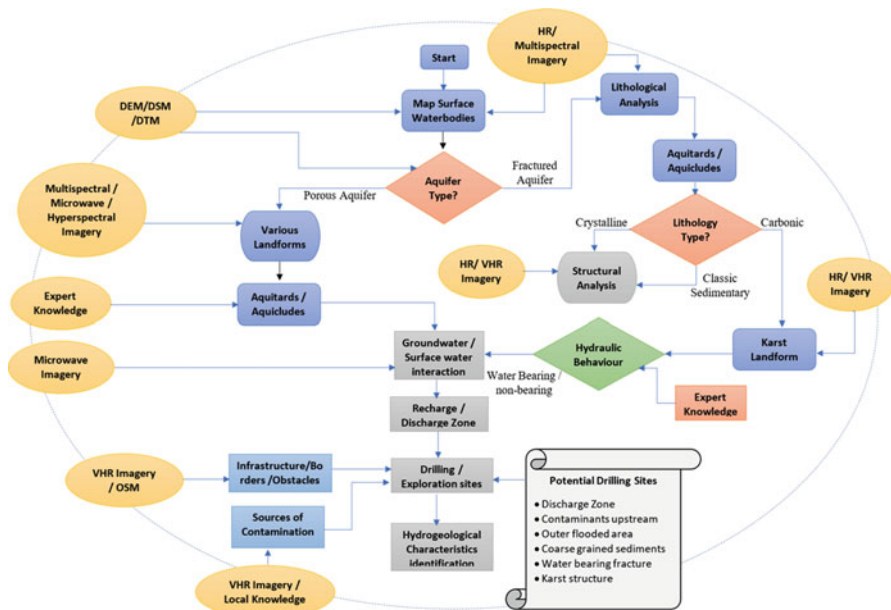


Fig. 3.3 Schematic diagram of groundwater exploration using remote sensing data. (Modified after Wendt et al. 2016)

thick vegetation. Mapping lineament in specific remote sensing imaging is a common step in the discovery of groundwater in hard rock areas.

Possible sources for groundwater exploration are therefore in widespread basis, deep reach and cross-sectional weak systems in regions such that (a) the hydrological drainage area is broad enough to have productive aquifers that are free from strong seasonal perturbations and (b) a long holding time between recharge and discharge to meet the criteria for efficiency. This involves a general topographic review, in which the river flow path and hence the approximate path of groundwater flow are measured. It involves the monitoring of water sources such as lakes and rivers, both permanently and seasonally. Vegetation may be a measure of the presence of groundwater at the soil, indicating the areas of wetlands, in arid or semi-arid environments. The development of vegetation index maps or soil moisture mapping may also be helpful when identifying appropriate sites for groundwater extraction. There is also a need to chart identified locations for groundwater withdrawals. Integration of surface waters and groundwater maps to identify the inundated areas of rivers and shorelines during different season. In conjunction with a digital elevation map, multitemporal satellite imagery to identify low-lying areas is used to this effect.

Depending on the surface material and environment conditions, temporary outflow-free lakes can contribute to groundwater infiltration. Discharge from a source of sediment to the river can be seen by an increased river depth, without visible impacts. Potential hazards may be human settlement and refugee communities where contaminants can reach the groundwater through latrines or animals but also mills, mines, site-sites or other possible waste sources. For a refugee or a major village to dig groundwater wells, access is typically required with an exhaust platform which is also placed on a truck. Therefore, it is important to recognize the existing paths, barriers and unpassable areas for ground vehicles.

3.3.2 Groundwater Potential Mapping

Remote sensing is becoming a key tool to target groundwater, because it has a direct link to the rock features and the surface geology conditions with its topographic and terrain characteristics. The study of sub-surface geological environments, identification of landscapes and lineaments, where there are sustainable groundwater potential zones, is a core aspect in sustainable groundwater planning.

The spectral differences of the surface features are shown by relative variations in the level of intensity between the bands. This technique is beneficial as human eyes can discern much more distinct colours than differences in grey tones, for instance, by analysing each channel independently or viewing bands side by side instead of as a Red-Green-Blue (RGB) fake colour composite. Because of high porosity and permeability, sandstone typically generates better plant cover. In visible-Near-infrared-Shortwave infrared (VIS-NIR-SWIR) imagery, it seems light-toned. They can be analogous to limestone, but do not have their characteristic absorption at 2.35 μm

(SWIR), particularly in the arid areas. In VIS-NIR-SWIR images, shales appear bright, with the exception of 2.1–2.4 μm , where clay minerals have an absorption characteristic. In VIS-NIR-SWIR images, carbonates typically contain light tones but approximately 2.35 μm ; residual iron bearing weathering can contribute to ultra-violet (UV) blue absorption bands. SAR data can help detect karst characteristics, as it reaches the sometimes-thick cover of vegetation. Some variations have been shown to differentiate various types of rock by their spectral characteristics. It should be recalled that these approaches only operate where there are no grass, regolith or charred areas on the rock surface. Mafic intrusive rocks are typically darker but look identical in remote sensing pictures and can be mistaken with granites. They are highly weather-dependent, particularly in wet conditions. The occurrence of rich iron minerals (pyroxenes, biotite, amphibolites) contributes to dark tones in the blue zone in particular. Alterations products may contain clay minerals between 2.1 and 2.4 μm with absorption bands. The choice of which band ratios to be used is once again arbitrary and includes matching outcrops of well-known rock forms with their performance (Table 3.2).

3.3.3 *Groundwater Modelling*

The “groundwater model” means a theoretical framework built using a computer code of choice adapted to a specific location using a series of control equations, parameters and boundaries. A groundwater model is a groundwater system approximation (Anderson et al. 2015). It simplifies a nuanced fact. Models of groundwater help users to consider the prevailing systems mechanisms and analyse the consequences of the management behaviour in that system (Bear and Cheng 2010). Groundwater models have been widely used in educated groundwater control for many decades (Barnett et al. 2012). Groundwater simulation should be used in order to explain water distribution and sub-surface absorption (distribution models), to explain and forecast water quality and contaminant transport (contaminant models), and in a particular location sea-water penetration models (density-dependent flow models). There are usually two types of mathematical codes describing hydrologic structures, theoretical models and computational models (Barnett et al. 2012). Analytical model codes define the physical mechanisms used by one or more governing equations for groundwater distribution and pollutant distribution. Although analytical model codes in space and time (DEQ 2014) are commonly not used to reflect changing situations, they are much easier to construct and operate than their quantitative predecessors. All this data is collected and viewed in a number of sizes like maps, graphic, table, electronic databases or graphs.

A Geographical Information System (GIS) is a versatile toolbox that can greatly enhance spatial data processing. Three approaches can be followed, loose coupling, close coupling and embedded attachment, using GIS and groundwater models (Gogu et al. 2001). Creation of models and algorithms for groundwater evaluations by combining remote sensing products and additional data. GIS tools enable spatial

Table 3.2 Band ratios for surface compositional discrimination

Spectral band ratio	Application	Spectral band ratio	Application
$\frac{SWIR_2}{SWIR_1}$	Argillic vs. non-argillic	$\left(\left(\frac{2.235-2.285 \mu m}{2.185-2.225 \mu m}\right) * \left(\frac{1.60-1.70 \mu m}{2.185-2.225 \mu m}\right)\right)$	OH-bearing minerals index (montmorillonite vs. mica)
$\frac{NIR/Red}$	Rocks vs. vegetation	$\left(\left(\frac{1.60-1.70 \mu m}{2.145-2.185 \mu m}\right) * \left(\frac{2.295-2.365 \mu m}{2.185-2.225 \mu m}\right)\right)$	Kaolinite index
$\frac{SWIR_1}{Blue}$	Iron-bearing vs. iron-free	$\left(\left(\frac{2.235-2.285 \mu m}{2.145-2.185 \mu m}\right) * \left(\frac{2.235-2.285 \mu m}{2.295-2.365 \mu m}\right)\right)$	Alumite index
$\frac{SWIR_1}{NIR}$	Argillic vs. Fe ²⁺	$\left(\left(\frac{2.235-2.225 \mu m}{2.295-2.365 \mu m}\right) * \left(\frac{2.360-2.430 \mu m}{2.295-2.365 \mu m}\right)\right)$	Calcite
$\frac{NIR}{SWIR_2}$	Argillic vs. Fe ³⁺	$\left(\left(\frac{8.475-8.825 \mu m}{8.125-8.475 \mu m}\right) * \left(\frac{8.475-8.825 \mu m}{8.925-9.275 \mu m}\right)\right)$	Quartzite
$\frac{Red/Blue}$	Fe ²⁺ vs. Fe ³⁺	$\left(\left(\frac{10.250-10.950 \mu m}{10.950-11.650 \mu m}\right)\right)$	Carbonate
		$\left(\left(\frac{8.925-9.275 \mu m}{10.250-10.950 \mu m}\right)\right)$	S ₂ O ₂

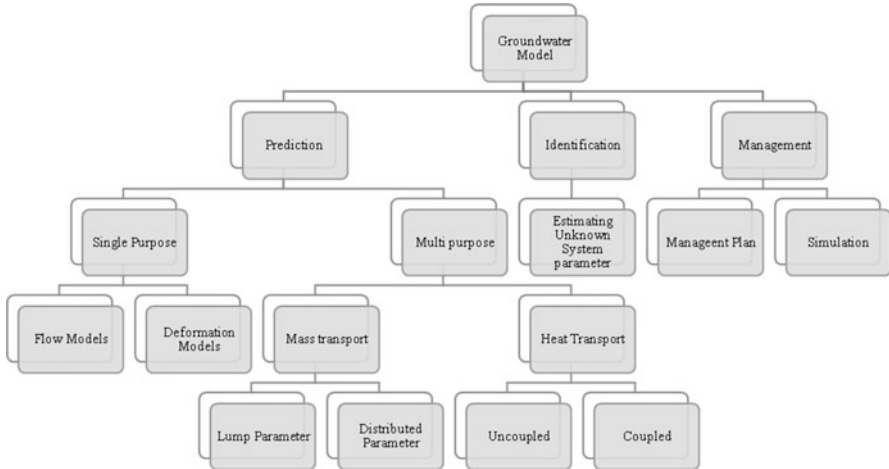


Fig. 3.4 Existing scenario of groundwater models used in research study

vision of the many factors which affect groundwater availability. GIS data layers can be merged and used for recharging, resource mapping and simulations to provide information on ground, erosion, soil, land use and land cover. Loose couplings occur when GIS and the model represent specific programme packets, and the conversion of data is done through predefined input/output configuration files. For the pre- and post-processing of spatial information, the GIS programme is used. The downside of this approach is that the merged programme solutions are separate programmes, which allow possible independent potential improvements. In tight coupling, the data is transmitted from GIS to the model, but the GIS tools are able to control subroutines of the input code interactively. Data transmission is fully automated in this situation. The relation between the spatial ERMA database scheme and MODFLOW, MODPATH, and MT3D Finite Software Difference applications (Steyaert and Goodchild 1994) is an example of the association. In CCRS, the EALCO (Ecological Assimilation of Land and Climate Observations) model assimilates the above EO products to simulate the aquifer refuelling period and evaluation. Its mechanical representation of physical, physiological and biogeochemical surface processes allows users to study the various impacts and input on surface water and groundwater interactions on climate and ecosystem management (Canisius et al. 2010). Figure 3.4 illustrates various types of groundwater models used in earlier research work.

MODFLOW, developed by the US Geological Survey (USGS), is an international model for simulating and modelling groundwater conditions and interactions between groundwater and surfacing water (Harbaugh et al. 2000). In GIS programming or in a basic GIS modelling framework, embedded coupling is used if a prototype is built in a GIS programming language. Examples of this method include the numerical simulation environment of Argus ONE (Argus Interware and Inc 1997) and the Groundwater Modelling System (GMS).

Several methods for the time interpolation and charging of time-series measurements have also been established and used. Arapahoe aquifer was used in the case study by Ruybal et al. (2019) for demonstrating that spatio-temporal crowding off a sparsely measured and poorly sampled aquifer is helpful to spatial weep. The spatial and temporal study of an Iranian aquifer was carried out by Ahmadi and Sedghamiz (2007), and the result is that the “spatial structure is substantially greater than the temporal structure”. Integrating temporal and spatial interpolation makes more precise forecasts by exploiting the connections between the measurement both temporal and spatial (Ruybal et al. 2019). In Canterbury, New Zealand, Bidwell (2005) has estimated groundwater volumes a month earlier using an ARMAX model based on its own aquifer complex structure. Oikonomou et al. (2018) used the stochastic exogenous seasonal autoregressive dynamic moving average (SARIMAX) to characterize the fluctuation in the virtual level of the groundwater of the regional physical soil water cycle and the Smoother Ensemble (ES) to estimate the level of groundwater.

3.3.4 *Geochemical Quality of Groundwater*

The groundwater includes numerous varieties of minerals that are supplied by solution, where their forms and quantities are largely depending on several influences, such as the rock composition, contact between surface and groundwater, the natural setup for groundwater flow requirements and some other cause of water contamination (Yousif and El-Aassar 2018). Both natural and anthropogenic forces regulate the composition of underground water. Natural influences that influence water chemistry include rainfall and number cycles, watershed and aquifer geological characteristics and meteorological conditions, as well as various aquifer mechanisms of rock–water interaction (Patel et al. 2016; Singh et al. 2015). Human practices impacting water quality include disposal of hazardous waste, domestic and agricultural waste, mining and farming (Singh et al. 2016). The composition of the groundwater is the end result of the contact between water and rocks of various geological periods.

Since groundwater chemistry is very complex in very close vicinity, and vary according to the season and climatic conditions (Ackah et al. 2011), evaluating the excellence of the groundwater is necessary to deduce the suitability of groundwater for household and agriculture. The water used in humans should be “clear and clean”, i.e. smell-less, colourless, tasty and free of dangerous chemicals and pathogens (Jinwal and Dixit 2008). The groundwater physicochemical parameters of the sample area shall deduce the suitability for human use and household use according to the recommendations by WHO (1997). Factor and cluster visualization are commonly used for the characterization of hydrochemical structures using traditional graphical techniques (Adewumi et al. 2018). The factor analysis helps to minimize data size in geological and related sciences (Adewumi et al. 2018) and

helps address different problems. This explains that groundwater includes numerous forms and amounts of certain dissolved chemical components.

Piper trilinear diagram is used as the basis of dominant ions to categorize water faces (Piper 1944). Significant ions are illustrated as major cations and major anions in two simple triangles of piper graphs. The trilinear piper diagram is used to separate the water faces into prevailing ions. Gibbs (1970) has suggested two models to explain hydrogeochemical procedures with respect for the precipitation of the atmosphere, rock–water interaction and groundwater evaporation. The rock–water interface in alluvial plains is the main method of controlling soil chemistry (Alam 2013). Statistical approaches provide data on identified concentrations of areal pollutants and offer characterization of the pollution potential of a particular geographic region by extrapolation from available knowledge in the field of interest.

In many geo-resources, such as mineral exploration, hydrogeology and other geological areas, remote sensing data is important. It is important to understand structural, geomorphological and lithological characteristics in hydrogeological identification. The details provided by RS increase our intelligence about the underground water. The consistency assessment of groundwater by analysing geological formations, geomorphic features and their hydrological characteristics is uniformly applicable to satellite images (Abdalla 2012; Moubark and Abdelkareem 2018). In order to measure the quality and the degree of groundwater contamination from the district of Wanaparthy, Telangana, a PIG system has been introduced by Subba Rao et al. (2018). Duraisamy et al. (2018) have carried out a report on the hydrochemical characterization and assessment of groundwater quality in Tamil Nadu, India, using the geographic information system (GIS). Drinking water quality index (DWQI) was used extensively in surfaces and sub-surface water quality measurements and has played an increasingly important role in the climate and management of water supplies (Sener et al. 2017). Figure 3.5 provides a schematic diagram for planning of a geographical distribution map using the Geographic Information System (GIS) to assess acceptable, inadequate groundwater quality areas for drinking purposes.

3.3.5 Identification of Suitable Areas for Groundwater Recharge Using GIS

Understanding the water balance of a groundwater system involves calculating the flow of charging and waste which usually varies with landscape morphology, climatic, land use and land use in time and space. In order to incorporate efficient approaches for minimizing salinity, surface water and groundwater quality conservation and habitat safety, defining groundwater drainage and runoff areas across catchments is essential. In exploring hydrogeological relations which define the groundwater systems, the geomorphic and geological existence of groundwater recharge areas and groundwater discharge areas are fundamental considerations. Remote sensing and GIS techniques involve on-the-ground knowledge to assess

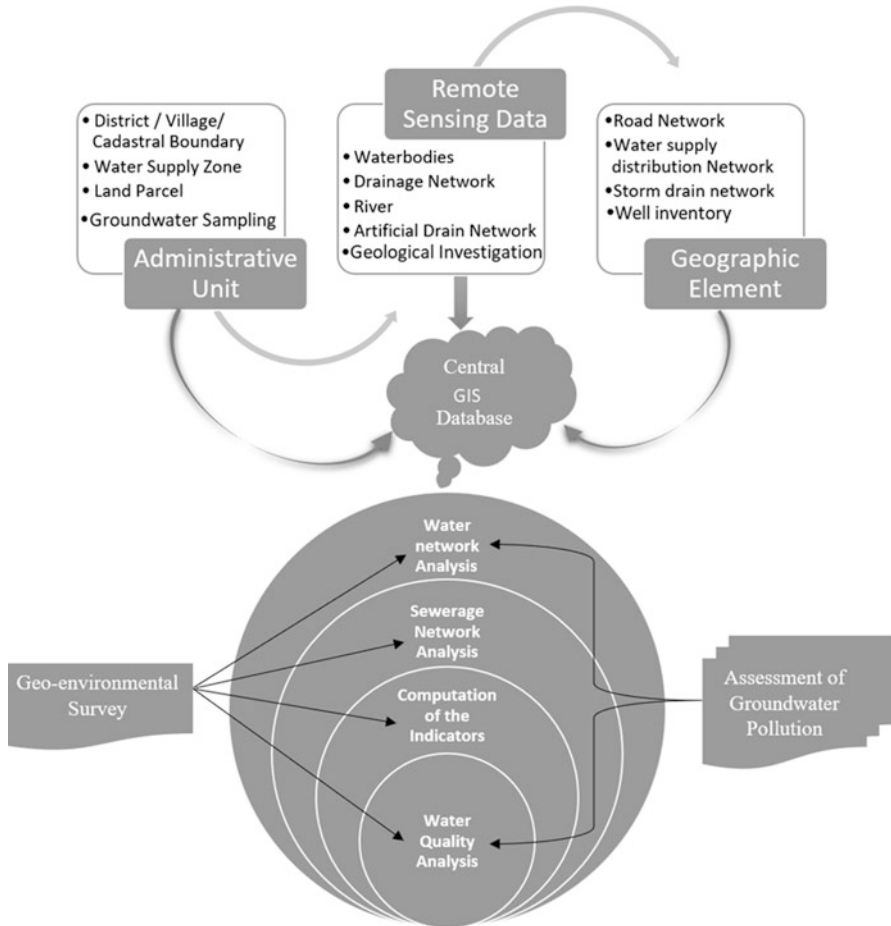


Fig. 3.5 Implementation of the integrated GIS in groundwater quality assessment

the effects of groundwater discharge and were used in many studies to classify the soil/vegetation type. Landsat (TM and ETM+) satellite data were used to identify groundwater discharge areas by detection of changes in the lake temperature (Tcherepanov et al. 2005) and through measuring groundwater spring channels (Sener et al. 2005). With on-the-ground hydrogeological surveys to map and discharge zones, Salama et al. (1994) detailed analysis of geomorphic and geological features from Landsat-TM and aerial image. Discharge mapping and identification of recharge areas can be analyzed depending upon different GIS (DEM field analysis; grid interpolation) and remote sensing (photosynthetic behaviour analysis, description of the images, basic threshold and airborne radiometry) techniques. Multi-source and multi-scale data systems including groundwater data, airborne (radiometric and aerial photos), satellites and GIS (soil map, DEMs, groundwater EC, flow and water table depth) maps were needed for remote sensing and GIS

techniques (Howari 2003; Spies and Woodgate 2005). Surface runoff is due to variations in soil composition, ground shape, slope and a loss or occurrence of the water level due to the normal soil wetness or dryness. The water level is high. Soils that are well drained (dry for long periods) would likely be strongly contaminated and thus considered an indication of favourable recharging areas.

The standard vegetation index deviation (SDVI) reflects the temporal variability of the photosynthetic plant development in all years. Lowest photosynthesis variability regions were observed using a basic SDVI image threshold technique. This mapping has only been applied to the dryer northerly region, where precipitation is the limited growth factor in summer. In addition to groundwater discharge zones, there are also poor SDVI concentrations on highways, urban areas and forests (Tweed et al. 2007). During the topographical depression and pitfalls in the entire basalt aquifer, two indices were created by a region's DEM, signalling possible saturation of groundwater. In both approaches, only if the depth to the water table is poor can the indicator reflect groundwater discharge zones. Moreover, the Wetness Index defined likely saturation zones in the base of concave slopes (a decrease in β ; Moore et al. 1991). The topographical depression and areas of possible groundwater leakage have been mapped using a basic threshold technique (>10). The GIS profile curvature function was used on the DEM to measure the break of slope of the field. The curvature of the profile is the curvature on the slope of the ground. A positive profile reveals that the surface of the cell is concave. A value of zero reveals a continuous slope of the surface. A basic technique threshold (>0.01) is used to measure the curvature values of the highest profile from the DEM and detect pitch breakage.

3.4 Recent Trend of Open Sources Data and Software in Groundwater Study

Open source data—a timely and reliable source, but still less addressed—is underused. Remote sensing has guided process observations and produced new data sets from a hydrological science perspective that cover the spectrum of water cycle components. In recent experiments, retrospective water cycle components and satellite-based hydrological improvement are examined; remotely sensed evaporation (Wang and Dickinson 2012), soil moisture (Wagner et al. 2007), precipitation (Kidd and Huffman 2011), surfaces (Alsdorf et al. 2007) and terrestrial water storage with more recent gravity-based methodological improvements are studied. The hydrological-based parameter of vegetation and the earth at different scales, including Landsat TM, AVHRR, MODIS, ENVISAT-ASAR and MERIS, RADARSAT-1 and -2, are obtained using a broad range of the satellite sensors. The recovered vegetation parameters include soil cover, land use and leaf area index (LAI). Previous research has used thermal images obtained from Landsat-5 (thematic mappers 10.45–12.4 μm) and Landsat-7 Enhanced Thematic Mappers+

(10.31–12.36 μm) to monitor areas of groundwater discharge zone (Sass et al. 2014). The full range of crop patterns and the intensities of irrigation (including groundwater and surface water) are characterized by satellite data with short return periods, such as the regular Moderate Resolution Imaging Spectrometer (MODIS) and its 8 days processed composites, e.g. MOD09Q1 data product (Gumma et al. 2011). Gravity experiments on the planet were carried out during the past decade by Gravity Recovery and the Climate Experiment (GRACE) (Tapley et al. 2004); the global complexity of this common topic of groundwater depletion has started to appear (Richey et al. 2015). This can be used to quantify improvements in overall water storage (ΔS). The Tropical Rainfall Mapping Mission (TRMM) has shown that precipitation can be measured at a period of 3 h + at a level of 50 ° N to 50 ° S and at a spatial resolution of 0.25 ° C (approximately 625 km² at Equator) (Huffman et al. 2007). Global Precipitation Measurement (GPM) provides greater (half-hour) and higher space resolution compared with TRMM (0.1°). This higher range GPM resolution is on the scale of local to regional aquifers (100 km² on Equator) and can aid to close down the equilibrium of water (Draper et al. 2015). By the end of the decade, NASA initiated with the collaboration of the Canadian Space Agency and of the French Space Agency (Durand et al. 2010) the SWOT (Surface Water and Ocean Topography) mission. SWOT is running at a space resolution of 10,000 m² and a time repeat of 22 days and represents a significant step towards remote sensing surface runoff. Other operations, such as the Suomi National Polar-Orbiting Partnership (Suomi NPP; launched in 2011) and Joint Polar Satellite System 1 (JPSS-1; scheduled for launch by the end of 2017), and future missions in the JPSS series are primarily aimed at atmospheric measurements, but they will all carry Visible Infrared Imaging Radiometer Suite (VIIRS) devices that accumulate visible and infrared images.

FREEWAT (FREE and open source tools for WATER resource management) software is then an advanced modelling framework for the public domain GIS that combines data analysis techniques and implements water management and planning frameworks for evaluating the usage of surface and groundwater in conjunction (Cannata et al. 2018). The FREEWAT framework was launched with a Free and Open Source Software licence (GPL v2) to ensure its longevity (no licencing fees and open community), its technical integrity (rights to review and change the source) and the capitalization of prior initiatives (use of current high-quality open source modules) (Rossetto et al. 2015). As internationally recognized as a standard for simulating groundwater conditions and their interaction with surface water, MODFLOW (USGS' modular groundwater model) and related programmes have been selected as the key modelling codes. The collection of FloPy is a function of the modelling codes selected. In reality, it's a specialized Python library designed specifically to create, run and post-process models that are part of the MODFLOW codes family. The time series pre-processing is performed in the modelling process, using individual tools such as Microsoft Excel, Matlab (Herring 2003) and R (Shumway and Stoffer 2006), or using such libraries in different coding languages such as PANDAS (McKinney 2015) for Python or ROOT (<https://root.cern.ch/>) for C++. TSPROC (Time Series PROCessor) (Westenbroek et al. 2010) which is a

simplified written language and includes features sometimes used for surface water models is a common time series analysis method supporting calibration of hydrological models. A software framework based on Python open source for visualizing, quantifying and using both temporal and spatial interpolation is developed by Evans et al. (2020). This method interpolates time series data on each individual well by interfacing with associations with other wells in the aquifer and spatially interplays these data to produce groundwater maps at selected time periods. This programme is beneficial for displaying time series and other details inside an aquifer and for visualizing aquifer-wide groundwater levels and animations at various times. Global Land Data Assimilation System (GLDAS) uses observationally based weather and radiation data to conduct 3-hour land surface simulation to address water and energy flows and store them globally (Rodell et al. 2004). Earth surface components were employed in monthly outputs from four GLDAS models, including Noah (NOAH) (Ek 2003), Variable Infiltration Capacity (VIC) (Liang et al. 1994), Common Land model (CLM) (Dai et al. 2003) and Mosaic (MOS) (Koster et al. 2000). Each LSM provides a different calculation of equal snow water, soil moisture and the availability of canopy vapour. The conservation of surface water including reservoirs, ponds and rivers does not address any of the GLDAS models explicitly. Each stock portion was transformed into an equal water height anomaly by extracting its time mean from April 2002 to January 2017 and dividing into a surface region to equate LSM and river routing performance with GRACE TWS anomalies (Purdy et al. 2019). The programme Satellite Hydrology Bits Analysis and Mapping (SHBAAM) software built here completes the pre- and post-processing tasks for GRACE TWS anomalies required for analysing and measuring terrestrial water cycles (Purdy et al. 2019). SHBAAM is the open source Python and bash shell-toolbox which is accessible online through GitHub (<https://github.com/c-h-david/shbaam>) or Docker (<https://hub.docker.com/r/chdavid/shbaam>). AkvaGIS application—GIS kit integrated with the FREEWAT framework—is user-friendly, free and open source (Criollo et al. 2019). AkvaGIS is designed to meet (i) management and visualization of structured hydrogeological and hydrochemical knowledge on different time and space scales, to promote the creation of the environmental conceptual model; (ii) the incorporation of data from various sources, obtained using different access techniques and formats; and (iii) the development of hydrogeologic input files in all formats available in QGIS for any numerical groundwater model. The GRACE and GLDAS data collection are downloaded and analysed by the toolbox for evaluating water storage improvements in every area around the world. The completion of NASA's SWOT mission in 2021 would deliver specific surface water rises of 90 per cent around the world twice every third week, allowing all surface water reserves and river flows to be measured. SWOT utilizes a large swath with a Ka-band interferometer to eliminate rivers 100 meters in width and lakes 250 m², wetlands or ponds 10 cm high and with a precision in the direction of 1 cm per kilometre. The latest rainfall results from only a fraction of the world's rivers are currently available mostly because of closed results policies in the developing world. The Groundwater Level Mapping Tool was created as a simple user interface Web application. The tool builds on Tethys Platform, an open source platform that reduces the barrier to

the creation of environmental web apps (Swain et al. 2016; Tethys 2020). The Groundwater Level Mapping Tool consists of two main parts, the user interface and the administrator interface. The administrator interface enables data to be uploaded to the app, and data processing to create interpolated groundwater level maps and animations. The tools used in this paper are all open source. The public can find the Web app code in <https://github.com/stevenwevans2/tethysapp-gw/tree/timeseries>. On Tethys Platform the web app was introduced (home page:<https://www.tethysplatform.org/>; source code: <https://github.com/tethysplatform/tethys>).

3.5 Conclusion

For groundwater management and scientists, sustainable yield remains a concern. Social analysts can make a significant contribution by defining how stakeholders identify or view “sustainable returns”, discussing them and maybe helping integrate various ways of thinking and interpreting their actions and their behaviours, and politics and management in turn. Satellite data inform about rock types, land types, geological formations, fault, folds, fracturing, dyke, weathering, soil types, erosion, land use/cover and water surface distribution and alteration. Such information when incorporated into a Geographic Information System (GIS) framework allows for groundwater recharge estimates; draft estimates; balance calculations; categorization of areas into highly developed, underdeveloped and undeveloped areas; identification and mapping of prospective groundwater zones; systematic groundwater planning and development; and identification of over-exploited areas. The recharge and discharge surface indicators should be important and capable of defining the dominant processes. The area’s best defined for groundwater disposal by mapping areas with relative low veggie variability. The mapping regions of comparatively low regions with basalt aquifer surface characteristics were effectively defined by preferential infiltration zones. Groundwater discharge areas were thus described by the mapping of impacts on surface characteristics (vegetation), while the mapping of surface characteristics’ influences on charging (infiltration) were classified as preferred recharge areas. However, the resolution and scope of information are improved for regional catchment by spatially identifying the priority recharge and discharge areas through the use of GIS and remote sensing visualization methods, thereby offering new hydrogeological knowledge for computational forecasting, water budget research and salinity reduction programmes.

References

- Abdalla, F. (2012). Mapping of groundwater prospective zones using remote sensing and GIS techniques: A casestudy from the Central Eastern Desert, Egypt. *J. Afr. Earth Sci.*, 70, 8–17.

- Ackah, M., Agyemang, O., Anim, A.K., Osei, J., Bentil, N.O., Klatch, L., ... Hanson, J.E.K. (2011). Assessment of groundwater quality for drinking and irrigation: The study of Teiman-Oyarifa Community, Ga East Municipality, Ghana. *Proceedings of the International Academy of Ecology and Environmental Sciences*, 1(3–4), 186–194.
- Adewumi AJ, Anifowose AYB, Olabode FO, Laniyan TA. (2018). Hydrogeochemical Characterization and Vulnerability Assessment of Shallow Groundwater in Basement Complex Area, Southwest Nigeria. *Contemp. Trends. Geosci.*, 7(1): 72-103
- Ahmadi SH, Sedghamiz A. (2007). Geostatistical analysis of spatial and temporal variations of groundwater level. *Environ. Monit. Assess.*, 129 (1–3): 277-294
- Alam F. (2013). Evaluation of hydrogeochemical parameters of groundwater for suitability of domestic and irrigational purposes: a case study from central Ganga Plain, India. *Arabian Journal of Geosciences*, 7, 4121–4131. doi:<https://doi.org/10.1007/s12517-013-1055-6>
- Alsdorf DE, Rodríguez E, and Lettenmaier DP. (2007). Measuring surface water from space, *Reviews of Geophysics*, 45, n/a–n/a, <https://doi.org/10.1029/2006RG000197>
- Anderson MP, Woessner WW, Hunt RJ. (2015). *Applied groundwater modeling, simulation of flow and advective transport*, Second Edition. Academic Press by Elsevier Inc
- Argus Interware, Inc. (1997). *Argus Open Numerical Environments – A GIS Modeling System*, Version 4, Argus Holdings, Limited
- Barnett, B., L.R. Townley, V. Post, R.E. Evans, R.J. Hunt, L. Peeters, S. Richardson, A.D. Werner, A. Knapton, and A. Boronkay. (2012). *Australian groundwater modeling guidelines*, Waterlines report, No. 82, National Water Commission, Canberra
- Bear, J., and A. H.-D. Cheng. (2010). *Modeling Groundwater Flow and Contaminant Transport*. Springer
- Bidwell VJ. (2005). Realistic forecasting of groundwater level, based on the eigenstructure of aquifer dynamics. *Math. Comput. Simulat.*, 69 (1–2): 12-20
- Bolin B, Collins T, Darby K. (2008). Fate of the Verde: water, environmental conflict, and the politics of scale in Arizona's central highlands. *Geoforum* 39(3):1494–1511
- Cannata, M., Neumann, J. Rossetto, R. (2018). Open source GIS platform for water resource modelling: FREEWAT approach in the Lugano Lake. *Spat. Inf. Res.* 26, 241–251, <https://doi.org/10.1007/s41324-017-0140-4>
- Canisius, F., Fernandes, R. and Chen, J. (2010). Comparison and evaluation of MERIS FR LAI products over mixed land use regions, *Remote Sensing of Environment*, doi:<https://doi.org/10.1016/j.rse.2009.12.010>
- Chau K. (2006). A review on integration of artificial intelligence into water quality modelling. *Mar Pollut Bull* 52:726–733
- Criollo R, Velasco V, Nardi A, de Vries LM, Riera C, Scheiber L, Jurado A, Brouyère S, Pujades E, Rossetto R, Vázquez-Suñé E. (2019). AkvaGIS: An open source tool for water quantity and quality management. *Computers and Geosciences*, 127: 123-132
- Cantor BA. (2009). Groundwater banking in aquifers that interact with surface water: aquifer response functions and double-entry accounting. *J Am Water Resour Assoc* 45 (6):1465–1474. doi: <https://doi.org/10.1111/j.1752-1688.2009.00378.x>
- Curtis A., Mitchell M., Mendham E. (2016). Social Science Contributions to Groundwater Governance. In: Jakeman A.J., Barreteau O., Hunt R.J., Rinaldo JD., Ross A. (eds) *Integrated Groundwater Management*. Springer, Cham. https://doi.org/10.1007/978-3-319-23576-9_19
- Dai, Y., Zeng, X., Dickinson, R. E., Baker, I., Bonan, G. B., Bosilovich, M. G., et al. (2003). The common land model. *Bull. Am. Meteorol. Soc.* 8:1013–1024. doi: <https://doi.org/10.1175/BAMS-84-8-1013>
- Department of Environmental Quality [DEQ], Michigan, (2014). *Groundwater Modeling: Remediation and Redevelopment Division Resource Materials*. Prepared by: Michigan Department of Environmental Quality Remediation and Redevelopment Division. RRD Resource Materials -25-2013-01. February, 2014.
- Draper, D., D. Newell, F. Wentz, S. Krimchansky, and G. Skofronick-Jackson. (2015). *The Global Precipitation Measurement (GPM) Microwave Imager (GMI): Instrument Overview and Early*

- On-Orbit Performance. *IEEE Journal of Selected Topics in Applied Earth Observations and Remote Sensing* 8, no. 7: 3452–3462. DOI:<https://doi.org/10.1109/JSTARS.2015.2403303>
- Duraisamy S., Govindhaswamy V., Duraisamy K., et al. (2018). Hydrogeochemical Characterization and Evaluation of Groundwater Quality in Kangayam Taluk, Tirupur District, Tamil Nadu, India, Using GIS Techniques *Environ Geochem Health*
- Durand, M., L.-L. Fu, D. P. Lettenmaier, D. E. Als, E. Rodriguez, and D. Esteban-Fernandez (2010), The surface water and ocean topography mission: Observing terrestrial surface water and oceanic submesoscale eddies, *Proc. IEEE*, 98(5), 766–779. <https://doi.org/10.1109/JPROC.2010.2043031>
- Ek, M. B. (2003). Implementation of Noah land surface model advances in the National Centers for Environmental Prediction operational mesoscale Eta model. *J. Geophys. Res.* 108:8851. doi: <https://doi.org/10.1029/2002JD003296>
- Elbeih SF. (2015). An overview of integrated remote sensing and GIS for groundwater mapping in Egypt. *Ain Shams Engineering Journal*, 6(1): 1-15
- Evens SW, Jones NL, Williams GP, Ames DP, Nelson EJ. (2020). Groundwater Level Mapping Tool: An open source web application for assessing groundwater sustainability. *Environmental Modelling and Software*, 131, 104782
- Fu B, Shi A, Zhang Z. (1999). Retrieval of temperature information of ground water enrichment belt using thermos-infrared remote sensing data, *Journal of Remote Sensing Technique and Application*, 14: 34 – 38
- Gibbs, R.J. (1970). Mechanism controlling world's water chemistry. *Science*, 170, 1088–1090. <https://doi.org/10.1126/science.170.3962.1088>
- Gogu R.G., Carabin G., Hallet V., Peters V., Dassargues A. (2001). GIS-based hydrogeological databases and groundwater modelling. *Hydrogeological Journal*, 9, pp. 555–569
- Gumma, M.K.; Thenkabail, P.S.; Nelson, A. (2011). Mapping Irrigated Areas Using MODIS 250 Meter Time-Series Data: A Study on Krishna River Basin (India). *Water*, 3, 113-131
- Guio Blanco, C. M., Brito Gomez, V. M., Crespo, P. Ließ, M. (2018). Spatial prediction of soil water retention in a Páramo landscape: Methodological insight into machine learning using random forest. *Geoderma*. 316, 100–114
- Harbaugh A. W., Banta E. R., Hill M. C. and McDonald M. G. (2000). "MODFLOW-2000, The US Geological Survey Modular Ground-water Model - User Guide to Modularization Concepts and the Ground-water Flow Process", US Geological Survey Open-File Report 00–92
- Herring, T. (2003). MATLAB tools for viewing GPS velocities and time series. *GPS Solutions*, 7 (3), 194–199
- Howari FM. (2003). The use of remote sensing data to extract information from agricultural land with emphasis on soil salinity. *Aust J Soil Res* 41:1243–1253
- Huffman, G., R. Adler, D. Bolvin, G. Gu, E. Nelkin, K. Bowman, Y. Hong, E. Stockerm, and D. Wolff. (2007). The TRMM multisatellite precipitation analysis (TMPA): quasi-global multi-year, combined-sensor precipitation estimates at fine scales. *Journal of Hydrometeorology* 8, no. 1: 38–55. DOI:<https://doi.org/10.1175/JHM560.1>
- Jaiswal R.K., Mukherjee S., Krishnamurthy J., Saxena R. (2003). Role of remote sensing and GIS techniques for generation of groundwater prospect zones towards rural development – an approach. *Int J Remote Sensing*, 24(5): 993-1008
- Jha MK, Chowdary VM. (2007). Challenges of using remote sensing and GIS in developing nations. *Hydrogeol J*, 15: 197-200
- Jinwal, A., Dixit, S. (2008). Pre- and post-monsoon variation in physico-chemical characteristics in groundwater quality of bhopal “The City of Lakes” India. *Asian Journal of Experimental Sciences*, 22(3), 311–316
- Kenda, K. et al. (2018). Groundwater modeling with machine learning techniques: Ljubljana polje Aquifer. *Proceedings 2*, 697, <https://doi.org/10.3390/proceedings2110697>
- Kidd C, and Huffman GJ (2011). Global precipitation measurement, *Meteorological Applications*, 18, 334–353, <https://doi.org/10.1002/met.284>

- Koster, R. D., Suarez, M. J., Ducharme, A., Stieglitz, M., and Kumar, P. (2000). A catchment-based approach to modeling land surface processes in a general circulation model I. Model structure. *J. Geophys. Res. Atmos.* 105, 24809–24822. doi: <https://doi.org/10.1029/2000JD900327>
- Kwarteng AY. (2002). Utilization of remote sensing and GIS for groundwater exploration in Kuwait. In: Sherif, Singh, Al-Rashed (Eds.), *Groundwater hydrology*, Balkema, The Netherlands, 157–178
- LeCun, Y., Bengio, Y. and Hinton, G. (2015). Deep learning. *Nature*. 521, 436–444
- Liang, X., Lettenmaier, D. P., Wood, E. F., and Burges, J. (1994). A simple hydrologically based model of land surface water and energy fluxes for general circulation models. *J. Geophys. Res.* 99 14415–14428
- Li W. (2010). MODIS-based remote sensing monitoring of desertification regional groundwater model, Master, Chang'an University, Xi'an, China
- Lockwood M, Davidson J, Curtis A et al (2010). Governance principles for natural resource management. *Soc Nat Resour* 23(10):986–1001. doi: <https://doi.org/10.1080/08941920802178214>
- Mazur N, Curtis A, Rogers M (2013). Do you see what I see? Rural landholders' belief in climate change. *Soc Nat Resour* 26(1):75–85. doi: <https://doi.org/10.1080/08941920.2012.686650>
- Meijerink AMJ, Bannert D, Batelaan O, Lubczynski MW, Pointet T. 2007. Remote sensing applications to groundwater. IHP-VI, Series on Groundwater No.16. Published in 2007 by the United Nations Educational, Scientific and Cultural Organization, Place de Fontenoy, 75352 Paris 07 SP
- McKinney, W. (2015). Python data analysis library. <http://pandas.pydata.org>. Accessed 12 Oct 2017.
- Moore ID, Grayson RB, Landson AR (1991). Digital terrain modelling: a review of hydrological, geomorphological, and biological applications. *Hydrol Process* 5:3–30
- Moubark, K.; Abdelkareem, M. (2018). Characterization and assessment of groundwater resources using hydrogeochemical analysis, GIS, and field data in southern Wadi Qena, Egypt. *Arabian J. Geosci.*, 11, 598
- Mukherji A, Shah T (2005). Groundwater socio-ecology and governance: a review of institutions and policies in selected countries. *Hydrogeol J*, 13(1):328–345. doi: <https://doi.org/10.1007/s10040-005-0434-9>
- Niu, W., Feng, Z., Cheng, C. and Zhou, J. (2018). Forecasting daily runoff by extreme learning machine based on quantum-behaved particle swarm optimization. *J. Hydrol. Eng.* 23, 1–10, [https://doi.org/10.1061/\(ASCE\)HE.1943-5584.0001625](https://doi.org/10.1061/(ASCE)HE.1943-5584.0001625).
- Oh HJ, Kim YS, Choi JK, Park E, Lee S. (2011). GIS mapping of regional probabilistic groundwater potential in the area of Pohang City, Korea. *J Hydrol*, 399: 158-172.
- Oikonomou PD, Alzraiee AH, Karavitis CA, Waskom RM. (2018). A novel framework for filling data gaps in groundwater level observations. *Adv Water Resour*, 119: 111-124
- Patel, P., Raju, N.J., Reddy, B.S.R., Suresh, U., Gossel, W., and Wycisk, P. (2016). Geochemical processes and multivariate statistical analysis for the assessment of groundwater quality in the Swarnamukhi River basin, Andhra Pradesh, India. *Environmental Earth Sciences*, 75(7), 611. <https://doi.org/10.1007/s12665-015-5108-x>
- Piper, A.M. (1944). A graphic procedure in the geochemical interpretation of water-analyses. *Transactions, American Geophysical Union*, 25, 914–923. <https://doi.org/10.1029/TR025i006p00914>
- Purdy AJ, David CH, Md. Sikder S, Reager JT, Chandanpurkar HA, Jones NL, Matin MA. (2019). An Open-Source Tool to Facilitate the Processing of GRACE Observations and GLDAS Outputs: An Evaluation in Bangladesh. *Frontiers in Environmental Science*, 7: 155
- Richey AS, Thomas BF, Lo MH, Reager JT, Famiglietti JS, Voss K et al. (2015). Quantifying renewable groundwater stress with GRACE. *Water Resour Res.* 51: 5217–5238. doi: <https://doi.org/10.1002/2015WR017349>


- Rodell M, Houser PR, Jambor U, Gottschalck J, Mitchell K, Meng CJ, et al. (2004). The global land data assimilation system. *Bull. Am. Meteorol. Soc.* 2004, 381–394. doi: <https://doi.org/10.1175/BAMS-85-3-381>
- Rossetto R, Borsi I, Foglia L. (2015). FREEWAT: FREE and open source software tools for WATER resource management. *Rendiconti Online Della Società Geologica Italiana*, 35, 252–255
- Ruybal CJ, Hogue TS, McCray JE. (2019). Evaluation of groundwater levels in the Arapahoe aquifer using spatiotemporal regression kriging. *Water Resour Res.*, 55 (4): 2820-2837
- Salama, R. B., G. A. Bartle, and P. Farrington (1994), Water use of plantation Eucalyptus camaldulensis estimated by groundwater hydrograph separation techniques and heat pulse method, *J. Hydrol.*, 156, 163–180.
- Sass GZ, Creed IF, Riddell J, Bayley SE. (2014). Regional-scale mapping of groundwater discharge zones using thermal satellite imagery. *Hydrological Processes* 28, 5662–5673
- Sener S, Sener E, Davraz A. (2017). Evaluation of water quality using water quality index (WQI) method and GIS in Aksu River (SW-Turkey). *Sci. Total Environ.*, 584, 131–144
- Sener E, Davraz A, Ozcelik M (2005). An integration of GIS and remote sensing in groundwater investigations: a case study in Burdur, Turkey. *Hydrogeol J* 13:826–834
- Shah T. (2007). *The Groundwater Economy of South Asia: An Assessment of Size, Significance and Socio-ecological Impacts*. Edited by M. Giordano and K.G. Villholth, *The Agricultural Groundwater Revolution: Opportunities and Threats to Development*, pp 7–36.
- Shumway, R. H., and Stoffer, D. S. (2006). *Time series analysis and its applications: with R examples*. New York: Springer Science and Business Media.
- Singh, S., Raju, N.J., and Ramakrishna, C. (2015). Evaluation of groundwater quality and its suitability for domestic and irrigation use in parts of the Chandauli-Varanasi region, Uttar Pradesh, India. *Journal of Water Resource and Protection*, 7(7), 572. <https://doi.org/10.4236/jwarp.2015.77046>
- Singh SK, Srivastava PK, Szilárd S, Petropoulos GP, Gupta M, Islam M (2016) Landscape transform and spatial metrics for mapping spatiotemporal land cover dynamics using earth observation data-sets. *Geocarto Int.* <https://doi.org/10.1080/10106049.2015.1130084>
- Sirat M (2013). Neural network assessment of groundwater contamination of US Mid-continent. *Arabian Journal of Geosciences*, 6(8):3149–3160
- Spies B, Woodgate P. (2005). Salinity mapping methods in the Australian context. Prepared for the Natural Resource Management Ministerial Council through Land and Water Australia and the National Dryland Salinity Program, Canberra, Australia
- Steyaert L.T., Goodchild M.F. (1994). Integrating geographic information systems and environmental simulation models: a status review. W.K. Michener, J.W. Brunt, S.G. Stafford (Eds.), *Environmental Information Management and Analysis: Ecosystem to Global Scales*, Taylor and Francis, Inc., Bristol, PA, USA, pp. 333–356
- Subba Rao N., Sunitha B., Rambabu R., Rao P.V.N., Rao P.S., Spandana B.D., Sravanthi M., Marghade D. (2018). Quality and degree of pollution of groundwater, using PIG from a rural part of Telangana State, India. *Appl. Water Sci.*, 8, p. 227, <https://doi.org/10.1007/s13201-018-0864-x>
- Swain, D. L., Horton, D. E., Swain, D. L., Horton, D. E., Singh, D., & Diffenbaugh, N. S. (2016). Trends in atmospheric patterns conducive to seasonal precipitation and temperature extremes in California. *Science Advances*, 2(4), e1501344.
- Swenson S, Wahr J, and Milly PCD. (2003). Estimated accuracies of regional water storage variations inferred from the Gravity Recovery and Climate Experiment (GRACE), *Water Resources Research*, 39, n/a–n/a, <https://doi.org/10.1029/2002WR001808>
- Taormina, R., Chau, K.-W. and Sethi, R. (2012). Artificial neural network simulation of hourly groundwater levels in a coastal aquifer system of the Venice lagoon. *Eng. Appl. of Artif. Intel.* 25, 1670–1676, <https://doi.org/10.1016/j.engappai.2012.02.009>
- Tapley, B. D., et al. (2004). GRACE measurements of mass variability in the Earth system, *Science*, 305, 503–505. <https://doi.org/10.1126/science.1099192>

- Tcherepanov EN, Zlotnik VA, Henebry GM (2005). Using Landsat thermal imagery and GIS for identification of groundwater discharge into shallow groundwater-dominated lakes. *Int J Remote Sens* 26(17):3649–3661.
- Tethys platform, 2020. Available at: <https://www.tethysplatform.org/>
- Tewari DD, Khanna S (2005). Building and energizing water institutions: a case study of irrigation management transfer in Gujarat. *J Environ Syst*, 31(3):201–221. doi: <https://doi.org/10.2190/ES.31.3.a>
- Thompson CL, Supalla RJ, Martin DL et al (2009). Evidence supporting cap and trade as a groundwater policy option for reducing irrigation consumptive use. *J Am Water Resour Assoc* 45(6):1508–1518. doi: <https://doi.org/10.1111/j.1752-1688.2009.00384.x>
- Thompson J C, Moore A D. Relations between topography and water table depth in a shallow forest soil, *Hydrological Process*, J. 10 (1996) 1513 - 1525.
- Tweed, S.O., Leblanc, M., Webb, J.A. et al. (2007). Remote sensing and GIS for mapping groundwater recharge and discharge areas in salinity prone catchments, southeastern Australia. *Hydrogeol J*, 15, 75–96 <https://doi.org/10.1007/s10040-006-0129-x>
- Vapnik, V. (2013). *The Nature of Statistical Learning Theory*. Springer science and business media
- Wang, X.; Linage, C.R.; Famiglietti, J.; Zender, C.S. (2011). Gravity Recovery and Climate Experiment detection of water storage changes in the Three Gorges Reservoir of China and comparison with in situ measurements. *Water Resour. Res.*, 47, 1–13
- Wang K, and Dickinson RE (2012). A review of global terrestrial evapotranspiration: Observation, modeling, climatology, and climatic variability, *Rev. Geophys*, 50, RG2005, <https://doi.org/10.1029/2011rg000373>,
- Wagner W, Naeimi V, Scipal K, de Jeu R, and Martínez-Fernández J (2007). Soil moisture from operational meteorological satellites, *Hydrogeol. J*, 15, 121–131, <https://doi.org/10.1007/s10040-006-0104-6>,
- Wendt L, Hilberg S, Robl J, Dirnberger D, Strasser T, Braun A. (2016). Remote Sensing in Hydrogeology: A short summary of methods and constraints for groundwater exploration. *DOC:HYDROGEOLOG. RS /08/2013, Issue:1.1. pp 1–57*
- Westenbroek, S.M., Kelson, V.A., Dripps, W.R., Hunt, R.J., and Bradbury, K.R., 2010, SWB—A modified Thornthwaite-Mather Soil-Water-Balance code for estimating groundwater recharge: *U.S. Geological Survey Techniques and Methods* 6–A31, 60 p.
- World Health Organization. (1997). *Guidelines for the drinking water quality, Revision of the 1984 guideline*, Final Task Group Meeting, 21–25 Sep 1992. Geneva: WHO
- Yamamoto S (2008). Groundwater management in rice terraces: a case study of a lakeside community in Shiga Prefecture, Japan. *Local Environ* 13(5):449–460. <https://doi.org/10.1080/13549830701809775>
- Yousif, M., El-Aassar, A.H.M. (2018). Rock-water interaction processes based on geochemical modeling and remote sensing applications in hyper-arid environment: cases from the southeastern region of Egypt. *Bull Natl Res Cent* 42, 4. <https://doi.org/10.1186/s42269-018-0004-7>

Chapter 4

Geospatial and Geophysical Approaches for Assessment of Groundwater Resources in an Alluvial Aquifer of India



Partha Pratim Adhikary , S. K. Dubey, Debashis Chakraborty,
and Ch. Jyotiprava Dash

Abstract Western Delhi is a peri-urban area and mainly produces cash crops like vegetables. For round the year vegetable production, the farmers in this area depend on groundwater for irrigation. Thus, widespread groundwater withdrawal for intensive vegetable cultivation is the primary cause of depletion of groundwater quantity in this part of Delhi. To understand sub-surface geologic condition and to assess groundwater availability, geophysical imaging of the sub-surface was carried out. Groundwater potential zones were found at 18–30 m below ground level, and the quality of groundwater seems to be of moderate to poor because of low resistivity values in the water potential zones. Geospatial mapping of the resistivity values of different sub-surface layers identified the geological formations like coarse fragments, clay, calcite and other formations. Longitudinal Unit Conductance (S value) and Transverse Unit Resistance (T value) and their combinations are found effective to identify groundwater potentiality. Geospatial maps prepared by ordinary kriging interpolation method indicated that 20.2% of the area has potential to get good quality groundwater. But these areas are scatteredly distributed at the east, west, and north side of west Delhi. The aquifer of the southern part of the study area showed low resistivity formation, which indicates groundwater pollution. The infiltrations of

P. P. Adhikary
ICAR-Indian Institute of Water Management, Bhubaneswar, India

S. K. Dubey (✉)
ICAR – Indian Agricultural Research Institute, New Delhi, India

ICAR – Indian Institute of Soil and Water Conservation, Research Centre, Agra, Uttar Pradesh,
India

D. Chakraborty
ICAR – Indian Agricultural Research Institute, New Delhi, India

Ch. J. Dash
ICAR – Indian Institute of Soil and Water Conservation, Research Centre, Koraput, Odisha,
India

highly polluted Najafgarh drain water and fertilizer laden surface water and their subsequent movements to the aquifer are mainly responsible for this. The study will help to identify the hotspots for periodic monitoring of groundwater quality. The study also suggests the directions of future research works for scientific development and management of groundwater resources in west Delhi.

Keywords Delhi · Geophysical imaging · Groundwater potentiality · Longitudinal Unit Conductance · Resistivity · Transverse Unit Resistance

4.1 Introduction

Monsoonal uncertainty and excessive withdrawal of groundwater over recharge are the main reasons of lowering of water table and also deterioration of groundwater quality in many parts of India (Adhikary et al. 2009). The problem is more acute in the alluvial aquifers where, nowadays, good quality water is primarily available in the deeper aquifers. The main geological formations in alluvial areas of North India are the deposition of weathered materials carried out by the rivers and wind; thus a regolith, normally produced by *ex situ* weathering, is highly deep. Hydro-geologically, the porosity of the weathered regolith is generally high and stores high amount of water; but it can show low permeability because of high clay content. Therefore, to get high water yield for a long duration, the bore well needs to be penetrated a large thickness of regolith. The farmers in the alluvial zones have the tendency to drill bore wells haphazardly without knowing the water bearing potential of the aquifer, resulting the failure of the bore wells. This may sometime increase the debt burden of the farmers.

Therefore, to help the farmers in the alluvial zone, proper appraisal of groundwater in terms of quantity and quality needs to be done. This is also needed to plan and manage groundwater scientifically for its multiple uses like irrigation, drinking, domestic and industrial uses, recreation, etc. In one hand, groundwater quality deterioration is generally linked to some point source activity like municipal and industrial waste depositions and non-point source activity like spraying of pesticides and fertilizers to the field in excess (Adhikary et al. 2010), and on the other hand, the quantity of groundwater available for different use is linked with indiscriminate withdrawal of groundwater for agriculture owing to no or very low electricity charge. The extent of groundwater withdrawal changes from year to year and season to season based on various issues and thus needs proper investigation for its efficient utilization.

The aquifer systems are very complex and the groundwater-related problems are very site specific. Therefore, a single approach for scientific evaluation and proper management of groundwater may not be sufficient and thus calls for an integrated

approach (Adhikary et al. 2014a, 2015a). To understand groundwater quality, the widely used method is hydro-chemical method (Adhikary et al. 2009, 2014b; 2015b; Prasanna et al. 2011). Geophysical technique, on the other hand, can easily assess and monitor spatio-temporal change of groundwater resources. It is a rapid, non-destructive, and cost-effective technique to monitor groundwater system as compared to conventional hydro-chemical technique (Adhikary et al. 2015a). Geophysical technique is the ensemble of four techniques, namely, geo-electrical, seismic, gravimetric, and electromagnetic. Among these, geo-electrical technique is the widely used technique to monitor aquifer characteristics (Skuthanet et al. 1986). Dependability and cost-effectivity are the two important issues of geo-electrical technique which have led to its widespread use in groundwater quality management (Mazac et al. 1987; Skuthan et al. 1986; Al Garni 2011; Adhikary et al. 2015a).

The zones of poor groundwater quality can be effectively monitored by geophysical imaging technique (Rao et al. 2011). It is the two-dimensional visualization of the variation of sub-surface resistivity and can be created by inverting the simultaneous measurement of many individual resistance (Adhikary et al. 2015a). Not only two-dimensional imaging, three-dimensional resistivity imaging is also widely used to monitor aquifer characteristics and groundwater pollution (Ustra et al. 2012). Geophysical imaging technique has widely been used for mapping of sub-surface configurations (Griffiths and Barker 1993; Loke and Barker 1996). The mapping of groundwater pollution plumes in the aquifer and their spatial and temporal movements can also be assessed by using geophysical imaging technique (Adhikary et al. 2015a).

For mapping of groundwater resources, the geospatial interpolation approach may be either deterministic, like inverse distance weighting (Varouchakis and Hristopulos 2013) and radial basis function (Arslan 2014) or stochastic, like ordinary kriging (Sun et al. 2009; Adhikary et al. 2010, 2012; Adhikary and Biswas, 2011; Arslan 2014), indicator kriging (Adhikary et al. 2011), and universal kriging (Sun et al. 2009; Adhikary and Dash 2017). But the widely used geospatial interpolation of groundwater resources is ordinary kriging (OK). OK was used by Prakash and Singh (2000) to determine optimum number of observation wells for monitoring of groundwater level spatially. Adhikary et al. (2015b) have used geostatistics for sustainable management of groundwater resources. OK has widely been used to optimize the groundwater level monitoring network and also to improve the quality of the monitored data (Theodossiou and Latinopoulos 2006). Ahmadi and Sedghamiz (2008) used OK to establish spatial and temporal structure of water level spatial variation. The application of OK to understand the spatial structure of water table data under non-uniformly spaced observation wells has been reported by Nikroo et al. (2010) in Iran. In a study in India, OK has been used to develop water table management network in an area where sufficient monitoring well is absent (Dash et al. 2010).

Thus, geophysical imaging along with ordinary kriging spatial interpolation technique has the capability to systematically assess and monitor the groundwater resources in a cost-effective way. The efficacy of these techniques has been

demonstrated in the southern part of Najafgarh block, which is situated at west Delhi, bordering Haryana state of India, which is a peri-urban area where huge amount of groundwater is being withdrawn for agricultural purpose. In this block, overexploitation of groundwater for growing mainly vegetable crops has been reported as the main cause of lowering of water table (CGWB 1996) and increasing of groundwater salinity (Adhikary et al. 2010, 2012, 2015c). In this context, geophysical imaging can become a handy tool to quantify the groundwater resources in this area. Therefore, the present study has been undertaken to assess the present status of groundwater through geophysical imaging of the sub-surface and subsequent spatial interpolation of groundwater quality using ordinary kriging interpolation technique.

4.2 Materials and Method

4.2.1 *The Study Area*

Delhi is a small state located at the juncture of the Indo-Gangetic plain and Aravalli range. It lies between north latitudes $28^{\circ}24'17''$ and $28^{\circ}53'00''$ and east longitudes $76^{\circ}50'24''$ and $77^{\circ}20'37''$. The location of the study area is the west side of Delhi state, that is the southern part of Najafgarh block. It lies between north latitude of $28^{\circ}30'14''$ and $28^{\circ}39'45''$ and east longitude of $76^{\circ}50'24''$ and $77^{\circ}02'15''$ with area-wise coverage of about 189 km^2 (Fig. 4.1). The Najafgarh drain flows along the south and east boundary, and Kultana Chhudani Bupania drain flows along the north boundary of the study area. It is surrounded by Jhajjar district and Nangloi block in the north, East Najafgarh block in the east, Gurgaon district in the south, and Jhajjar district in the west.

4.2.2 *Physiography, Relief, and Drainage*

Three types of physiographic units are found in the study area. They are undulating plains, piedmont plains, and the Aravalli ridge. Undulating plains are formed from the fluvio-aeolian deposits coming from Yamuna River and Rajasthan desert. In some areas, colluvial deposits from the Aravalli ranges also form the undulating plains. Piedmont plains are formed at the foothills of the Aravalli range, and these plains are modified by aeolian deposits or by fluvian deposits. The Aravalli ridge is a long, narrow continuation of the Aravalli range and dissects Delhi state from south to north.

The topography of Delhi is undulating in nature with an average elevation of 227 m above mean sea level. The elevation ranges between 198 and 326 m above mean sea level, and the average slope is from south-west to north-east direction. The drainage is important to remove excess water from the land surface as well as

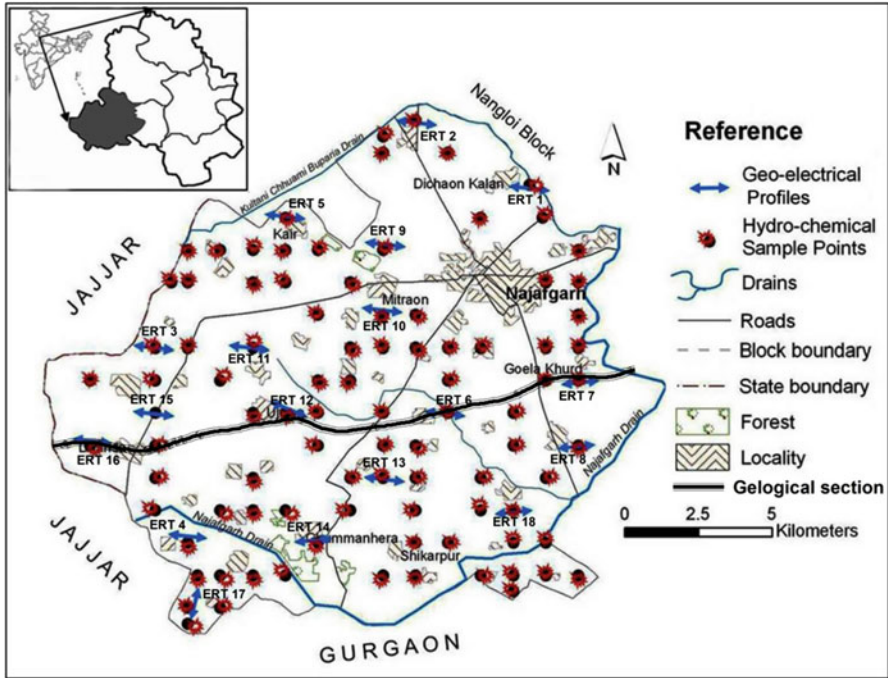


Fig. 4.1 Study area map showing the location of the geophysical survey points and hydro-chemical sampling points

sub-surface. With the drainage water, salt and other harmful chemicals are also being removed from the productive fertile land. The Najafgarh drain, originated from Najafgarh *jheel*, is the main drainage system of the area forming the southern boundary. Kultana Chhudani Bupania drain forms the northern boundary of the study area and drains the water to the Najafgarh drain, which ultimately meets the Yamuna River. A small *nala* originates from the western part bifurcate the study area and meets the Najafgarh drain.

4.2.3 Climate

The study area belongs to sub-tropical semi-arid climatic condition. In this area, dry hot summer and cold winter are the characteristic features. The average annual temperature of the study area is 25.6 °C. Mean maximum temperature is nearly 45 °C observed in the month of June, whereas mean minimum is nearly 7 °C observed in the month of January. Rainfall is unimodal, and monsoon is the main rainy season when more than 80% of rainfall occurs. According to IMD (1991), the long-term average annual rainfall of the area is 611.8 mm occurring in 27 rainy days.

During summer season the average relative humidity ranges between 20 and 30%, whereas during monsoon season the same varies between 62.5 and 75%.

4.2.4 Soils and Geology

The USDA Soil Taxonomy is coarse loamy, mixed, hyperthermic Typic Haplustepts. The soil texture is sandy loam to loamy sand. In some pockets, loam-textured soil has also been found. The soil series is Palam series having the characteristic of very deep, yellowish-brown alluvial material. Calcium carbonate concretions are also present in the sub-soil. Quartzite sandstone and mica schist are the main lithology of the study area. At the foothills piedmont plain is found and formed from the deposition of alluvial materials. Granite, schist, and ferruginous lime quartzite are the predominant minerals from which the surface soil is developed. Epidote-zoisite (32–50%), hornblende (17–34%), iron oxide (10–20%), garnet-kyanite-zircon-titanite (9–14%), tourmaline (1–3%), and mica (1–2%) are the dominant minerals of fine sand (Sen 1952).

4.2.5 Natural Vegetation and Land Use

Dry deciduous trees are the types of natural vegetation found in the study area. The common vegetations comprise Babool (*Acacia arabica*), Dhak (*Butea monosperma*), Doob (*Cynodon dactylon*), Jand (*Prosopis cineraria*), Jharberi (*Ziziphus nummularia*), Kikar (*Acacia catechu*), Moonj (*Sacharum munja*), Neem (*Azadirachta indica*), Pipul (*Ficus religiosa*), and Shisham (*Dalbergia sissoo*). Agriculture is the dominating land use comprising 75% of the study area. Forests habitats, ponds, roads, etc. are the other land uses. Pearl millet, chick pea, and green gram are grown in the rainy season, and wheat and mustard are cultivated during the winter season. Now widespread cultivation of vegetables is the main agricultural practice. Irrigation by deep tube well is a common practice. Sprinkler and drip irrigation are also being practiced by few farmers.

4.2.6 Geophysical Imaging Investigation

Geophysical imaging was done by using Lund imaging technique. This imaging technique was primarily based on resistivity measurement of the sub-surface. Resistivity meter is the instrument which is used to measure sub-surface resistivity. The principle involves two current and two potential electrodes inserted into soil along a

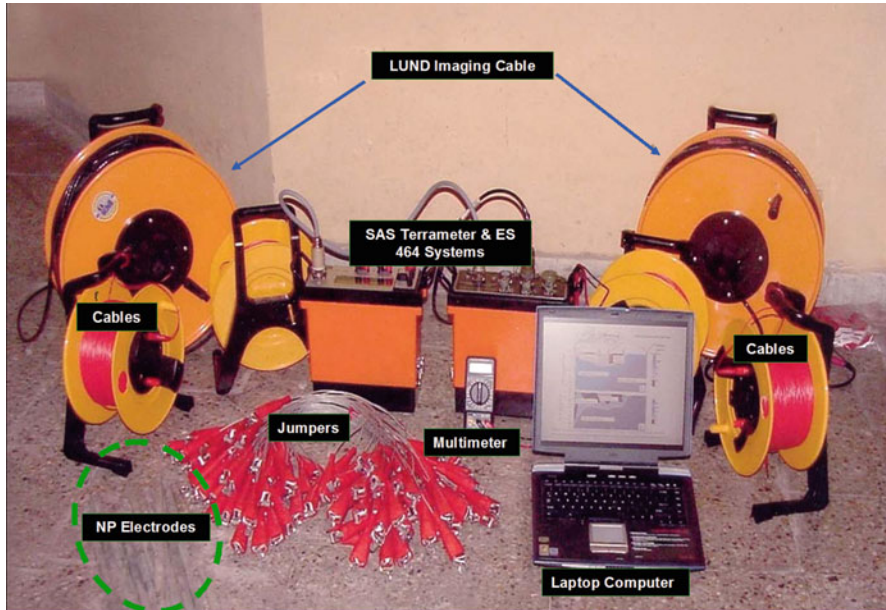


Fig. 4.2 Geophysical instruments (Lund Imaging System) for groundwater survey

straight line with some particular distance apart. The potential difference between the potential electrodes is measured and interpreted as a result of the controlled current that is passed through the current electrodes. Depending on actual electrode configuration, the separation distances between the electrodes are changed. By this way a series of apparent resistivity (ρ_a) was obtained, which is the resistivity of an equivalent homogeneous medium where the same current is used to produce the same potential drop (Bhattacharya and Patra 1968). The geological matrixes of the sub-surface govern the resistivity value. Generally, the compact rock shows very high resistivity value, and the fractured rocks with water shows very low resistivity value (Verma *et al.* 1980).

In the present study, Lund Imaging System was used where separation distance between two electrodes was increased with each successive pass. By increasing the electrode spacing, the depth of penetration has been increased. The equipment used for Lund imaging are shown in Fig. 4.2.

The lateral and vertical apparent resistivity variation of the underlying sub-surface matrix was used to make a 2D pseudo-section. It was constructed by plotting the apparent resistivity on vertical section at a depth equivalent to the median depth of investigation (Edwards 1977). The data are contoured to form a pseudo-section. RES2DINV software was used to determine a 2D resistivity model of sub-surface for the data obtained from electrical imaging survey (Griffiths and Barker, 1993). A forward modeling subroutine was used to calculate the apparent

resistivity values, and a non-linear least squares optimization technique was used for the inversion routine (De Groot_Hedlin and Constable 1990; Loke and Barker 1996). Inversion routine used by the program is based on the smoothness constrained in Least Squares method (De Groot_Hedlin and Constable 1990; Sasaki 1992).

4.2.7 Interpretation of Geophysical Data

The data coming out of geophysical imaging was interpreted to calculate the thickness and the resistivity of different sub-surface layers. The apparent resistivity data was interpreted for this purpose using Schlumberger configuration (Dorbin 1960) from the following formula:

$$\rho_a = \frac{\frac{\pi}{4} \times \frac{(e^2 - p^2)}{p^2}}{\frac{V}{I}} \quad (4.1)$$

where “e” is the distance between current electrodes and “p” is the distance between potential electrodes.

For better assessment of potential groundwater zones in the study area along with true resistivity data, Dar Zarrouk parameters S (Longitudinal Unit Conductance) and T (Transverse Unit Resistance) were calculated. True resistivity data (combining resistivity and thickness) of each geophysical image was interpreted, and the corresponding values of longitudinal unit conductance (S) and transverse unit resistance (T) parameters for each geophysical image were computed. The formula to calculate Dar Zarrouk parameters are given below:

For a sequence of horizontal, homogeneous, and isotropic layers of resistivity ρ_i and thickness h_i , where S and T are defined by:

$$S = \sum_{i=1}^n \frac{h_i}{\rho_i} \quad (4.2)$$

and

$$T = \sum_{i=1}^n h_i \times \rho_i \quad (4.3)$$

where ρ_i is the resistivity of a homogeneous and isotropic layer, h_i is the thickness of a homogeneous and isotropic layer, and n is the number of layers.

4.2.8 Geospatial Approach in Development of Spatial Variability Models

The spatial variability map of the sub-surface configuration can be visualized through apparent resistivity contours. These iso-resistivity contours of various layers were interpolated through ordinary kriging technique. Kriging is the mostly used spatial interpolation technique because of its flexibility to understand the spatial autocorrelation of the variables. It can give option to estimate interpolation error. Thus, we can get estimation accuracy and reliability of the spatial distribution of the variable. The spatial dependence can be quantified from semivariogram (Burgess and Webster 1980). It is the mean square variability between two neighboring points of distance h as shown in Eq. (4.5):

$$\gamma(h) = \frac{1}{2N(h)} \sum_{i=1}^{N(h)} [z(x_i + h) - z(x_i)]^2 \quad (4.4)$$

where $\gamma(h)$ is the semivariogram expressed as a function of the magnitude of the lag distance or separation vector h between two points, $N(h)$ is the number of observation pairs separated by distance h , and $z(x_i)$ is the random variable at location x_i .

The experimental semivariogram $\gamma(h)$ can be fitted in a theoretical model such as spherical, exponential, linear, or Gaussian to determine three parameters, such as the nugget (c_0), the sill (c), and the range (A_0). These models are defined as follows (Issaks and Srivastava 1989):

Spherical model:

$$\begin{aligned} \gamma(h) &= c_0 + \left[1.5 \left(\frac{h}{A_0} \right) - 0.5 \left(\frac{h}{A_0} \right)^3 \right] & h \leq A_0 \\ \gamma(h) &= c_0 + c, & h > A_0 \end{aligned} \quad (4.5)$$

Exponential model:

$$\gamma(h) = c_0 + c \left[1 - \exp \left(-3 \frac{h}{A_0} \right) \right] \quad (4.6)$$

Gaussian model:

$$\gamma(h) = c_0 + c \left[1 - \exp \left[- \left(\frac{3h}{A_0} \right)^2 \right] \right] \quad (4.7)$$

Linear model:

$$\gamma(h) = c_0 + h\left(\frac{c}{A_0}\right) \tag{4.8}$$

Based on R2 and RSS, we determine which model needs to be used.

4.3 Result and Discussion

4.3.1 Geophysical Imaging

Eighteen profiles of geophysical imaging of the sub-surface were carried out at the southern part of Najafgarh block of Delhi. The resulting geophysical images for groundwater are presented from Figs. 4.3, 4.4, 4.5, 4.6, 4.7, 4.8, 4.9, 4.10, 4.11, 4.12, 4.13, 4.14, 4.15, 4.16, 4.17, 4.18, 4.19, and 4.20.

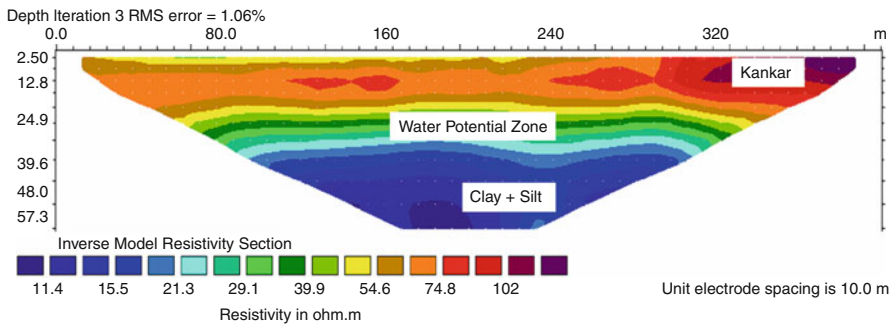


Fig. 4.3 Geophysical image of the sub-surface obtained at Dichaon Kalan village of Delhi showing various geological layers and groundwater potential zones (Profile 1)

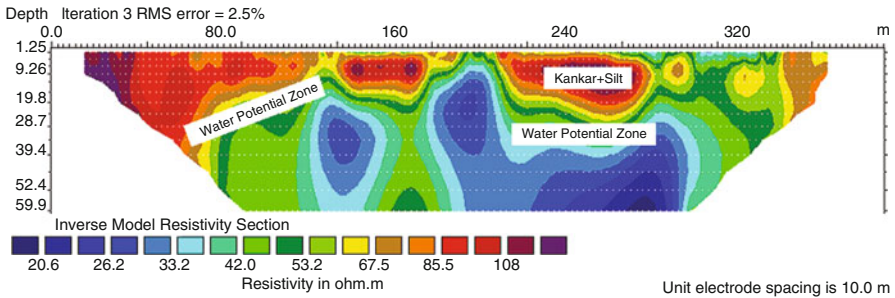


Fig. 4.4 Geophysical image of the sub-surface obtained at Jharoda Kalan village of Delhi showing various geological layers and groundwater potential zones (Profile 2)

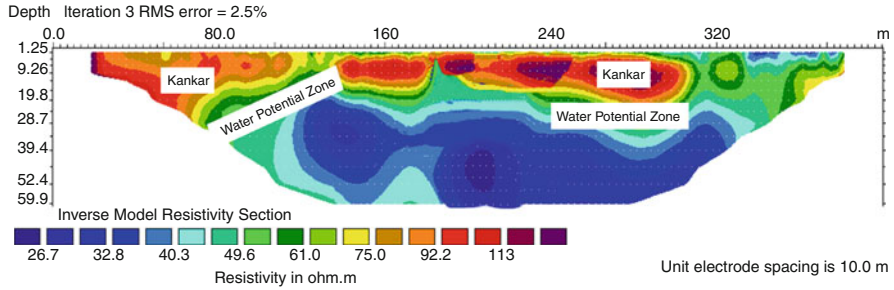


Fig. 4.5 Geophysical image of the sub-surface obtained at Bagargarh village of Delhi showing various geological layers and groundwater potential zones (Profile 3)

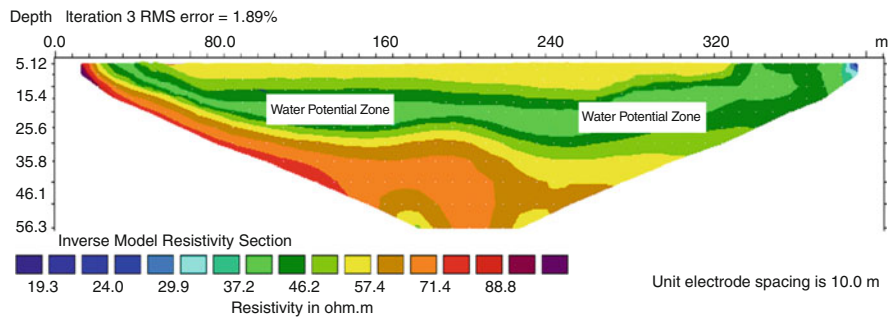


Fig. 4.6 Geophysical image of the sub-surface obtained at Goela Khurd village of Delhi showing various geological layers and groundwater potential zones (Profile 4)

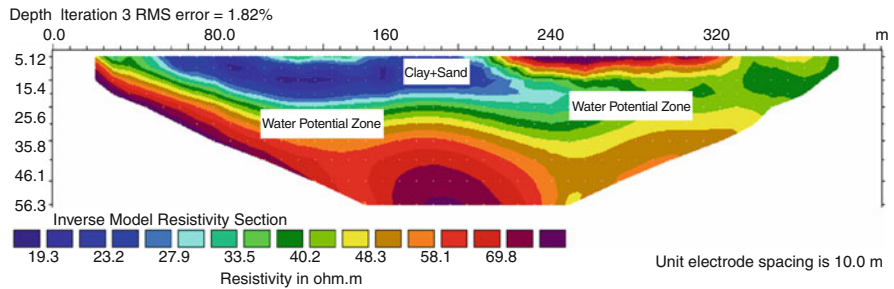


Fig. 4.7 Geophysical image of the sub-surface obtained at Kair village of Delhi showing various geological layers and groundwater potential zones (Profile 5)

4.3.1.1 Geophysical Imaging Through Profile 1

In the south west side of Dichaon Kalan village, the first geophysical imaging was done. The first electrode to get the sub-surface geophysical profile was inserted just side of a road, and the other electrodes went through an agricultural field. The value of resistivity ranges between 10 and 130 ohm-m. Figure 4.3 indicates that at the

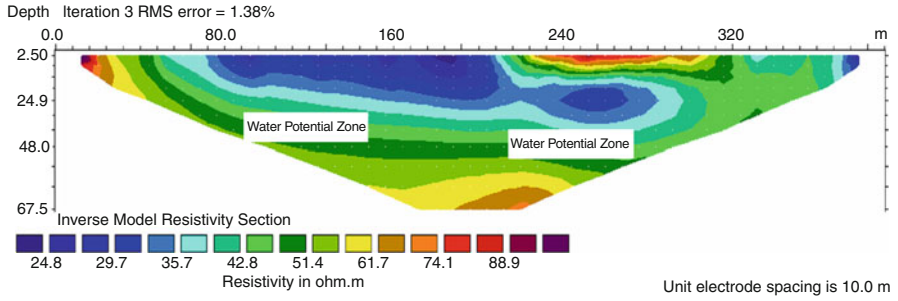


Fig. 4.8 Geophysical image of the sub-surface obtained at Pindwala Kalan village of Delhi showing various geological layers and groundwater potential zones (Profile 6)

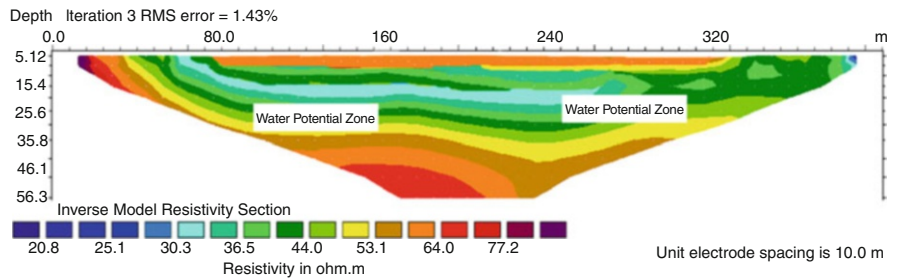


Fig. 4.9 Geophysical image of the sub-surface obtained at Qazipur village of Delhi showing various geological layers and groundwater potential zones (Profile 7)

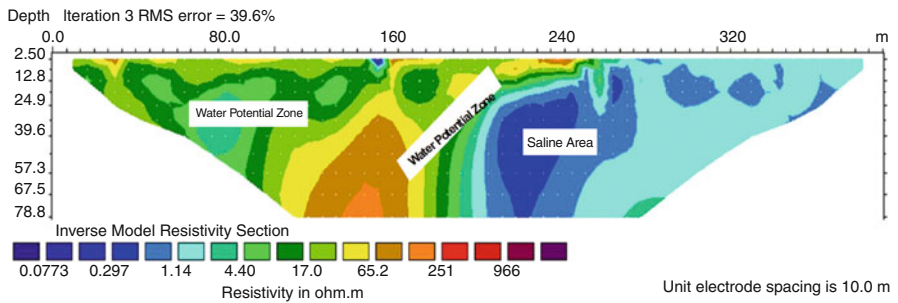


Fig. 4.10 Geophysical image of the sub-surface obtained at Daurala village of Delhi showing various geological layers and groundwater potential zones (Profile 8)

upper depth kankar is the predominating geological material with a resistivity value of 60–115 ohm-m. The absence of any bed rock is also evidenced from this profile. At a lower depth (more than 40 m bgl) low resistivity materials are found which may be made up of clay and silt. Within the sub-surface profile, the geological layers are distinctly separated from each other in the vertical direction. In the horizontal direction the variation of resistivity is very low. This is a clear indication of alluvial

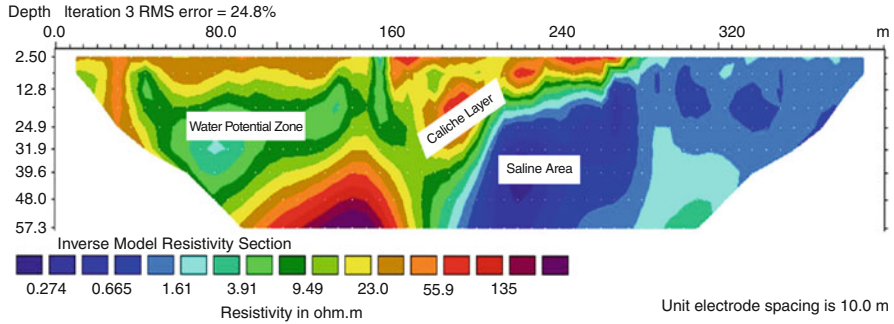


Fig. 4.11 Geophysical image of the sub-surface obtained at Ghalibpur village of Delhi showing various geological layers and groundwater potential zones (Profile 9)

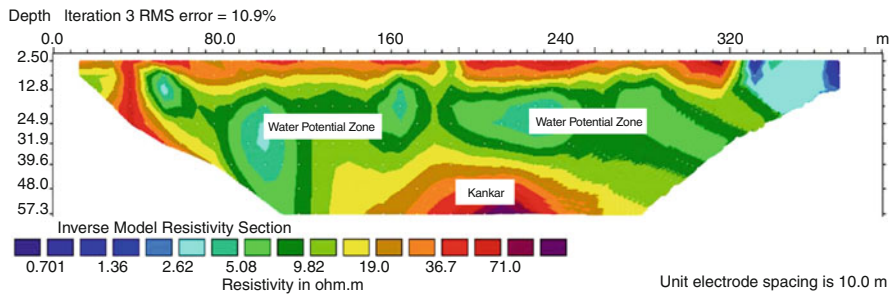


Fig. 4.12 Geophysical image of the sub-surface obtained at Mitraon village of Delhi showing various geological layers and groundwater potential zones (Profile 10)

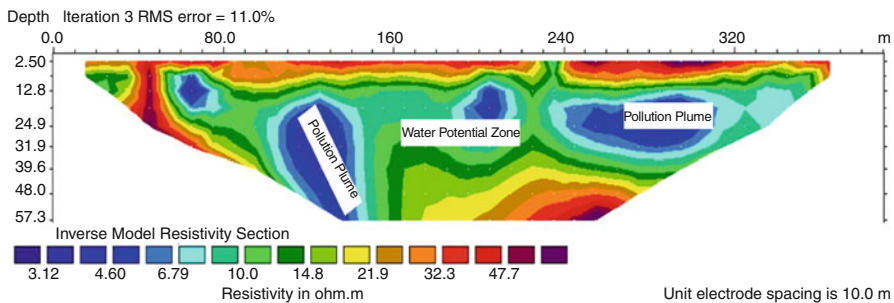


Fig. 4.13 Geophysical image of the sub-surface obtained at Jaffarpur Kalan village of Delhi showing various geological layers and groundwater potential zones (Profile 11)

deposits under different geological era, as the area is coming under the flood plain of River Yamuna. Groundwater potential zones are expected within the depth of 20–30 m below ground level (bgl) where the resistivity value varies between 28 and 48 ohm-m.

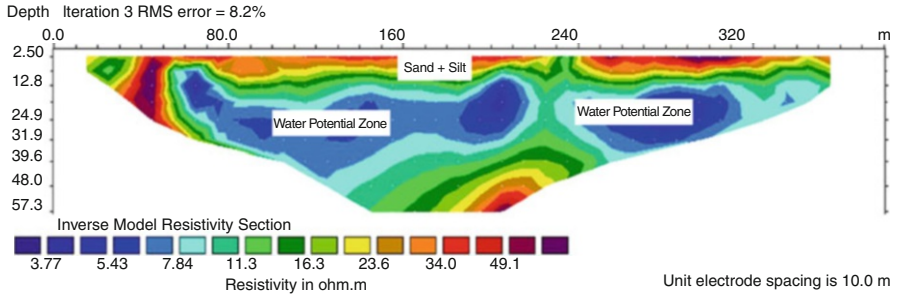


Fig. 4.14 Geophysical image of the sub-surface obtained at Ujwah village of Delhi showing various geological layers and groundwater potential zones (Profile 12)

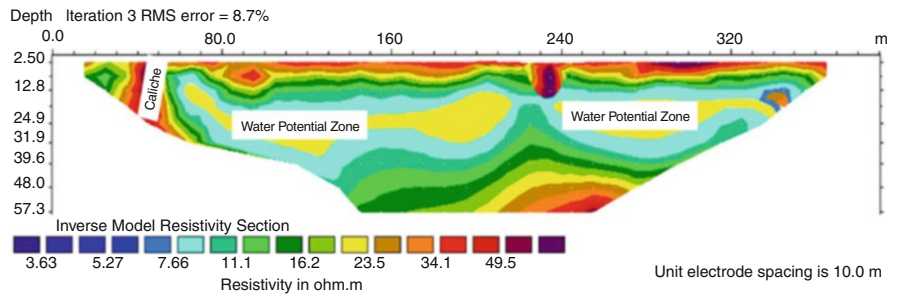


Fig. 4.15 Geophysical image of the sub-surface obtained at Surkhpur village of Delhi showing various geological layers and groundwater potential zones (Profile 13)

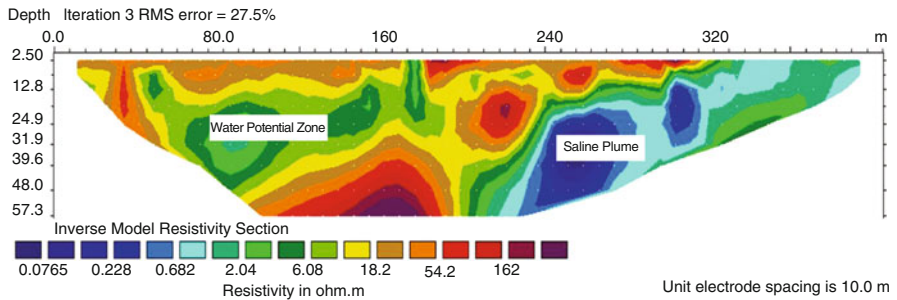


Fig. 4.16 Geophysical image of the sub-surface obtained at Ghummanhera village of Delhi showing various geological layers and groundwater potential zones (Profile 14)

4.3.1.2 Geophysical Imaging Through Profile 2

The second geophysical imaging was done at Jharoda Kalan village of Delhi. The entire sub-surface resistivity profile run through a farmer’s field situated at the side of a village road (Fig. 4.4). The value of resistivity ranges between 15 and 140 ohm-m. The upper part of the sub-surface with the depth ranging from 2 to

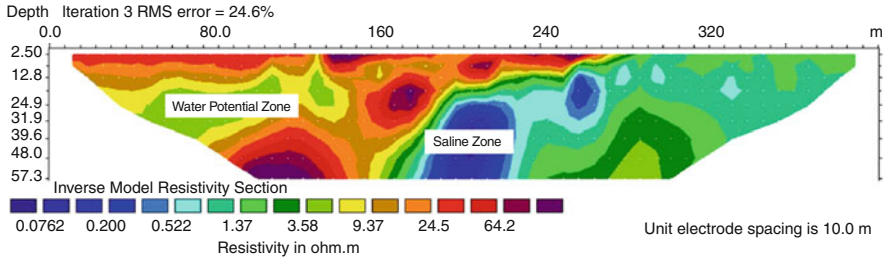


Fig. 4.17 Geophysical image of the sub-surface obtained at Chhawala village of Delhi showing various geological layers and groundwater potential zones (Profile 15)

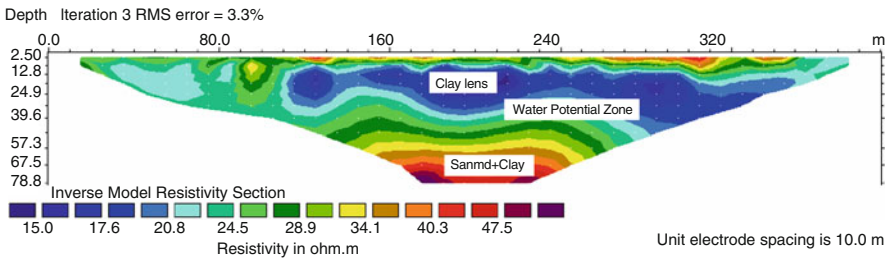


Fig. 4.18 Geophysical image of the sub-surface obtained at Hasanpur village of Delhi showing various geological layers and groundwater potential zones (Profile 16)

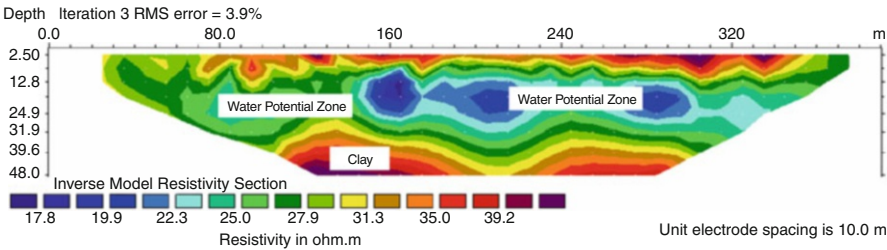


Fig. 4.19 Geophysical image of the sub-surface obtained at Dhansa village of Delhi showing various geological layers and groundwater potential zones (Profile 17)

15 m bgl mainly comprises course materials like kankar and kankar plus silt. The resistivity of this zone is somewhat high and ranges between 100 and 140 ohm-m. This kankar layer is predominantly found at the start of the profile and up to 300 m from the starting point. After that the sub-surface configuration changes and it becomes slightly finer. Clay lenses are observed in between 200 and 300 m away from the starting point and at a depth of 40–50 m bgl. Water bearing layer may be expected at a depth of 20–30 m bgl, and the resistivity of this layer varies between 32 and 53 ohm-m. This profile is very much helpful to identify the location of a potential bore hole.

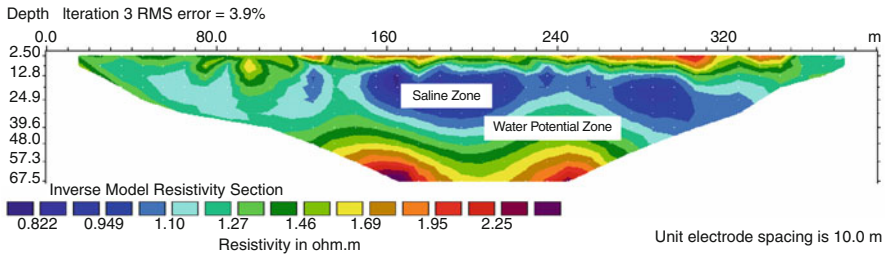


Fig. 4.20 Geophysical image of the sub-surface obtained at Kanganheri village of Delhi showing various geological layers and groundwater potential zones (Profile 18)

4.3.1.3 Geophysical Imaging Through Profile 3

The geophysical image along with profile 3 was obtained near the side of a monument in the village Bagargarh of Delhi and partially along the road side (Fig. 4.5). The value of resistivity ranges between 15 and 140 ohm-m and showing wide vertical and horizontal variation. The coarse textured materials are dominant at the upper part of the sub-surface which mainly consist of kankar. Between 13 and 28 m bgl, water bearing formation is expected, and beyond that the presence of low resistivity zone is an indicator of the dominance of clay, kankar, and silt. The presence of clay lens at 30 m to 40 m depth is indicative of the formation of a confined aquifer beneath 40 m in this area.

4.3.1.4 Geophysical Imaging Through Profile 4

The geophysical image along profile 4 has been obtained at a vegetable field in the Goela Khurd village of Delhi (Fig. 4.6). The vegetable field was located just side of a farm road. The value of resistivity ranges between 15 and 100 ohm-m. The horizontal variation of resistivity is insignificant in this case, and the vertical variation is also very low. The groundwater may be available at a depth of 14 m to 25 m bgl. High resistivity values below the aquifer indicate that aquifer may be overlaying on a calcitic bed rock.

4.3.1.5 Geophysical Imaging Through Profile 5

The geophysical image along profile 5 was obtained from an orchard field located at the south-eastern part of the village Kair (Fig. 4.7). The arrangement of the profile is along with a road. The resistivity values of the sub-surface range between 17 and 91 ohm-m. In the sub-surface, the upper part is dominated with clay and sand. The expected groundwater depth is 16 to 31 m below ground level. The resistivity value of the water bearing layers indicates the presence of good quality groundwater in this area. The hydro-chemical parameters also support the fact. At a deeper depth of more

than 40 m below ground level, high resistivity vale has been observed. The presence of dolomite and calcite at deeper layer may be the reason for high resistivity of this zone. The presence of high calcium and magnesium ion in the groundwater of deep tube wells also supports this fact.

4.3.1.6 Geophysical *Imaging Through Profile 6*

The geophysical image along profile 6 was obtained from a government field lying along the main road which is situated just eastern part of Pindwala Kalan village (Fig. 4.8). The arrangement of the profile is also along the main road. The resistivity value of the sub-surface geological materials ranges between 18 and 110 ohm-m. At the upper part of the sub-surface geologic material, the resistivity varies widely in the horizontal direction. In the vertical direction the resistivity value increases gradually. Low resistivity at the upper part of the vadose zone indicates that there may be accumulation of soil moisture at this part of the vadose zone. This may be because of capillary movement of water to the soil surface from the underneath saturated zone. Water bearing layers are expected at a depth of 25–40 m bgl. The groundwater quality in this area is good to moderate as evidenced from the resistivity value of the water bearing layers. The hydro-chemical data is also indicative of the same.

4.3.1.7 Geophysical *Imaging Through Profile 7*

The geophysical image along profile 7 was laid at the outside boundary of an orchard situated at the southern portion of the village Qazipur (Fig. 4.9). The arrangement of the profile is along the direction of the orchard but perpendicular to the main road. The value of resistivity in this profile ranges from 14 ohm-m to 102 ohm-m. The geo-electrical layers in this profile are quite parallel to each other, and more than 45 m of depth below ground level there is a material of high resistivity, which may be the bed rock made up of lime stones. Presence of high concentration of calcium and bicarbonate in the groundwater is an indicative of the same. Water potential zone is expected at a depth of 16 to 30 m bgl. At the surface layer, the high resistivity value is an indication of the presence of coarse textured soil like sandy soil. The resistivity value of the water potential zone shows that the quality of groundwater is good to moderate and which is also evidenced from the hydro-chemical data.

4.3.1.8 Geophysical *Imaging Through Profile 8*

The geo-electrical image along profile 8 was obtained from a farmer's field lying along the village road situated at the western part of the village Daurala (Fig. 4.10). The arrangement of the profile is along the direction of the road. There is a wide variation of resistivity in this profile both for horizontal and vertical direction. The range of resistivity is also very high, ranging from 0.0773 ohm-m to 250 ohm-m. The

potential water bearing zone is expected at a depth of 15 to 35 m below ground level. The resistivity values of the sub-surface features are clearly revealing that the groundwater is saline in nature and the level of salinity is increasing after 200 m from the start of the profile. The hydro-chemical data are also confirming the result. An interesting finding from the image is that the pollution plume is migrating from right side of the profile to the left side. In real sense, the direction is toward the depression area of the Najafgarh drain.

4.3.1.9 Geophysical Imaging Through Profile 9

The geo-electrical image along profile 9 was obtained from the western side of a horticultural farm situated at the eastern part of the village Ghalibpur (Fig. 4.11). The resistivity variations of different layers are very complex, and for both the horizontal and vertical direction a wide variation of resistivity has been found. The value of resistivity varies from 0.274 ohm-m to 210 ohm-m. The very low resistivity value is an indication of salinity, and the hydro-chemical data are also showing that the groundwater is of highly saline in nature. Water bearing layers are expected at a depth of 20 to 40 m below ground level. At a distance of 220 m from the start of the profile, a highly saline zone is expected. The abrupt change of high resistivity near the surface and the vadose zone is an indication of the presence of caliche (CaCO_3) layer in the sub-surface. This is quite possible in the sub-surface layers of the arid and semi-arid regions of India.

Geophysical Imaging Through Profile 10

The geophysical image along profile 10 was laid in a farmer's field just side of the main road situated at the south-western part of the village Mitraon (Fig. 4.12). The resistivity value varies from 0.701 ohm-m to 110 ohm-m, and the variation is showing a very clear trend. A good amount of groundwater can be expected at a depth of 15 m to 40 m below ground level. The groundwater quality at Mitraon village can be expected as moderate to poor because of very low resistivity of the water potential zone. Hydro-chemical investigation supports this result where moderate groundwater quality is observed. At the upper part of the vadose zone and at a depth more than 50 m, moderate to high resistivity value is observed. Coarse textured materials like sand and *kankar*'s presence at those layers may be responsible for this high resistivity value.

4.3.1.10 Geophysical Imaging Through Profile 11

The geophysical image along profile 11 was laid on a farmer's field cultivated with seasonal vegetables just side of a shallow tube well situated at the northern part of the village Jaffarpur Kalan (Fig. 4.13). The profile is along the north-south direction.

The resistivity of the sub-surface varies from 1.02 to 72 ohm-m, and the degree of variation is very high in both the horizontal and vertical directions. Groundwater can be available in the layers situated at a depth of 25 to 40 m below ground level. The groundwater quality is expected to be poor because of very low resistivity of the water potential zone. The same conclusion was drawn from the results of hydro-chemical investigations. Very low resistivity zones within the water bearing layers may be the pollution slugs having high electrical conductivity. A layer of high resistivity was observed near the surface. This indicates the presence of coarse fragments like sand and *kankar* in that layer.

4.3.1.11 Geophysical Imaging Through Profile 12

The geophysical image along profile 12 was also laid on a farmer's field by the side of a village road at the eastern part of the village Ujwah (Fig. 4.14). The arrangement of the profile is along the east-west direction. The profile is also similar to the previous one that is like Jaffarpur Kalan. The resistivity value of this profile varies between 1.54 and 74 ohm-m. The value of resistivity varies more along the vertical direction, and along the horizontal direction it remains somewhat consistent. The availability of water bearing layers can be expected at a depth of 15 to 40 m below ground level. The groundwater quality is poor because of very low observed resistivity of the water bearing layers. The hydro-chemical investigations also support this result. A high resistivity value near the surface is the result of presence of coarser material like *kankar* in that layer. A similar high resistivity value has also been observed at the lower depth, which may also indicate the presence of dolomite and calcite bed rock.

4.3.1.12 Geophysical Imaging Through Profile 13

The geophysical image along profile 13 was laid on a field at the eastern side of a farm house which is situated at the eastern part of the village Surkhpur (Fig. 4.15). The arrangement of the profile is along the east-west direction. The resistivity value of the sub-surface configuration varies from 2.33 to 73 ohm-m. The geological layers bearing water may be situated at a depth of 15 to 37 m below ground level. The groundwater quality is poor as indicated by the very low resistivity of the water bearing layers in the sub-surface, and this is also confirmed from the hydro-chemical data. A high resistivity value near the surface is an indication of presence of coarse fragments like sand and silt in that layer. A layer of calcium carbonate (caliche layer) has been observed at a horizontal distance of 40 m and 220 m from the point of initiation of the profile.

4.3.1.13 Geophysical Imaging Through Profile 14

The geophysical image along profile 14 was taken from a forest area across a footpath within the forest which is situated at the west side of Ghummanhera village (Fig. 4.16). The arrangement of the profile is along the east-west direction. The resistivity in the sub-surface material is highly variable, and it varies from 0.0765 to 230 ohm-m. The potential water bearing zone may be expected in between 19 and 47 m depth below ground level. The groundwater quality is anticipated to be very poor because of very low resistivity of the water bearing layers. The salinity level increases after 200 m distance from the start of the profile. This poor quality of groundwater is also evidenced from the hydro-chemical data. A high resistivity value is observed near the surface which may be either a coarse texture soil or a layer of calcium carbonate, but the secondary data revealed that it is due to the surface soil of coarse textured.

4.3.1.14 Geophysical Imaging Through Profile 15

The geophysical image along profile 15 was laid in a fallow land along with a road which is situated at the side of a big village pond in the northern part of the village Chhawala (Fig. 4.17). The arrangement of the profile is of north-east and south-west direction. The resistivity in the profile is somewhat low and varies from 0.0762 to 104 ohm-m. The depth of geological layers where groundwater can be available was found at a depth of 20 to 35 m below ground level. The groundwater quality of this layer seemed to be very poor as envisaged from the observed very low resistivity value of this layer. The hydro-chemical data is also confirming the same. A highly saline pollution plume is present nearly 200 m away from the start of the profile.

4.3.1.15 Geophysical Imaging Through Profile 16

The geophysical image along profile 16 was laid on a farmer's field situated at the western side of an orchard in the northern part of the village Hasanpur (Fig. 4.18). The profile is arranged along a village road of north-south direction. The resistivity value in the profile varies between 13 and 57 ohm-m. The water bearing geological layers are expected at a depth of 30 to 45 m below ground level. The low resistivity values at the water bearing layers are telling that the quality of water stored in those layers is moderate, and this is confirmed by the hydro-chemical data obtained from those layers. Above the water potential zone, a clay-enriched layer has been found which may be formed at the time of formation of sedimentary rocks at the ancient times.

4.3.1.16 Geophysical Imaging Through Profile 17

The geophysical image along profile 17 was taken from a farmer's field situated at the side of the main road in the eastern part of the village Dhansa (Fig. 4.19). The profile is arranged along the road at east-west direction. The resistivity value of the sub-surface geological materials within the profile varies from 14 to 52 ohm-m. The expected aquifer depth in this area is about 20 m below ground level. At deeper depth (>35 m below ground level) *kankar* and clay-enriched layer is expected as inferred from their resistivity value within the profile.

4.3.1.17 Geophysical Imaging Through Profile 18

The geophysical image of profile 18 was taken from a farmer's field which is located along the main road at the north-eastern part of the village Kanganheri (Fig. 4.20). The profile is arranged at the north-south direction. The overall resistivity value of the sub-surface geological materials in the profile is very low, and the same is ranging between 0.822 and 3.57 ohm-m. The water bearing geological formations are observed at a depth of 25 to 40 m below ground level. Very low observed resistivity of the water bearing layers indicates the quality of groundwater seems to be very poor. Groundwater is situated in the unconfined aquifer, and capillary rise of water to the upper part of the vadose zone is the main cause of soil salinity in this area. The hydrostatic pressure of the aquifer also helped in this process to raise soil salinity.

4.3.2 Iso-resistivity Contours

The apparent resistivity (ρ_a) values have been interpreted using RES2DINV software. Then the localized model was generated for getting true resistivity data (h_n and ρ_n). Altogether five geophysical layers have been obtained based on Lund imaging data. The true resistivity values were interpreted, and iso-resistivity contours of these geophysical layers were mapped.

4.3.2.1 Geophysical Layer 1

The first geophysical layer varies from the surface to 7 m bgl. Resistivity values vary widely from 7 to 190 ohm-m. The iso-resistivity map of this layer is shown in Fig. 4.21. From low to high, the resistivity values of this layer are classified in to five classes, namely, <10, 10–20, 20–30, 30–40, and > 40 ohm-m. The resistivity class of <10 ohm-m indicates the presence of fine textured materials like clay. Low resistivity areas are found nearby Chhawala and Surkhpur villages. Resistivity class

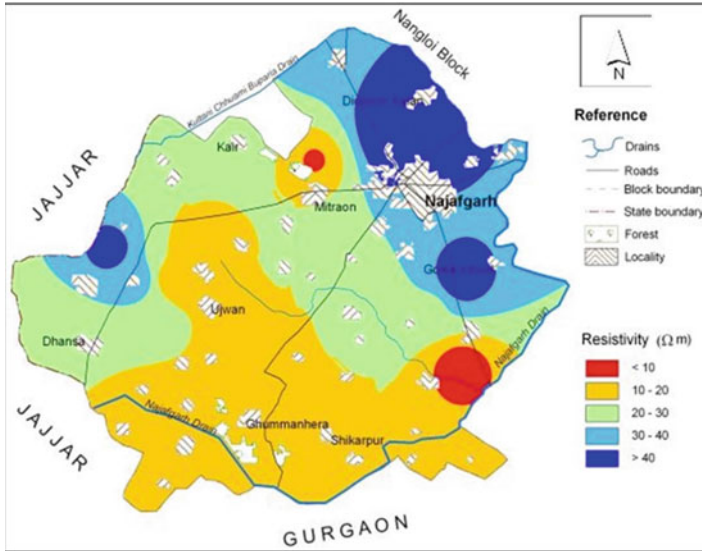


Fig. 4.21 Spatial variation of resistivity of the upper part of the sub-surface (0–7 m bgl) showing the moisture distribution pattern in the vadose zone of the study area

of 10–20 ohm-m indicates the moist soil with some amount of salts and has been located at the southern portion of the study area covering nearly 30% of the total area. The resistivity range of 30–40 ohm-m indicates moist soil and is located in the western, northern, and the middle portion of the study area. Next two ranges of resistivity values indicate relatively dry soil and predominantly found at the north and west side of the study area. Therefore, the first geophysical layer tells about the spatial pattern of soil moisture within the study area.

4.3.2.2 Geophysical Layer 2

The second geophysical layer varies from a depth of 7–15 m bgl. The variation of resistivity value of this layer is of similar magnitude of the first layer. It varies from 7 to 173 ohm-m (Fig. 4.22). This layer is also classified as that of the first layer. It has been observed that fine textured materials like clay along with some moisture are the dominating materials of the south and south eastern part of the study area covering the villages Ghummanhera and Ujwah. The resistivity values and its pattern of this layer are the typical signature of the unsaturated zone. This layer is mainly dominated by sand and *kankar* as the geologic material. Capillary movement of water is there in this layer but this layer does not store groundwater.

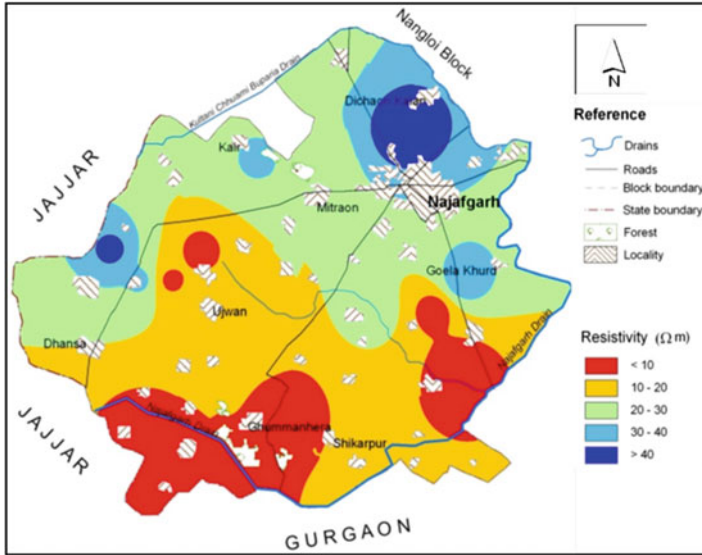


Fig. 4.22 Spatial variation of resistivity at the second geophysical layer of the sub-surface (7–15 m bgl) showing the presence of sand and *kankar* as the geologic material

4.3.2.3 Geophysical Layers 3 and 4

The geophysical layer 3 varies from 15 to 28 m bgl and the layer 4 varies from 28 to 40 m bgl. Although these are two separate layers, considering the widespread overlapping of the resistivity values of these two layers, these layers have been discussed together (Figs. 4.23 and 4.24). The zones of low resistivity value (<10 ohm-m) represent saline groundwater. The slightly low resistivity values (10–20 ohm-m) indicate the presence of water with clay. The zones of medium resistivity values (20–30 ohm-m) represent the presence of water with sand and clay. Presence of groundwater along with sand can be represented by the resistivity values of 30–40 ohm-m. In zones where high resistivity values (>40 ohm-m) are there, groundwater is available in the sand and gravelly aquifer material. Water bearing layers with better availability of groundwater mainly are formed by sand and gravel. Therefore, it may be inferred that the areas adjoining Goela Khurd village, surrounding Bagargarh village, and areas north of Jharoda Kalan village and Kair village are expected to get good amount of groundwater. As a whole, moderate quality of groundwater is expected at some pockets of north, west, and east side of the study area.

The fifth geophysical layer contains the geological materials with high resistivity values in major parts of the study area. This may represent the presence of calcite and other types of bed rock formation.

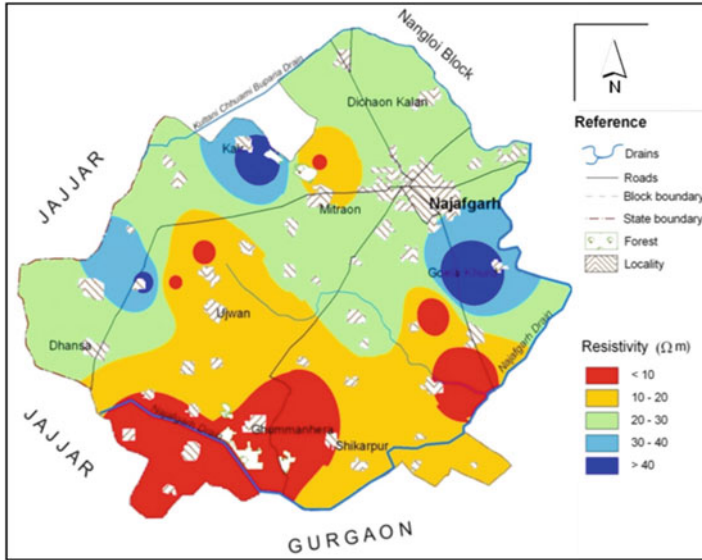


Fig. 4.23 Spatial variation of resistivity at the third geophysical layer of the sub-surface (15–28 m bgl) showing the presence of groundwater

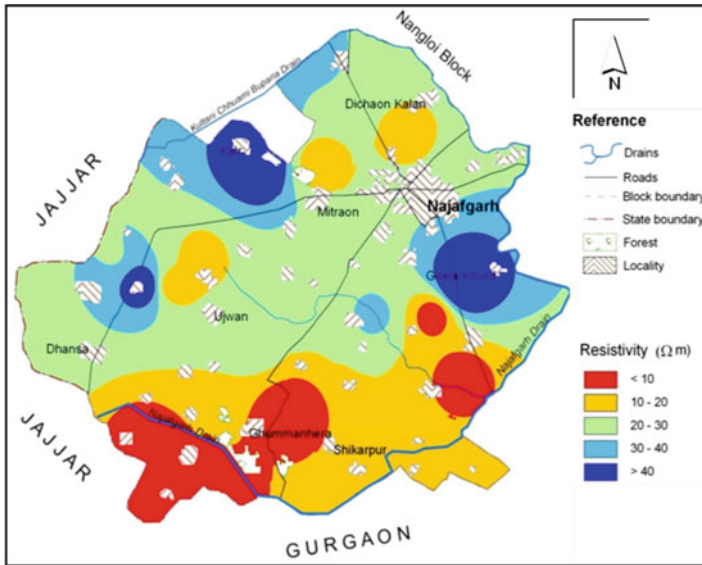


Fig. 4.24 Spatial variation of resistivity at the fourth geophysical layer of the sub-surface (28–40 m bgl) showing the presence of sand and gravel as the geologic material

4.3.3 Delineation of Water Potential Zones

For better assessment of potential groundwater zones in the study area along with true resistivity data, Dar Zarrouk parameters (S and T parameters) were used. True resistivity data (combining resistivity and thickness) of each geophysical image was interpreted, and the corresponding values of longitudinal unit conductance (S) and transverse unit resistance (T) parameters for each geophysical image were computed. The spatial distributions of these two parameters were mapped using geostatistical wizard of Arc GIS® 10.2 package.

Spatial variation map of S parameter is shown in Fig. 4.25. The S parameter was divided into five classes, and the classification scheme of S parameter with regard to the present study area is S values 0–0.5 dS (very low), 0.5–1.0 dS (low), 1.0–2.0 dS (medium), 2.0–5.0 dS (high), and > 5.0 dS (very high). It has been observed that in the study area very low and low classes of S parameter are distributed in a scattered manner. In few pockets (geophysical imaging locations of 2, 4, 5, and 17) low and very low S parameter values are observed. Higher values of S parameter (1.0–2.0, 2.0–5.0, and > 5.0 dS) cover a major portion of the study area. Spatial location of the S parameter in the range of 1.0–2.0 dS is predominantly concentrated in a strip spreading at the north side of the study area and in few selected places at the middle part of the study area, and the S parameter in the range of 2.0–5.0 dS is observed in a strip spreading at the middle portion of the study area where S parameter >5.0 dS is observed at the southern portion of the study area.

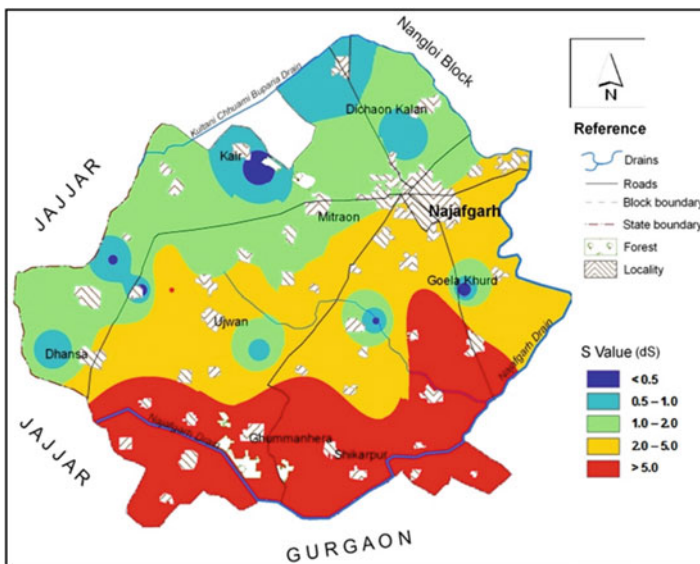


Fig. 4.25 Spatial map showing the variation of longitudinal unit conductance (S) of the groundwater in the study area

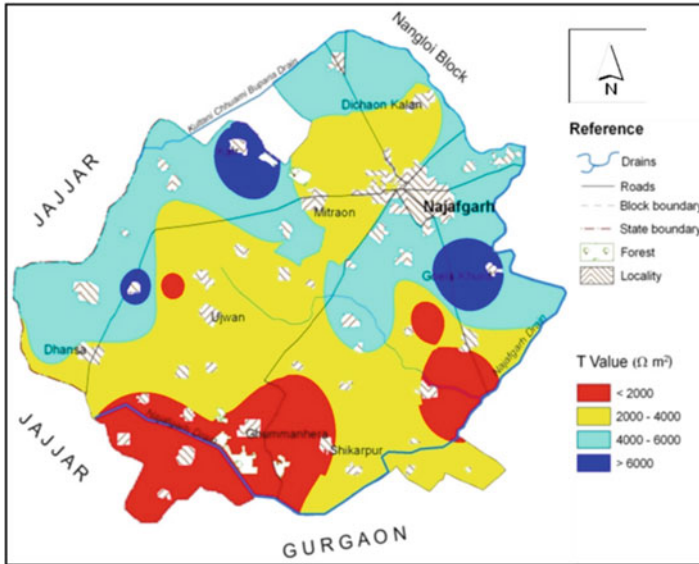


Fig. 4.26 Spatial map showing the variation of transverse unit resistance (T) of the groundwater in the study area

Spatial map of T parameter (Fig. 4.26) has been prepared taking the range of $<2000\ \text{ohm}\cdot\text{m}^2$, $2000\text{--}4000\ \text{ohm}\cdot\text{m}^2$, $4000\text{--}6000\ \text{ohm}\cdot\text{m}^2$, and $> 6000\ \text{ohm}\cdot\text{m}^2$. So, there are four classes of T parameter. It has been found that medium values of T parameter, i.e., in the range of $2000\text{--}4000\ \text{ohm}\cdot\text{m}^2$ and $4000\text{--}6000\ \text{ohm}\cdot\text{m}^2$, cover a major part of the study area. T value of $<2000\ \text{ohm}\cdot\text{m}^2$ is practically concentrated at the southern part of the study area.

A combination of Dar Zarrouk parameters (S and T parameters) has been widely used to delineate potential water bearing layers in the sub-surface. Chandra and Athavale (1979) studied various combinations of Dar Zarrouk parameters and concluded that the combination of high T and low S will be the indicator of potential water bearing layers in the sub-surface, provided that the spatial variations of water quality in that region remain more or less uniform. Transmissivity ($T_r = K \cdot b$; K, hydraulic conductivity; b, aquifer thickness) of the aquifer and transverse unit resistance (T) can also be used to identify potential aquifer, and the relationship between these two is linear (Kelley 1977). As the transmissivity is directly related to the characteristics of the aquifer, T parameter indirectly shows water potential zones. Keeping all these findings the criteria table as proposed by Adhikary et al. (2012) (Table 4.1) has been followed to classify the area in terms of high, moderate, and poor water potential zones. Based on this criteria table these two thematic maps (S and T) were overlaid to get the combination of S and T parameters (Fig. 4.27), which will directly show the hotspots where we can expect better groundwater.

Table 4.1 Criteria table by using different combinations of Dar Zarrouk parameters for delineating water potential zones (Adhikary et al. 2012)

S parameter (dS)	T parameter (Ω meter ²)	Category
1.0–2.0	<2000	2 (moderate)
	2000–4000	1 (good)
	>4000	1 (good)
2.0–5.0	<2000	3 (poor)
	2000–4000	2 (moderate)
	>4000	1 (good)
>5.0	<2000	3 (poor)
	2000–4000	3 (poor)
	>4000	2 (moderate)

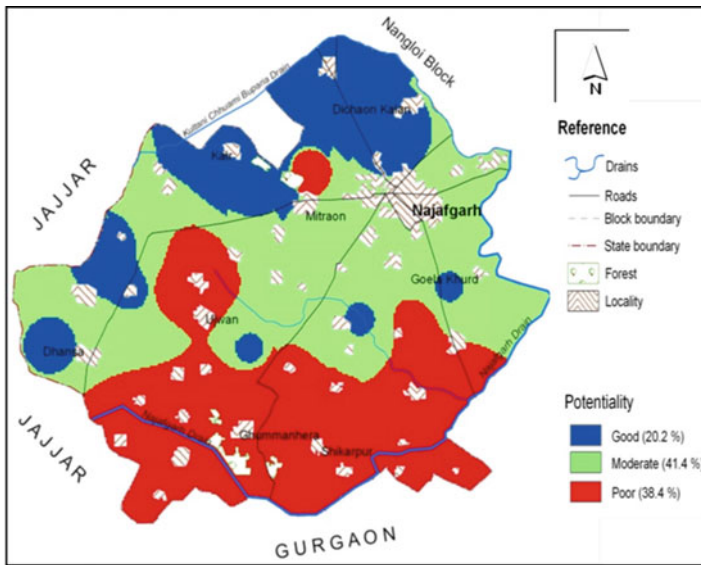


Fig. 4.27 Overlay map of S and T parameters indicating potential groundwater zones of the study area

In the study area better water potential zones are found at the north side covering the villages Dichaon Kalan, Kair, etc. In few pockets at the west side of study area, good amount of water is also available. Poor water potential zones are mainly concentrated at the southern border of the study area where Najafgarh drain is flowing. Area wise it has been observed that nearly 41.4% of the study area is coming under moderate water potential zones. In 38.4% of the area poor water potentiality has been observed, and only 20.2% of the area is having good water potentiality. Therefore, for sustainable vegetable cultivation, rain water harvesting and consumptive use of surface and groundwater may be adopted.

4.4 Conclusion

In this study geophysical imaging technique has been proved as an effective technique to delineate the sub-surface configuration. The geophysical investigation reveals that the potential groundwater zones are expected at a depth of 20–30 m below ground level. On spatial scale good groundwater potential zones are mainly found at the north and west side of Najafgarh covering 20.1% of the study area. Bagargarh, Ghasipura, Goela Khurd, Jharoda Kalan, and Kair are the few villages where intensive vegetable cultivation may be possible because of availability of good amount of groundwater. The groundwater quality of the study area is moderate to poor, and poor-quality zones are mainly found in the villages Ghummanhera and Ujwah. For sustainable vegetable production, rain water harvesting and consumptive use of surface and groundwater may be adopted.

References

- Adhikary, P.P., Chandrasekharan, H., Chakraborty, D., Kamble, K. (2010). Assessment of groundwater pollution in west Delhi, India using geostatistical approach. *Environmental Monitoring and Assessment* 167:599-615.
- Adhikary, P.P., Chandrasekharan, H., Chakraborty, D., Kumar, B., Yadav, B.R. (2009). Statistical approaches for hydrogeochemical characterization of groundwater in West Delhi, India. *Environmental Monitoring and Assessment* 154:41-52.
- Adhikary, P.P., Dash, C.J., Chandrasekharan, H., Rajput, T.B.S., Dubey, S.K. (2012). Evaluation of groundwater quality for irrigation and drinking using GIS and geostatistics in a peri-urban area of Delhi, India. *Arabian Journal of Geosciences* 5:1423-1434.
- Adhikary, P.P. and Biswas, H. (2011). Geospatial assessment of groundwater quality in Datia district of Bundelkhand. *Indian Journal of Soil Conservation* 39(2): 108-116.
- Adhikary, P.P., Chandrasekharan, H., Dash, C.J., Jakhar, P. (2014a). Integrated isotopic and hydrochemical approach to identify and evaluate the source and extent of groundwater pollution in west Delhi, India, *Indian Journal of Soil Conservation* 42 (1), 17-28.
- Adhikary, P.P., Chandrasekharan, H., Dash, C.J., Kumar, G. (2015c). Hydrogeochemical investigation of groundwater quality in west Delhi, India, *Indian Journal of Soil Conservation* 43 (1), 15-23.
- Adhikary, P.P., Chandrasekharan, H., Dubey, S.K., Trivedi, S.M., Dash, C.J. (2015a). Electrical resistivity tomography for assessment of groundwater salinity in west Delhi, India, *Arabian Journal of Geosciences* 8 (5), 2687-2698.
- Adhikary, P.P., Chandrasekharan, H., Trivedi, S.M., Dash, C.J. (2015b). GIS applicability to assess spatio-temporal variation of groundwater quality and sustainable use for irrigation, *Arabian Journal of Geosciences* 8 (5), 2699-2711.
- Adhikary, P.P., Dash, C.J. (2017). Comparison of deterministic and stochastic methods to predict spatial variation of groundwater depth, *Applied Water Science* 7 (1), 339-348.
- Adhikary, P.P., Dash, C.J., Bej, R., Chandrasekharan, H. (2011). Indicator and probability kriging methods for delineating Cu, Fe, and Mn contamination in groundwater of Najafgarh Block, Delhi, India, *Environmental Monitoring and Assessment* 176 (1-4), 663-676.
- Adhikary, P.P., Dash, C.J., Sarangi, A., Singh, D.K. (2014b). Hydrochemical characterization and spatial distribution of fluoride in groundwater of Delhi state, India. *Indian Journal of Soil Conservation* 42 (2), 170-173.

- Ahmadi SH, Sedghamiz A (2008) Application and evaluation of kriging and cokriging methods on groundwater depth mapping. *Environmental Monitoring and Assessment* 138:357–368.
- Al Gami MA (2011) Magnetic and DC resistivity investigation for groundwater in a complex subsurface terrain. *Arabian Journal of Geosciences* 4:385–400.
- Arslan H (2014) Estimation of spatial distribution of groundwater level and risky areas of seawater intrusion on the coastal region in Çarşamba Plain, Turkey, using different interpolation methods. *Environmental Monitoring and Assessment* doi:<https://doi.org/10.1007/s10661-014-3764-z>.
- Bhattacharya, R.K. and Patra, H.P. (1968). *Direct current geoelectric sounding*. Elsevier Publishing Co., Amsterdam, pp. 135.
- Burgess TM, Webster R (1980) Optimal interpolation and isarithmic mapping of soil properties I: The semivariogram and punctual kriging. *Journal of Soil Science* 31:315-331.
- CGWB (1996) Development and augmentation of groundwater resources in National Capital Territory of Delhi. Ministry of Water Resources, Government of India 42p.
- Chandra, P.C. and Athavale, R.N. (1979). Close grid resistivity survey for demarcating the aquifer encountered in bore well at Koyyur in lower Maner basin. Tech. Report No. GH-11-Gp-7, Hyderabad, pp. 16.
- Dash JP, Sarangi A, Singh DK (2010) Spatial variability of groundwater depth and quality parameters in the National Capital Territory of Delhi. *Environmental Management* 45(3):640-650.
- De Grooth-Hedlin C, Constable S (1990) Occm's inversion to generate smooth, two-dimensional models from magneto-telluric data. *Geophysics* 55:1613-1624.
- Dorbin, M.B. (1960). *Introduction to geographical prospecting*. McGraw Hill Book Co., pp. 466.
- Edwards, L.S. (1977). A modified pseudosection for resistivity and induced polarization. *Geophysics*, 42: 1020-1036.
- Griffiths DH, Barker RD (1993) Two-dimensional resistivity imaging and modeling in areas of complex geology. *Journal of Applied Geophysics* 29:211–226.
- IMD (1991). *Climate of Haryana and Union Territories of Delhi and Chandigarh*. India Meteorological Department, Govt. of India Report. pp. 92-98.
- Isaaks EH, Srivastava RM (1989) *An Introduction to Applied Geostatistics*. Oxford University, New York.
- Kelley, W.E. (1977). Geo-electric sounding for estimating aquifer hydraulic conductivity. *Ground Water*, 15(6): 420-425.
- Loke MH, Barker RD (1996) Rapid least-squares inversion of apparent resistivity pseudo sections by a quasi-Newton method. *Geophysical Prospect* 44:499–524.
- Mazac O, Kelly WE, Landa I (1987) Surface geo-electrics for ground water pollution and protection studies. *Journal of Hydrology* 93:277-294.
- Nikroo L, Kompani-Zare M, Sepaskhah A, Fallah Shamsi S (2010) Groundwater depth and elevation interpolation by kriging methods in Mohr Basin of Fars province in Iran. *Environmental Monitoring and Assessment* 166(1–4):387–407.
- Prakash MR, Singh VS (2000) Network design for groundwater monitoring – A case study. *Environmental Geology* 39:628–632.
- Prasanna, M.V., Chidambaram, S., Senthil Kumar, G., Ramanathan, A.L. and Nainwal, H.C. 2011. Hydrogeochemical assessment of groundwater in Neyveli Basin, Cuddalore District, South India, *Arabian Journal of Geosciences* 4: 319–330.
- Rao VVSG, Rao GT, Surinaidu L, Rajesh R, Mahesh J (2011) Geophysical and Geochemical Approach for Seawater Intrusion Assessment in the Godavari Delta Basin, A.P., India. *Water Air and Soil Pollution* 217:503–514.
- Sasaki Y (1992) Resolution of resistivity tomography inferred from Numerical Simulation. *Geophysical Prospect* 40: 453–464.
- Sen, N. (1952). Geomorphological evaluation of Delhi area. *Current Science*, 21: 157-159.
- Skuthan B, Mazac O, Landa I (1986) The importance of geophysical methods for protecting ground water from agricultural pollution. *Proc. J. Geol. Sci., Sect. Appl. Geophys* 11:27-39.

- Sun Y, Kang S, Li F, Zhang L (2009) Comparison of interpolation methods for depth to groundwater and its temporal and spatial variations in the Minqin oasis of Northwest China. *Environmental Modelling and Software* 24:1163-1170.
- Theodossiou N, Latinopoulos P (2006) Evaluation and optimization of groundwater observation networks using the kriging methodology. *Environmental Modelling and Software* 21:991-1000.
- Ustra AT, Elis VR, Mondelli G, Zuquette LV, Giacheti HL (2012) Case study: a 3D resistivity and induced polarization imaging from downstream a waste disposal site in Brazil. *Environmental Earth Sciences* 66:763-772.
- Varouchakis EA, Hristopulos DT (2013) Comparison of stochastic and deterministic methods for mapping groundwater level spatial variability in sparsely monitored basins. *Environmental Monitoring and Assessment* 185:1-19.
- Verma, R.K., Rao, M.K. and Rao, C.V. (1980). Resistivity investigations for ground water in metamorphic area near Dhanbad, India. *Ground Water*, 18: 46-55.

Chapter 5

Groundwater and Space Technology: Issues and Challenges



**Gouri Sankar Bhunia, Pravat Kumar Shit, Harsha Das Gupta,
and Partha Pratim Adhikary**

Abstract Most of the world's freshwater resources are known as groundwater. In just a few areas, increased groundwater depletion causes significant consequences for a water table fall, water quality deterioration, stream base flow loss, etc. Water resources, especially in developing countries, are poorly controlled and hydrologically educated offer valuable metrics for groundwater resources recognition. This chapter explains the capabilities of various satellite sensors to derive specific primary and secondary parameters associated with soil water studies. Different spatial models have been studied to demonstrate how spectral indices, digital elevation models (DEM) and their potential as passive, low-cost investigation techniques for groundwater studies are. Possible application of space technology in assessment, monitoring, and use of groundwater resources was established. This chapter also explains the specific problems and challenges associated with space and groundwater study. Also possible potentials of groundwater space technology are briefly summarized.

Keywords Geographical information system · Groundwater management · Remote sensing · Satellite sensor · Spatial modelling · Spectral indices

G. S. Bhunia (✉)

RANDSTAD India Pvt Ltd., New Delhi, Delhi, India

Department of Geography, Seacom Skill University, Bolpur, West Bengal, India

P. K. Shit

PG Department of Geography, Raja N.L. Khan Women's College (Autonomous), Medinipur, West Bengal, India

H. D. Gupta

Department of Geography, Seacom Skill University, Bolpur, West Bengal, India

P. P. Adhikary

ICAR-Indian Institute of Water Management, Bhubaneswar, India

e-mail: partha.adhikary@icar.gov.in

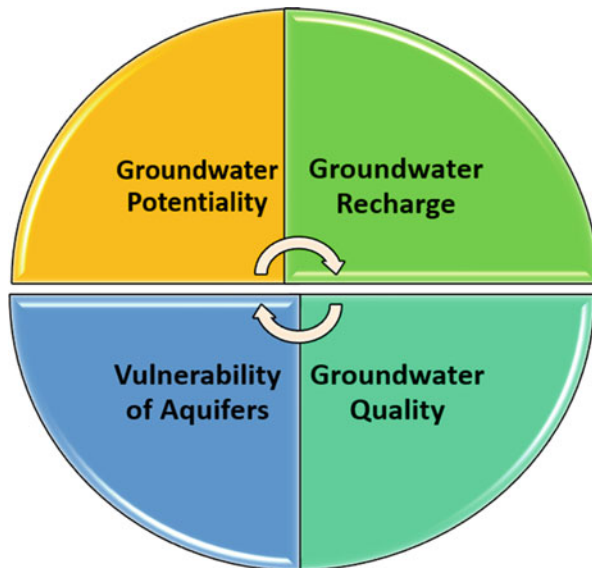
5.1 Introduction

The problems associated with groundwater management in India (Adhikary and Dash 2017) are water tables, water depressions, groundwater contamination, water extraction, water salinity and salt intrusion, and salt water infringement. The source of the current water crisis must be acknowledged that it is not a monsoon irregularity as the Indian media says. Today, the government is incompetent, the myths are incorrect, and the country's water resources are completely misappropriated. In the following decades, climate change will intensify Indian water scarcity. The declining water table rate is reported to be 1–2 m/year in several parts of India. According to the World Bank report (2018), the total annual water withdrawal by India was 761 billion m³, out of which agricultural irrigation accounts for 90% (688 billion m³) of India's freshwater extractions. The World Bank also estimated that 21 Indian cities would run out of water by the end of 2020 and that about 50% of the population will not have access to drinking water by 2030, with 6% losing their GDP by 2050 in the wake of the catastrophe.

Recently, increased arsenic content has created fear among groundwater users in shallow aquifers in West Bengal. To accomplish this, numerous preventive and legislative steps were undertaken in India to resolve groundwater management issues; however, none of the measures have significant effects on the lack of awareness and political and administrative will. The NITI Aayog, a government-renowned think tank, announced in July of last year that it was affected by the biggest water crisis in the past, and the “Composite Water Management Index (CWMI)” includes about 600 million Indians or about 55% of Indians, a national water measurement tool. India's most important plants—the most water-consuming plants are rice, wheat and sugarcane. For one kilogram of grain produced, rice, which is a major export crop, uses around 3500 liters of water. Punjab, the third largest rice producer, relies entirely on groundwater for rice production. Government procurement policies and subsidized energy are making rice lucrative for farmers, while farmers in Bihar, Western Bengal, Assam, and Tripura, more rainfall-driven, have no such opportunities. Farmers in Maharashtra use groundwater as a source of sugarcane because they are marketed in the sugar mills, while Bihar that is better suited for sugarcane production produces just 5% of the total sugarcane production in this region. State governments must therefore promote less water-intensive cultivations, such as hulls, millets, and oleaginous seeds, in areas under water stress, as well as water scrub crops. Rice should only be grown in areas that are water-rich.

Groundwater is the subsurface phenomenon, largely controlled by the primary and secondary porosity prevalence and orientation, and is protected by understanding from above. In groundwater modelling, four categories of data, namely, (i) the aquifer system stress factors (i.e., effective recharge, pumping volumes, water surface flow exchanges), (ii) aquifer system and strata geometry (i.e., geological information, topographic maps, and contour maps), (iii) the hydrogeological parameter of the simulated process (i.e., hydraulic conductivity, storage coefficient, dispersivity), and (iv) main measured variables (Gogu et al. 2001), are required

Fig. 5.1 Major application of remote sensing and GIS in groundwater studies



5.2 Electromagnetic Spectrum and Waterbody Extraction

The physical basis for distant determination of earth materials is used for better understanding the characteristics of rock formations by means of spectral reflection of minerals forming rocks (Bishop 2018). At the sensor resolution pixel scale, spectral signatures are recorded. Compared to other earth surface objects, a waterbody shows a weak reflectivity, manifested in the wavelength range of visible light (580 ~580 nm), its reflectivity is about 5% ~5%, while at 880 nm it decreases to 2% ~3%, because waterbody has strong absorption characteristic in near-IR band and mid-IR band (750 ~2500 nm). This can be used to differentiate water from soil, trees, houses, and other artifacts on the ground. The shortwave infrared (SWIR) is a water-absorbed wavelength (1.55–1.75 μm) that enables the presence of waterbodies to be retrieved.

5.3 Remote Sensors in Groundwater Applications

The variations between spectral responses can be identified by satellite images (Gupta 2018). Such images are of different wavelengths and are usually analyzed by breaking down the image in different stripes to find additional detail (Bishop 2018). At present, there are several satellite platforms that provide useful evidence in groundwater study, comprising with Landsat 7, Landsat 8, IKONOS, WorldView-5, Pleiades, KOMPSAT, QuickBird, ALOS, or Sentinel-2, among others (Table 5.2). Koch et al. (2013) employed and funded ground measurement (ground penetration

Table 5.2 Satellite used for groundwater studies

Sensor	Launch year	Ground resolution (m)	Precipitation	Surface temperature	Soil moisture	Water storage	Snow water	Land cover	Topography
AMSE-E	2002	5500–56000	√	√	√		√		
ASTER	1999	15, 30, 90		√				√	√
AVHRR	1991–2003	1100	√	√	√		√		
GRACE	2002	300000				√			
IRS LISS-III		23.5						√	
ENVISAT RA-1	2002	1000		√					√
Landsat 7	1999	30, 30		√				√	
Landsat 8	2013	30, 15, 100		√				√	
MODIS	1999	250, 500, 1000		√				√	
OrbView-2	1997	1100		√				√	
OrbView-3	2003	1, 5		√				√	
RADARSAT-1	1995	8–100			√				√
SRTM	2000	30, 90							√

Source: After Becker (2006)

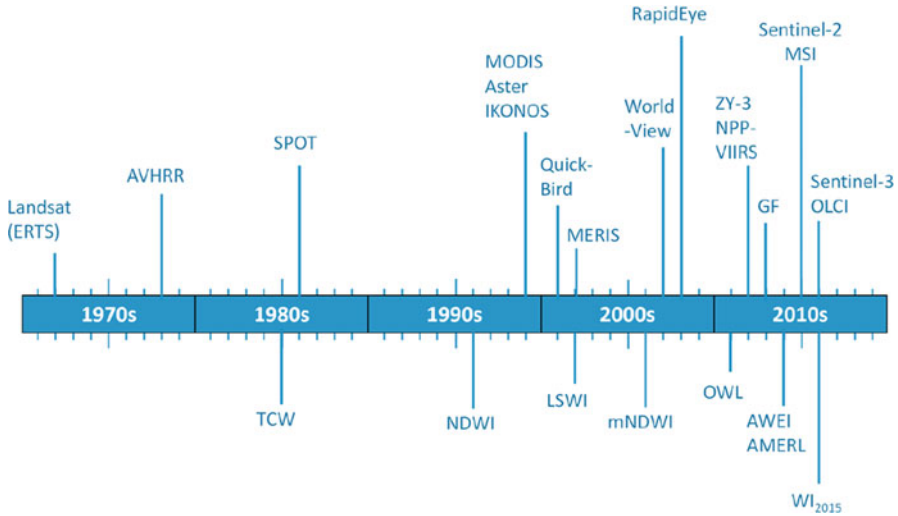


Fig. 5.2 Timeline diagram of development of major water indices and launch of satellites/sensors. (Source: Huang et al. 2018)

radar, field spectrometer, magnetometer, etc.) optical and microwave RS techniques coupled with multi-spectrum, thermal, and microwave (ASTER and PALSAR) data to identify the potential areas for groundwater accumulation. The Gravity Recovery and Climate Experiment (GRACE) satellite detects earth gravity field changes by monitoring distance variations in orbits on the earth. The GRACE satellite data explicitly monitors changes in total water storage (TWS) and does not alter hydrological features (such as surface water, land, and moisture). Figure 5.2 shows a timeline diagram of various applied water indices to find an automatic and universal method for extracting water area along with satellite sensors. However, new methods will start in the near future for surface water extraction.

5.4 Remote Sensing Data in Groundwater Studies

The key element in groundwater capacity was defined by most of the documents in the database. Approximately, 20 parameter groups, almost 50% consistent with the majority of studies, included lithology, geomorphology, soil, terrestrial use, topography, linear drainage, height, slope, precipitation, and surface water level (Table 5.1). There are several applications of remotely sensed data in groundwater studies:

- Airborne geophysical surveys aids to classify faults and dikes, lithology and magnetic characteristics competence changes (Danielsen et al. 2003). This knowledge helps to build a more accurate aquifer model.

- Lineaments have already been established as groundwater flow in broken aquifers and, thus, are aimed at the site of production wells (Tam et al. 2005). With the use of GIS, it is possible to introduce the overlaying of lineaments mapped from traditional remote sensing techniques and those derived from airborne geophysical methods.
- Spatial gravity surveys along with GRACE (Gravity Recovery and Weather Experiment) can be worn to identify temporary variations in overall water storage (e.g., surface water, soil water, and groundwater). The changes of the total water storage system (TWS) in the earth system is unswervingly commensurate with the sequential changes in the acceleration measured. Based on its structural characteristics, the concept of a hydraulic unit generally supports lineament mapping (Adeyeye et al. 2015), which plays a significant role in the absorption and flow of groundwater (Assatse et al. 2016).
- The area of the ground is also the upper limit of the aquifer and restricts its level of groundwater for a phreatic aquifer. Airborne platforms, such as LiDAR (Microwave and Radar Institute 2006), stereo orthophoto, or satellite array interferometry (Slater et al. 2006), can be used to assess surface altitudes. For environmental reasons, groundwater depth including water for plant supplies or salinization by phreatic evaporation is needed in a number of studies. DEM will estimate this surface distance and groundwater depth.
- Accurate surface height estimates determine regional decay caused by piezometric depression around wellfields (Hoffmann et al. 2001) or periodic groundwater level changes (Chang et al. 2005). Once a relationship between subsidence and drawdown has been developed, the surface subsidence observed can be used to spatially distribute drawdown.
- Radar satellites can be used to measure surfaces like river, lake, paleochannel, and ponds and low-lying areas (Berry et al. 2005). Data obtained may be relevant to groundwater-level determination hydrology.
- The presence of water and its depth to groundwater surface are two important indicators for vegetation. Vegetation provides useful information, which can be linked to shallow groundwater. For example, in the dry season, extensive planting of a permanent spring or a shallow water table may be used as a proxy. Previous studies indicated that hydrological aspects decide the form, density, and condition of vegetation (Fensholt et al. 2006) and proxy for evapotranspiration (Loukas et al. 2005). The vegetation cover and its temporal pattern were extracted from several spectral indicators, such as ratio vegetation index (RVI), vegetation index number (VIN), difference vegetation index (DVI), and normalized difference vegetation index (NDVI) (Xue and Su 2017).
- A remote sensing and multispectral characterization of a water surface in the landscape can be detected by RADAR (Roshier and Rumbachs 2005). Density and dispersion suggest the distribution of the regional recharge.
- Hydrological elements, such as alluvial fans, are the paleo-channel, paleo-lakes and the paleo-shorelines that can be buried (Sternberg and Paillou 2015). The spaceborne low-frequency synthetic aperture radar (SAR) with space support

leads to discovery of paleo-hydrological and tectonic systems concealed beneath the earth's crust.

- The thermal inertia of subversive water can also be used as a measure of groundwater temperature incongruities in land surface. Cool thermal variances are characterized as settings in which the temperatures of the land area under normal circumstances are lower than those in the neighborhood.
- The intersection of surface and groundwater is essential for understanding the behavior of wetlands. Water surface layout and overtime flood patterns are a useful information for model calibration (Bauer et al. 2006).
- Salt crusts indicate high water tables with phreatic evaporation. Multi-spectrum satellite data can be mapped to show phreatic fluxes and depth in the soil (Brunner et al. 2007).
- Satellite data can be used as a kind of lenient knowledge for groundwater charging in the form of prior understanding in the conventional zone-based model calibration strategy (Carrera and Neuman 1986).

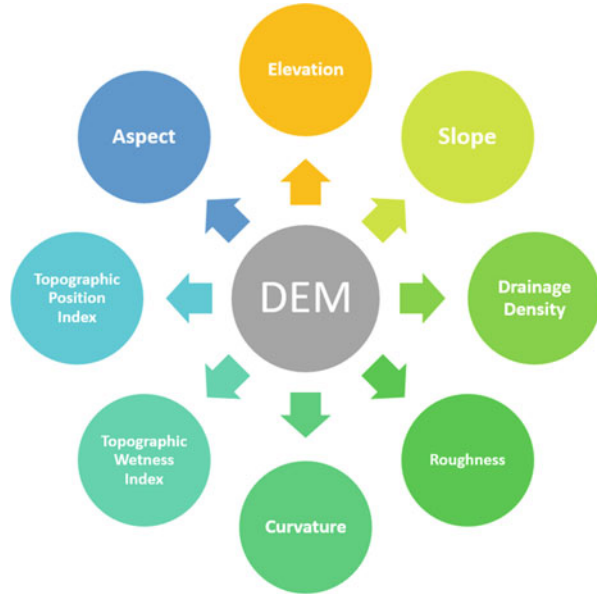
5.5 Spectral Indices and Water Assessment

Surface waterbodies are determined by water indices derived from satellite data. First developed by McFeeters (1996), normalized differential water index (NDWI) was used to classify open-source features using the near-infrared (NIR) spectroscopy and the green bands given by Landsat thematic mappers (TM). Xu (2006) changed NDWI and renamed it to MNDWI to eliminate errors in buildup, vegetation and soil from NIR band by replacing the shortwave infrared (SWIR) band. In view of multiple spectral ranges, Feyisa (2015) established the automated water extraction index (AWEI). In order to delineate surface waterbodies, Fisher (2016) established a water index using surface reflection bands of Landsat data. Other spectral indices such as the Tassled Cap (TC) transformation (Crist 1985) and normalized difference vegetation index (NDVI) were proven effective in the detection of the water surface.

5.6 Digital Elevation Model and Groundwater Investigation

A major source to gather information about hydrological and geomorphological conditions of soil water mapping and interpretation is the digital elevation model (DEM), as well as the digital terrain model (DTM) and the digital surface model (DSM) (Solomon 2003). In general, DEMs vary in their production in different resolution with either active or passive optical sensors (GeoEye-1, WorldView-1, WorldView-2, IKONOS, Pleiades-1, SPOT-5, SPOT-6, or SPOT-7); also, in vertical and horizontal precision (RADAR, LiDAR, ASTER, ALOS, TanDEM), DEMs vary from one sensor to the other. DEMs also provide an excellent example of cross-discipline applications. SRTM and ASTER GDEM are available freely and currently

Fig. 5.3 Use of digital elevation model (DEM) in groundwater application



provide accurate global data with a 1-arcsecond (30 m) spatial resolution (Wendt et al. 2016). Topography helps to control flooding and plays a large role in the geographical circulation of hydrological parameters, such as soil infiltration or soil moisture (Sorensen et al. 2006).

Satellite imagery DEMs data can be used to map lineaments. DTMs would be used to evaluate the lineament in first order (slope, look) or second order (skyline profile and curvature plane), since these represent better the undulations of the earth's surface (Wendt et al. 2016). The side-looking SAR machine geometry offers subtle lineament extraction structures due to low RADAR wave incidence angles. Landsat data with edge enhancement filters, such as the Sobel operator or the Canny filter, have currently been used to determine the perceptibility or detectability of lineaments by reducing the data redundancy with main component analysis. DEM data is also useful to extract drainage network, topographic wetness index (TWI), Topographic Position Index (TPI) through various hydrology tools of GIS software (Fig. 5.3). The TWI can be prepared, for example, on the basis of TOPMODEL index (Beven 1997), and the Jenness algorithm can be used to prepare the TPI (Yeh et al. 2016). The TWI is the draining zone logarithm up to the point and mean gradient of the drainage system. A higher TWI index indicates a lower slope and a larger area (Misi et al. 2018). DEMs can also be used for drainage density, since the high drainage density indicates that runoff can be diverted rapidly, less probability of infiltration (Fashae et al. 2015).

5.7 Spatial Modelling and Groundwater Evaluation

A number of scientific methods for hydrological modelling and predicting, including the most popular ‘data-based’ or ‘data-driven’ method, have been used today. Mathematical equations derived not from the physical process in the water basin but from a contemporary time series input and data are included in these modeling methods (Solomatine and Ostfeld 2008). A key point in the modeling of groundwater is the aggregation of data, for the “numeric score” or “weight” to each pixel in each thematic map. Two main components, namely, the weights comparative and intrinsic, exist in each of the variables on groundwater potential (Das et al. 2017). This process is based on an expert evaluation that always requires a certain degree of subjectivity (Martín-Loeches et al. 2018; Govindaraj et al. 2017). Previous researchers used probabilistic models, for example, frequency ratio (Ozdemir 2011; Razandi et al. 2015), multi-criteria decision analysis (Chowdhury et al. 2009; Rahmati et al. 2015), weight of evidence (Corsini et al. 2009; Pourghasemi and Beheshtirad 2015), logistic regression (Pourtaghi and Pourghasemi 2015), evident belief function (Mogaji et al. 2015), artificial neural network model (Lee et al. 2012), certainty factor (Razandi et al. 2015), Shannon’s entropy (Naghbi et al. 2015), decision tree (Chenini and Ben 2010), machine learning techniques such as random forest (RF), maximum entropy (ME) (Rahmati et al. 2016), and so on to delineate the groundwater potential zone.

MCDM offers the choice of parameters and decision-making options and provides an efficient instrument for the management of groundwater resources by bringing structure, auditability, transparency, and precision to decision-making (Adiat et al. 2012; Mallick et al. 2015). Furthermore, Professor Thomas L. Saaty’s analytic hierarchy process (AHP) developed in the 1977s was commonly used as an alternative to or criterion for the MCDM method for groundwater management to solve the problem of independence. In addition, several researchers subsequently suggested the analytical network process (ANP) to resolve dependence on alternatives/criteria (Dagdeviren and Ihsan 2007; Agarwal et al. 2013). In the sense of decision-making, ANP is more accurate than AHP, because priority should be given to both the elements and community or clusters of elements which is usually needed in the real world (Saaty 1999).

Multi-influencing factor (MIF) techniques are the most common approaches to analyze the weight of each variable in groundwater (Das et al. 2017; Nasir et al. 2018). That element, in order to create a hierarchy, is independently connected against each other. Factors having major influence were marked as major effect and were assigned a weight of 1.0 whereas, minor influence were marked as a minor effect with a weight of 0.5. The relative value of the variables is added, and the weight as the share of the total values of all variables is estimated (Thapa et al. 2017a, b).

Close association with groundwater machine training based on evidence that concentrates on revealing occult patterns in large data sets (Naghbi et al. 2015; Chen et al. 2018). The majority of studies in groundwater are based mainly on supervised learning, i.e., a sequence of variables which can illuminate a known

output. The machine learning methods comprise weights of evidence (Madani and Niyazi 2015), frequency ratio (Abrams et al. 2018), logistic regression (Odzemir 2011), functional tree models (Chen et al. 2018), evidential belief function model (Mogaji and Lim 2018), regression trees (Naghbi et al. 2017), and others.

The Ecological Assimilation of Land and Climate Observations (EALCO) model developed by CCRS simulates the relationship between ground and surface water, in order to support water quality assessments, sustainable yields, and regional aquifer susceptibility to environment and land use schemes under expected climate change scenarios. The flow analysis model was used by Baker et al. (1993) to develop soil water protection strategies in conjunction with hydrogeological mapping of well-head protection areas (WHPAs). A wellhead was developed as a features-based system by Adams et al. (1993) using an object-based data model to interactively and specifically calculate and retrieve subsurface data. A density-dependent FEM transport and flow model based on the hydraulics of the aquifer has been developed by Roaza et al. (1993) using SWICHA code. Salama et al. (1996) developed the most practical research and areas of groundwater dumping techniques for the H-GIS (manual, geostatistic, and hydrogeological GIS-based technology). In order to optimize parameters for the best agreement between simulated and observed groundwater elevations, Harbaugh et al. (2000) developed a 3-D finite difference method for the groundwater model using the program MODFLOW-2000. Dubey et al. (2002) have developed a Factor Analysis Model (FAM) groundwater pollution potential to develop a decision-making support system to allocate a groundwater-polluting surface and subsurface environmental parameter. In order to build a physical and very detailed recharging boundary for groundwater modeling, Jyrkama et al. (2002) built a HELP-3 model. In order to quantify renewable water resources which calculate long-term water flow over the wide basin, the US Department of Agriculture (USDA) has developed a Soil and Water Assessment Tool (SWAT) (Yan et al. 2010). Jin and Feng (2013) derived the global terrestrial water storage (TWS) from GRACE observation over a span of approximately 10 years and obtained groundwater storage by subtracting simulated surface water from the Global Land Data Assimilation System (GLDAS) and WaterGAP Global Hydrology Model (WGHM).

The groundwater modeling system is a powerful instrument in the hydrogeological basin for the pre- and post-processing operation. The Computer Graphics Laboratory Technology (1998) has developed a computational model through the use of finite-element tools from SUFT3D and MODFLOW. The combination of groundwater and SVAT models greatly improved MODFLOW's representation of the soil airflow to delineate the recharge and discharge area (Levine and Salvucci 1999).

GIS provides an array of groundwater applications, because of its capacity to display specific applicable characteristics spatially according to need (Lilly 2016). Advanced GIS software engineering capabilities provide an adequate framework for managing hydrological databases, for spatial analysis of continuous groundwater data, and for standardizing aquifer models, explore the capacities of groundwater storage, and build networks to collect and cross-polline groundwater data (Khazaz et al. 2015). The spatial interpolation can be performed either probabilistically (e.g.,

when calculating weight values, the degree of similarity observed is considered) or deterministically (e.g., directly correlated with the distance from the point data observed).

5.8 Need for Future Research and Development

For groundwater studies, implementations of geospatial technologies are very poor due to their inherent limitations. Remote sensing technology has a long way to go in order to develop and manage groundwater resources effectively.

- A key challenge for remote sensing is to increase the precision and reliability of several hydrological parameters in hydrological studies. The steps should therefore be taken with the refinement of analysis and with better calculation, the production and deployment of newer and enhanced sensors.
- Remote sensing can only detect changes on the ground or a shallow layer (< 1 m) of the ground in hydrogeology. Nevertheless, as withdrawal increase and the groundwater level decreases, the normal remote sensing data does not use, except for the GPR (Ground-Penetrating Radar) information obtained. The emphasis of the research should therefore be considered in quantifying the concentration of subsurface water and in seeing the movement and conveyance of the fluids in hydrogeological thinking.
- The usefulness of microwave satellite data in multi-temporal and spatial environments will accompany the viewing and modelling of groundwater recharging in order to detect parameters and land classes using these technologies. Furthermore, it can be expected to soon visualize the cyclical groundwater recharge over large areas based on the synergistic use of the earth's gravity field satellites.
- For the computerization and extension of custom and user-friendly GISs to sub-surface flow and transport modelling, multi-disciplinary investigation is required.
- The management of groundwater is slowly being given attention. Emphasis on soil humidity, evapotranspiration, and snowmelt rushing needs to be in place. Therefore, geospatial technology will perceive through irrigated areas and use them for transient state modelling.
- Enhancement of recharge and ET compliance estimates by remote ET and soil moisture sensing by calibration and assimilation models.
- In order to understand the data structure and data analyses on expertise of GIS, future modelling is necessary for other GIS applications for parameter assessment, grid design, sensitivity, and evaluating reliability.
- Apart from the calculative pressure, the most daunting obstacle is to obtain sufficient and reliable data for the use of class mechanistic flow and transport models for field examinations. Enhanced space servers that rely on RDBMS,

which allow end users to know how to provide a huge volume of data that is important as input in models.

- Field datasets often include physically impaired information, which can result in incorrect results and a less detailed image of a given region. The definition of variables and the likelihood that the groundwater will occur must therefore be determined based on different aspects of each environment.
- Enhanced data collection and optimization using uncertainty studies. Model and remote sensing tests can be examined to calibrate model forecasts with field-based observations in the most appropriate locations.
- GIS has not been so much incorporated with expert systems (ES) and spatial decision support systems (SDSS) in water resource engineering and hydrology. Such a program can simplify a regional water issue resolution mechanism and help identify cost-effective management alternatives.
- An effective tool for hydrological simulation can be artificial intelligence (AI) with correct inputs and optimal configuration of the network. The integration of the AI into GIS expertise can offer practitioners with easy-to-interpret water quality maps and models for sustainable groundwater management. Integration of AI models such as Fuzzy Logic, ANN, neuro-fuzzy, Sugeno Fuzzy Logic (SFL), Mamdani Fuzzy Logic (MLF), committee machine artificial intelligence (CMAI), and supervised committee machine artificial intelligence (SCMAI) can be done to assess groundwater vulnerability.

5.9 Conclusion

Groundwater studies take time, and cost-effective and geospatial technology offers a practical mode of assimilating many data sources to facilitate the sustainable development of groundwater. Data on geology, hydraulics, geomorphology, and satellite technology plays an important role in identifying reliable groundwater potential areas. In the eyes of shareholders and decision-makers, this knowledge has a natural propensity to replace a fact which means that the end user understands the snares. Most of the literatures deal with semi-tropical and tropical climates; however, in colder environments (e.g., snow-related factors), it has seldom been discussed. For RS-based groundwater analysis, there may be several margins for the number of nuanced variables. An up-to-date overview is given of groundwater studies based on literary analysis using geospatial technology. A few studies have, however, checked the findings with basic facts. Hence, the main competition in the evolving high-quality maps for the evaluation of water policy is misleading. Methodology indicates an exhilarating development in the near future of machine learning techniques.

References

- Abdalla, F. (2012). Mapping of groundwater prospective zones using remote sensing and GIS techniques: a case study from the central Eastern Desert. *Egyptian Journal African Earth Science*, 70, 8–17.
- Abrams, W., Ghoneim, E., Shew, R., LaMaskin, T., Al-Bloushi, K., Hussein, S., AbuBakr, M., Al-Mulla, E., Al-Awar, M. & El-Baz, F. (2018). Delineation of groundwater potential (GWP) in the northern United Arab Emirates and Oman using geospatial technologies in conjunction with simple additive weight (SAW), analytical hierarchy process(AHP), and probabilistic frequency ratio (PFR) techniques. *Journal of Arid Environment*, <https://doi.org/10.1016/j.jaridenv.2018.05.005>.
- Adams, T.M., Tang, A.Y.S. & Wiegand, N. (1993). Spatial data models for managing subsurface data. *Journal of Computation in Civil Engineering*, ASCE, 7(3), 260–277.
- Adeyeye, O.A., Ikpokonte, A.E. & Arabi, A.S. (2015). The dual use of drainage characteristics in groundwater potential modelling using remote sensing and GIS: an example from Dengi area, northcentral Nigeria. *Sustainable Water Resources Management*, <https://doi.org/10.1007/s50899-018-0261-5>.
- Adhikary, P.P., & Dash, C.J. (2017). Comparison of deterministic and stochastic methods to predict spatial variation of groundwater depth. *Applied Water Science* 7 (1), 339–358.
- Adiat, K.A.N., Nawawi, M.N.M. & Abdullah. (2012). Assessing the accuracy of GIS-based elementary multi criteria decision analysis as a spatial prediction tool—A case of predicting potential zone of sustainable groundwater resources. *Journal of Hydrology*, 550, 75–89.
- Agarwal, E., Agarwal, R., Garg, R.D. & Garg, P.K. (2013). Delineation of groundwater potential zone: An AHP/ANP approach. *Journal of the Earth System Science*, 122(3), 887–898.
- Agarwal, R. & Garg, P.K. (2016). Remote sensing and GIS based groundwater potential & recharge zones mapping using multi-criteria decision-making technique. *Water Resources Management*, 30, 253–260.
- Ahmed, R. & Sajjad, H. (2018). Analyzing factors of groundwater potential and its relation with population in the lower Barpani watershed, Assam, India. *Natural Resource Research*, 27(5), 503–515.
- Akbar, T.A., Lin, H. & Degroote, J. (2011). Development and evaluation of GIS-based Arc PRZM-3 system for spatial modelling of groundwater vulnerability to pesticide contamination. *Computer Geosciences*, 37(7), 822–830.
- Akinlalu, A.A., Adegbuyiro, A., Adiat, K.A.N., Akeredolu, B.E. & Lateef, W.Y. (2017). Application of multi-criteria decision analysis in prediction of groundwater resources potential: a case of Oke-Ana, Ilesa area southwestern Nigeria. *NRIAG Journal of Astronomy Geophysics*, 6, 185–200.
- Al Abadi, A.M. (2015). Groundwater potential mapping at northeastern Wasit and Missan governorates, Iraq using a data-driven weights of evidence technique in framework of GIS. *Environmental Earth Sciences*, 75, 1109–1125. <https://doi.org/10.1007/s12665-015-5097-0>.
- Al Shaheeb, A.A., Al-Adamat, R., Al-Fugara, A., Al-Amoush, H. & AlAyyash, S. (2018). Delineating groundwater potential zones within the Azraq Basin of central Jordan using multi-criteria GIS analysis. *Groundwater Sustainable Development*, 7, 82–90.
- Ali, H., Priju, C.P. & Prasad, N.B.N. (2015). Delineation of groundwater potential zones in deep Midland aquifers along Bharathapuzha River basin, Kerala using geophysical methods. *Aquatic Procedia*, 5, 1039–1056.
- An, Y., Wang, Y., Zhang, H. & Wu, X. (2012). GIS-based suitability assessment for shallow groundwater development in Zhangye Basin. *Procedia Environ Science*, 12, 1397–1503.
- Assatse WT, Nouck PN, Tabod CT, Akame JM, Biringanine GN. (2016). Hydrogeological activity of lineaments in Yaounde Cameroon region using remote sensing and GIS Techniques. *Egypt J Remote Sens Space Sci*, 19: 49-60, <https://doi.org/10.1016/j.ejrs.2015.12.006>

- Baker, C.P., Bradley, M.D. & Bobiak, S.M.K. (1993). Well head protection area delineation: linking flow model with GIS. *Journal of Water Resources Planning and Management, ASCE*, 119(2), 275–287.
- Balamurugan, G., Seshan, K. & Bera, S. (2017). Frequency ratio model for groundwater potential mapping and its sustainable management in cold desert, India. *Journal of King Saud University Science*, 29, 333–357.
- Bashe, B.B. (2017). Groundwater potential mapping using remote sensing and GIS in Rift Valley Lakes Basin, Weito Sub Basin, Ethiopia. *International Journal of Science and Research*, 8(2), 53–51.
- Bauer, P., Gumbricht, T. & Kinzelbach, W. (2006). A regional coupled surface water/ground water model of the Okavango Delta, Botswana. *Water Resources Research*, 52, W05503. <https://doi.org/10.1029/2005WR005235>.
- Bayewu, O.O., Oloruntola, M.O., Mosuro, G.O., Laniyan, T.A., Ariyo, A.O. & Fatoba, J.O. (2018). Assessment of groundwater prospect and aquifer protective capacity using resistivity method in Olabisi Onabanjo University campus. *NRIAG Journal of Astronomy Geophysics*, <https://doi.org/10.1016/j.nrjag.2018.05.002>.
- Becker, M.W. (2006). Potential for Satellite Remote Sensing of Ground Water. *Ground Water*, 55 (2), 306–318.
- Berry PAM, Garlick JD, Freeman JA, Mathers EL, 2005. Global inland water monitoring from multi-mission altimetry, *Geophys. Res. Lett.*, 32, L16401, <https://doi.org/10.1029/2005GLO22814>
- Beven, K. (1997). TOPMODEL: a critique. *Hydrological Processes*. 11, 1069–1085.
- Bishop, C. (2018). Geological remote sensing. *International Journal of Applied Earth Observation and Geoinformation*, 65, 267–275.
- Brunner, P., Hendricks Franssen, HJ., Kgotlhang, L. et al. (2007). How can remote sensing contribute in groundwater modeling?. *Hydrogeol J* 15, 5–18. <https://doi.org/10.1007/s10040-006-0127-z>
- Carrera, J. & Neuman, S.P. (1986). Estimation of aquifer parameters undertransient and steady state conditions. 2. Uniqueness, stability, and solution algorithms. *Water Resources Research*, 22(2), 211–227.
- Chang, C.P., Chang, T.Y., Wang, C.T., Kuo, C.H. & Chen, K.S. (2005). Land surface deformation corresponding to seasonal ground-water fluctuation, determined by SAR interferometry in SW Taiwan. *Mathematics and Computers in Simulation*, 67(5–5), 351–359.
- Chen, W., Li, H., Houa, E., Wang, S., Wang, G., Panahi, M., Li, T., Peng, T., Guo, C., Niua, C., Xiao, L., Wang, J., Xie, X., Ahmad, B.B. (2018). GIS-based groundwater potential analysis using novel ensemble weights of evidence with logistic regression and functional tree models. *Science of Total Environment*, 635, 853–867.
- Chenini, I., Ben, M.A. (2010). Groundwater recharges study in arid region: an approach using GIS techniques and numerical modeling. *Computer Geosciences*, 36, 801–817.
- Chowdhury, A., Jha, M.K., Chowdary, V.M. & Mal, B.C. (2009). Integrated remote sensing and GIS based approach for assessing groundwater potential in West Medinipur district, West Bengal, India. *International Journal of Remote Sensing*, 30, 231–250.
- Corsini, A., Cervi, F. & Ronchetti, F. (2009). Weight of evidence and artificial neural networks for potential groundwater spring mapping: an application to the Mt. Modino area (Northern Apennines, Italy). *Geomorphology*, 111, 79–87.
- Crist, E.P.A.T.M. 1985. Tasseled Cap equivalent transformation for reflectance factor data. *Remote Sensing Environment*.
- Dagdeviren, M. & Ihsan, Y. (2007). Personnel selection using analytic network process; Istanbul Ticaret "Universitesi Fen Bilimleri Dergisi Yil, 6(11), 99–118.
- Danielsen, J.E., Auken, E., Jorgensen, F., Sondergaard, V. & Sorensen, K.I. (2003). The application of the transient, electromagnetic method in hydrogeophysical surveys. *J Appl Geophys*, 53, 181–198.

- Dar, I.A., Sankar, K., Dar, M.A. (2010). Remote sensing technology and geographic information system modeling: An integrated approach towards the mapping of groundwater potential zones in hard rock terrain, Mamundiyar basin. *J Hydrol* 395, 285–295.
- Das, S., Gupta, A. & Ghosh, S. (2017). Exploring groundwater potential zones using MIF technique in semi-arid region: a case study of Hingoli district, Maharashtra. *Spat Inf Res*, 25(6), 759–756.
- Díaz-Alcaide, S., Martínez-Santos, P. (2019). Review: Advances in groundwater potential mapping. *Hydrogeology Journal*. <https://doi.org/10.1007/s10050-019-02001-3>.
- Díaz-Alcaide, S., Martínez-Santos, P., Villarroya, F. (2017). A commune-level groundwater potential map for the Republic of Mali. *Water*, 9,839. <https://doi.org/10.3390/w9110839>.
- Dinesan, V.P., Gopinath, G. & Ashitha, M.K. (2015) Application of geoinformatics for the delineation of groundwater prospect zones: a case study for Melattur Grama Panchayat in Kerala, India. *AquaticProced*, 5(105), 1389–1396.
- Dubey CS, Pattanayak SK, Sharma BK, Sirohi A (2002) Groundwater pollution in the satellite city Faridabad, India. In: Dubey CS and Saklani PS (eds) *Geoindicators and related environmental studies: focus on India (KB Powar Volume)*. Pilgrims Publishers, ISBN: 81-7769-187-2, Kathmandu, Nepal, pp 47–56
- Elbeih, S.F. (2015). An overview of integrated remote sensing and GIS for groundwater mapping in Egypt. *Ain Shams Eng J*, 6, 1–15.
- Fashae, O.A., Tijani, M.N., Talabi, O.A., Adediji, O.I. (2015). Delineation of groundwater potential zones in the crystalline basement terrain of SW-Nigeria: an integrated GIS and remote sensing approach. *Appl Water Sci*, 5, 19–38. <https://doi.org/10.1007/s13201-013-0127-9>.
- Fensholt, R., Sandholt, I., Stisen, S., Tucker, C. (2006). Analysing NDVI for the African continent using the geostationary meteosat second generation SEVIRI sensor. *Remote Sens Environ*, 101 (2), 212–229.
- Feyisa, G.L., Meilby, H., Fensholt, R. Proud, S.R. (2015). Automated Water Extraction Index: A new technique for surface water mapping using Landsat imagery. *Remote Sens. Environ.*, 150, 23–35.
- Fisher, A., Flood, N., Danaher, T. (2016). Comparing Landsat water index methods for automated water classification in eastern Australia. *Remote Sens. Environ.*, 175, 167–182.
- Gabriel, B.O., Olusola, O.M., Omowonuola, A.F., Lawrence, A.O. (2015). A preliminary assessment of the groundwater potential of Ekiti state, southwestern Nigeria, using terrain and satellite imagery analyses. *J Environ Earth Sci*, 5(18), 33–53.
- García-Rodríguez, M., Antón, L., Martínez-Santos, P. (2015). Estimating groundwater resources in remote desert environments by coupling geographic information systems with groundwater modeling (ErgChebbi, Morocco). *J Arid Environ*, 110, 19–29.
- Gogu, R.C., Carabin, G., Hallet, V., Peters, V., Dassargues, A. (2001). GIS-based hydrogeological databases and groundwater modelling. *Hydrogeology Journal*, 9, 555–569.
- Govindaraj, V., Karthick, P., Lakshumanan, C. (2017). Assessment of groundwater potential zones using remote sensing and GIS techniques in Gomukhi River basin of Tamil Nadu, India. *Int Res J Earth Sci*, (11), 1–12.
- Gumma, M.K., Pavelic, P. (2013). Mapping of groundwater potential zones across Ghana using remote sensing, geographic information systems, and spatial modeling. *Environ Monit Assess*, 185, 3561–3579. <https://doi.org/10.1007/s10661-012-2810-y>
- Gupta, R.P. (2018). *Remote sensing geology*, 3rd edn. Springer, Berlin, 528 p.
- Harbaugh, A. W., Banta, E. R., Hill, M. C., and McDonald, M. G. *MODFLOW-2000, the US Geological Survey modular groundwater model-user guide to modularization concepts and the ground-water flow process*, US Geological Survey 2000; openfile report: 00-92, 2000.
- Hoffmann, J., Zebker, H.A., Galloway, D.L., Amelung, F. (2001). Seasonal subsidence and rebound in Las Vegas Valley, Nevada, observed by synthetic aperture radar interferometry. *Water Resour Res*, 37(6), 1551–1566.
- Huang G, Liu C, Sun J, Zhang M, Jing J, Li L. 2018. A regional scale investigation on factors controlling the groundwater chemistry of various aquifers in a rapidly urbanized area: A case study of the Pearl River Delta. *The Science of the Total Environment*, 7, 625:510–518.

- Hussein, A.A., Govindu, V., Nigusse, A.G.M. (2017). Evaluation of groundwater potential using geospatial techniques. *Appl Water Sci*, 7, 2557–2561. <https://doi.org/10.1007/s13201-016-0533-0>.
- Ibrahim-Bathis, K., Ahmed, S.A. (2016). Geospatial technology for delineating groundwater potential zones in Doddahalla watershed of Chitradurga district, India. *Egypt J Remote Sens Space Sci*, 19, 223–235.
- Jahan, C.S., Rahaman, M.F., Arefin, R., Ali, M.S., Mazumder, Q.H. (2018). Delineation of groundwater potential zones of Atrai–Sib river basin in north-west Bangladesh using remote sensing and GIS techniques. *Sustain Water Resour Manag.*, <https://doi.org/10.1007/s50899-018-0250-x>.
- Jenifer, M.A., Jha, M.K. (2017) Comparison of analytic hierarchy process, catastrophe and entropy techniques for evaluating groundwater prospect of hard-rock aquifer systems. *J Hydrol*, 558, 605–625.
- Jin, S., Feng, G. (2013). Large-scale global groundwater variations from satellite gravimetry and hydrological models, 2002–2012. *Glob. Planet. Chang.*, 106, 20–30.
- Jyrkama, M.I., Sykes, J.F., Normani, S.D. (2002). Recharge estimation for transient ground water modeling. *GroundWater*, 50(6), 638–658.
- Khazaz, L., Oulidi, H. J., Moutaki, S. E., & Ghafiri, A. (2015). Comparing and Evaluating Probabilistic and Deterministic Spatial Interpolation Methods for Groundwater Level of Haouz in Morocco. *Journal of Geographic Information Systeme*, 7, 631–65.
- Koch, M., Gaber, A., Gereish, M.H., Zaghoul, E., Arafat, S.M., AbuBakr, M. (2013). Multisensor characterization of subsurface structures in a desert plain area in Egypt with implications for groundwater exploration. In: SPIE remote sensing conference, Dresden, Germany; 23–26 September 2013.
- Konkul, J., Rojborwornwittaya, W., Chotpantarat, S. (2015). Hydrogeologic characteristics and groundwater potentiality mapping using potential surface analysis in the Huay Sai area, Phetchaburi province, Thailand. *Geosci J*, 18(1), 89–103. <https://doi.org/10.1007/s12303-013-0057-6>.
- Kumar, P., Herath, S., Avtar, R., Takeuchi, K. (2016). Mapping of groundwater potential zones in Killinochi area, Sri Lanka, using GIS and remote sensing techniques. *Sustain Water Resour Manag*, 2, 519–530. <https://doi.org/10.1007/s50899-016-0072-5>.
- Lee, S., Kim, Y.S. & Oh, H.J. (2012). Application of a weights-of-evidence method and GIS to regional groundwater productivity potential mapping. *J. Environ. Manage.*, 96, 91–105.
- Levine, J.B., and Salvucci, G.D. (1999). Equilibrium analysis of groundwater–vadose zone interactions and the resulting spatial distribution of hydrologic fluxes across a Canadian prairie. *Water Resources Research*, 35(5), 1369–1383.
- Lilly, J.O. (2016). A GIS Approach to Modeling Groundwater Levels in the Mississippi River Valley Alluvial Aquifer. Theses and Dissertations. 1827. University of Arkansas, Fayetteville. Available at: <http://scholarworks.uark.edu/etd/1827>.
- Liu, T., Yan, H., Zhai, L. (2015). Extract relevant features from DEM for groundwater potential mapping. *The International Archives of the Photogrammetry, Remote Sensing and Spatial Information Sciences*, volume XL-7/W5. International Workshop on Image and Data Fusion, Kona, Hawaii, 21–23 July 2015.
- Loukas, A., Vasiliades, L., Domenikiotis, C., Dalezios, N.R. (2005). Basin-wide actual evapotranspiration estimation using NOAA/AVHRR satellite data. *Phys Chem Earth*, 30(1–3), 69–79.
- Madani, A., Niyazi, B. (2015). Groundwater potential mapping using remote sensing techniques and weights of evidence GIS model: a case study from Wadi Yalamlam basin, Makkah Province, Western Saudi Arabia. *Environ Earth Sci*, 75, 5129–5152.
- Magaia, L.A., Goto, T.N., Masoud, A.A., Koike, K. (2018). Identifying groundwater potential in crystalline basement rocks using remote sensing and electromagnetic sounding techniques in central western Mozambique. *Nat Resour Res*, 27(3). 275–298.

- Magesh, N.S., Chandrasekar, N., Soundranayagam, J.P. (2012). Delineation of groundwater potential zones in Theni district, Tamil Nadu, using remote sensing, GIS and MIF techniques. *Geosci Front*, 3(2), 198–196.
- Mallick, J., Singh, C.K., Al-Wadi, H., Ahmed, M., Rahman, A., Shashtri, S., Mukherjee, S. (2015). Geospatial and geostatistical approach for groundwater potential zone delineation. *Hydrological Processes*, <https://doi.org/10.1002/hyp.10153>.
- Martin-Loeches, M., Reyes-López, J., Ramírez-Hernández, J., Temiño-Vela, J., Martínez-Santos, P. (2018). Comparison of RS/GIS analysis with classic mapping approaches for siting low-yield boreholes for hand pumps in crystalline terrains: an application to rural communities of the Caimbambo province, Angola. *J Afr Earth Sci*, 138, 22–31.
- McFeeters, S.K. (1996). The use of the Normalized Difference Water Index (NDWI) in the delineation of open water features. *Int. J. Remote Sens.*, 17, 1525–1532.
- Microwave and Radar Institute. (2006). TanDEM-X: a new high resolution interferometric SAR mission. <http://www.dlr.de/hr/tmx>. Cited 29 October 2006.
- Misi, A., Gumindoga, W., Hoko, Z. (2018). An assessment of groundwater potential and vulnerability in the upper Manyame sub-catchment of Zimbabwe. *Phys Chem Earth*, 105:72–83.
- Mogaji, K.A., Lim, H.S. & Abdullah, K. (2015). Regional prediction of groundwater potential mapping in a multifaceted geology terrain using GIS-based Dempster–Shafer model. *Arab. J. Geosci.*, 8, 3235–3258.
- Mogaji, K.A., Lim, H.S. (2018). Application of Dempster-Shafer theory of evidence model to geoelectric and hydraulic parameters for groundwater potential zonation. *NRIAG J Astron Geophys*, 7, 135–158.
- Naghibi, S.A., Moghaddam, D.D., Kalantar, B., Pradhan, B., Kisi, O. (2017). A comparative assessment of GIS-based data mining models and a novel ensemble model in groundwater well potential mapping. *JHydrology*, 558, 571–583.
- Naghibi, S.A., Pourghasemi, H.R., Pourtaghi, Z.S., Rezaei, A. (2015). Groundwater quantity potential mapping using frequency ratio and Shannon’s entropy models in the Moghan watershed, Iran. *Earth Sci. Informatics*, 8, 171–186.
- Nampak, H., Pradhan, B., Manap, M.A. (2015). Application of GIS based data driven evidential belief function model to predict groundwater potential zonation. *J Hydrology*, 513, 283–300.
- Nanda, S., Annadurai, R., Barik, K.K. (2017). Geospatial decipherment of groundwater potential of Kattankolathur block of Tamil Nadu using MCDM techniques. *Remote Sens Appl Soc Environ*, 8, 250–250.
- Nicolas, M., Selles, S., Bour, O., Maréchal, J.C., Chandra, S., Mohanty, A., Ahmed, M.S. (2017). Delineation of groundwater potential zones using noninvasive techniques to improve conceptual modelling of recharge in a non-instrumented weathered crystalline aquifer in South India. 53rd IAH Congress. Montpellier, France, December 2017.
- Nsiah, E., Appiah-Adjei, E.K., Adjei, K.A. (2018). Hydrogeological delineation of groundwater potential zones in the Nabogo basin, Ghana. *J Afr Earth Sci*, 153, 1–9.
- Oh, H.J., Kim, Y.S., Choi, J.K., Park, E., Lee, S. (2011). GIS mapping of regional probabilistic groundwater potential in the area of Pohang City, Korea. *J Hydrology*, 399, 158–172.
- Oikonomidis, D., Dimogianni, S., Kazakis, N., Voudouris, K. (2015). A GIS/remote sensing-based methodology for groundwater potentiality assessment in Tirnavos area, Greece. *J Hydrology*, 525, 197–208.
- Omosuyi, G.O., Oseghale, A., Bayode, S. (2013). Hydrogeophysical delineation of groundwater prospect zones at Odigbo, southwestern Nigeria. *Academic J*, 8(15), 596–608. <https://doi.org/10.5897/SRE2013.5359>.
- Ozdemir, A. (2011). GIS-based groundwater spring potential mapping in the Sultan Mountains (Konya, Turkey) using frequency ratio, weights of evidence and logistic regression methods and their comparison. *J. Hydrology*, 511, 290–308.
- Pandey, V.P., Shrestha, S., Kazama, F. (2013). A GIS-based methodology to delineate potential areas for groundwater development: a case study from Kathmandu Valley, Nepal. *Applied Water Sci.*, 3, 553–565.

- Parks, S., Byrnes, J., Abdelsalam, M.G., Dávila, D.A.L., Atekwana, E.A., Atya, M.A. (2017). Assessing groundwater accessibility in the Kharga Basin, Egypt: a remote sensing approach. *J Afr Earth Sci*, 136, 272–281.
- Patra, S., Mishra, P., Mahapatra, S.C. (2018). Delineation of groundwater potential zone for sustainable development: a case study from Ganga alluvial plain covering Hooghly district of India using remote sensing, geographic information system and analytic hierarchy process. *J Clean Prod*, 172, 2585–2502.
- Pourghasemi, H.R., Beheshtirad, M. (2015). Assessment of a data-driven evidential belief function model and GIS for groundwater potential mapping in the Koohrang Watershed, Iran. *Geocarto Int.*, 30, 662–685.
- Pourtaghi, Z.S., Pourghasemi, H.R. (2015). GIS-based groundwater spring potential assessment and mapping in the Birjand Township, southern Khorasan Province, Iran. *Hydrogeol. J.*, 22, 653–662.
- Rahmati, O., Melesse, A.M. (2016). Application of Dempster–Shafer theory, spatial analysis and remote sensing for groundwater potentiality and nitrate pollution analysis in the semi-arid region of Khuzestan, Iran. *Sci Total Environ*, 568, 1110–1123.
- Rahmati, O., Pourghasemi, H. R. & Melesse, A. M. (2016). Application of GIS-based data driven random forest and maximum entropy models for groundwater potential mapping: a case study at Mehran Region, Iran. *Catena*, 137, 360–372.
- Rahmati, O., Samani, A. N., Mahdavi, M., Pourghasemi, H. R. & Zeinivand, H. (2015). Groundwater potential mapping at Kurdistan region of Iran using analytic hierarchy process and GIS. *Arab. J. Geosci.*, 8, 7059–7071.
- Razandi, Y., Pourghasemi, H. R., Neisani, N. S. & Rahmati, O. (2015). Application of analytical hierarchy process, frequency ratio, and certainty factor models for groundwater potential mapping using GIS. *Earth Sci Inf* 8(4):867–883. <https://doi.org/10.1007/s12145-015-0220-8>.
- Roaza, H., Roaza, R.M., Wagner, J.R. (1993). Integrating geographic information systems in groundwater applications using numerical modeling techniques. *Water Resources Bulletin*. *AWRA*, 29(6), 981–988.
- Roshier, D.A., Rumbachs, R.M. (2005). Broad-scale mapping of temporary wetlands in arid Australia. *J Arid Environ*, 56(2), 259–263.
- Saaty, T.L. (1999). Fundamentals of the analytic network process; International Symposium of the Analytic Hierarchy Process (ISAHP), Kobe, Japan.
- Salama, R.B., Ye, L., Broun, J.L. (1996). Comparative study of methods of preparing hydraulic-head surfaces and the introduction of automated hydrogeological-GIS techniques. *Journal of Hydrology*, 185(1–5), 115–136.
- Sener, E., Sener, S., Davraz, A. (2018). Groundwater potential mapping by combining fuzzy-analytic hierarchy process and GIS in Beyşehir Lake Basin, Turkey. *Arab J Geosci*, 11, 187.
- Siddha, S., Sahu, P. (2018). Assessment of groundwater potential of Gandhinagar region. *Gujarat. J Geol Soc India*, 91, 91–98.
- Slater, J.A., Garvey, G., Johnston, C., Haase, J., Heady, B., Kroenung, G., Little, J. (2006). The SRTM data “finishing” process and products. *Photogramm Eng Remote Sens*, 72(3), 237–257.
- Solomatine, D.P., Ostfeld, A. (2008). Data-driven modelling: some past experiences and new approaches. *J. Hydroinform.*, 10 (1): 3–22.
- Solomon, S. (2003). *Remote Sensing and GIS: Applications for Groundwater Potential Assessment in Eritrea*. Environmental and Natural Resources Information Systems, Royal Institute of Technology, SE-100 55 Stockholm, Sweden. ISBN 91-7283-557-9. Available at: <http://www.diva-portal.org/smash/get/diva2:9296/FULLTEXT01.pdf>.
- Sorensen, R., Zinko, U., Seibert, J. (2006). On the calculation of the topographic wetness index: evaluation of different methods based on field observations. *Hydrol Earth Syst Sci*, 10, 101–112.
- Sternberg, T., Paillou, P. (2015). Mapping potential shallow groundwater in the Gobi Desert using remote sensing: Lake UlaanNuur. *J Arid Environ*, 118, 21–27.

- Sultan, S.A., Essa, K.S.A.T., Khalil, M.H., El-Nahry, A.E.H., Galal, A.N.H. (2017). Evaluation of groundwater potentiality survey in south Ataq northwestern part of Gulf of Suez by using resistivity data and site-selection modeling. *NRIAG J Astron Geophys.* 6, 230–253.
- Tam, V.T., De Smedt, F., Batelaan, O., Dassargues, A. (2005). Study on the relationship between lineaments and borehole specific capacity in a fractured and karstified limestone area in Vietnam. *Hydrogeol J*, 12(6), 662–673.
- Thapa, R., Gupta, S., Guin, S., Kaur, H. (2017a). Assessment of groundwater potential zones using multi-influencing factor (MIF) and GIS: a case study from Birbhum district, West Bengal. *Appl Water Sci*, 7, 5117–5131. <https://doi.org/10.1007/s13201-017-0571-z>.
- Thapa, R., Gupta, S., Gupta, A., Reddy, D.V., Kaur, H. (2017b). Use of geospatial technology for delineating groundwater potential zones with an emphasis on water-table analysis in Dwarka River basin, Birbhum, India. *Hydrogeol J*, 26, 899–922.
- Venkatesan, V., Krishnaveni, M., Karunakaran, K., Ravikumar, G. (2010). GIS-based multi-criteria analysis for assessment of groundwater potential and land suitability. *Int J Earth Sci Eng*, 3(2), 207–225.
- Venkateswaran, S., Ayyandurai, R. (2015). Groundwater potential zoning in upper Gadilam River basin. Tamil Nadu. *Aquatic Procedia*, 5, 1275–1282.
- Vishwakarma J, Sinha MK, Verma MK, Ahmad I (2015) Application of remote sensing and GIS in groundwater prospect mapping. *Int J Eng Res Technol*, 3(10), 559–555.
- Wahyuni, S., Oishi, S., Sunada, K. (2008). The estimation of the groundwater storage and its distribution in Uzbekistan. *Annual Journal Hydraulic Engg.*, 52, 31–36.
- Wendt, L., Hilberg, S., Rob, J., Dimberger, D., Strasser, T., Braun, A. (2016). Remote sensing in hydrogeology: a short summary of methods and constraints for groundwater exploration. Technical report, University of Salzburg and University of Tübingen, Germany, 57 pp
- Wendt, L., Hilberg, S., Robl, J., Dimberger, D., Strasser, T., Braun, A. EO5HumEn – Earth Observation based services to support humanitarian operations: monitoring population and natural resources in refugee/IDP camps, funded by the Austrian Research Promotion Agency FFG (ASAP 9, Nr. 850081).
- World Bank. (2018). Beyond Crop per Drop Assessing Agricultural Water Productivity and Efficiency in a Maturing Water Economy. World Bank Publications, The World Bank Group, 1818 H Street NW, Washington, DC 20533. ISBN: 978-1-5658-1298-9. <http://documents.worldbank.org/curated/en/-352321530075399351/pdf/127625-PUB-Date-6-28-2018-PUB-LIC-Beyond-Crop-per-Drop.pdf>
- Xu, H. (2006). Modification of normalised difference water index (NDWI) to enhance open water features in remotely sensed imagery. *Int. J. Remote Sens.*
- Xue, J., Su, B. (2017). Significant remote sensing vegetation indices: are view of developments and applications. *J Sensors*. <https://doi.org/10.1155/2017/1353691>.
- Yan, E., Milewski, A., Sultan, M., Abdeldayem, A., Soliman, F., Gelil, K.A. (2010). Remote-Sensing Based Approach to Improve Regional Estimation of Renewable Water Resources for Sustainable Development. US – Egypt Workshop on Space Technology and Geo-information for Sustainable Development, Cairo, Egypt 15-17 June, 2010
- Yeh, H.F., Cheng, Y.S., Lin, H.I. & Lee, C.H. (2016). Mapping groundwater recharge potential zone using a GIS approach in Hualian River, Taiwan. *Sustain. Environ. Res.* 26, 33–53.

Part II
Groundwater Availability, Quality
and Pollution

Chapter 6

Groundwater Quality Through Multi-Criteria-Based GIS Analysis: Village Level Assessment



Baisakhi Chakraborty, Sambhunath Roy, Gouri Sankar Bhunia, Debashish Sengupta, and Pravat Kumar Shit

Abstract Groundwater quality deterioration is becoming a very vital issue among various environmental problems in the present decades. Good quality of groundwater helps in healthy living status and high crop yield. A village level study is the need of the hour. The present study analyzes the groundwater quality of different villages in Kashipur block of Purulia district in West Bengal. Water samples were collected from 52 bore wells in this study area in two different seasons (pre-monsoon and post-monsoon). Chemical properties of the water samples (pH, EC, TDS, TH, TA, Na^+ , Ca^{2+} , Mg^{2+} , SO_4^{2-} , HCO_3^- , CO_3^{2-} , Fe, K^+ , and F^-) were measured by various methods, and these values were analyzed to indicate different irrigation water quality by SSR, SSP, MAR, and KR method. The overall groundwater quality was analyzed by the PIG (Pollution Index of Groundwater) method for both the seasons. PIG values vary from 0.46 to 1.50 in the pre-monsoon season and from 0.38 to 1.38 in the post-monsoon season. 73.07% of the samples indicate insignificant pollution, 26.92% of the samples indicate low pollution, and only 0.01% of the samples show high pollution in the pre-monsoon season. The spatial distribution map was prepared using kriging interpolation technique on ArcGIS platform. PIG values of post-monsoon season show 67.30% of samples fall under the insignificant pollution zone, 32.69% of samples fall under the low pollution zone, and only 0.01% of samples indicate a high pollution zone. A statistical method such as summary statistics and correlation matrix was used to understand the interdependence or magnitude of each variable to the others in two climatic seasons. Results clearly defined that anthropogenic and geogenic conditions mainly determine the quality of

B. Chakraborty (✉) · S. Roy · P. K. Shit
PG Department of Geography, Raja N.L. Khan Women's College (Autonomous), West Bengal, India

G. S. Bhunia
RANDSTAD India Pvt Ltd., New Delhi, Delhi, India

D. Sengupta
Department of Geology & Geophysics, Indian Institute of Technology (IIT), Kharagpur, West Bengal, India

groundwater. Mapping of the PIG zone by GIS techniques helps to show the influence of geological and anthropogenic sources on the quality of groundwater in the study area.

Keywords Chemical parameters · Correlation matrix · GIS · Irrigation water quality · Ordinary kriging · PIG · Statistical methods

6.1 Introduction

Groundwater is a precious and important resource of water in the earth, naturally occurred by the hydrological processes. Groundwater is less contaminated than the surface water and generally bacteria-free; therefore, it is very useful for drinking and other consumption purposes (Nag and Das 2017). In developing countries, about 80% of diseases are associated with the poor sanitary conditions and unhealthy drinking water (UNESCO 2007). In India, with the rising number of the human population, the demand for groundwater usage is increasing abruptly. Thus, human health is directly related to the quality of groundwater. Surface and subsurface water have been deteriorated by increasing anthropogenic wastes, untreated sewerage, and related unconscious public activities (Shanmugasundharam et al. 2015). This practice changes the overall quality of groundwater which deteriorates the standards of water quality used for drinking and irrigation purposes. Therefore, assessment on the quality of groundwater is important to measure the suitability for different uses especially for drinking and irrigational purpose (Nag and Das 2017).

Several research works have been carried out to measure the groundwater quality as the characteristics of soil and rock media influenced the chemical quality of groundwater (Raji and Alagbe 1997; Acheampong and Hess 1998; Foster et al. 2000). Hydro-chemical characteristics of water quality have been conducted by various researchers in the different river basins (Umar et al. 2006; Raju 2007; Rao et al. 1997; Subramani et al. 2005). The source of groundwater and the ion-exchange process determines the hydrochemistry of water (Mercado 1985). Quality of groundwater and its usefulness to drinking as well as irrigation purpose has been assessed by many scholars (Jalali 2006; Rivers et al. 1996; Nag and Lahiri 2012; Nag and Das 2017). Groundwater quality zonation map has been prepared using GIS techniques in the Nalgonda district (Brindha and Elango 2012). Water quality assessment by hierarchical cluster analysis method and CCME index method of Damodar river in south Bengal was done by Halder et al. (2014). The groundwater potential zone has been documented using MIF (multi-influencing factor) by weighted method in Birbhum district by Thapa et al. (2017). Quality and degree of groundwater pollution have been analyzed by PIG (Pollution Index of Groundwater) and ANOVA test, correlation, and piper diagram in a rural part of Telangana state, India, by Rao et al. (2018). Fluoride laden groundwater appraisal in Suri-I and Suri-II blocks of Birbhum district, West Bengal, was conducted by geochemical model PHREEQC and piper diagram (Das and Nag 2017). An investigation on crystalline rocks for the

development of groundwater resources has been analyzed by Ahmed (2007) and Wright and Burges (1992). Potential lineaments of groundwater and impacts on regional subsidence and vulnerability to groundwater pollution have been analyzed by GIS techniques (Taheri et al. 2015; Singh et al. 2015). Spatial distribution mapping of the different parameters is generated by ordinary kriging (OK) and irrigational water quality threshold limit which is obtained by indicator kriging (IK) (Masoomah et al. 2014).

Several studies have been carried out to investigate the groundwater quality using GIS platform. But the relation between groundwater quality with its geomorphologic structure and various physical factors using GIS techniques has not been done yet. Therefore, the present study is to analyze the quality of groundwater for drinking and irrigation purpose with its different bio-chemical parameter and find the relation of its variation with different geogenic conditions in two different climatic seasons using GIS techniques to determine the suitability of use in domestic as well as agricultural purpose.

The present study area (Kashipur block of Purulia district) is situated on the eastern part of the Chotanagpur plateau of the Indian peninsula with semi-arid climate. People of this area use groundwater for mainly drinking and irrigation purpose. Water samples were collected from the hand-dug wells and bore wells. But the shallow aquifers of this area are mostly contaminated by storm water and human activities, which bring changes in the physio-chemical parameters of water quality. According to WHO and BIS if the dilution of any parameter is above the standard limit, there can be health problems. In the Kashipur block geological, lithological, vegetation, soil, and human livelihood characteristics influenced the quality of groundwater (Kundu and Nag 2018). Therefore, the assessment of the Water Quality Index (WQI) with geospatial techniques is very essential for further management of groundwater resource in this area.

6.2 Study Area

Kashipur block (Purulia district of West Bengal) is located in the part of eastern fringe of Chotanagpur plateau extended between $23^{\circ}18' N$ to $23^{\circ}31' N$ latitude and $86^{\circ}34' E$ to $86^{\circ}52' E$ longitude (Fig. 6.1) with an area of 430 km^2 (Kundu and Nag 2018). Kashipur block lies under the Raghunathpur subdivision, and it consisted of thirteen Gram Panchayats. From the topographical point of view, this block experienced an undulating surface with rough terrain and moderately weathered pediplain in western and south-western part. Some residual denudated hills are also found there. The average altitude of the study area is recorded as 190 m. The general slope lies from the west to east. Climatologically, the study area is semi-arid and drought-prone. The highest temperature hits up to $48^{\circ} C$ in the months of March to June. On the other hand, winter temperature falls up to $4-5^{\circ} C$ between November to February times. Rainfall occurs mainly from S to W Monsoon winds with annual average rainfall from 1000 to 1400 mm. Geologically, Purulia district is the part of

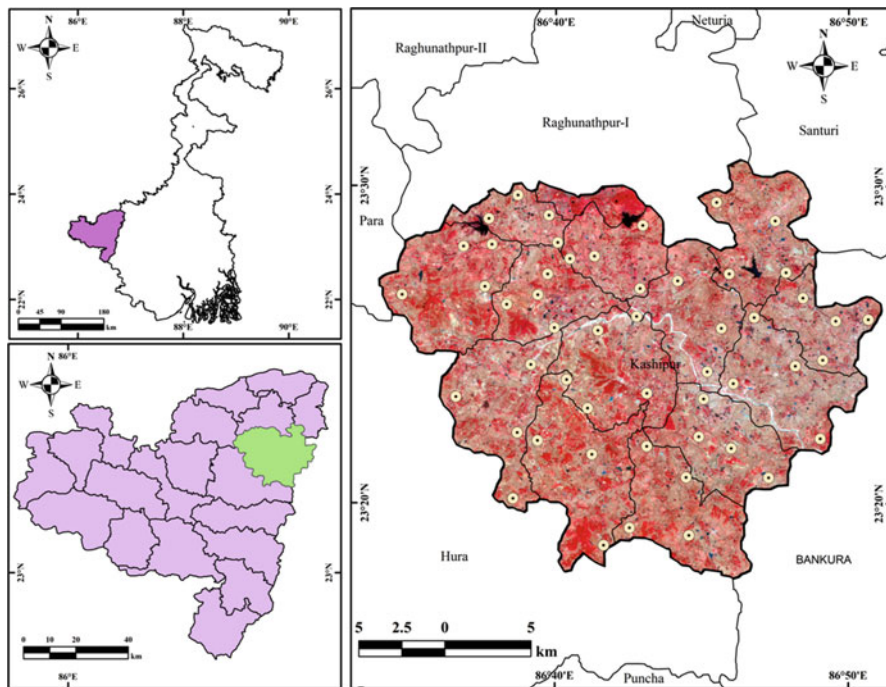


Fig. 6.1 Location map of the study area and sapling sites

Gondwanaland and the rock formation are pre-Cambrian age. In this study area granite gneiss and mica schist are the dominating rock types (Fig. 6.2). The gravel conglomerate of sijua formation is found beside the Dwarakeswar River. Different intrusions as well as lineaments are also found. Amphibolites are also found dispersedly. Various fractures and weathering rocks help to percolate water to reach the groundwater zone more easily. Upper layer of soils is made from weathered granitic rocks, and thus lateritic soils with acidic contents are formed in this region (Fig. 6.2). This creates secondary aquifer in the underlying strata. Many rain faded streams originated from Chotanagpur plateau and are flowing toward the east over this region with numerous short tributaries. Some of those main rivers are Kangsabati, Dwarakeswar, and Silabati are observed with a dendritic drainage pattern (Kundu and Nag 2018).

In the Kashipur block, the main source of water supply for drinking and irrigation are hand-dug wells and bore wells. But human activities polluted the hand-dug wells and surface water by dumping waste which has contaminated the water of lower aquifers. In this semi-arid region most of the surface and dug wells dried up in the dry seasons. Thus, deep tube well or bore well is the most dependable source of groundwater.

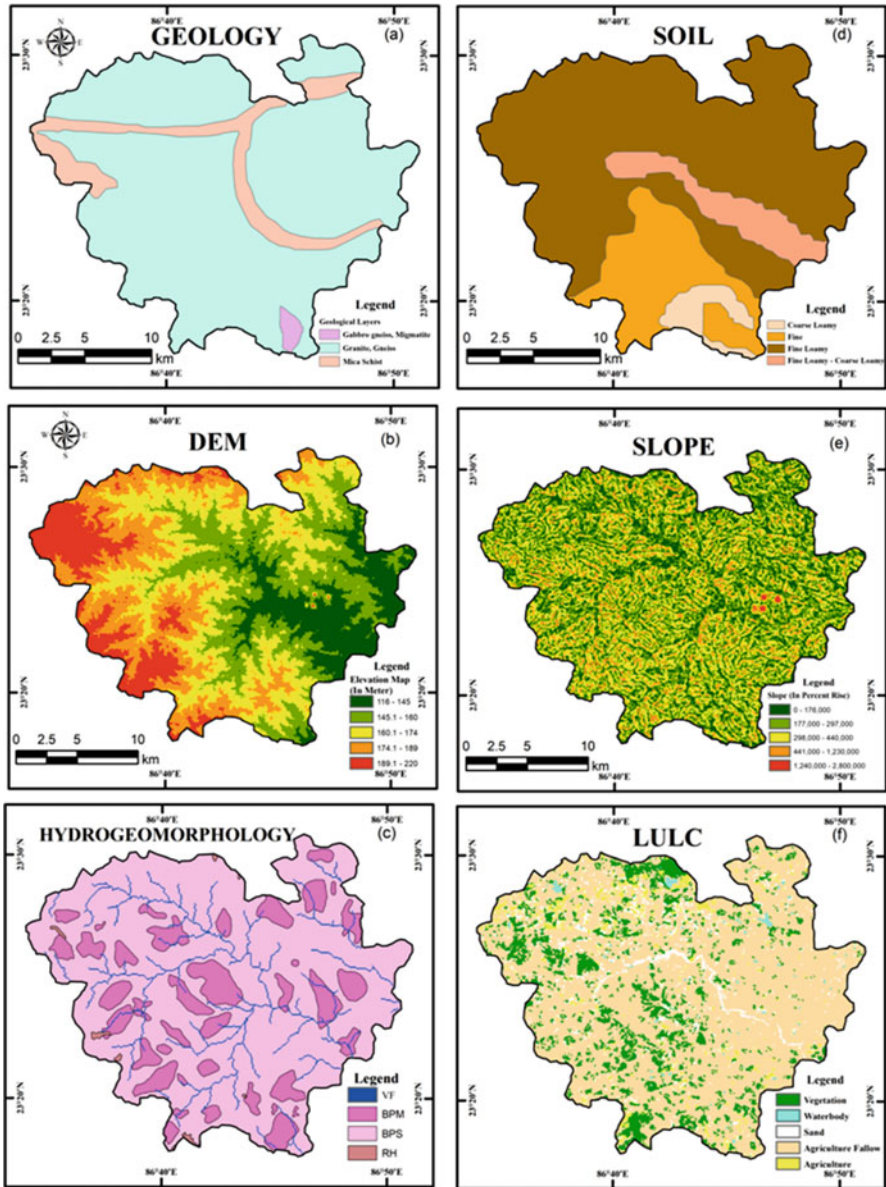


Fig. 6.2 Surface and sub-surface factors maps of the study area

6.3 Materials and Methods

6.3.1 Collection of Samples and Chemical Analysis

Village level groundwater samples were collected from 52 bore wells from 13 Gram Panchayats. These samples were collected for both the pre-monsoon and post-monsoon season. Half liter of clean containers made by plastics has been used for collecting the water samples. Plastic containers were treated by 1:1 hydrochloric acid (HCL) for about 24 h and then washed by distilled water for deionizing. Each sample location was labelled on each container, and all those were suitably preserved up to chemical analysis in the laboratory.

To assess the quality of groundwater such as pH, EC (electrical conductivity) has been measured by portable meters. Total Dissolved Solids (TDS) were computed after measuring the EC of each sample (Hem 1991). EDTA Titration method was used for calculating the quantity of total hardness (TH) of the groundwater samples. The concentration of sodium, calcium, chloride, magnesium, carbonate, fluoride, and potassium was analyzed by the standard methods of the American Public Health Association (APHA 2012). The HCO_3 was analyzed by HCl volumetric method. Na and K were calculated by the flame photometer method. UV spectrophotometric techniques are used for measuring SO_4 , NO_3 , and F. All concentration was expressed in mg/l, except pH.

6.3.2 Pollution Index of Groundwater (PIG)

Pollution Index of Groundwater (PIG) was used for measuring the impact of each chemical property in the groundwater quality for irrigation and drinking purpose by Subba Rao (2012). To compute PIG, each parameter was assigned by its relative weight (R_w) from 1 to 5. These weights were given by the relative impact of chemicals to the suitability of drinking and irrigation purpose. Table 6.1 shows the details relative weight (R_w) and weight parameter (W_p).

Weight parameter (w_p) was calculated for each chemical component in the second step to assess the impact on overall water quality. In the third step, S_c (status of concentration) was calculated by dividing the quantity of each chemical parameter of each sample by its respective safe limit for drinking water quality. In the next step o_w (overall chemical quality of water) was measured by the product of W_p and S_c . Finally, all o_w values for each parameter were added (sum total).

$$W_p = R_w / \sum R_w \quad (6.1)$$

$$S_c = C / D_s \quad (6.2)$$

Table 6.1 List of relative weight (R_w), weight parameter (W_p), and drinking water quality standards (D_s)

Chemical parameter	R_w	W_p	D_s
pH	5	0.104	7.5
TDS	5	0.104	500
Ca^{2+}	2	0.042	75
Mg^{2+}	2	0.042	30
Na^{+}	4	0.083	200
K^{+}	1	0.021	10
HCO_3^{-}	3	0.062	300
Cl^{-}	4	0.083	250
So_4	5	0.104	150
F	5	0.104	1.5
EC	2	0.042	730
TA	2	0.042	200
TH	2	0.042	200
Fe	3	0.062	3
CO_3	3	0.062	100
SUM	48	1.000	

Source: Subba Rao (2012), BIS (2012)

Table 6.2 Classification of pollution index of groundwater (PIG) (Subba Rao 2012)

PIG Range	Classification
<1.0	Insignificant pollution
1.0–1.5	Low pollution
1.5–2.0	Moderately pollution
2.0–2.5	High pollution
>2.5	Very high pollution

$$O_w = W_p * S_c \tag{6.3}$$

$$PIG = O_w \tag{6.4}$$

For calculating PIG, the contribution of each chemical parameter to the groundwater quality of each sample was taken into account (Table 6.2). If overall quality of water (chemical) is greater than 0.1 (O_w), it means 10% value of 1.0 of the PIG. There are four categories that have been put for analyzing PIG.

To analyze the irrigation water quality, different exponents were calculated such as sodium adsorption ratio (SAR), soluble sodium percentage (SSP), magnesium adsorption ratio (MAR), and Kelly’s ratio (KR) for suitability of groundwater for agriculture usages in the study area. For details measurement of variation in water quality of various chemical parameters was analyzed by descriptive statistics and correlation matrix tools.

6.3.3 Spatial Interpolation

The dataset of physico-chemical parameters was imported into the GIS database. Kriging interpolation model was used to generate a set of predicted values at known location. Kriging model was used subjected to semivariogram with smoothing factor under exponential and spherical tuning techniques (Fahid et al. 2011).

6.3.4 Statistical Analysis

Descriptive statistics was calculated for all the physico-chemical parameters of groundwater samples. The correlation analysis is also performed among the groundwater samples through Pearson's correlation co-efficient (r). The statistical analysis has been performed through Microsoft Excel. All the statistical analysis was performed at 0.05 significance level.

6.4 Results and Discussion

6.4.1 Groundwater Quality and Chemistry

The physio-chemical analysis of water parameters is compared with the standard drinking water quality measured by BIS (2012). The use of the ordinary kriging method helps to generate a spatial distribution of those chemical parameters (Figs. 6.3, 6.4, 6.5, and 6.6).

6.4.1.1 pH

Water quality very much depends on the characteristics of dissolved hydrogen ion in the water. In this study area, pH values vary between 6.15 to 7.94 and 6.24 to 7.35 with an average value of 6.88 and 6.75 in pre-monsoon and post-monsoon season correspondingly. Thus, the quality of groundwater seems to be neutral to saline condition. According to BIS, the permissible limit of pH is 7.5. In the study area, 4 (7.69%) groundwater samples are found as higher values than the standard limit. Otherwise, 48 (92.30%) samples are below than standard limit in the pre-monsoon season. In the post-monsoon season, samples are not higher than the permissible limit. Thus 100% of samples lie under the safe limit to drinking purpose. The ordinary kriging tool helps to detect the concentration of pH in the study area which indicates central and north of this block (parts of Sonathale, Rangamati, Gourangdi, Gagnabad, Kaliada, Kashipur, Gram Panchayat), and a few villages of Sonajuri GP are affected by a higher concentration of pH value. A wide portion of

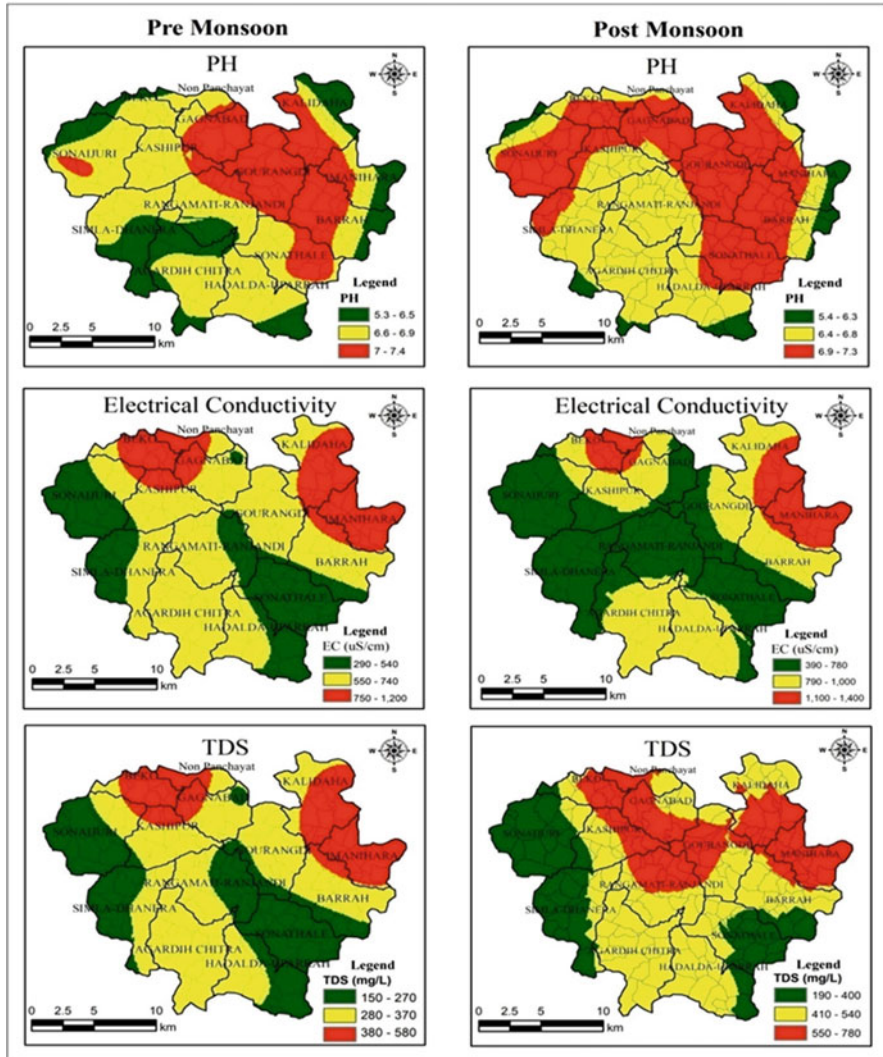


Fig. 6.3 Physio-chemical parameters (pH, EC, and TDS) zonation using ordinary kriging method

western, southern, and few villages of north, eastern, central locations (e.g., villages of Sonajuri, Beko, Kashipur, Gagnabad, Rangamati-Ranjandi, Simla-Dhanara, Agardih-Chitra, Hadalda-Uparrah, Sonathale, Barrah, Manihara, and Kaliada) shows their pH values in moderate condition. Some villages of south-western, north-eastern, and eastern fringe of Kashipur block, few villages of Simla-Dhanara, Sonajuri, Beko, Kaliada, Manihara, Barrah and Hadalda-Uparrah show low concentration of pH in their groundwater samples in pre-monsoon season. On the other hand, most of the villages of Kashipur block were located in eastern, northern, north-

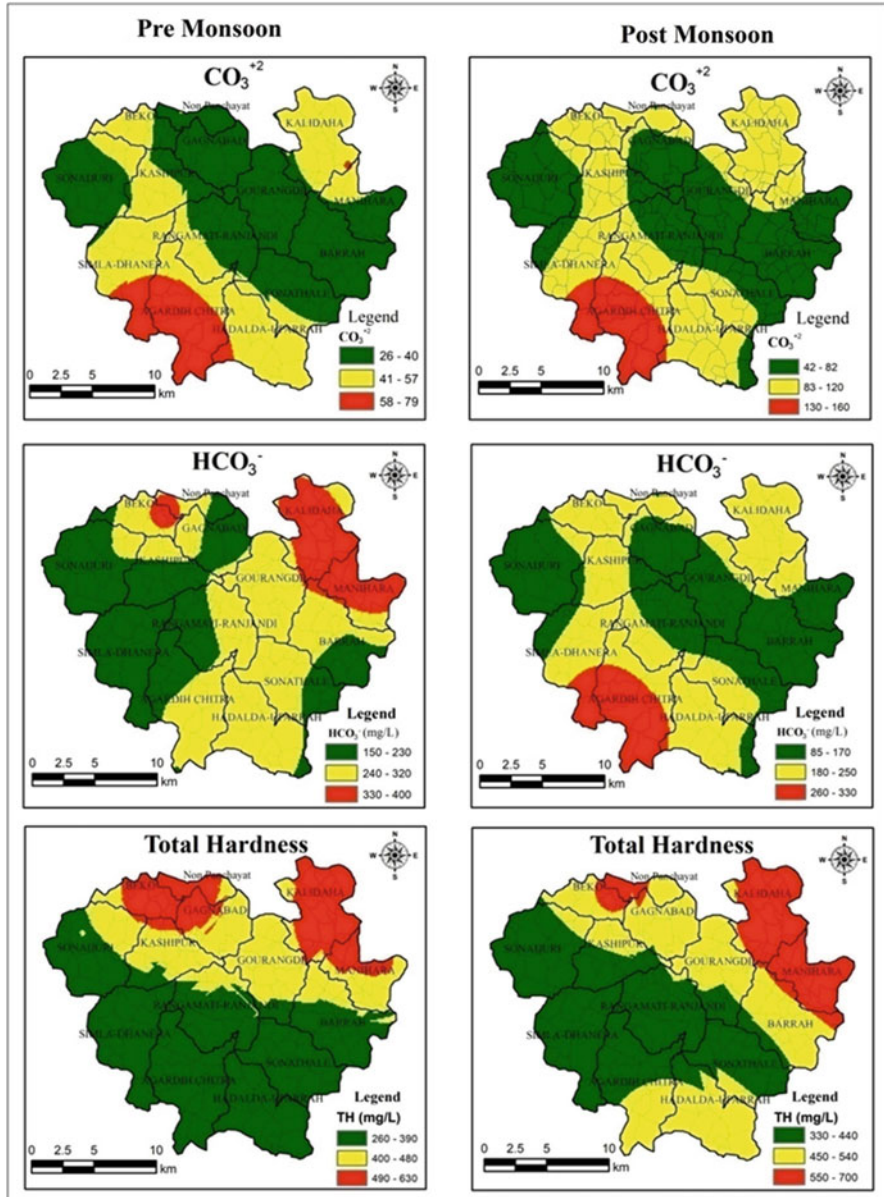


Fig. 6.4 Physio-chemical parameters (CO_3 , HCO_3 , and total hardness) zonation using ordinary kriging method

eastern, and western parts of the villages of Sonajuri, Beko, Gagnabad, Gourangdi, Barrah, Sonathale, Manihara, and Kaliada GP and are affected in the high concentration of pH. Other wide parts of central, southern, and few villages of eastern and

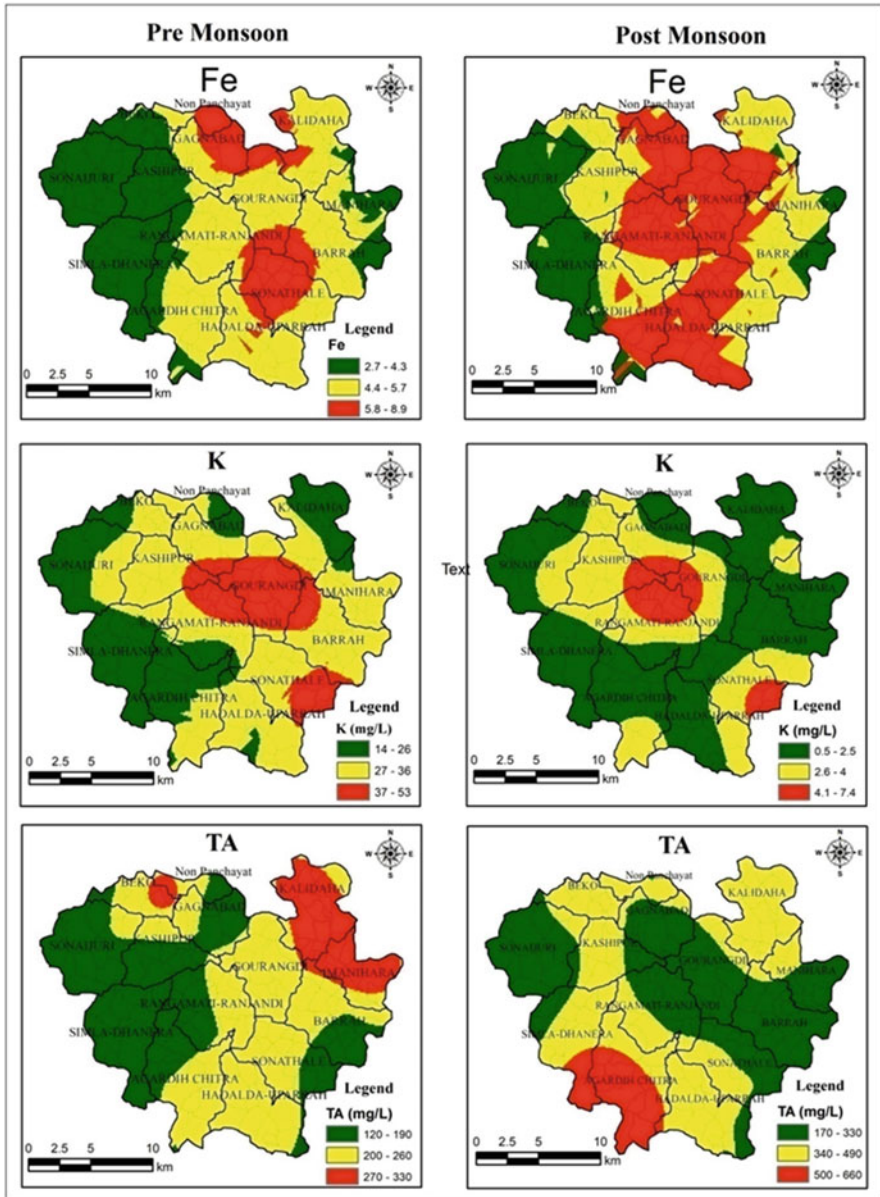


Fig. 6.5 Physico-chemical parameters (Fe, K, and TA) zonation using ordinary kriging method

north-western parts of various Gram Panchayats such as Kashipur, Rangamati-Ranjandi, Agardih-Chitra, Simla-Dhanara, Hadalda-Uparrah, Sonajuri, Barrah, Manihara, Beko, and Kaliada GP have moderate concentration of pH. Very few villages of this Kashipur block mainly located in fringing parts of eastern, southern,

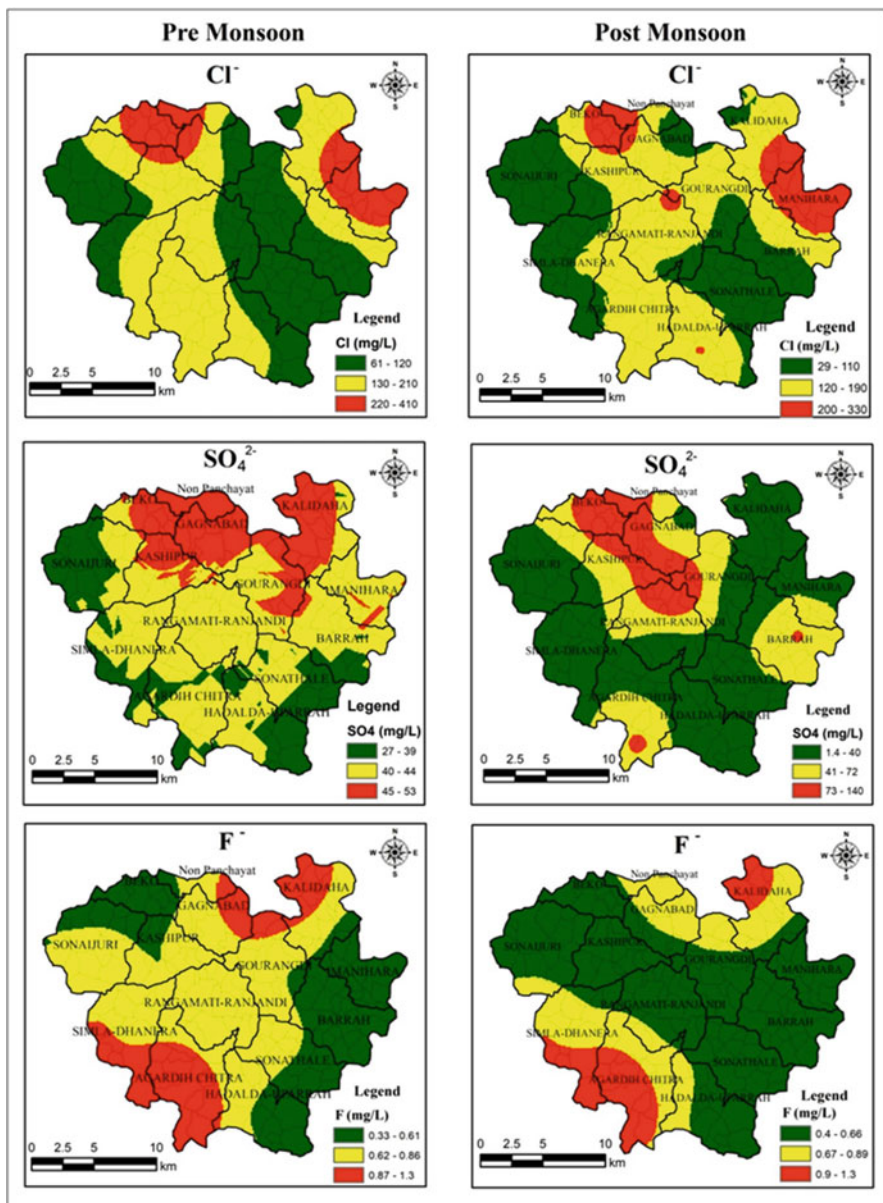


Fig. 6.6 Physico-chemical parameters (Cl, SO₄, and F⁻) zonation using ordinary kriging method

north-western locations (Sonajuri, Simla-Dhanara, Agardih-Chitra, Hadalda-Uparrah, Barrah, Manihara, Kaliada GP) have lower pH values than safe limit in post-monsoon season (Fig. 6.3).

6.4.1.2 TDS

Total dissolved solids (TDS) are directly related to electric conductivity. Mainly animal waste, dumping, and soluble minerals enhance the concentration of TDS in groundwater (Kumar et al. 2014). The range of TDS in post-monsoon season is varying between 130 and 1170 mg/l with average value of 555.76 mg/l and 100–910 mg/l with average value of 350.38 mg/l in pre-monsoon and post-monsoon season, respectively. According to BIS, the safe limit of TDS in water is 500 mg/l. In pre-monsoon season 10 (19.23%) samples are found as higher than safe limit in Kashipur block, and 42 (80.77%) samples are found as below than the standard limit. In the post-monsoon season, 22 (42.30%) water samples lie above the permissible limit, and 30 (57.69%) water samples lie below the permissible limit in the study area. It is clearly identified that high mixing of polluted water with the groundwater in the rainy season increases the concentration of TDS in the post-monsoon season. In the pre-monsoon season, kriging shows some part of the northern region and some part of the eastern region of Kashipur block (many villages of Kaliada, Manihara, Beko, Gagnabad, Kashipur GP) have groundwater with high TDS particles. In this season, mostly the central and southern parts of this block (villages of Kashipur, Gagnabad, Sonajuri, Simla-Dhanara, Rangamati-Ranjandi, Agardih-Chitra, Hadalda-Uparrah, Barrah, Gourangdi, Kaliada, GP) fall under the medium concentration of TDS. Subsequently, the western and south eastern parts of Kashipur block (i.e., the villages of Sonajuri, Simla-Dhanara, Agardih-Chitra, Sonathale GP) and Kuardi village of Gagnabad GP have lower concentration of TDS in their groundwater samples. In the post-monsoon season, some villages of the northern, eastern, and central regions (Beko, Gagnabad, Kashipur, Gourangdi, Rangamati-Ranjandi, Manihara, and Kaliada GP) show high values of TDS in their groundwater sample. Most of the samples collected from southern and some pockets of northern and eastern parts (Beko, Kashipur, Rangamati-Ranjandi, Agardih-Chitra, Hadalda-Uparrah, Sonathale, Gourangdi, Kaliada, Gagnabad GP) of Kashipur block indicate moderate concentration of TDS in water samples. Few villages of western and south-eastern location (Sonajuri, Simla-Dhanara, Sonathale, Hadalda-Uparrah GP) lie under low concentration of groundwater TDS in Kashipur block in post-monsoon season (Fig. 6.3).

6.4.1.3 EC

BIS identified as 730 μ s/cm of electric conductivity is the standard limit for drinking purpose of groundwater. In the pre-monsoon and post-monsoon season, the values range from 200 to 1820 μ s/cm and 260 to 2210 μ s/cm, respectively. The average value of EC in pre-monsoon and post-monsoon season is calculated as 700.19 μ s/cm and 976.34 μ s/cm, respectively. 37 (71.15%) samples are found beyond the permissible limit, and 15 (28.84%) samples lie under the limit which are safe for drinking purpose in post-monsoon season. On the other hand, 14 (26.92%) samples are higher

than the BIS limit, and 38 (73.07%) samples fall under the limit in the pre-monsoon season. In the pre-monsoon season, the spatial distribution of EC by kriging shows about the same pattern as TDS. In pre-monsoon season some villages of north and north-eastern parts (Beko, Gagnabad, Manihara, Kaliada GP) show higher concentration of EC in water samples (Fig. 6.3). Most of the villages under Kashipur block which are located mainly in northern, central, southern, and eastern locations (Rangamati- Ranjandi, Simla-Dhanara, Agardih-Chitra, Barrah, Gourangdi, Kaliada GP) indicate moderate concentration of EC, and some parts of western, south-eastern locations (villages of Sonajuri, Simla-Dhanara, Rangamati-Ranjandi, Sonathale, Agardih-Chitra GP) and Kuardi village of Gagnabad GP have low concentration of EC in pre-monsoon season. In the post-monsoon season, the spatial distribution of high EC concentration in groundwater shows quite the same as pre-monsoon season. The moderate concentration of EC is distributed in various parts of south, north-eastern, eastern, and northern areas (Beko, Kashipur, Gagnabad, Kaliada, Gourangdi, Barrah, Agardih-Chitra, Hadalda-Uparrah GP) of Kashipur block. However, the distribution of low concentration of EC spread continues over northern, central, western, and south-eastern areas (villages of Sonajuri, Simla-Dhanara, Rangamati-Ranjandi, Sonathale, Barrah, Gourangdi, Gagnabad GP).

6.4.1.4 TA

Total alkalinity (TA) is measured for showing the power of water to neutralize strong acid. Pipe lines and dumping waste are the main sources of alkalinity in the study area. 200 mg/l is the permissible limit for TA in drinking water (BIS 2012). TA value ranges between 130 and 750 mg/l with an average of 395.21 mg/l in pre-monsoon season. In the post-monsoon season, estimated TA values range between 134 and 938.2 mg/l, with an average of 433.95 mg/l in the study. In the Kashipur block 43 (82.69%) samples are higher than standard value for drinking and irrigation purpose, and 9 (17.30%) samples lie under the permissible limit in pre-monsoon season. In the post-monsoon season 38 (73.07%) samples are higher than standard value, and 14 (26.92%) are lower than permissible value. If the value of TA increases than 60 mg/l, then the water becomes hard. The spatial distribution (OK) of TA shows that the eastern parts (villages of Kaliada, Manihara GP) are more affected by a high amount of TA in the pre-monsoon season. Few villages of Beko GP also show high concentration of TA in the Kashipur block. Moderate range of TA is concentrated in central, northern, and eastern portions (villages of Gourangdi, Rangamati-Ranjandi, Barrah, Sonathale, Agardih-Chitra, Kashipur, Beko GP) . Most of the western side and a small portion of south-eastern side of Kashipur block (Sonajuri, Simla-Dhanara, Rangamati-Ranjandi, Sonathale, Barrah GP) and some villages of Gagnabad GP located in the north side show low amount of TA concentration . In the post-monsoon season, kriging shows only the south-western part of Kashipur block (villages of Agardih-Chitra and Simla-Dhanara GP) which shows high concentration of TA . Villages in central part and northern part (Beko, Kashipur, Simla-Dhanara, Rangamati-Ranjandi, Agardih-Chitra, Sonathale, Manihara, Kaliada, Gagnabad GP)

indicate moderate concentration of TA in water samples. Some villages of western and central and south-eastern parts (Sonajuri, Gagnabad, Sonathale, Manihara, Rangamati-Ranjandi, Manihara, Gourangdi GP) have low concentration of TA (Fig. 6.5).

6.4.1.5 TH

Total hardness (TH) is the concentration of calcium and magnesium which is supplied to the groundwater by leaching process. It reduces by the cleansing power of soap. In pre-monsoon season, the estimated TH values in the study area range between 100.9 and 1435.2 mg/l with an average value of 504.08 mg/l. In the post-monsoon season, the TH value varies between 146.3 and 1265.6 mg/l with an average of 2.04 mg/l. 200 mg/l is the permissible limit of TH as per BIS (2012) standard. In the pre-monsoon season, 40 (76.92%) samples fall above the permissible limit, and 12 (23.07%) samples fall below the permissible limit. 44 (84.61%) samples are higher than the permissible value, and 8 (15.38%) samples are lower than the permissible value in Kashipur block. The spatial map shows the distribution of high values of TH is located in north and north-eastern sections (villages of Beko, Gagnabad, Kaliada, Manihara GP) of Kashipur block in pre-monsoon season (Fig. 6.4). In this season, moderate concentration of TH is found in a longitudinal section spread from west to east (villages of Sonajuri, Kashipur, Gourangdi, Gagnabad, Manihara, Barraha, GP) of the Kashipur block. Entire villages of southern part (Sonajuri, Simla-Dhanara, Agardih-Chitra, Sonathale, Hadalda-Uparraha, Rangamati-Ranjandi, Barraha GP) extending from east to west of the Kashipur block show low concentration of TH of their spatial distribution in pre-monsoon season. In the post-monsoon season, the spatial distribution of high concentration is more or less same as the pre-monsoon period. The extreme southern part (Hadalda-Uparraha, Agardih-Chitra GP) and a linear patch from north-west to north-east (Beko, Gagnabad, Kashipur, Gourangdi, Barraha, GP) of Kashipur block show medium values of TH. Subsequently, the western and central area of the Kashipur block shows low concentration of TH (Sonajuri, Simla-Dhanara, Agardih-Chitra, Sonathale, Rangamati-Ranjandi GP) in post-monsoon season.

6.4.1.6 Ca and Mg

Two most important cations which affect the water quality are calcium (Ca) and magnesium (Mg). The main cause of calcium contamination with groundwater is the limestone especially crystalline and feldspars (Hem 1991; Todd 1980). Traditional activities of agriculture may also help increase calcium contamination in groundwater (Bohlke 2002). In the pre-monsoon season, the Ca varies from 21.84 to 387.4 mg/l with an average value of 100.94 mg/l. In the post-monsoon season, the Ca varies from 11.76 to 288.96 mg/l with an average value of 97.88 mg/l. According to BIS standard (2012), the upper limit of Ca should not be exceeding 75 mg/l. In our study

area, 32 (61.54%) samples of Ca crossed the boundary limit, and 20 (38.46%) samples lie under the safe zone in pre-monsoon season.

Weathered minerals such as dolomite, hornblende, and mica are the influential source of magnesium in the groundwater (Nag and Suchetana, 2016). It decreases the power of the detergent. The magnesium in pre-monsoon varies from 3.1 to 166.72 mg/l, with an average concentration of 61.79 mg/l. In the post-monsoon season, the value of Mg is varied between 16.61 and 159.63 mg/l with an average of 60.66 mg/l. BIS set the upper limit of magnesium as 30 mg/l. Our results suggest that 43 (82.69%) groundwater samples exceed the highest limit and only 9 (17.30%) samples come under the safe limit in both the pre-monsoon and post-monsoon season.

6.4.1.7 Na and K

Sodium (Na) and potassium (K) are important cations of groundwater among all those components. Excess intake of sodium may increase kidney problems, heart disease, etc. (Kundu and Nag, 2018). Feldspars evaporate the sodium bearing minerals (Kundu and Nag, 2018). According to BIS, the maximum permissible limit of sodium is 200 mg/l. In the post-monsoon season, the concentration of sodium in groundwater varies from 14 to 104 mg/l with an average value of 68.84 mg/l. On the other hand, the concentration of sodium varies from 9 to 56 mg/l, with an average of 32.44 mg/l in the pre-monsoon. In the Kashipur block, all these samples are within the permissible limit in both pre-monsoon and post-monsoon season (Fig. 6.5).

Potassium (K) is a very vital nutrient for human growth as it control muscles and normalizes blood pressure. BIS set the upper limit of K as 10 mg/l in pre-monsoon season, and the concentration of K varies from 9 to 63 mg/l with a mean value of 28.48 mg/l. In the study area, 51 (98.07%) samples exceed the highest limit, and only one sample (1.92%) lies under the permissible limit in pre-monsoon season. In the post-monsoon, the value ranges from 0.5 to 7.4 mg/l with an average value of 2.92 mg/l. In this season, all samples are within the safe limit. The spatial distribution map derived through kriging shows high concentrations of K are found in the central and south-east (villages of Gourangdi, Rangamati-Ranjandi, Barrah, Sonathale GP) of Kashipur block. The moderate values of K are found in eastern, southern, northern, and central parts (Beko, Sonajuri, Kashipur, Rangamati-Ranjandi, Sonathale, Hadalda-Uparrah, Barrah, Manihara, Gagnabad GP) of this block, and low values are found in some areas of western and north-eastern parts (Sonajuri, Simla-Dhanara, Agardih-Chitra, Beko, Kaliada, Gagnabad GP) in pre-monsoon season. In the post-monsoon season, high concentration is found in central and south-eastern parts (villages of Rangamati-Ranjandi, Gourangdi, Kashipur, Gagnabad, Sonathale GP) of this study area. Moderate concentrations of K are found in some areas of northern, central, eastern, and southern parts (villages of Beko, Kashipur, Rangamati-Ranjandi, Gourangdi, Gagnabad, Sonathale, Hadalda-Uparrah, Agardih-Chitra GP) of Kashipur block. Subsequently, the low

concentration of K in the post-monsoon season is distributed in western, eastern, north-eastern, and southern regions (villages of Beko, Sonajuri, Simla-Dhanara, Agardih-Chitra, Sonathale, Hadalda-Uparrah, Barrah, Manihara, Kaliada, Gagnabad, Gourangdi GP) at Kashipur block.

6.4.1.8 Cl and CO₃

Chloride (Cl) generally occurred from weathered sedimentary rocks and leaching of salts. Saline water is created due to a mixture of sodium (Na) and Cl minerals. The concentration of Cl in the post-monsoon ranges from 10 to 374.88 mg/l with an average of 147.49 mg/l. In the pre-monsoon season, the calculated value of Cl varies from 59.98 to 414.87 mg/l with an average of 203.58 mg/l. The permissible limit of Cl is 250 mg/l set by BIS (2012). In Kashipur block 18 (34.00%) samples crossed the limit of Cl, and another 34 (65.38%) samples fall under the safe limit in pre-monsoon season. Otherwise, 11 (21.15%) samples fall above the safe limit, and 41 (78.84%) samples are under the safe limit in the post-monsoon season.

High concentrations of Cl⁻ are found in north and eastern parts (villages of Beko, Gagnabad, Kashipur, Kaliada, Manihara GP) of Kashipur block in pre-monsoon season. Moderate concentrations of Cl are shown in southern, small pockets of north-eastern, eastern, and northern regions (Beko, Kashipur, Rangamati-Ranjandi, Gagnabad, Simla-Dhanara, Agardih-Chitra, Hadalda-Uparrah, Sonathale, Kaliada, Barrah, Manihara GP) of Kashipur block, and low values are found in western (Sonajuri, Simla-Dhanara GP) and central parts along with north-south direction (Gourangdi, Gagnabad, Rangamati-Ranjandi, Barrah, Sonathale, Hadalda-Uparrah GP) and Lohat village of Kaliada GP in pre-monsoon season. On the other hand, high concentration of Cl⁻ are found in small parts of north, east, and central regions (villages of Beko, Kashipur, Manihara, Kaliada, Rangamati-Ranjandi GP) in post-monsoon season of Kashipur block. A vast area of central, southern, and some parts of north-eastern, northern, and eastern regions indicates moderate concentration of Cl ion in groundwater samples. Regions of west, south-east, and northern parts of Kashipur block show lower value of Cl⁻ in water sample.

High concentrations of CO₃ are found in the south-western part (Agardih-Chitra, Simla-Dhanara GP) of Kashipur block. The moderate concentrations of CO₃ are found in southern, western, north-western, and north-eastern areas (Simla-Dhanara, Rangamati-Ranjandi, Beko, Kaliada, Kashipur, Agardih-Chitra GP), and low concentrations are found in western, northern, central, and eastern parts (Beko, Gagnabad, Sonajuri, Kashipur, Gourangdi, Rangamati-Ranjandi, Sonathale, Barrah, Manihara GP) in pre-monsoon season. The spatial distribution of CO₃ is about the same as pre-monsoon period in the study block.

6.4.1.9 HCO_3^- , SO_4 , and F^-

The concentrations of bicarbonate (HCO_3^-), sulfate (SO_4), and fluoride (F^-) are collected as 146.4–402.6 mg/l, 5.15–143.44 mg/l, and 0.24–1.69 mg/l, respectively. In the pre-monsoon season, the calculated average values of HCO_3^- , SO_4 , and F^- are 271.68 mg/l, 49.99 mg/l, and 0.81 mg/l, respectively. The value of HCO_3^- , SO_4 , and F^- ranges between 73.2 and 478 mg/l, 1.14 and 143.09 mg/l, and 0.25 and 2.05 mg/l in the post-monsoon season. The estimated average values of HCO_3^- , SO_4 , and F^- are recorded as 216.47 mg/l, 46.97 mg/l, and 0.96 mg/l, respectively, in the post-monsoon in Kashipur block. The standard limit of HCO_3^- is 300 mg/l, and 19 (36.53%) samples are beyond the critical limit in the pre-monsoon season, and 33 (63.46%) samples are under the safe limit set by BIS. 12 (23.07%) samples exceed the critical limit, and 40 (76.92%) samples are under the safe limit in the post-monsoon season. The upper limit of SO_4 is 150 mg/l. In the study area, all the samples are under the safe limit according to BIS in both pre- and post-monsoon season.

Fluoride is a very essential element for strong teeth and bones. But the excess concentration of it causes harm to humans. The upper limit of F^- is 1.5 mg/l. In Kashipur block 4 (7.69%) samples exceed fluoride contamination, and 48 (92.30%) samples are under the safe limit in the pre-monsoon season. 13 (25%) samples are higher than the safe limit, and 39 (75.00%) samples are shown below the safe limit in the post-monsoon season. The spatial distribution map shows high values of HCO_3^- are portrayed in the north-eastern region (Kaliada, Manihara GP) and some villages of Beko GP in pre-monsoon season. Moderate concentration of HCO_3^- is noticed in central and southern Gourangdi, Rangamati-Ranjandi, Agardih-Chitra, Hadalda-Uparrah, and Sonathale GP and few parts of northern and eastern regions (Beko, Kashipur, Gagnabad, Barrah, Manihara GP) of the study area. Low values of HCO_3^- are found in western part and eastern part (villages of Sonajuri, Simla-Dhanara, Rangamati-Ranjandi, Kashipur, Sonathale, Barrah GP) of Kashipur block in pre-monsoon season. In post-monsoon season, high concentrations of HCO_3^- are found in south-western part of Kashipur block (villages of Simla-Dhanara, Agardih-Chitra GP). Moderate concentrations of HCO_3^- are shown in northern, central, and southern parts of this block (Beko, Kashipur, Rangamati-Ranjandi, Simla-Dhanara, Hadalda-Uparrah, Sonathale, Kaliada, Manihara GP), and lower values of HCO_3^- are found in western, central, and eastern parts (villages of Sonajuri, Gagnabad, Rangamati-Ranjandi, Barrah, Sonathale, Manihara, Gourangdi GP) of Kashipur block in post-monsoon season (Fig. 6.6).

High concentration of SO_4 is found in the northern part (villages of Beko, Gagnabad, Kashipur, Gourangdi, Kaliada GP) of Kashipur block in pre-monsoon season. The entire central and eastern, western, southern areas (Rangamati-Ranjandi, Sonajuri, Simla-Dhanara, Sonathale, Barrah, Manihara, Gourangdi GP) indicate moderate concentration of SO_4 , and parts of western, south-west, and south-eastern regions (Sonajuri, Simla-Dhanara, Hadalda-Uparrah, Sonathale GP) indicate lower concentration of SO_4 in the pre monsoon season. In the post-monsoon season, high

values of SO_4 are found in north-western part (Beko, Kashipur, Rangamati-Ranjandi, Gourangdi, Gagnabad GP), Sirjam village of Barrah GP, and Pabra Pahari village of Agardih-Chitra GP of Kashipur block. Moderate concentrations of SO_4 are found in eastern, south-western, and central parts of this block (Barrah, Agardih-Chitra, Rangamati-Ranjandi, Kashipur, Sonajuri, Gourangdi GP), and low values of SO_4 are found in western, south-eastern, and north-eastern parts (some villages of Sonajuri, Simla-Dhanara, Agardih-Chitra, Sonathale, Manihara, Kaliada, Barrah GP) of Kashipur block.

The spatial distribution map shows the concentration of F^- higher in north-eastern and south-western parts (villages Of Gagnabad, Gourangdi, Kaliada, Simla-Dhanara, Agardih-Chitra GP) of the Kashipur block in pre-monsoon season. The entire central and some parts of west, south, north, and north-east indicate moderate values of fluoride concentration in this Kashipur block. The low concentrations of F^- are found in north-western and south-eastern parts (villages of Sonajuri, Beko, Kashipur, Hadalda-Uparrah, Sonathale, Barrah, Manihara GP) of the study area in pre-monsoon period. On the other hand, high concentrations of F^- are found in few parts of north-eastern and south-western regions (villages of Kaliada, Simla-Dhanara, Agardih-Chitra GP) in the Kashipur block in post-monsoon season. Moderate concentrations are found in two crescentic shape area located southwest and northeast (villages of Simla-Dhanara, Agardih-Chitra, Hadalda-Uparrah GP And Gagnabad, Gourangdi, Kaliada GP) in Kashipur block. Low concentrations of F^- are found in north-west and east (villages of Sonajuri, Beko, Kashipur, Gagnabad, Gourangdi, Rangamati-Ranjandi, Hadalda-Uparrah, Sonathale, Barrah, Manihara GP) in pre-monsoon season.

6.4.2 Statistical Analysis

The descriptive statistics of physico-chemical parameters in pre-monsoon and post-monsoon seasons are illustrated in Tables 6.3 and 6.4, respectively. In this analysis, it is found that except pH, Na, and SO_4 , all other parameters have maximum values than the permissible limit in the pre-monsoon season. As such, except Na and SO_4 all other parameters have the maximum values than the safe limit of drinking and irrigational water in the post-monsoon season. The mean values of EC, TA, TH, Ca, Mg, Fe, and K are higher than the upper limit of drinking water. Thus, it is clearly understood that the most samples of those parameters lie under the unsafe quality of groundwater in the pre-monsoon season. In the post-monsoon season, the mean values of TDS, EC, TA, TH, Ca, and Mg lie above the permissible limit, according to BIS.

The correlation analysis for pre- and post-monsoon season groundwater quality parameters is presented in Tables 6.5 and 6.6, respectively. In the study area, pH has negative correlation with TDS, EC, TA, TH, Na^+ , Ca^{2+} , Mg^{2+} , CO_3^{2+} , HCO_3^- , and SO_4^{2-} and positive relation with Fe, K^+ , Cl, and F^- in the pre-monsoon season. TDS is highly correlated (regression value greater than 0.5) with EC, TH, Ca, Mg, HCO_3^- ,

Table 6.3 Descriptive statistics of pre-monsoon season of Kashipur block

	pH	TDS	EC	TA	TH	Na+	Ca ²⁺	Mg ²⁺	Fe	K+	CO ₃ ²⁻	HCO ₃	Cl-	SO ₄	F-
Mean	6.89	350.38	700.19	395.21	504.09	32.44	100.94	61.79	4.03	28.48	49.27	271.68	203.59	49.99	0.82
Standard error	0.06	27.87	53.48	23.75	46.32	1.43	11.85	5.73	0.35	1.83	4.43	10.17	16.04	4.02	0.06
Median	6.84	305	635	352	417.7	32	78	51.44	3.34	25	44.5	269.65	161.8	50.64	0.72
Mode	6.84	340	660	254	#N/A	40	55.44	#N/A	3.24	15	28	219.6	59.98	48.2	1.24
Standard deviation	0.4	201.01	385.66	171.27	334	10.28	85.42	41.3	2.53	13.19	31.94	73.36	115.7	28.96	0.43
Sample variance	0.16	40403.77	148731.33	29333.82	111558.4	105.7	7296.95	1705.68	6.39	173.94	1020.4	5381	13385.8	838.86	0.18
Kurtosis	-0.22	1.17	1.69	-0.65	1.24	-0.36	2.49	1.08	7.84	0.81	0.51	-1	-1.21	1.72	-0.95
Skewness	0.49	1.3	1.39	0.45	1.33	0.1	1.81	1.34	2.73	1.06	0.91	0.03	0.49	0.88	0.51
Range	1.79	810	1620	624	1334.3	47	365.56	163.62	13.59	54	136	256.2	354.89	138.29	1.45
Minimum	6.15	100	200	130	100.9	9	21.84	3.1	0.7	9	0	146.4	59.98	5.15	0.24
Maximum	7.94	910	1820	754	1435.2	56	387.4	166.72	14.29	63	136	402.6	414.87	143.44	1.69
Sum	358.14	18,220	36,410	20,551	26212.5	1687	5249.04	3213.24	209.72	1481	2562	14127.4	10586.48	2599.67	42.56

Table 6.4 Descriptive statistics of post-monsoon season of Kashipur block

	pH	TDS	EC	TA	TH	Na+	Ca ²⁺	Mg ²⁺	Fe	K+	CO ₃ + 2	HCO ₃	Cl-	SO ₄	F-
Mean	6.76	555.77	976.35	433.96	561.09	68.85	97.89	60.67	2.05	2.93	79.54	216.47	147.50	46.98	0.97
Standard error	0.04	41.71	70.08	36.17	43.53	3.13	8.40	4.58	0.18	0.21	5.64	15.15	15.54	5.02	0.08
Median	6.71	465.00	865.00	375.10	467.40	73.50	88.20	53.75	1.63	2.55	69.00	176.90	97.78	36.27	0.78
Mode	6.58	450.00	760.00	145.20	#N/A	98.00	57.12	64.20	1.19	2.50	84.00	73.20	64.98	8.47	1.74
Standard deviation	0.28	300.75	505.33	260.84	313.93	22.55	60.61	33.06	1.32	1.54	40.68	109.25	112.04	36.20	0.56
Sample variance	0.08	90452.34	255356.98	68039.33	98553.14	508.45	3673.21	1093.04	1.73	2.38	1655.12	11935.79	12553.79	1310.34	0.32
Kurtosis	-0.56	-0.99	-0.14	-0.58	-0.68	-0.29	0.88	1.25	0.25	0.14	2.25	-0.87	-0.83	0.18	-1.13
Skewness	0.48	0.39	0.70	0.79	0.58	-0.58	0.94	1.15	1.08	0.73	1.50	0.50	0.74	0.86	0.52
Range	1.11	1040.00	1950.00	849.20	1119.30	90.00	277.20	143.02	4.98	6.90	187.00	404.80	364.88	141.95	1.80
Minimum	6.24	130.00	260.00	134.00	146.30	14.00	11.76	16.61	0.28	0.50	17.00	73.20	10.00	1.14	0.25
Maximum	7.35	1170.00	2210.00	983.20	1265.60	104.00	288.96	159.63	5.26	7.40	204.00	478.00	374.88	143.09	2.05
Sum	351.29	28900.00	50770.00	22565.80	29176.90	3580.00	5090.18	3154.62	106.40	152.30	4136.00	11256.60	7669.77	2442.94	50.39

Table 6.5 Correlation matrix of pre-monsoon season

	pH	TDS	EC	TA	TH	Na ⁺	Ca ²⁺	Mg ²⁺	Fe	K ⁺	CO ₃ ²⁺	HCO ₃ ²⁻	Cl ⁻	SO ₄ ²⁻	F ⁻
pH	1.00														
TDS	-0.09	1.00													
EC	-0.11	0.99	1.00												
TA	0.00	0.15	0.16	1.00											
TH	-0.07	0.97	0.97	0.19	1.00										
Na ⁺	-0.45	0.39	0.43	0.04	0.34	1.00									
Ca ²⁺	-0.32	0.63	0.64	0.30	0.72	0.28	1.00								
Mg ²⁺	-0.17	0.92	0.92	0.15	0.93	0.30	0.74	1.00							
Fe	0.09	-0.29	-0.29	-0.03	-0.33	-0.12	-0.27	-0.32	1.00						
K ⁺	0.18	-0.05	-0.03	0.15	-0.03	-0.12	0.03	-0.06	-0.09	1.00					
CO ₃ ²⁻	-0.12	0.24	0.26	0.23	0.23	0.23	0.17	0.24	-0.12	-0.02	1.00				
HCO ₃	-0.02	0.54	0.54	0.30	0.49	0.16	0.35	0.48	-0.17	0.11	0.13	1.00			
Cl ⁻	0.14	0.25	0.27	0.20	0.24	0.16	0.09	0.24	-0.37	-0.24	0.14	0.12	1.00		
SO ₄ ²⁻	-0.13	0.51	0.50	0.29	0.52	0.36	0.59	0.51	-0.26	-0.05	0.18	0.32	0.51	1.00	
F ⁻	0.19	-0.21	-0.21	0.17	-0.17	-0.13	-0.09	-0.20	0.08	-0.10	0.20	-0.21	0.16	0.07	1.00

Table 6.6 Correlation matrix of post-monsoon season

	pH	TDS	EC	TA	TH	Na+	Ca ²⁺	Mg ²⁺	Fe	K+	CO ₃ ²⁺	HCO ₃ ²⁻	Cl ⁻	SO ₄ ²⁻	F ⁻
pH	1.00														
TDS	-0.43	1.00													
EC	-0.29	0.82	1.00												
TA	-0.12	-0.05	-0.11	1.00											
TH	-0.37	0.89	0.84	0.05	1.00										
Na ⁺	-0.36	0.78	0.68	0.12	0.70	1.00									
Ca ²⁺	-0.30	0.59	0.56	0.36	0.69	0.54	1.00								
Mg ²⁺	0.01	0.45	0.52	-0.05	0.51	0.32	0.34	1.00							
Fe	0.12	-0.12	-0.27	0.20	-0.07	0.02	0.07	-0.35	1.00						
K ⁺	0.12	0.19	-0.03	0.02	0.13	0.19	0.06	-0.04	0.02	1.00					
CO ₃ ²⁻	-0.11	-0.13	-0.01	0.31	-0.03	0.11	0.09	0.00	-0.11	-0.15	1.00				
HCO ₃	-0.30	0.25	0.23	0.34	0.24	0.27	0.02	0.06	0.07	0.06	0.26	1.00			
Cl ⁻	-0.16	0.62	0.64	-0.21	0.56	0.41	0.32	0.61	-0.38	0.13	0.04	0.14	1.00		
SO ₄ ²⁻	-0.20	0.44	0.26	0.15	0.29	0.51	0.37	0.20	-0.12	0.26	0.09	0.22	0.22	1.00	
F ⁻	-0.13	0.05	-0.04	0.27	0.09	0.07	0.12	-0.27	0.26	0.27	0.01	0.32	-0.04	-0.06	1.00

and SO_4 . Total hardness (TH) is highly correlated to Ca^{2+} , Mg^{2+} , and SO_4 . Concentration of CO_2 is positively related with Mg^{2+} , SO_4^{2-} , K^+ , HCO_3 , and Cl . Mg and Cl have very strong positive correlation with SO_4 in the pre-monsoon season. In the post-monsoon season, pH has positive correlation with TA, Mg^{2+} , Fe, and K^+ . TDS is strongly correlated with EC, TH, Na^+ , Ca, and Cl. TH values are highly influenced by Na^+ , Ca^+ , Mg^{2+} , and Cl^- . Sodium is positively correlated with calcium ($r = 0.54$). Magnesium is positively correlated with Cl values in Kashipur block in post-monsoon season.

6.4.3 Irrigation Water Quality Assessment

Saline or alkaline quality of water determines the agricultural production of an area. Assessment of the overall quality of water used in agriculture for irrigation purpose are derived by certain indicators, namely, SAR, SSP, MAR, and KR (Obeifuna and Sheriff 2011). The calculated parameters are shown in Tables 6.7 and 6.8.

6.4.3.1 Sodium Adsorption Ration (SAR)

The hazard of alkaline water is generally known as sodium adsorption ratio (SAR). Analysis of sodium concentration is necessary for irrigation purpose because it's deformed soil structure and the permeability capacity of water (Todd 1980). The following equation was used to find the SAR values of water quality for irrigation of different GP in Kashipur block (Richards 1954).

$$\text{SAR} = (\text{Na}^+) / \left\{ \frac{[(\text{Ca}^{2+}) + (\text{Mg}^{2+})]}{2} \right\}^{1/2}.$$

All ion concentrations have been defined in mg/l.

High concentration of sodium leads to alkaline type soil which is difficult to crop production. In the study area, the low infiltration capacity of soils makes water to runoff, and thus in dry period of crop production it is very tough without proper irrigation and well drainage system. SAR values are categorized under two sub-groups. Values less than 10 are indicated as suitable, and values greater than 10 are considered as unsuitable. In the present study, village level SAR values range from 1.23 to 9.13 in the pre-monsoon season and varied between 2.27 and 15.89 in post-monsoon season. All SAR values of pre-monsoon seasons are below 10 and all fall under suitable category, and 10 samples of post-monsoon show SAR values higher than 10 (Rugri, Chakalta, Kapistha, Lapara, Lajhna, Jiara, Haridih, Kalapathar, Sirjam, and Rampur) which are highlighted by using Arc GIS treated as unsuitable. The zonation mapping shows that the villages with unsuitable water are distributed scatteredly in the central and eastern region of Kashipur block in post-monsoon season (Fig. 6.7).

Table 6.7 Estimation of irrigation water quality in pre-monsoon season of different blocks in Kashipur

GP	Villages name	SAR	SSP	KR	MAR
Kalidaha	Lohat	4.08	28.63	0.24	40.59
	Kelahi	3.73	26.85	0.22	46.57
	Bhatulkend	3.23	15.64	0.13	55.36
	Indrabil	3.00	23.89	0.17	46.28
Manihara	Manihara	2.76	21.92	0.14	71.49
	Adali	1.96	14.53	0.09	49.15
	Rampur	1.53	14.98	0.08	52.57
	Agrabad	3.76	24.90	0.18	44.39
Barrah	Sirjam	6.91	42.71	0.50	42.59
	Rajra	3.37	40.09	0.27	41.70
	Kadori	5.50	37.31	0.42	49.94
	Paharpur	6.29	42.94	0.52	45.96
Sonathale	Kalapatthar	9.13	61.38	1.04	8.08
	Balarampur	2.76	56.02	0.25	40.08
	Jibanpur	5.92	41.18	0.50	40.86
	Sonathol	4.23	47.85	0.37	39.04
Hadalda-Upparah	Hadalda	2.80	22.42	0.15	37.86
	Kaliada	3.94	21.70	0.16	27.82
	Ichamara	3.01	13.61	0.12	24.29
	Jiara	1.23	7.72	0.04	26.32
Agardih-Chitra	Pabra Pahari	5.78	38.57	0.36	39.01
	Chaka	4.82	37.98	0.34	45.38
	Saharbera	1.87	18.06	0.07	20.59
	Tara	2.31	12.49	0.09	21.36
Simla-Dhanara	Simla	4.77	28.12	0.28	40.26
	Damankiri	5.02	30.04	0.30	43.49
	Liya	4.10	38.62	0.40	39.13
	Shiulibari	5.77	41.81	0.45	56.52
Simla-Dhanara	Rudra	2.99	36.58	0.21	42.19
	Kalyajhor	1.45	23.71	0.12	41.27
	Bhalagara	5.40	61.84	0.61	38.73
	Daldali	6.25	60.85	0.67	29.47
Beko	Jorisha	4.20	25.45	0.23	38.55
	Palaskola	3.66	16.89	0.12	35.67
	Rugri	3.63	15.34	0.12	35.60
	Jibanpur	3.04	14.52	0.10	35.86
Gagnabad	Kuardi	4.27	39.81	0.46	50.18
	Chakalta	5.86	56.63	0.55	50.81
	Dhobari	3.25	33.24	0.21	39.75
	Gagnabad	3.19	28.46	0.21	38.64
Kashipur	Lapara	5.83	45.61	0.44	39.89
	Rangiladi	4.47	37.56	0.32	32.88

(continued)

Table 6.7 (continued)

GP	Villages name	SAR	SSP	KR	MAR
	Sidpur	5.19	38.66	0.34	34.62
	Gopalpur	6.32	35.92	0.42	35.71
Rangamati-Ranjandi	Ranjandi	4.61	29.50	0.30	36.58
	Patpur	3.87	40.23	0.23	37.53
	Tilabani	5.07	32.18	0.31	40.66
	Lajhna	4.55	32.60	0.28	40.89
Gourangdi	Kapistha	4.26	48.99	0.31	40.17
	Talajuri	3.23	37.78	0.19	38.35
	Sutabani	2.86	26.79	0.16	35.16
	Jamkuri	2.44	27.75	0.14	37.74

6.4.3.2 Soluble Sodium Percentage (SSP)

Irrigation water with high concentration of sodium ion is absorbed by clay components in the soil which decreased the porosity of soil and affects the agricultural production (Nag and Das 2017). Thus the soluble sodium percentage is calculated by the following equation:

$$SSP = [(Na^+ + K^+) \times 100] / [Ca^{2+} + Mg^{2+} + Na^+ + K^+]$$

In Kashipur block, the values of SSP range from 7.72 to 61.83 in the pre-monsoon season and from 16.69 to 62.72 in the post-monsoon season. The SSP values which are <50 are indicated “good,” and values >50 are indicated “unsafe” for irrigation purpose (USDA 1954). In the present study, 5 (9.62%) samples of pre-monsoon season (Lohat, Rampur, Manihara, Ichamara, Hadalda) and 4 (7.69%) samples of post-monsoon season (Rampur, Kalapathar, Haridih, Jaira) have SSP values of >50. The details of calculated SSP values are given in Table 6.9. It is clearly observed that concentrations of villages with high SSP values are situated in extreme southern and north-eastern parts of Kashipur block in pre-monsoon season. In the post-monsoon season higher concentrations of SSP values are distributed in south-eastern region (Fig. 6.7).

6.4.3.3 Magnesium Adsorption Ratio (MAR)

Magnesium (Mg) is a very important component for plant growth. But higher concentration of Mg leads to damage of leaves, reduces plant growth, and decreases the crop production. It is calculated by the following equation followed by (Raghunath 1987):

Table 6.8 Estimation of water quality in relation to irrigation in post-monsoon of different blocks in Kashipur

GP	Village name	SAR	SSP	KR	MAR
Kalidaha	Lohat	8.42	34.64	0.52	36.94
	Kelahi	7.19	29.92	0.42	43.17
	Bhatulkend	5.62	18.15	0.21	43.31
	Indrabil	8.01	28.99	0.40	41.17
Manihara	Manihara	8.53	26.30	0.35	53.68
	Adali	6.71	25.34	0.33	23.21
	Rampur	11.17	50.72	1.01	58.12
	Agrabad	7.35	27.61	0.36	33.71
Barrah	Sirjam	10.95	44.40	0.78	42.19
	Rajra	6.72	26.77	0.35	48.13
	Kadori	5.38	20.69	0.25	37.24
	Paharpur	8.53	35.05	0.51	33.77
Sonathale	Kalapatthar	15.89	62.72	1.64	74.95
	Balarampur	5.15	37.11	0.49	45.09
	Jibanpur	7.38	38.98	0.58	64.98
	Sonathol	13.20	52.05	1.03	77.44
Hadalda-Uparrah	Hadalda	6.99	24.27	0.31	38.67
	Kaliada	8.03	30.05	0.41	45.17
	Ichamara	9.37	43.92	0.72	49.88
	Jiara	13.13	53.13	1.05	25.00
Agardih-Chitra	Pabra Pahari	8.47	32.35	0.46	37.67
	Chaka	8.08	31.55	0.43	35.94
	Saharbera	8.37	31.83	0.44	10.14
	Tara	8.49	27.74	0.37	9.54
Simla-Dhanara	Simla	8.93	35.83	0.55	37.21
	Damankiri	9.99	37.67	0.59	37.07
	Liya	6.90	41.97	0.70	34.23
	Shiulibari	4.17	23.25	0.28	69.08
Simla-Dhanara	Rudra	4.92	29.49	0.38	42.45
	Kalyajhor	2.27	16.69	0.18	35.78
	Bhalagara	3.25	19.95	0.21	54.22
	Daldali	4.42	21.54	0.26	66.03
Beko	Jorisha	8.37	34.83	0.52	38.32
	Palaskola	6.75	19.41	0.23	31.44
	Rugri	12.17	43.01	0.73	79.94
	Jibanpur	8.41	26.88	0.36	46.90
Gagnabad	Kuardi	7.07	43.48	0.76	53.70
	Chakalta	10.86	38.53	0.62	11.44
	Dhobari	8.11	34.09	0.51	26.75
	Gagnabad	9.49	35.34	0.54	60.09
Kashipur	Lapara	10.92	44.98	0.78	41.03
	Rangiladi	6.92	30.41	0.41	39.06

(continued)

Table 6.8 (continued)

GP	Village name	SAR	SSP	KR	MAR
Rangamati-Ranjandi	Sidpur	6.39	22.39	0.28	23.52
	Gopalpur	8.92	29.80	0.41	19.54
	Ranjandi	7.28	29.16	0.40	20.32
	Patpur	4.51	24.56	0.31	51.82
	Tilabani	8.42	28.02	0.37	27.14
Gourangdi	Lajhna	10.49	36.68	0.56	24.16
	Kapistha	11.45	41.85	0.67	42.65
	Talajuri	7.69	33.75	0.49	28.21
	Sutabani	5.82	24.72	0.31	43.35
	Jamkuri	7.94	32.60	0.46	38.95

$$\text{MAR} = (\text{Mg}^{2\pm} \times 100) / (\text{Ca}^{2\pm} + \text{Mg}^{2\pm})$$

The concentration of MAR is calculated in mg/l.

The computed MAR values ranged from 8.07 to 71.49 mg/l in the pre-monsoon and 9.54 to 79.94 mg/l in the post-monsoon season. MAR values <50 mg/l are taken as suitable for irrigation, while MAR values of >50 mg/l are considered as unsuitable for irrigation. In the present study, 6 (11.54%) samples of MAR in Kashipur block are >50 in pre-monsoon season (Bhatulkend, Manihara, Rampur, Shiulibari, Kuardi, Chakalta) and are indicated as unsuitable for irrigation. On the other hand, 12 (23.07%) samples in post-monsoon season are >50 mg/l (Manihara, Rampur, Kalapathar, Jibanpur, Sonathol, Shiulibari, Bhalagara, Daldali, Rugri, Kuardi, Gagnabad, Patpur) (Table 6.9). The spatial distribution map shows villages with high MAR values located at northern, eastern, and western parts of the Kashipur block in pre-monsoon season.. In this post-season, spatial distribution map shows that unsafe villages are distributed scatteredly over the Kashipur block. (Fig. 6.8).

6.4.3.4 Kelly's Ratio

This is used to calculate the sodium concentration with respect to Ca and Mg in water (Nag and Das 2017; Kelly 1976) as follows:

$$\text{KR} = \text{Na}^{\pm} / (\text{Ca}^{2\pm} + \text{Mg}^{2\pm})$$

KR value of <1 is taken as suitable for crop production. 99% of the sample value is lower than the safe limit. 48 (92.31%) samples of post-monsoon season are less than the safe limit, and 7.69% of samples (Kalapathar, Haridih, Jaira, Rampur) are >1 in the study area, indicating unsuitable condition for agriculture production (Table 6.9). The spatial mapping shows that only one village (Kalapathar) situated

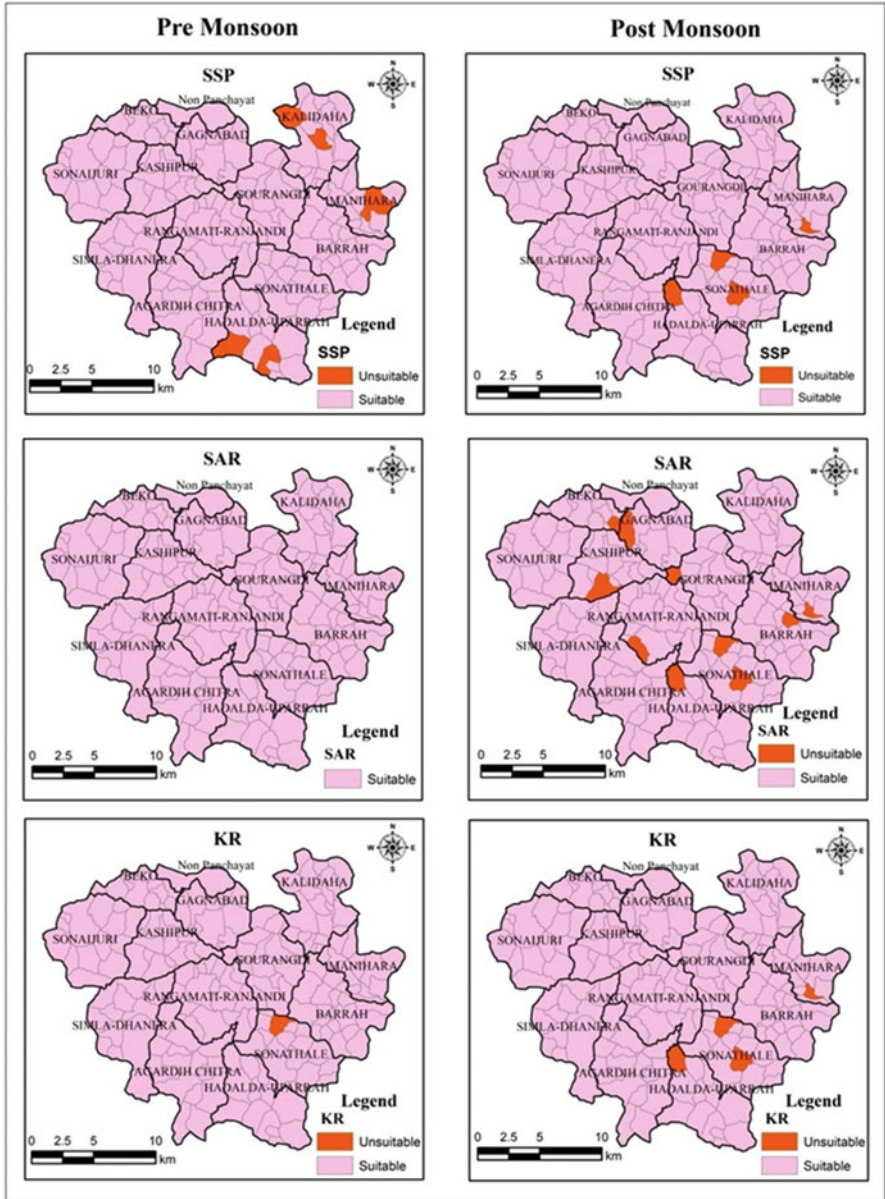


Fig 6.7 Village level irrigation water quality parameters zonation by using ArcGIS software

at south-east location of the study area is affected by higher KR and is indicated as unsuitable for agriculture in pre-monsoon season. In post-monsoon season, the unsafe villages are located in the south-eastern part of Kashipur block (Fig. 6.7).

Table 6.9 Standardized parameters of irrigation water quality classification

Parameters	Range (mg/l)	Category	No. of samples (pre-monsoon)	No. of samples (post-monsoon)
SAR	<10	Suitable	52	42
	>10	Unsuitable	0	10
SSP	<50	Suitable	47	48
	>50	Unsuitable	5	4
KR	<1	Suitable	51	48
	>1	Unsuitable	1	4
MAR	<50	Suitable	46	40
	>50	Unsuitable	6	12

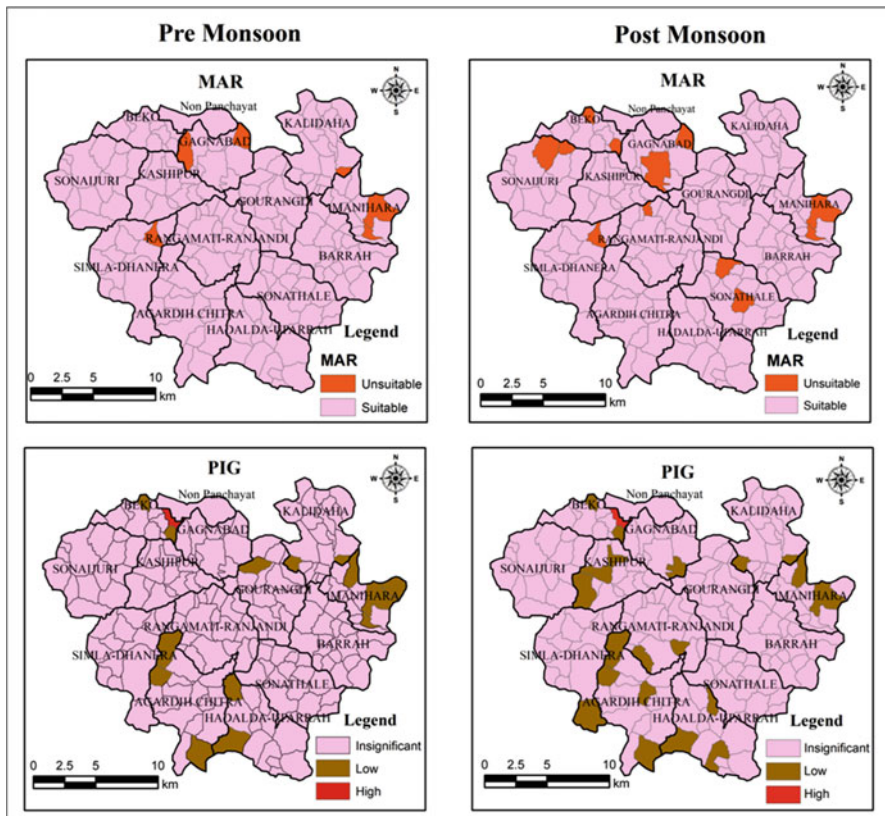


Fig. 6.8 Village level PIG zonation using ArcGIS software

6.4.4 Analysis of Groundwater Pollution Zone by PIG Method

For the assessment of groundwater quality, contribution of each chemical variable was considered to calculate the PIG of each sample. A higher value of PIG indicates greater pollution intensity of groundwater sample. Here, the PIG value was divided into three major divisions, such as (i) <1 as insignificant pollution zone, (ii) $1-1.5$ as low pollution zone, and (iii) >1.5 as high pollution zone (Tables 6.10 and 6.11). In this study area, PIG values range between 0.46 and 1.50, with an average value of 0.85 in the pre-monsoon period. 38 (73.07%) samples scored <1 , and these zones fall under insignificant pollution and which are very safe to drink or for irrigation. 14 (26.92%) samples come under the low pollution zone, and only one sample (Palaskola) is above the value of 1.5 which is a highly polluted zone indicated by PIG method in the pre-monsoon season.

In the post-monsoon season, the PIG values range from 0.38 to 1.38, with an average value of 0.84. About 35 (67.30%) groundwater samples indicate insignificant pollution in Kashipur block with good water quality. 17 (32.69%) groundwater samples indicate low pollution. One sample (Palaskola) shows higher than 1.5. It may be due to dense population with high living standards and effects by sewage runoff from nearby railway settlement colony. Thus, it clearly indicates that groundwater quality of Palaskola village is highly polluted by various anthropogenic sources such as metallic wastes of railway department, liquid sewage of residential settlement, etc. in the soil (Fig. 6.8).

6.4.5 Water Quality Assessment in Relation with Physical Condition of the Study Area

In the present study area, overall water quality has been assessed by the various physico-chemical conditions. The chemical parameters such as pH, TDS, EC, and TH are directly related to high elevation region. Greater elevation indicates highlands with weathered granitic gneissic formation with low to moderate pH in most regions and low elevation with high to moderate pH and TH condition. Weather-resistant rocks supply low amount of TDS and EC to the groundwater, and these resistant rocks produce uplands; thus, elevation with greater values shows low TDS and EC in the water samples of the study area. Fine loamy soils of the study area also indicate low concentration of cations such as CO_3^{2-} , HCO_3^- , and Fe^- in the groundwater samples. Potassium is highly found in the fine loamy to coarse loamy soil zone in the study area. The geogenic condition directly affects the soil formation, and types of rocks and minerals greatly influenced the quality of groundwater and its usability to drinking and irrigation purpose.

Table 6.10 Groundwater Pollution Zones (PIG) classification of different GP of Kashipur block, Purulia district in pre-monsoon season

Insignificant pollution (<1)	Low pollution (1–1.5)	High pollution (>1.5)
Lohat	Bhatulkend	Palaskola
Kelahi	Indrabil	
Sirjam	Manihara	
Rajra	Adali	
Kadori	Rampur	
Paharpur	Agrabad	
Kalapathar	Jiara	
Balarampur	Saharbera	
Jibanpur, Sonathale	Tara	
Sonathol	Rugri	
Hadalda	Jibanpur, beko	
Kaliada	Ichamara	
Bhalagara	Pabra - pahari	
Chaka	Jamkuri	
Simla		
Damankiri		
Liya		
Shiulibari		
Rudra		
Kalyajhor		
Bhalagara		
Daldali		
Jorisha		
Kuardi		
Chakalta		
Dhobari		
Gagnabad		
Lapara		
Rangiladi		
Sidpur		
Gopalpur		
Ranjandi		
Patpur		
Tilabani		
Lajhna		
Kapistha		
Talajuri		
Sutabani		

Table 6.11 Groundwater Pollution Zones (PIG) classification of different GP of Kashipur block, Purulia district in post-monsoon season

Insignificant pollution (<1)	Low pollution (1–1.5)	High pollution (>1.5)
Lohat	Bhatulkend	Palaskola
Kelahi	Indrabil	
Adali	Manihara	
Rampur	Agrabad	
Sirjam	Chaka	
Rajra	Pabra- pahari	
Kadori	Tara	
Paharpur	Damankiri	
Kalapathar	Dhobari	
Balarampur	Rugri	
Jibanpur (Sonathale)	Jibanpur , (beko)	
Sonathol	Tilabani	
Kaliada	Lajhna	
Hadalda	Saharbera	
Ichamara	Rangiladi	
Jiara	Sidpur	
Simla	Gopalpur	
Liya		
Shiulibari		
Rudra		
Kalyajhor		
Bhalagara		
Daldali		
Jorisha		
Kuardi		
Chakalta		
Dhobari		
Gagnabad		
Lapara		
Ranjandi		
Patpur		
Kapistha		
Talajuri		
Sutabani		
Jamkuri		

6.5 Conclusion

The assessment of overall groundwater quality of different villages in Kashipur block of Purulia district gives some important knowledge about its spatial variation in the study area: A total of 52 samples were collected from bore wells of 52 different villages. Physico-chemical parameters were analyzed in laboratory by authentic

methods. The analysis shows that the concentration of pH is moderate to safe for drinking use.

Concentration of TDS is positively correlating with the EC values which are affected by various anthropogenic activities in the study area (agricultural, industrial, domestic runoff). The cationic and anionic concentrations are determined by geochemical characteristics of the aquifer zone.

In this study area, the values of Na^+ and SO_4^{+} are safe to drinking and agricultural usages, where the high concentration of Mg indicates richness of ferromagnesian minerals in the underlying rocks and mixing of waste or sewage water to the underground water in both pre-monsoon and post-monsoon seasons. Concentration of calcium in the groundwater generally depends upon the source of calcium feldspars. The groundwater samples of the study area indicate most of the samples are rich in calcium concentration for its geogenic conditions. High percentage of Ca and Mg increases the values of TH. Due to low presence of biotitic, hornblende-like minerals, the mixing of fluoride is limited in some parts of the study area. The PIG method shows the overall quality of groundwater where most of the samples are under insignificant pollution zone (73.07%) and few are moderately polluted (26.92%) and only one sample (0.01%) falls under high pollution zone in pre-monsoon season. On the other hand, 67.30% samples of post-monsoon season fall under the insignificant pollution zone, 32.69% samples show low pollution, and 0.01% of samples indicate high pollution in the Kashipur block. The irrigation water quality assessment techniques (SAR, SSP, KR, MAR) show that most of the samples are safe to use for agricultural production. Some samples indicate high values of SSP, MAR, KR, and SAR which are unsafe for irrigation practice in the study area.

Ordinary kriging method is used to generate spatial concentration of different chemical parameters in the Kashipur block. Modern GIS techniques are used to delineate the overall groundwater quality in the study area. Zonation by PIG method indicates northern, north-eastern, and southern parts of Kashipur block are moderately affected by their physico-chemical conditions in the pre-monsoon season. Eastern, central, southern, and south-western parts of Kashipur block are affected by moderate to high groundwater pollution zone. Thus, it is helpful to further assess groundwater quality and measures to enhance the usefulness of the valuable groundwater resource to the Kashipur block of Purulia district.

References

- Acheampong SY, Hess JW (1998) Hydro geologic and hydro chemical framework of the shallow groundwater system in the southern Voltaian Sedimentary Basin, Ghana. *J Hydrogeol* 6 (4):527–537
- Ahmed AA (2007) Using lithologic modeling techniques for aquifer characterization and groundwater flow modeling of Sohag area, Egypt. Second International Conference on Geo-Resources in the Middle East and North Africa. 24–28 Feb. 2007, Cairo University, Egypt
- APHA (2012) Standard methods for the examination of water and wastewater, 22nd edn. American Public Health Association, Washington, DC

- BIS (2012) Drinking water specifications. Bureau of Indian Standards, IS 10500, New Delhi, India
- Bohlke JK (2002) Groundwater recharge and agricultural contamination. *Hydrogeol j* 10:153–179
- Chapman D (Ed) (1996) On the behalf of UNESCO, WHO. UXEP. Water quality assessments—a guide to use biota, sediments and water in environmental monitoring. F & F Spoil, London, Chapter 9
- Das S and Nag SK (2017) Geochemical appraisal of fluoride-laden groundwater in Suri I and II blocks, Birbhum district, West Bengal. *Appl Water Sci.* 7:2559–2570. <https://doi.org/10.1007/s13201-016-0452-x>.
- Fahid K.J. Rabah, Said M. Ghabayen and Ali A. Salha, 2011. Effect of GIS Interpolation Techniques on the Accuracy of the Spatial Representation of Groundwater Monitoring Data in Gaza Strip. *Journal of Environmental Science and Technology*, 4: 579–589.
- Foster S, Chilton J, Moench M, Cardy F, Schiffer M (2000) Groundwater in rural development, World Bank technical paper, 463
- Haldar D, Halder S, Das P, Halder G, (2014) Assessment of water quality of Damodar river in south Bengal region of India by Canadian Council of Ministers of Environment (CCME) water quality index: a case study. <https://doi.org/10.1080/19443994.2014.987168>.
- Hem JD. 1991 study and interpretation of the chemical characteristics of natural water. Scientific publishers: jodhpur. India ; 2254.
- Jalali M (2006) Chemical characteristics of groundwater in parts of mountainous region, Alvand, Hamadan, Iran. *Environ Geol* 51:433–446
- Kelly WP (1976) Use of saline irrigation water. *Soil Sci* 95(4):355–391
- Kumar VS, Amarender B, Dhakate R, Sankaran S, Kumar KR (2014) Assessment of groundwater quality for drinking and irrigation use in shallow hard rock aquifer of Pudunagaram, Palakkad District, Kerala. *Appl water sci* 6:149–167
- Kundu A, Nag SK, (2018) assessment of groundwater quality in kashipur block, purulia district, west Bengal. *Appl water sci* 8:33. <https://doi.org/10.1007/s13201-018-0675-0>
- Masoomeh D, Meysam A, Masoud BM (2014) Assessing groundwater quality for irrigation using indicator kriging method . *Appl water sci* 6:371–381
- Mercado A (1985) Use of hydrochemical pattern in carbonate, sand and sandstone aquifers to identify intrusion and flushing saline water. *Groundwater* 23(5):635–645
- Nag SK, Das A (2017) Assessment of groundwater quality from bankura I and bankura II blocks, Bankura district, West Bengal, India. *Appl water sci* 7:3447–3467. <https://doi.org/10.1007/s13201-017-0530-8>
- Nag SK, Lahiri A (2012) Hydrochemical characteristics of groundwater for domestic and irrigation purposes in Dwarakeswar watershed area, India. *Am J Clim Change* 1(4):217–230
- Nag SK, Suchetana B (2016) Groundwater quality and its suitability for irrigation and domestic purposes: a study in rajnagar block, Birbhum district, West Bengal India. *J Earth Sci Clim Change* 7:337. <https://doi.org/10.4172/2157-7617.1000337>.
- Obiefuna GI, Sheriff A (2011) Assessment of shallow ground water quality of Pindiga Gombe area, Yola area, NE, Nigeria for irrigation and domestic purposes. *Res J Environ Earth Sci* 3 (2):131–141
- Raghunath HM (1987) *Groundwater*, 2nd edn. Wiley eastern limited, New Delhi, India, pp. 344–369
- Raji BA, Alagbe SA (1997) Hydrochemical facies in parts of the Nigerian basement complex. *Environ Geol* 29(1–2):46–49
- Raju NJ (2007) Hydrogeochemical parameters for assessment of groundwater quality in the upper Gunjanaeru River Basin, Cuddapah District, Andhra Pradesh, South India. *Environ Geol* 52 (2007):1067–1074
- Rao SN, Sunita B, Rao PVN, Rao PS, Spandana BD, Sravanthi M, Marghade D (2018) Quality and degree of pollution of groundwater , using PIG from a rural part of Telangana state, India. *Appl water sci* 8:227. <https://doi.org/10.1007/s13201-018-0864-x>.
- Rao YS, Reddy TVK, Nayudu PT (1997) Ground-water quality in the Niva River basin, Chittoor district, Andhra Pradesh, India. *Environ Geol* 31(1):56–63

- Richards LA (1954) Diagnosis and improvement of saline and alkali soils; agric handbook, vol 60. USDA and IBH Publ. Coy Ltd., New Delhi, pp 98–99
- Rivers CN, Hiscock KM, Feast NA, Barrett MH, Dennis PF (1996) Use of nitrogen isotopes to identify nitrogen contamination of the Sherwood sandstone aquifer beneath the city of Nottingham, UK. *Hydrol J* 4(1):90–102
- Shanmugasundharam A, Kalpana G, Mahapatra SR, Sudharson ER (2015) Assessment of groundwater quality in Krishnagiri and Vellore districts in Tamilnadu, India. *Appl water sci* doi <https://doi.org/10.1007/s13201-015-0361-4>
- Singh A, Srivastav SK, Kumar S, Chakrapani GJ (2015) A modified DRASTIC model (DRASTICA) for assessment of groundwater vulnerability to pollution in an urbanized environment in Lucknow, India. *Environ Earth Sci* 74(7):5475–5490. Doi:<https://doi.org/10.1007/s12665-015-4558-5>
- Subba Rao N (2012) PIG: a numerical index for dissemination of groundwater contamination zones. *Hydrol Process* 26:3344–3350
- Subramani T, Elango L, Damodarasamy SR (2005) Groundwater quality and its suitability for drinking and agricultural use in Chithar River Basin, Tamil Nadu, India. *Environ Geol* 47(8):1099–1110
- Taheri K, Gutierrez F, Mohseni H, Raeisi E, Taheri M (2015) Sinkhole susceptibility mapping using the analytical hierarchy process (AHP) and magnitude-frequency relationships: a case study in Hamadan province, Iran. *Geomorphology* 234:64–79. Doi:<https://doi.org/10.1016/j.geomorph.2015.01.005>
- Thapa R, Gupta S, Guin S, Kaur H (2017) Assessment of groundwater potential zones using Multi – Influencing factor (MIF) and GIS: a case study from Birbhum district, West Bengal. *Appl water sci* 7:4117–4131
- Todd DK (1980) *Groundwater hydrology*. Wiley, New York, p 535
- Umar R, Khan MMA, Absar A (2006) Groundwater hydrochemistry of a sugarcane cultivation belt in parts of Muzaffarnagar District, Uttar Pradesh, India. *Environ Geol* 49(7):999–1008
- UNESCO (2007) UNESCO water portal newsletter no. 161. Water related diseases. [Http://www.unesco.org/water/news/newsletter/161.shtml](http://www.unesco.org/water/news/newsletter/161.shtml)
- USDA (1954) diagnosis and improvement of saline and alkali soils. U.S. salinity laboratory staff, government printing office, Washington, dc
- Wright EP, Burgess WG (eds) (1992) *The hydrogeology of crystalline basement aquifers in Africa*. Soc Spl Publ N, Geol

Chapter 7

Analysis of Groundwater Potentiality Zones of Siliguri Urban Agglomeration Using GIS-Based Fuzzy-AHP Approach



Suraj Kumar Mallick and Somnath Rudra

Abstract Availability of sustainable potable water and its efficient utilisation is one of the major challenges in urban planning to meet the everincreasing demand for expanding urban population. In the present study, the groundwater resource potential zones were evaluated based on integrated GIS-based Fuzzy Analytical Hierarchy Process (AHP) approach on Siliguri urban agglomeration (SUA), West Bengal, India. For that purpose, eight different thematic layers (DEM, slope, soil, LULC, annual precipitation, lineament density, moisture index and geology) were integrated by geospatial techniques, and the resulting values are put into the Saaty's AHP to detect Groundwater Potentiality Zone (GPZ). Finally, five major classes of GPZ were identified based on water potentiality, namely, low, medium, medium-high, high and very high. The results were validated through a standard method namely precision Receiver Operating Characteristics (ROC) curve and the calculated AUC value was 87.7%. The study area had 33.19% good groundwater potentiality area at the South-Western and Western part, and low potentiality zone had shared 6.76% of the total area. The study concludes that the overall study area has carried out suitable groundwater potentiality. The zonation of groundwater potentiality may be useful for urban area development over Siliguri in the near future.

Keywords Groundwater potential zone · Precision accuracy assessment · Saaty's AHP · Thematic layers · Urban planning

7.1 Introduction

The growing population in India with increasing unpredicted human demand on water becomes a critical issue, while we have only 4% freshwater availability (Aayog 2017). Annually, India has available replenishable groundwater resources, but the maximum volume of groundwater is used for agriculture purposes and the

S. K. Mallick · S. Rudra (✉)

Department of Geography, Vidyasagar University, Midnapore, West Bengal, India

© The Author(s), under exclusive license to Springer Nature Switzerland AG 2021

P. K. Shit et al. (eds.), *Groundwater and Society*,

https://doi.org/10.1007/978-3-030-64136-8_7

141

rest of the groundwater resources are used through domestic and natural discharge purposes (CGWB 2017). Consequently, surpass withdrawal of groundwater and deficiency of surface water resources has created a negative impact on the environment, resulting in water stress in major parts of India (Jha et al. 2010).

Moreover, cities or urban areas have certain limited resources, and majority of people are attracted towards the urban areas to find their job and better livelihood, thus expanding cities promptly. Census survey report of India shows at the beginning of the twentieth century (1901) only 1/10 of the population of India lived in urban areas, but now (2011), 1/3 of the population of India lived in urban areas (Chandramouli and General 2011). Therefore, sustainable potable water and its efficient use is one of the major challenges in urban planning to ensure sufficient demand for the growing population in an urban area. The number of people with increasing demand on water, including poor management, has become an issue for any urban bodies. Potential groundwater aquifers help the urban areas to sustain good quality of water supply for drinking purposes throughout the year, including available surface water resources (Singh et al. 2013).

Although it is crucial that each and every urban body must have efficient use of groundwater resource, it still requires Groundwater Potential Zone (GPZ) assessment to identify the site suitability for urban residential zone development in the future. Availability of the groundwater in any urban region has been influenced by the different climatic and hydrological features and its interrelationship (Tiwari et al. 2019). This hydrological feature depends on physical settings like slope, elevation, soil type, geology, geomorphology, drainage and lineament, etc. (Ozdemir 2011; Rahmati et al. 2014). The climatic features such as precipitation and moisture have governed the physical attributes for the analysis and mapping of GPZ (Tiwari et al. 2019).

Since the 1970s, geospatial techniques of remote sensing (RS) and geographical information system (GIS) have been fruitfully projected for mapping on physical structures and their features (altitude and slope), geological structures, land use/land cover, drainage system, recharge and discharge, geomorphology, soil, etc. (Mogaji 2016). Satellite images can be effectively handled by GIS. RS and GIS both are used as spatial evaluation measures associated with beleaguered spatial decision problems. GIS can also integrate with the multi-criteria decision analysis (MCDA) method which generates an influential tool for spatial decision-making processes. Past few decades, the MCDA has been established and denoted to the developmental decisions through accuracy assessment, structure analysis and suitability analysis (Ozdemir 2011; Tiwari et al. 2019). Saaty's analytic hierarchy process (AHP) is one of the worldwide conventional MCDA-based numerical method to resolve problems of multiple attribute-based domains such as site suitability analysis and mapping (Saaty 1980), healthcare assessment (Reddy et al. 2014; Thokala et al. 2016), hazard mapping (Matori et al. 2014; Hoque et al. 2017), mapping on groundwater delineation (Jenifer and Jha 2017), etc. In the beginning of the twenty-first century, various new approaches have emerged in addition to AHP, such as data-driven model using fuzzy logic (Liggett and Talwar 2009; Boughriba et al. 2010), knowledge-driven model-like statistical index (SI) (Nag and Ghosh 2012), frequency ratio

(FR) (Ozdemir 2011; Park et al. 2013), weights of evidence (WoE) (Machiwal et al. 2011), artificial neural network (ANN) (Lee et al. 2012) and support vector machines (SVMs) (Naghbi et al. 2017), which are used to study the geospatial data for generating groundwater potentiality zone map which has a great role to develop urban land use site suitability.

A knowledge-driven model like Fuzzy-based mapping is a kind of model where users are often faced with some difficulties in selecting a membership function (Al-Abadi et al. 2018). Even some statistical models such as SI and WoE have shown some problems in measuring the interrelationship between training factors and groundwater event (Yilmaz 2009; Ozdemir 2011). Moreover, the modified advance data-driven machine learning techniques, such as ANN, RF, SVM and BRT, have some restrictions, namely, the neural network opacity and its dependency on outliers of logistic regression for understanding (Tiwari et al. 2019). But, AHP technique can agree the amalgamation of fundamental elements (Rahmati et al. 2014). Furthermore, it can decompose the observation into hierarchy and ensure that the combining aspects of qualitative and quantitative analysis have been integrated. Hence, AHP deals with the issues of generalisation in human decision-making processes (Emrouznejad and Marra 2017). In recent times, Fuzzy-based MCDA (Ishizaka and Labib 2011; de FSM Russo and Camanho 2015) combined with AHP is established as a parsimonious and an appropriate tool to delineate groundwater zone and its management (Pani et al. 2016; Pinto et al. 2017; Kumar and Krishna 2018). So, we have concentrated on the Fuzzy-based AHP approach using geospatial and statistical techniques to delineate GPZ of Siliguri urban agglomeration (SUA).

A large number of studies on delineation of GPZ using Fuzzy-AHP had been done by Murthy (2000), Jaiswal et al. (2003), Anbazhagan et al. (2005), Kumar et al. (2007), Gupta and Srivastava (2010), Rahmati et al. (2016), Tiwari et al. (2019), etc. The result helps us to identify the water potential area to support future urban commercial and residential land use planning.

7.2 Study Area

Siliguri, a metropolitan city, is basically known as the gateway of north-east India. In 1901, it was a mere village, but within a few decades it has developed as the largest urban agglomeration of North Bengal. The Siliguri urban agglomeration (SUA) is located at the junction of New Jalpaiguri district and the foothills of Darjeeling Himalaya on the bank of Mahananda and Balason River extending from $88^{\circ}23'15''$ E to $88^{\circ}28'01''$ E longitude and from $26^{\circ}40'38''$ N to $26^{\circ}46'40''$ N latitude (Fig. 7.1), with an average elevation of 120 metres from the mean sea level (MSL). Urbanisation is gradually going on throughout the entire North Bengal, but in the case of Siliguri it is faster mainly due to its geographical location and communication importance. The study area is covered by 99.60 sq. km (Census 2011). The total population of SUA is 1,057,438 with the population density of 11,171 per square

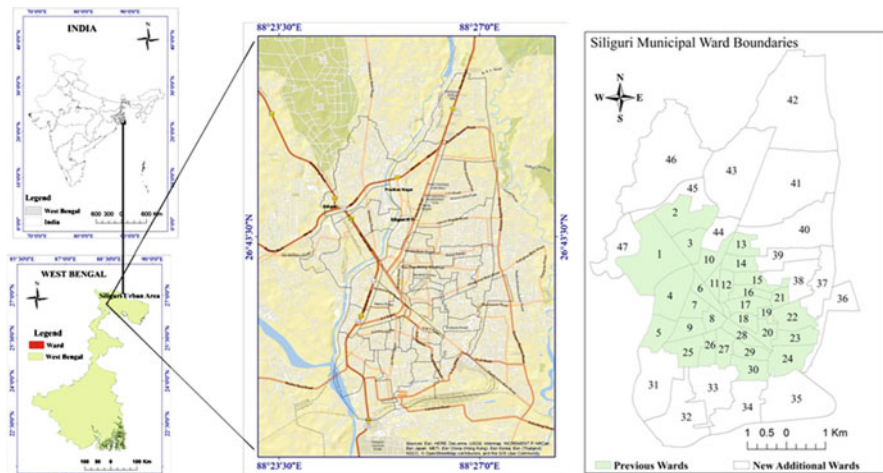


Fig. 7.1 Location map of the Siliguri urban agglomeration (SUA) with open street map and increasing ward boundaries

Table 7.1 Detail information of Landsat-8 imagery and ASTER DEM data

Acquisition date	Satellite	Path/row	Resolution	Referencing system
07/03/2018	Landsat-8 OLI	139/42	30 m, 100 m	UTM 45°N and WGS 84
15/03/2011	ASTER DEM	NA	30 m	

km. The sharp increase in population occurred due to the partition of Bengal in 1947 and further during the political unrest in 1971. Also, due to administrative problems in Nepal and China, people started to settle permanently in Siliguri. It was given a status of Municipal Corporation by the government in 1994, while 17 new wards were added with existing 30 wards in SUA and the total scenario has been changed (Fig. 7.1). Although the whole area was developed over the alluvium flood plain but some portion in the northern part of the study area was covered by the impervious surface. As various urban issues are coming in the forefront with the increasing trends of urban population, groundwater has become one of the issues.

7.3 Materials and Methods

7.3.1 Data Used

In this study we have applied multi-spectral satellite imagery of Landsat-8-(OLI/TIRS) and Advanced Spaceborne Thermal Emission and Reflection Radiometer (ASTER)-digital elevation model (DEM) data obtained from satellite. Table 7.1 provides detail information about the data acquisition. Landsat data and DEM data

were derived from the US Geological Survey (USGS) Earth Explorer web portal (<http://earthexplorer.usgs.gov>).

7.3.2 Data Processing and Creation of Thematic Layers

Methodological flow chart was used in this present study to give the better understanding for developing groundwater potential zone map (Fig. 7.2). Firstly, we had used the ASTER DEM data to generate the slope map. The generated slope map was categorised into five specified land classes using natural break method. Then Landsat-OLI/8 image had been composed, clipped and finally classified using supervised maximum likelihood classification method and categorised into six predetermined classes, water body, bare surface, crop land, open pasture, vegetation cover and built-up, to generate the LULC map. Moisture index map was obtained from the Landsat-OLI/8 satellite data of 2018 using modified normalised difference moisture index (MNDMI) to show the soil moisture content rate instead of drainage density. The geological map was prepared with the help of Geological Survey of India (GSI), Kolkata. Firstly, the scanned image was rectified and then digitised using ArcGIS software. With the help of density module in ArcGIS spatial analyst tool, lineament density map also was prepared in the similar way. The soil map was collected from the National Bureau of Soil Survey and Land Use Planning

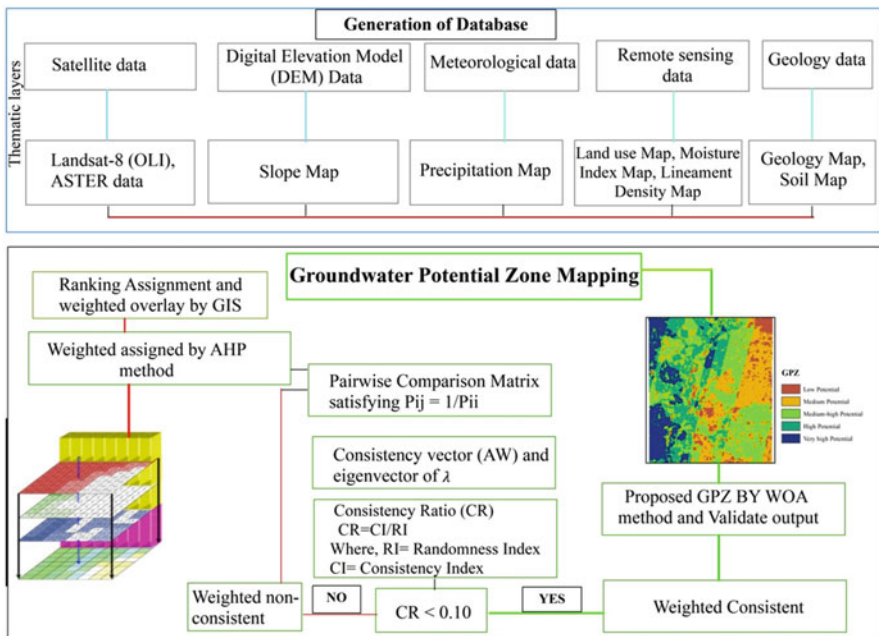


Fig. 7.2 Flowchart of the study

(NBSS&LUP), Kolkata, West Bengal. Then, station data for rainfall distribution over 17 years (2001–2018) was obtained from India Meteorological Department (IMD) to generate the annual rainfall distribution map using spatial interpolation method like nonlinear inverse distance weighting (IDW). IDW is used to represent the proximity of an unobserved point which is computed in reverse considering the distance to the points (Wu et al. 2010) classification. Various maps were validated with Siliguri perspective plan 2025 proposed by Siliguri Jalpaiguri Development Authority (SJDA).

7.3.3 Fuzzy-AHP and Assignments of Normal Weighted Overlay of the Selected Thematic Layers

Analytic hierarchy process (AHP) is applied to define the weights of the thematic layers (Saaty 1980). Remarkably, the GIS-based Fuzzy weighted overlay analysis (WOA) method including AHP has been an essential technique to evaluate the multifaceted longitudinal decision problems. The judgement rating value is ranged between 1 and 9 scales (Saaty 1980) shown in Table 7.2. Therefore, weighted values of each thematic layer are needed for developing GPZ with the help of ArcGIS software.

Firstly, the problem was designed based on criteria and objectives in a hierarchical process. Secondly, comparison and gradation numbers had been given into the weighted criteria to assume its intensities with specific importance. Weights were given to each category of selected layers from earlier knowledge of the factor characteristics, local experts, personal observation (Machiwal et al. 2011) and

Table 7.2 Comparison and gradation number for alternatives in AHP (Saaty 1980)

Intensity of importance ^a	Characteristics	Explanation
1	Not suitable	Two activities contribute equally to the objective
3	Moderately suitable	Judgement slightly favours one activity over another
5	Suitable	Judgement strongly favours one activity over another
7	Very suitable	Activity is favoured very strongly over another
9	Extremely suitable	Highest possible order of favouring one activity over another
2, 4, 6, 8	Judgemental value	When compromise is needed
Reciprocals of the above numbers	If it is assigned one of the numbers when comparing with <i>j</i> , then <i>j</i> has the reciprocal value when compared with <i>i</i>	Reasonable assumption

^aLess importance <- (1/9-1/8-1/7-1/6-1/5-1/4-1/3-1/2-1-2-3-4-5-6-7-8-9) -> More importance

urban planning expert of Siliguri Municipality Corporation. Thirdly, relative weightage was allocated to each factor, and in this way, pairwise comparison matrix had been formed (Table 7.5). Then, the allocated value of every factor was normalised into 1 by eigenvector method of AHP, and finally, the summation of one column value was divided by column total. In this way, normalisation of pairwise matrix was completed. Thereafter, the influence of the allocated weights of the thematic layers was examined for consistency measurement through the normalisation processes (Saaty 1980). Thereafter, each standard corresponding weight was given based on average value of individual row; thus final normalised pairwise weighted matrix has been formulated (Table 7.6).

$$AW = \begin{pmatrix} P_{11} & P_{12} & P_{13} & \dots & P_{1n} \\ P_{21} & P_{22} & P_{23} & \dots & P_2 \\ \dots & \dots & \dots & \dots & \dots \\ \dots & \dots & \dots & \dots & \dots \\ P_{n1} & P_{n2} & P_{n3} & \dots & P_{nn} \end{pmatrix} \times \begin{pmatrix} W_1 \\ W_2 \\ \dots \\ \dots \\ W_n \end{pmatrix} = P_{ij} \times W_i \quad (7.1)$$

where P_{ij} ($i = 1, 2, 3, \dots, n$) and ($j = 1, 2, 3, \dots, n$) denote pairwise comparison matrix; $P_{ii} = 1$ and $P_{ij} = 1/P_{ji}$. W_i ($i = 1, 2, \dots, n$) denotes ranking weight.

The consistency vector can be denoted by the term AW which is measured with the help of equivalent weight values of λ . The sum of AW when divided by ranking weights is called λ_{max} (Tiwari et al. 2019).

$$\lambda_{max} = \frac{1}{n} \sum_{W_i=0}^n \frac{AW}{W_i} \quad (7.2)$$

where W denotes the corresponding eigenvector of λ_{max} , W_i ($i = 1, 2, 3, \dots, n$) denotes the ranking weight (Machiwal et al. 2011), AW denotes the consistency vector and n represents the number of classes (Table 7.3).

$$CI = \frac{\lambda_{max} - n}{n - 1} \quad (7.3)$$

where n represents the frequency of classes, λ_{max} is the maximum eigenvalue and CI is the consistency index.

$$CR = \frac{CI}{RI} \quad (7.4)$$

Table 7.3 Random index for different values of n (Saaty 1980)

n	1	2	3	4	5	6	7	8	9	10
RI	0	0	0.58	0.89	1.12	1.24	1.32	1.41	1.45	1.49

where the CR (consistency ratio) represents the denominator of CI and RI. The CR value should be less than 0.10 that reflects the consistency in each of the factors' weightage during pairwise comparison matrix (Sener et al. 2011).

7.3.4 Delineation of the GPZ

Groundwater potentiality zones were delineated using geospatial and statistical approach. Weighted overlay analysis (WOA) method is used to calculate the GPZ by combining all the possible factors and giving weightage to each of the selected factors (Eq. 7.5).

$$GPZ = \sum_{W=1}^m \sum_{i=1}^n (W_i \times X_j) \quad (7.5)$$

where W_i is the normalised weight of the i thematic layer and X_j is the rank value associated with the j layer, while m and n denote the entire number of selected thematic layers and overall classes used in each thematic layer, respectively. The GPZ is calculated with the help of Eq. 7.6 below:

$$GPZ = E_w E_r + SL_w SL_r + S_w S_r + LULC_w LULC_r + P_w P_r + LD_w LD_r + MI_w MI_r + G_w G_r \quad (7.6)$$

where w and r represent the normalised weight index and AHP rating of the individual classes, respectively. E is the elevation, SL is denoted as slope, S represented the distribution of soil, $LULC$ is denoted land use land cover of SUA, P specifies volume of rainfall, LD is the lineament density, MI is the moisture index and G represented geological and topographical condition of the study area (Table 7.2).

7.4 Result and Discussion

7.4.1 Thematic Layers

Various important factors were incorporated to classify the GPZ in SUA, viz. elevation, geological structure, land use/land cover (LULC), annual precipitation, soil, moisture index and lineament density for GPZ analysis (Jaiswal et al. 2003). These thematic layer factors were calculated by giving importance gradation score (Table 7.5.) and then used the value for pairwise comparison matrix (Table 7.6). Moreover, each significant weight of assigned value was used to calculate and validate each of the individual factor. We used the consistency index (CI) and consistency ratio (CR) to mitigate the validation problem. Detailed information of

each thematic layer and its sub-classes, including groundwater suitability rating, was used to identify the GPZ map (Table 7.7). The detailed information about the individual thematic layer is as follows.

7.4.1.1 DEM

Digital elevation model (DEM) is the 3-D digital illustration of any kind of topography (Fig. 7.3). The current DEM showed mostly South-Western and Southern parts of SUA have almost flat topography. Therefore, maximum weight had been given to that part of the urban area due to the high potentiality of recharge including minimum runoff, while the northern part had highest elevation and it had very high opportunities of runoff rather than groundwater recharging. For that reason, it was given minimum weight.

7.4.1.2 Slope

Slope is the degree of inclination of any topographical surface, and aspect denoted the directions of the physical slope faces. Slope map was generated with the help of ASTER-DEM data of SUA. Plane areas are able to control the precipitation and supply groundwater recharge compared to the steep slope area. The area was categorised into five classes, which were (1) 0–0.45, (2) 0.45–1.21, (3) 1.21–2.15, (4) 2.15–3.19 and (5) 3.19–5.32 (Fig. 7.3). The maximum percentage of the slope was ranged from 1.21 to 2.15 degree. Higher rank was assigned to the gentle slope or flat slope, where the class was ranged from 3.19 to 5.32 degree and was assigned into lowest rank due to the steep slope.

7.4.1.3 Soil

Soil component was used to find out the actual moisture content into the soil and its nature. In this study area, four major soil classes were identified, i.e. (1) Clay loam, (2) Inceptisols-I, (3) Inceptisols-II and (4) Entisols (Fig. 7.3). Clay loam had constituted the most extensive soil, covering approximately 22.13% of area along the Mahananda basin at the north to the Balason basin at the South-west. Inceptisols-I-type soil basically falls under *tropest* sub-groups, more or less freely drained Inceptisols of humid tropics. It was found in the South-eastern part of the Mahananda basin with a thin to moderately deep profile (50–120 cm), developed mostly on steep slopes along the northern hilly area and the foothill around Marionbari and Panighatta. Inceptisols-II was found at the whole Debagram census town and adjacent part of the study area. The Inceptisols, including both I and II types, were covering 39.96% of the study area. But, Entisols have held a little evidence of soil profile development due to inadequate deposition of new alluvium layer at Balason and Mahananda basin area, and thus, it was given less weight. The

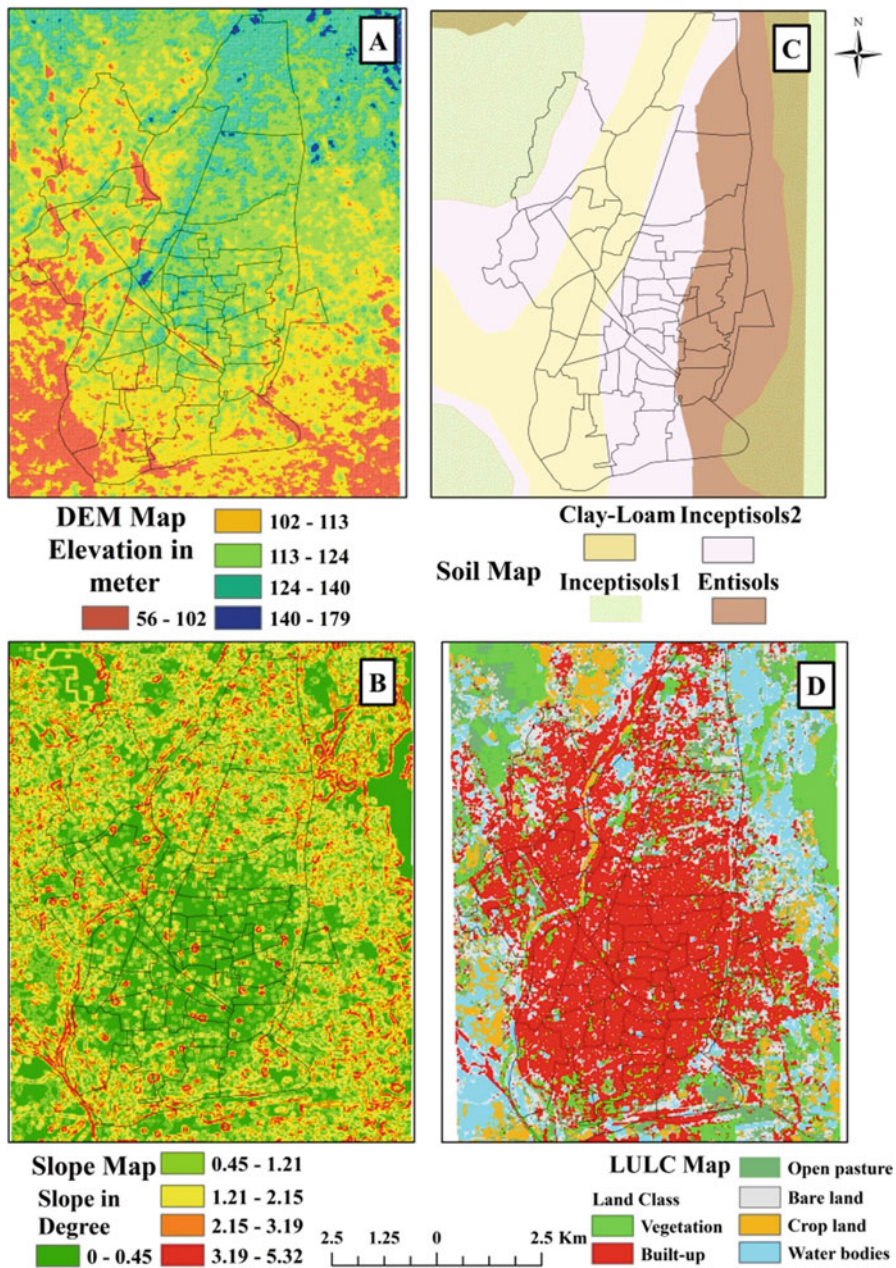


Fig. 7.3 Thematic layers: (a) DEM map; (b) slope map; (c) soil map; (d) LULC map of the study area

whole SMC was under this type of soil groups. These soils are typical humid soils possessing a wide variety of physical and chemical properties which are varying with depth, colour, texture, structure, organic carbon, porosity and permeability. Significance of soil characteristics was controlled by the infiltration level, and depending on local geological structure, the weightage was assigned (Table 7.7). Clay soil had greater control capacity which was extended from 0.00 to 0.06 inch/hour; hence, clay soil had assigned less importance and highest weightage than Inceptisols-I soil.

7.4.1.4 Land Use and Land Cover (LULC)

The land use and land cover (LULC) map of SUA 2018 was used to identify the distribution of total area including percentage of every land class (Figs. 7.3 and 7.4). LULC map was classified and generated using unsupervised and supervised processes using ERDAS 15.0 amalgamation with ArcGIS 10.1. Thus, six different types of LULC were found with a proportion of area shared by each land class, i.e. bare land (16.16%), built-up area (32.40%), crop land (10.91%), open pasture (15.72%), vegetation (12.66%) and water body (12.14%). Built-up area shared the maximum percentage (32.40%) and resulted into huge demand on water day by day. Consequently, water availability becomes a question, and urban people are facing some water stress (Table 7.4).

7.4.1.5 Precipitation

Precipitation or rainfall is a key factor for groundwater recharge. The nature of groundwater potentiality depends on duration and volume of precipitation which controls discharge and the balance between all the components of the hydrological cycle. Precipitation map was prepared using spatial interpolation method based on two meteorological stations data in around 15 km range. Nowadays, spline polynomial function has been carried out an important role to represent the interpolation of annual precipitation in monthly and yearly basis (Peel et al. 2009). Two precipitation zones 2500–3000 mm and above 3000 mm were identified in the annual precipitation map (Fig. 7.4). Southeast and western parts of Siliguri urban area were recorded above 3000 mm rainfall per annum that have been given maximum weightage.

7.4.1.6 Lineament Density

The lineament is a linear feature on the earth's surface defined as the fault with distortion in the geomorphic features due to adjustment of constant tension in the geological structure. It reflects a general surface expression of underground fractures like cracking, folding, faulting, etc. (Pradhan and Youssef 2010). Lineament is a key factor to determine the groundwater potentiality depending on the permeability and

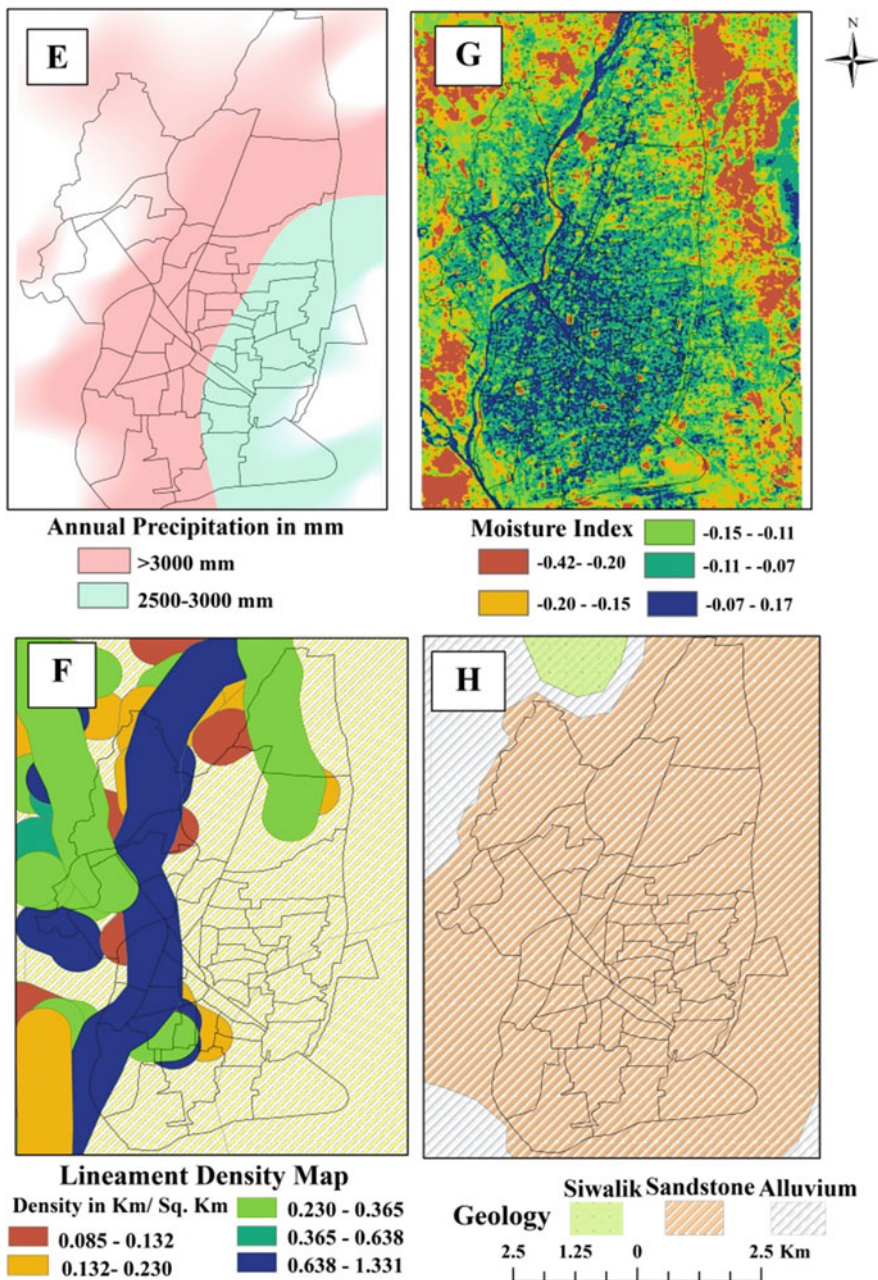


Fig. 7.4 Thematic layers: (e) precipitation map; (f) lineament density map; (g) moisture index map; (h) geology of the study area

Table 7.4 Land use/cover with percentage of land use share in 2018

LULC types	2018	
	Area	% of area
Bare land	16.10	16.16
Built-up area	32.27	32.40
Crop land	10.87	10.91
Open pasture	15.66	15.72
Vegetation	12.61	12.66
Water body	12.09	12.14
Total area	99.60	100.00

penetrability (Sreedevi et al. 2006). The lineament density (L_d) was formulated using the web linkage method which is shown in Eq. 7.7. Areas with higher lineament density values were denoted higher recharge zones, and thus lower value indicated the lower groundwater potential zone. The calculated lineament density values of the SUA were classified into five zones, 0–0.13 (very low), 0.13–0.23 (low), 0.23–0.36 (moderate), 0.36–0.63 (high) and 0.63–1.33 km/km² (very high) (Fig. 7.4), and weightage was also given as per nature of lineament.

$$L_d = \sum_{i=1}^{i=n} \frac{L_i}{A} \quad (7.7)$$

where $\sum L_i$ is represented the lineament length of i th class (km) and A is represented the area in km².

7.4.1.7 Moisture Index (MI)

Moisture index (MI) is a GIS-based bio-physical composition where we used Middle Infrared (MIR) instead of Near Infrared (NIR) because MIR is more absorbent of light giving clear identification of water bodies. Therefore, band 5 in OLI/8 was denoted the MIR. The high positive value represents the higher water or moisture content, and middle to zero value represents the bare land while value close to zero or negative shows the presence of vegetation or soil. It can be shown in Eq. 7.8.

$$MI = \frac{(\text{band3} - \text{band5})}{(\text{band3} + \text{band5})} \quad (7.8)$$

In this study, MI map was classified into five classes (Table 7.7) where the highest moisture value was 0.17, which was found along the Mahananda river basin, and the lowest moisture value was found at the northeast part of SUA.

Table 7.5 Different factors and pairwise comparison matrix of eight thematic layers for GPZ

	E	Slope	Soil	LULC	P	LD	MI	G
DEM (E)	1	1/3	1/2	1/2	1/3	1/4	1/3	1/5
Slope	3	1	1/3	4	5	1/3	3	1/4
Soil	2	3	1	3	1/5	1/2	1/6	1/7
LULC	2	1/4	5	1	6	4	2	1/4
Precipitation (P)	3	1/5	2	1/6	1	6	1/2	2
Lineament density (LD)	4	3	6	1/4	1/6	1	1/5	3
Moisture index (MI)	3	1/3	7	1/2	2	5	1	2
Geology(G)	5	4	4	4	1/2	1/3	1/2	1

Table 7.6 AHP with normalised pairwise weight matrix of eight thematic layers for GPZ

	E	Slope	Soil	LULC	P	LD	MI	G	Weight	λ
DEM (E)	0.09	0.15	0.1	0.17	0.05	0.07	0.03	0.12	0.9	7.8
Slope	0.08	0.09	0.02	0.04	0.03	0.05	0.02	0.08	0.05	8.2
Soil	0.02	0.03	0.06	0.04	0.05	0.04	0.08	0.05	0.04	7.4
LULC	0.15	0.14	0.06	0.13	0.15	0.11	0.12	0.02	0.11	8.0
Precipitation (P)	0.12	0.08	0.19	0.21	0.09	0.02	0.05	0.06	0.1	8.2
Lineament	0.17	0.12	0.04	0.05	0.14	0.06	0.04	0.09	0.09	7.9
Moisture index (MI)	0.11	0.10	0.21	0.28	0.13	0.05	0.04	0.07	0.12	8.2
Geology(G)	0.05	0.12	0.22	0.08	0.07	0.02	0.21	0.15	0.11	8.4

Value of lambda max = 8.35, consistency index = 0.05, consistency ratio = 0.04

7.4.1.8 Geology

Geology is defined the solid features of earth surface and describes the structure of the earth on and beneath it. It has an important role to control the groundwater recharge including the infiltration of water. In this study, authors had found three types of geology, namely, alluvium, sandstone and Siwaliks (Fig. 7.4). Alluvium, mostly abundant and identical topographical layer, was characterised as typically fine-grained and greyish in colour. It was given maximum weightage because of maximum recharge possibility and holding capacity of groundwater was higher enough compared to sandstone and Siwaliks (Tables 7.5, 7.6, and 7.7).

7.4.2 GPZ Map

The groundwater potential zone (GPZ) map of SUA was prepared with Fuzzy weighted overlay analysis. Selected eight thematic layers were assigned in ArcGIS raster calculator. The GPZ result is shown in Fig. 7.5 and area is given in Table 7.8. The map was classified into five different classes based on weighted matrix analysis and AHP which were 3–7, 7–8, 8–9, 9–10 and 10–14 following the natural Jenks

Table 7.7 Different factors and classes with relative weighted index (W_i) of eight thematic layers for GPZ

Factors	Class/value	Potentiality for groundwater storage	Rating	W_i
DEM (m)	56–102	Very good	5	0.90
	102–113	Good	4	
	113–124	Moderate	3	
	124–140	Poor	2	
	140–179	Very poor	1	
Slope (degree)	0–0.45	Very good	5	0.05
	0.45–1.21	Good	4	
	1.21–2.15	Moderate	3	
	2.15–3.19	Poor	2	
	3.19–5.32	Very poor	1	
Soil	Clay-loam	Very good	5	0.04
	Entisols	Poor	4	
	Inceptisols-I	Very good	3	
	Inceptisols-II	Good		
LULC	Vegetation	Good	4	0.11
	Open pasture	Poor	2	
	Bare surface	Moderate	3	
	Crop lands	Very good	5	
	Water bodies	Very good	5	
	Built-up	Poor	1	
Lineament density (Km/Km ²)	0.08–0.13	Very poor	1	0.10
	0.13–0.23	Poor	2	
	0.23–0.36	Moderate	3	
	0.36–0.63	Good	4	
	0.63–1.33	Very good	5	
Precipitation (mm)	2500–3000	Good	4	0.09
	>3000	Very good	5	
Moisture index	–0.42–0.20	Very poor	1	0.12
	–0.20–0.15	Poor	2	
	–0.15–0.11	Poor	2	
	–0.11–0.07	Poor	2	
	–0.07–0.17	Good	4	
Geology	Alluvium	Very good	5	0.11
	Sandstone	Good	4	
	Siwaliks	Poor	2	

method. The GPZ value was presented in the form of low, medium, medium-high, high and very high potential zone categories. Medium potential groundwater zone and medium-high potential groundwater zone covering 33.89% and 26.02%, respectively, spread over the northern and eastern sections, while the western and south-western parts were a huge potentiality of groundwater till now.

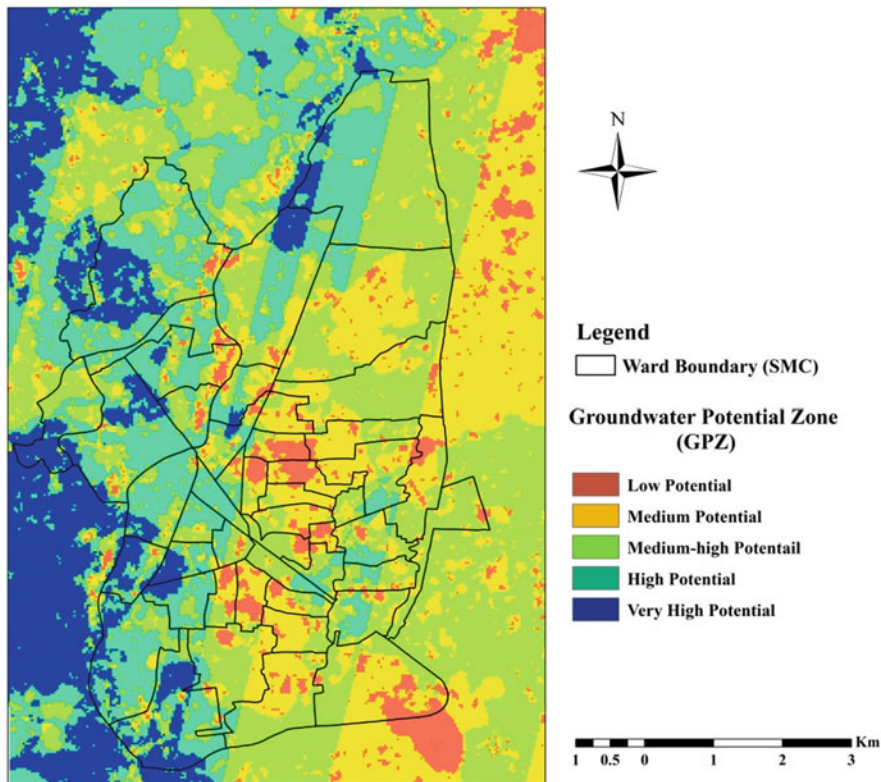


Fig. 7.5 Calculated GPZ map of Siliguri urban area

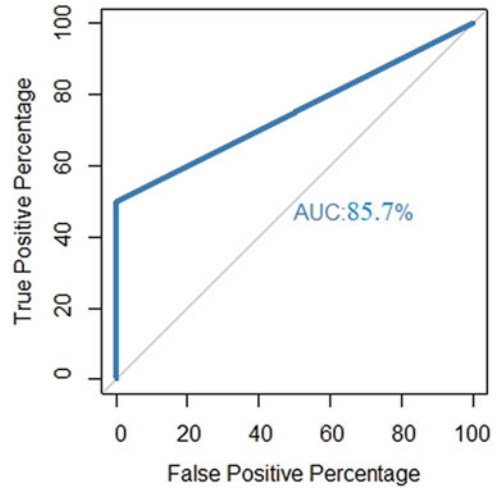
Table 7.8 Calculated GPZ with area and percentage of area shared of each zone

GPZ	Area (Km ²)	Percentage of area
Low potential	6.73	6.76
Medium potential	33.76	33.89
Medium-high potential	25.92	26.02
High potential	16.67	16.74
Very high potential	16.52	16.59

7.4.3 Validation of GPZ Map

Validation is the most important technique for any kind of model for the assessment of the accuracy of the result. For the validation of GPZ, we used Mahananda and Balason river water data and bore well data derived from West Bengal Pollution Control Board (WBPCB) and then analysed the yield data with the groundwater potentiality values. The collected groundwater yield data was classified accordingly as high (above 0.6 litres per second), medium (3–6 litres per second) and low (below 3 litres per second) categories (Tiwari et al. 2019). The GPZ result was validated

Fig. 7.6 Validation of GPZ using precision ROC curve



using Precision Accuracy through Receiver Operating Characteristics (ROC) curve (Fig. 7.6). Assessment (PAA) techniques.

Area Under Curve (AUC)

$$\begin{aligned}
 &= (\text{Number of observed water samples and expected water samples}) \\
 &\quad / (\text{Number of groundwater sample data collected through GPS}) \\
 &= 12/14 * 100 = 85.71\%
 \end{aligned}$$

The calculated AUC value replicates that the classified GPZ may be relevant for the residential planning and development over SUA in the near future. This method was used by different scholars (Tehrany et al. 2013; Rahmati et al. 2014; Tiwari et al. 2019).

7.5 Conclusion

In this study, authors demonstrated the distributed groundwater potential zones of Siliguri urban agglomeration (SUA), West Bengal, India, with the help of MCDA like GIS-based Fuzzy-AHP approach. Here, eight thematic layers were chosen for the delineation GPZ, and these were elevation (DEM), slope, soil, LULC, precipitation, lineament density, moisture index and geology assigning different weightage on the basis of field experience and expert's knowledge. These layers were brought a high consistency index that was 0.05 with consistency ratio of 0.04 denoting strong interrelation between climatic variables and physical attributes. On the basis of result, we delineated the GPZ of SUA into five water potentiality zones. The area

has had 16.74% (16.67 Km²) of high potential water and 16.59% (16.52 Km²) of very high potential water at the south-western part. But, the low potential groundwater zone (6.73 km²) at the city centre and near to New Jalpaiguri Junction area needed some proper management due to less resistivity, the sandy nature of soil with less permeability, groundwater susceptibility and steep slope. The total 58.68 sq.km areas have covered by medium potential groundwater and medium-high potential groundwater zone which is covered by the northern and southern portion of SUA. Thus, SUA has carried out suitable groundwater potentiality due to enormous source of the groundwater recharge and physical characteristics of the land. The PAA value of the classified GPZ was 85.71% that reflected excellent arrangement of groundwater zonation (Hasmadi et al. 2017).

The combination of modern GIS-based and AHP techniques provided a comprehensive outcome of GPZ that is really helpful for urban land use residential planning, industrial development and city development planning of SJDA-2030 with the growing urban population and expansion of the urban area. But still the quality of water, specially drinking water, becomes a question. Therefore, the achievement of sustainable groundwater utilisation can assist decision-makers to convey the effective and efficient groundwater management through rooftop rainwater harvesting and establishment of different groundwater recharge and recovery solutions of Mahananda and Balason river basin and that will be the best strategy for the management of future groundwater of this urban area.

Acknowledgement The authors would like to express their sincere thanks to the University Grants Commission for providing fund and DST-FIST (Department of Science and Technology – Fund for Improvement of S&T Infrastructure in Universities and Higher Educational Institutions) to conduct the research and field study, and finally thanks to the Siliguri Jalpaiguri Development Authority (SJDA) and Siliguri Municipal Corporation (SMC) for providing some important data and information related to the study.

Conflict of Interest The authors declare that they have no conflict of interest.

References

- Al-Abadi, A. M., Al-Bhadili, S. A., & Al-Ghanimy, M. A. (2018). A comparative assessment of fuzzy logic and evidential belief function models for mapping artesian zone boundary in an arid region, Iraq. *Journal of Hydro informatics*, 20(2), 497–519.
- Anbazhagan, S., Ramasamy, S.M., & Gupta, D.S. (2005) Remote sensing and GIS for artificial recharge study, runoff estimation and planning in Ayyar basin, Tamil Nadu, India. *Environ Geol* 48, 158–170.
- Boughriba, M., Barkaoui, A., Zarhlouly, Y., Lahmer, Z., & Verdoya, M. (2010). Groundwater vulnerability and risk mapping of the Angad transboundary aquifer using DRASTIC index method in GIS environment. *Arabian Journal of Geosciences*, 3(2), 207–220.
- CGWB Groundwater Year Book—India 2016–17 (Central Groundwater Board, Ministry of Water resources, Government of India, 2017).
- Chandramouli, C., & General, R. (2011). Census of India 2011. Provisional population totals. New Delhi: Government of India.

- De FSM Russo, R., & Camanho, R. (2015). Criteria in AHP: A systematic review of literature. *Procedia Computer Science*, 55, 1123–1132.
- Emrouznejad, A., & Marra, M. (2017). The state of the art development of AHP (1979–2017): A literature review with a social network analysis. *International Journal of Production Research*, 55(22), 6653–6675.
- Gupta, M., & Srivastava, P.K. (2010) Integrating GIS and remote sensing for identification of groundwater potential zones in the hilly terrain of Pavagarh, Gujarat, India. *Water International*, 35(2), 233–245.
- Hasmadi, M., Pakhriazad, H.Z., & Shahrin, M.F. (2017). Evaluating supervised and unsupervised techniques for land cover mapping using remote sensing data. *Geogr. - Malays. J. Soc. Sp.* 5(1).
- Hoque, M. A. A., Phinn, S., Roelfsema, C., & Childs, I. (2017). Tropical cyclone disaster management using remote sensing and spatial analysis: A review. *International Journal of Disaster Risk Reduction*, 22, 345–354.
- Ishizaka, A., & Labib, A. (2011). Review of the main developments in the analytic hierarchy process. *Expert Systems with Applications*, 38(11), 14336–14345.
- Jaiswal, R. K., Mukherjee, S., Krishnamurthy, J., & Saxena, R. (2003). Role of remote sensing and GIS techniques for generation of groundwater prospect zones towards rural development: An approach. *International Journal of Remote Sensing*, 24(5), 993–1008.
- Jenifer, M. A., & Jha, M. K. (2017). Comparison of Analytic Hierarchy Process, Catastrophe and Entropy techniques for evaluating groundwater prospect of hard-rock aquifer systems. *Journal of Hydrology*, 548, 605–624.
- Jha, M. K., Chowdary, V. M., & Chowdhury, A. (2010). Groundwater assessment in Salboni Block, West Bengal (India) using remote sensing, geographical information system and multi-criteria decision analysis techniques. *Hydrogeology Journal*, 18(7), 1713–1728.
- Kumar, A., & Krishna, A. P. (2018). Assessment of groundwater potential zones in coal mining impacted hard-rock terrain of India by integrating geospatial and analytic hierarchy process (AHP) approach. *Geocarto International*, 33(2), 105–129.
- Kumar, P.K., Gopinath, G., & Seralathan, P. (2007). Application of remote sensing and GIS for the demarcation of groundwater potential zones of a river basin in Kerala, southwest coast of India. *Int J Remote Sens*, 28(24), 5583–5601.
- Lee, S., Song, K. Y., Kim, Y., & Park, I. (2012). Regional groundwater productivity potential mapping using a geographic information system (GIS) based artificial neural network model. *Hydrogeology Journal*, 20(8), 1511–1527.
- Liggett, J. E., & Talwar, S. (2009). Groundwater vulnerability assessments and integrated water resource management. *Streamline Watershed Management Bulletin*, 13(1), 18–29.
- Machiwal, D., Jha, M. K., & Mal, B. C. (2011). Assessment of groundwater potential in a semi-arid region of India using remote sensing, GIS and MCDM techniques. *Water Resources Management*, 25(5), 1359–1386.
- Matori, A. N., Lawal, D. U., Yusof, K. W., Hashim, M. A., & Balogun, A. L. (2014). Spatial analytic hierarchy process model for flood forecasting: An integrated approach. In IOP conference series: *Earth and environmental science*, 20 (1), 12–29.
- Mogaji, K. A. (2016). Combining geophysical techniques and multicriteria GIS-based application modeling approach for groundwater potential assessment in southwestern Nigeria. *Environmental Earth Sciences*, 75(16), 1167–1181.
- Murthy, K.S.R. (2000). Groundwater potential in a semi-arid region of Andhra Pradesh: a geographical information system approach. *Int J Remote Sens*, 21(9), 1867–1884.
- N.I.T.I. Aayog (2017). Government of India. Nourishing India— National Nutrition Strategy.
- Nag, S. K., & Ghosh, P. (2012). Delineation of groundwater potential zone in Chhatna Block, Bankura District, West Bengal, India using remote sensing and GIS techniques. *Environmental Earth Sciences*, 70(5), 2115–2127.
- Naghbi, S. A., Ahmadi, K., & Daneshi, A. (2017). Application of support vector machine, random forest, and genetic algorithm optimized random forest models in groundwater potential mapping. *Water Resources Management*, 31(9), 2761–2775.

- Ozdemir, A. (2011). GIS-based groundwater spring potential mapping in the Sultan Mountains (Konya, Turkey) using frequency ratio, weights of evidence and logistic regression methods and their comparison. *Journal of Hydrology*, 411(3–4), 290–308.
- Pani, S., Chakrabarty, A., & Bhadury, S. (2016). Groundwater potential zone identification by analytical hierarchy process (AHP) weighted overlay in GIS environment: A case study of Jhargram block, Paschim Medinipur. *International Journal of Remote Sensing and Geoscience*, 5(3), 1–10.
- Park, S., Choi, C., Kim, B., & Kim, J. (2013). Landslide susceptibility mapping using frequency ratio, analytic hierarchy process, logistic regression, and artificial neural network methods at the Inje area, Korea. *Environmental Earth Sciences*, 68, 1443–1464.
- Peel, M. C., McMahon, T. A., & Pegram, G. G. S. (2009). Assessing the performance of rational spline-based empirical mode decomposition using a global annual precipitation dataset. *Proceedings of the Royal Society A Mathematical, Physical and Engineering Sciences*, 465(2106), 1919–1937.
- Pinto, D., Shrestha, S., Babel, M. S., & Ninsawat, S. (2017). Delineation of groundwater potential zones in the Comoro watershed, Timor Leste using GIS, remote sensing and analytic hierarchy process (AHP) technique. *Applied Water Science*, 7(1), 503–519.
- Pradhan, B., & Youssef, A. M. (2010). Manifestation of remote sensing data and GIS for landslide hazard analysis using spatial-based statistical models. *Arab J Geosci*, 3(3), 319–326.
- Rahmati, O., Pourghasemi, H. R., & Melesse, A. M. (2016). Application of GIS-based data driven random forest and maximum entropy models for groundwater potential mapping: A case study at Mehran Region, Iran. *Catena*, 137, 360–372.
- Rahmati, O., Samani, A. N., Mahdavi, M., Pourghasemi, H. R., & Zeinivand, H. (2014). Groundwater potential mapping at Kurdistan region of Iran using analytic hierarchy process and GIS. *Arabian Journal of Geosciences*, 8(9), 7059–7071.
- Reddy, B. P., Kelly, M. P., Thokala, P., Walters, S. J., & Duenas, A. (2014). Prioritising public health guidance topics in the National Institute for Health and Care Excellence using the Analytic Hierarchy Process. *Public Health*, 128(10), 896–903.
- Saaty, T. L. (1980). *The analytic hierarchy process*. New York: McGraw-Hill.
- Sener, S., Sener, E., & Karagüzel, R. (2011). Solid waste disposal site selection with GIS and AHP methodology: A case study in Senirkent-Uluborlu (Isparta) Basin, Turkey. *Environmental Monitoring and Assessment*, 173(1–4), 533–554.
- Singh, S. K., Srivastava, P. K., Pandey, A. C., & Gautam, S. K. (2013). Integrated assessment of groundwater influenced by a confluence river system: Concurrence with remote sensing and geochemical modelling. *Water Resources Management*, 27(12), 4291–4313.
- Sreedevi, P. D., Subrahmanyam, K., & Ahmed, S. (2006). The significance of morphometric analysis for obtaining groundwater potential zones in a structurally controlled terrain. *Environmental Geology*, 47(3), 412–420.
- Tehrany MS, Pradhan B, Jebur MN (2013). Spatial prediction of flood susceptible areas using rule based decision tree (DT) and a novel ensemble bivariate and multivariate statistical models in GIS. *J Hydrol*, 504, 69–79.
- Thokala, P., Devlin, N., Marsh, K., Baltussen, R., Boysen, M., & Kalo, Z. (2016). Multiple criteria decision analysis for health care decision making: An introduction: report 1 of the ISPORMCDA Emerging Good Practices Task Force. *Value in Health*, 19(1), 1–13.
- Tiwari, A., Ahuja, A., Vishwakarma, B. D., & Jain, K. (2019). Groundwater Potential Zone (GWPZ) for Urban Development Site Suitability Analysis in Bhopal, India. *Journal of the Indian Society of Remote Sensing*.(doi:<https://doi.org/10.1007/s12524-019-01027-0>).
- Wu, G., De, L.J., Skidmore, A.K., Liu, Y., & Prins, H. H. (2010) Comparison of extrapolation and interpolation methods for estimating daily photosynthetically active radiation (PAR). *Geospatial Information Science*, 13(4), 235–242.
- Yilmaz, I. (2009). Landslide susceptibility mapping using frequency ratio, logistic regression, artificial neural networks and their comparison: a case study from Kat landslides (Tokat—Turkey). *Computers and Geosciences*, 35(6), 1125–1138.

Chapter 8

Assessing the Groundwater Potentiality of the Gumani River Basin, India, using Geoinformatics and Analytical Hierarchy Process



Sadik Mahammad and Aznarul Islam

Abstract Groundwater is vital for human life and development activities. Thus, proper evaluation and management of groundwater resource are required at the village level. The present study aims to assess the groundwater potentiality of the Gumani River Basin (GRB), India, using geoinformatics and analytical hierarchy process (AHP). Ten thematic layers, viz., lithology, geomorphology, slope, relief, drainage density, distance from the river, land use and land covers (LULC), lineament density, soil types, and average rainfall, were used to assess groundwater potentiality. The thematic maps and their classes were assigned weight according to their relative importance to groundwater recharge based on Saaty's 9-point scale and normalized by eigenvector techniques. Groundwater potential index (GPI) was prepared applying the weighted linear combination (WLC) method in GIS environment. The produced groundwater potential map (GPM) was categorized into four classes on the basis of the score of GPI such as low (3–4), moderate (4–5), high (5–6), and very high (6–8). The low potential zone covers ~26% of the GRB with an area of ~3345 km². The moderate potential zone accounts for ~416 km² which is ~32% of the total basin area. The high potential zone accounts for ~305 km² which is ~23% of the total area of the GRB. The very high potential zone comprises ~252 km² which is ~19% of GRB. The produced GPM was validated using the groundwater depth of the 20 locations which depicts the overall producer accuracy of ~80% and overall user accuracy of ~82% coupled with a statistically significant relation ($R^2 = 0.68$) between the observed and predicted water depth.

Keywords Groundwater depth · Groundwater potential index · Multi-criteria decision-making · Weighted linear combination

S. Mahammad · A. Islam (✉)
Department of Geography, Aliah University, Kolkata, India

8.1 Introduction

Groundwater is vital for human life and development activities. Nowadays, the exponential growth of the human population has accelerated the demand for water in the domestic, agricultural, and industrial sectors which diminishes the quantity and quality of groundwater. To address this challenge, proper evaluation and management of groundwater resource are required through the village-level study. The groundwater resource having its occurrence in complex subsurface formations cannot be observed on the earth's surface; hence, its spatiotemporality is difficult to gauge (Nejad et al. 2017). Some parameters like geology, relief, drainage, slope, lineament, soil, vegetation, and land use and land cover of a region may indicate potential storage of groundwater.

Geophysical and geospatial studies have been carried out for groundwater exploration throughout the world (Adhikary et al. 2015). Though geophysical techniques provide proper information about the potentiality of groundwater storage in an aquifer system, it requires huge cost, time, and skilled manpower. However, geospatial techniques proved a very useful tool in assessing, monitoring, and conserving groundwater resources of a large, even an inaccessible, area in a short period of time by dint of its multi-temporal, multispectral high-resolution data and management (Sener et al. 2005; Venkateswaran and Ayyanduraib 2015).

Therefore, many studies have been conducted across the world about the groundwater potential zone using remote sensing (RS) and geographic information system (GIS) techniques (Dar et al. 2011; Magesh et al. 2011; Kumar et al. 2012). Besides, groundwater studies have also been undertaken using geophysical techniques. For example, Vertical Electrical Sounding (VES) integrated with GIS facilitates delineation of groundwater potential zones by assessing the depth of occurrence of groundwater, thickness of the aquifer system, and probable well locations (Sree Devi et al. 2001; Rao et al. 2003; Srivastava and Bhattacharya 2006; Venkateswaran et al. 2014; Ali et al. 2015). Furthermore, various thematic layers such as rainfall, geology, lineaments, soil, drainage density, slope, relief, vegetation cover, and land use and land cover (LULC) have been extracted from the conventional maps and RS data using geospatial techniques and assigned weights according to their relative importance (Ibrahim-Bathis and Ahmed 2016; Ardakani and Ekhtesasi 2016; Singh et al. 2014; Kumar and Dev 2014; Manjare 2014; Periyasamy et al. 2014; Shekhar and Pandey 2014; Elmahdy and Mohamed 2014; Biswas et al. 2013; Reghu et al. 2013; Nag and Ghosh 2012).

Recently, the application of various models such as the frequency ratio (FR) (Manap et al. 2014; Moghaddam et al. 2015; Naghibi et al. 2015; Balamurugan et al. 2017), logistic regression (LR) (Park et al. 2017), weights of evidence (WOE) (Al-Abadi 2015; Lee et al. 2012a, b; Tahmassebipoor et al. 2016), analytical hierarchy process (AHP) (Kumar and Krishna 2016; Al-Abadi and Al-Shamma'a 2014; Rahmati et al. 2015; Sahoo et al. 2015; Shekhar and Pandey 2014), Evidential Belief Function (EBF) (Park et al. 2014; Nampak et al. 2014), fuzzy logic (Şener et al. 2018; Ghayoumian et al. 2007), and artificial neural networks (ANN) (Lee et al.

2012a, b, 2017) is widely noted for demarcating the groundwater potential zones across the world. Besides, different models and their relative applicability have been illustrated in the context of preparing groundwater potential maps as well (Das 2019; Nejad et al. 2017; Chen et al. 2018; Falah et al. 2016; Naghibi and Pourghasemi 2015; Ozdemir 2011; Sahoo et al. 2015; Zeinivand and Nejad 2017).

Previous works carried out at the international framework indicate that most of the studies intend to delineate groundwater potential zones based on such features as geological, geomorphological, and meteorological. Many of the studies (e.g., Ball 1877; Rao and Purushottam 1962; Khan 1987; Singh and Singh 1996; Sanyal and Sengupta 2012; Bhattacharji 2012) related to geological, geomorphological, and paleogeographical aspects were carried out for the present study area. However, a review of the previous literature indicates that there is a gap in the field of groundwater potentiality for the Gumani River Basin (GRB). Therefore, the present study would be a pioneering effort for the GRB to delineate the potentiality of groundwater using AHP. Keeping the above view in mind, the present paper would address the systematic objectives as follows:

- (i) To analyze the thematic layers including lithology, geomorphology, slope, relief, drainage, rainfall, lineaments soil type, and land use and land cover properties of the study area
- (ii) To delineate groundwater potential zones based on the integration of all thematic layers according to their relative importance using AHP

8.2 Study Area

The Gumani River Basin (GRB), the study area, is located in the northeastern part of Jharkhand State of India comprising some portions of the three districts, Sahibganj, Godda, and Pakur. It extends from $24^{\circ}37'20''\text{N}$ to $25^{\circ}13'20''\text{N}$ latitude and $87^{\circ}21'14''\text{E}$ to $87^{\circ}54'40''\text{E}$ longitude, covering an area of $\sim 1307 \text{ km}^2$ (Fig. 8.1). The topographic elevation of the study area ranges from 24 to 590 m above mean sea level (MSL). Lithologically, the study area is mostly constituted by Rajmahal trap (Reddy 2013; Toppo 2013). The soils in the study area are characterized by mainly fine texture. The GRB has dry and humid to sub-humid climate with a normal average rainfall of about 140 cm, most of which is contributed by the SW monsoon from July to September. The maximum temperature rises up to 45°C during the summer months (April–May), while the minimum record of about 7°C is observed during winter (December–January). Gumani, the principal river of the study area, originates from Chota Nagpur Plateau region and flows toward the northeast direction. Morang River, the main tributary of the Gumani River, flows from North to the south to join the Gumani River at Barhait. The combined flow runs toward the east and finally falls into the river Ganga. The GRB depicts a dendritic drainage pattern. The basin is a semi-critical tract, and hence groundwater potentiality assessment becomes significant especially in the context of an agrarian base of economy and huge population pressure.

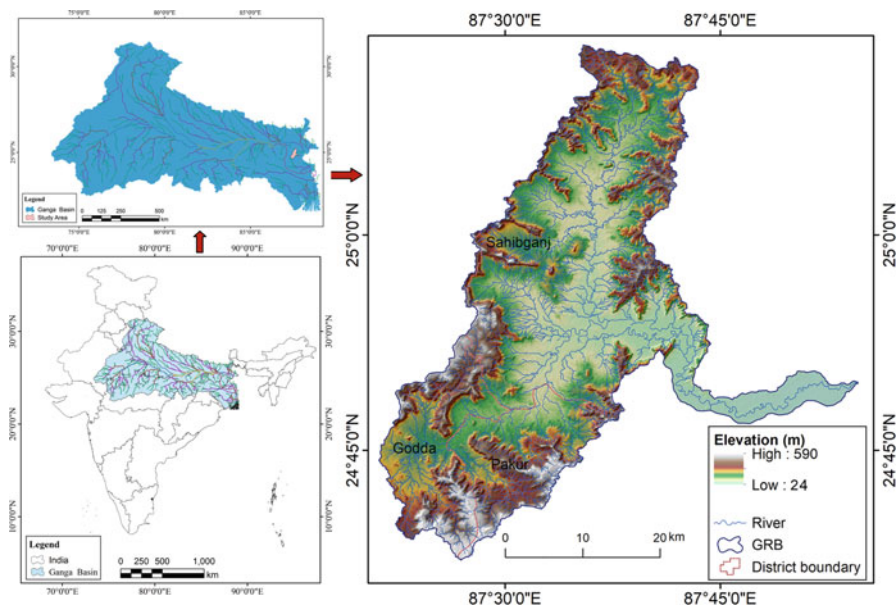


Fig. 8.1 Location of the study area

8.3 Dataset and Methodology

8.3.1 Dataset

The present work is principally based on geospatial data. The quantitative information of basin parameters and properties of the ten thematic parameters such as lithology, geomorphology, slope, relief, drainage density, distance from the river, LULC, lineament density, soil types, and average rainfall have been derived using the RS and GIS. The study utilized the Shuttle Radar Topography Mission (SRTM) Digital Elevation Model (DEM) of 30 m resolution dated 23 September 2014 downloaded from the US Geological Survey (USGS) EarthExplorer to delineate the basin relief and slope properties. A multispectral image of Landsat 8 Operational Land Imager (OLI) (row, 43; path, 139, dated 15 January 2017) was acquired from GloVis USGS for preparing the LULC map. In addition, to get the geomorphic units and arrangements of lineament, the web map service (WMS) was used in ArcGIS toolbox from the Bhuvan website (<https://bhuvan-vec2.nrsc.gov.in/bhuvan/wms>). Survey of India (SOI) topographical maps (72O/8, 72O/12, 72P/5, 72P/6, 72P/9, 72P/10, and 72P/13) of 1974 with the contour interval of 20 meters and scale of 1:50000 were collected. Besides, the geological map with a scale of 1:25000 was collected from the Geological Survey of India (GSI). District-wise soil maps with a scale of 1:50000 were downloaded from the website of the Agriculture Department of Jharkhand (<http://agri.jharkhand.gov.in/>). The average annual rainfall data from

1996 to 2016 have been computed from India-WRIS’s website for Sahibganj, Godda, and Pakur districts. To validate the delineated groundwater potential zone, groundwater level data from May 2015 to January 2016 of the available groundwater wells (only four) have been collected from the groundwater yearbook of Jharkhand for the year 2015–2016 published by the Central Groundwater Board (CGWB 2016). Furthermore, as the Gumani river basin is a data-sparse environment, the groundwater depth data of another 16 validation sites were derived using an interpolation method coupled with the hydro-geomorphic observations of the basin and its surroundings. The interpolation was based on the four CGWB wells within the basin and another 14 CGWB wells from the surrounding areas.

8.3.2 Methodology

8.3.2.1 Methodological Design

A robust and integrated methodology has been adopted to execute this current research (Fig. 8.2). This work is a three-step research. First, the database has been

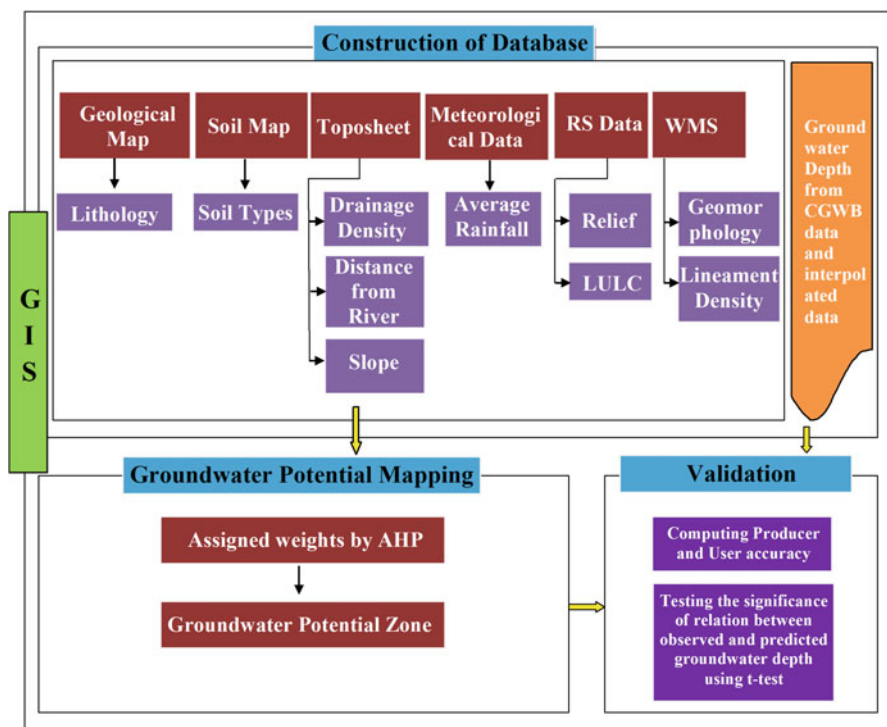


Fig. 8.2 Methodological design to explore groundwater potential zone

constructed using the geological map, soil map, toposheet, rainfall data, satellite image, and data from WMS in GIS.

Second, groundwater potential zones have been delineated using AHP, and third, potential zones have been validated using groundwater depth data.

8.3.2.2 Processing of Geospatial Data

For the extraction of morphometric characteristics such as drainage, relief, and slope properties of the river basin, SRTM DEM and SOI topographical maps have been used. The SRTM DEM has been corrected using the “fill” tool in ArcGIS 10.3.1 software to avoid the local effect on elevation and employed to extract relief of the basin using the software. All topographical maps, geological maps, and soil maps have been geo-referenced adding the longitudinal and latitudinal values of ground control points (GCPs) with total root mean square (RMS) error of <0.02 for better accuracy. Projection systems of topographical maps and conventional maps have been defined as projected coordinate system (PCS) with the Universal Transverse Mercator (UTM) and datum with WGS 1984 and finally rectified in IMAGINE Image format. All the rectified topographical maps are used to make a combined mosaic map using ArcGIS software. The drainage network of the basin has been digitized from the topographical maps and drainage density map generated using the formula after Horton (Horton 1932, 1945). The slope map of the study area is prepared following the algorithm of “Slope” from the toolbox of ArcGIS using DEM. The theme distance from the river is generated using “Euclidean distance” tool in arc toolbox. The relief map is generated from SRTM DEM. Lithology and soil types of the basin have been digitized in vector format from the respective geo-referenced map in ArcGIS software. The arrangements of lineament and the geomorphology of the study area have been extracted from web-based mapping techniques through the GIS server tools in ArcGIS from the thematic services of Bhuvan, Indian Geo-Platform of ISRO (<https://bhuvan-vec2.nrsc.gov.in/bhuvan/wms>), and thus lineament density map is generated. The LULC map of the basin has been prepared from the multispectral image of Landsat 8 OLI in GIS environment. Bands of 5, 4, and 3 have been applied to create a false-color composite (FCC) image. The FCC image has been used to execute supervised classification based on maximum likelihood classification for assessing the five LULC classes of the study area such as vegetation cover, agricultural land, built-up area, waterbody, and fallow land. The average rainfall map has also been created by the interpolation method of rainfall data of Sahibganj, Godda, and Pakur district using inverse distance weighted (IDW) tool in ArcGIS.

8.3.2.3 Assignment Weights and Weights Normalization

In the present study, to delineate groundwater potential zones, ten thematic features, viz., lithology, geomorphology, slope, relief, drainage density, distance from the

Table 8.1 Scale of relative importance

1	Equal importance
3	Moderate importance
5	Strong importance
7	Very strong importance
9	Extreme importance
2,4,6,8	Intermediate value
1/3, 1/5, 1/7, 1/9	Reciprocal value

Table 8.2 Value of random consistency index

n	1	2	3	4	5	6	7	8	9	10
RI	0.00	0.00	0.58	0.90	1.12	1.24	1.32	1.41	1.45	1.49

river, LULC, lineament density, soil types, and average rainfall, were considered. The analytical hierarchy process (AHP) by Saaty (1980) was used to assign the weight of all thematic layers according to their relative importance. It is one of the widely used MCDM techniques in natural resource management (Rahmati et al. 2015). AHP is a multiple-criteria decision-making technique that helps subjective as well as objective features to be taken into account in the decision-making process (Al-Abadi and Al-Shamma'a 2014). The weights were decided based on field experience and on the basis of the literature survey. The weight of all thematic features ranges from 1 (equally significant) to 9 (absolutely significant) (Table 8.1), considering the two features on the basis of the relative importance of groundwater recharge at a time. Pairwise comparison matrices of themes have been done using AHP (Saaty 1980). The pairwise comparison matrix was normalized by the eigenvector technique. The calculated values of normalized weights of the thematic layers were verified for accuracy using consistency ratio (CR) as recommended by Saaty (1980). CR value should be less than 0.10. If the CR value is more than 0.10, the corresponding weights should be re-evaluated to avoid inconsistency (Saaty 1977). To compute for the CR for each theme and feature, the following steps have been followed:

Step 1: Principal eigenvalue (λ) was computed by the eigenvector technique.

Step 2: Consistency index (CI) was calculated from the following equation (Saaty 1980):

$$CI = \lambda_{\max} - n/n - 1$$

where n is the number of criteria or factors.

Step 3: Finally, CR was calculated as (Saaty 1980):

$$CR = CI/RI$$

where RI = random consistency index.

The value of RI was obtained from the Saaty's 1–10 scale (Table 8.2).

8.3.2.4 Delineation of Groundwater Potential Zone

Groundwater potential index (GPI) is an integration of all the thematic layers using the weighted linear combination method:

$$\text{GPI} = L_w L_r + G_w G_r + SL_w SL_r + RE_w RE_r + DD_w DD_r + DR_w DR_r + LULC_w LULC_r + LD_w LD_r + S_w S_r + R_w R_r$$

where “L” stands for lithology, “G” for geomorphology, “SL” for slope, “RE” for relief, “DD” for drainage density, “DR” for distance from the river, “LULC” for land use and land cover, “LD” for lineament density, “S” for soil types, and “R” for rainfall; subscripts $_w$ and $_r$ denote weight and rank, respectively, of each parameter.

8.3.2.5 Validation Techniques

Validation of the delineated groundwater potential zone was carried out with groundwater depth data using accuracy index and significance test (t-test) of the relationship between observed and predicted water depth.

The proposed groundwater potential index is compared to the actual groundwater depth of the selected 20 validation points of the study area using the accuracy index (Story and Congalton 1986):

$$\text{User's accuracy} = \frac{\text{Number of correct pixels in each category}}{\text{Total number of pixels in that category (the row total)}} \times 100$$

$$\text{Producer's accuracy} = \frac{\text{Number of correct pixels in each category}}{\text{Total number of pixels in that category (the column total)}} \times 100$$

$$\text{Overall accuracy} = \frac{\text{Number of all correct pixels (Diagonal total)}}{\text{Total number of reference pixels}} \times 100$$

Furthermore, the Student's t-test technique has been employed to examine the goodness of the relationship between observed groundwater depth and the groundwater potential index of the 20 validation points in the GRB. The t-test (Islam 2016) is performed using the following expression:

$$\text{Student's } t - \text{test}(t) = r \sqrt{\frac{n-2}{1-r^2}}$$

where r is the coefficient of correlation and n is the number of observation.

8.4 Results and Discussion

8.4.1 The Pattern of Factorial Behavior

The major factors influencing the potentiality of the groundwater in the GRB are investigated in the following sections.

8.4.1.1 Lithology

The occurrence and flow of groundwater highly depend on porosity and permeability of the geological horizons that may store and permit to move water (Nair et al. 2017). The study area consists of five lithological units such as alluvium (27.62%), Chota Nagpur gneiss (0.41%), laterites (0.10%), lower Gondwana system (5.39%), and Rajmahal trap (66.47%) (Fig. 8.3a). The basaltic lava flow of Rajmahal trap is the dominant lithological unit in the GRB. The massive rock with low porosity has a little influence on groundwater recharge compared to the weathered rocks associated with high porosity. The vascular litho units and weathered zone and joint and fractured zone of basalt are the limited prospects of groundwater (Toppo 2013; Reddy 2013). The quaternary alluvium is composed of sand and subordinate clay mainly located in northern patches; the middle and eastern part of the basin has good yield prospects of groundwater (Toppo 2013; Reddy 2013). The laterites of Tertiary age group found in the southwestern portion of the basin being originated in situ conditions provide a limited yield prospect of groundwater (Toppo 2013; Reddy

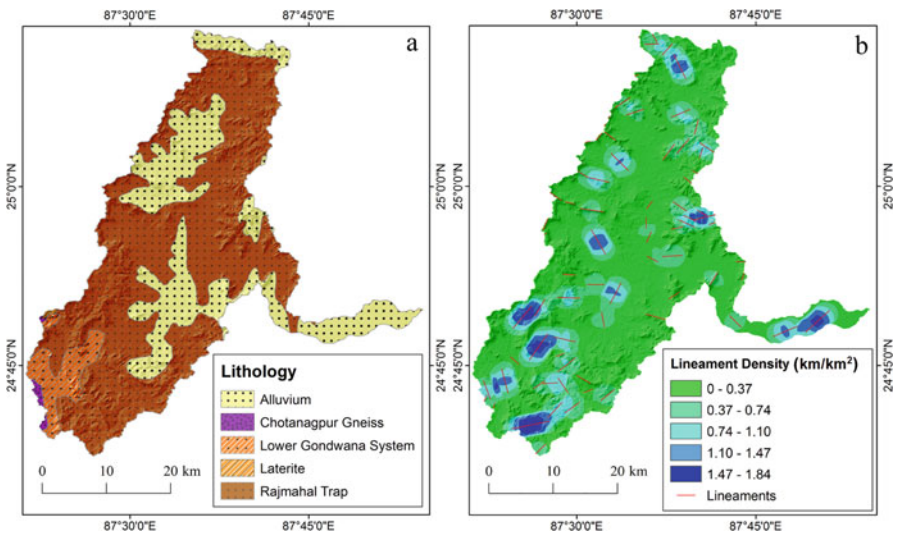


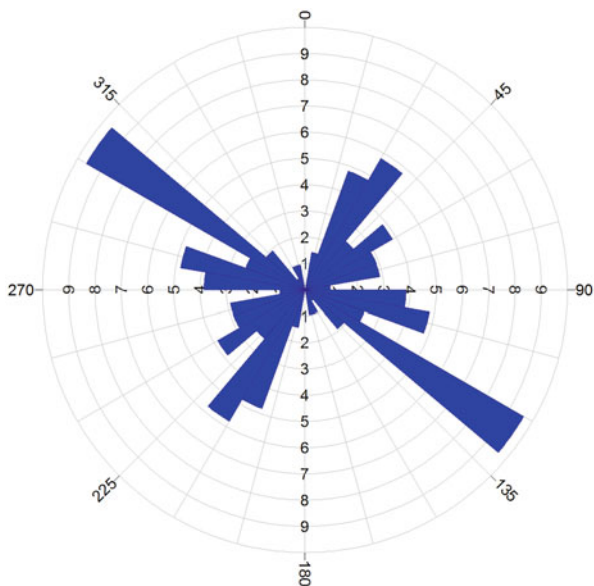
Fig. 8.3 Lithological and structural properties of the study area. (a) Lithology, (b) lineament density

2013). The Gondwana super group formation consisting of sandstone, shale, siltstone, and coal seams is traced in the southwestern portion of the basin and characterized by very good yield prospect of groundwater (Toppo 2013; Reddy 2013). The Precambrian Chota Nagpur gneiss formation consisting of granite gneiss, mica schist amphibolites, etc. is located in the southwestern edge of the basin and associated with moderate yield prospect of groundwater (Toppo 2013; Reddy 2013).

8.4.1.2 Lineaments Density

Lineaments are the surface manifestations of structurally controlled linear or curvilinear features found mainly in hard rock terrains (Kumar and Pandey 2016). Lineaments provide a pathway for groundwater movement and are hydrogeologically very important (Sankar 2002; Mukherjee et al. 2012). In the Gumani River Basin, 124 lineaments have been traced representing mainly joints, fractures, break-in-slope, ridge parallel, and drainage parallel from the Bhuvan portal (Fig. 8.3b). Trend analysis of the percentage frequency of the lineaments reveals that prominent directions of the lineaments of the study have been found from NWW to SSE and from NNE to SWW (Fig. 8.4). Furthermore, the statistical summary indicates that the maximum bin population is 8.13%, the mean bin population is 2.78%, and the standard deviation of bin population is 2.15%. Similarly, maximum bin length is 7.32%, mean bin length is 2.78%, and standard deviation of the bin length is 1.54%. Besides, the vector mean is 65.1 degrees with a confidence interval of 26.1 degrees (80%).

Fig. 8.4 Rose diagram of lineaments within the study area



The lineament density signifying the porosity and permeability of an area is measured as a ratio of the total length of all the lineaments in the basin to the total area of that basin (Nair et al. 2017). Therefore, it can be revealed that the higher the lineament density, the higher the potentiality of groundwater recharges. The lineament density of the GRB varies from 0 to 1.84 km per km². Thus, it has been categorized into five classes such as very high (1.47–1.84 km/km²), high (1.10–1.47 km/km²), moderate (0.74–1.10 km/km²), low (0.37–0.74 km/km²), and very low (0–0.37 km/km²) (Fig. 8.3b).

8.4.1.3 Soil Texture

Soil type is an important factor in groundwater recharge and runoff because the water holding capacity of an area is largely influenced by soil types and their permeability (Murthy 2000). The study area reveals the three types of soil texture such as fine (94.84%), fine loamy (3.61%), and loamy skeletal (1.55%) as shown in the thematic layer of soil (Fig. 8.5a). From the thematic map, it is apparent that fine soil comprises the whole basin except the SW part and NE edge of the basin characterized by low groundwater recharge potentiality due to poor infiltration rate. Fine loamy soil, located on the SW part of the basin, permits a moderate rate of infiltration; hence groundwater potential is higher than fine soil. The loamy-skeletal soil, found on the NE edge of the basin, induces the rate of infiltration, and therefore, the potentiality of groundwater recharge is high. Briefly, the potentiality of groundwater recharge is high for loamy-skeletal soil, moderate for fine loamy soil, and low for fine soil.

8.4.1.4 Geomorphology

The geomorphic imprints may indicate about the status of the surficial characteristics of a terrain that may aid in the identification of subsurface water conditions (Preeja et al. 2011). The GRB consists of various geomorphic features ranging from moderately dissected hills and valleys of structural origin to fluvial origin active floodplains extracted from the web map service (WMS) layer of Bhuvan. Nine geomorphic units have been identified such as moderately dissected hills and valleys of structural origin (42.07%), moderately dissected upper plateau of structural origin (0.19%), dissected lower hills and valleys of structural origin (0.03%), moderately dissected hills and valleys of denudational origin (0.16%), moderately dissected lower plateau of denudational origin (0.01%), pediment-pediplain complex of denudational origin (55.27%), older floodplain of fluvial origin (1.06%), active floodplain of fluvial origin (0.12%), and water bodies (1.08%) (Fig. 8.5b). The geomorphological units of the GRB are a result of the geological evolution, and its distribution varies with respect to lithology, elevation, and proximity to the river systems. Moderately dissected hills and valleys of structural origin, characterized by steep slope on all directions, high elevation, dense forest cover, and high drainage

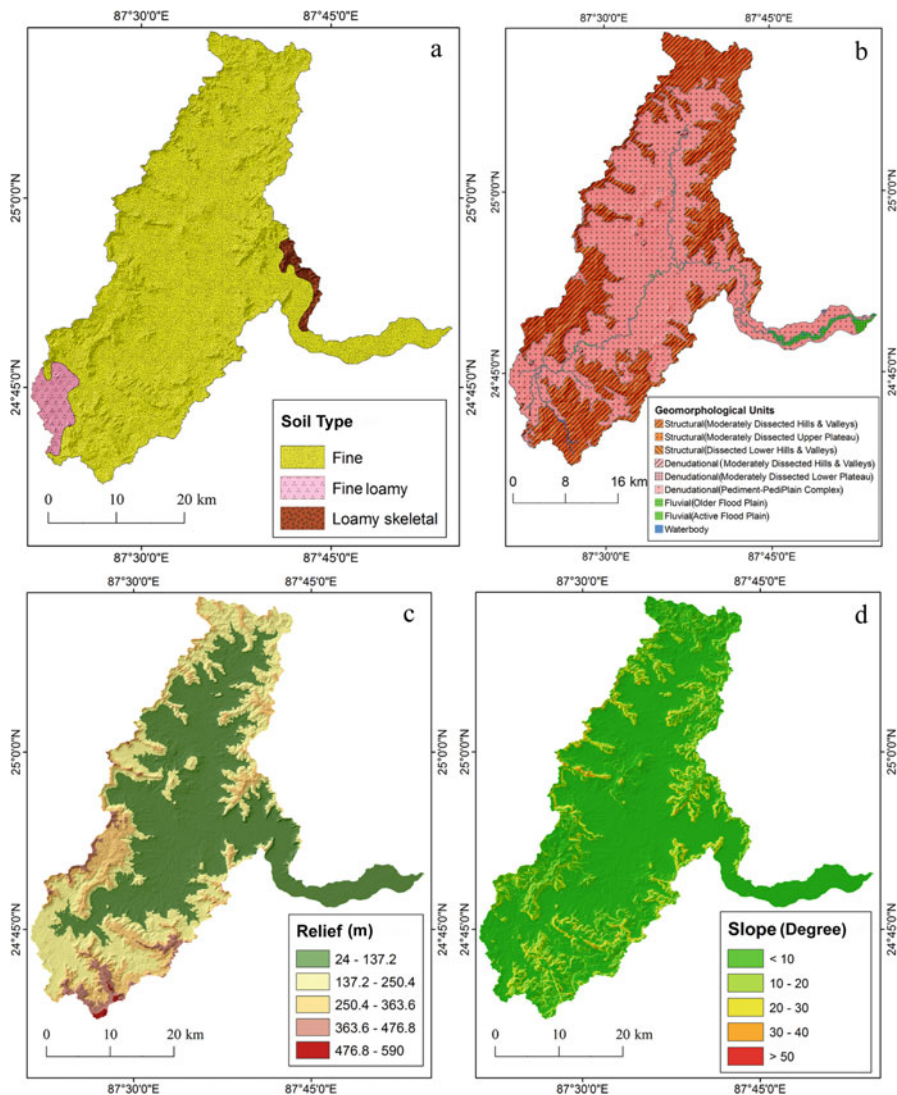


Fig. 8.5 Pedo-geomorphological characteristics: (a) Soil type, (b) geomorphological units, (c) relief, (d) slope

density, have bounded the GRB on every side except SW portion and lower reach of the basin. Moderately dissected upper plateau and dissected lower hills and valleys of structural origin are isolated in the middle part and SW part of the basin, respectively. The dominant geomorphic unit of the GRB located in upper, middle and SW parts of the basin is the denudationally originated pediment and pediplain complex with a gentle slope, flat topography, and low elevation. It is associated with moderately dissected hills, valleys, and lower plateau of denudational origin. The

floodplains are depositional landforms constituted by gravel, sand, and clay carried by the river system. The fluvial origin older floodplain is situated on the banks of the Gumani River especially near the confluence point of the lower reaches and the active floodplains. The potentiality of groundwater recharge is good to excellent in a waterbody, older and active floodplain of fluvial origin, and pediment-pediplain complex of denudational origin.

8.4.1.5 Relief

Relief, the difference in elevation from highest to lowest altitude of the basin (Smith 1935), plays an important role in groundwater recharge, for high relief coupled with steep slope increases runoff and thereby decreases infiltration. On the other hand, lower relief with the gentle slope decreases runoff and helps more water to infiltrate. Therefore, the area of high relief has less potential for groundwater recharge, while the area with low relief has a high potential for groundwater recharge. The relief of the study area is categorized into five equal classes such as very low (24–137.2 m), low (137.2–250.4 m), moderate (250.4–363.6 m), high (363.6–476.8 m), and very high (476.8–590 m) (Fig. 8.5c).

8.4.1.6 Slope

Slope is a dominant factor that strongly affects groundwater recharge. For example, the area with gentle slope offers more resistance time for the percolation of rainwater. However, the area with high slope increases surface runoff allowing less resistance time for rainwater (Prasad et al. 2008). Therefore, the area with a gentle slope has more potential than that of a steep slope. The slope of the study area has been grouped into five equal categories ranging from very gentle to very steep slope (Fig. 8.5d). The distributional pattern depicts that the slope gradually increases from the center to the fringe area of the basin except in lower reaches and the SW section. The very gentle slope (<10 degree) is located in the middle portion and lower reaches of the basin and also SW part with a very high potentiality of groundwater. The gentle slope (10–20 degrees) is located around the very gentle slope area with high potentiality. The moderate slope (20–30 degrees) is located on the fringe area of the basin and characterized by moderately potential zone. The steep slope (30–40 degree) is located on the eastern and western edges of the south part of the basin, while the very steep slope (>50 degree) is found on the western-eastern fringe and southern part of the basin. The steep and very steep slope is characterized by the low and very low potential of groundwater recharge, respectively.

8.4.1.7 Average Rainfall

Rainfall is a major source of water that determines the amount of water that would be available to percolate into the groundwater system (Agarwal et al. 2013). Therefore, the area with higher rainfall induces higher potentiality for groundwater recharge than the area with lower rainfall. The average annual rainfall from 1996 to 2016 ranges from 1492.69 to 1617.62 mm; most of which occurs in monsoon season. The distribution of rainfall is grouped into three classes such as high (1575.97–1617.62 mm), moderate (1534.33–1575.97 mm), and low (1492.69–1534.33 mm) (Fig. 8.6a). The amount of rainfall is higher in the northern part and gradually decreases toward the south of the study area.

8.4.1.8 Drainage Density

Drainage density is the length of streams per unit area of a basin (Horton 1932). The hard rock terrain, characterized by a low infiltration rate, has high drainage density, while the alluvial terrain with a high permeability rate has low drainage density (Kale and Gupta 2010). So the relationship between drainage density and groundwater recharge potentiality is inversely related. Based on the relationship, it should be noted that the higher the drainage density, the lower the degree of groundwater recharge potential and vice versa. The drainage density of the basin is classified into five classes such as very low (0–0.68 km/km²), low (0.68–1.36 km/km²), moderate (1.36–2.03 km/km²), high (2.03–2.71 km/km²), and very high (2.71–3.39 km/km²) (Fig. 8.6b). Therefore, very low drainage density has very high potential of groundwater.

8.4.1.9 Distance from the River

Distance from the river represented by the proximity of the rivers and drainages in the area (Nejad et al. 2017) is an important factor in groundwater recharge. The area close to the river has more groundwater potential than the area far away from the streams. In the present study, this factor is grouped into five classes, namely, very low (0–300 m), low (300–600 m), moderate (600–900 m), high (900–1200 m), and very high (1200–1500 m) (Fig. 8.6c).

8.4.1.10 Land Use and Land Cover

Land use and land cover (LULC) of an area plays a significant role in groundwater recharge. Vegetation cover is an effective factor in the enhancement of the recharge rate because it reduces the rate of surface runoff and percolates more water through roots (Islam and Guchhait 2015), while man-made constructions have the

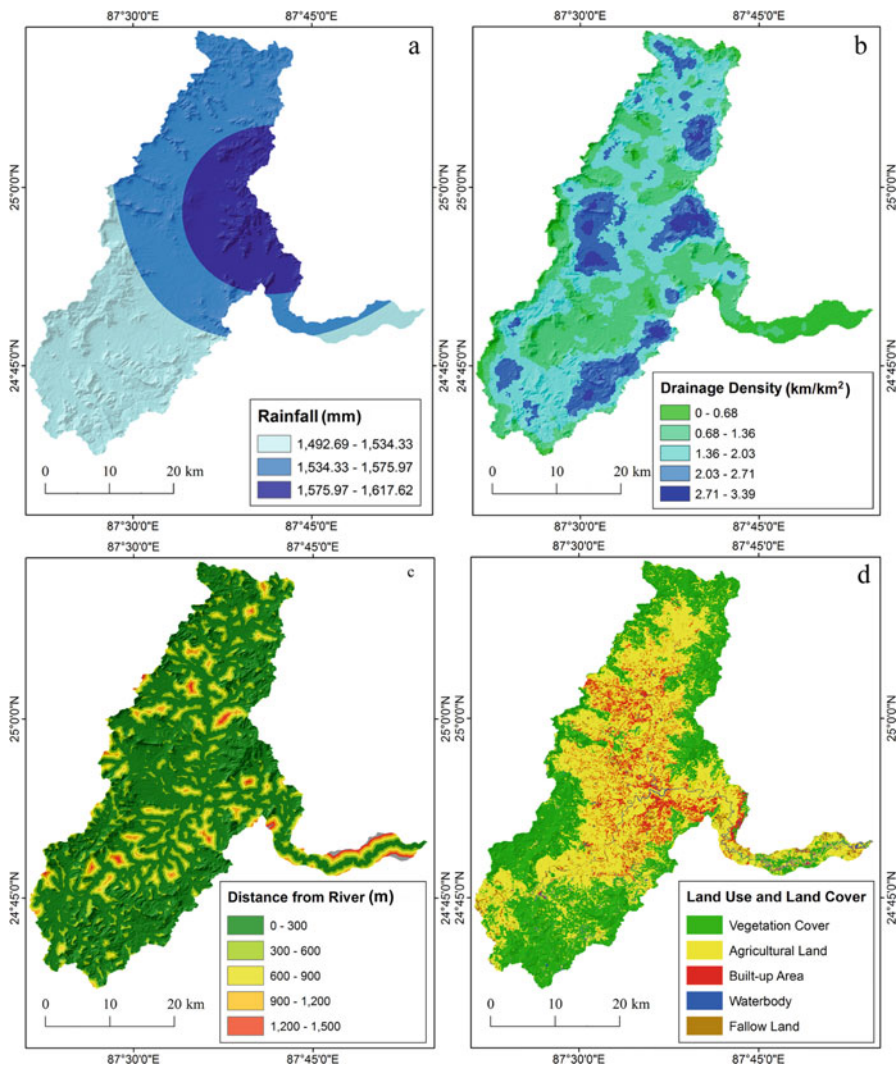


Fig. 8.6 Climate, drainage, and LULC. (a) Average rainfall, (b) drainage density, (c) distance from the river, (d) LULC

characteristic of low groundwater recharge (Shaban et al. 2006). The study area consists of five types of land use and land cover such as vegetation cover, agricultural land, built-up area, fallow land, and waterbody (Fig. 8.6d). The thematic map reveals that agricultural land (48.27%) is the dominant LULC type followed by vegetation cover (40.86%), built-up area (7.62%), fallow land (1.62%), and waterbody (1.62%). The accuracy index of the LULC has been done in which the overall accuracy of supervised classification is 92% and Kappa coefficient is 0.9 which indicates the high precision of image classification (Table 8.3). In terms of

Table 8.3 Accuracy index for land use and land cover

LULC	Vegetation cover	Agricultural land	Built-up area	Waterbody	Fallow land	Total	User's accuracy (%)
Vegetation	37	1	0	0	0	38	97.36
Agricultural land	2	39	3	1	6	51	76.47
Built-up area	0	0	37	1	1	39	94.87
Waterbody	1	0	0	38	0	39	97.43
Fallow land	0	0	0	0	33	33	100
Total	40	40	40	40	40		
Product's accuracy (%)	92.5	97.5	92.5	95	82.5		
Overall accuracy = $(37 + 39 + 37 + 38 + 37)/400 = 92\%$, Kappa coefficient = 0.9							

user's accuracy, all the classes except agricultural land are over 90%, and in the case of producer's accuracy, all the classes are above 90% except fallow land (82.5%).

8.4.2 Groundwater Potential Zones

The groundwater potential zone of the GRB has been delineated using the integration of all thematic layers like lithology, geomorphology, slope, relief, drainage density, distance from the river, lineament density, land use and land cover, soil types, and average annual rainfall according to their relative importance to groundwater recharge. Assessment of the final GPI using the ten thematic features has been done following a three-step process: pairwise comparison matrix, normalized pairwise comparison matrix, and integrated individual ranks of each class with the normalized weight of the respective theme. In the pairwise comparison matrix (Table 8.4), developments of the hierarchical structure of all the themes have been done based on the relative importance of different features with respect to groundwater recharge.

In the matrix table, the value of the column theme was defined based on how it is important with respect to the row theme and listed as the value row elements divided by the value column element, while the value of row elements is listed as the value of column element divided by the value of row element. The values of diagonal elements are 1 because the theme of the column is equally important to the same theme of the row. The normalized pairwise matrix is computed as all the elements of the column divided by the sum of the column (Table 8.5).

The criteria weights are calculated by averaging all the elements of the row. Therefore, it can be found that the lithology has the maximum normalized weight as 0.277582 followed by geomorphology (0.173482), slope (0.140833), relief

Table 8.4 Pairwise comparison matrix

Themes	Lithology	Geomorphology	Slope	Relief	Drainage density	Distance from the river	LULC	Lineament density	Soil types	Rainfall
Lithology	1	2	3	4	5	5	5	5	6	7
Geomorphology	0.5	1	2	2	2	3	4	5	6	6
Slope	0.33	0.5	1	2	2	3	4	4	5	6
Relief	0.25	0.5	0.5	1	2	2	3	4	5	6
Drainage density	0.2	0.5	0.5	0.5	1	2	3	3	4	5
Distance from the river	0.2	0.33	0.33	0.5	0.5	1	2	3	4	4
LULC	0.2	0.25	0.25	0.33	0.33	0.5	1	2	3	4
Lineament density	0.2	0.2	0.25	0.25	0.33	0.33	0.5	1	2	3
Soil types	0.16	0.16	0.2	0.2	0.25	0.25	0.33	0.5	1	2
Rainfall	0.14	0.16	0.16	0.16	0.2	0.25	0.25	0.33	0.5	1

Table 8.5 Normalized pairwise comparison matrix

Themes	Lithology	Geomorphology	Slope	Relief	Drainage density	Distance from the river	LULC	Lineament density	Soil types	Rainfall	Criteria weights
Lithology	0.31	0.35	0.37	0.37	0.37	0.29	0.22	0.18	0.16	0.16	0.28
Geomorphology	0.15	0.17	0.24	0.18	0.15	0.17	0.17	0.18	0.16	0.14	0.17
Slope	0.10	0.09	0.12	0.18	0.15	0.17	0.17	0.14	0.14	0.14	0.14
Relief	0.07	0.09	0.06	0.09	0.15	0.12	0.13	0.14	0.14	0.14	0.11
Drainage density	0.06	0.09	0.06	0.05	0.07	0.12	0.13	0.11	0.11	0.11	0.09
Distance from the river	0.06	0.06	0.04	0.05	0.04	0.06	0.09	0.11	0.11	0.09	0.07
LULC	0.06	0.04	0.03	0.03	0.02	0.03	0.04	0.07	0.08	0.09	0.05
Lineament density	0.06	0.04	0.03	0.02	0.02	0.02	0.02	0.04	0.05	0.07	0.04
Soil types	0.05	0.03	0.02	0.02	0.02	0.01	0.01	0.02	0.03	0.05	0.03
Rainfall	0.04	0.03	0.02	0.02	0.01	0.01	0.01	0.01	0.01	0.02	0.02
Consistency ratio = 0.041379											

(0.112891), drainage density (0.09081), distance from the river (0.069764), LULC (0.050968), lineament density (0.037584), soil types (0.026257), and rainfall (0.019831) (Table 8.6).

Each class of the thematic layer is assigned a rank as per Saaty's 1–9-point scale (Table 8.1), and GPI was defined by multiplying the class rank with the respective theme normalized weights. The consistency ratio (Table 8.5) has been calculated to check the accuracy of the calculated value. The final map of the groundwater potentiality of the basin depicts the GPI ranges from 3 to 8. It has been categorized into four classes on the basis of the natural breaks (Jenks) of the GPI such as low (3–4), moderate (4–5), high (5–6), and very high (6–8) (Fig. 8.7). The area distribution of the groundwater potential zones reveals that the GRB occupies the highest area of the moderate potential zone. It accounts for ~416.09 km² (31.84%) of the total area of the GRB. The lowest area is occupied by very high potential zone which accounts for an area of ~251.65 km² (19.25%) of the GRB. The low potential zone accounts for an area of ~334.67 km² (25.61%) of the GRB. The high potential zone covers an area of ~304.63 km² (23.31%) of the total basin area (Table 8.7).

8.4.3 Validation

The study area consists of twenty validation points located in the four groundwater potential zones (Fig. 8.7). Out of the twenty points, seven (Sundarpahari, Ranga, Borio, Pokharia, Chhota Banguon, Kadma, and Chandpur) are located in the very high potential zone, four wells (Sabaiya, Jhimuli, Barhait, and Dariapur) are located in the high potential zone, five wells (Hiranpur, Dharampur, Busjori, Mugdi, and Manjhladih) are located in the moderate potential zone, and four wells (Dumeri, Chhota Paktoli, Jampata, and Matia Bedo) are located in the low potential zone. The accuracy index of the groundwater potential map (GPM) has been done in which the user's accuracy of the low, moderate, and high potential zones portrays an overall level of 75% precision, while the very high potential zone shows a 71.43% precision. In terms of the producer's accuracy, all the classes have precision levels above 80%, except for the class of high potential (60%). Overall accuracy is 80%, which indicates the high precision of GPM (Table 8.8).

Furthermore, a bivariate correlation was run between the observed groundwater depth and potential groundwater depth as expressed through the GPI which gleans out that there is a strong correlation ($R^2 = 0.68$) between the variables under consideration (Fig. 8.8).

The analysis of goodness of the relationship between groundwater depth and the GPI of the 20 validation points in the GRB has been examined with the help of the Student's t-test. At 18 degrees of freedom ($df = n-2$), the computed t-value is 6.124, while the tabulated t-value is 2.101 for the 0.05 level of significance, implying a statistically significant relationship between the observed and predicted water depth at 95% level of confidence. It may be inferred that the potential zones are in good order with reality.

Table 8.6 Assigned and normalized weights of different classes of ten thematic layers for delineation of groundwater potential zone

Themes	Class	Rank	Normalized weight
Lithology	Lower Gondwana system	7	0.277582
	Alluvium	6	
	Laterites	5	
	Chota Nagpur gneiss	3	
	Rajmahal trap	2	
Geomorphology	Structural (moderately dissected hills and valleys)	1	0.173482
	Structural (moderately dissected upper plateau)	2	
	Structural (dissected lower hills and valleys)	3	
	Denudational (moderately dissected hills and valley)	4	
	Denudational (moderately dissected lower plateau)	5	
	Denudational (pediment-pediplain complex)	6	
	Fluvial (older floodplain)	7	
	Fluvial (active floodplain)	8	
	Waterbody	8	
Slope	<10	9	0.140833
	10–20	7	
	20–30	5	
	30–40	3	
	>40	1	
Relief	24–137.2	9	0.112891
	137.2–250.4	7	
	250.4–363.6	5	
	363.6–476.8	3	
	476.8–590	1	
Drainage density	0–0.68	9	0.09081
	0.68–1.36	7	
	1.36–2.03	5	
	2.03–2.71	3	
	2.71–3.39	1	
Distance from the river	<300	9	0.069764
	300–600	7	
	600–900	5	
	900–1200	3	
	>1500	1	
LULC	Waterbody	7	0.050968
	Vegetation cover	7	
	Agricultural land	5	
	Fallow land	2	
	Built-up area	1	

(continued)

Table 8.6 (continued)

Themes	Class	Rank	Normalized weight
Lineament density	0–0.37	1	0.037584
	0.37–0.74	3	
	0.74–1.10	5	
	1.10–1.47	7	
	1.47–1.84	9	
Soil types	Fine	3	0.026257
	Fine loamy	5	
	Loamy skeletal	7	
Rainfall	1492.69–1534.33	3	0.026257
	1534.33–1575.97	5	
	1575.97–1617.62	7	

8.5 Conclusion

With the specific contribution of the ten thematic layers and their classes, the groundwater potential zone of GRB has been delineated. The weighted overlay techniques were used to ingrate the relative importance of each thematic layer and its constituting classes. The final output of the groundwater potential zone has been categorized into four classes based on the GPI such as low (3–4), moderate (4–5), high (5–6), and very high (6–8). The low potential zone covers 25.61% GRB having an area of $\sim 334.67 \text{ km}^2$. The moderate potential zone accounts for $\sim 416.09 \text{ km}^2$ which is 31.83% of the total basin area. The high potential zone accounts for $\sim 304.63 \text{ km}^2$ which is 23.31% of the total area of GRB. The very high potential zone consists of $\sim 251.65 \text{ km}^2$ which is 19.25% of GRB. The delineated groundwater potential zone is highly correlated with lithology geomorphology relief and slope of the basin. The delineated potential zone has been validated by the groundwater depth of the validation points using accuracy assessment and Student's t-test which reveals significant accuracy of the validation. Therefore, the present study unearths that RS and GIS are important tools to assess groundwater potentiality through different thematic layers using AHP techniques, and it will be used in the context of future development and planning activity of the basin.

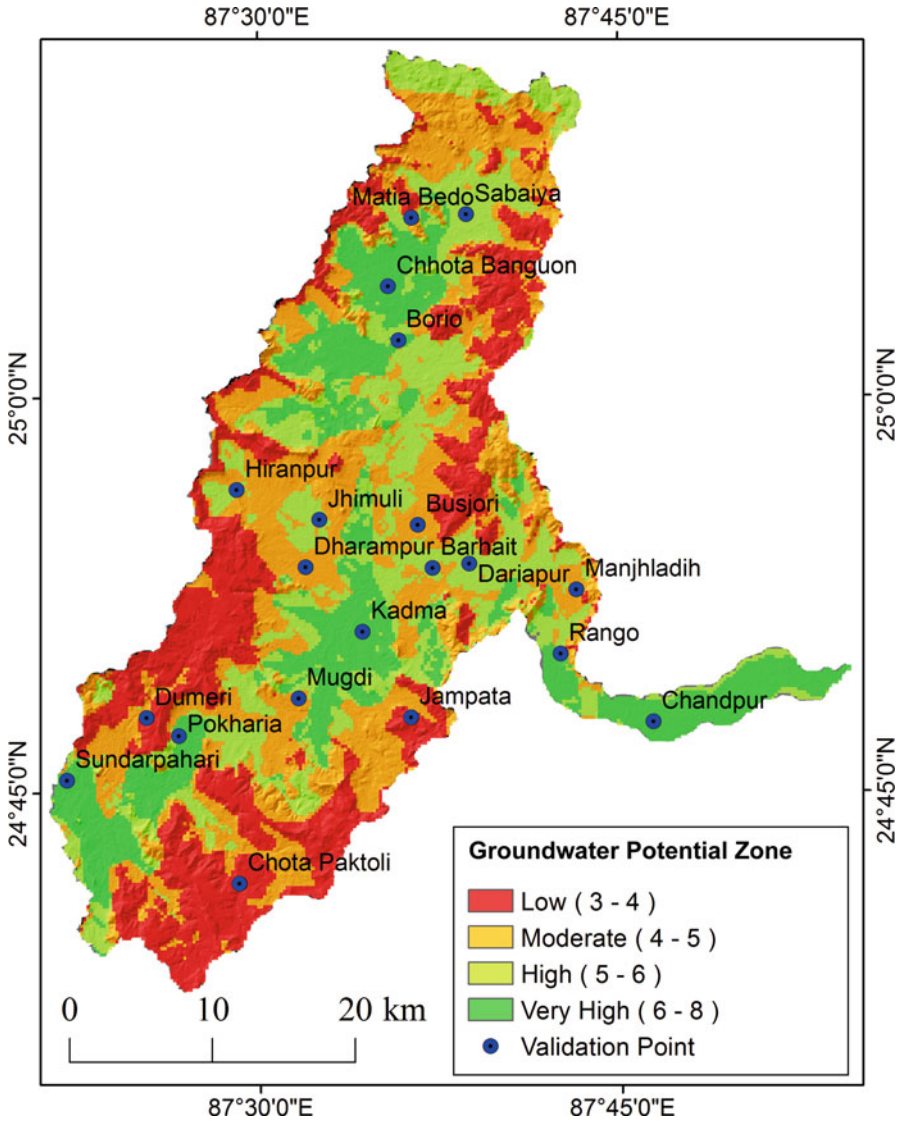


Fig. 8.7 Groundwater potential map of the study area

Table 8.7 Areal distribution of groundwater potential zone

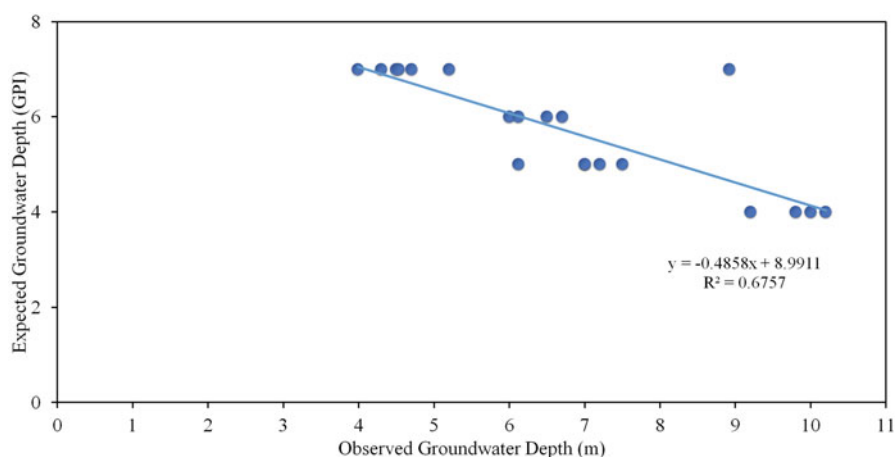
Groundwater potential zone	Area (km ²)	Area (%)
Low	334.666094	25.60506
Moderate	416.088664	31.83464
High	304.626729	23.30677
Very high	251.6495369	19.25352
Total	1307.031024	100

Table 8.8 Accuracy index for groundwater potential zone

Groundwater potential zone	Low	Moderate	High	Very High	Total	User's accuracy (%)
Low	4	0	0	0	4	100
Moderate	0	4	1	0	5	80
High	0	1	3	0	4	75
Very high	1	0	1	5	7	71.4286
Total	5	5	5	5		
Producer's accuracy (%)	80	80	60	100		

Overall accuracy = $4 + 4 + 3 + 5/20 = 80\%$

Source: Computed by the authors based on Groundwater Yearbook, Jharkhand (2015–2016), and field observation

**Fig. 8.8** Correlation between GPI and groundwater depth

References

- Adhikary, P.P., Chandrasekharan, H., Dubey, S.K., Trivedi, S.M., Dash, C.J. (2015). Electrical resistivity tomography for assessment of groundwater salinity in west Delhi, India, *Arabian Journal of Geosciences* 8 (5), 2687–2698.
- Agarwal, E., Agarwal, R., Garg, R. D., & Garg, P. K. (2013). Delineation of groundwater potential zone: An AHP/ANP approach. *J. Earth Syst. Sci.*, 122 (3), 887–898.
- Al-Abadi, A. M. (2015). Groundwater potential mapping at northeastern Wasit and Missan governorates, Iraq using a data-driven weights of evidence technique in framework of GIS. *Environ Earth Sci*, 74, 1109–1124.
- Al-Abadi, A., & Al-Shamma'a, A. (2014). Groundwater Potential Mapping of the Major Aquifer in Northeastern Missan Governorate, South of Iraq by Using Analytical Hierarchy Process and GIS. *Journal of Environment and Earth Science*, 4 (10), 125–150.
- Ali, Y. H., Prijju, C. P., & Prasad, N. N. (2015). Delineation of Groundwater Potential Zones in Deep Midland Aquifer along Bharathapuzha River Basin, Kerala using Geophysical Method. *Science Direct*, 4, 1039–1046.

- Ardakani, A. H., & Ekhtesasi, M. R. (2016). Groundwater potentiality through Analytic Hierarchy Process (AHP) using remote sensing and Geographical Information System (GIS). *JGeope*, 6 (1), 75–88.
- Balamurugan, G., Seshan, K., & Bera, S. (2017). Frequency ratio model for groundwater potential mapping and its sustainable management in cold desert, India. *Journal of King Saud University – Science*, 29, 333–347.
- Ball, V. (1877). *Geology of Rajmahal Hills Mem. Geol Surv Ind.*, 13 (1).
- Bhattacharji, M. (2012). Topographic features of the Gumani River Basin, Rajmahal volcanic province, Jharkhand: An example of exhumed of topography or palaeotopographic control? *Journal of Indian Geomorphology*, 1, 45–54.
- Biswas, A., Jana, A., & Mandal, A. (2013). Application of Remote Sensing, GIS and MIF technique for Elucidation of Groundwater Potential Zones from a part of Orissa coastal tract, Eastern India. *Research Journal of Recent Science*, 2 (11), 42–49.
- Chen, W., Li, H., Hou, E., Wang, S., Wang, G., Panahi, M., et al. (2018). GIS-based groundwater potential analysis using novel ensemble weights-of-evidence with logistic regression and functional tree models. *Science of the Total Environment*, 634, 853–867.
- CWGB. (2016). *Ground Water Year Book, Jharkhand (2015-2016)*. Central Ground Water Board.
- Dar, I. A., Sankar, K., & Dar, M. A. (2011). Deciphering groundwater potential zones in hard rock terrain using geospatial technology. *Environ Monit Assess*, 173, 597–610.
- Das, S. (2019). Comparison among influencing factor, frequency ratio and analytical hierarchy process techniques for groundwater potential zonation in Vaitarna basin, Maharashtra, India. *Groundwater for Sustainable Development*, 8, 617–629.
- Elmahdy, S. I., & Mohamed, M. M. (2014). Groundwater potential modelling using remote sensing and GIS: a case study of the Al Dhaid area, United Arab Emirates. *Geocarto International*, 29 (4), 433–450.
- Falah, F., Nejad, S. G., Rahmati, O., Daneshfar, M., & Zeinivand, H. (2016). Applicability of generalised additive model in groundwater potential modelling and comparison its performance by bivariate statistical methods. *Geocarto International*, <https://doi.org/10.1080/10106049.2016.1188166>.
- Ghayoumian, J., Saravi, M. M., Feiznia, S., Nouri, B., & Malekian, A. (2007). Application of GIS techniques to determine areas most suitable for artificial groundwater recharge in a coastal aquifer in southern Iran. *Journal of Asian Earth Sciences*, 30, 364–374.
- Horton, R. E. (1932). *Drainage Basin Characteristics*. Transactions American Geophysical Union, 350–361.
- Horton, R. E. (1945). *Erosional Development of Streams and Their Drainage Basin; Hydrophysical Approach to Quantitative Morphology*. Geological Society of America Bulletin, 56 (3), 275–370.
- Ibrahim-Bathis, K., & Ahmed, S. A. (2016). Geospatial technology for delineating groundwater potential zones in Doddahalla watershed. *The Egyptian Journal of Remote Sensing and Space Sciences*, 19, 223–234.
- Islam, A and Guchhait, SK (2015). Integrating channel instability, bank erosion and land use planning along the left bank of River Bhagirathi in Nadia district, West Bengal. *River Behaviour & Control*, Vol.34, 2013–14 - pages 11–26
- Islam, A. (2016). *River Bank Erosion and Its Impact on Economy and Society A Study Along the Left Bank of River Bhagirathi in Nadia District West Bengal*. An Unpublished PhD thesis. The University of Burdwan.
- Kale, V. S., & Gupta, A. (2010). *Introduction to geomorphology*. Hyderabad: Universities Press (India) Private Limited.
- Khan, Z. A. (1987). *Paleodrainage and Paleochannel Morphology of A Barakar River (Early Permian) in the Rajmahal Gondwana Basin, Bihar, India*. *Palaeogeography, Palaeoclimatology, Palaeoecology*, 58, 235–247.
- Kumar, A., & Krishna, A. P. (2016). Assessment of groundwater potential zones in coal mining impacted hard-rock terrain of India by integrating geospatial and analytic hierarchy process (AHP) approach. *Geocarto International*, <https://doi.org/10.1080/10106049.2016.1232314>.

- Kumar, A., & Pandey, A. C. (2016). Geoinformatics based groundwater potential assessment in hardrock terrain of Ranchiurban environment, Jharkhand state (India) using MCDM–AHP techniques. *Groundwaterfor Sustainable Development*, 2 (3), 27–41.
- Kumar, D., & Dev, P. (2014). Groundwater Potential Zone Identification of Karwi Area, Mandakini River Basin, Uttar Pradesh Using Remote Sensing and GIS Techniques. *International Journal of Engineering Science Invention*, 10–19.
- Kumar, S. K., Chandrasekar, N., Seralathan, P., Godson, P. S., & Magesh, N. S. (2012). Hydrogeochemical study of shallow carbonate aquifers, Rameswaram Island, India. *Environ Monit Assess*, 184, 4127–4138.
- Lee, S., Kim, Y.-S., & Oh, H.-J. (2012a). Application of a weights-of-evidence method and GIS to regional groundwater productivity potential mapping. *Journal of Environmental Management*, 96, 91–105.
- Lee, S., Song, K.-Y., Kim, Y., & Park, I. (2012b). Regional groundwater productivity potential mapping using a geographic information system (GIS) based artificial neural network model. *Hydrogeology Journal*, 20, 1511–1527.
- Leea, S., Hong, S.-M., & Jung, H.-S. (2017). GIS-based groundwater potential mapping using artificial neural network and support vector machine models: the case of Boryeong city in Korea. *Geocarto International*, <https://doi.org/10.1080/10106049.2017.1303091>.
- Magesh, N. S., Chandrasekar, N., & Soundranayagam, J. P. (2011). Morphometric evaluation of Papanasam and Manimuthar watersheds, parts of Western Ghats, Tirunelveli district, Tamil Nadu, India: a GIS approach. *Environ Earth Sci*, 64, 373–381.
- Manap, M. A., Nampak, H., Pradhan, B., Lee, S., Sulaiman, W. N., & Ramli, M. F. (2014). Application of probabilistic-based frequency ratio model in groundwater potential mapping using remote sensing data and GIS. *Arab J Geosci*, 7, 711–724.
- Manjare, B. S. (2014). Identification of groundwater prospecting zones using Remote Sensing and GIS techniques in upper Vena river watersheds Nagpur district, Maharashtra, India. 15th Esri India User Conference (pp. 1–14). Esri India.
- Moghaddam, D. D., Rezaei, M., Pourghasemi, H. R., Pourtaghie, Z. S., & Pradhan, B. (2015). Groundwater spring potential mapping using bivariate statistical model and GIS in the Taleghan Watershed, Iran. *Arab J Geosci*, 8, 913–929.
- Mukherjee, P., Singh, C. K., & Mukherjee, S. (2012). Delineation of Groundwater Potential Zones in Arid Region of India—A Remote Sensing and GIS Approach. *Water Resour. Manage.*, 26, 2643–2672.
- Murthy, K. S. R. (2000). Ground water potential in a semi-arid region of Andhra Pradesh – a geographical information system approach. *International Journal of Remote Sensing*, 21 (9), 1867–1884.
- Nag, S. K., & Ghosh, P. (2012). Delineation of groundwater potential zone in Chhatna Block, Bankura District, West Bengal, India using remote sensing and GIS techniques 2012. *Environ Earth Sci*, <https://doi.org/10.1007/s12665-012-1713-0>
- Naghibi, S. A., & Pourghasemi, H. R. (2015). A Comparative Assessment Between Three Machine Learning Models and Their Performance Comparison by Bivariate and Multivariate Statistical Methods in Groundwater Potential Mapping. *Water Resour Manage*, 29, 5217–5236.
- Naghibi, S. A., Pourghasemi, H. R., Pourtaghi, Z. S., & Rezaei, A. (2015). Groundwater qanat potential mapping using frequency ratio and Shannon’s entropy models in the Moghan watershed, Iran. *Earth Sci Inform*, 8, 171–186.
- Nair, H. C., Padmalal, D., Joseph, A., & Vinod, P. G. (2017). Delineation of Groundwater Potential Zones in River Basins Using Geospatial Tools—an Example from Southern Western Ghats, Kerala, India. *J geovis spat anal*, <https://doi.org/10.1007/s41651-017-0003-5>.
- Nampak, H., Pradhan, B., & Manap, M. A. (2014). Application of GIS based data driven evidential belief function model to predict groundwater potential zonation. *Journal of Hydrology*, 513, 283–300.
- Nejad, S. G., Falah, F., Daneshfar, M., Haghizadeh, A., & Rahmati, O. (2017). Delineation of groundwater potential zones using remote sensing and GIS-based data-driven models. *Geocarto International*, 32 (2), 167–187.

- Ozdemir, A. (2011). GIS-based groundwater spring potential mapping in the Sultan Mountains (Konya, Turkey) using frequency ratio, weights of evidence and logistic regression methods and their comparison. *Journal of Hydrology*, 411, 290–308.
- Park, I., Kim, Y., & Lee, S. (2014). Groundwater Productivity Potential Mapping Using Evidential Belief Function. *Groundwater*, 52, 201–207.
- Park, S., Hamm, S.-Y., Jeon, H.-T., & Kim, J. (2017). Evaluation of Logistic Regression and Multivariate Adaptive Regression Spline Models for Groundwater Potential Mapping Using R and GIS. *Sustainability*, <https://doi.org/10.3390/su9071157>.
- Periyasamy, P., Sudalaimuthu, M., Nanda, S., & Sundaram, A. (2014). Application of RS and GIS Technique for Identifying Groundwater Potential Zone in Gomukhi Nadi Sub Basin, South India. *International Journal of Environment, Chemical, Ecological, Geological and Geophysical Engineering*, 8 (12), 867–873.
- Prasad, R. K., Mondal, N. C., Banerjee, P., Nandakumar, M. V., & Singh, V. S. (2008). Deciphering potential groundwater zone in hard rock through the application of GIS. *Environ Geol*, 55, 467–475.
- Preeja, R. K., Joseph, S., & Thomas, J. (2011). Identification of Groundwater Potential Zones of a Tropical River Basin (Kerala, India) Using Remote Sensing and GIS Technology. *J Indian Soc Remote Sens*, 39 (1), 83–94.
- Rahmati, O., Samani, A. N., Mahdavi, M., Pourghasemi, H. R., & Zeinivand, H. (2015). Groundwater potential mapping at Kurdistan region of Iran using analytic hierarchy process and GIS. *Arab J Geosci*, 8, 7059–7071.
- Raja Rao, C. S., & Purushottam, A. (1962). Pitchstone flows in the Rajmahal hills, Santhal Parganas, Bihar. *Rec. Geol Surv Ind*, 91 (2), 341–146.
- Rao, P. J., Rao, B. S., Rao, M. J., & Harikrishna, P. (2003). Geo-Electrical data analysis to demarcate groundwater pockets and recharge zones in Champavathi River Basin, Vizianagaram District, Andhra Pradesh. *J. Ind. Geophys. Union*, 7 (2), 105–113.
- Reddy, K. R. (2013). Ground Water Information Booklet Godda District, Jharkhand State. Central Ground water Board.
- Reghu, S., Gopinath, G., Srinivas, R., Raghunath, R., & Sajan, K. (2013). Demarcation of Groundwater Prospective Zones in Humid Tropical River Basin: A Geospatial Approach. *Iranian Journal of Earth Sciences*, 5, 13–20.
- Saaty, T. L. (1977). A scaling method for prioritized in hierarchical structures. *Journal of Mathematical Psychology*, 15, 234–281.
- Saaty, T. L. (1980). *The analytic hierarchy process: planning, priority setting, resource allocation*. New York: McGraw-Hill.
- Sahoo, S., Jha, M. K., Kumar, N., & Chowdary, V. M. (2015). Evaluation of GIS-based multi-criteria decision analysis and probabilistic modeling for exploring groundwater prospects. *Environ Earth Sci*, 74, 2223–2246.
- Sankar, K. (2002). Evaluation of groundwater potential zones using remote sensing data in upper Vaigai river basin, Tamil Nadu, India. *J Indian Soc Remote Sens*, 30 (3), 119–129.
- Sanyal, S., & Sengupta, P. (2012). Gneiss Complex of the East Indian Shield: current Gneiss Complex of the East Indian Shield: current status. *Geological Society*, 365, 117–145, <https://doi.org/10.1144/SP365.7>.
- Sener, E., Davraz, A., & Ozcelik, M. (2005). An integration of GIS and remote sensing in groundwater investigations: A case study in Burdur, Turkey. *Hydrogeology Journal*, 13, 826–834.
- Şener, E., Şener, Ş., & Davraz, A. (2018). Groundwater potential mapping by combining fuzzy-analytic hierarchy process and GIS in Beyşehir Lake Basin, Turkey. *Arabian Journal of Geosciences*, 11 (187), <https://doi.org/10.1007/s12517-018-3510-x>.
- Shaban, A., Khawlie, M., & Abdallah, C. (2006). Use of remote sensing and GIS to determine recharge potential zones: the case of Occidental Lebanon. *Hydrogeology Journal*, 14, 433–443.
- Shekhar, S., & Pandey, A. C. (2014). Delineation of groundwater potential zone in hard rock terrain of India using remote sensing, geographical information system (GIS) and analytical hierarchy

- process (AHP) techniques. Geocarto International, <https://doi.org/10.1080/10106049.2014.894584>.
- Shekhara, S., & Pandey, A. C. (2014). Delineation of groundwater potential zone in hard rock terrain of India using remote sensing, geographical information system (GIS) and analytic hierarchy process (AHP) techniques. Geocarto International, <https://doi.org/10.1080/10106049.2014.894584>.
- Singh, E. P., Singh, E. A., & Vijhani, A. (2014). Groundwater Potential Zone Mapping Approach in Chandraprabha Basin U.P. Using Remote Sensing & GIS Technology. 15th Esri India User Conference (pp. 1–8). Esri India.
- Singh, M. P., & Singh, P. K. (1996). Petrographic characterization and evolution of the Permian coal deposits of the Rajmahal basin, Bihar, India. *International Journal of Coal Geology*, 29, 93–118.
- Smith, G. H. (1935). The relative relief of Ohio. *Geographical review*, 25(2), 272–284. <https://doi.org/10.2307/209602>.
- Sree Devi, P. D., Srinivasulu, S., & Raju, K. K. (2001). Delineation of groundwater potential zones and electrical resistivity studies for groundwater exploration. *Environmental Geology*, 40, 1252–1264.
- Srivastava, P. K., & Bhattacharya, A. K. (2006). Groundwater assessment through an integrated approach using remote sensing, GIS and resistivity techniques: a case study from hard rock terrain. *International Journal of Remote Sensing*, 27 (20), 4599–4620.
- Story, M., & Congalton, R. G. (1986). Accuracy assessment: A user's perspective. *Photogrammetric Engineering and Remote Sensing*, 52, 397–399.
- Tahmassebipoor, N., Rahmati, O., Noormohamadi, F., & Lee, S. (2016). Spatial analysis of groundwater potential using weights-of-evidence and evidential belief function models and remote sensing. *Arab J Geosci*, 9 (79), <https://doi.org/10.1007/s12517-015-2166-z>.
- Toppo, S. (2013). Ground Water Information Booklet Sahibganj District, Jharkhand State. Central Ground water Board.
- Venkateswaran, S., & Ayyandurai, R. (2015). Groundwater Potential Zoning in Upper Gadilam River Basin Tamil Nadu. *ScienceDirect*, 4, 1275–1282.
- Venkateswaran, S., Prabhu, M. V., & Karuppannan, S. (2014). Delineation of Groundwater Potential zones using Geophysical and GIS Techniques in the Sarabanga Sub Basin, Cauvery River, Tamil Nadu, India. *International Journal of Current Research and Academic Review*, 2 (1), 58–75.
- Zeinivand, H., & Nejad, S. G. (2017). Application of GIS-based data-driven models for groundwater potential mapping in Kuhdasht region of Iran. Geocarto International, <https://doi.org/10.1080/10106049.2017.1289560>.

Chapter 9

Application of AHP for Groundwater Potential Zones Mapping in Plateau Fringe Terrain: Study from Western Province of West Bengal



Manas Karmakar, Monali Banerjee, Mrinal Mandal , and Debasis Ghosh 

Abstract The water-stressed Joyponda river basin is situated on the hard rock terrain of *Chotanagpur Granite Gneiss Complex* of Archean age and older alluvium of Quaternary. An assessment is carried out to delineate the groundwater prospect zones for this densely populated river basin taking into account eleven hydro-geological factors, namely, geology, lineament, geomorphology, slope, curvature, drainage, rainfall, soil, infiltration number, topographic wetness index and land use land cover. To prepare the thematic layers of all these parameters, different maps, satellite images and data are collected from various national and international organizations and analysed in different Remote Sensing (RS) and Geographical Information System (GIS) softwares. The Analytical Hierarchy Process (AHP) model is considered in this study to assign weight for all factors depending upon their influencing capacities in the development of groundwater. The map of groundwater prospect zones is prepared integrating all the factors in GIS software. The applied model is also validated computing overall accuracy assessment and Kappa co-efficient. The study confirms that an area of 37.49% of the Joyponda river basin bears good to very good groundwater potentiality. Around 10.97% of the basin is delineated as very poor groundwater prospect zones. A significant proportion of basin area of 28.93% is moderately potential for groundwater. The result of accuracy assessment of the study ensures the 85% validity of the model. Moreover, the Kappa co-efficient is calculated as 0.81 and describes an almost perfect agreement between simulated model and reference points.

Keywords AHP · Groundwater assessment · Hydro-geology · Joyponda river basin · RS and GIS

M. Karmakar · M. Banerjee · D. Ghosh (✉)

Department of Geography, University of Calcutta, Kolkata, West Bengal, India

M. Mandal

Department of Geography, Sidho-Kanho-Birsha University, Purulia, West Bengal, India

9.1 Introduction

Water is the most precious natural resource for all living organisms in the world. But in the last few decades, a rapid population growth, unsustainable use of water and climate change altogether have decreased the volume of freshwater across the globe (Hinrichsen and Tacio 2002; Lakshmi et al. 2018). It is estimated that around 844 million people in the world are devoid of fresh drinking water, and 3 out of 10 people cannot use safely managed drinking water (Gun 2012). The amount of available freshwater in the world is 2.50%, and 1.5% of this total freshwater is recorded as groundwater (Chow et al. 2008). This little amount of freshwater, i.e. groundwater, is considered as the only source of potable water supply to the half of the world population (World Water Assessment Programme 2009); and around 15 million people of the world use it as the main source of freshwater supply for their multi-purpose activities (Agarwal et al. 2013; Teixeira et al. 2013). Even most of the rural (about 90%) settlements of the world directly depend on the groundwater for drinking purpose (Jaiswal et al. 2003; Sar et al. 2015). The excessive rate of groundwater exploitation to keep parity with the demands of ever-increasing populations has been taking the world towards the serious crisis of freshwater (Suhag 2016; Guru et al. 2017). It is reported by the Central Water Commission (CWC) of India that around 1800 million people of the world will suffer from the severe freshwater crisis in the near future (Central Water Commission 2010). It is estimated that the Asian countries withdraw around two-thirds of the globally explored groundwater, and India is the largest user in this regard (World Bank 2010), because 80% of rural areas and 50% of urban areas in India directly bank on groundwater for the domestic purposes (Lakshmi and Reddy 2018). According to the Central Ground Water Board (CGWB) of India, around 230 billion cubic meter groundwater is withdrawn every year in India (Central Ground Water Board 2017), out of which 89% and 9% are used for agricultural irrigation and domestic purposes, respectively, and remaining groundwater is used for industrial and other activities of the country (Suhag 2016). If the rate of groundwater exploitation maintains this present trend, a drastic decline of groundwater table will be experienced by 60% of districts of India in the coming two decades compromising Indian agricultural productions not less than 25% (World Bank 2010). Extensive rate of groundwater extraction will definitely be decreasing the storage of the aquifers in the near future. In India, most of the aquifers (53.31%) are found in hard rocks terrain (Groundwater Estimation Committee 2017), where around 65% of India's geographical areas are made of hard rocks with less than 5% of porosity level (Saraf and Choudhury 1998). Generally, groundwater in hard rocks terrain is mainly concentrated in different fractured zones, and it becomes very difficult to account the availability of groundwater without proper assessment of aquifers (Sivaramakrishnan et al. 2015). Broadly, there are two types of groundwater assessment methods, namely, conventional and advanced methods (Goldman and Neubauer 1994; Lakshmi and Reddy 2018). The geophysical technique of conventional method is used to explore the aquifer characteristics and identification of sites

for borehole drilling (Lakshmi and Reddy 2018; Etikala et al. 2019). The main drawbacks of conventional method to delineate groundwater potential zones are expensive instruments, extensive field visits, more labour supports and time requirements (Mukherjee et al. 2012). In contrast, the geospatial technologies of advanced method are proved to be more cost-effective and less time consuming in preliminary estimation of groundwater prospect zones (Faust et al. 1991; Hinton 1996; Jha et al. 2007; Razandi et al. 2015; Santharam and Elangovan 2018). The Remote Sensing (RS) and Geographical Information System (GIS) are the indirect means in groundwater exploration using several directly related hydro-geological factors, which determine the availability of groundwater (Javed and Wani 2009). These factors are geomorphology, slope, soil, geology, rainfall, lineament, infiltration number, drainage, land use land cover, curvature and topographic wetness index (Subba Rao 2006; Magesh et al. 2012; Rajaveni et al. 2017; Santharam and Elangovan 2018; Arulbalaji et al. 2019). In recent past, several researchers from various disciplines have successfully integrated different hydro-geological factors in RS and GIS environment to delineate groundwater prospect zones employing different statistical and mathematical models, such as Analytical Hierarchy Process (AHP) (Mandal et al. 2016; Maity and Mandal 2017; Panahi et al. 2017; Aydi 2018), Frequency Ratio Model (FRM) (Ozdermir 2011; Trabelsi et al. 2019), Multi-Influencing Factor (MIF) (Magesh et al. 2012; Nasir et al. 2018; Ghosh et al. 2020), Certainty Factor Model (CRM) (Razandi et al. 2015; Hou et al. 2018) and Artificial Neural Network (ANN) (Baghapour et al. 2016; Lee et al. 2019). The AHP model is one of the most popular Multi-Criteria Decision-Making (MCDM) techniques and has been used with RS and GIS techniques more widely for its capacity to simplify the complex system of groundwater occurrence in various natural environments (Mandal et al. 2016; Arulbalaji et al. 2019; Kumar et al. 2020), such as in hard rocks regions (Shekhar and Pandey 2014; Maity and Mandal 2017; Murmu et al. 2019), semi-arid regions (Machiwal et al. 2011; Kumar et al. 2014; Singh et al. 2018; Rajasekhar et al. 2019) and also for coastal regions (Gangadharan et al. 2016; Swetha et al. 2017). In general, the western part of West Bengal experiences the high intensity rainfall for short period of time followed by high rate of runoff due to high topographic slope that leads to water scarcity during hot dry season (Nag and Das 2017; Government of West Bengal 2017). The present study deals with the delineation of groundwater prospect zones of Joyponda river basin situated on the plateau fringe zone of *Chotanagpur Granite Gneiss Complex* (CGGC) of Bankura district in the state of West Bengal, India. The uniqueness of the basin is that it is composed of heterogeneous lithology. The upper reach is mainly comprised of hard rocks, and the lower reach is composed of alluvium. This region has already been identified as one of the drought-prone areas in West Bengal (Government of West Bengal 2017). The demand for freshwater remains always high among the people of the river basin throughout the year because the population density of the basin ($528/\text{km}^2$) is much higher than the national average ($382/\text{km}^2$) of India (Census of India 2011), though the total groundwater withdrawal of Bankura district is 40% out of the total net available groundwater (Central Ground Water Board 2017). This report indicates that there are plenty scopes of groundwater exploration, and it can only be done by

the proper investigations. There have several works already been carried out in different parts of CGGC to assess the availability of groundwater. Majority of the studies mention that the abundance of groundwater varies from space to space depending upon the different hydro-geological factors (Chowdhury et al. 2010; Shekhar and Pandey 2014; Ghosh et al. 2015, 2020; Das 2017; Nag and Das 2017; Maity and Mandal 2017; Das et al. 2019; Murmu et al. 2019). In this context, an attempt has been made here to delineate groundwater potential zones of the Joyponda river basin considering various significant hydro-geological parameters of the study of interest using the RS and GIS techniques along with the AHP model.

9.2 Study Area

The river Joyponda, a left-hand tributary of the Shilabati River, originates near Boga village of Indpur Community Development (C.D.) block of Bankura district, West Bengal. The river flows over the four C.D. blocks of Bankura district, such as Indpur, Onda, Taldangra and Simlapal, and meets the river Shilabati at Chakrasol village of Simlapal C.D. block. The total stretch of the river is 60.63 km covering the basin area of 396.69 km². The shape of the basin is elongated, and the river Joyponda starts its journey from north-west direction to south-east direction, almost in a diagonal path. The geographical extension of the basin is 22°53'33.87" N to 23°10'31.68" N and 86°50'56.035" E to 87°12'52.68" E (Fig. 9.1). The basin area is mainly consisted of Pre-Cambrian metamorphic rocks of CGGC and older alluvium of Lalgarrh formation and Sijua formation (Vaidyanadhan and Ghosh 1993; Geological Survey of India 2001). The presence of the pediment-pediplain complex makes the upper part of the basin more undulating (Sen et al. 1998). The hot and dry tropical climate prevails over the study area with maximum temperature of 45 °C and minimum temperature of 7 °C. The rainfall of this area, blessed by the South-West Monsoon, is recorded as 1353 mm, which takes place mostly in between June to September (Government of West Bengal 2014). The hard rock terrain with rolling topography and less permeability increases the surface runoff during the Monsoon period, and the area encounters severe shortage of surface water (Maity and Mandal 2017; Ghosh et al. 2020). Thus, the non-perennial Joyponda river basin experiences semi-arid type of climatic conditions except rainy season. This adverse nature of the region helps to grow the deciduous type of natural vegetation, namely, sal (*Shorea robusta*), palash (*Butea monosperma*), mahua (*Madhuca longifolia*) and babla (*Vachellia nilotica*). Moreover, different types of cactus, shrubs and bushes in bare land of the study area are also found (Forest Survey of India 1985). A total number of 244 villages with 209,522 populations come under the jurisdiction of the Joyponda river basin. The river basin shares 5.83% of the total population of Bankura district (Census of India 2011).

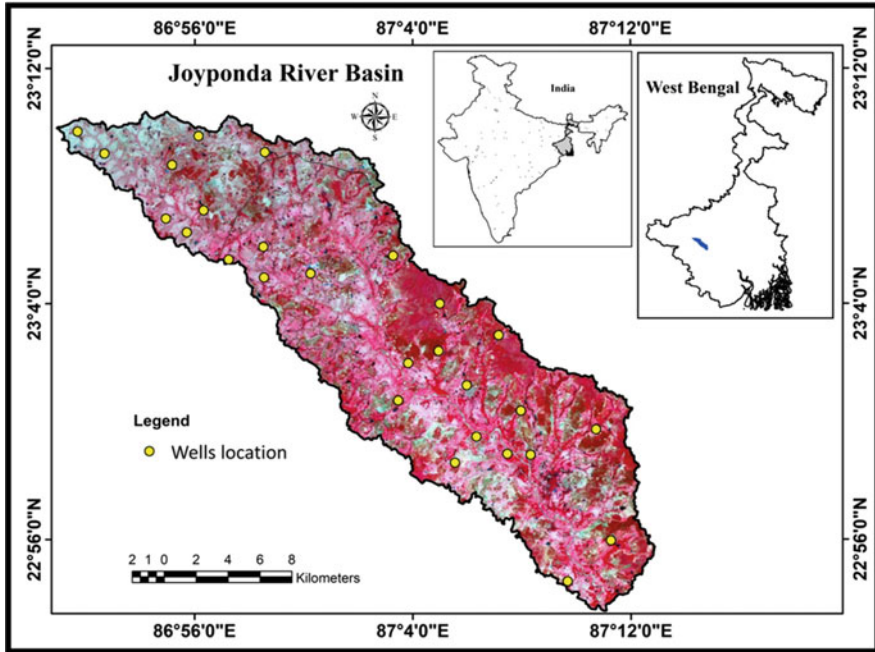


Fig. 9.1 Location map of the Joyponda river basin

9.3 Materials and Methods

9.3.1 Data Sources

To assess the groundwater prospect zones of the Joyponda river basin, a total number of eleven influential hydro-geological factors, such as geology, lineament, geomorphology, slope, curvature, drainage, rainfall, soil, infiltration number, topographic wetness index and land use land cover, are taken into consideration. We obtain different data sets for these selected factors from various sources, such as Digital Elevation Model (DEM) of Shuttle Radar Topography Mission (SRTM) with spatial resolution of 1-Arc second (downloaded from <https://earthexplorer.usgs.gov>) acquired on 23 September 2014; Landsat-8 Operational Land Imager (OLI) satellite image with 30 m spatial resolution acquired on 24 April 2018 (downloaded from <https://earthexplorer.usgs.gov>); district resource map of the Geological Survey of India (GSI) on a 1:50000 scale; geomorphology map of GSI on a 1:250000 scale; soil map of National Bureau of Soil Survey and Land Use Planning (NBSS&LUP) of India on a 1:250000 scale; and station-wise rainfall data of Central Water Commission (CWC) of India to prepare individual thematic layer. The application of RS and GIS softwares is done here using Erdas Imagine 2014, PCI Geomatica 2016 and ArcGIS 10.3.1 to process and analyse different data.

9.3.2 Preparation of Thematic Layers

The drainage basin of the Joyponda River, which is the base map of the present study, is delineated from SRTM-DEM using hydrology tool in ArcGIS software. The drainage density and infiltration number of thematic layers are prepared using hydrology tool of spatial analyst in ArcGIS software using SRTM-DEM. On the contrary, the surface tool of spatial analyst is adopted to create slope, curvature and topography wetness index thematic layers employing the SRTM-DEM. The OLI satellite image of Landsat-8 is taken to produce land use land cover thematic layer applying the raster tool in Erdas Imagine software. The OLI image is then classified into different categories of land use land cover types using maximum likelihood algorithm of supervised classification. To prepare the lineament density map, a Principle Component Analysis (PCA) of OLI image is performed in Erdas Imagine software adopting spectral tool. The extracted lineaments based on the output of PCA of the study of interest are produced adopting line algorithm tool of PCI Geomatica software. The thematic layer of lineament is also verified with 'lineament (50k) theme layer' of the study area prepared by the National Remote Sensing Centre (NRSC) of India, and it is freely available on NRSC portal (downloaded from <https://bhuvan.nrsc.gov.in>) at 'Thematic Services' option. Moreover, the prepared lineament density map is also validated with the district resource map of GSI. The geology and geomorphology maps of the Joyponda river basin are reproduced from the GSI maps using the editor tool of ArcGIS software. The CWC data of rainfall from 2014 to 2018 of four nearby rain gauge stations of the basin are considered to prepare the rainfall map interpolating the rainfall data adopting Inverse Distance Weighted (IWD) method of spatial analyst tool in ArcGIS software. The editor tool of ArcGIS software is also used to make a soil map of the study area from the map of NBSS&LUP. During the preparation of different thematic layers, the maps are geo-coded following Universal Transverse Mercator (UTM) projection, World Geodetic Survey-84 (WGS-84) and 45 N zone as per requirements.

9.3.3 Application of AHP Model

All the eleven selected hydro-geological factors are mutually interrelated, and the groundwater development almost depends on these factors. The AHP model is used in this study to assign weight to each factor and their respective sub-classes depending upon the gravity of influence of each factor in the occurrence and movement of groundwater.

The AHP model developed by T. Saaty in 1980 is an effective multi-criteria decision-making technique, which helps to quantify the weight of a selected factor in numerical form. This model can easily solve many complexities in resource exploration and planning adopting the best possible opportunities (Olson 1988; Chowdhury et al. 2010; Shekhar and Pandey 2014; Malik et al. 2014; Pintu et al.

2017; Maity and Mandal 2017; Waris et al. 2019; Kumar et al. 2020). To assign weight considering the nine-point scale of Saaty (1980), all the eleven factors are now arranged in a hierarchical structure based on priorities. Each score of nine-point scale (Saaty 1990) has a specific definition of importance, such as (1) equal, (2) weak, (3) moderate, (4) moderate plus, (5) strong, (6) strong plus, (7) very strong, (8) very, very strong and (9) extreme. The priority of employing weight to each factor is done based on proper field investigations and review of literatures. In the next step, a pair-wise comparison matrix is formed to compute the normalized weight of an individual factor (Table 9.1).

The justification of assigned weight of each factor given by the decision-maker can be verified with the help of consistency index, and it is the best part of this model (Saaty and Vargas 1982; Ramanathan 2001; Arulbalaji et al. 2019; Das et al. 2019; Waris et al. 2019). The consistency index is calculated using the following equation (formula 9.1):

$$CI = \frac{(\lambda_{\max} - n)}{(n - 1)} \tag{9.1}$$

where *CI* simply denotes consistency index. The λ_{\max} represents the principle eigenvalue, which is calculated using eigenvector technique (Malik et al. 2014), and *n* is the total number of factors used in the study. The Consistency Ratio (CR) is computed for the verification of judgement coherence. If the value of CR happens to be more than 0.1, the judgement value cannot be accepted. Thus, it becomes necessary to consider new judgement values for all factors to reach the CR value less than 0.1. The following expression is used to calculate the CR (formula 9.2), where *RCI* is the random consistency index, which is proposed by Saaty in 1980 (Saaty 1990):

$$CR = \frac{CI}{RCI} \tag{9.2}$$

9.3.4 Calculation of Groundwater Potential Zones Index and Accuracy Assessment

The Groundwater Potential Zones Index (GPZI) is computed taking into account all the 11 thematic layers of selected parameters adopting weighted linear combination method of map algebra tool in ArcGIS software. The derived GPZI is dimensionless. Formula 9.3 is used to calculate the GPZI. Here, W_i is the normalized weight of i^{th} factor, R_j represents the rank of j^{th} sub-class in respective i^{th} factor, m denotes the total number of factors, and n is the total number of sub-classes of all factors. Finally, obtained GPZI values are divided into five distinct classes, such as very poor, poor, moderate, good and very good using natural break classification system in ArcGIS

Table 9.1 Pair-wise comparison matrix of considered factors and normalized weight

	Geology	Geomorphology	Slope	Land use land cover	Lineament density	Soil	Infiltration number	Drainage density	Rainfall	Topographic wetness index	Curvature	Geometric mean	Normalized weight
Geology	9/9	9/8	9/7	9/7	9/6	9/6	9/5	9/5	9/4	9/3	9/3	1.67	0.14
Geomorphology	8/9	8/8	8/7	8/7	8/6	8/6	8/5	8/5	8/4	8/3	8/3	1.48	0.13
Slope	7/9	7/8	7/7	7/7	7/6	7/6	7/5	7/5	7/4	7/3	7/3	1.29	0.11
Land use land cover	7/9	7/8	7/7	7/7	7/6	7/6	7/5	7/5	7/4	7/3	7/3	1.29	0.11
Lineament density	6/9	6/8	6/7	6/7	6/6	6/6	6/5	6/5	6/4	6/3	6/3	1.11	0.10
Soil	6/9	6/8	6/7	6/7	6/6	6/6	6/5	6/5	6/4	6/3	6/3	1.11	0.10
Infiltration number	5/9	5/8	5/7	5/7	5/6	5/6	5/5	5/5	5/4	5/3	5/3	0.93	0.08
Drainage density	5/9	5/8	5/7	5/7	5/6	5/6	5/5	5/5	5/4	5/3	5/3	0.93	0.08
Rainfall	4/9	4/8	4/7	4/7	4/6	4/6	4/5	4/5	4/4	4/3	4/3	0.74	0.06
Topographic wetness index	3/9	3/8	3/7	3/7	3/6	3/6	3/5	3/5	3/4	3/3	3/3	0.56	0.05
Curvature	3/9	3/8	3/7	3/7	3/6	3/6	3/5	3/5	3/4	3/3	3/3	0.56	0.05

Saaty's CR = (<0.1); CR = 0.0001507, the computed matrix is accepted based on derived CR value

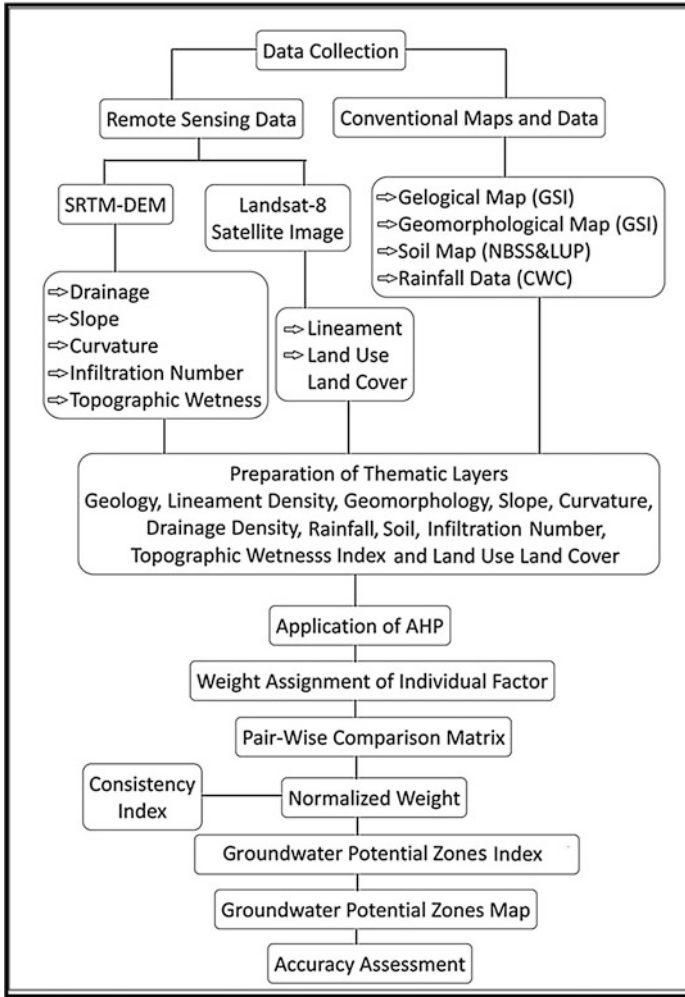


Fig. 9.2 Flow chart showing the methodology adopted

software. The final Groundwater Potential Zones (GPZ) map is validated with the Pre-Monsoon groundwater level data, which are collected from 27 pre-existing dug wells distributed across the river basin. The groundwater level data of 14 dug wells are collected from CGWB, and remaining groundwater level data of 13 dug wells are gathered during the field investigation in the month of March 2020. The overall accuracy assessment is computed to understand the accuracy level of the applied model, and the Kappa co-efficient is also calculated to validate the model. The complete description of used methodology of this present study is shown by a flow chart diagram for better understanding (Fig. 9.2).

$$GPZI = \sum_{i=1}^n \sum_{w=1}^m (W_i \times R_j) \quad (9.3)$$

9.3.5 Groundwater Recharge Estimation

The identification of potential groundwater recharge zones can be delineated with the help of GPZ map. If the amount of potential recharge is estimated for the present river basin, it will be easy to identify good groundwater potential zones, and ultimately it will facilitate in groundwater planning and management (Reese and Risser 2010; Nemaxwi et al. 2019). The spatial distribution of natural groundwater recharge is calculated adopting the rainfall infiltration factor method of Groundwater Estimation Committee (GEC) 2015 of Government of India (formula 9.4). R_r is the amount of natural groundwater recharge, ppt denotes the average annual rainfall and R_{np} represents the rainfall infiltration factor, which is obtained from GEC-1997 norms (Groundwater Estimation Committee 2017). Now, IDW method of spatial analyst tool is used in ArcGIS software to prepare the map of potential groundwater recharge amount.

$$R_r = (ppt \times R_{np} \times \text{area}) \quad (9.4)$$

9.4 Results and Discussions

9.4.1 Geological Setting

Geological setting of an area plays a significant role in determining the thickness of groundwater bearing strata (Arulbalaji et al. 2019). The Joyponda river basin area is consisted of different rock types of various geological ages ranging from Proterozoic to Quaternary (Sen et al. 1998; Geological Survey of India 2001). The entire basin area can be divided almost into two broad equal halves in general. The upper portion consists of granitic gneiss (45.34%) of extended part of Chota Nagpur Plateau of Archean age with a couple of scattered concentration of lateritic patches (Lalgarh formation), while the lower portion of the basin (51.74%) is mainly developed by the accumulation of alluviums (Table 9.2). The concentration of older alluvium is observed more in the basin with smaller amount of deposition of newer alluviums near the confluence point of the Joyponda and Shilabati rivers (Fig 9.4). The laterite deposition in the lower basin area is seen in some small pockets from east to west direction (Fig. 9.3). From the hydro-geological point of view, the older and newer

Table 9.2 Classification of factors and assignment of rank for sub-classes on the basis of influencing capacity in development of groundwater

Factors	Normalized weight	Sub-classes	Area (%)	Rank
Geology	0.14	Granitic gneiss	45.34	3
		Laterite	2.24	4
		Older alluvium	51.74	5
		Newer alluvium	0.69	6
Geomorphology	0.13	Upland plain	60.61	4
		Pediment-pediplain complex	34.79	3
		Flood plain	2.50	5
		Water bodies	2.09	6
Slope (degree)	0.11	<1.04	29.86	6
		1.04–2.26	39.69	4
		2.26–3.78	23.73	3
		3.78–12.04	6.72	2
Land use land cover	0.11	Agricultural land	62.12	5
		Forest cover	5.42	5
		Shrub land	23.42	4
		Barren land	6.56	3
		Water bodies	1.00	6
		Fallow land	1.48	2
Lineament density (km/km ²)	0.1	0.11–0.31	24.84	2
		0.31–0.39	46.78	3
		0.39–0.49	19.38	5
		0.49–0.74	9.00	6
Soil	0.1	Fine-fine silty	38.29	4
		Fine loamy	28.65	5
		Coarse loamy	23.78	6
		Loamy skeletal	2.99	3
		Clayey skeletal	6.29	2
Infiltration number	0.08	0.11–0.73	27.65	2
		0.73–1.06	35.79	3
		1.06–1.42	29.33	5
		1.42–2.14	7.23	6
Drainage density (km/km ²)	0.08	0.63–0.95	13.62	6
		0.95–1.09	47.35	4
		1.09–1.25	30.12	3
		1.25–1.51	8.91	2
Rainfall (mm)	0.06	1147–1178	12.62	2
		1178–1201	17.40	3
		1201–1222	25.87	5
		1222–1241	44.11	6

(continued)

Table 9.2 (continued)

Factors	Normalized weight	Sub-classes	Area (%)	Rank
Topographic wetness index	0.05	5.01–7.95	56.11	2
		7.95–10.39	26.27	3
		10.39–14.05	14.43	4
		14.05–23.31	3.18	5
Curvature	0.05	(−1.58) – (−0.23)	10.27	1
		(−0.23) – 0.00	53.62	2
		0.00–0.23	24.45	4
		0.23–2.38	11.66	6

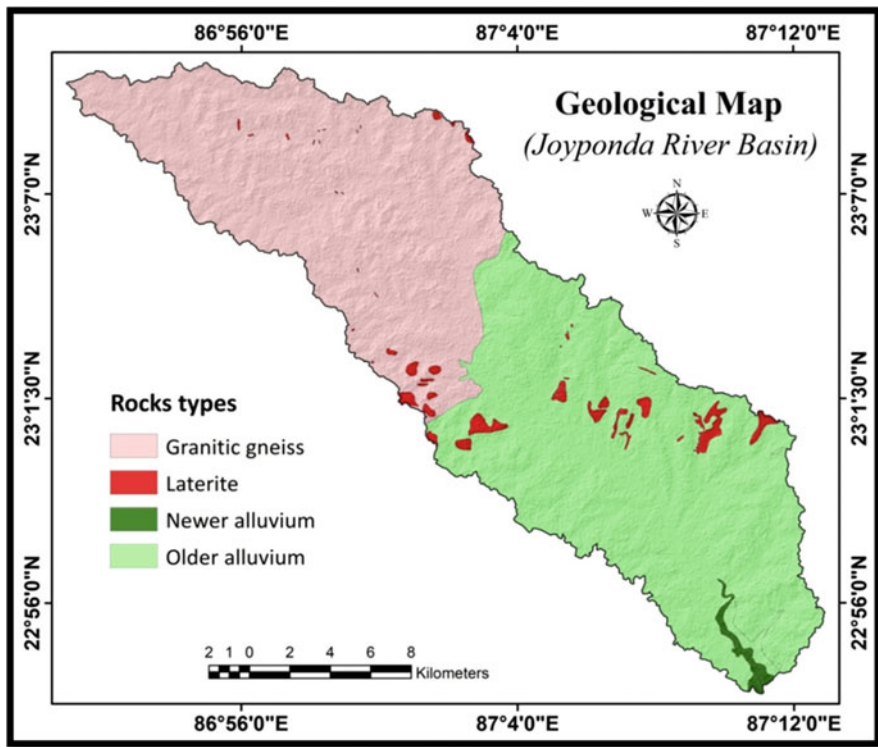


Fig. 9.3 Geological setting of the study area

alluviums are considered as the major water bearing aquifers in the basin area followed by the laterite and granitic gneiss (Groundwater Estimation Committee 2017) (Fig. 9.4).



Fig. 9.4 Field photographs of the Joyponda river basin

9.4.2 Lineament Density

The groundwater potentiality in hard rocks terrain is largely controlled by the discontinuity of rock surface, such as joints, fractures, faults and shear zones. These linear or curvilinear tectonically deformed features create favourable conditions for downward movement of water through the hard rocks surface and ultimately that gives rise to the development of pocket aquifers (Chandra et al. 2006; Acharya and Malik 2012; Shailaja et al. 2019). The permeability and secondary porosity are highly influenced by the areas of high lineaments (Arulbalaji et al. 2019; Ghosh et al. 2020). The high lineament density zones are observed in different pockets of the basin in circular, semi-circular and elongated patterns covering an area of 28.38% of the total basin (Fig. 9.5). The moderate type of lineament density is seen along the basin almost from source to sink of the river, while some portion of the basin boundary (24.84%) shares low amount of lineament density (Table 9.2).

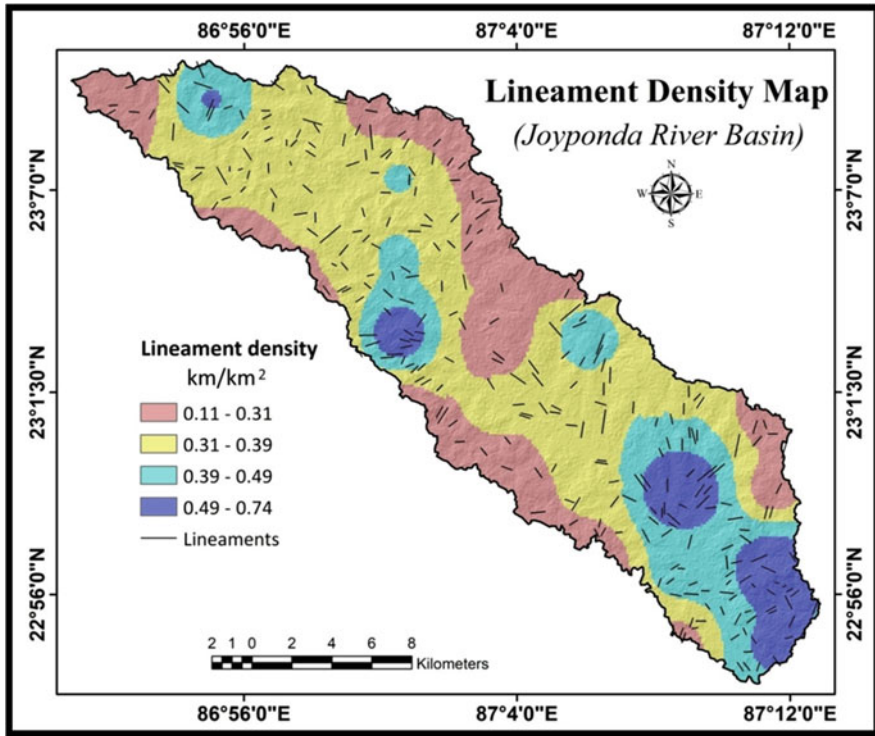


Fig. 9.5 Lineament density of the study area

9.4.3 Geomorphology

Geomorphology is the science which tries to understand the evolution of landforms of complex diversity and different geomorphic processes acting upon them (Summerfield 1999; Goudie 2004; Huggett 2007). It also provides details about the distribution of weathered zones, processes of water movement and characteristics of underlying lithology (Murmu et al. 2019). The geomorphic features of the area are divided into four distinct categories. The upper portion of the basin, which is pediment-piedplain complex, occupies 34.79% area of the total basin, and this complex is considered as less favourable for groundwater recharge due to its undulating topographical characteristics. The upland plain (60.61%) mainly dominates the entire basin from upper-middle course of the Joyponda river up to the confluence point (Table 9.2). There are plenty numbers of small water bodies observed across the river basin randomly. A small proportion of flood plain area is contributed by the river Joyponda from its middle reach to sink (Fig. 9.6). The weathered and loose materials of upland plain and alluvium of flood plain are more suitable in the movement and occurrence of groundwater (Krishnamurthy et al. 1996).

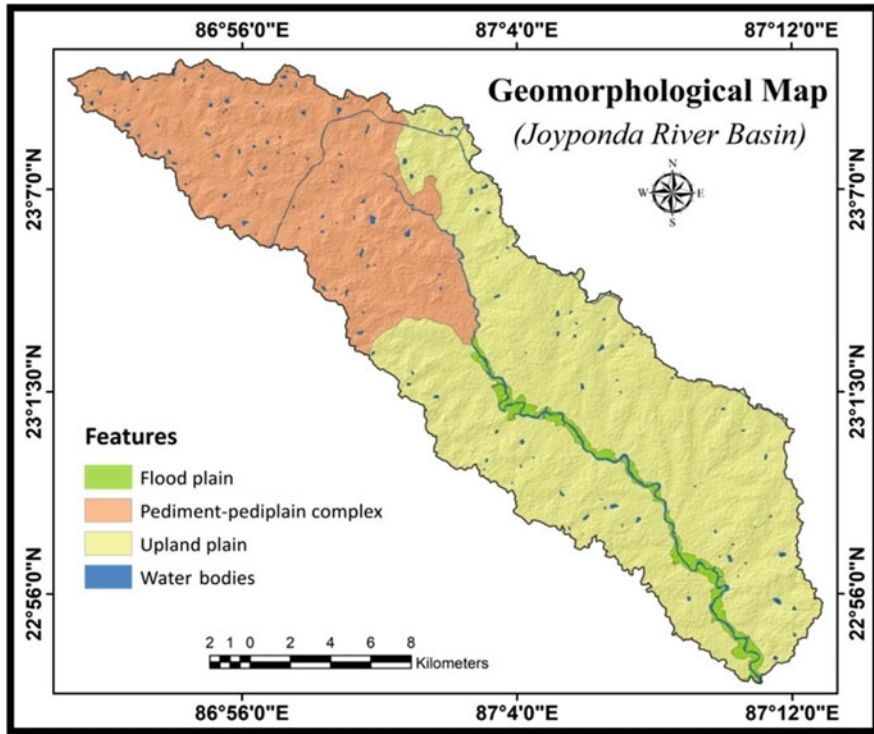


Fig. 9.6 Geomorphological map of the study area

9.4.4 Slope

The steepness of topography is a very crucial factor in groundwater development of an area. The degree of slope is directly proportional to the surface runoff and inverse to the infiltration rate (Siva et al. 2017). The higher amount of slope reduces the chance of water percolation into the soil and resulting less amount of groundwater recharge (Singh et al. 2013). The high degree of slope covering an area of 6.72% is observed across the basin due to concentration of low dissected residual hills (Fig. 9.7). The low degree of slope (i.e. less than 1.04 degree) is mainly found in the riverine areas of lower course sharing an area of 29.86% of the total basin. This area is most favourable for groundwater recharge due to loose sediments. A significant proportion of the basin area (63.42%) experiences moderate type of slope varying from 1.04 to 3.78 degree (Table 9.2).

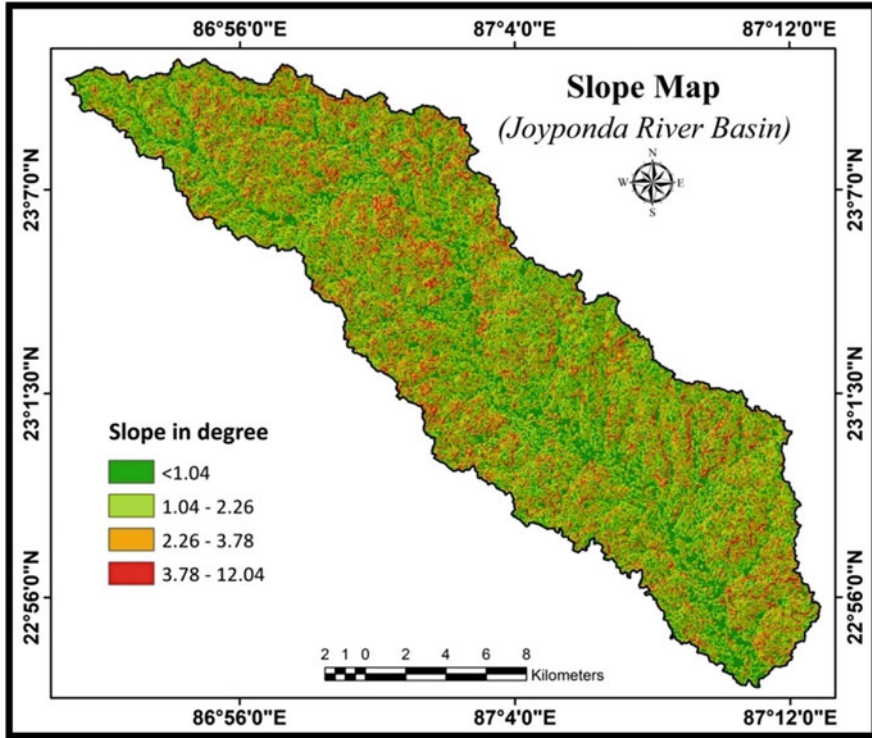


Fig. 9.7 Slope map of the study area

9.4.5 Curvature

Curvature refers to the amount of bend of topographic surface from being a horizontal plain. The shapes of bend or curve of topography are considered as convex profile, when it is curved upward, and concave profile, when it is curved downward (Benjmel et al. 2020). The concave upward profile has the highest potentiality in groundwater recharge (Arulbalaji et al. 2019). High curvature value represents the deceleration of runoff and enhancement in water infiltration rate. The curvature values of the study area lie in between -0.23 and 2.38 . The concave surface occupies around 36.11% of the total basin area (Table 9.2), and it reflects a good signature of high amount of water accumulation though most part of the river basin area experiences convex surface (Fig. 9.8).

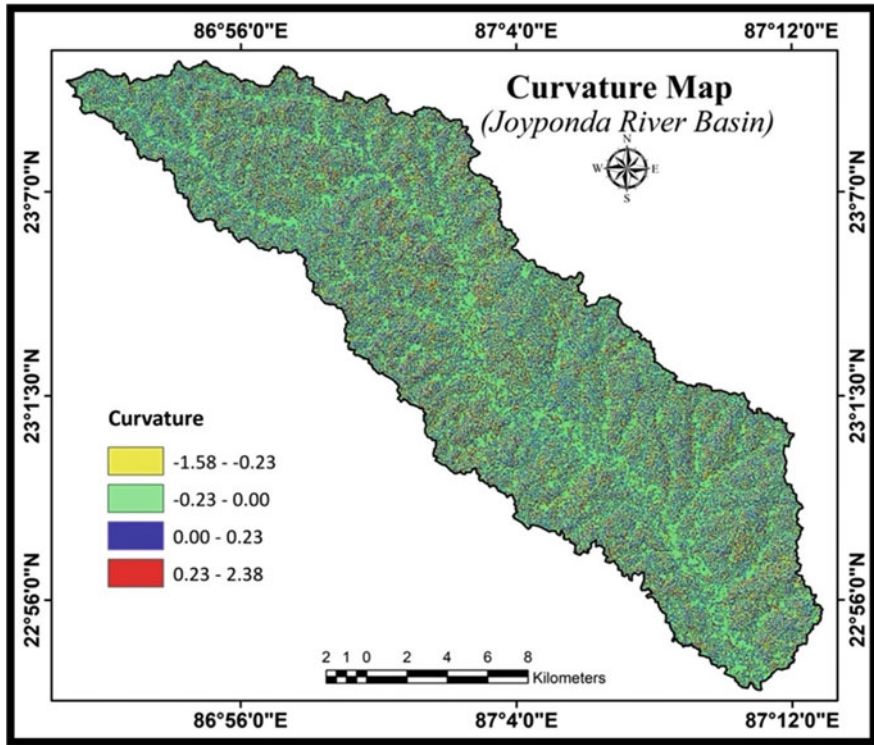


Fig. 9.8 Curvature map of the study area

9.4.6 Drainage Density

Drainage density of an area is expressed as a ratio between sum of the total stream lengths considering all stream orders of a unit to the total unit area (Horton 1932; Kale and Gupta 2001). There is a positive relation of drainage density with slope, altitude and rainfall, while negative relation exists with vegetation cover and infiltration rate (Chorley and Morgan 1962; Morisawa 1962; Hugget 2007). The higher drainage density is an indicator of high runoff and less groundwater recharge. In contrast, the lower drainage density areas are suitable for groundwater recharge (Magesh et al. 2012). The drainage density of the river basin is classified into four distinct categories. Most of the drainage basin (60.97%) enjoys almost low drainage density, i.e. less than 1.09 km/km² (Table 9.2), and it is mainly found in the entire middle portion of the basin. The higher degree of drainage density is observed either in elongated pattern or circular pattern over the river basin, and the lower order streams are mainly incipient ephemeral in nature along with short life span in terms of their perennial character (Fig. 9.9).

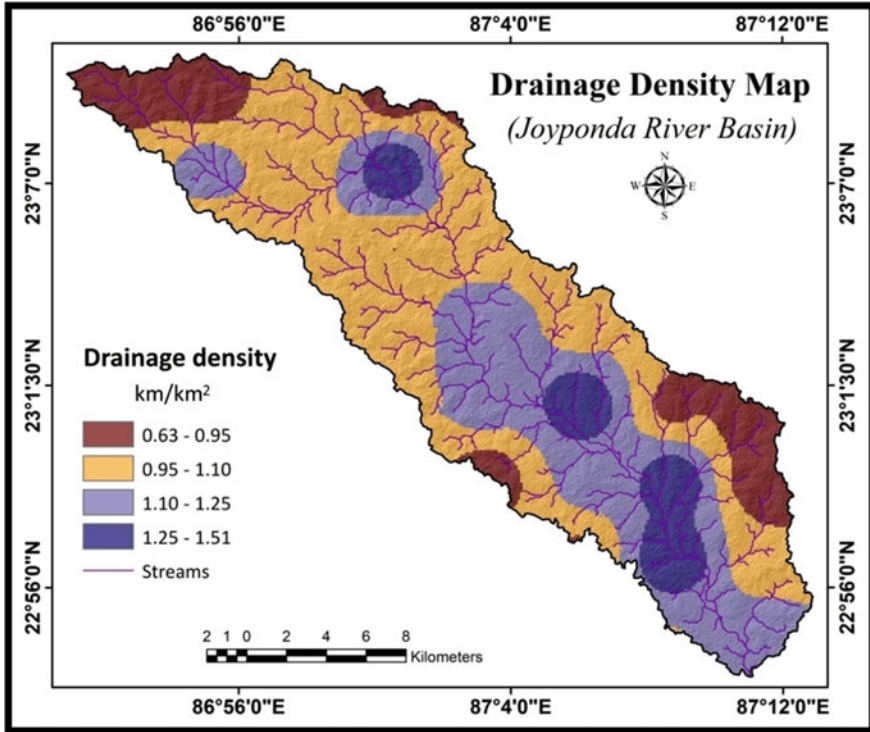


Fig. 9.9 Drainage density map of the study area

9.4.7 Rainfall

Rainfall is the main source of groundwater recharge in this area. The maximum rainfall is received in between June to September by the entire area due to advent of Monsoon (Nag and Ray 2015). According to the CGWB more than 80% of precipitation flows away as runoff of this hard rocks terrain due to low rate of permeability and topographical irregularities (CGWB 2017). Thus, the low intensity rainfall of longer duration is more preferable in groundwater recharge compared to the high intensity rainfall of short period (Nasir et al. 2018). The annual average rainfall of the basin varies from 1147 mm to 1241 mm as per the CWC database. The entire river basin has divided itself into four distinct rainfall categories from north-west to south-east direction like a stair case (Fig. 9.10). The higher amount of rainfall is enjoyed by the upper portion of the basin, whereas the amount of rainfall decreases gradually towards the lower catchment area of the basin. Most of the basin area (69.98%) enjoys more than 1201 mm rainfall (Table 9.2).

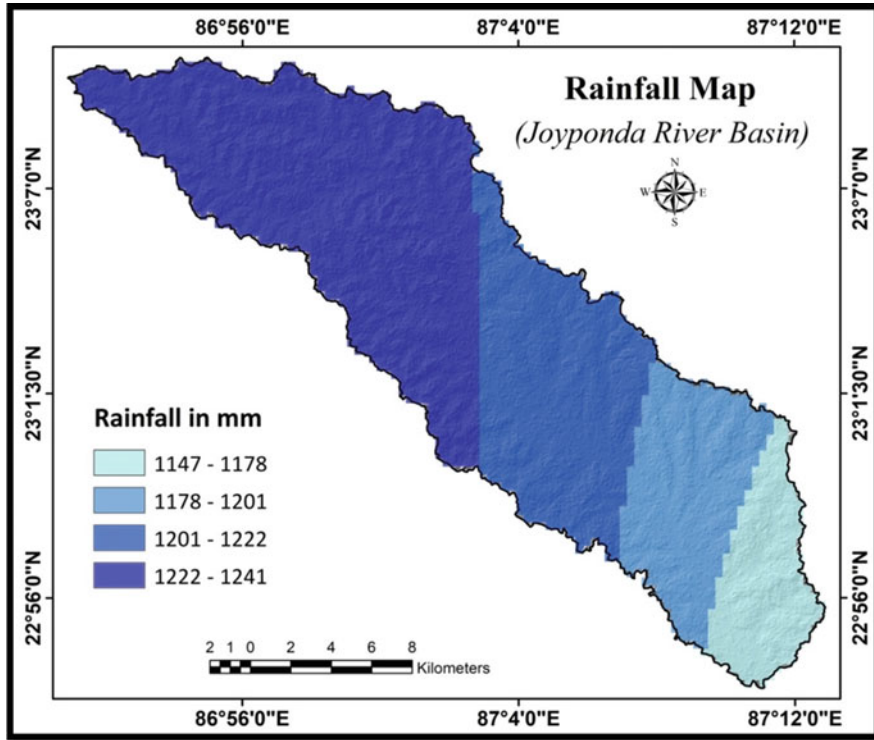


Fig. 9.10 Rainfall distribution map of the study area

9.4.8 Soil

The groundwater recharge is determined by a number of properties of soil, such as soil type, texture, water infiltration, percolation, permeability and water holding capacity (Shekhar and Pandey 2014; Murmu et al. 2019). The coarse texture of soil is more favourable for groundwater recharge followed by fine texture (Maity and Mandal 2017; Ghosh et al. 2020). There are five types of soils found in the study area (Fig. 9.11), and the coarse loamy soil covers an area of 23.78% of the Joyponda river basin, followed by fine loamy soil (28.65%) and fine-fine silty soil (38.29%). The clayey skeletal soil and loamy skeletal soil account for 6.29% and 2.99% of the basin area, respectively (Table 9.2).

9.4.9 Infiltration Number

The infiltration number is used to understand the potential infiltration capacity of an area, and it is the result of stream frequency and drainage density (Prabhakaran and

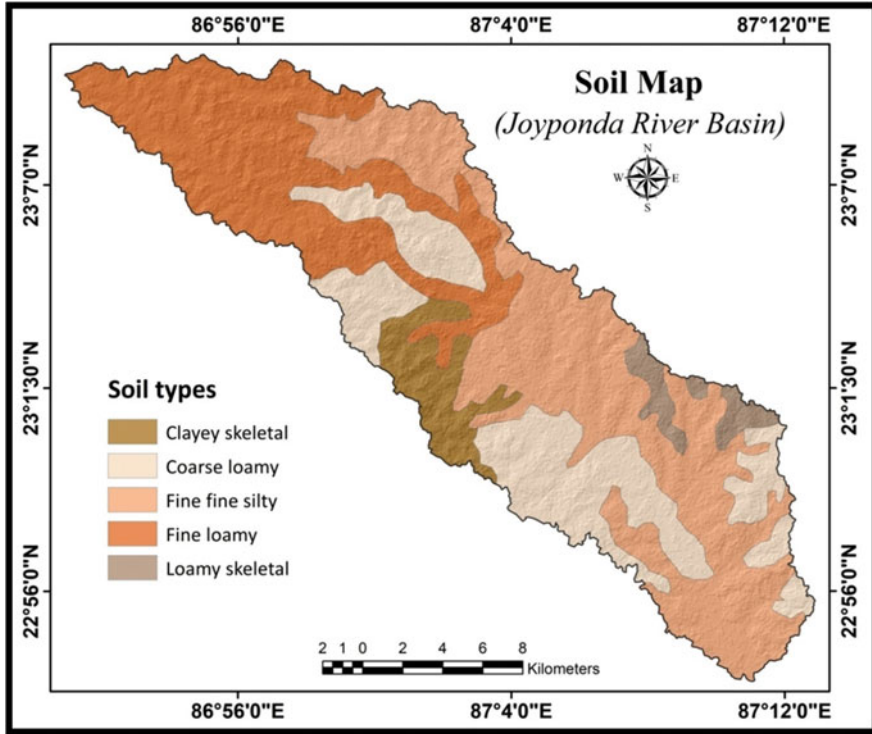


Fig. 9.11 Soil map of the study area

Raj 2018). There is an inverse relation between infiltration number and groundwater recharge. The higher infiltration number is unfavourable for groundwater recharge and leads to high runoff. Less infiltration number increases the chances of high groundwater recharge (Joji et al. 2013; Ghosh and Jana 2018; Prabhakaran and Raj 2018). Infiltration number of the basin varies from 0.11 to 2.14. Most of the basin area (63.44%) comes under the less infiltration number, i.e. less than 1.06 (Table 9.2). Areas of higher infiltration number of more than 1.42 are mainly found in circular pattern from middle to lower reach of the basin, while medium infiltration number is highly concentrated in elongated pattern almost in the middle of the basin (Fig. 9.12).

9.4.10 Topographic Wetness Index

Topographic wetness index helps to perceive the role of topography in controlling the potential groundwater infiltration. It is computed considering the propensity of water to be stored up at any point of the basin and the propensity of water to move

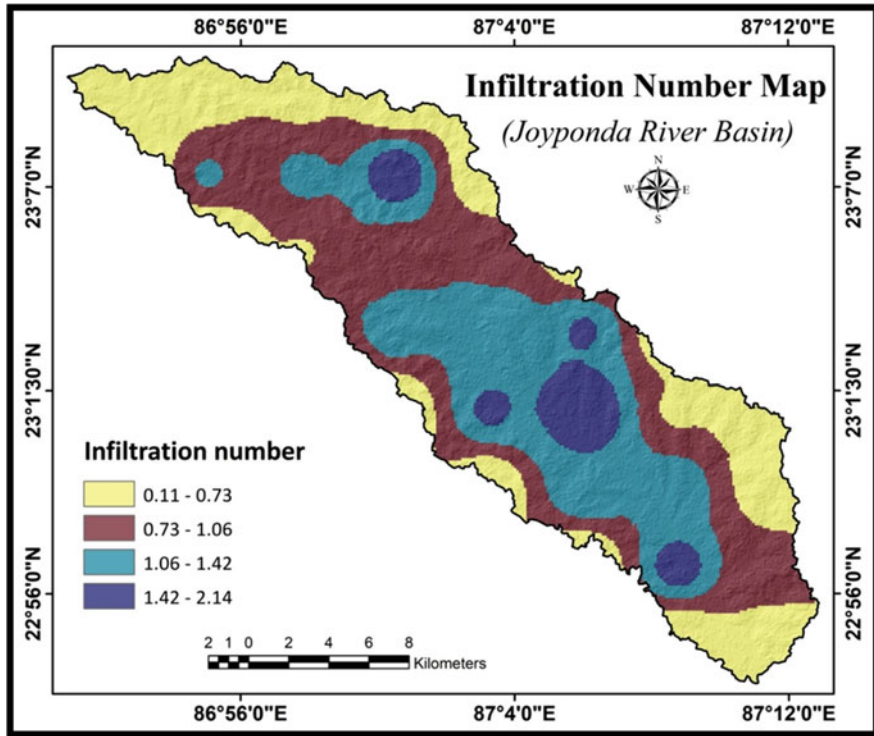


Fig. 9.12 Infiltration number map of the study area

down due to gravitational force (Nampak et al. 2014; Arulbalaji et al. 2019). This index of the basin varies from 5.01 to 23.31. The higher index value of an area over the river basin indicates good potentiality of groundwater, and vice-versa. An area of 17.61% of the river basin enjoys higher topographic wetness index, i.e. more than 10.39 (Table 9.2). The rest of the basin area experiences low to moderate topographic wetness index (Fig. 9.13).

9.4.11 Land Use Land Cover

In the process of groundwater development, the role of land use land cover is indisputable, and it also portrays the details about the surface water, groundwater, infiltration, soil moisture, water holding capacity and runoff rate (Singh et al. 2017). The entire basin area is categorized into six classes based on land use land cover. Most of the basin area (62.12%) is utilized for agricultural practices, which bear good potentiality of groundwater recharge. Forest cover and shrub land share 28.84% of total basin area (Table 9.2). This vegetation cover is found to be good

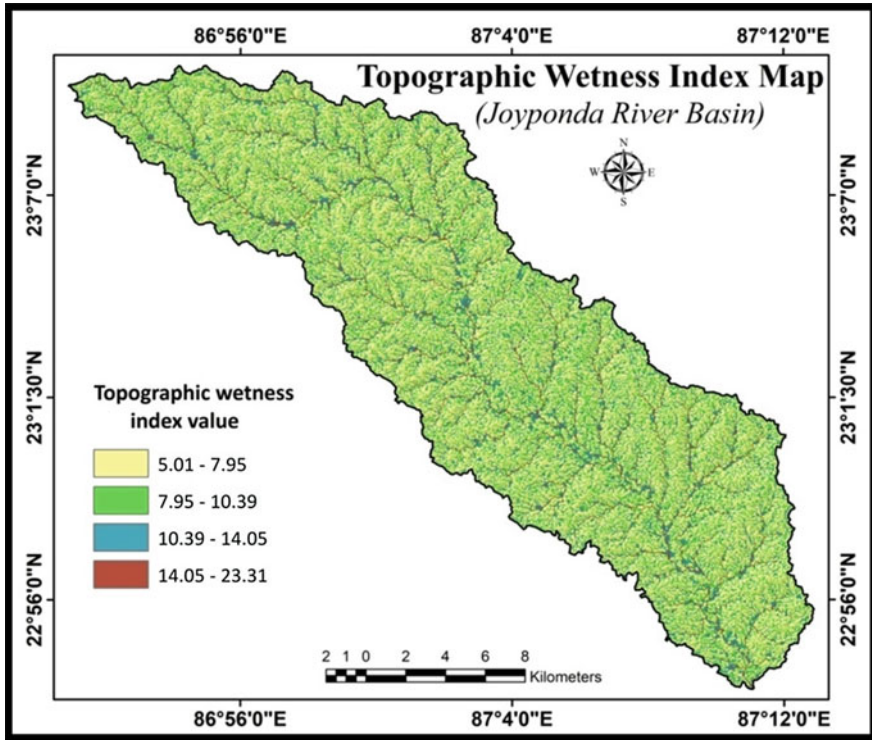


Fig. 9.13 Topographic wetness index map of the study area

transmitter of water into the ground creating routes for water percolation unfastening the soils and rocks by their roots (Murmu et al. 2019). There is a very small amount of water bodies (1.00%) existing over the basin. The main concentration of barren land is located at the top of the river basin, and a few numbers of patches of barren land are observed in small semi-circular pattern scattering over the basin (Fig. 9.14)

9.4.12 GPZ of the Joyponda River Basin

The prospect zones of groundwater of Joyponda river basin are delineated using the integrated approach of AHP and geospatial techniques considering a total number of eleven hydro-geological factors. It is estimated that the basin enjoys 12.62% of area as very good GPZ followed by good (24.47%). The moderate prospect zone of groundwater is recorded as 28.93%. Only 10.97% area of the river basin experiences very poor groundwater potentiality followed by poor potential zones (Table 9.3). The prospect zones of good to very good lie mainly in between middle to lower reach of the river basin (Fig. 9.15).

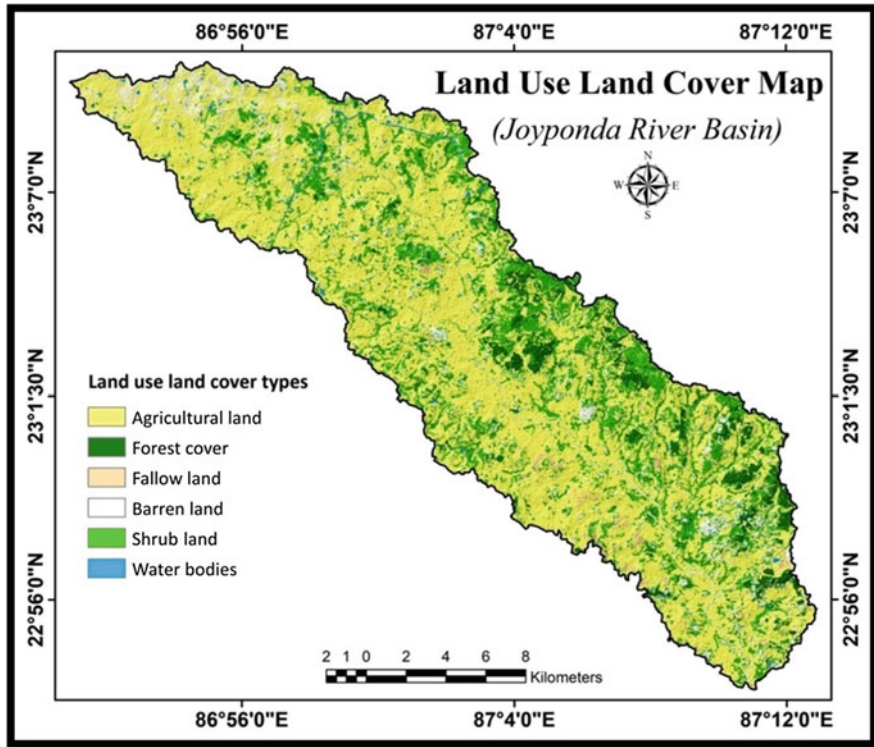


Fig. 9.14 Land use land cover map of the study area

Table 9.3 Descriptive statistics of groundwater potential zones

Groundwater potential zones	Area (km ²)	Area (%)	No. of reference dug wells
Very poor	43.5	10.97	4
Poor	89.69	22.61	4
Moderate	114.78	28.93	7
Good	98.67	24.87	4
Very good	50.05	12.62	8

9.4.13 Accuracy Assessment of GPZ Map

Before the judicious use of the GPZ map, it is a prerequisite condition to assess the accuracy level and validity of the applied model. To do the same, the Pre-Monsoon groundwater level data of 27 dug wells distributed over the river basin are taken into account. These individual dug wells are considered as reference points to investigate groundwater prospect. The range of the groundwater level data lies in between 0.90 mbgl and 9.97 mbgl, and the data are classified into five different categories in ArcGIS software adopting natural break classify system, namely, very poor (7.25

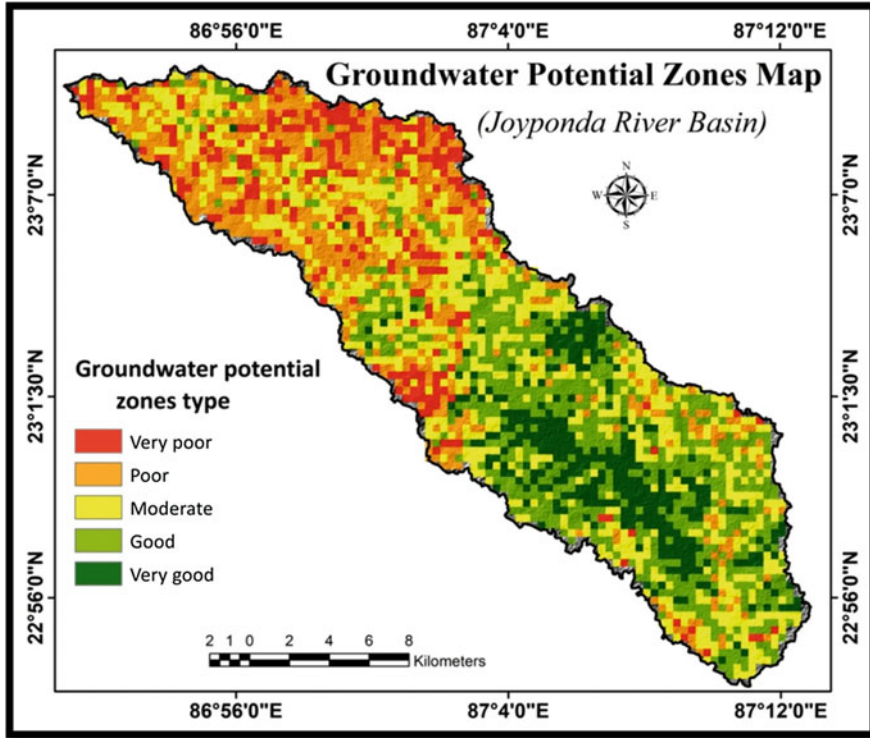


Fig. 9.15 Groundwater potential zones map of the study area

mbgl to 9.97 mbgl), poor (6.39 mbgl to 7.25 mbgl), moderate (4.39 mbgl to 6.39 mbgl), good (2.89 mbgl to 4.39 mbgl) and very good (0.90 mbgl to 2.89 mbgl). The calculated value of the overall accuracy assessment of the study is found to be 85%, which certainly upholds the implication of the used model. The study shows that the higher depth of water level of dug wells is found at the upper part of the basin, while the lower depth of water level of dug wells is observed at the lower part of the river basin. Here, the Kappa co-efficient is also computed to understand the level of agreement between simulated GPZ map and reference points of dug wells. Generally, the value of the Kappa co-efficient belongs to 0 to 1, where 1 represents almost perfect agreement and 0 denotes less than chance of agreement (Viera and Garrett 2005). The Kappa co-efficient value of the present study is computed as 0.81, which indicates towards the almost perfect agreement between simulated model and observed value of reference points.

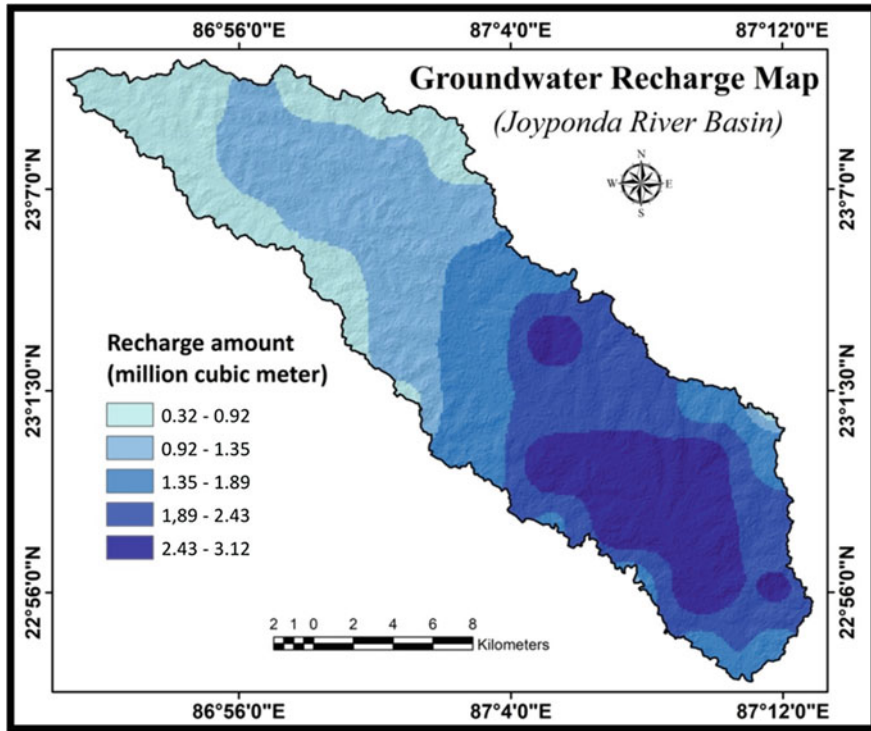


Fig. 9.16 Spatial distribution of natural groundwater recharge amount

9.4.14 Estimation of Natural Groundwater Recharge

In the present day, identification of groundwater recharge zones emerges with great importance to quantify the amount of infiltrated water into the ground for amplification of groundwater storage (Oke et al. 2015). The amount of recharge highly depends on the characteristics of hydro-geological unit. The duration and intensity of rainfall amount, pore space of soil, permeability, slope, etc. are primarily key determinants of groundwater recharge. The average annual rainfall of the study area varies from 1147 mm to 1241 mm. To calculate the amount of groundwater recharge from rainfall, the specified method of GEC 2015 is applied using raster calculator in ArcGIS software. It is estimated that the whole basin area receives average annual rainfall of $4.77 \times 10^8 \text{ m}^3$. Of the total volume of obtained rainfall, only 13.78% water, i.e. $6.5 \times 10^7 \text{ m}^3$, is credited to groundwater storage. The lower river basin area provides more rainfall for groundwater recharge compared to the upper catchment area (Fig. 9.16), which receives highest amount of rainfall in the basin. It is the topography which influences the variation of groundwater recharge by its inherent characteristics.

9.5 Conclusion

The study reveals that an area of 148.73 km² (37.49%) of the total Joyponda river basin enjoys good to very good potentiality of groundwater. These zones are mainly observed at lower basin areas, where older alluvium, gentle slope and high lineament density coexist. The areas of very poor to poor groundwater prospect occupy 133.19 km² (36.03%) area of the total basin. This area is mainly situated at the upper reach of the basin, which is characterized by high drainage density, high degree of slope, less lineament density, hard granitic gneiss rocks and high runoff. To meet the demands for water of populations of the basin mainly during the scorching dry summer, the groundwater exploration is required to be made when there is no such option left. Many a time, it was witnessed that the people of this region were discouraged due to the failing of borehole drillings in search of groundwater. Only the delineated GPZ are required to explore to minimize the risk of failures. This work may also help in disclosing many ways of new researches related to estimation of groundwater storage, rate of recharge, nature of aquifers, etc.

Acknowledgements The authors are beholden to Mr. Sushanta Mandi, State Aided College Teacher in the Department of Geography of Arsha College, Purulia of West Bengal, for his assistance during the data collection from the field. They are indebted to the United States Geological Survey (USGS) of the United States Government; Geological Survey of India (GSI) of the Government of India; National Bureau of Soil Survey and Land Use Planning (NBSS&LUP) of the Government of India; and Central Water Commission (CWC) of the Government of India for providing their satellite images, geological maps, soil maps and rainfall data, respectively.

References

- Acharya T, Mallik SB (2012) Analysis of lineament swarms in a Precambrian metamorphic rocks in India. *J Earth Syst Sci* 121:453–462. <https://doi.org/10.1007/s12040-012-0164-z>
- Agarwal E, Agarwal R, Garg RD, Garg PK (2013) Delineation of groundwater potential zone: An AHP/ANP approach. *J Earth Syst Sci* 122:887–898. <https://doi.org/10.1007/s12040-013-0309-8>
- Arulbalaji P, Padmalal D, Sreelash K (2019) GIS and AHP techniques based delineation of groundwater potential zones: a case study from Southern Western Ghats, India. *Sci Rep* 9:2082. <https://doi.org/10.1038/s41598-019-38567-x>
- Aydi A (2018) Evaluation of groundwater vulnerability to pollution using a GIS-based multi-criteria decision analysis. *Groundwater for Sustainable Development* 7:204–211. <https://doi.org/10.1016/j.gsd.2018.06.003>
- Baghapour MA, Fadaei Nobandegani A, Talebbeydokhti N, et al (2016) Optimization of DRASTIC method by artificial neural network, nitrate vulnerability index, and composite DRASTIC models to assess groundwater vulnerability for unconfined aquifer of Shiraz Plain, Iran. *J Environ Health Sci Engineer* 14:13. <https://doi.org/10.1186/s40201-016-0254-y>
- Benjmel K, Amraoui F, Boutaleb S, et al (2020) Mapping of groundwater potential zones in crystalline terrain using remote sensing, GIS techniques, and multicriteria data analysis (case of the Ighrem region, Western Anti-Atlas, Morocco). *Water* 12:471. <https://doi.org/10.3390/w12020471>

- Census of India (2011) C.D. block wise primary census abstract data (PCA) - West Bengal. Directorate of Census, Government of India, New Delhi, New Delhi
- Central Ground Water Board (CGWB) (2017) Groundwater year book of West Bengal & Andaman & Nicobars Island 2015-2016. Ministry of Water Resource, Government of India, Kolkata
- Central Water Commission (2010) Water and related statistics 2010. Ministry of Water Resources, River Development and Ganga Rejuvenation. Government of India, New Delhi
- Chandra S, Rao VA, Krishnamurthy NS, et al (2006) Integrated studies for characterization of lineaments used to locate groundwater potential zones in a hard rock region of Karnataka, India. *Hydrogeol J* 14:1042–1051. <https://doi.org/10.1007/s10040-006-0097-1>
- Chorley RJ, Morgan MA (1962) Comparison of Morphometric Features, Unaka Mountains, Tennessee and North Carolina, and Dartmoor, England. *Geol Soc America Bull* 73:17. [https://doi.org/10.1130/0016-7606\(1962\)73\[17:COMFUM\]2.0.CO;2](https://doi.org/10.1130/0016-7606(1962)73[17:COMFUM]2.0.CO;2)
- Chow VT, Maidment DR, Mays LW (2008) Applied hydrology, [Nachdr.], internat. ed. 1988. McGraw-Hill, New York
- Chowdhury A, Jha MK, Chowdary VM (2010) Delineation of groundwater recharge zones and identification of artificial recharge sites in West Medinipur district, West Bengal, using RS, GIS and MCDM techniques. *Environ Earth Sci* 59:1209–1222. <https://doi.org/10.1007/s12665-009-0110-9>
- Das B, Pal SC, Malik S, Chakraborty R (2019) Modeling groundwater potential zones of Puruliya district, West Bengal, India using remote sensing and GIS techniques. *Geology, Ecology, and Landscapes* 3:223–237. <https://doi.org/10.1080/24749508.2018.1555740>
- Das S (2017) Delineation of groundwater potential zone in hard rock terrain in Gangajalghati block, Bankura district, India using remote sensing and GIS techniques. *Model Earth Syst Environ* 3:1589–1599. <https://doi.org/10.1007/s40808-017-0396-7>
- Etikala B, Golla V, Li P, Renati S (2019) Deciphering groundwater potential zones using MIF technique and GIS: A study from Tirupati area, Chittoor District, Andhra Pradesh, India. *HydroResearch* 1:1–7. <https://doi.org/10.1016/j.hydrres.2019.04.001>
- Faust NL, Anderson WH, Star JL (1991) Geographic information systems and remote sensing future computing environment. *Photogrammetric Engineering and Remote Sensing* 57:655–668
- Forest Survey of India (1985) Forest resources of Bankura district, West Bengal. Ministry of Environment and Forests, New Delhi
- Gangadharan R, Nila Rekha P, Vinoth S (2016) Assessment of groundwater vulnerability mapping using AHP method in coastal watershed of shrimp farming area. *Arab J Geosci* 9:107. <https://doi.org/10.1007/s12517-015-2230-8>
- Geological Survey of India (2001) District resource map of Purulia
- Ghosh D, Mandal M, Karmakar M, et al (2020) Application of geospatial technology for delineating groundwater potential zones in the Gandheswari watershed, West Bengal. *Sustain Water Resour Manag* 6:14. <https://doi.org/10.1007/s40899-020-00372-0>
- Ghosh PK, Bandyopadhyay S, Jana NC (2015) Mapping of groundwater potential zones in hard rock terrain using geoinformatics: a case of Kumari watershed in western part of West Bengal. *Model Earth Syst Environ* 2:1. <https://doi.org/10.1007/s40808-015-0044-z>
- Ghosh PK, Jana NC (2018) Groundwater potentiality of the Kumari River Basin in drought-prone Purulia upland, Eastern India: a combined approach using quantitative geomorphology and GIS. *Sustain Water Resour Manag* 4:583–599. <https://doi.org/10.1007/s40899-017-0142-3>
- Goldman M, Neubauer FM (1994) Groundwater exploration using integrated geophysical techniques. *Surv Geophys* 15:331–361. <https://doi.org/10.1007/BF00665814>
- Goudie A (ed) (2004) Encyclopedia of geomorphology. Routledge: International Association of Geomorphologists, London; New York
- Government of West Bengal (2014) District statistical handbook, Purulia 2014. Bureau of Applied Economics and Statistics, Kolkata
- Government of West Bengal (2017) Annual flood report for the year 2017. Irrigation & Waterways Directorate, Government of West Bengal, Kolkata

- Ground Water Resource Estimation Committee (GEC) (2017) Methodology. Ministry of Water Resources, River Development & Ganga Rejuvenation, Government of India, New Delhi
- van der Gun J (2012) Groundwater and global change: trends, opportunities and challenges. UNESCO, Paris
- Guru B, Seshan K, Bera S (2017) Frequency ratio model for groundwater potential mapping and its sustainable management in cold desert, India. *Journal of King Saud University - Science* 29:333–347. <https://doi.org/10.1016/j.jksus.2016.08.003>
- Hinrichsen D, Tacio H (2002) Finding the source: The coming freshwater crisis is already here. Woodrow Wilson International Center for Scholars, Washington, DC
- Hinton JC (1996) GIS and remote sensing integration for environmental applications. *International journal of geographical information systems* 10:877–890. <https://doi.org/10.1080/02693799608902114>
- Horton RE (1932) Drainage-basin characteristics. *Trans AGU* 13:350. <https://doi.org/10.1029/TR013i001p00350>
- Hou E, Wang J, Chen W (2018) A comparative study on groundwater spring potential analysis based on statistical index, index of entropy and certainty factors models. *Geocarto International* 33:754–769. <https://doi.org/10.1080/10106049.2017.1299801>
- Huggett RJ (2007) Fundamentals of geomorphology, 2nd ed. Routledge, London ; Madison Avenue, N.Y
- Jaiswal RK, Mukherjee S, Krishnamurthy J, Saxena R (2003) Role of remote sensing and GIS techniques for generation of groundwater prospect zones towards rural development—an approach. *International Journal of Remote Sensing* 24:993–1008. <https://doi.org/10.1080/01431160210144543>
- Javed A, Wani MH (2009) Delineation of groundwater potential zones in Kakund watershed, Eastern Rajasthan, using remote sensing and GIS techniques. *J Geol Soc India* 73:229–236. <https://doi.org/10.1007/s12594-009-0079-8>
- Jha MK, Chowdhury A, Chowdary VM, Peiffer S (2007) Groundwater management and development by integrated remote sensing and geographic information systems: prospects and constraints. *Water Resour Manage* 21:427–467. <https://doi.org/10.1007/s11269-006-9024-4>
- Joji VS, Nair ASK, Baiju KV (2013) Drainage basin delineation and quantitative analysis of Panamaram watershed of Kabani river basin, Kerala using remote sensing and GIS. *J Geol Soc India* 82:368–378. <https://doi.org/10.1007/s12594-013-0164-x>
- Kale VS, Gupta A (2001) Introduction to geomorphology. Universities Press, New Delhi
- Krishnamurthy J, Venkatesa Kumar N, Jayaraman V, Manivel M (1996) An approach to demarcate ground water potential zones through remote sensing and a geographical information system. *International Journal of Remote Sensing* 17:1867–1884. <https://doi.org/10.1080/01431169608948744>
- Kumar T, Gautam AK, Kumar T (2014) Appraising the accuracy of GIS-based Multi-criteria decision making technique for delineation of Groundwater potential zones. *Water Resour Manage* 28:4449–4466. <https://doi.org/10.1007/s11269-014-0663-6>
- Kumar VA, Mondal NC, Ahmed S (2020) Identification of groundwater potential zones using RS, GIS and AHP techniques: A case study in a part of Deccan Volcanic Province (DVP), Maharashtra, India. *J Indian Soc Remote Sens* 48:497–511. <https://doi.org/10.1007/s12524-019-01086-3>
- Lakshmi SV, Reddy VK (2018) Identification of groundwater potential zones using GIS and remote sensing. *International Journal of Pure and Applied Mathematics* 119:3195–3210
- Lakshmi V, Fayne J, Bolten J (2018) A comparative study of available water in the major river basins of the world. *Journal of Hydrology* 567:510–532. <https://doi.org/10.1016/j.jhydrol.2018.10.038>
- Lee S, Hyun Y, Lee M-J (2019) Groundwater potential mapping using data mining models of big data analysis in Goyang-si, South Korea. *Sustainability* 11:1678. <https://doi.org/10.3390/su11061678>

- Machiwal D, Jha MK, Mal BC (2011) Assessment of groundwater potential in a semi-arid region of India using remote sensing, GIS and MCDM techniques. *Water Resour Manage* 25:1359–1386. <https://doi.org/10.1007/s11269-010-9749-y>
- Magesh NS, Chandrasekar N, Soundranayagam JP (2012) Delineation of groundwater potential zones in Theni district, Tamil Nadu, using remote sensing, GIS and MIF techniques. *Geoscience Frontiers* 3:189–196. <https://doi.org/10.1016/j.gsf.2011.10.007>
- Maity DK, Mandal S (2017) Identification of groundwater potential zones of the Kumari river basin, India: an RS & GIS based semi-quantitative approach. *Environ Dev Sustain* 21:1013–1034. <https://doi.org/10.1007/s10668-017-0072-0>
- Mallick J, Singh CK, Al-Wadi H, et al (2014) Geospatial and statistical approach for groundwater potential zone delineation. *Hydrol Process* 29:395–418. <https://doi.org/10.1002/hyp.10153>
- Mandal U, Sahoo S, Munusamy SB, et al (2016) Delineation of groundwater potential zones of coastal groundwater basin using multi-criteria decision making technique. *Water Resour Manage* 30:4293–4310. <https://doi.org/10.1007/s11269-016-1421-8>
- Morisawa ME (1962) Quantitative geomorphology of some watersheds in the Appalachian plateau. *GSA Bulletin* 73:1025–1046. [https://doi.org/10.1130/0016-7606\(1962\)73\[1025:QGOSWI\]2.0.CO;2](https://doi.org/10.1130/0016-7606(1962)73[1025:QGOSWI]2.0.CO;2)
- Mukherjee P, Singh CK, Mukherjee S (2012) Delineation of groundwater potential zones in arid region of India—A remote sensing and GIS approach. *Water Resour Manage* 26:2643–2672. <https://doi.org/10.1007/s11269-012-0038-9>
- Murmu P, Kumar M, Lal D, et al (2019) Delineation of groundwater potential zones using geospatial techniques and analytical hierarchy process in Dumka district, Jharkhand, India. *Groundwater for Sustainable Development* 9:100239. <https://doi.org/10.1016/j.gsd.2019.100239>
- Nag SK, Das S (2017) Assessment of groundwater quality from Bankura I and II Blocks, Bankura District, West Bengal, India. *Appl Water Sci* 7:2787–2802. <https://doi.org/10.1007/s13201-017-0530-8>
- Nag SK, Ray S (2015) Deciphering groundwater potential zones using geospatial technology: A study in Bankura block I and block II, Bankura district, West Bengal. *Arab J Sci Eng* 40:205–214. <https://doi.org/10.1007/s13369-014-1511-y>
- Nampal H, Pradhan B, Manap MA (2014) Application of GIS based data driven evidential belief function model to predict groundwater potential zonation. *Journal of Hydrology* 513:283–300. <https://doi.org/10.1016/j.jhydrol.2014.02.053>
- Nasir MJ, Khan S, Zahid H, Khan A (2018) Delineation of groundwater potential zones using GIS and multi influence factor (MIF) techniques: a study of district Swat, Khyber Pakhtunkhwa, Pakistan. *Environ Earth Sci* 77:367. <https://doi.org/10.1007/s12665-018-7522-3>
- Nemawwi P, Odiyo JO, Makungo R (2019) Estimation of groundwater recharge response from rainfall events in a semi-arid fractured aquifer: Case study of quaternary catchment A91H, Limpopo Province, South Africa. *Cogent Engineering* 6:. <https://doi.org/10.1080/23311916.2019.1635815>
- Oke MO, Martins O, Idowu OA, Aiyelokun O (2015) Comparative analysis of groundwater recharge estimation Value obtained using empirical methods in Ogun and Oshun river basins. *Ifé Journal of Science* 17:53–63
- Olson DL (1988) Topics in theory of the analytical hierarchy process. *Mathematical and Computer Modelling* 11:206–209
- Ozdemir A (2011) GIS-based groundwater spring potential mapping in the Sultan Mountains (Konya, Turkey) using frequency ratio, weights of evidence and logistic regression methods and their comparison. *Journal of Hydrology* 411:290–308. <https://doi.org/10.1016/j.jhydrol.2011.10.010>
- Panahi MR, Mousavi SM, Rahimzadegan M (2017) Delineation of groundwater potential zones using remote sensing, GIS, and AHP technique in Tehran–Karaj plain, Iran. *Environ Earth Sci* 76:792. <https://doi.org/10.1007/s12665-017-7126-3>

- Pinto D, Shrestha S, Babel MS, Ninsawat S (2017) Delineation of groundwater potential zones in the Comoro watershed, Timor Leste using GIS, remote sensing and analytic hierarchy process (AHP) technique. *Appl Water Sci* 7:503–519. <https://doi.org/10.1007/s13201-015-0270-6>
- Prabhakaran A, Raj N Jawahar (2018) Drainage morphometric analysis for assessing form and processes of the watersheds of Pachamalai hills and its adjoinings, Central Tamil Nadu, India. *Appl Water Sci* 8:31. <https://doi.org/10.1007/s13201-018-0646-5>
- Rajasekhar M, Sudarsana Raju G, Sreenivasulu Y, Siddi Raju R (2019) Delineation of groundwater potential zones in semi-arid region of Jilledubanderu river basin, Anantapur District, Andhra Pradesh, India using fuzzy logic, AHP and integrated fuzzy-AHP approaches. *HydroResearch* 2:97–108. <https://doi.org/10.1016/j.hydres.2019.11.006>
- Rajaveni SP, Brindha K, Elango L (2017) Geological and geomorphological controls on groundwater occurrence in a hard rock region. *Appl Water Sci* 7:1377–1389. <https://doi.org/10.1007/s13201-015-0327-6>
- Ramanathan R (2001) A note on the use of the analytic hierarchy process for environmental impact assessment. *Journal of Environmental Management* 63:27–35. <https://doi.org/10.1006/jema.2001.0455>
- Razandi Y, Pourghasemi HR, Neisani NS, Rahmati O (2015) Application of analytical hierarchy process, frequency ratio, and certainty factor models for groundwater potential mapping using GIS. *Earth Sci Inform* 8:867–883. <https://doi.org/10.1007/s12145-015-0220-8>
- Reese SO, Risser DW (2010) Summary of groundwater-recharge estimates for Pennsylvania: Pennsylvania Geological Survey, Harrisburg
- Saaty TL (1990) How to make a decision: The analytic hierarchy process. *European Journal of Operational Research* 48:9–26. [https://doi.org/10.1016/0377-2217\(90\)90057-1](https://doi.org/10.1016/0377-2217(90)90057-1)
- Saaty TL, Vargas LG (1982) *The Logic of Priorities: Applications in Business, Energy, Health, and Transportation*. The Hague, Boston
- Sar N, Khan A, Chatterjee S, Das A (2015) Hydrologic delineation of ground water potential zones using geospatial technique for Keleghai river basin, India. *Model Earth Syst Environ* 1:25. <https://doi.org/10.1007/s40808-015-0024-3>
- Saraf AK, Choudhury PR (1998) Integrated remote sensing and GIS for groundwater exploration and identification of artificial recharge sites. *International Journal of Remote Sensing* 19:1825–1841. <https://doi.org/10.1080/014311698215018>
- Sen A, Das B, Nandi M (1998) Tectono – stratigraphic studies of the supracrustal rocks at the southern contact of the Chhotanagpur granite gneiss with proterozoic mobile belt in Bankura and Purulia districts, West Bengal extending upto the northern flank of the Dalma volcanics. Geological Survey of India, Government of India, New Delhi
- Shailaja G, Kadam AK, Gupta G, et al (2019) Integrated geophysical, geospatial and multiple-criteria decision analysis techniques for delineation of groundwater potential zones in a semi-arid hard-rock aquifer in Maharashtra, India. *Hydrogeol J* 27:639–654. <https://doi.org/10.1007/s10040-018-1883-2>
- Shantharam Y, Elangovan K (2018) Groundwater potential zones delineation using geo-electrical resistivity method and GIS for Coimbatore, India. *Indian Journal of Geo-Marine Sciences* 47:1088–1095
- Shekhar S, Pandey AC (2014) Delineation of groundwater potential zone in hard rock terrain of India using remote sensing, geographical information system (GIS) and analytic hierarchy process (AHP) techniques. *Geocarto International* 30:402–421. <https://doi.org/10.1080/10106049.2014.894584>
- Singh LK, Jha MK, Chowdary VM (2018) Assessing the accuracy of GIS-based Multi-Criteria Decision Analysis approaches for mapping groundwater potential. *Ecological Indicators* 91:24–37. <https://doi.org/10.1016/j.ecolind.2018.03.070>
- Singh P, Thakur JK, Kumar S (2013) Delineating groundwater potential zones in a hard-rock terrain using geospatial tool. *Hydrological Sciences Journal* 58:213–223. <https://doi.org/10.1080/02626667.2012.745644>

- Singh SK, Laari PB, Mustak Sk, et al (2017) Modelling of land use land cover change using earth observation data-sets of Tons River Basin, Madhya Pradesh, India. *Geocarto International* 33:1202–1222. <https://doi.org/10.1080/10106049.2017.1343390>
- Siva G, Nasir N, Selvakumar R (2017) Delineation of groundwater potential zone in Sengipatti for Thanjavur district using analytical hierarchy process. *IOP Conf Ser: Earth Environ Sci* 80:012063. <https://doi.org/10.1088/1755-1315/80/1/012063>
- Sivaramakrishnan J, Asokan A, Sooryanarayana KR, et al (2015) Occurrence of ground water in hard rock under distinct geological setup. *Aquatic Procedia* 4:706–712. <https://doi.org/10.1016/j.aqpro.2015.02.091>
- Subba Rao N (2006) Groundwater potential index in a crystalline terrain using remote sensing data. *Environ Geol* 50:1067–1076. <https://doi.org/10.1007/s00254-006-0280-7>
- Suhag R (2016) Overview of ground water in India. PRS India, New Delhi
- Summerfield MA (1999) *Global geomorphology: an introduction to the study of landforms*, [8.] repr. Addison Wesley Longman, Harlow
- Swetha TV, Gopinath G, Thirvikramji KP, Jesiya NP (2017) Geospatial and MCDM tool mix for identification of potential groundwater prospects in a tropical river basin, Kerala. *Environ Earth Sci* 76:428. <https://doi.org/10.1007/s12665-017-6749-8>
- Teixeira J, Chaminé HI, Carvalho JM, et al (2013) Hydrogeomorphological mapping as a tool in groundwater exploration. *Journal of Maps* 9:263–273. <https://doi.org/10.1080/17445647.2013.776506>
- Trabelsi F, Lee S, Khlifi S, Arfaoui A (2019) Frequency ratio model for mapping groundwater potential zones using GIS and remote sensing; Medjerda watershed Tunisia. In: Chaminé HI, Barbieri M, Kisi O, et al. (eds) *Advances in Sustainable and Environmental Hydrology, Hydrogeology, Hydrochemistry and Water Resources*, Springer International Publishing, Cham, pp. 341–345
- Vaidyanadhan R, Ghosh RN (1993) Quaternary of the East Coast of India. *Current Science* 64:804–816
- Viera AJ, Garrett JM (2005) Understanding interobserver agreement: the kappa statistic. *Fam Med* 37:360–363
- Waris M, Panigrahi S, Mengal A, et al (2019) An application of analytic hierarchy process (AHP) for sustainable procurement of construction equipment: Multicriteria-based decision framework for Malaysia. *Mathematical Problems in Engineering* 2019:1–20. <https://doi.org/10.1155/2019/6391431>
- World Bank (2010) *Deep wells and prudence : towards pragmatic action for addressing groundwater overexploitation in India* (English). Washington, DC
- World Water Assessment Programme (United Nations), UN-Water, Unesco (eds) (2009) *Water in a changing world*, 3rd ed. UNESCO Publishing; Earthscan, Paris: London

Chapter 10

Performance of Frequency Ratio Approach for Mapping of Groundwater Prospect Areas in an Area of Mixed Topography



Subhas Garai and Pulakesh Das

Abstract Assessment of groundwater potential zones is important to ensure the sustainable use of limited groundwater resources in dry subtropical regions. The increased freshwater demand for households, irrigation during the drier seasons for multiple cropping, economic development, and industrial use imposing threats to water resources, which may continue under the projected change scenarios. The geospatial analysis allows the integration of several proxy variables in demarcating the groundwater potential zones based on the importance of each factor in a GIS environment. In the current study, we have added a number of spatial layers as land use land cover, vegetation density, slope, altitude, rainfall, soil, geology, geomorphology, hydrogeology, drainage density, lineament density, and aquifer to estimate groundwater potential for the Paschim Medinipur and Jhargram district, West Bengal, India. The frequency ratio (FR) method was applied to derive the groundwater potential zones, indicated well-accepted performance judged by the AUC value of 0.732. The study indicated a higher importance of geomorphology, soil, slope, hydrogeology, and aquifer. The high and moderate groundwater potential zones are identified in around 30.15% and 40% of the area, respectively. These areas are mostly observed in the eastern and northern parts of the study area. Moreover, 25.59% of the total area is identified as lower potential zones, mostly distributed in the western part.

Keywords Aquifer · Frequency ratio · Groundwater potential · Jhargram · Paschim Medinipur

S. Garai · P. Das (✉)

Department of Remote Sensing & GIS, Vidyasagar University, Mindapore, West Bengal, India

10.1 Introduction

Ground water is one of the important sources of the natural freshwater stored in the subsurface geological formations. Alteration in the climate condition and over-exploitation of the groundwater for various purposes causing a significant reduction in the groundwater level. The increased demand for groundwater for households, agriculture irrigation, and industrial use imposes an immense pressure on the groundwater resources. The scarcity of groundwater is more severe in the drier sub-tropical, arid, and semi-arid regions with high population density and cropping intensity. Moreover, the regions with intense and recurrent drought events cause degradation in the groundwater level (Pandey and Srivastava 2019). Significant depletion in groundwater resources imposes threats to agricultural productivity and water security. About 68% of the annual groundwater recharge in India is dependent on the rainfall, and another 32% is contributed by the other resources as canal seepage, excess water from cropland, recharge from tanks, ponds, and water conservation structures (Groundwater Yearbook 2013–14). In India, around 62% of the water used in irrigation is extracted from groundwater, while around 85% and 45% of rural and urban water use are extracted from the groundwater resources, respectively (Saha and Ray 2019). According to a study conducted in India's groundwater indicated that more than 54% of the total geographic area experiences high to extremely high water stress (WRI India report 2015). The reduction in precipitation has shown a direct and indirect impact on the groundwater storage, indicated the rate of reduction by $2 \text{ cm}\cdot\text{year}^{-1}$ and increase by $1\text{--}2 \text{ cm}\cdot\text{year}^{-1}$ in northern and southern India, respectively, during the period 2002–2013 (Asoka et al. 2017).

The occurrence and distribution of groundwater are primarily regulated by surface and sub-surface soil's porosity and permeability with the underlying lithology (Shahid et al. 2000). The groundwater potentiality is decided based on the different lithology and geomorphic units. The percolation of rainwater, different water channels, and resources through the soil is stored in porous soils and rocks. When the soil zone becomes saturated, water percolates downward. A zone of saturation occurs where all the interstices are filled with water. Groundwater is also recharged when there is a leakage in water supply systems and a surplus of water in agricultural land. Groundwater is stored in the aquifer's zone, which is a geological formation consisting of permeable material capable to store/yield significant quantities of water. Aquifers are composite of unconsolidated sands and gravels, permeable sedimentary rocks (e.g., sandstones or limestones), fractured volcanic and crystalline rocks, etc. The rock contains water-filled pore spaces, and, when the spaces are connected, the water can flow through the matrix of the rock. Aquifers are categorized into four types as (i) confined, (ii) unconfined, (iii) perched, and (iv) leaky, which are having different storage capacities. Groundwater storage also encompasses a variety of chemical processes including dissolution, hydrolysis, and precipitation reactions, adsorption, and ion exchange. The major chemical components of groundwater are sodium ion, potassium ion, magnesium ion, calcium ion, bicarbonate ion, sulfate ion, chloride ion, and hydrogen silicate.

Groundwater studies are important for monitoring seasonal changes, demand assessment, targeting groundwater potential zones, and conservation. The traditional approaches for groundwater assessment use ground surveys employing geophysical, geological, and hydrogeological tools. However, such methods are time-consuming, are costly, and have scale limitation. However, the geospatial technique is an alternative approach that allows seasonal and long-term monitoring in the geographical area. The optical remote sensing system has a limitation in collecting data of the subsurface parameters; however, the suitable microwave sensors can penetrate surface soil layers enabling the proxy measure of the groundwater resource. The latest GRACE data measures the changes in the gravity field, which provides a proxy measure of groundwater storage. Rodell et al. (2009) analyzed the GRACE data and employed a hydrological model to simulate changes in groundwater storage and reported an annual depletion rate of 4 ± 1 cm.year⁻¹ in Rajasthan, Punjab, and Haryana states of India.

Alternatively, the presence of groundwater can be inferred by integrating different proxy indicators on surface features derived from satellite imagery (i.e., land use land cover, surface water bodies, river network) and surveyed maps (i.e., geology, landforms, soils) (Todd 1980; Jha and Peiffer 2006). The assessment of groundwater potentiality using geospatial technology requires the study or integration of causative factors and field observations. Such factor mostly includes the layers as rainfall, topographic factors (slope, aspect), lithology, aquifer thickness, drainage density, lineaments, and land use land cover. The land utilization practice and vegetation cover play important roles in groundwater recharge processes (Leduc et al. 2001). The land slope determines the flow of water and residing time for water enabling groundwater recharge. The lower slope allows high groundwater recharge, while a higher slope leads to poor groundwater potential zones. Rainfall is one of the major sources for groundwater recharging through the hydrologic processes for a fractured aquifer (Ettazarini 2007). The soil texture regulates the percolation of water, where the fine-grained soil has lower permeability than coarse-grained. The sandy and coarse sandy clay soil are more suitable due to the higher infiltration rate that influences the groundwater recharge (Srivastava and Bhattacharya 2006), while clay soil is considered as poor due to being poorly drained, lower permeability, and hydraulic conductivity (Chowdhury et al. 2009).

The importance or influence of different data layers is either decided based on the expert's knowledge or derived through integrated analysis based on the field observed values. The obtained equation is then used to estimate values for other known location enabling validation of the developed model. Several methods have been adopted in various studies, i.e., analytical hierarchical process (AHP), frequency ratio (FR), multi-criteria decision analysis (MCDA), logistic regression (LR), decision tree (DT), and machine learning approaches as artificial neural network (ANN), Support Vector Machine (SVM), and random forest (RF) (Arulbalaji et al. 2019; Machiwal et al. 2011; Park et al. 2017; Duan et al. 2016; Lee et al. 2018; Naghibi et al. 2017). Shahid et al. (2000) adopted Analytical Hierarchy Process (AHP) method for assessing the groundwater potential zone deriving the Groundwater Potential Index (GWPI) based on seven factors, where

the existing borehole and pumping data was used to estimate the modeling accuracy. Gupta and Srivastava (2010) integrated various GIS layers on topography, geological structures, the extent of fractures, secondary porosity, slope, drainage pattern, landforms, LULC, and climatic conditions to estimate the groundwater potential in Pavagarh, Gujarat, India. Razandi et al. (2015) used FR and AHP to assess the groundwater potential zones, where they have followed three basic steps as (i) development of a spatial database on the various factors to regulate groundwater potential, (ii) spatial analysis of well locations and groundwater conditioning factors, and (iii) extrapolation and validation. Guru et al. (2017) assessed the groundwater potential zone in Leh valley using the FR model employing eight factors, including land use land cover map derived from LISS-IV data. For validation, the area under the curve was employed considering the cumulative percentage of spring wells and percent of groundwater potentiality index value. The FR model has been utilized in several studies for the demarcation of potential groundwater zones (Manap et al. 2013; Ozdemir 2011; Pourtaghi and Pourghasemi 2014).

Das et al. (2019) employed AHP and pair-wise comparison matrix to map the groundwater potential zone in Purulia district of West Bengal, India, and observed 60.92% and 16.53% of the study area under the moderate and lower potential zones. Chowdhury et al. (2009) delineated the groundwater potential zones in Paschim Medinipur (earlier Jhargram and Paschim Medinipur) employing the AHP technique and reported around 55% and 30% of the total area is residing in moderate and low potential zones. In the current study, we have demarcated the groundwater potential zones in two cropland- and forest-dominated districts as Jhargram and Paschim Medinipur, West Bengal, India, using the FR model.

10.2 Study Area

The Paschim Medinipur and Jhargram districts of West Bengal state are considered for the current study. The study regions are situated in the southern part of West Bengal. Geographically the area extension is in between latitude $21^{\circ}45'39''\text{N}$ and $22^{\circ}56'54''\text{N}$, and longitude $87^{\circ}53'20''\text{E}$ and $86^{\circ}3'11''\text{E}$ falls under the Gangetic region (Fig. 10.1). The total area of the study region is 9393.15 km². Agriculture is the predominant land use class followed by dense forest. The main three rivers in this region are as follows: Subarnarekha flows in the south part, the Kasai River flows in the heart of West Midnapore and Jhargram district, and the Silavati river creates a green stretch in the upper portion of the study area. The study region is classified as the sub-tropical climate zone. The mean annual precipitation is about 1560 mm, and the majority (~74%) of the precipitation occurs during the Monsoon, whereas the mean annual temperature varies from 9 °C in the winter to 44 °C in the summer.

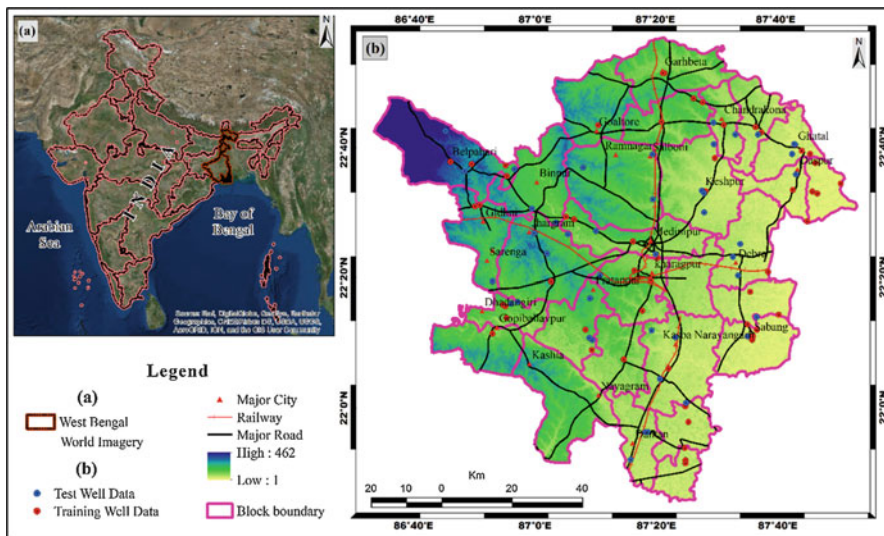


Fig. 10.1 Location map with SRTM elevation data of the study area

10.3 Data and Methodology

10.3.1 Data Collection

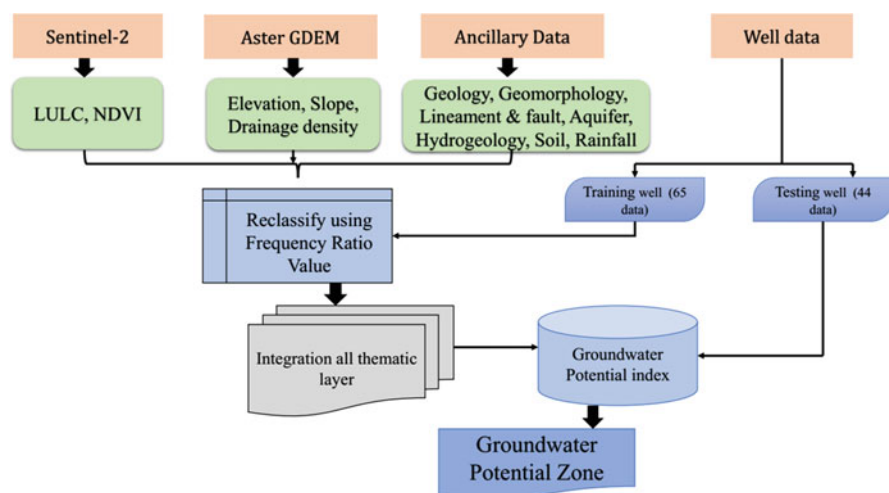
For potential groundwater zones demarcation, various spatial layers are integrated into the current study. Sentinel-2 optical remote sensing data has been accessed from sentinel-hub portal to generate the land use land cover map and vegetation density map and identify the geomorphic units for the study area. The Shuttle Radar Topography Mission (SRTM) data derived digital elevation model (DEM; 30 m spatial resolution) is used to create the topographic variables (elevation and slope). The details of various other layers included in the current study are given in Table 10.1.

10.3.2 Methodology

The Sentinel-2 bands having 10 m and 20 m spatial resolution were stacked to create the land use land cover map. The maximum likelihood classifier method was applied in the supervised classification, and the output map was verified with the high-resolution Google Earth imagery. The Sentinel-2 data is further used to derive the vegetation density map using the normalized difference vegetation index (NDVI). The SRTM DEM data is used to prepare the altitude map and derive the topographic slope map. The DEM data is further used for hydrological analysis to create the

Table 10.1 Data used for identifying the groundwater potentiality

Data	Scale/ resolution	Source
Soil	1:250,000	National Bureau of Soil Survey and Land Use Planning (NBSS & LUP)
Geology	1:250,000	Geological Survey of India (GSI)
Geomorphological	1:50,000	The National Geomorphological and Lineament Mapping (NGLM)
Hydrogeology and well data	1:250,000	Central Groundwater Board (CGWB) and Geological Survey of India (GSI)
Rainfall	1 × 1 km	Climate Hazards Group InfraRed Precipitation with Station (CHIRPS) data
Lineament	1:50,000	The National Geomorphological and Lineament Mapping (NGLM)
Aquifer		India Water Resources Information System

**Fig. 10.2** Overall methodology flowchart

stream or drainage network and corresponding density map. Similarly, the obtained lineament map is used to generate the lineament density map.

The frequency ratio (FR) method is used to estimate the groundwater potential. The FR method employs a bivariate statistical approach to determine the probabilistic relationship between the independent variables or factors and the dependent variable (Oh et al. 2011). Based on the literature survey, twelve important variables are selected, and corresponding criteria maps have been prepared. The selected criteria are elevation, slope, rainfall, drainage density, aquifer, geology, geomorphology, LULC, NDVI, soil, lineament density, and hydrogeology. The overall data analysis for groundwater potential zone mapping is depicted in Fig. 10.2. The FR is defined as the ratio of the area where groundwater wells (high groundwater

productivity) occurred in the total study area. FR model structure is based on the correlation and observed relationships between each groundwater conditioning factor and distribution of groundwater well locations. The following equation is used to compute the FR:

$$FR = \frac{W/G}{M/T} \quad (10.1)$$

where W is the number of pixels with groundwater well for each factor, G is the number of total groundwater wells in the study area, M is the number of pixels in the class area of the factor, and T is the number of total pixels in the study area.

Each map is then reclassified using the frequency ratio value, which was then overlaid to find out the Groundwater Potential Zone (GPZ) use the following equation:

$$GWPI = \sum_{R=1}^{R=n} FR \quad (10.2)$$

10.4 Results and Discussion

The details of the various thematic layers on land use land cover, vegetation, slope, altitude, rainfall, soil, geology, geomorphology, hydrogeology, drainage density, lineament density, and aquifer used in the current study are described as follows.

10.4.1 Land Use Land Cover (LULC)

Land use land cover (LULC) plays an important role in groundwater recharge. The Sentinel-2 data derived LULC map includes the classes as dense and open forest, agriculture fallow, cultivated land, settlement, sand, wetland, and water body (Fig. 10.3). The vegetation cover enables groundwater recharge via several ways as biological decomposition of the roots helps loosen the rock and soil and allows water to percolate the surface, while vegetation prevents runoff and direct evaporation of water from the soil. Moreover, the agriculture fallow (cultivated in monsoon season) and cultivated land enables groundwater recharge of the excess water standing on the ground.

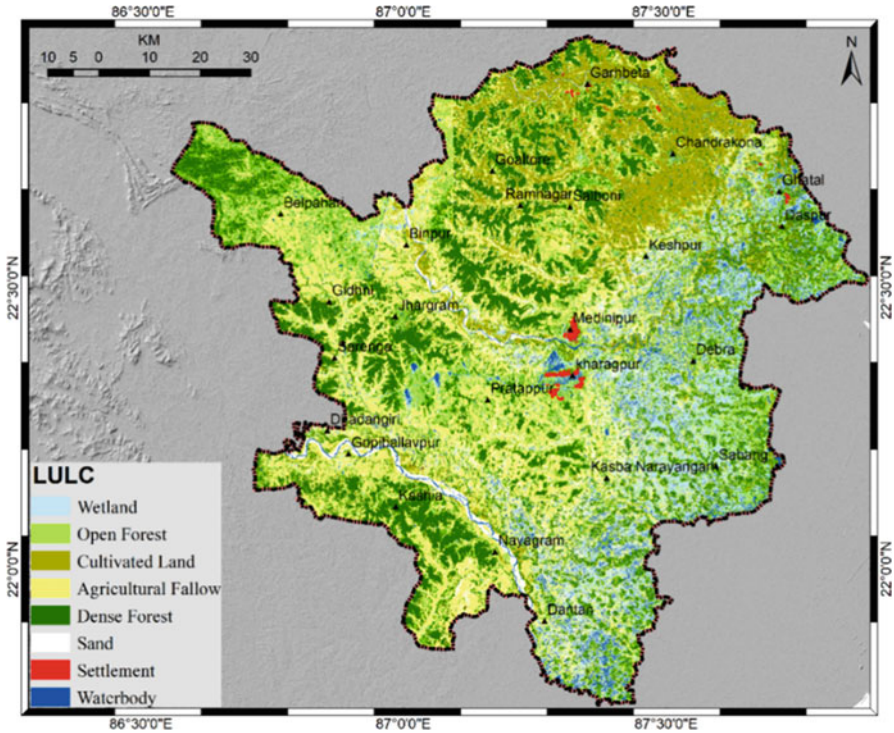


Fig. 10.3 Land use land cover (LULC) map of the study area

10.4.2 Vegetation

In addition to the LULC map, the Normalized Difference Vegetation Index (NDVI) map has been prepared using the red and NIR band of Sentinel 2 imagery to indicate the vegetation coverage in the terrain. The NDVI image was reclassified into five classes, where 0.16–0.24 indicates moderate vegetation density and the class with >0.24 NDVI values indicated dense vegetation and cropland during the post-monsoon rabi season (Fig. 10.4). However, the negative and low positive values indicated the water body and barren land areas. Dense vegetation is observed in the middle, the western, and upper parts of the region.

10.4.3 Altitude

The SRTM DEM data is used to prepare the altitude map indicating the height of any place from the datum. The altitude for the study area varies between 1 m and 462 m, where the altitude of the eastern part is observed lower than the western part. The

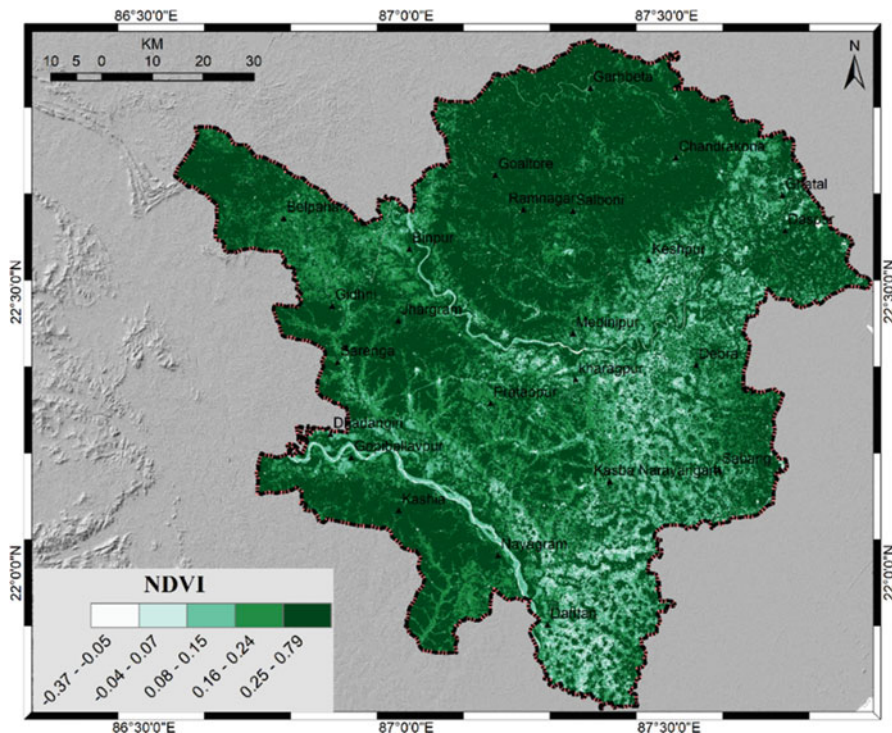


Fig. 10.4 Vegetation greenness map of the study area

altitude data is reclassified into five classes as 1–34 m, 34.01–65 m, 65.01–118 m, 118.01–193 m, and 193.01–462 m (Fig. 10.5).

10.4.4 Slope

Slope indicates the variations in topography and relates the local and regional relief setting, which determines the surface runoff and movement of water, and also regulates groundwater recharge. The observed slope (in degree) is divided into five classes as 0–2.33, 2.34–4.66, 4.67–7.58, 7.59–12.63, and 12.64–49.55 (Fig. 10.6). The majority of the study area belongs to the plain land where a few regions in the western part indicated a higher slope. The eastern part is dominated by alluvial plain, indicated a lower slope. On the other hand, the western part belongs to the hilly region with dominant gravels.

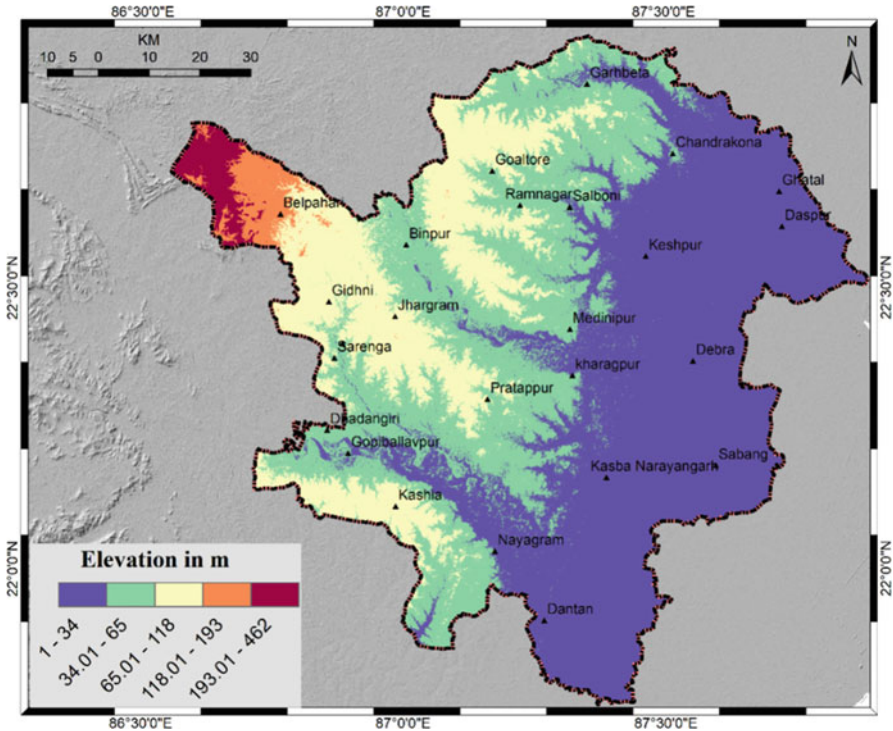


Fig. 10.5 Altitude map of the study area

10.4.5 Rainfall

The annual rainfall and its seasonality are considered as one of the main factors of the hydrologic process that act as a source of groundwater recharge. The high-resolution satellite CHIRPS precipitation data integrated with the ground-based observations is used to prepare the annual rainfall map. The monthly rainfall range is divided into five classes as 170.00–178 mm, 178.01–188 mm, 188.01–193 mm, 193.01–198 mm, and 198.01–207.9 mm (Fig. 10.7). The relationship between rainfall distribution and well location indicated a positive correlation.

10.4.6 Soil

The soil layers regulate the percolation of water through pore spaces. The soil texture dominantly controls the infiltration of surface water into an aquifer, which is determined by the soil texture. The soil map at 1:25000 scale published by the National Bureau of Soil Survey and Land Use Planning (NBSS & LUP) is used in

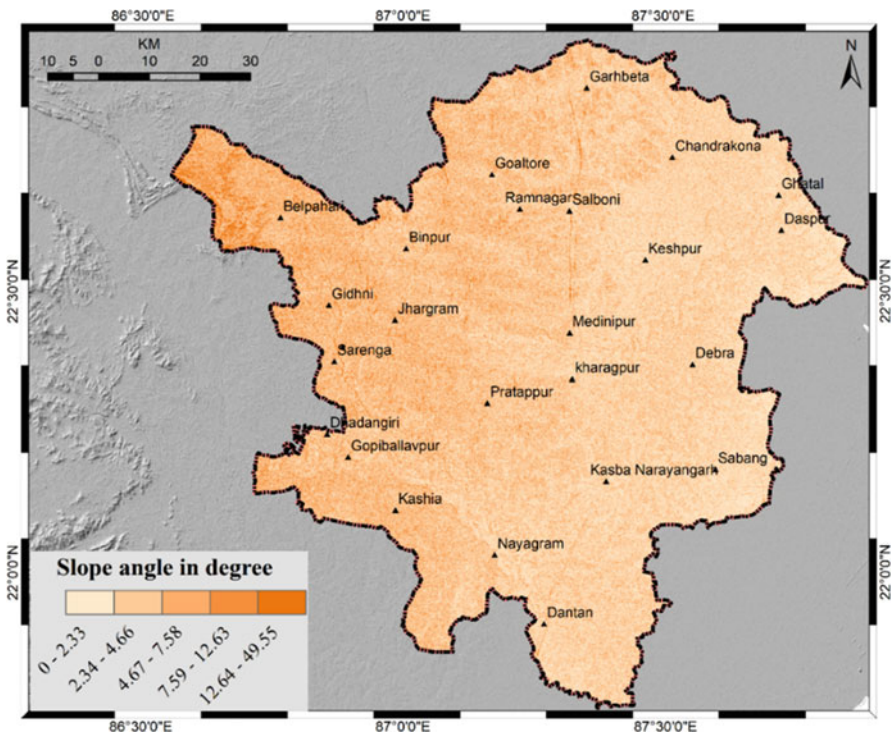


Fig. 10.6 Slope map of the study area, derived from Aster GDEM elevation data

the current study. The infiltration rate also depends on soil thickness and grain size. The coarse-grained soils have high permeability than fine-grained, such as sandy and coarse sandy clay. On the contrary, clay soil has low permeability and checks the groundwater recharge. The dominant soil types observed in this area are lateritic, older alluvial, red gravelly, red sandy, and younger alluvial (Fig. 10.8).

10.4.7 Geology

The type of rock exposed on earth’s surface plays an important role in groundwater recharge. Similar to the soil, the lithology also regulates the groundwater recharge by controlling the percolation of water. The geology map shown as Fig. 10.9 is accessed from the Geological Survey of India (GSI) indicating the occurrences of laterite and bauxite, Kuilpal granite, gravel and sandstone, Gangpur Gp, Dalma volcanic, coastal, and glacial sediments.

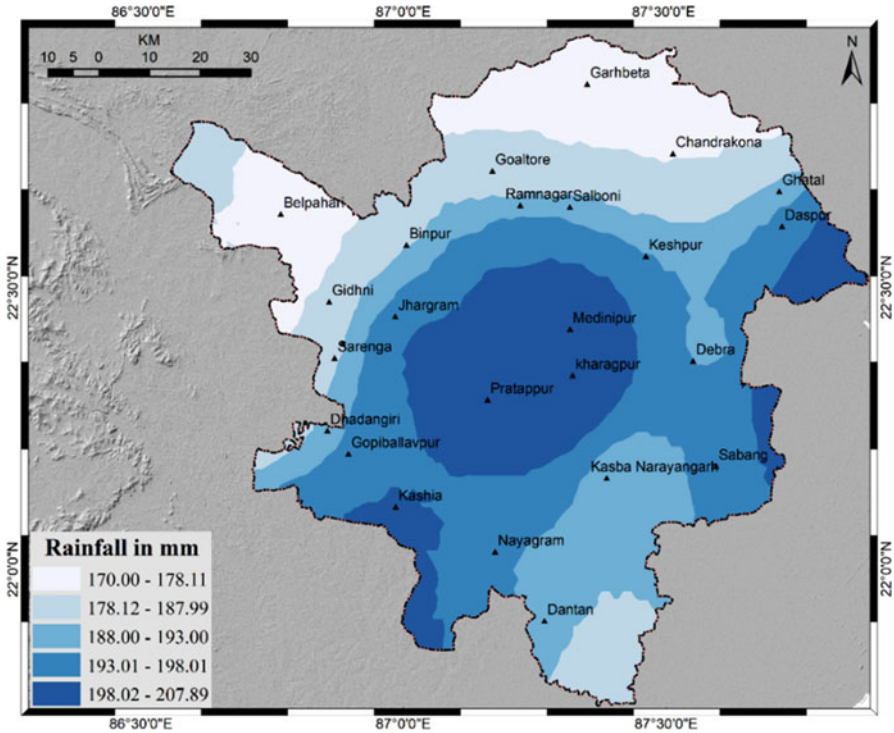


Fig. 10.7 Rainfall map of the study area

10.4.8 Geomorphology

The geomorphic features are indicated by the different landforms developed by the dynamic action of different geological processes as temperature change (freezing and thawing), chemical reactions, seismic shaking, and direction of wind and water (Ramaiah et al. 2012). The geomorphic features of the study area include (i) deep buried pediments, (ii) deep to moderately buried pediments with lateritic capping, (iii) denudational terrace and rocky outcrops, (iv) flood plain deposits, (v) moderately buried pediments with lateritic cropping, (vi) pediments, and (vii) valley fill deposits (Fig. 10.10).

10.4.9 Hydrogeology

Hydrogeology indicates the geological area that deals with the movement and redistribution of [groundwater](#). It regulates the water stored in aquifers and determines the pathways of flow and recharge. The different hydrogeological features

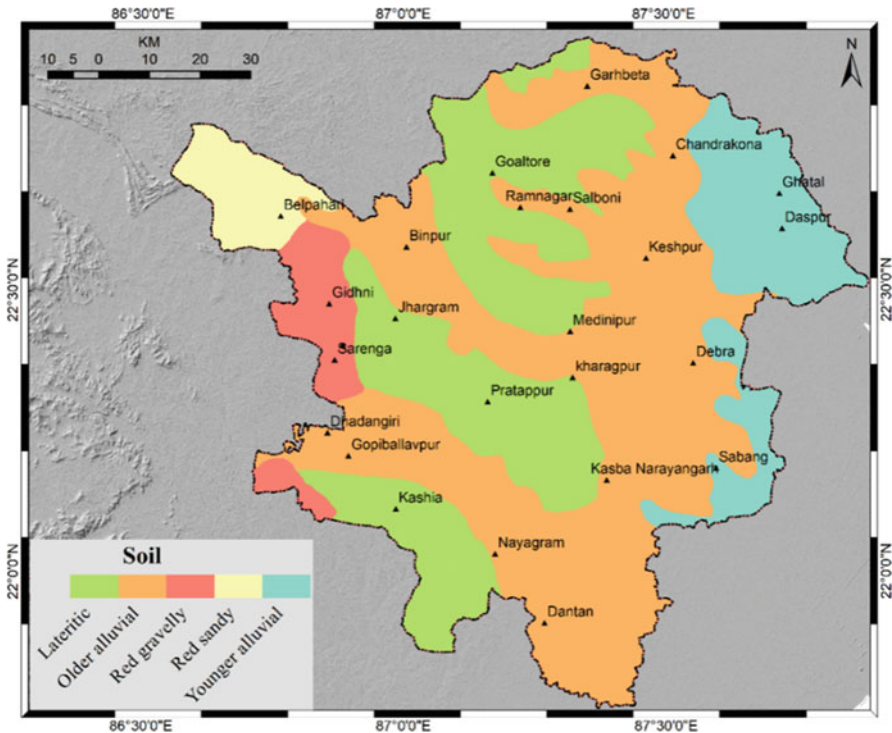


Fig. 10.8 Soil type map of the study area. (Source: NBSS & LUP)

present in the study area include quartz, phyllite, granite, pebbles, gravels, and sands with silts, clay impregnated with caliche nodules, etc., listed in Table 10.2 (Fig. 10.11).

10.4.10 Drainage Density

The rate of groundwater recharge depends on the distribution of the drainage network. The stream network is a function of lithology and density function to the rate that rainfall or water infiltrates. Drainage density is inversely proportional to groundwater potential, where regions with high drainage density are unfavorable for groundwater existence, and, alternatively, regions with lower drainage density represent high groundwater potential zones. Low densities areas allow for longer

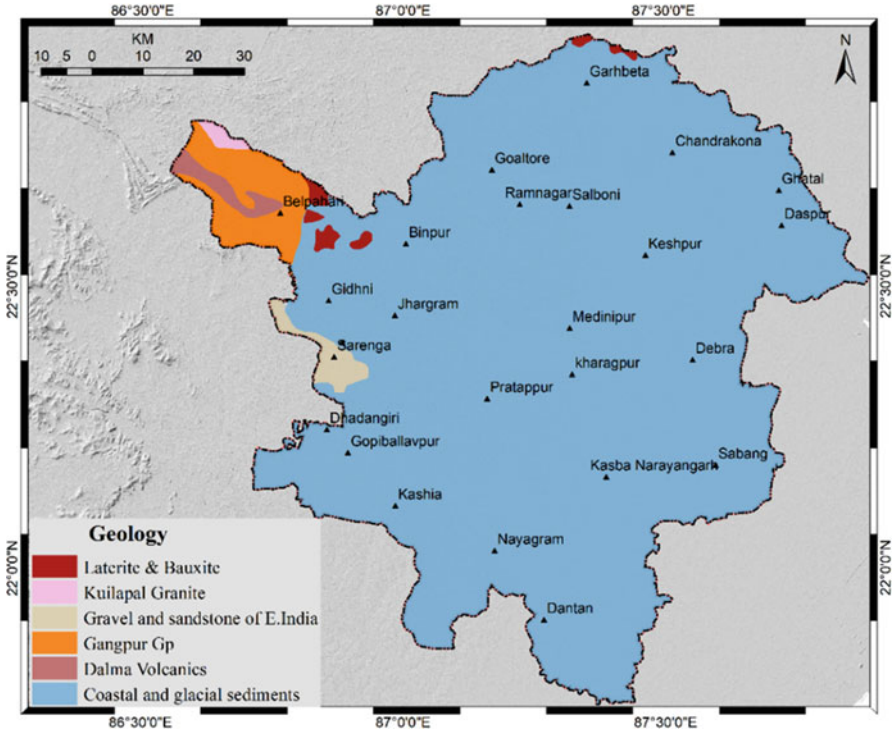


Fig. 10.9 Geological map of the study area. (Source: GSI)

residence time, which allows the abstraction mechanisms to have more time to remove water (Gupta and Srivastava 2010). The drainage density is classified into five classes as 0–0.35, 0.36–0.55, 0.56–0.69, 0.70–0.83, and 0.84–1.19 (Fig. 10.12).

10.4.11 Lineament Density

Lineaments are the structurally controlled linear or curvilinear features, enabling groundwater recharge through the fractures, fissures, joints, and faults (Sahoo et al. 2017). These features exhibit surface expression or topographic variations due to the underlying structural features and represent the potential zones of faulting and fracturing resulted from the increased secondary porosity and permeability. The lineaments are one of the most significant features in groundwater recharge which facilitate the pathways for groundwater flows. Lineament density is thus directly proportional to groundwater potential or recharge zones. The lineament data is accessed from the National Mission on Geomorphological and Lineament Mapping (NMGLM). The observed lineaments were used to generate the lineament density

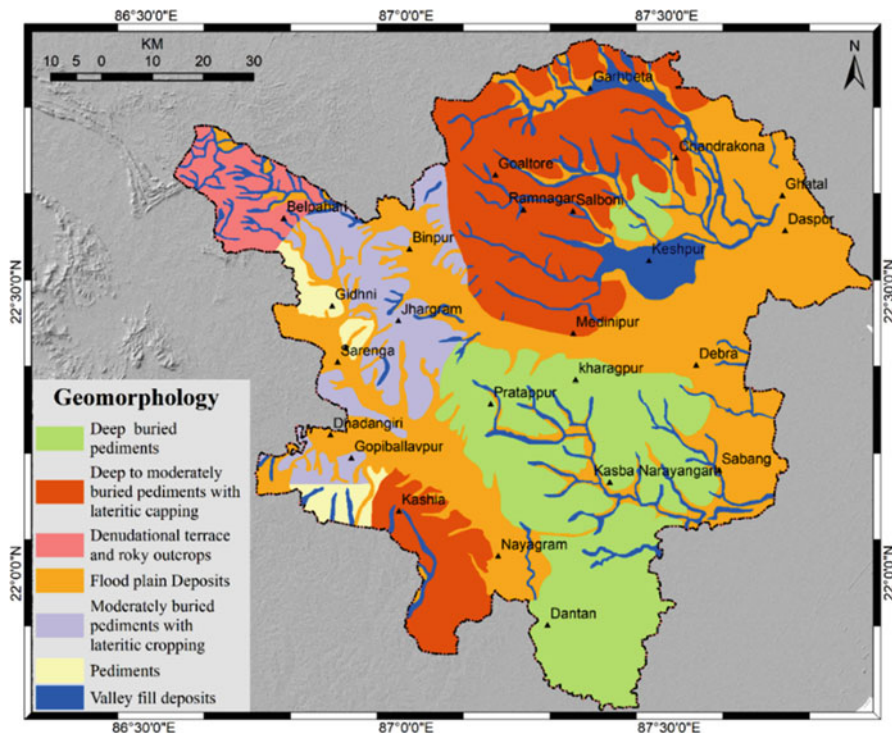


Fig. 10.10 Geomorphology map of the study area. (Source: NGLM)

Table 10.2 Hydrogeology classes and areas

Name	Area (km ²)	Name	Area (km ²)
Quart, phyllite, granite pebbles, and gravels	3639.81	Mica schist	167.98
Sands with silts, clays associated with Fe-nodules	1522.56	Carbon phyllite	37.36
Sands with silts, clay impregnated with caliche nodules	3379.52	Laterite with occasional ring-like growth of silica	0.80
River	161.71	Quartzite	2.86
Phyllite	222.83	Granite-staurolite schist with kyanite	4.63
Gravels of different size	123.54	Clay, grit, and conglomerate	26.64
Sands, silts, and clays	49.82	Sands with silts, clay impregnated with caliche nodules	14.67
Kuilapal granite	38.38		

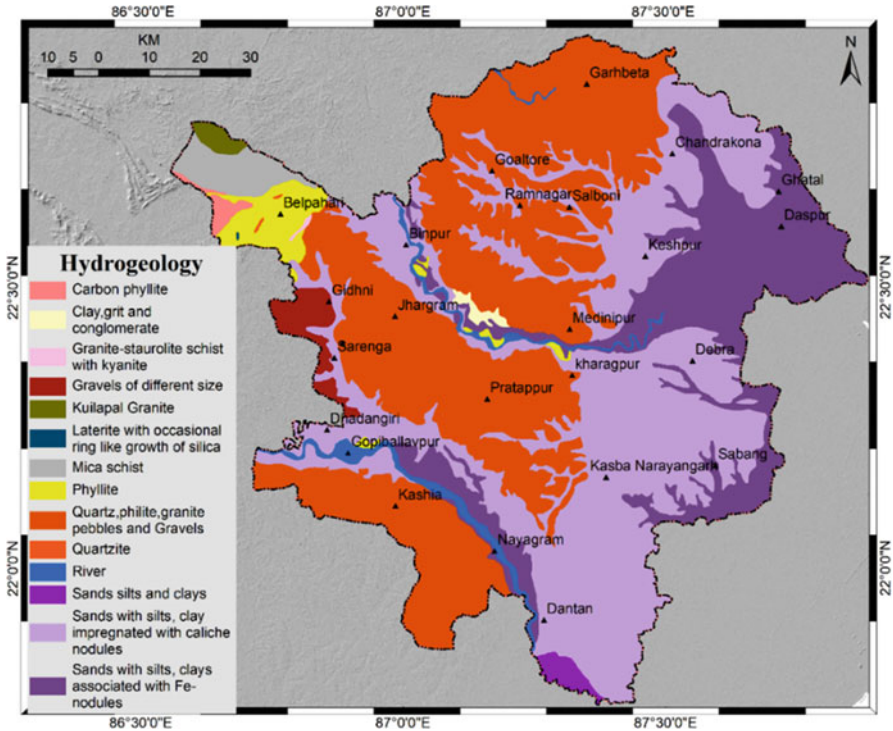


Fig. 10.11 Hydrogeology map of the study area. (Source: Central Groundwater Board (CGWB) and GSI)

map, which has been classified into five classes, viz., 0–0.03, 0.04–0.09, 0.1–0.15, 0.16–0.21, and 0.22–0.29 (Fig. 10.13).

10.4.12 Aquifer

An aquifer is an underground layer of water-bearing rock, where the permeable layers allow liquids and gasses to pass through, while the saturated permeable layers carry movable water and act as an instant groundwater source. Aquifer thickness is an important hydrogeological factor used to demarcate the groundwater potential zone. The four major aquifer systems are observed in the study area, viz., laterite, phyllite, schist, and younger alluvium, as depicted below in Fig. 10.14.

All the thematic layers were further reclassified using the frequency ratio method, which was further integrated to generate the groundwater potential zone for the study area. The calculation for the frequency ratio is shown in Table 10.3. The relation

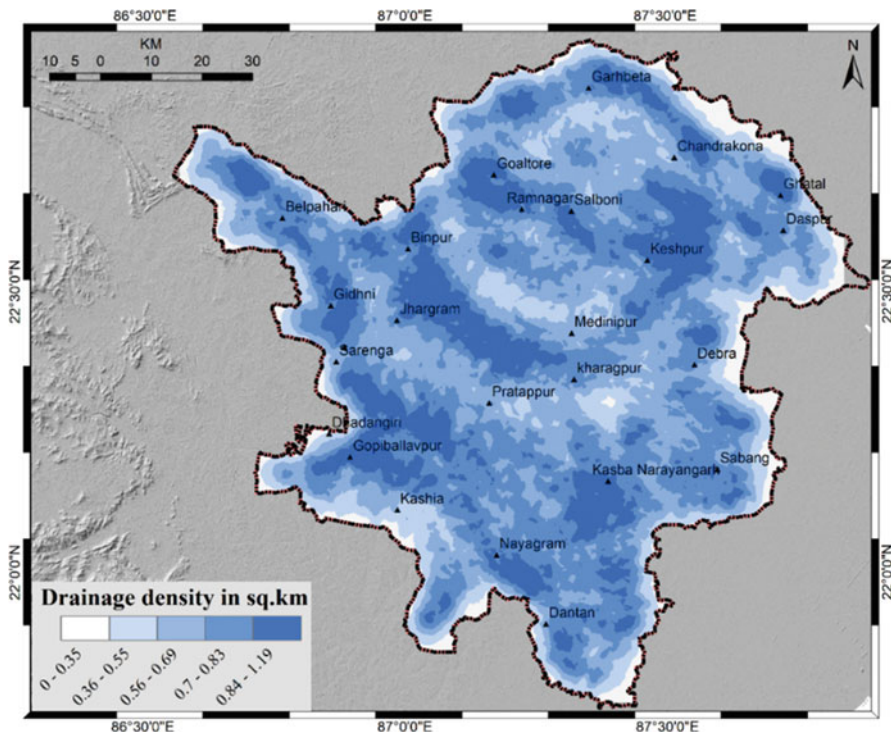


Fig. 10.12 Drainage density map of the study area

between percent (%) of class area, percent (%) of well in the class, and the frequency ratio (FR) value is shown as a line graph (Fig. 10.15).

The ROC curve is created by plotting the true-positive rate (TPR) against the false-positive rate (FPR) at various threshold settings. The true-positive rate indicates sensitivity, recall, or probability of detection. The obtained ROC curve indicated well-accepted accuracy of modeling (Fig. 10.16).

The groundwater potential zone map has been classified into four classes, viz., low, moderate, high, and very high potential zone. The eastern and central region of the study area is observed to have moderate and high groundwater potential covering ~40% and 30.15% of the total area, respectively. The lower potential zones observed in the north-west, west, and south-west regions cover 25.59% of the total area (Fig. 10.17). However, very high potential zones are observed in small patches in and around two major urban areas as Midnapore and Kharagpur city, including other urban areas. The number of wells per unit area is maximum for the very high groundwater potential zones having 14.68% (16 numbers) of the total wells. The majority of the wells around 44% (48 numbers) are observed in high potential zones,

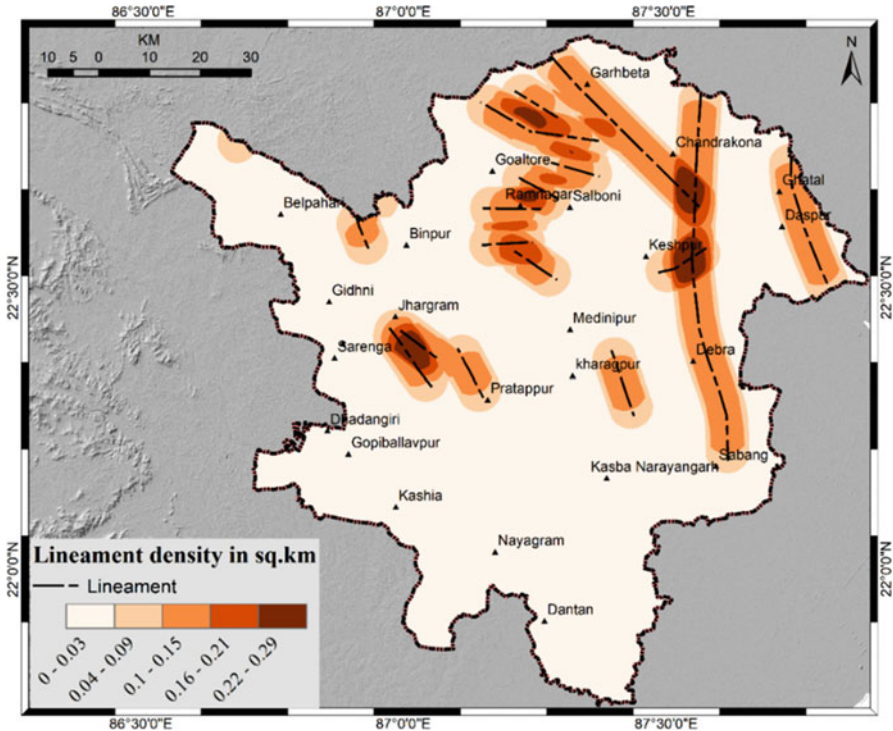


Fig. 10.13 Lineament density map of the study area. (Source: National Mission on Geomorphological and Lineament Mapping; NMGLM)

whereas 33% (36 numbers) of wells are observed in the moderate potential zone. The least number of wells at 8.26% (9 numbers) is observed in the low potential zone (Table 10.4). The dominant contributors to moderate and high potential zones include the geomorphology (flood plain deposit), alluvial soil layer, lower slope, hydrogeology (coarse texture sands with silt), and aquifer (younger alluvium). The estimated groundwater potential map and area statistics in the current study corroborates the similar studies carried out in this region by Chowdhury et al. (2009), where they have reported nearly similar distribution of moderate and good as well as poor potential zones. The majority of the areas as identified under the moderate and high potential zones indicate suitable zones, for artificial groundwater recharge zones as assessed by Chowdhury et al. (2010).

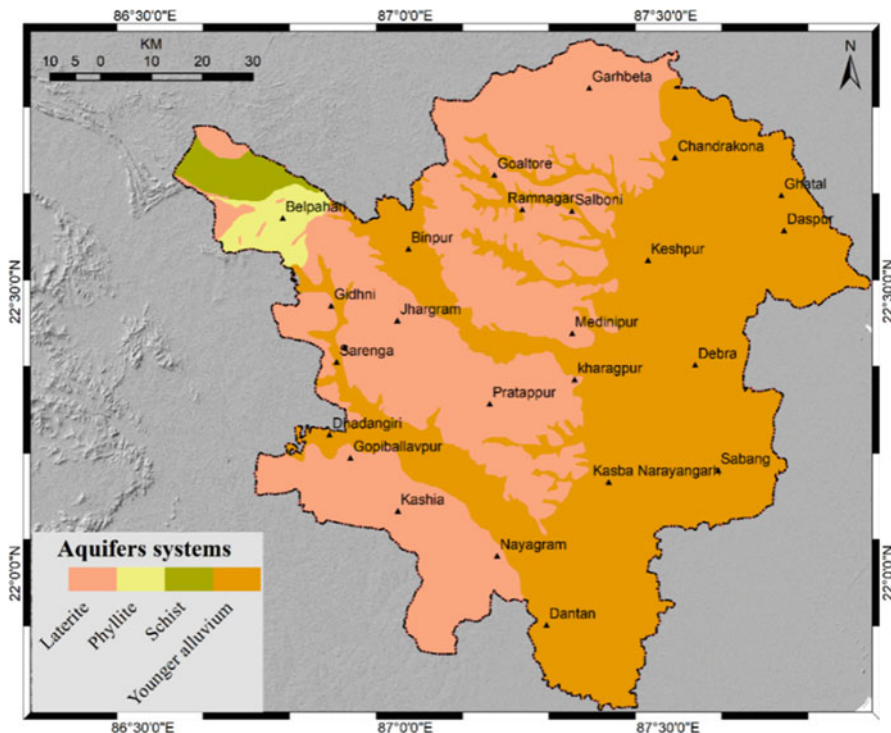


Fig. 10.14 Aquifer distribution of the study area. (Source: India WRIS)

10.5 Conclusion

The current study area is classified under the sub-tropical climate region, where the majority of the population is dependent on agriculture and the allied sector. Vast areas in these two districts are used for multiple cropping, where rice is cultivated in monsoon. On the contrary, the drier pre- and post-monsoon cropping (vegetables and cash crops) is primarily dependent on limited river and canal network for irrigation, while the groundwater is used for irrigation in the majority of the study area. Thus, assessment of groundwater potential is essential for the agriculture and water resource managers to adopt suitable measures ensuring the sustainable use of groundwater resources. For this, a number of factors are used, indicating the contributions of each theme and the sub-classes in estimating the groundwater potential zones for the study area. The dominant factors that lead to moderate and high potential zones include geomorphology, soil, slope, hydrogeology, and aquifer. The regions with flood plain deposits, dominated with alluvial coarse texture soil, located at a lower slope with younger alluvium aquifer, indicating moderate and high groundwater potential zones, were identified in around 40% and 30.15% of the area, respectively. The very high potential zones are identified in the minimal area in this

Table 10.3 The calculation for frequency ratio

Attribute	Class	Class area	Class area %	No of wells	% of well	FR
Aquifer	Laterite	4,503,051	43.16	20	30.77	0.71
	Younger alluvium	5,528,807	52.99	42	64.62	1.22
	Phyllite	215,235	2.06	3	4.62	2.24
	Schist	186,653	1.79	0	0	0
LULC	Wetland	1,198,024	11.48	12	18.46	1.61
	Open forest	1,554,433	14.89	16	24.62	1.65
	Cultivated land	1,372,071	13.15	5	7.69	0.59
	Agricultural fallow	2,903,745	27.82	15	23.08	0.83
	Dense forest	2,592,458	24.84	12	18.46	0.74
	Sand	338,351	3.24	0	0	0
	Settlement	28,706	0.28	5	7.69	27.97
	Waterbody	448,995	4.3	0	0	0
Geology	Coastal and glacial sediments	9,840,211	94.31	63	96.92	1.03
	Gangpur Gp	463,885	4.45	2	3.08	0.69
	Laterite and bauxite	29,392	0.28	0	0	0
	Gravel and sandstone of E. India	100,594	0.96	0	0	0
Geomorphology	Deep buried pediments	2,315,682	22.19	15	23.08	1.04
	Denudational terrace and rocky outcrops	318,006	3.05	1	1.54	0.5
	Deep to moderately buried pediments with lateritic capping	2,249,177	21.55	7	10.77	0.5
	Valley fill deposits	928,096	8.89	6	9.23	1.04
	Flood plain deposits	3,596,672	34.46	32	49.23	1.43
	Pediments	215,714	2.07	0	0	0
	Moderately buried pediments with lateritic cropping	813,487	7.79	4	6.15	0.79
Hydrogeology	Quartz, phyllite, granite pebbles, and gravels	4,044,272	38.75	18	27.69	0.71
	Sands with silts, clays associated with Fe-nodules	1,691,678	16.21	14	21.54	1.33
	Sands with silts, clay impregnated with caliche nodules	3,770,279	36.13	30	46.15	1.28
	River	179,564	1.72	0	0	0
	Phyllite	247,639	2.37	2	3.08	1.3
	Gravel size	137,221	1.31	0	0	0
	Sand, silt, and clay	55,362	0.53	0	0	0
	Kuilapal granite	42,647	0.41	0	0	0
	Mica schist	186,653	1.79	0	0	0
	Carbon phyllite	41,503	0.4	0	0	0
	888	0.01	0	0	0	

(continued)

Table 10.3 (continued)

Attribute	Class	Class area	Class area %	No of wells	% of well	FR
	Laterite with occasional ring-like growth of silica					
	Quartzite	3179	0.03	0	0	0
	Granite-staurolite schist with kyanite	5134	0.05	0	0	0
	Clay, grit, and conglomerate	29,615	0.28	1	1.54	5.42
Lineament density	0–0.03	7,667,175	73.46	41	63.08	0.86
	0.04–0.09	981,221	9.4	7	10.77	1.15
	0.10–0.15	1,371,136	13.14	15	23.08	1.76
	0.16–0.21	259,800	2.49	2	3.08	1.24
	0.22–0.29	157,472	1.51	0	0	0
NDVI	–0.32	50,390	0.48	0	0	0
	–0.11	366,678	3.51	4	6.15	1.75
	0.08–0.15	1,135,984	10.89	12	18.46	1.7
	0.16–0.24	2,440,609	23.39	12	18.46	0.79
	0.25–0.79	6,441,774	61.73	37	56.92	0.92
Soil	Red sandy	453,869	4.35	1	1.54	0.35
	Red gravelly	501,765	4.81	2	3.08	0.64
	Lateritic	3,140,607	30.09	10	15.38	0.51
	Older alluvial	5,063,651	48.52	35	53.85	1.11
	Younger alluvial	1,276,918	12.23	17	26.15	2.14
Drainage Density	0.02–0.52	813,992	7.8	3	4.62	0.59
	0.53–0.73	1,884,140	18.05	11	16.92	0.94
	0.74–0.87	3,583,328	34.33	16	24.62	0.72
	0.88–1.02	3,202,668	30.69	31	47.69	1.55
	1.03–1.64	952,676	9.13	4	6.15	0.67
Slope	0–2.33	3,578,823	34.29	29	44.62	1.3
	2.34–4.66	4,156,950	39.83	22	33.85	0.85
	4.67–7.58	1,963,869	18.82	12	18.46	0.98
	7.59–12.63	639,984	6.13	2	3.08	0.5
	12.64–49.55	96,707	0.93	0	0	0
Altitude	<34	4,903,794	46.99	37	56.92	1.21
	34.01–65	3,172,837	30.4	20	30.77	1.01
	65.01–118	1,945,785	18.64	7	10.77	0.58
	118.01–193	224,476	2.15	1	1.54	0.72
	193.01–462	189,441	1.82	0	0	0
Rainfall	170.00–178.11	406,590	3.9	2	3.08	0.79
	178.12–187.99	2,939,568	28.17	18	27.69	0.98
	188.00–193.00	1,935,041	18.54	7	10.77	0.58
	193.01–198.01	1,319,452	12.64	12	18.46	1.46
	198.02–207.89	3,835,114	36.75	26	40	1.09

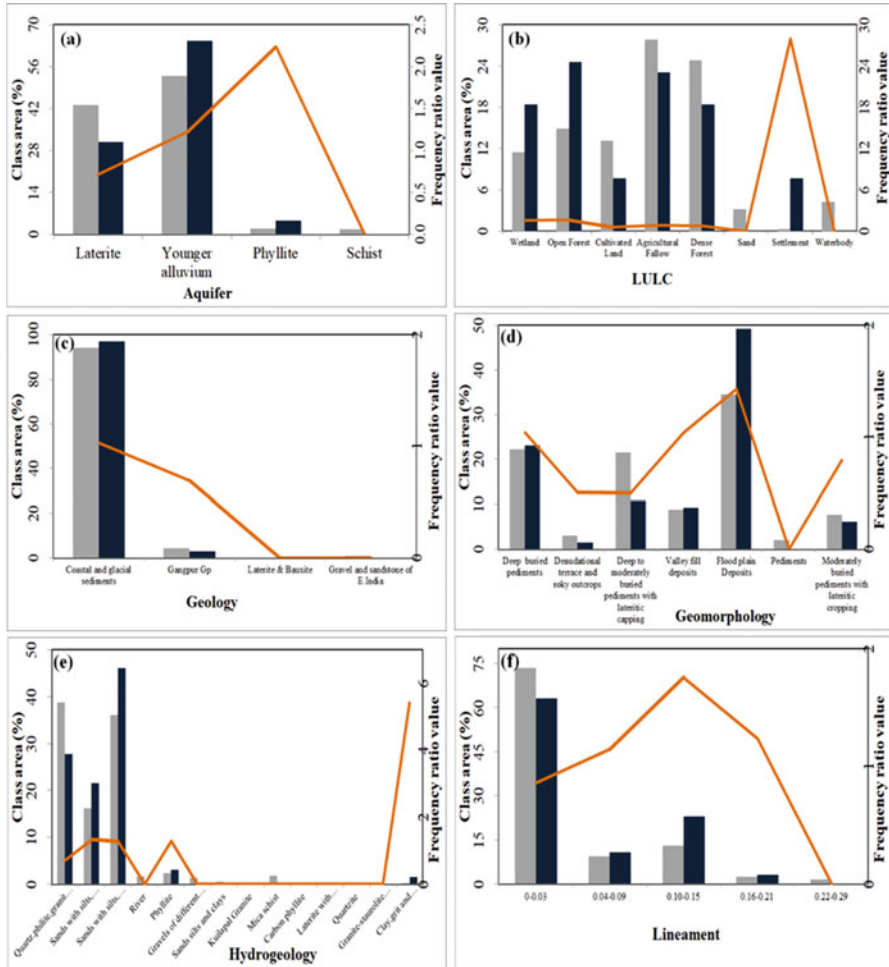


Fig. 10.15 Frequency ratio plot of different parameters

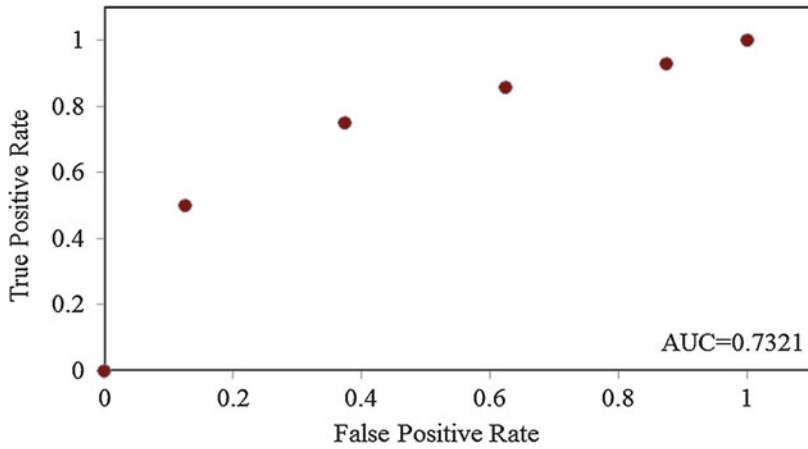


Fig. 10.16 ROC curve showing the false-positive rate with true-positive rate

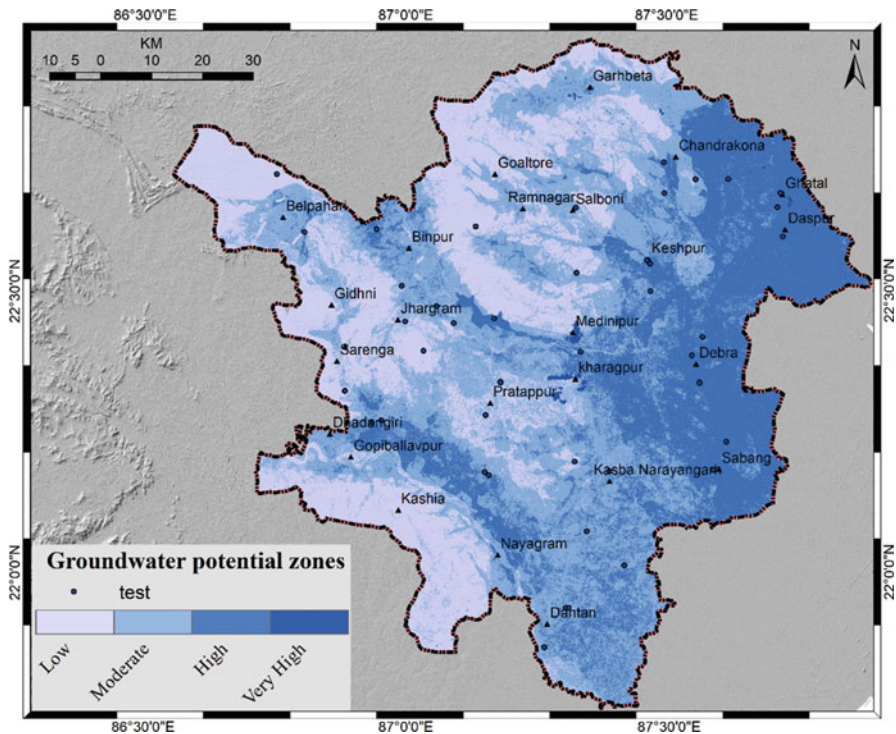


Fig. 10.17 Groundwater potential zone map of the study area

Table 10.4 Area statistics of potentiality map

Class	Area	% Area	No. of well
Low	2780	29.59	9
Moderate	3755	39.98	36
High	2832	30.15	48
Very high	26	0.8	16
Total	9393		109

region, mostly observed in and around the two major cities as Midnapore and Kharagpur. The accuracy as observed from the ROC curve specified the consistency of the frequency ratio method in demarcating groundwater zones. The obtained spatial map also corroborates similar studies in this region, where the moderate and high potential zones indicated a higher potential for artificial groundwater recharge.

References

- Arulbalaji, P., Padmalal, D., & Sreelash, K. (2019). GIS and AHP techniques based delineation of groundwater potential zones: a case study from southern Western Ghats, India. *Scientific reports*, 9(1), 1–17.
- Asoka, A., Gleeson, T., Wada, Y., & Mishra, V. (2017). Relative contribution of monsoon precipitation and pumping to changes in groundwater storage in India. *Nature Geoscience*, 10 (2), 109–117.
- Chowdhury, A., Jha, M. K., & Chowdary, V. M. (2010). Delineation of groundwater recharge zones and identification of artificial recharge sites in West Medinipur district, West Bengal, using RS, GIS and MCDM techniques. *Environmental Earth Sciences*, 59(6), 1209.
- Chowdhury, A., Jha, M. K., Chowdary, V. M., & Mal, B. C. (2009). Integrated remote sensing and GIS-based approach for assessing groundwater potential in West Medinipur district, West Bengal, India. *International Journal of Remote Sensing*, 30(1), 231–250.
- Das, B., Pal, S. C., Malik, S., & Chakraborty, R. (2019). Modeling groundwater potential zones of Purulia district, West Bengal, India using remote sensing and GIS techniques. *Geology, Ecology, and Landscapes*, 3(3), 223–237.
- Duan, H., Deng, Z., Deng, F., & Wang, D. (2016). Assessment of groundwater potential based on multicriteria decision making model and decision tree algorithms. *Mathematical Problems in Engineering*, 2016.
- Ettazarini, S. (2007). Groundwater potentiality index: a strategically conceived tool for water research in fractured aquifers. *Environmental Geology*, 52(3), 477–487.
- Groundwater Yearbook 2013–14, July 2014, Central Groundwater Board. Govt. of India.
- Gupta, M., & Srivastava, P. K. (2010). Integrating GIS and remote sensing for identification of groundwater potential zones in the hilly terrain of Pavagarh, Gujarat, India. *Water International*, 35(2), 233–245.
- Guru, B., Seshan, K., & Bera, S. (2017). Frequency ratio model for groundwater potential mapping and its sustainable management in cold desert, India. *Journal of King Saud University-Science*, 29(3), 333–347.
- <http://india-wris.nrsc.gov.in/LithologApp.html?UType=R2VuZXJhbA==?UName = 08 may 2018>
- <https://www.un-igrac.org/what-groundwater> 17/04/2018

- Jha, M. K., & Peiffer, S. (2006). Applications of remote sensing and GIS technologies in groundwater hydrology: past, present and future (p. 201). Bayreuth: BayCEER.
- Leduc, C., Favreau, G., & Schroeter, P. (2001). Long-term rise in a Sahelian water-table: The Continental Terminal in south-west Niger. *Journal of hydrology*, 243(1–2), 43–54.
- Lee, S., Hong, S. M., & Jung, H. S. (2018). GIS-based groundwater potential mapping using artificial neural network and support vector machine models: the case of Boryeong city in Korea. *Geocarto international*, 33(8), 847–861.
- Machiwal, D., Jha, M. K., & Mal, B. C. (2011). Assessment of groundwater potential in a semi-arid region of India using remote sensing, GIS and MCDM techniques. *Water resources management*, 25(5), 1359–1386.
- Manap, M. A., Sulaiman, W. N. A., Ramli, M. F., Pradhan, B., & Surip, N. (2013). A knowledge-driven GIS modeling technique for groundwater potential mapping at the Upper Langat Basin, Malaysia. *Arabian Journal of Geosciences*, 6(5), 1621–1637.
- Naghbi, S. A., Ahmadi, K., & Daneshi, A. (2017). Application of support vector machine, random forest, and genetic algorithm optimized random forest models in groundwater potential mapping. *Water Resources Management*, 31(9), 2761–2775.
- Oh, H. J., Kim, Y. S., Choi, J. K., Park, E., & Lee, S. (2011). GIS mapping of regional probabilistic groundwater potential in the area of Pohang City, Korea. *Journal of Hydrology*, 399(3–4), 158–172.
- Ozdemir, A. (2011). GIS-based groundwater spring potential mapping in the Sultan Mountains (Konya, Turkey) using frequency ratio, weights of evidence and logistic regression methods and their comparison. *Journal of Hydrology*, 411(3–4), 290–308.
- Pandey, V., & Srivastava, P. K. (2019). Integration of microwave and optical/infrared derived datasets for a drought hazard inventory in a sub-tropical region of India. *Remote Sensing*, 11(4), 439.
- Park, S., Hamm, S. Y., Jeon, H. T., & Kim, J. (2017). Evaluation of logistic regression and multivariate adaptive regression spline models for groundwater potential mapping using R and GIS. *Sustainability*, 9(7), 1157.
- Pourtaghi, Z. S., & Pourghasemi, H. R. (2014). GIS-based groundwater spring potential assessment and mapping in the Birjand Township, southern Khorasan Province, Iran. *Hydrogeology Journal*, 22(3), 643–662.
- Ramaiah, S. N., Gopalakrishna, G. S., Vittala, S. S., & Najeeb, K. M. (2012). Geomorphological Mapping for Identification of Ground Water Potential Zones in Hard Rock Areas Using Geospatial Information-A Case Study in Malur Taluk, Kolar District, Karnataka, India. *Nature Environment and Pollution Technology*, 11(3), 369.
- Razandi, Y., Pourghasemi, H. R., Neisani, N. S., & Rahmati, O. (2015). Application of analytical hierarchy process, frequency ratio, and certainty factor models for groundwater potential mapping using GIS. *Earth Science Informatics*, 8(4), 867–883.
- Rodell, M., Velicogna, I., & Famiglietti, J. S. (2009). Satellite-based estimates of groundwater depletion in India. *Nature*, 460(7258), 999–1002.
- Saha, D., & Ray, R. K. (2019). Groundwater resources of India: Potential, challenges and management. In *Groundwater Development and Management* (pp. 19–42). Springer, Cham.
- Sahoo, S., Munusamy, S. B., Dhar, A., Kar, A., & Ram, P. (2017). Appraising the Accuracy of Multi-Class Frequency Ratio and Weights of Evidence Method for Delineation of Regional Groundwater Potential Zones in Canal Command System. *Water Resources Management*, 31(14), 4399–4413.
- Shahid, S., Nath, S., & Roy, J. (2000). Groundwater potential modelling in a soft rock area using a GIS. *International Journal of Remote Sensing*, 21(9), 1919–1924.
- Srivastava, P. K., & Bhattacharya, A. K. (2006). Groundwater assessment through an integrated approach using remote sensing, GIS and resistivity techniques: a case study from a hard rock terrain. *International Journal of Remote Sensing*, 27(20), 4599–4620.

- Teixeira, J., Chaminé, H. I., Carvalho, J. M., Pérez-Alberti, A., & Rocha, F. (2013). Hydrogeomorphological mapping as a tool in groundwater exploration. *Journal of Maps*, 9 (2), 263–273.
- Todd, D. K. (1980). *Groundwater Hydrogeology* ed. 2nd. John Willey and Sons, New York, 537.
- WRI India report, 2015: <https://www.wri.org/blog/2015/02/3-maps-explain-india-s-growing-water-risks>; visited on 20/09/2020

Chapter 11

Artificial Neural Network for Identification of Groundwater Potential Zones in Part of Hugli District, West Bengal, India



Shashank Yadav and Chalantika Laha Salui

Abstract Adequate availability of groundwater for the rural and urban population is essential because groundwater is an important source of drinking water and agricultural irrigation. This study analyzes groundwater potentiality in part of the Hugli District (Goghat-II, Goghat-I, Arambag, Khanakul-I, Khanakul-II, Pursurah, and Tarakeswar blocks) using artificial neural network model (ANN), on GIS platform, and using remote sensing data and some secondary data sources. Factors like elevation, slope, drainage density, flow accumulation, geology, geomorphology, soil, land use land cover, rainfall, pre-monsoon, post-monsoon, and recharge rate were considered to be influencing the groundwater occurrence over this area. Sentinel-2 satellite data, SRTM data processing techniques, and GIS spatial analysis tools were used to prepare these maps. Groundwater depth level data from 34 wells were considered as ground truth data and randomly divided into training and test sets. An ANN based on the relationship between groundwater potential data and the above factors was implemented on R-studio. Each factor's weight and relative importance was determined by the back-propagation training method. Then the groundwater potential indices were calculated, and the final map was created using GIS tools. The resulting groundwater potential map was validated using Area-Under-Curve analysis with data that had not been used for training. An accuracy of 77.78% was obtained. Five categories ("very high," "high," "moderate," "low," "very low") of groundwater potential zones have been demarcated. This groundwater potential information will be useful for effective groundwater management and exploration.

Keywords ANN · Groundwater potential · Sentinel data · SRTM data

S. Yadav · C. L. Salui (✉)

Indian Institute of Engineering Science and Technology, Shibpur, Howrah, West Bengal, India

11.1 Introduction

Groundwater is one of the most valuable natural resources and supports human health, economic development, and ecological diversity. Due to consistent temperature, widespread and continuous availability, excellent natural quality, limited vulnerability, low development cost, and drought reliability, it has become an essential and dependable source of water supplies in all climatic regions (Todd and Mays 2005). But, due to frequent failures in monsoon, undependable surface water, and rapid urbanization and industrialization, considerable risk to this valuable resource was created (Ramamoorthy and Rammohan 2015). Ever-increasing population of the world leads to the increasing demand for surface as well as sub-surface water supply. To meet the demand, there has been indiscriminate exploitation of groundwater resources. Due to the lack of planned groundwater withdrawal approach, random drilling of bore wells results in decrease in groundwater potential, lowering of water level, and deterioration in groundwater quality. Thus it is necessary to develop a sustainable groundwater management system to properly utilize these important resources. The occurrence of groundwater at any place on the earth is a consequence of the interaction of the climatic, geological, hydrological, physiographical, and ecological factors (Acharya and Nag 2013; Antony 2012) and hence is dependent on the correct interpretation of the hydrological indicators and evidence (Biswas et al. 2012). Identification of groundwater potential zones is an essential step to an effective groundwater management. There are several methods for the identification of groundwater potential zones. Remote sensing technique with its advanced features facilitates largely for the purpose. Remote sensing (RS) and geographic information system (GIS) have proven to be efficient, rapid, and cost-effective techniques producing valuable data on geology, geomorphology, lineaments, and slope as well as a systematic integration of these data for exploration and delineation of groundwater potential zones (Fashae et al. 2014; Kumar et al. 2016). This study was taken up to identify different groundwater potential zones by artificial neural network (ANN) where simulation was based on factors influencing the availability of groundwater along with their test sites. The study was conducted for the part of Hugli district (Fig. 11.1). Understanding the groundwater potential of the area is useful to regulate and optimize water use without adversely impacting water resources for future use in this area. In the Hugli district, the alluvium in the area forms a rich repository of groundwater. Each aquifer system consists of two to three aquifers separated by thin clay layers, which are not regionally extensive (CGWB). The material of the shallow aquifer is fine to medium-grained sands in the upper part and coarser in the lower part. Sand is the dominant lithological unit in the aquifer system of the Hugli district.

Generally, the first aquifer is restricted within 60–80 mbgl (meters below ground level) depth. However, at some places like Tarakeswar (Tarakeswar block) and Bhadreswar (Serampore-Uttarpara block), the first aquifer has been noticed to continue down to 127 mbgl and 113 mbgl depth and further continuing downward, and the second aquifer system starts below 90 mbgl (CGWB). Groundwater occurs

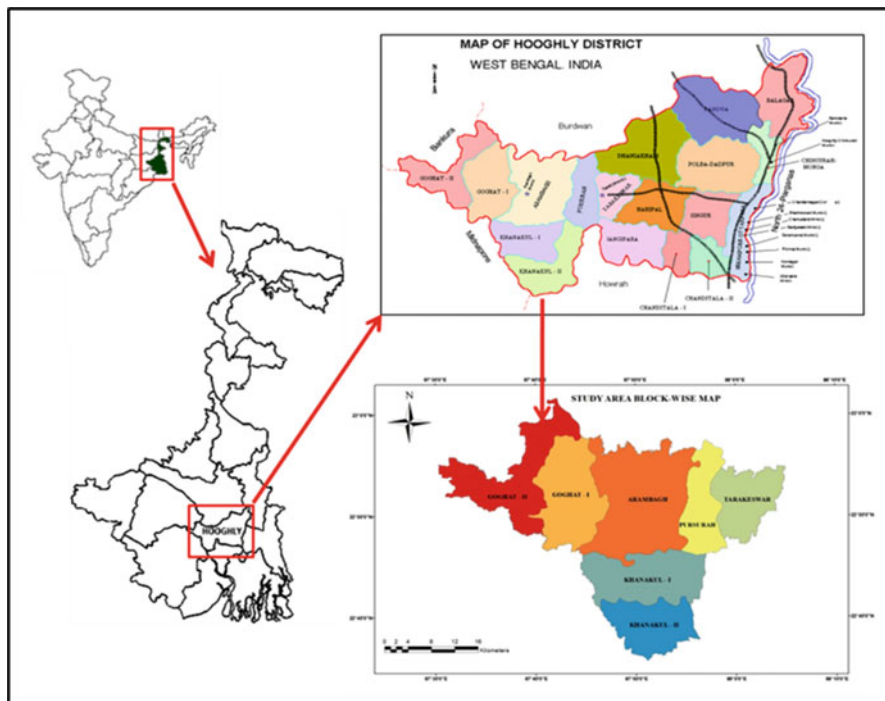


Fig. 11.1 Map showing the location of the study area

in a thick zone of saturation within the alluvium, existing under water-table conditions in the entire area except for a small portion to the west beyond the river Darakeswar.

11.2 Data and Methodology

The data used for this analysis was obtained from the following sources and later modified to meet the requirements of the study using software like ESRI ArcGIS, ERDAS Imagine, QGIS, and R-Studio. For determining groundwater potential zone in the study area, 12 thematic maps, viz., geology, geomorphology, soil, land use/land cover, elevation, slope, drainage density, flow accumulation, recharge, rainfall, and groundwater table depth of pre-monsoon and post-monsoon, were generated using satellite imagery and various conventional datasets (Fig. 11.2). The Digital Elevation Model used in this study is SRTM DEM (Shuttle Radar Topography Mission) and was classified into five elevation classes. Then using Spatial Analyst tool, the slope map was created from this SRTM DEM. For the analysis, it was further sliced into five classes. For the drainage density data, drainages were taken from SOI topographical sheets and were updated from satellite

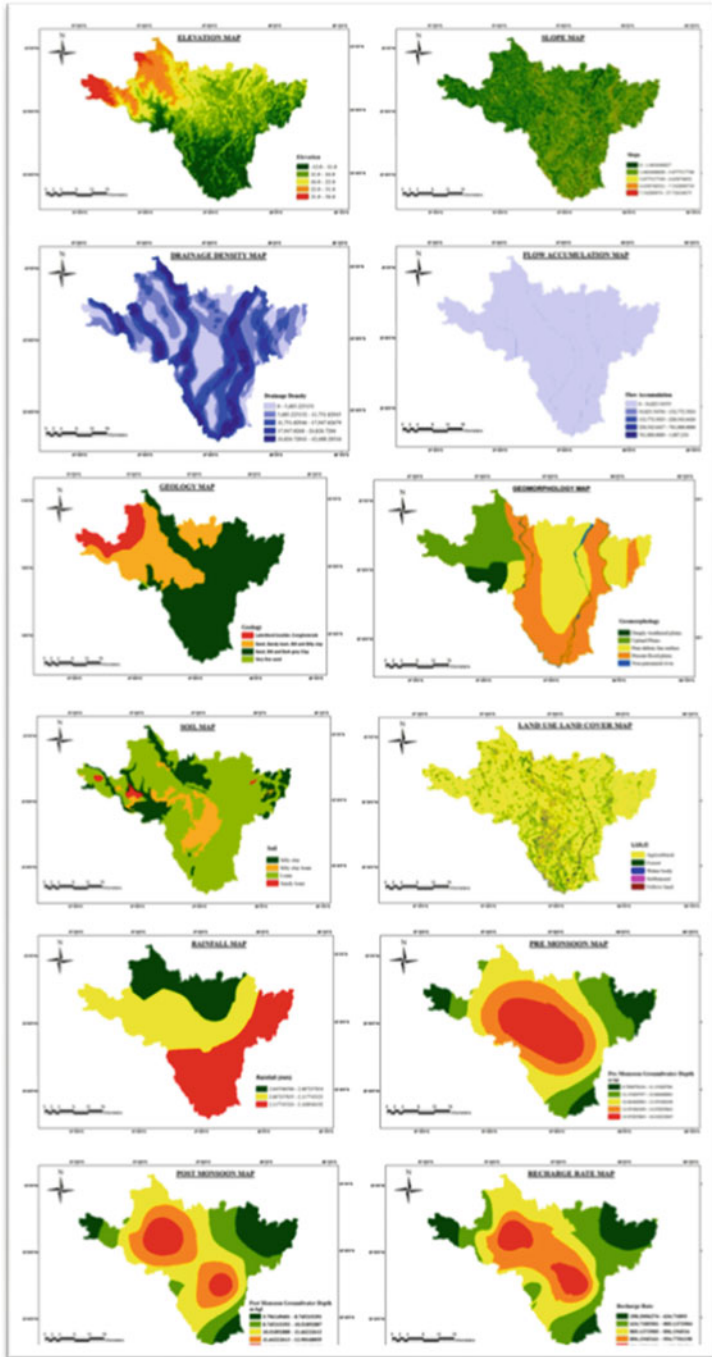


Fig. 11.2 Factors influencing groundwater potential

imagery. Then the line density was calculated for each cell. From the combined effect of slope and drainage, flow direction mapping was done followed by the flow accumulation mapping using Arc-hydro tool. The geology information was acquired from the Geological Survey of India; scale of map is 1:250,000. Laterized boulder/conglomerate, sand/sandy loam, silt and silty clay, sand/silt/dark gray clay, and very fine sand are found in this area. Geomorphological units present here are deeply weathered plain, upland plains, para-deltaic fan surface, present flood plains, and non-perennial rivers. The soil map was acquired from the National Bureau of Soil Survey and Land Use Planning (NBSS&LUP) at a scale of 1:500,000. Soil categories like silty clay, silty clay loam, loam, and sandy loam are found in this area. Processing of satellite data was done, so as to make data free from all the errors caused by atmosphere, geometry, and radiometric distortions during the acquisition of data.

Groundwater observation well (especially, depth to the water table) data on spatio-temporal fluctuations of groundwater (with respect to pre and post-monsoon depth) in the study area and its adjoining parts are collected from Central Ground Water Board (CGWB). The annual average pre- and post-monsoon groundwater depth maps were generated by geo-statistical interpolation technique. In this case, the interpolation method was selected to produce pre- and post-monsoon groundwater depth maps and has been extensively used to produce groundwater depth maps.

Annually estimating groundwater storage is based on the water level fluctuation and specific yield approach:

$$\Delta S = \Delta h \times A \times S_y \quad (11.1)$$

where ΔS =change in groundwater storage, Δh =change in water table elevation during a given period of time, and s_y =specific yield.

In this computational formula, the difference between the highest and the lowest level is taken as the fluctuation of the groundwater level is used for estimating the change in groundwater storage. The area in Eq. (11.1) is the area of influence of the respective monitoring wells in the concerned study area.

11.2.1 Methodology

All of the generated thematic layers were used as independent variables in an artificial neural network for finding the groundwater potential zones (Fig. 11.3). After defining the input and output parameters and then training, validation, and test data set, the learning algorithm was defined, and the network was trained and validated. If results are unsatisfactory, then updating the parameters for the training of the network were followed. After obtaining the best neural network architecture

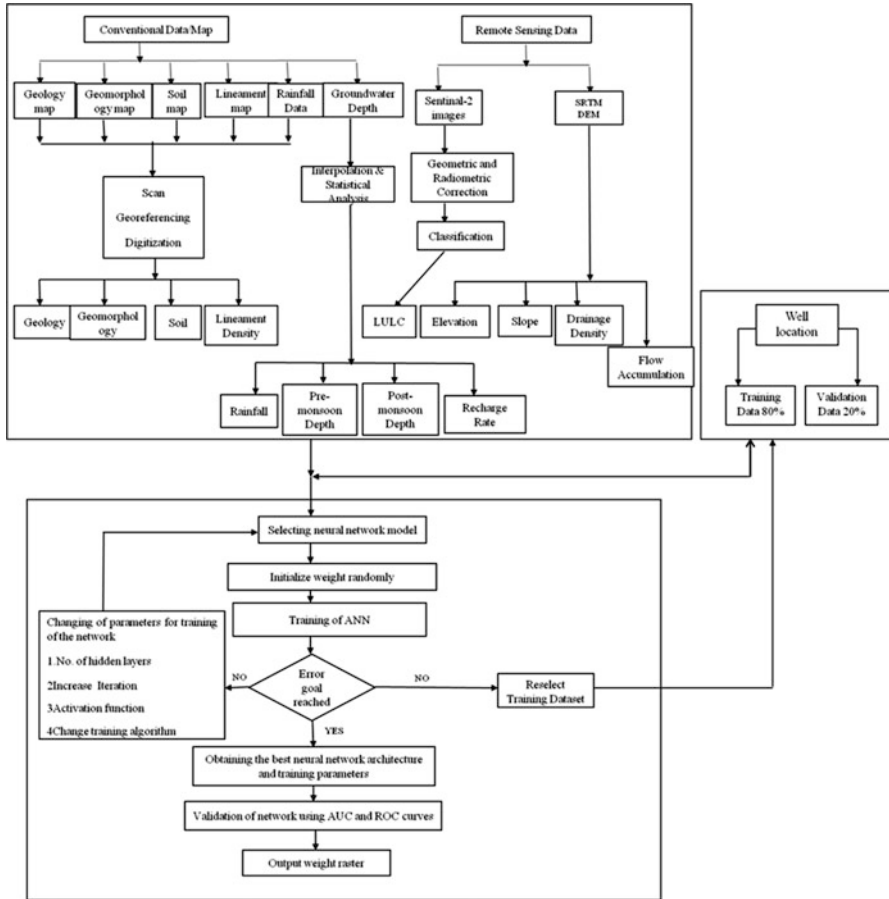


Fig. 11.3 Methodology flowchart

and training parameters with a satisfactory level of accuracy, the final output weight raster was generated and that was classified into various potential zones.

11.3 Results and Discussion

Groundwater well data were collected for pre-monsoon and post-monsoon (34 wells). The main use of the groundwater in this area is agricultural, so our data was obtained between April–June and October–December. Locations considered likely and unlikely to have groundwater were selected as training sites. To select the

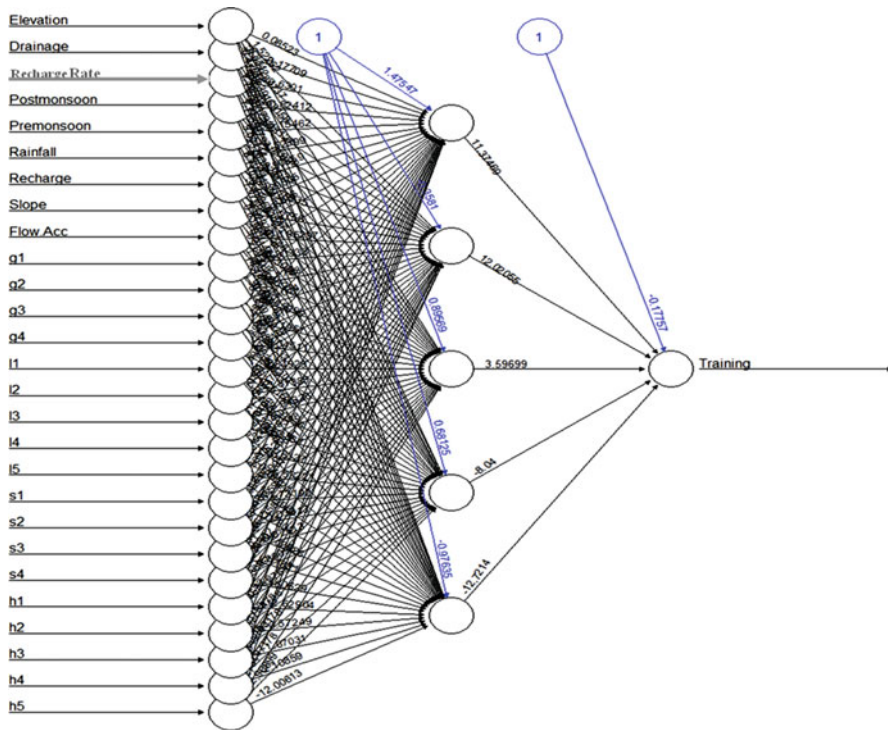


Fig. 11.4 The artificial neural network

training sites based on scientific and objective criteria, pre-monsoon groundwater level was used. 80% of groundwater level values were classified into a groundwater potential training dataset that was randomly selected and used for training. The remaining 20% of groundwater level values were used for validation. csv files of training and testing data were prepared for modelling the Artificial Neural Network in R Studio (Fig. 11.4).

The training and testing data were cleaned up in R Studio. The clean-up process involves removal of empty cells in the data and the conversion of categorical data into numeric data for scaling and computation. The categorical variables of Geology, Geomorphology, Soil, and Land cover were converted to numeric variables of 0s and 1s. The 0s represent the absence of a category in a particular subclass, and the 1s represent the presence of a category in a particular sub-class.

A total of 27 variables were finally available in the training data after conversion of the categorical data into numeric. These variables were then normalized using Z-score standardization or Min-Max scaling as typical neural network algorithms require data that are on a 0–1 scale. The same procedure was applied to the testing data involving reading of testing .csv file, conversion of categorical variables to numeric, and scaling.

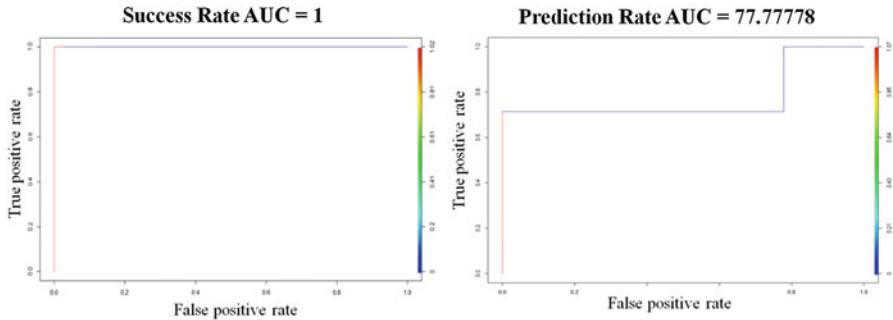


Fig. 11.5 AUC of success and prediction rate ROC

The neural network architecture was set with these parameters:

- (i) No. of hidden layers → 5
- (ii) Error Function (cost function) → Cross entropy
- (iii) Activation Function → Sigmoid (by default)
- (iv) Algorithm → Resilient Back Propagation (RPROP+ by default)
- (v) Maximum number of steps → $1e+08$
- (vi) Threshold → 0.01 (by default)
- (vii) Startweights → NULL (by default)
- (viii) learningrate.limit → NULL (by default)
- (ix) learningrate.factor → list(minus = 0.5, plus = 1.2) (by default)

The training error in the artificial neural network was found to be 0.054477 and a threshold of 0.009988.

The trained model was validated with the AUC of the ROC curve. A Receiver Operating Characteristic curve, or ROC curve, is a graphical plot that illustrates the diagnostic ability of a binary classifier system as its discrimination threshold is varied. The ROC curve is created by plotting the true-positive rate (TPR) against the false-positive rate (FPR) at various threshold settings. The true-positive rate is also known as sensitivity, recall, or probability of detection in machine learning. The false-positive rate is also known as probability of false alarm.

Firstly, the ANN model prediction was checked on the training data itself to see if the model could predict its own data accurately. For this, a code was written in R to compute the output of the ANN model with the training dataset and compare it with the original training data itself, and produce an output table that showed how many 0s were classified as 0s and how many 1s were classified as 1s. The same procedure was then repeated with the testing data to see how many 0s and 1s in the testing dataset were correctly classified and how many were incorrectly classified. After this, the ROCs were plotted, and the AUCs were computed to determine to accuracy of the model (Fig. 11.5).

The success rate represents the accuracy with which the ANN Model predicted the training data itself. This model has a success rate of 1, i.e., 100%. The Prediction

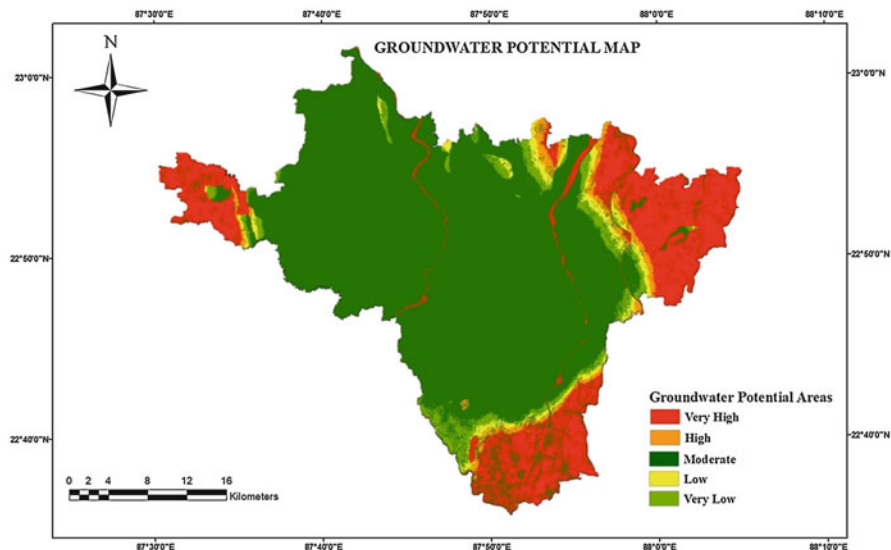


Fig. 11.6 Groundwater potential zone map

rate represents the accuracy with which the ANN Model predicted the testing data. This model has a Prediction rate of 77.78% (Fig. 11.5).

The primary objective of using the groundwater potential map is to effectively predict and display groundwater potential areas. In this study, groundwater potential weight raster was created using the neuron architecture as shown in Fig. 11.6. It is showing three distinct classes representing “good,” “moderate,” and “poor” groundwater potential zones in the study area. Normally, the “good” groundwater potential zone coincides with high groundwater table which is determined by various factors. River or water bodies are generally considered as the vital sources of recharge of the groundwater table. However, if too many rivers flow in an area, it increases the density of drainage which simultaneously generates high surface runoff and promotes limited infiltration rate. The good groundwater potential zone mainly encompasses Holocene age deposition which is under the present-day flood plain and older flood plain zones around the major river systems. It demarcates the areas where the terrain (flat, gentle slope, soft, unconsolidated) is most suitable for groundwater storage. The “good” groundwater potential zone of the study area covers the north, north-eastern, south, and south-western part, respectively. The “moderate” area of groundwater potential zone is mainly concentrated in the central part and scatter patches randomly distributed over the study area. The hydro-geomorphic feature available in this portion is mainly Holocene to Upper Pleistocene age deposition (western part), a zone of calcareous concentration is present in the upper part of the clay horizon, and the sandy layer often exhibits small sigmoidal, which also suggests moderate capacity of groundwater storage. The “poor” groundwater potential zone

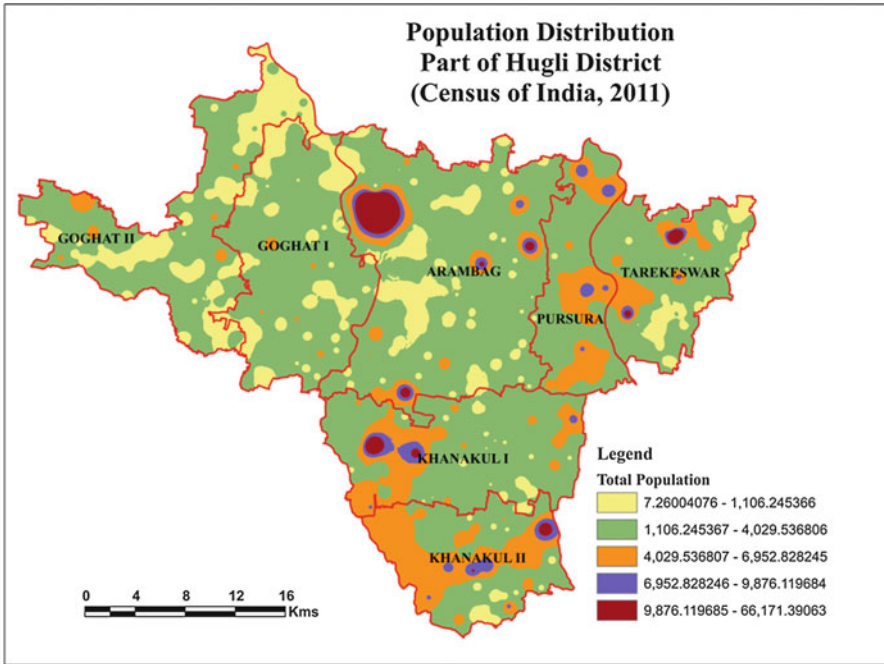


Fig. 11.7 Population density of the study area

has a low discharge (extraction) rate (volume/unit time) as compared to good and moderate groundwater potential zone.

In the study area, the village-wise population was interpolated (Fig. 11.7). High density of population leads to high demand of groundwater. High groundwater potential zones are found in western part of Goghat-II, eastern part of Khanakul-II, and Tarakeswar blocks. High demand areas of Arambag and Khanakul-I are coming under moderate groundwater potential zone. These areas should be taken under groundwater planning and management scheme. Pursurah block should also be monitored as the density of population is moderate for most of the portion of the block with moderate groundwater potentiality.

11.4 Conclusion

In order to sustain long-term agricultural as well as socio-economic development in the Ganga alluvial plain area, judicious use of groundwater is necessary. In this paper, the integrated RS and GIS-based ANN methodology are used to identify groundwater potential zones. By applying these methods, the study area is classified (Hugli district) into five groundwater potential zones, “very high,” “high,” “moderate,” “low,” and “very low.” The result shows that most parts of the areas with

favorable geology, soil, slope, and optimum rainfall condition have a high potential for groundwater. Identification and selection of a suitable number of thematic layers and justifiable assignment of weights are keys to the benefit of RS and GIS application in determining the potential zone of groundwater resources. Since the methodology adopted in this study is based on logical conditions and it is generic in nature, the same can also be applied in other regions of India or abroad with/without suitable modifications. In addition to designing appropriate policies and institutions toward judicious use and extraction of groundwater resources, there is also a need for a collective approach, particularly by the government organizations, the NGOs, and the common people. The integration of groundwater potential zone, policies, and institutions and the removal of imperfections existing in groundwater use can play a crucial role in this regard. However, a decentralized and participatory planning process is necessary for this purpose.

References

- Acharya, T., Nag, S.K., (2013) Study of groundwater prospects of the crystalline rocks in Purulia District, West Bengal, India using remote sensing data. *Earth Resource* 1(2), 54–59.
- Antony, R.A., (2012) Azimuthal square array resistivity method and groundwater exploration in Sanganoor, Coimbatore District, Tamilnadu, India. *Res J Recent Sci* 1(4), 41–45
- Biswas, A., Adarsa, J., Prakash, S.S., (2012) Delineation of Groundwater Potential Zones using Satellite Remote Sensing and Geographic Information System Techniques: A Case study from Ganjam district, Orissa, India *Research Journal of Recent Sciences* 1(9), 59–66.
- Fashae, O.A., Tijani, M.N., Talabi, A.O., Adedeji, O.I., (2014) Delineation of groundwater potential zones in the crystalline basement terrain of SW-Nigeria: an integrated GIS and remote sensing approach. *App. Wat. Sci.J.* 4(1), 19–38.
- Kumar, J.R., Dushiyanthan, C., Thiruneelakandan, B., Suresh, R., Vasanth Raja, S., Kumar, S.M., Karthikeyan, K., (2016) Evaluation of Groundwater Potential Zones using Electrical Resistivity Response and Lineament Pattern in Uppodai Sub Basin, Tambaraparani River, Tirunelveli District, Tamilnadu, India. *J GeolGeophys* 5(2).
- Ramamoorthy P., Rammohan V., (2015) Assessment of Groundwater potential zone using remote sensing and GIS in Varahanadhi watershed, Tamilnadu, India, *International Journal for Research in Applied Science & Engineering Technology* 3(V), 695–702
- Todd, D. and Mays, L. (2005) *Groundwater Hydrology*. 3rd Edition, John Wiley and Sons, Inc., Hoboken.

Chapter 12

Multi-criteria Analysis for Groundwater Quality Assessment: A Study in Paschim Barddhaman District of West Bengal, India



Payel Das and Niladri Das

Abstract Groundwater, one of the most valued natural hydrological resources, plays an important character in various sectors, i.e. agriculture, industry, and household. With increasing population pressure, its quality and quantity are affected enormously. Therefore, groundwater quality assessment is of prime necessity to confirm the availability of safe water for consumption and utilization in agriculture purpose. The present study was conducted on Paschim Barddhaman district of West Bengal based on 14 physico-chemical parameters, i.e. pH, EC, TH, Ca, Mg, Na, K, HCO_3 , Cl, SO_4 , PO_4 , F, Fe and SiO_2 of 43 groundwater samples. Multi-criteria analysis, such as factor analysis and cluster analysis, has been done to extract the principal controlling factors of groundwater chemistry. Factor analysis shows that four factors explain the total variance of 71.358%, and it implies that the hydro-geochemistry of groundwater is influenced not only by the interaction of groundwater and geology but also by contamination by the chemical fertilizer, industrial effluent and urban sewage. From the hierarchical cluster analysis, three clusters are identified from the region on the basis of homogenous groundwater chemistry. Gibbs diagram indicates that groundwater hydrochemistry is mainly influenced by the nature and composition of rocks. Water quality indices reveal that the groundwater of the district is safe for drinking purposes except very few locations. Based on irrigation suitability analysis, i.e. sodium percentage, sodium absorption ratio and permeability index, majority of the sample villages show that groundwater is suitable for irrigation purpose except a few villages.

Keywords Hydrochemistry · Hierarchical cluster analysis · Irrigation suitability · Principal component analysis · Water quality index

P. Das (✉)

Department of Geography, Visva-Bharati, Santiniketan, West Bengal, India

N. Das

Department of Geography, Hiralal Bhakat College, Nalhati, West Bengal, India

12.1 Introduction

Groundwater plays a crucial part in human life, and it has a strong importance in agriculture, industry and household sectors. With increasing population pressure, the worldwide demand for groundwater resource is gradually escalating. The global population was recorded as 7.6 billion in 2018 and is projected to reach 9.6 billion in 2050 (United Nations 2013). Therefore, in the future, there will be a safe drinking water scarcity. In India, annually about 230 cubic kilometres of groundwater is abstracted for different purposes, i.e. irrigation, drinking, industrial, etc., and greater than 60% of agricultural irrigation and 85% of drinking water supply rely upon the groundwater resource (World Bank 2012). Although groundwater is considered as a replenishable resource, it is not renewed very quickly. The average time of subsurface water renewal is about 14000 years (World Water Balance 1978). So, monitoring of groundwater chemistry and water quality assessment are required for better planning. Jain et al. (2000), Meenakumari and Hosmani (2003), Jain (2004), Gupta et al. (2008), Banoeng-Yakubo et al. (2009), Singh et al. (2010), Nosrati and Eeckhaut (2012), Dhakate et al. (2013), Ghosh and Kanchan (2014), Pazand and Javanshir (2014), Kumar et al. (2015), Adhikary et al. (2015), Bencer et al. (2016), Boateng et al. (2016), Hassen et al. (2016), Longanathan and Ahamed (2017), Kazakis et al. (2017) and some other distinguished persons have deeply studied the groundwater hydro-geochemistry in different slices of the world and evaluated the quality of groundwater for domestic and agricultural purposes.

Groundwater contamination is an urgent matter of concern because people largely depend on the groundwater source for different purposes. Consumption of contaminated groundwater is dreadful for all the biota (Jain et al. 2000; Baba and Tayfur 2011). On a global scale, about three million people die in every year due to the consumption of contaminated water (WHO 2004). Scientific management of groundwater resource is poor in the developing countries. Groundwater quality assessment is important in this context. Surface water quality is severely affected by the intensive use of chemical fertilizer and pesticide in agriculture, industrial wastage, domestic sewage, etc., but the groundwater quality is influenced not only by the agricultural actions and industrial effluents but also geological formation, groundwater level, flow pattern, degree of chemical weathering, etc. Knowledge of subsurface water chemistry is inevitable to detect the source of chemical compounds of groundwater like geogenic or anthropogenic (Srinivasamoorthy et al. 2008; Chenini et al. 2010; Das et al. 2019).

Gupta et al. (2008) studied the hydro-chemical properties of groundwater of the entire Burdwan district to assess the irrigation suitability. Singh et al. (2010) studied about the groundwater quality of Raniganj coal mining area. Thapa et al. (2018a) investigated the manganese-contaminated zones of Burdwan district using the frequency ratio model, and they (2018b) also demarcated the iron-contaminated zone of Burdwan district. For this investigation, Paschim Barddhaman is selected as the study area. Paschim Barddhaman is a mining-based industrial and urbanized district. Asansol and Durgapur Municipal Corporation and Raniganj, Jamuria and Kulti

municipalities collectively generate about 696 tons per day of solid waste (Department of Municipal Affairs 2013). Municipal solid wastes, hazardous wastes and biomedical wastes are being openly dumped in the waste disposal sites (Kalipahari, Asansol, Samdihi, Burnpur) and non-engineered municipal solid waste landfill site (Durgapur) which causes infiltration of leachates in subsurface water (Adhikari and Pal 2016). Urban sewage, untreated industrial effluents, solid wastes and mining wastes are some major vectors of groundwater contamination in the industrial belt of Paschim Bardhaman (Holt 2000; Tiwary 2001). Moreover, in the eastern share of the test area mainly, Kanksa block has been endowed with massive agricultural production. So, the application of chemical fertilizer to obtain more agriculture production may cause the deterioration of groundwater quality. As consumption of contaminated water is harmful for human health, groundwater quality assessment is very urgent to this district. It will help to plan for supportable water resource management. The main aims of this study are to assess the hydro-geochemistry using multivariate statistical techniques like factor analysis and cluster analysis and evaluate the groundwater quality for drinking and irrigation purposes using the parameters sodium percentage (Na%), sodium absorption ratio (SAR), permeability index (PI), magnesium ratio (MR), etc.

12.2 Test Area

Paschim Bardhaman district is located between $23^{\circ}24'10.25''\text{N}$ to $23^{\circ}52'40.16''\text{N}$ latitude and $86^{\circ}47'46.41''\text{E}$ to $87^{\circ}31'33.81''\text{E}$ longitude, encompassing an area of 1603.17 km^2 , and it consists of 2 municipal corporations and 8 community development (CD) blocks (Fig. 12.1). Administratively, the test area is surrounded by the Jharkhand state in the west and north-west, Birbhum district in north, Purba Bardhaman district in the east and Purulia and Bankura district in south. Damodar marks the southern boundary; Barakar forms the western boundary and Ajay separates the district from Birbhum district. Physically, this region is a part of the 'Rarh' Bengal.

In geological point of view, this district comprises many rock formations, e.g. dissected plateau composed of granitic gneissic complex of Archaean age is present in the north-western portion of the district, while the eastern part of the district is made up of laterite of tertiary period and a few patches of the quaternary alluvium, and in between these two, a large tract is covered by Gondwana deposition (Fig. 12.2). Archaean granite gneiss and migmatite of Chota Nagpur granite gneissic complex are bared in the north-western fringe of the test area constituting the oldest basement rock. Gondwana supergroup sedimentary sequence is deposited within a faulted, subsided semi-graben-type structural trough over the basement rock. Talchair, Barakar, Barren Measure, Raniganj and Panchet formation constitutes the lower Gondwana group composing sandstone, shale, conglomerate and siltstone with coal seams. Raniganj formation is predominant in coal supplying in the district (Table 12.1). Groundwater resource of the study area is largely guided by the

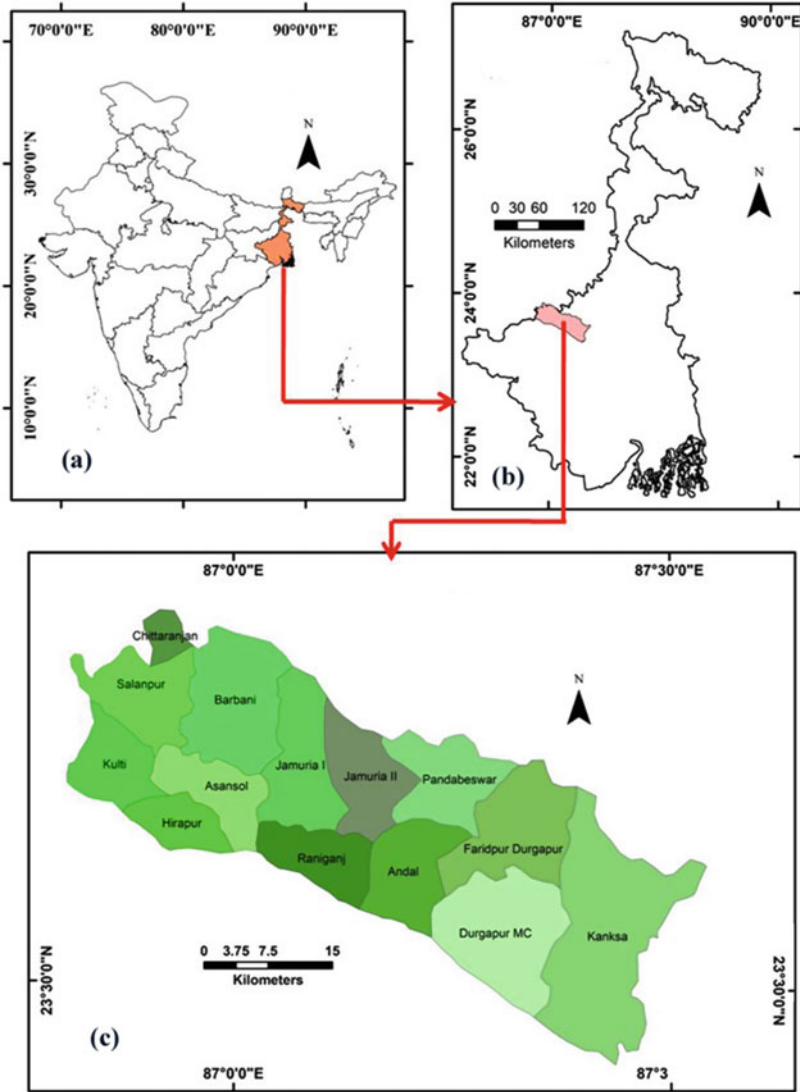


Fig. 12.1 Location map of (a) India, (b) West Bengal and (c) Paschim Bardhaman district

geology and geomorphology of the district (Gupta et al. 2008). Except the east margin, the entire study area is characterized by limited yield prospect (below 50 m²/h). Tertiary and quaternary deposits of the eastern section of the test area have a large yield potential (above 150 m²/h). In the westernmost section of the test area, groundwater is restricted under phreatic condition in the weathered residuum and secondary porosities like joints, faults, fractures, etc. (Thapa et al. 2018b). In the

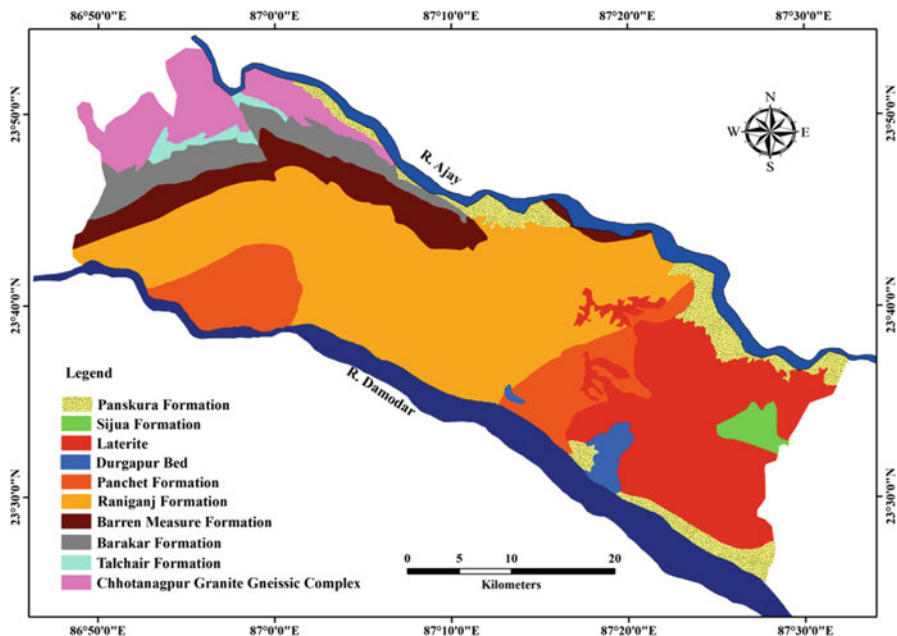


Fig. 12.2 Major geological units of Paschim Bardhaman district

Table 12.1 Major geological succession of Paschim Bardhaman district

Formation	Geological time period	Lithology
Panskura formation	Middle to upper Holocene	Clay alternating with silt and sand
Sijua formation	Upper Pleistocene to middle Holocene	Clay with caliche concretion
Laterite	Cainozoic	Laterite
Durgapur bed	Jurassic	Very coarse sandstone
Panchet formation	Triassic	Red shale, sandstone
Raniganj formation	Permian	Fine-grained sandstone, siltstone with coal seams
Barren Measure formation	Permian	Micaceous shale, sandstone
Barakar formation	Permian	Gritty pebbly sandstone with coal seams
Talchair formation	Carboniferous-Permian	Sandstone, conglomerate
Chota Nagpur granite gneissic complex	Archaean-Proterozoic	Granite gneiss and migmatite

Source: Geological Survey of India

eastern section of the district, groundwater occurs under both confined and unconfined aquifers in tertiary and quaternary deposits (Dutta 2016).

In general, the district is under subtropical monsoon-type climate and receives an average annual rainfall of 1300 mm. Generally the temperature varies between 39°C

in summer and 12°C in winter. But during summer time, the district suffers from very high temperature due to penetration of hot westerly wind from central India.

12.3 Materials and Method

For the entire analysis, 14 parameters, viz. pH, EC, TH, Ca, Mg, Na, K, HCO₃, Cl, SO₄, PO₄, F, Fe and SiO₂, have been taken as test parameters from the groundwater year book of West Bengal and Andaman and Nicobar Islands for the year of 2015–2016, and it has been published by Central Groundwater Board, Government of India. The data was collected for the month of April from 43 bore wells from the entire district.

From the quantitative point of view, multivariate statistical technique has been used for hydro-chemical analysis; principal component analysis (PCA) is one of the important multivariate statistical techniques which help to deduct the dimensionality of a data set consisting of a large number of interconnected variables (Zhang et al. 2009; Bencer et al. 2016; Kazakis et al. 2017). PCA has been calculated by using IBM SPSS version 25 statistical software. This method helps to extract major chemical components which affect groundwater of this region. Here, PCA has been made through varimax rotation with Kaiser normalization. According to the Guttman-Kaiser rule, the factors having the eigenvalue >1 have been taken as major factors (Dhakate et al. 2013; Bencer et al. 2016; Noshadi and Ghafourian 2016). PCA can be expressed through the following equation (Eq. 12.1):

$$Z_{ij} = pc_{i1}x_{1j} + pc_{i2}x_{2j} + \dots \dots pc_{im}x_{mj} \quad (12.1)$$

Hierarchical cluster analysis (HCA) helps to identify the grouping of associated variables of groundwater chemistry (Dhakate et al. 2013; Hassen et al. 2016). The Euclidean distance has been used here to measure the similarity level within the sample sites. Ward's method has been implied to generate dendrogram, which graphically represents the clusters (Gibrilla et al. 2011). HCA has been computed by using the following formula (Eq. 12.2):

$$d^2_{mn} = \sum_{k=1}^x (Z_{m,k} - Z_{n,k}) \quad (12.2)$$

where d_{mn} is the Euclidean distance, Z_{mk} and Z_{nk} are the variable k for objects m and n , respectively, and x is the number of variables.

Pearson's correlation matrix has been prepared to identify the bivariate relationship between various groundwater controlling factors (Chapman 1996; Hassen et al. 2016; Das and Nag 2017), and scatter plots have been constructed to represent the trend of correlation between two variables. The co-relation value of >0.5 specifies a

strong correlation between variables, <0.5 indicates a poor correlation between variables, and the value of 0.5 means moderate co-relation between variables (Vasantavigar et al. 2013). For the spatial analysis of the 14 groundwater chemical parameters and the 4 significant factors and magnesium hazard, inverse distance weighting (IDW) technique in spatial analysis tool of ArcGIS 10.5 software has been used and here weighing factors are the chemical parameters, which have been already mentioned. Wilcox diagram, USSL diagram and Gibbs diagram have been plotted using AquaChem v. 2011.1 software (evaluation copy) to identify the groundwater suitability for irrigation.

12.4 Result and Discussion

12.4.1 *Spatial Distribution of pH*

Concentration of pH value in groundwater is varying from 7.4 to 8.1 that indicates that the nature of groundwater is slightly alkaline. The very low standard deviation value of 0.17 indicates that the pH value of all the sample wells is very close to the average value of 7.5 of the test area, which shows negatively skewed distribution (-0.35) and the kurtosis value (0.5) is moderately positive. About 97.67% of the sample wells are within the safe limit as approved by the WHO (2004). Concentration of pH value is low in the eastern section (Kanksa) of the test area. Higher concentration of pH is mainly observed in a few pockets of Kulti, Brabant, Andal and Raniganj (Fig. 12.3a).

12.4.2 *Electrical Conductivity (EC)*

EC in groundwater indicates the ion concentration which comes from dissolved salts and inorganic chemicals like chloride, calcium, sodium and magnesium (Prasanth et al. 2012). The EC value is ranging from 115 μS to 2020 μS with an average of 781.42 and very high standard deviation of 387.61 (Table 12.2). Both the skewness and kurtosis values are positive. Throughout the study area, distribution of EC value is low except the sample well of Dakshin Khanda of Andal (Fig. 12.3b). As per WHO's guideline (2004), 97.67% of the sample well are within the safe limit and only 2.32% under moderate electrical conductivity. As the pH value in groundwater is slightly alkaline, it retards the solubility of chemical compounds. Presence of low soluble materials causes low concentration of electrical conductivity (Prasanth et al. 2012). EC value becomes low due to the presence of insoluble rock types.

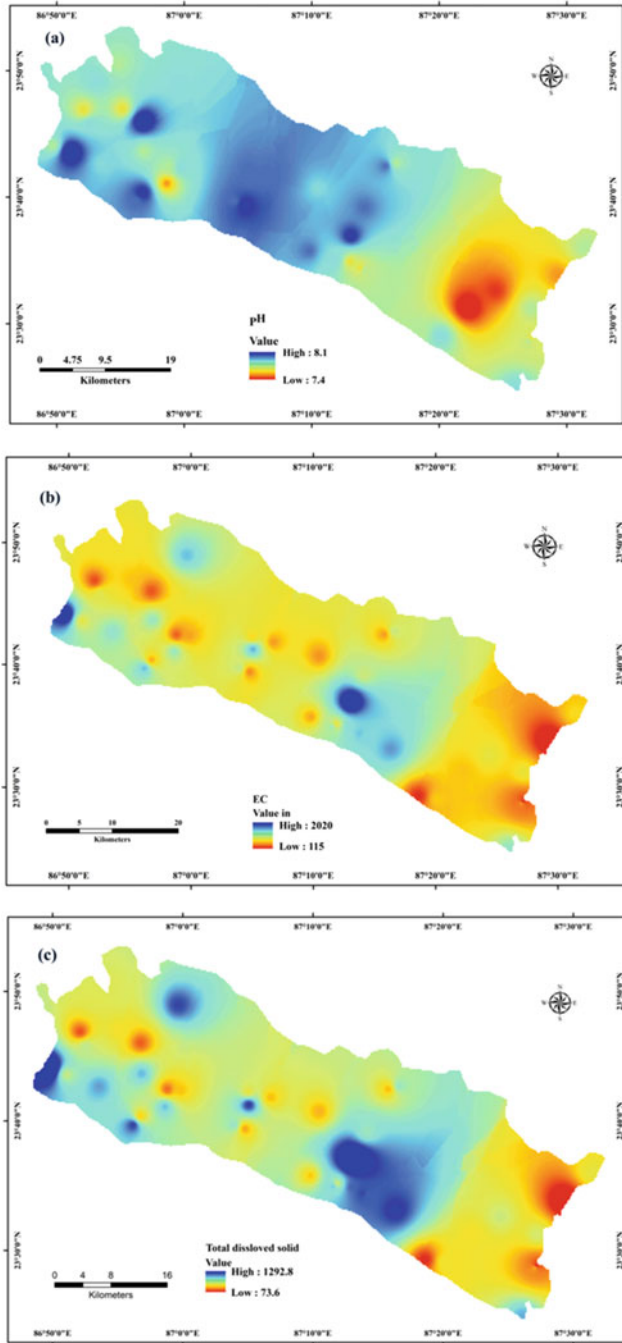


Fig. 12.3 Spatial map of (a). pH (b). Electrical conductivity (c). Total dissolved solid (d). Total hardness (e). Calcium (f). Magnesium (g). Sodium (h). Potassium (i). Calcium bicarbonate (j). Chloride (k). Fluoride (l). Iron (m). Sulphate (n). Phosphate (o). Silicon oxide

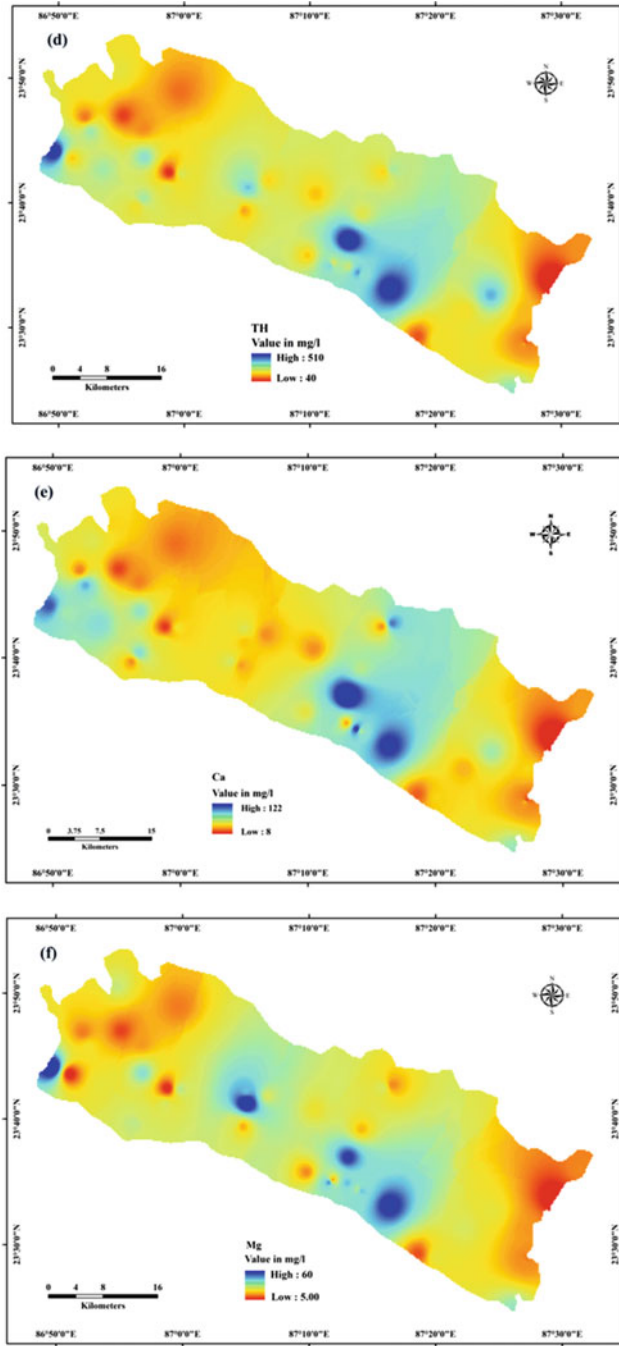


Fig. 12.3 (continued)

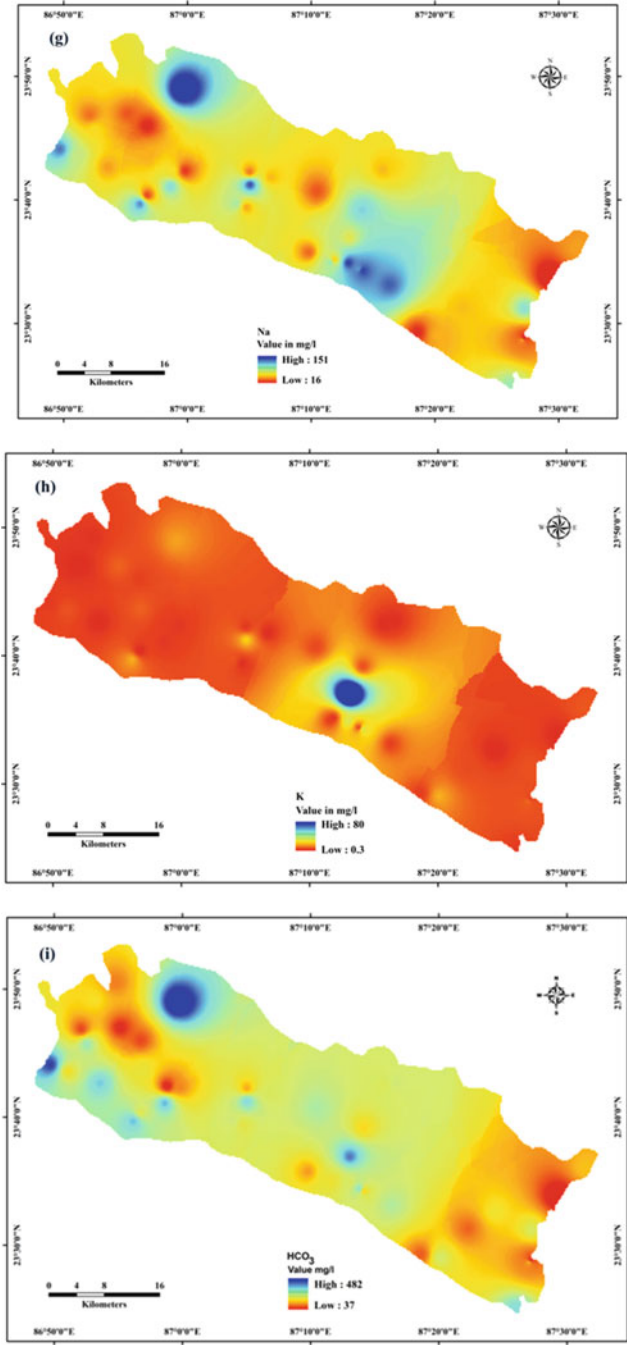


Fig. 12.3 (continued)

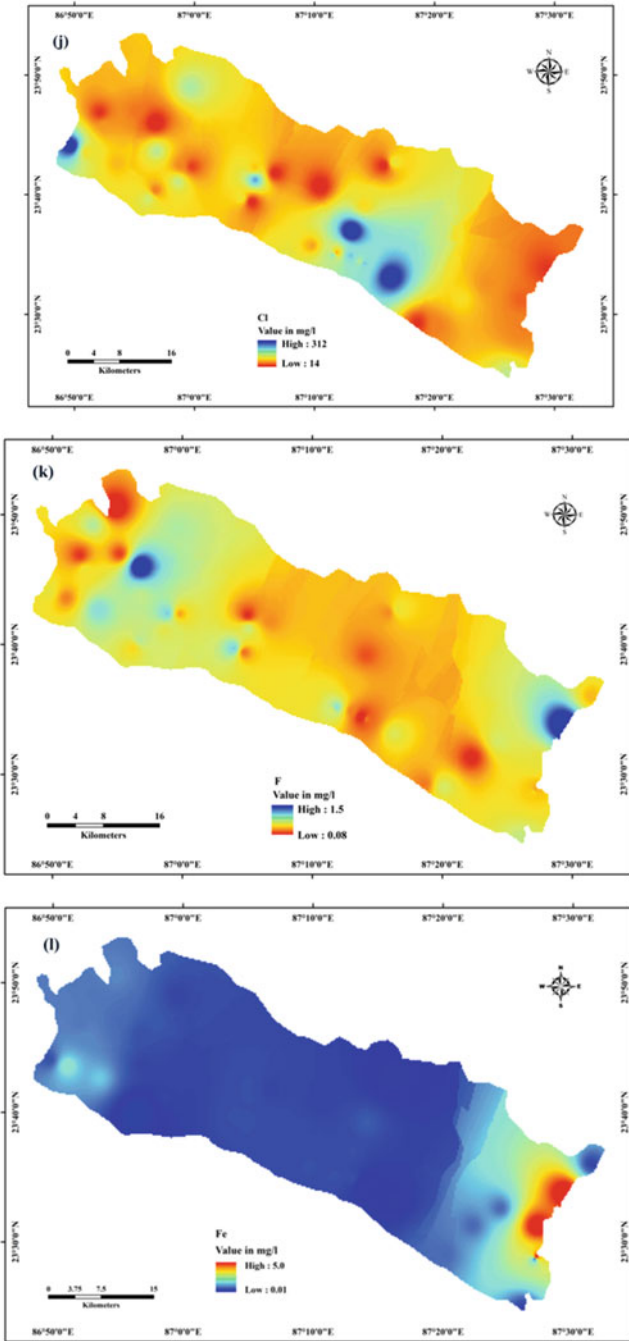


Fig. 12.3 (continued)

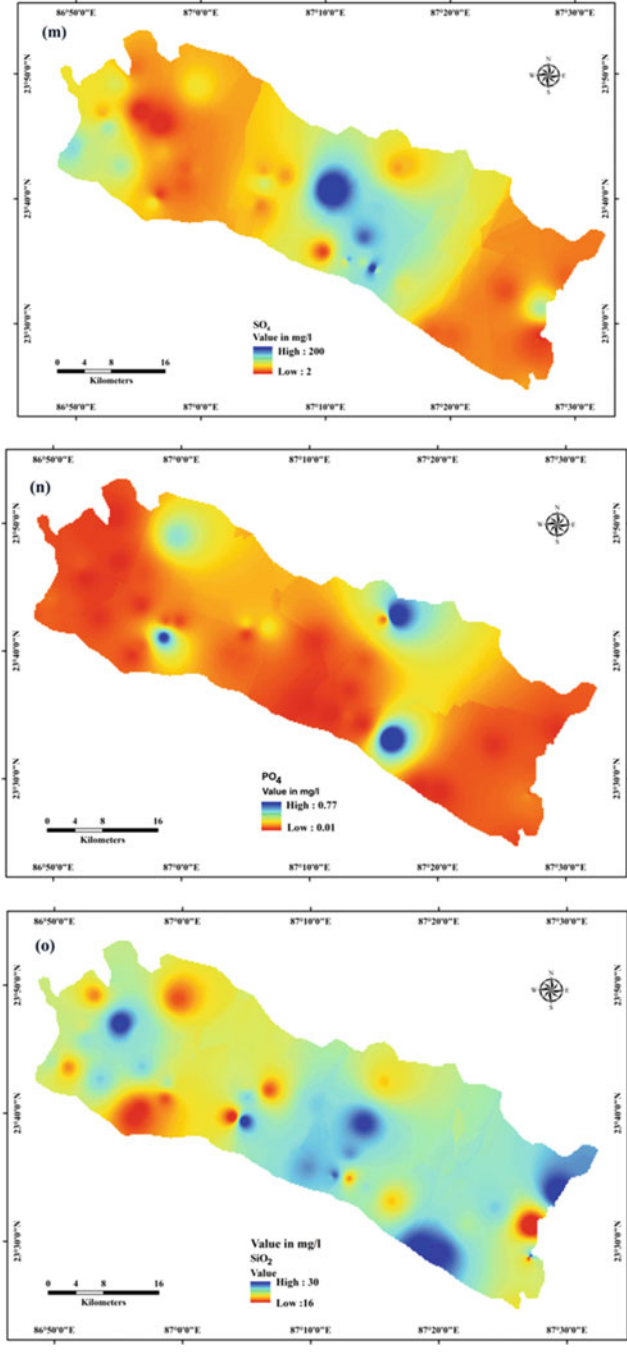


Fig. 12.3 (continued)

Table 12.2 Classification of groundwater based on EC concentration

EC	Type of water	Percentage of sample well
<1500	Low enrichment of salt	97.67
1500–3000	Moderate enrichment of salt	2.32
>3000	High enrichment of salt	0

Table 12.3 Classification of groundwater based on TH concentration (Sawyer and McCarty 1967)

TH	Type of water	Percentage of sample well
<75	Soft	2.32
75–150	Moderately hard	20.93
150–300	Hard	62.79
>300	Very hard	13.95

12.4.3 Total Dissolved Solid (TDS)

Total dissolved solid varies from 73.6 to 1292.8 mg/l with an average value of 523.14 mg/l. As per WHO's guideline, all the sample wells are within the permissible limit, but 44.18% of sample wells are beyond the maximum desirable limit (500 mg/l). Concentration of TDS is high in Andal, Durgapur municipality, Kulti and Barabani blocks (Fig. 12.3c).

12.4.4 Total Hardness (TH)

The presence of cations like magnesium and calcium and anions like carbonate, bicarbonate, sulphate and chloride is the prime cause of total hardness in groundwater (Ravikumar et al. 2010; Dhakate et al. 2013; Das and Nag 2017; Boateng et al. 2016). Total Hardness ranging from 40 to 510 mg/l with an average value of 216.82 mg/l and high standard deviation of 101.15, which shows a huge variation in the concentration of TH in the study area. Both skewness (0.85) and kurtosis (0.89) values are highly positive. According to Sawyer and McCarty's classification (1967), only 2.32% of sample wells are soft; 20.93% are moderately hard; 62.79% are hard and 13.95% are very hard (Table 12.3). Throughout the study area, TH has been concentrated in a few patches of Kanksa, Salanpur, Barabani and Asansol (Fig. 12.3d).

12.4.5 Calcium and Magnesium (Ca and Mg)

Concentration of calcium is ranging from 8 to 122 mg/l with a mean value 46.59 mg/l and standard deviation of 23.54. According to the WHO (2004), the permissible

limit of calcium concentration in groundwater is 200 mg/l which indicates that all the sample wells are within the safe limit. Magnesium concentration in groundwater is observed between 5 and 60 mg/l with an average value of 24.48 mg/l. The permissible limit of magnesium is 150 mg/l recommended by the WHO (2004). Therefore, all the sample wells are under permissible limit of magnesium concentration. The major source of calcium and magnesium is the leaching process of silicate minerals (Srinivasamoorthy et al. 2008).

12.4.6 Sodium and Potassium (Na and K)

Sodium is a vital element for human life, but high sodium content in drinking water causes numerous health complications like high blood pressure, hypertension, nervous system disorder, etc. (Gupta et al. 2008). Higher amount of sodium causes unsuitability for irrigation purpose also. Here, sodium concentration is ranging from 16 to 151 mg/l with a mean value of 64.45 mg/l and standard deviation of 32.97. All the sample wells are within the permissible limit (200 mg/l) by the WHO (2004). Na^+ concentration is relatively higher in Barabani, Durgapur and Andal (Fig. 12.3g) blocks. Sodium is formed here from both natural, i.e. presence of gneissic rocks like feldspar, pyroxene, amphiboles, etc., and anthropogenic sources, i.e. industrial waste, leaching from landfill and sewage, etc. (Gupta et al. 2008; Srinivasamoorthy et al. 2008; Baba and Tayfur 2011).

Potassium, an important natural-occurring element, is formed due to the presence of orthoclase, hornblende and microcline in igneous rock (Gupta et al. 2008). High concentration of potassium causes several health hazards like heart disease, coronary diseases, artery attack, hypertension, etc. (WHO 2009). Potassium concentration in groundwater is found between 0.3 and 80 mg/l. The uppermost permissible limit of potassium concentration in drinking water is 12 mg/l (WHO 2004). Two sample wells, located in Andal and Faridpur Durgapur, are beyond the permissible limit of the WHO (Fig. 12.3h).

12.4.7 Bicarbonate (HCO_3)

Presence of high bicarbonate in groundwater reduces the irrigational suitability of water. According to WHO (2003) recommended that the maximum permissible limit of HCO_3 is 180 mg/l. HCO_3 concentration in groundwater is high in the north-western section of the study area due to the presence of Chota Nagpur granite gneissic complex made up of granite gneiss and migmatite. In the study area, the value of HCO_3 varies from 37 to 482 mg/l. About 61% of the sample well beats the permissible limit of the WHO. Due to weathering of silicate minerals (quartz, feldspar, etc.), HCO_3 concentration is high (Boateng et al. 2016) in the study region.

12.4.8 Chloride (Cl)

Higher concentration of chloride causes bad taste in drinking water and may result in hypertension and osteoporosis (McCarthy 2004). Chloride, mixing with sodium (Na), forms NaCl which makes the water saline. Chloride is coming from different anthropogenic sources like industrial effluent and sewage and agricultural application, i.e. inorganic fertilizer (Karanth 1987). The concentration of chloride ranges from 14 to 312 mg/l with an average value of 98.18 mg/l and standard deviation of 72.02 which indicates that concentration of Cl varies throughout the region. Concentration is low to moderate except a few patches like Durgapur Municipality Corporation, Andal and Kult, where the amount is higher than the WHO's permissible limit (250 mg/l) (Fig. 12.3j). As the chloride ion is highly mobile, it can be easily transported. There is a strong positive co-relation with the concentration of chloride and EC (Prasanth et al. 2012).

12.4.9 Fluoride (F)

In drinking water, low level of fluoride concentration (below 1.5 mg/l) is good for human health because it helps in bone development and prevents dental decay. High level of fluoride concentration causes serious health problems like dental fluorosis, skeletal fluorosis, hyperparathyroidism, etc. (Thapa and Reddy 2017). In the present test area, concentration of fluoride varies from 0.08 to 1.5 mg/l. In all the sample wells, fluoride concentration is within the permissible limit recommended by the WHO (2004). Concentration of fluoride is relatively high near Kanksa, Barabani and Salanpur (Fig. 12.3k). Natural sources like alkaline soil and presence of caliche nodules in lateritic soil and the anthropogenic sources like application of phosphate fertilizer in agro-field occur fluoride contamination in groundwater in this area.

12.4.10 Iron (Fe)

Iron is another major element in our human body, but concentration of high amount of iron, i.e. >0.3 mg/l (WHO 2011), in drinking water results in serious health problems, viz. haemochromatosis, digestion problem, diabetes, skin diseases, etc. (WHO 2011). Iron concentration is relatively high in the lateritic terrain of the eastern section of the study area due to presence of iron nodules (Thapa et al. 2018b).

12.4.11 Sulphate (SO₄) and Phosphate (PO₄)

Sulphate does not create any health hazard, but the presence of higher concentration of sulphate makes water bitter taste and bad odour. Concentration of sulphate varies from 2 to 200 mg/l with standard deviation of 45.64 and a mean value of 59.84 mg/l. All the sample wells are within the allowable limit (400 mg/l) of the WHO (2004). Sulphate has been originated both naturally and anthropogenically. Although sulphate-bearing minerals, i.e. gypsum, are absent in the test area, the concentration of SO₄ is high (Fig. 12.3m). Here, seepage of chemical fertilizer, organic material, industrial effluent and sewage collectively influence the sulphate concentration (Baruah et al. 2008; Jeevanandam et al. 2012).

Phosphate concentration is low to average throughout the area except a few pockets near Durgapur, Pandabeswar, Asansol and Barabani. The concentration of phosphate ranges between 0.01 and 0.7 mg/l with a mean value of 0.1. The rocks, containing phosphate ion, apatite, amphibolite, biotite and garnet, all have a significant influence on the occurrence of PO₄ in the present study area (Srinivasa Rao and Rajendra Prasad 1997). Agricultural fertilizers, industrial effluents and sewage rich with phosphate are other important sources of PO₄ in groundwater (Akpabli and Drah 2001; Sinha et al. 2000; Akoto et al. 2010). Figure 12.3n shows that high concentration is mainly found in the industrial area.

12.4.12 Silica (SiO₂)

Silica concentration varies from 16 to 30 mg/l with a standard deviation of 3.98. Weathering of silicate minerals within rocks and agricultural activities are major responsible factors for silica dissolved in subsurface water. In the study area, maximum silica concentration is observed in the plateau fringe area (Fig. 12.3o), where weathering of silicate minerals is predominant.

12.4.13 Co-relation Analysis

Table 12.4 shows the correlation matrix of the chemical parameters of groundwater which depicts the linear relationship between two or more variables (Rawat and Tripathi 2015). The result illustrates a strong positive association between TH and EC (0.817), Ca (0.887) and Mg (0.848) and moderate correlation with HCO₃ (0.557) and SO₄ (0.477). Those parameters are responsible for permanent hardness of groundwater. The ions Cl, TH, Ca, Mg and Na all are positively associated with EC, and there is a moderate positive association between EC and K (0.561) and SO₄ (0.538) (Table 12.4). It confirms that the electrical conductivity is fully controlled by the presence of soluble salt content. The correlation matrix shows the significant

Table 12.4 Correlation matrix showing the relation between groundwater quality parameters

Correlation	pH	TDS	EC	TH	Ca	Mg	Na	K	HCO ₃	Cl	F	Fe	SO ₄	PO ₄	SiO ₂
pH	1.000	0.101	0.101	0.082	0.156	0.076	-0.007	0.216	0.216	-0.023	0.152	-0.246	0.127	-0.135	-0.118
TDS	0.101	1.000	1.000	0.817	0.718	0.750	0.744	0.561	0.786	0.914	-0.108	-0.335	0.538	0.196	-0.190
EC	0.101	1.000	1.000	0.817	0.718	0.750	0.744	0.561	0.786	0.914	-0.108	-0.335	0.538	0.196	-0.190
TH	0.082	0.817	0.817	1.000	0.887	0.848	0.450	0.420	0.557	0.798	-0.135	-0.363	0.477	0.189	-0.086
Ca	0.156	0.718	0.718	0.887	1.000	0.543	0.307	0.410	0.507	0.662	-0.103	-0.302	0.527	0.246	-0.073
Mg	0.076	0.750	0.750	0.848	0.543	1.000	0.520	0.357	0.501	0.789	-0.151	-0.342	0.349	0.107	-0.111
Na	-0.007	0.744	0.744	0.450	0.307	0.520	1.000	0.176	0.669	0.712	-0.139	-0.240	0.418	0.276	-0.392
K	0.216	0.561	0.561	0.420	0.410	0.357	0.176	1.000	0.297	0.550	-0.084	-0.094	0.303	-0.110	0.104
HCO ₃	0.216	0.786	0.786	0.557	0.507	0.501	0.669	0.297	1.000	0.583	0.006	-0.316	0.502	0.280	-0.344
Cl	-0.023	0.914	0.914	0.798	0.662	0.789	0.712	0.550	0.583	1.000	-0.075	-0.240	0.403	0.283	-0.118
F	0.152	-0.108	-0.108	-0.135	-0.103	-0.151	-0.139	-0.084	0.006	-0.075	1.000	0.221	-0.173	0.024	0.003
Fe	-0.246	-0.335	-0.335	-0.363	-0.302	-0.342	-0.240	-0.094	-0.316	-0.240	0.221	1.000	-0.103	-0.151	0.127
SO ₄	0.127	0.538	0.538	0.477	0.527	0.349	0.418	0.303	0.502	0.403	-0.173	-0.103	1.000	-0.098	0.004
PO ₄	-0.135	0.196	0.196	0.189	0.246	0.107	0.276	-0.110	0.280	0.283	0.024	-0.151	-0.098	1.000	-0.343
SiO ₂	-0.118	-0.190	-0.190	-0.086	-0.073	-0.111	-0.392	0.104	-0.344	-0.118	0.003	0.127	0.004	-0.343	1.000

relationship between Cl, SO₄, Na, Mg, Ca and K which indicates the subsurface hydrology is largely controlled by the leaching process and dissolution of soluble salts. Due to the presence of soluble substances, the nature of groundwater is mild alkaline.

12.4.14 Factor Analysis

To extract the factors, here, principal component analysis was performed using varimax rotation with Kaiser normalization. In this method, four significant factors were extracted with eigenvalue of greater than one (Davis 1986) which explain total variance of 71.358%. Factor 1 has 42.456% of total variance with positive loadings on electrical conductivity (0.936), total hardness (0.890), calcium (0.794), magnesium (0.792), sodium (0.597), potassium (0.650), bicarbonate (0.663), chloride (0.907) and sulphate (0.634) (Table 12.5). Factor 1 can be considered as salinity factor. Those chemical components represent the contribution of both natural (dissolution of rocks and minerals) and anthropogenic sources (chemical fertilizer, industrial effluent, sewage, etc.). Factor 2 explains 11.796% of total variance with strong positive loadings on phosphate (0.728) and sodium (0.597), and the negative loading is on SiO₂ (−0.781), which implies that the geochemistry of groundwater is controlled not only by the interaction with geology but also by contamination by the chemical fertilizer, industrial effluent and urban sewage. Third and fourth factors explain 9.099% and 8.007% of total variance, respectively. Factor 3 shows a very

Table 12.5 Rotated component matrix

	Component			
	1	2	3	4
pH	0.082	−0.046	0.920	0.073
TDS	0.952	0.220	0.052	−0.045
EC	0.952	0.220	0.052	−0.045
TH	0.880	0.070	0.027	−0.199
Ca	0.782	0.035	0.113	−0.140
Mg	0.789	0.112	−0.008	−0.207
Na	0.625	0.538	−0.066	−0.049
K	0.645	−0.339	0.165	0.092
HCO ₃	0.685	0.448	0.253	0.045
Cl	0.916	0.198	−0.142	−0.004
F	−0.088	0.089	0.208	0.841
Fe	−0.228	−0.235	−0.442	0.638
SO ₄	0.625	−0.125	0.125	−0.071
PO ₄	0.097	0.724	−0.210	−0.022
SiO ₂	−0.017	−0.781	−0.205	−0.001

Extraction method: Principal component analysis

Rotation method: Varimax with Kaiser normalization^a

strong positive value of pH (0.920), and factor 4 has a strong positive loading on fluoride (0.850) and iron (0.636). pH is controlled by the presence of soluble ions like Na^+ , Ca^{2+} , Mg^{2+} , Cl^- , HCO_3^- and SO_4 . Presence of clay minerals, i.e. kaolinite and illite, also controls the pH level of groundwater. Fluoride and iron both are originated due to dissolution of minerals and rocks.

12.4.15 Hierarchical Cluster Analysis

Cluster is also a multivariate statistical measure for the categorization of homogeneous groups of the variables. In statistics, there are various methods to prepare clustering, viz. K-means cluster, step clustering, hierarchical cluster, etc. In this study, hierarchical cluster has been applied to identify the homogeneous grouping as it has been a widely accepted technique, and for grouping of homogeneous chemical variables, it is the most applied method (Davis 1986).

With the help of Euclidean distance method, hierarchical cluster programming has been done using the of 43 subsurface chemical water samples data, and the dendrogram shows three clusters on the basis of homogeneous chemical composition. Within cluster 1, there are 13 villages with higher amount of TH (301.54), Ca (60.31), Mg (36.77), Cl (175.85), SO_4 (76.69) and PO_4 (0.22). Cluster 2 is comprised of 67.44% of sample villages with higher concentration of F (0.58 mg/l) and Fe (0.12 mg/l). Cluster 3 shows that only one sample falls under this group due to high concentration of pH (8.00), TDS (794.88), EC (1242), Na (112), K (9.80), HCO_3 (323.0) and SiO_2 (27.0) (Fig. 12.4).

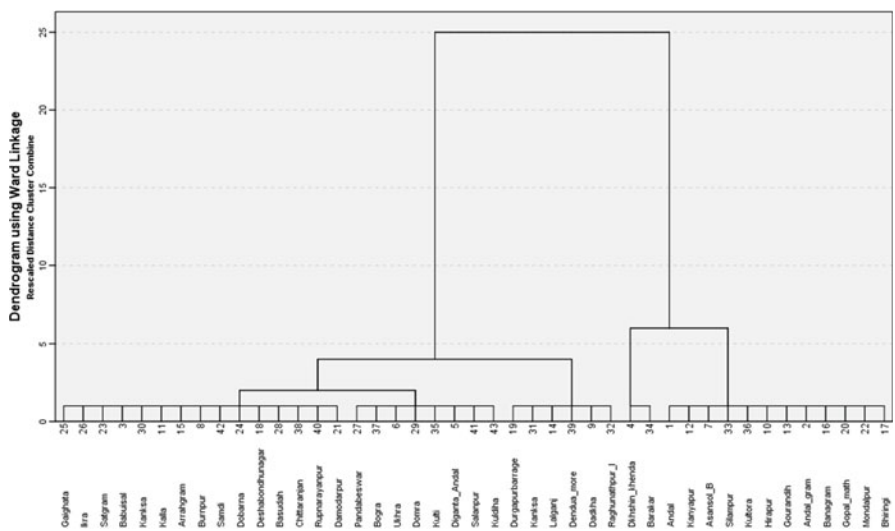


Fig. 12.4 Hierarchical cluster analysis

12.4.16 Mechanism Regulating the Groundwater Chemistry

With the help of Gibbs diagram, one can easily assess the mechanism which regulates the groundwater chemistry. In the year 1970, Gibb depicted three functional sources, i.e. evaporation dominance, rock dominance and precipitation dominance, which affect the groundwater chemistry as well as the quality (Loganathan and Ahamed 2017). Gibbs ratio was represented in formulas 12.3 and 12.4:

$$\text{Gibbs Ratio I (for anions)} = \frac{\text{Cl}^-}{(\text{Cl}^- + \text{HCO}_3^-)} \quad (12.3)$$

$$\text{Gibbs Ratio II (for cations)} = \frac{\text{Na}^+ + \text{K}^+}{(\text{Na}^+ + \text{K}^+ + \text{Ca}^{2+})} \quad (12.4)$$

Figures 12.5 and 12.6 reveal that above 90% samples fit to the category of rock dominance. So, this result designates that almost all samples of the study area are influenced by the rock weathering.

12.4.17 Evaluation of Groundwater Quality

12.4.17.1 Water Quality Index

To extract the quality of groundwater for drinking propose, water quality index has been widely used (Tiwari and Mishra 1985; Subba Rao 1997; Mishra and Patel 2001). Here, 12 chemical parameters (pH, EC, Ca, Mg, Na, K, HCO₃, Cl, F, SO₄, PO₄, TDS) of 43 sample villages from Paschim Barddhaman district have been used to regulate the water quality of subsurface water. There are five steps to calculate the WQI.

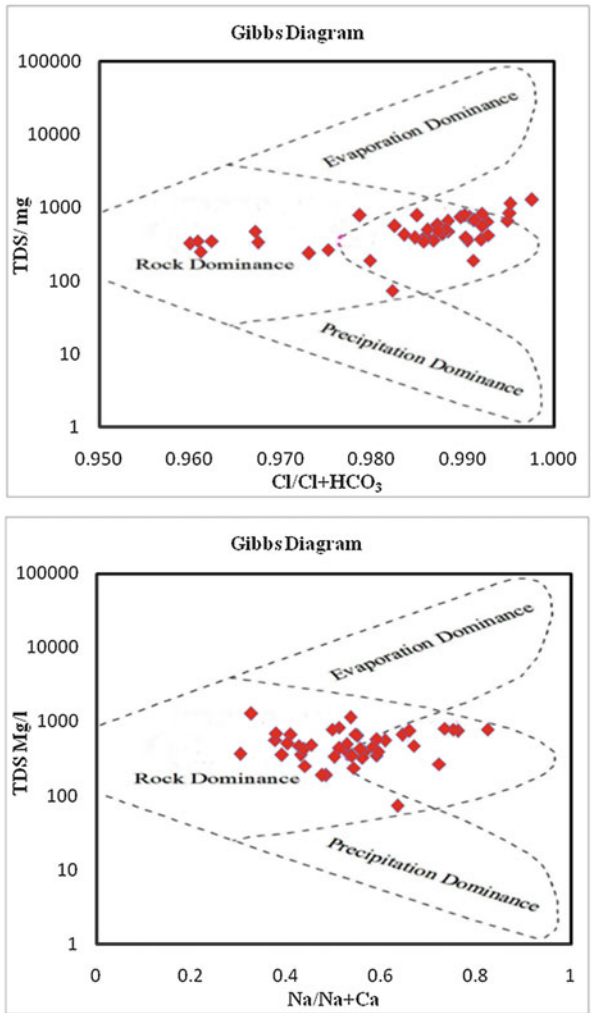
In the **first step**, weightage (w_i) has been given to all the parameters in referenced to their importance. Higher weight has been given to parameter which has a major importance in water quality and vice versa.

In the **second step**, the relative weightage (Rw_i) has been calculated using equation no. 12.5:

$$Rw_i = w_i / \sum w_i \quad (12.5)$$

where w_i is the weightage of the individual parameter and $\sum w_i$ is the summation of individual parameter.

Figs. 12.5 and 12.6 Mechanism controlling the chemistry of groundwater. (After Gibbs 1970)



In the **third step**, quality rating scale (Q_i) has been calculated from the following equation:

$$Q_i = (A_i/S_i) * 100 \tag{12.6}$$

where A_i is the actual value of the parameter and S_i is the drinking water quality standard prescribed by the WHO (2011).

In the **fourth step**, Sub indices (SI) has been calculated by $SI = R_{w_i} * Q_i$ (12.7)

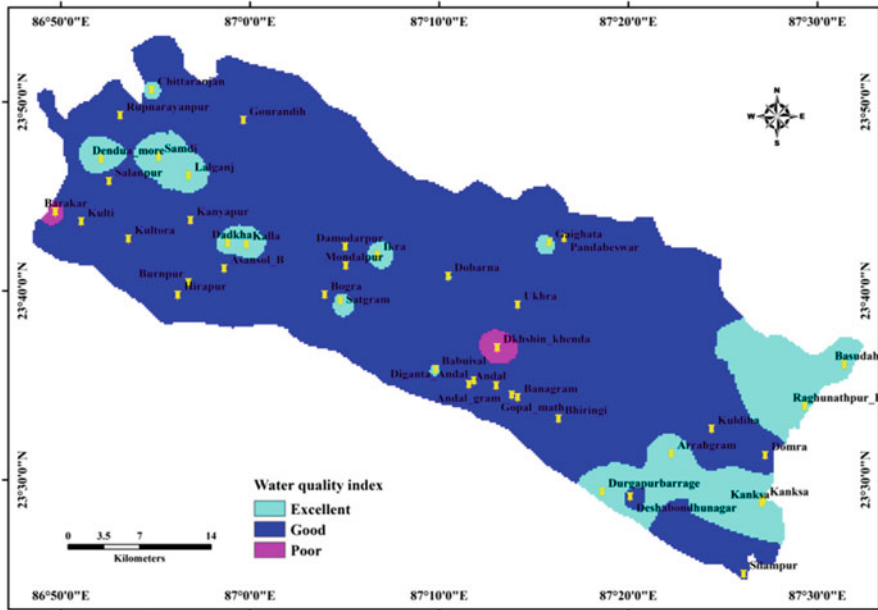


Fig. 12.7 Drinking water quality map

And finally WQI has been computed using the following formula:

$$WQI = \sum SI_i \tag{12.8}$$

Groundwater quality indices are ranging from 30.60 to 136.05 value, and on the basis of WQI value, 39.53% of the sample villages fall under excellent category, and 55.81% of samples fall into good category, and only 4.65% of samples are under poor category (Fig. 12.7).

12.4.17.2 Irrigation Suitability

As Indian rainfall is irregular and seasonal, irrigation is a prime factor for the agricultural development of a region and groundwater accounted as the secure source of irrigation. The quality of groundwater largely affects the cropping yield. Therefore, the evaluation of groundwater suitability is very much needed for the irrigation potentiality analysis (Prasanth et al. 2012; Nagarajua et al. 2014; Singh et al. 2015). The parameters like sodium percentage (Na%), sodium absorption ratio (SAR) and permeability index (PI) have been applied to evaluate the groundwater suitability for irrigation purpose.

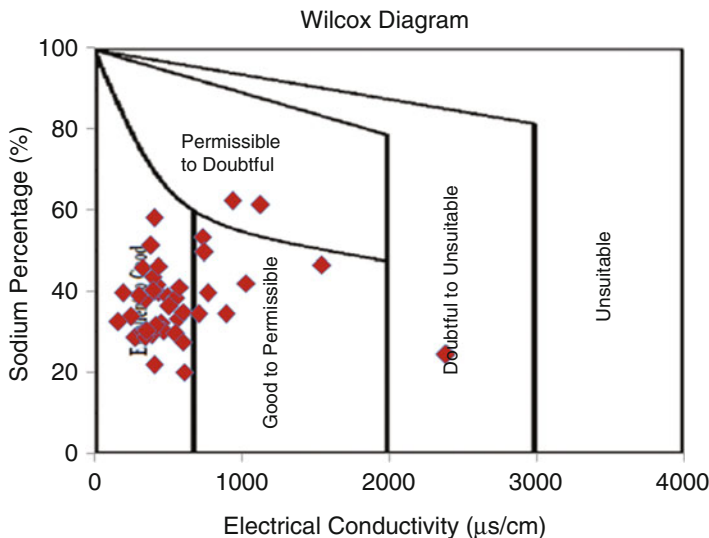


Fig. 12.8 Quality for irrigation through the Wilcox diagram

(i) Sodium Percentage

For irrigation purpose, the determination of sodium percentage of water is urgent because excessive sodium content affects the soil structure which has a negative impact on agriculture (Gupta et al. 2008). Sodium percentage is calculated as

$$Na\% = \frac{(Na^+ + K^+) \times 100}{(Ca^+ + Mg^+Na^+ + K^+)} \tag{12.9}$$

According to sodium percentage, the groundwater can be categorized into five groups, i.e. excellent (<20%), good (20–40%), permissible (40–60%), doubtful (60–80%) and unsuitable (>80%) (Wilcox 1955). Here sodium percentage ranges from 21.21 to 72.06%. About 67.44% of samples fit to the good category, 27.90% in permissible category, and only 4.65% in doubtful category (Fig. 12.8). Single one sample falls neither in the excellent nor unsuitable category. Here, the Wilcox diagram has been taken up to classify the groundwater for irrigation purpose. It shows that groundwater samples occupy the field of excellent to good (76.74%), good to permissible (16.28%), permissible to doubtful (4.65%) and doubtful to unsuitable (2.33%) for irrigation.

(ii) Salinity and Alkalinity Hazard

Highest concentration of salinity content in irrigation water stunts the plants’ growth because of the osmotic pressure in soil and specific ion toxicities (Läuchli and Epstein 1990). High amount of sodium in groundwater decreases the soil permeability which reduces the soil infiltration capacity and leads to water

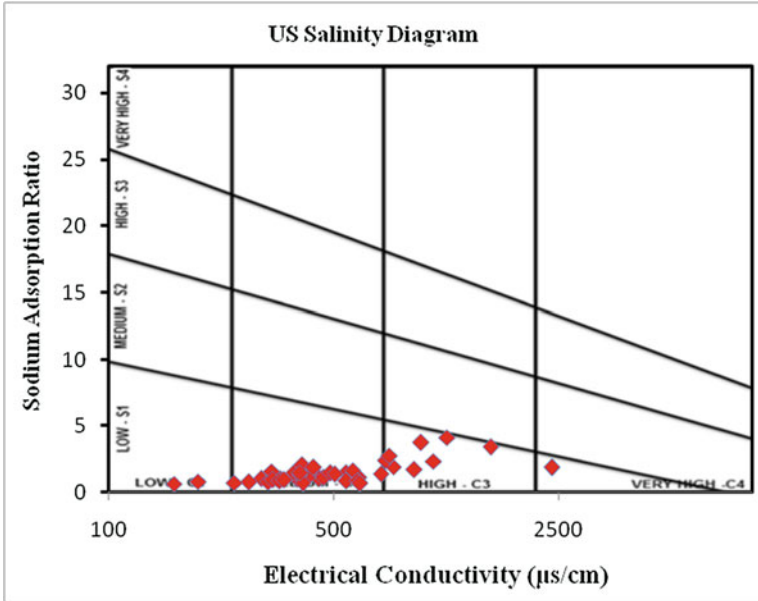


Fig. 12.9 US salinity diagram indicating the groundwater quality for irrigation

stagnation. High sodium content also affects the soil structure because it displaces calcium and magnesium ion in soil which diminishes the soil aggregation capability (Arveti et al. 2011). To determine the sodium hazard, sodium absorption ratio (SAR) is one of the most significant criteria (Todd and Mays 2005). The sodium absorption ratio has been computed using the following equation:

$$\text{SAR} = \frac{\text{Na}^+}{[(\text{Ca}^{2+} + \text{Mg}^{2+})/2]^{0.5}} \quad (12.10)$$

In the study area, SAR value ranges between 0.89 and 5.72 which indicates that most of the samples belong to excellent category (Richards 1954). The US Salinity Laboratory Diagram (US Salinity Laboratory Staff 1954) has been employed to classify the groundwater based on salinity and alkalinity or sodium hazard, and it shows that the ion part of the samples (95.34%) falls within the group of C3S1 (high salinity and low alkalinity) and C2S1 (medium salinity and low alkalinity). Only two samples, i.e. Raghunathpur and Gourandhi, belong to the group of C1S1 (low salinity and low alkalinity) and C3S2 (high salinity and medium alkalinity), respectively. Salt-tolerant crops should be cultivated in those areas where groundwater falls in the group of C3S2 and C3S1. Land with a good drainage status is needed for that category of water (Fig. 12.9). The samples belonging to the C1S1 and C2S1 categories are favourable for irrigation purpose in all types of soil.

(iii) Permeability Index

Based on PI, irrigation water can be classified into three categories good, moderate and poor (Donnen 1964). Permeability index has been calculated using the following formula:

$$PI = \frac{\{NA + (HCO_3)^{0.5}\} \times 100}{(Na + Ca + Mg)} \quad (12.11)$$

In the study area, PI value ranges from 22.78 to 74.69, which reveals that all the samples are under the good category.

(iv) Magnesium Hazard

Calcium and magnesium collectively conserve the equilibrium of water. Excess amount of magnesium in irrigational water causes low agricultural production (Nagarajua et al. 2014). To calculate the magnesium ratio, the following formula has been computed (Paliwal 1972):

$$\text{Magnesium ratio} = \frac{Mg^{2+} \times 100}{(Ca^{2+} + Mg^{2+})} \quad (12.12)$$

In the present study area, MH varies from 16.11 to 72.22. About 34.88% of samples belong to the unsuitable category, and 65.12% are suitable for irrigation. Irrigational water is unsuitable for agriculture in Jamuria I and II.

12.5 Conclusion

Groundwater hydro-geochemistry of Paschim Barddhaman district has been evaluated to identify groundwater quality for domestic and agricultural purposes and also to identify the major determinants of groundwater quality. Hydro-chemical data of sample villages reveal that the nature of subsurface water is slightly alkaline and most of the parameters are within the allowable limit recommended by the WHO for drinking water purpose. But the concentration of bicarbonate, chloride and potassium is beyond the permissible limit of the WHO in a few sample villages. The PCA results determine that the physico-chemical character of groundwater is not only controlled by the dissolution of rocks and minerals but also the leaching process from chemical fertilizers, industrial effluents, sewage, etc. due to anthropogenic activities. Gibbs plot shows that the hydrochemistry of the groundwater is influenced by rock weathering as the major part of the test area belongs to plateau fringe of Chota Nagpur. Water quality index informs that about 93% of the sample villages have excellent to good category of water. Majority of the sample villages show that groundwater is suitable for irrigation purpose except a few villages. Therefore, this

kind of study not only help to assess the present quality of groundwater, but also it may help the decision makers to take appropriate policy design in management of subsurface water quality in such kind of problematic region.

References

- Adhikari, K. and Pal, S. (2016). Assessment of pollution potential of soil and groundwater in a non-engineered MSW landfill site. *International Journal of Environmental Science and Development*, 7(3), 207-2010.
- Adhikary, P.P., Chandrasekharan, H., Trivedi, S.M., Dash, Ch.J. (2015). GIS applicability to assess spatio-temporal variation of groundwater quality and sustainable use for irrigation, *Arabian Journal of Geosciences* 8 (5), 2699-2711.
- Akoto, O., Bruce T.N., Darko G. (2010). Chemical and biological characteristics of streams in the Owabi watershed. *Environ Monit Assess*, 161,413-422.
- Akpabli, C.K. and Drah, G.K. (2001). Water quality of the main tributaries of the Densu stream. *JGSA* 3(2):84-94.
- Arveti, N., Sarma, M.R.S., Aitkenhead-Peterson, J.A., Kumar, S.K. (2011). Fluoride incidence in groundwater: a case study from Talupula, Andhra Pradesh, India. *Environ Monit Asses*, 172, 427-443.
- Baba, A. and Tayfur, G.(2011). Groundwater contamination and its effect on health in Turkey. *Environ Monit Asses*, 183, 77-94, <https://doi.org/10.1007/s10661-011-1907-z>.
- Banoeng-Yakubo, B.K., Yidana, S.M., Emmanuel, N. Akabzaa, T. (2009). Analysis of groundwater quality using water quality index and conventional graphical methods: The Volta region, Ghana. *Environmental Earth Science*, 59(4), 867-879. <https://doi.org/10.1007/s12665-009-0082-9>
- Baruah, M., Bhattacharyya, K.G., Patgiri, A.D. (2008). Water quality of shallow groundwater of core city area of Guwahati. In: Proceedings of sixteenth national symposium on environment, Haryana, India, pp. 101-106.
- Bencer, S., Boudoukha, A., Mouni, L. (2016). Multivariate statistical analysis of the groundwater of Ain Djacer area (Eastern of Algeria). *Arab J Geosci*, 9,248, <https://doi.org/10.1007/s12517-015-2277-6>
- Boateng, T.K., Opoku, F., Osafo Acquah, S. (2016). Groundwater quality assessment using statistical approach and water quality index in ejisu-juaben municipality, Ghana. *Environ earth sci*, 75:489, <https://doi.org/10.1007/s12665-015-5105-0>
- Chapman, D.V. World Health Organization, Unesco & United Nations Environmental Programme. (1996). Water quality assessments: a guide to the use of biota, sediments and water in environmental monitoring. 2nd ed. London: E & FN Spon. <http://www.who.int/iris/handle/10665/41850>.
- Chenini, I., Farhat, B., Mammou, A.B. (2010). Identification of major sources controlling groundwater chemistry from a multilayered aquifer system. *Chemical Speciation and Bioavailability*, 22(3),183-189.
- Das, S. and Nag S.K. (2017). Application of multivariate statistical analysis concepts for assessment of hydrogeochemistry of groundwater- a study in Suri I and Suri II blocks of Birbhum District, West Bengal, India. *Appl water Sci*, 873-888, <https://doi.org/10.1007/s13201-015-0299-6>.
- Das, N., Mondal, P., Ghosh, R., Sutrarshar, S. (2019). Groundwater quality assessment using multivariate statistical technique and hydro-chemical facies in Birbhum district, West Bengal, India. *SN Appl. Sci.* 1, 825. <https://doi.org/10.1007/s42452-019-0841-5>
- Davis, J.C. (1986). *Statistics and data analysis in geology*, 2nd edn. Wiley, New York
- Department of urban development and municipal affairs (2013). <https://www.wbdma.gov.in> accessed 1April 2019.

- Dhakate, R., Mahesh, J., Sankaran, S., Gurunadha Rao, V. V. S. (2013). Multivariate Statistical Analysis for Assessment of Groundwater Quality in Talcher Coalfield Area, Odisha. *Journal Geological Society of India*, 82,403-412.
- Donnen, L.D. (1964). Water quality for agriculture, Department of Irrigation, University of California, Davis.48.
- Dutta, S. (2016). Cause-effect analysis between irrigation and agricultural expansion on sub-surface water resources: a case study of Kanksa Block in Ajay–Damodar Interfluvium of Bardhaman District, West Bengal, India Sustain. Water Resour. Manag., <https://doi.org/10.1007/s40899-017-0128-1>.
- Ghosh, T. and Kanchan, R. (2014). Geoenvironmental appraisal of groundwater quality in Bengal alluvial tract, India: a geochemical and statistical approach. *Environ Earth Sci*, <https://doi.org/10.1007/s12665-014-3155-3>.
- Gibbs, R.J. (1970). Mechanisms controlling world water chemistry. *Science*, 170, 1088-1090.
- Gibrilla A., Bam, E.K.P., Adomako, D. Ganyaglo, S., Osae, S., Akiti, T.T., Achoribo, E., Ahiale, E., Ayano, G., Agyeman, E.K. (2011). Application of Water Quality Index (WQI) and Multivariate Analysis for Groundwater Quality Assessment of the Birmanian and Cape Coast Granitoid Complex: Densu River Basin of Ghana. *Water Qual Expo Health*, 3, 63-78, <https://doi.org/10.1007/s12403-011-0044-9>
- Gupta, S., Mahato, A., Roy, P., Datta, J.K., Saha, R.N. (2008). Geochemistry of groundwater, Burdwan District, West Bengal, India. *Environ Geol*, 53(6),1271–1282. <https://doi.org/10.1007/s00254-007-0725-7>
- Hassen, I., Hamzaoui-Azaza, F., Bouhlila, R. (2016). Application of multivariate statistical analysis and hydrochemical and isotopic investigations for evaluation of groundwater quality and its suitability for drinking and agriculture purposes: case of Oum Ali-Thelepte aquifer, central Tunisia. *Environ Monit Assess*, 188,135, <https://doi.org/10.1007/s10661-016-5124-7>.
- Holt, M.S. (2000). Sources of Chemical Contaminants and Routes into the Freshwater Environment, *Food and Chemical Toxicology*, 38, S21-S27.
- Jain, C. K. (2004). Ground water quality of District Dehradun, Uttaranchal. *Indian Journal of Environment and Eco planning*, 8(2), 475–484.
- Jain, C. K., Bhatia, K. K. S., & Kumar, V. (2000). Ground water quality in Sagar district, Madhya Pradesh. *Indian Journal of Environmental Health*, 42(4), 151–158.
- Jeevanandam M, Nagarajan R, Manikandan M, Senthilkumar M, Srinivasulu S, Prasanna MV (2012) Hydrogeochemistry and microbial contamination of groundwater from Lower Ponnaiyar Basin, Cuddalore District, Tamil Nadu, India. *Environ Earth Sci* 67(3):867–887
- Karanth, K.R. (1987). *Groundwater assessment, development and management*. Tata McGraw Hill publishing Company Limited, New Delhi
- Kazakis, N., Mattas, C., Pavlou, A., Patrikaki, O., Voudouris, K. (2017). Multivariate statistical analysis for the assessment of groundwater quality under different hydrogeological regimes. *Environ Earth Sci*, 76:349, <https://doi.org/10.1007/s12665-017-6665-y>.
- Kumar, D.L. , Sateesh, K., Saxena, P.R., Satyanarayana, E. and Edukondal, A. (2015). Assessment of Groundwater Quality and its suitability for drinking and irrigation purpose in Maheshwaram area, Ranga Reddy District, Telangana State, India. *J. Environ Res Develop* 9(3), 523-529.
- Läuchli, A., and Epstein, E. (1990). Plant responses to saline and sodic conditions. In: Tanji KK (ed.) *Agricultural salinity assessment and management*. ASCE New York. ASCE manuals and reports on engineering practice No, 71,113–137.
- Longanathan, K., Ahamed, A.J. (2017). Multivariate statistical techniques for the evaluation of groundwater quality of Amaravathi River Basin: South India. 7, 4633–4649. <https://doi.org/10.1007/s13201-017-0627-0>.
- McCarthy MF. (2004) Should we restrict chloride rather than sodium? *Med Hypotheses* 63:138–148
- Meenakumari, H. R., & Hosmani, S. P. (2003). Physico-chemical and biological quality of ground water in Mysore City, Karnataka. *Indian. Journal of Environment and Ecoplanning*, 7(1), 79–82.

- Mishra, P. C., & Patel, R. K. (2001). Study of the pollution load in the drinking water of Rairangpur. A small tribal dominated town of North Orissa. *Indian Journal of Environment and Ecoplanning*, 5(2), 293–298.
- Nagarajua, A. Kumar, S.K., Thejaswi, A. (2014). Assessment of groundwater quality for irrigation : a case study from Bandalamottu lead mining area, Guntur District, Andhra Pradesh, South India. *Appl Water Sci*, <https://doi.org/10.1007/s13201-014-0154-1>.
- Noshadi, M. and Ghafourian, A.(2016). Groundwater quality analysis using multivariate statistical techniques (case study: Fars province, Iran). *Environ Monit Assess*, 188,419, <https://doi.org/10.1007/s10661-016-5412-2>.
- Nosrati, K. and Eeckhaut, M.V.D. (2012) Assessment of groundwater quality using multivariate statistical techniques in Hashtgerd plain, Iran. *Environmental Earth Sciences*. 65(1). <https://doi.org/10.1007/s12665-011-1092-y>.
- Paliwal, K. V. (1972). *Irrigation with saline water* (p. 198) Monogram No.2 (New series). IARI, New Delhi.
- Pazand, K. and Javanshir, A.R. (2014). Rare earth element geochemistry of spring water, north western Bam, NE Iran. *Applied Water Science*. 4(1), 1-9. <https://doi.org/10.1007/s13201-013-0125-y>
- Prasanth, S. V.S. , Magesh, N.S., Jitheshlal, K.V., Chandrasekar, N., Gangadhar, K. (2012). Evaluation of groundwater quality and its suitability for drinking and agricultural use in the coastal stretch of Alappuzha District, Kerala, India. *Appl Water Sci*, 2, pp.165-175.
- Ravikumar, P., Venkatesharaju, K., Somashekar, R.K. (2010), Major ion chemistry and hydrochemical studies of groundwater of Bangalore South Taluk, India. *Environ Monit Assess*, 163, 643–653.
- Rawat, K.S. and Tripathi, V.K. (2015). Hydro-chemical survey and quantifying spatial variations of groundwater quality in Dwarka, subcity of Delhi, India. *The Institution of Engineers (India)*, <https://doi.org/10.1007/s40030-015-0116-0>.
- Richards, L.A. (1954). (Ed.) *Diagnosis and improvement of saline and alkali soils*. USDA Handbook, No. 60, 160.
- Sawyer C.N. and McCarty, P.L. (1967). *Chemistry for sanitary engineers*. 2nd Ed., McGraw-Hill, New York, pp. 518.
- Singh, A.K., Mahato, M.K., Neogi, B., Singh, K.K.(2010). Quality Assessment of Mine Water in the Raniganj Coalfield Area, India. *Mine Water Environ*, 29:248–262 <https://doi.org/10.1007/s10230-010-0108-2>.
- Singh, S., Raju N.J., Ramkrishna, Ch. (2015). Evaluation of Groundwater Quality and Its Suitability for Domestic and Irrigation Use in Parts of the Chandauli-Varanasi Region, Uttar Pradesh, India. *J Water Res and Prot* 7, 572-587, <https://doi.org/10.4236/jwarp.2015.77046>.
- Sinha A.K., Srivastava K.P., Sexena J. (2000). Impact of urbanization on groundwater of Jaipur, Rajasthan. In: Sinha AK, Shrivastava PK (eds) *Earth resources and environmental issues*. ABD Publishers, Jaipur, pp. 173–179.
- Srinivasa Rao, N. and Rajendra Prasad, P.(1997). Phosphate Pollution In The Groundwater Of Lower Vamsadhara River Basin, India. *Environmental Geology*, 31 (1/2) , Q Springer-Verlag, 117-122.
- Srinivasamoorthy, K., Chidambaram, S., Prasanna, V., Vasanthavihar, M., Peter, J., Anandhan, P. (2008). Identification of major sources controlling groundwater chemistry from a hard rock terrain – A case study from Mettur taluk, Salem district, Tamil Nadu, India. *J. Earth Syst. Sci.*, 117(1), 49–58.
- Subba Rao, N. (1997). Studies on water quality index in hard rock terrain of Guntur District, Andhra Pradesh, India. In National Seminar on Hydrology of Precambrian Terrains and Hard Rock Areas, 129–134.
- Thapa, R. and Reddy, D.V. (2017). Application of geospatial modelling technique in delineation of fluoride contamination zones within Dwarka Basin, Birbhum, India. *Geoscience Frontiers*. 8(5), 1105-1114. <https://doi.org/10.1016/j.gsf.2016.11.006>

- Thapa, R., Gupta, S., Kaur, H., Mandal, R. (2018a). Assessment of manganese contamination in groundwater using frequency ratio (FR) modeling and GIS: a case study on Burdwan district, West Bengal, India) Modeling Earth Systems and Environment, <https://doi.org/10.1007/s40808-018-0433-1>
- Thapa, R., Gupta, S., Kaur, H., Rajak, S. (2018b). Search for potential iron contamination zones in Burdwan district: an approach through fuzzy logic. Sustainable Water Resource Management, <https://doi.org/10.1007/s40899-018-0277-x>
- Tiwari, T. N. and Mishra, M. A. (1985). A preliminary assignment of water quality index of major Indian rivers. *Indian Journal of Environmental Protection*, 5, 276–279.
- Tiwary, R.K. (2001). Environmental impact of coal mining on water regime and its management. *Water, Air, and Soil Pollution*, 132, 185–199.
- Todd, D.K. and Mays, L.W. (2005). Groundwater Hydrology, 3rd edition, John Wiley and Sons, Inc. Hoboken.
- United Nations. (2013). World population prospects: The 2012 revision— key findings and advance tables. Working paper no. ESA/P/WP 227. United Nations: Population Division.
- US Salinity Laboratory Staff (1954). Diagnosis and improvement of saline and alkali soils. US Department of Agricultural soils. US Department of Agricultural Hand Book 60, Washington.
- Vasantavigar, M., Srinivasamoorthy, K., Prasanna, M.V. (2013). Identification of groundwater contamination zones and its sources by using multivariate statistical approach in Thirumanimuthar sub-basin, Tamil Nadu, *India. J Hydro*, 68, 1783–1795.
- WHO (2003). Guideline for drinking water quality. World Health Organization, Geneva.
- WHO (2004). Guideline for drinking water quality. World Health Organization, Geneva.
- WHO (2009). Guideline for drinking water quality. World Health Organization, Geneva.
- WHO (2011). Guideline for drinking water quality, 4th edn. World Health Organization, Geneva.
- Wilcox, L.V. (1955). Classification and use of irrigation waters. USD Circular No. 969, p 19
- World Bank. (2012). Report: India groundwater: a valuable but diminishing resource. www.worldbank.org.
- World Water Balance and Water Resources of the Earth. (1978) U.S.S.R. Committee for the International Hydrological Decade, UNESCO, Paris, France.
- Zhang Q., Li Z., Zeng G., Li J., Fang Y., Yuan Q., Wang Y., Ye F. (2009). Assessment of surface water quality using multivariate statistical techniques in red soil hilly region: a case study of Xiangjiang watershed, China. *Environ Monit Assess* 152: 123-131. <https://doi.org/10.1007/s10661-008-0301>.

Chapter 13

Performance of WQI and HPI for Groundwater Quality Assessment: Study from Sangramgarh Colliery of West Burdwan District, West Bengal, India



Tanushree Paul and Manas Nath

Abstract This chapter attempts to study the groundwater quality of abandoned Sangramgarh colliery area using the weighted arithmetic water quality index method and heavy metal pollution index method. The present study also draws attention toward the seasonal changes of some water parameters and groundwater level of the study area. Scarcity of clean and potable drinking water is one of the most serious issues in this study area. The result of hydrochemical analysis shows the water quality rating as per weighted arithmetic water quality index method is 59.58, which indicates poor water quality of the groundwater, and it also shows near-neutral to alkaline conditions of the groundwater in abandoned Sangramgarh colliery area. Land filling materials, huge overburden dumps, mine waste and heavy metal leaching during the rainy season contaminate the groundwater and deteriorate drinking water quality, which is a serious human health issue. Therefore, a periodic assessment of groundwater quality is necessary in order to ascertain the quality for human consumption purpose and to take better planning for sustainable management of groundwater.

Keywords Abandoned colliery · AMD · HPI · WQI

13.1 Introduction

Water is an essential commodity to living things and nonliving things, and it is important in all aspects of human life (Tiwarly and Dhar 1994; WHO 1984, 1997). Chemically, the combination of oxygen and hydrogen forms water. As water penetrates through the ground surface to the subsurface as groundwater, impurities get into it. Access to safe drinking water remains an urgent necessity, as 30% of urban and 90% of the rural Indian population still depend completely on untreated

T. Paul (✉) · M. Nath
Department of Geography, Burdwan University, Bardhaman, WB, India

surface or groundwater resources. Scarcity of clean and potable drinking water has emerged in recent years as one of the most serious developmental issues in many parts of West Bengal, Jharkhand, Orissa, Western Uttar Pradesh, Andhra Pradesh, Rajasthan and Punjab (Tiwari and Singh 2014). The rate of depletion of groundwater level and deterioration of groundwater quality is of immediate concern in major cities and towns of country (Tiwarly and Abhishek 2004, 2005; Ramakrishnaiah et al. 2009; Singh et al. 2011, 2013, 2014a; Tiwari and Singh 2014).

Mining is a major anthropogenic activity causing water pollution and environmental degradation (Abhishek and Sinha 2006). In abandoned coal mines, acid mine drainage (AMD) results from the oxidation of iron sulphide minerals which are associated with coal deposits. Huge overburden dumps or mine waste, resulting from the excavation process in open cast and underground mining operations, could also contain sulphide minerals (Bernd 2007). These materials are normally dumped on the surface, and water infiltrating through these materials can enhance the generation of AMD. But, AMD creation did not happen in all abandoned mines. The effect of this depends on the nature of the rocks. If coal seams have iron pyrites, sulphate and soluble metal ions are exposed to air and due to oxidation of the sulphide minerals form sulphuric acid which is called AMD. If they contain calcite or other carbonate minerals, the acidic mine water can be neutralized, and metals may stay immobile. In many abandoned mines, groundwater in hard-rock aquifers becomes vulnerable that may have a serious impact on human health. Besides, mining activities also released both major and trace elements into the environment. Trace elements or the heavy metals are classified among the most dangerous groups of pollutants due to their toxicity and persistence in the environment. Metals in the contaminated soils and water may reach the human body through agricultural products (Sponza and Karaoğlu 2002). Leaching of these heavy metals from the mine spoils during the rainy season contaminates the groundwater and deteriorates drinking water quality, which are serious human health issues. Groundwater contamination is one of the most important environmental problems in the present world where metal contamination is a major concern due to its high toxicity even at low concentration (Marcovecchio et al. 2007; Momudu and Anyakora 2010). According to the WHO, about 80% of all diseases in human beings are caused by water (Ramakrishnaiah et al. 2009). Therefore a periodic assessment of groundwater quality is necessary in order to ascertain the quality for human consumption purpose and to take better planning for sustainable management of groundwater.

The major objectives of the current study are (1) to measure the water quality of study area, (2) to assess the heavy metal contamination and (3) to reveal the seasonal fluctuation of some important water parameter and groundwater level.

13.2 Study Area

Sangramgarh colliery is located in the north-central part of Raniganj Coalfield and falls under Salanpur Area of Eastern Coalfields and West Burdwan district of West Bengal (Fig. 13.1). The colliery is to the north of GT Road and around 15 km from Asansol City. The latitudinal and longitudinal extensions of the mine are 23°47'N–23°48'N and 86°54'E–86°57'E. A total of 261 ha area is under leasehold of ECL. The leasehold area of the property being worked by underground is about 150 ha.

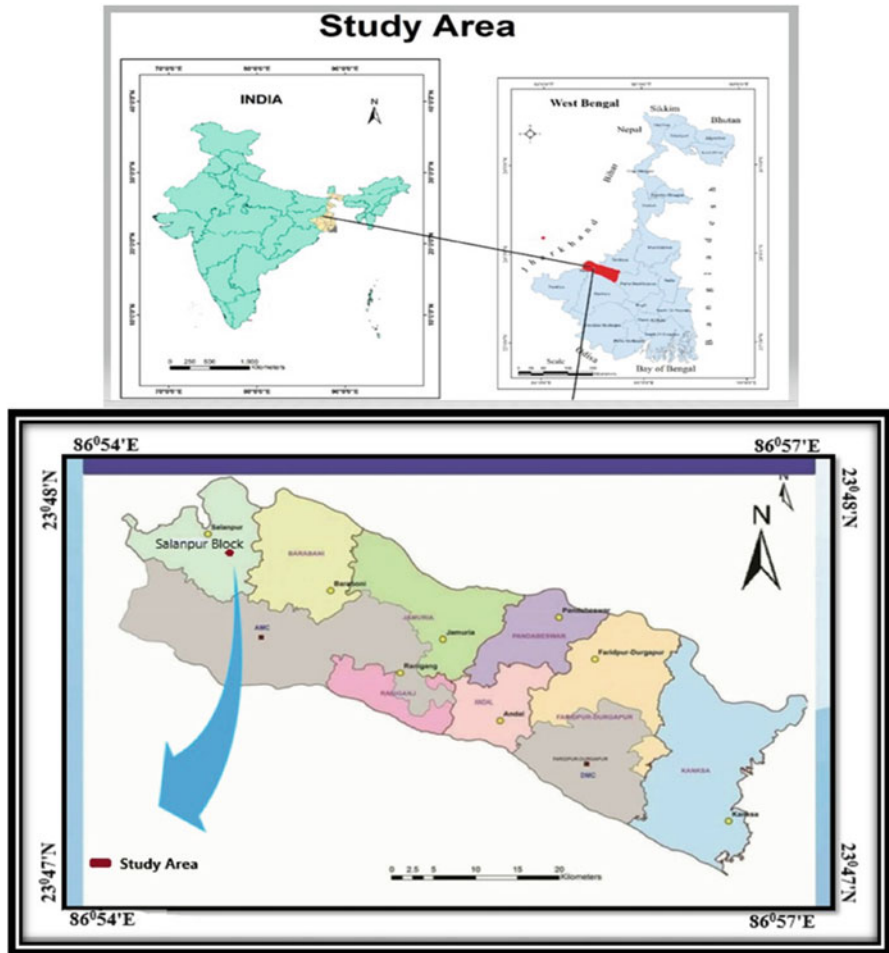


Fig. 13.1 Location map of the study area

13.3 Materials and Methods

13.3.1 Selection of Parameters

Firstly, study the Indian standard (BIS 2003) for drinking water specification. Here, the physicochemical parameters along with the desirable limits and related health effects are given. A parameter has to be selected based on its impact in the overall quality of water and health effects. 24 parameters like pH, BOD, COD, total dissolved solids (TDS), arsenic, lead (Pb), turbidity, iron, chlorides, Res free chlorine, calcium, copper, manganese, sulphate, nitrate, fluoride, selenium, zinc, chromium, boron, phenolics, alkalinity and total hardness have been selected.

13.3.2 Sample Collection and Analysis

Water samples are collected from CMPDI (Central Mine Planning and Design Institute) report, 2015–2016. Water quality of study area was evaluated by water quality index (WQI) technique. WQI indicates the quality of water in terms of index number which represents the overall quality of water for any intended use. A water quality index provides a single number that expresses overall water quality at a certain location and time based on several water quality parameters. In order to calculate WQI, 24 parameters have been selected. Water quality index was calculated for assessing the suitability of water for biotic communities and also drinking purposes.

13.3.3 Calculation of Water Quality Index (WQI)

The WQI has been applied for evaluating the water quality of study area. The WQI result represents the level of water quality in a given water basin such as lake, river or stream. WQI indicates the quality of water in terms of index number which represents the overall quality of water for any intended use. The indices are among the most effective ways to communicate the information on water quality trends to the general public or to the policy makers and in water quality management. Mostly it is done from the point of view of its suitability for human consumption.

Weighted Arithmetic Water Quality Index Method

In this paper the WQI was calculated using the weighted arithmetic water quality index (WAWQI) method which was proposed by Horton (1965), developed by Brown et al. (1970) and then by Cude (2001) in which water parameters are multiplied by a weighting factor and are then aggregated using a simple arithmetic mean by the following three equations.

Table 13.1 Water quality rating as per different water quality index methods

National Sanitation Foundation Water Quality Index (NSFWQI)	
91–100	Excellent water quality
71–91	Good water quality
51–71	Medium water quality
26–50	Bad water quality
0–25	Very bad water quality
Canadian Council of Ministers of the Environment Water Quality Index (CCME WQI)	
95–100	Excellent water quality
80–94	Good water quality
60–79	Medium water quality
45–59	Bad water quality
0–44	Very bad water quality
Oregon Water Quality Index (OWQI)	
90–100	Excellent water quality
85–89	Good water quality
80–84	Fair water quality
60–79	Marginal water quality
0–59	Poor water quality

1. Relative Weight

For water quality index calculation, assigning a weight for each groundwater parameter (*w_i*) for computing the relative weight (*W_i*) is needed. The assigned *w_i* values for each parameter are shown in Table 13.1. Weighted values are assigned according to relative importance in the overall quality of water for drinking purposes (weight may be from 1 to 5). The highest weight of 5 was assigned to parameters which have the major effects on water quality. TDS and nitrate are assigned the highest weight because of their importance in the water quality assessment (Ramakrishnaiah et al. 2009). Chloride is given the minimum weight of 1 as it plays an insignificant role in the water quality assessment. The relative weight (*W_i*) of the chemical parameter is computed using the following equation:

$$W_i = w_i / \sum w_i \quad (i = 1 \text{ to } n) \tag{1}$$

where *W_i* is the relative weight, *w_i* is the weight of each parameter and ‘n’ is the number of parameters.

Relative weight (*W_i*) of each parameter is calculated as a value inversely proportional to the Bureau of Indian Standards’ drinking water specifications. Factors which have higher permissible limits are less harmful because they can harm the quality of water when they are present in very high quantity.

2. Rating Scale

Rating scale (Table 13.1) was prepared for a range of values of each parameter. The quality rating scale (*Q_i*) for each parameter is calculated by using this expression:

Table 13.2 Water quality rating as per weight arithmetic water

WQI value	Rating of water quality	Grading
0–25	Excellent water quality	A
26–50	Good water quality	B
51–75	Poor water quality	C
76–100	Very poor water quality	D
Above 100	Unsuitable for drinking purpose	E

Table 13.3 HPI value classes

HPI value	Class of pollution intensity
<15	Low
15–30	Medium
>30	High

$$Qi = 100 \times [(Vi - Vo)/(Si - Vo)] \tag{2}$$

where

Qi is the quality rating scale.

Vi is the estimated concentration of *i*th parameter in the analysed water or observed value.

Vo is the ideal value of this parameter in pure water, *Vo* = 0 (the ideal value for pH = 7, dissolved oxygen = 14.6 mg/l, and for other parameters, it is equal to zero).

Si is the recommended standard value of *i*th parameter or the guideline value/desirable limit as given in Indian drinking water standard (BIS 2003).

3. Water Quality Index (WQI)

WQI is a compilation of a number of parameters that can be used to determine the overall quality of water. The numerical value is multiplied by a weighting factor that is relative to the significance of the test to water quality. The values of *Qi*, *Wi* and *QiWi* are given in Tables 13.2 and 13.3. Hence by multiplying *Wi* and *QiWi*, we can get the value of WQI. It is basically a mathematical means of calculating a single value from multiple test results:

$$WQI = \sum QiWi / \sum Wi \tag{3}$$

Based on the calculated WQI, the category of water quality types is shown in Table 13.2 according to Tyagi et al. (2013).

13.3.4 Calculation of Heavy Metal Pollution Index (HPI)

A heavy metal is any metallic element that has a relatively high density and is toxic or poisonous even at low concentrations. Heavy metals exist as natural constituents

of the earth crust and are persistent environmental contaminants, because these cannot be degraded or destroyed. Human exposure to harmful heavy metals can occur in many ways. Consumption of contaminated water is one of them. Water quality and its suitability for drinking purpose can be examined by determining its quality index (Mohan et al. 1996; Prasad and Sangita 2008; Prasad and Mondal 2008; Tiwari et al. 2013) by heavy metal pollution index methods. The HPI represents the total quality of water with respect to heavy metals. The HPI is also based on weighted arithmetic quality mean method. The HPI model proposed is given by Mohan et al. (1996):

$$\text{HPI} = \sum_{i=1}^n \text{WiQi} / \sum_{i=1}^n \text{Wi} \quad (1)$$

$$\text{Qi} = 100 \times \{[M_i(-)I_i] / [S_i(-)I_i]\} \quad (2)$$

where M_i is the monitored or observed value of heavy metal of the i th parameter

I_i is the ideal value (maximum desirable value for drinking water)

S_i is the standard value (maximum permissible value for drinking water)

The $(-)$ indicates the numerical difference of the two values, ignoring the algebraic sign. A modified scale is used in the present study after Edet and Offiong (2002). The scale is in the following table (Table 13.3).

13.4 Results and Discussion

13.4.1 Water Quality Index (WQI)

Finally, overall WQI was calculated according to the following expression:

$$\text{WQI} = \sum QiWi / \sum Wi$$

Water quality rating as per weighted arithmetic water quality index method is 59.58 which indicates a poor water quality in the study area.

The important water quality parameters and the water quality index are given in Table 13.4. pH is an important parameter which determines the suitability of water for various purposes having a desirable limit of 6.5–8.5 as specified by IS 10500. The pH of water is a measure of the acid-base equilibrium, and mostly natural water is controlled by the CO_2 -bicarbonate-carbonate equilibrium system. An increased CO_2 concentration will therefore lower pH, whereas a decrease will cause it to rise. Acid deposition has many harmful ecological effects. But in the abandoned Sangramgarh colliery area, the result of hydrochemical analysis shows the annual mean pH value is 7.65 which indicates neutralization of the groundwater.

Table 13.4 Calculation of water quality index as per weighted arithmetic water quality index method

No.	Parameter	Unit	Standard value (Si)	Ideal value (Vo)	Observed values (Vi)	Weight (wi)	Relative Weight (Wi)	Quality Rating (Qi)	Sub Index (SI) $W_i \times Q_i$
1	BOD	mg/L	5	0	3	4	0.054	60	3.24
2	COD	mg/L	10	0	24.3	4	0.054	243	13.12
4	TDS	mg/L	500	0	689	5	0.068	137.8	9.37
5	pH	pH units	7.5	7	7.53	4	0.054	106	5.72
6	Arsenic	mg/L	0.05	0	0.005	5	0.068	10	0.68
7	Lead (Pb)	mg/L	0.05	0	0.005	5	0.068	10	0.68
8	Turbidity	NTU	5	0	4.0	4	0.054	80	4.32
9	Iron	mg/L	0.30	0	0.06	4	0.054	20	1.08
10	Chlorides	mg/L	250	0	91	1	0.014	36.4	0.510
11	Res free chlorine	mg/L	0.20	0	0.02	2	0.027	10	0.27
12	Calcium	mg/L	75	0	49.6	2	0.027	66.1	1.78
13	Copper	mg/L	0.05	0	0.03	3	0.041	60	2.46
14	Manganese	mg/L	0.1	0	0.02	3	0.041	20	0.82
15	Sulphate	mg/L	200	0	62	4	0.054	31	1.67
16	Nitrate	mg/L	45	0	3.99	5	0.068	8.87	0.603
17	Fluoride	mg/L	1.0	0	0.62	3	0.041	62	2.54
18	Selenium	mg/L	0.01	0	0.005	2	0.027	50	1.35
19	Zinc	mg/L	5.0	0	0.02	3	0.041	0.4	0.016
20	Chromium	mg/L	0.05	0	0.01	3	0.041	20	0.82
21	Boron	mg/L	1.0	0	0.01	1	0.014	1	0.014
22	Phenolics	mg/L	0.001	0	0.001	1	0.014	100	1.4
23	Alkalinity	mg/L	200	0	208	4	0.054	104	5.62
24	Total hardness	mg/L	300	0	196	3	0.041	65.3	2.68
						$\sum w_i = 74$	$\sum W_i = 1.019$	$\sum Q_i = 1300.6$	$\sum W_i \times Q_i = 60.713$

Data source: CMPDI (Central Mining Planning and Design Institute) records, 2015–2016

Alkalinity is a measure of the ability of the water to neutralize acids. The predominant chemicals present in natural water are carbonates, bicarbonates and hydroxides. Alkaline content in water is 208 mg/L which exceeded the desirable limit (200 mg/L). This value indicates non-acidic water of the study area. Alkalinity is not considered detrimental to humans, but high alkalinity water may have a distinctly flat and unpleasant taste.

The effect of this depends on the nature of the rocks. If coal seams have iron pyrites, sulphate and soluble metal ions are exposed to air and due to oxidation of the sulphide minerals form sulphuric acid which is called AMD. If they contain calcite or other carbonate minerals, the acidic mine water can be neutralized and metals may stay immobile. Commonly, however, the water dissolves any metal compounds present resulting in high concentrations of metals, particularly iron, zinc, copper, lead, cadmium, manganese and aluminium. The quality of mine waters varies considerably; they may be alkaline, acidic, ferruginous and highly saline or clean (Abandoned mines and the water environment Science project SC030136-41). However, carbonate minerals are not common in the study area. The anthropogenic sources may be the main sources of it. These sources can be related to the materials used in sealing of the coal mines, overburden dump consisting mainly of mining waste and lesser content of ash, garbage, slag, sludge, construction waste and industrial residue household waste (GLA-NRW, 1988). These materials often have a low amount of calcite. Dissolution of these carbonates reduces the oxidation of sulphide and changes the mine water from acidic to neutral conditions. In non-acidic mines, water quality shows high hardness, TSS, TDS bacterial contaminants and some heavy metals. These features are shown in the study area.

High TSS (*total suspended solids*) indicates mud, fine sand and microorganisms or decaying plants and animals. High TSS parameter indicates high level of pollution of water. The TSS value is 34 in summer season which exceeded the permissible limit of 25 mg/L, and annual mean value is 17 mg/L.

TDS (*total dissolved solids*) are the terms used to describe the inorganic salts and small amounts of organic matter present in water. If the TDS value is 500 mg/L, the water is considered as disagreeable (Indian standard IS 10500, 2012 by BIS). In the study area, the annual mean of TDS is 689 mg/L which exceeded the desirable limit. In this respect this water is not very suitable for drinking purposes. But due to lack of water resources, people of the study area have to drink this type of water.

COD (*chemical oxygen demand*) test is helpful in indicating toxic condition and presence of biologically resistant organic substances. In the present study, the annual mean of COD value is 24.3 mg/L which exceeded the standard value of 10 mg/L.

Turbidity is the degree of clarity to which the water loses its transparency due to presence of suspended particulates such as sediment and other contaminants. Turbidity is an indication of the presence of suspended inorganic matter. Turbidity nature of the study area's groundwater is 4.0 NTU which is below the permissible limit of 5–10 NTU. Higher turbidity results in increased BOD.

The BOD (biochemical oxygen demand) test is required to measure the amount of oxygen required by an organic matter for their decomposition. It gives a measure of the amount of organic matter in the water sample and their strength. It helps in assessing the pollution levels of the water sample. BOD >5 mg/L signifies the water is impure. In the study area, BOD value is found to be 3 mg/L which is less than the permissible limit.

Total hardness of water is a measure of the ability of water to cause precipitation of insoluble calcium and magnesium salts of higher fatty acids from soap solutions. The principal hardness-causing cations are calcium, magnesium bicarbonate, carbonate, chloride and sulphates. The hardness values of the present study were found to be 196 mg/L, whereas the permissible limit is 300 mg/L. The value of carbonate, chloride and sulphate of the present study is found within permissible limit, i.e. 49.6 mg/L (IS: 75 mg/L), 91 mg/L (IS: 250 mg/L) and 62 mg/L (IS: 200 mg/L).

13.4.2 Heavy Metal Pollution Index (HPI)

HPI is a very useful tool in evaluating the overall pollution of water bodies with respect to heavy metals (Prasad and Sangita 2008). Considering the classes of HPI, the study area falls under the low class (HPI < 15) 7.24. The present study reveals that groundwater sample is found less polluted with respect to heavy metal contamination (Table 13.5). The concentration of all heavy metals is within the desirable limit except for Mn content. Therefore this indicates the groundwater is not critically polluted with respect to heavy metal in Sangramgarh colliery area.

Table 13.5 Heavy metal pollution calculation for groundwater

Sl. No.	Heavy metals	Monitored value (M_i)	Ideal value	Highest permissible value	w_i	Q_i	$W_i \times Q_i$
1	Chromium	0.04	0.05	0.05	20	1	20
2	Copper	0.03	0.05	1.5	0.67	1.38	0.93
3	Zinc	0.06	5.0	15.0	0.067	49.4	3.31
4	Manganese	0.20	0.1	0.3	3.33	50	166.5
5	Iron	0.12	0.30	1.00	1.0	25.7	25.7
6	Arsenic	0.005	0.05	0.05	20	4.5	90
7	Lead	0.005	0.05	0.05	20	4.5	90
8	Nickel	0.10	3.0	6.0	0.17	96.67	16.4
9	Cadmium	0.001	0.003	0.005	20	100	2000
						$\Sigma 333.15$	$\Sigma 2412.84$

Data source: CMPDI (Central Mining Planning and Design Institute) records, 2015–2016

13.4.3 Seasonal Fluctuation of Water Parameters

The pH values of groundwater sample ranged from 6.79 in summer to 8.18 in pre-winter with an annual mean value for all periods of 7.65. TDS showed highest range of 865.5 mg/L in spring and lowest range of 475 mg/L in winter with an annual mean value of 689 mg/L, whereas TSS value is shown a high range of 34 mg/L in summer and low range of 6 mg/L in autumn with annual mean value of 17 mg/L. All studied parameters showed significant temporal differences of water quality (Table 13.6). The seasonal change in water quality is mostly influenced by trophicity, organic pollution, oxide-related process, erosion as well as anthropogenic activities (Fig. 13.2).

13.4.4 Groundwater Level

The groundwater level is a key parameter for evaluating spatial and temporal changes in groundwater environments. In Fig. 13.3, it is clearly shown that precipitation and evaporation affected the groundwater level in the study area. There is a positive correlation with precipitation and negative correlation with the evaporation of the groundwater level. During dry season, on January, November and May, a downward trend of the groundwater level is shown, whereas during wet season, on August, the groundwater level is increased gradually as most of rainfall falls in July–August month. Climate change, as reflected in precipitation and evaporation rates, influences the groundwater level fluctuation.

13.5 Conclusion

It is concluded that WQI can be used as a tool to assess the water quality of any area. Water quality index (WQI) is valuable and unique rating to depict the overall water quality status in a single term that is helpful for the selection of appropriate treatment technique to meet the concerned issues. HPI is also a very useful tool in evaluating the overall pollution of water bodies with respect to heavy metals. These all values give the public a general idea of the possible problems with water in a particular region and communicate the information on water quality trends to the policy makers and water quality management.

With the help of Weighted Water Quality Index Method, it is shown that WQI is 59.58 which indicates a poor water quality as per weighted arithmetic water quality index method, whereas HPI value is low ($HPI < 15$) (7.24) which indicates the groundwater is not critically polluted with respect to heavy metals in the study area. The groundwater quality in this mining area is significantly affected by abandoned Sangramgarh coal mines. Leaching of materials from overburden dumps, land

Table 13.6 Season-wise simple statistical analysis of some important water parameters

Water parameter	Seasons																		Annual Mean value	
	Summer			Rainy			Autumn			Pre-winter			Winter			Spring				Standard Value
	Min	Max	Mean	Min	Max	Mean	Min	Max	Mean	Min	Max	Mean	Min	Max	Mean	Min	Max	Mean		
pH	6.79	7.58	7.19	7.68	7.94	7.81	7.94	7.98	7.96	7.88	8.18	8.03	7.87	7.88	7.88	6.99	7.10	7.05	7.5	7.65
TSS	25	34	29.5	25	26	25.5	6	25	15.5	8	13	10.5	6	10	8	8	14	11	25 mg/l	17
TDS	798	823	810.5	812	825	818.5	518	810	664	484	506	495	475	486	480.5	861	870	865.5	500 mg/l	689
COD	20	24	22	16	32	24	16	32	24	12	28	20	24	32	28	24	32	28	10 mg/l	24.3

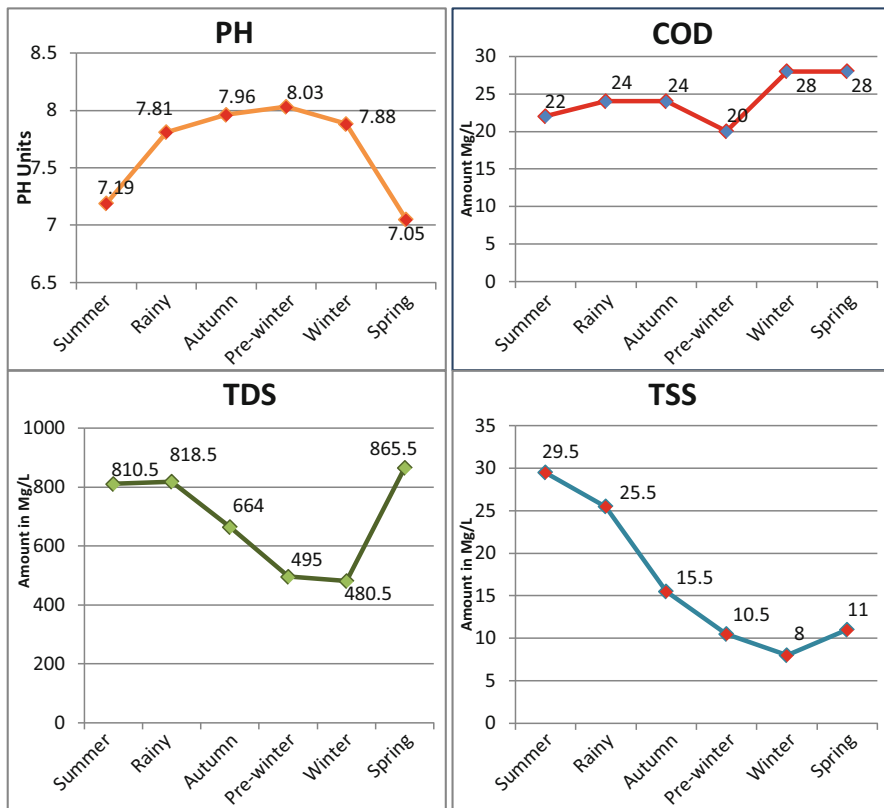


Fig. 13.2 Seasonal fluctuation of water parameters

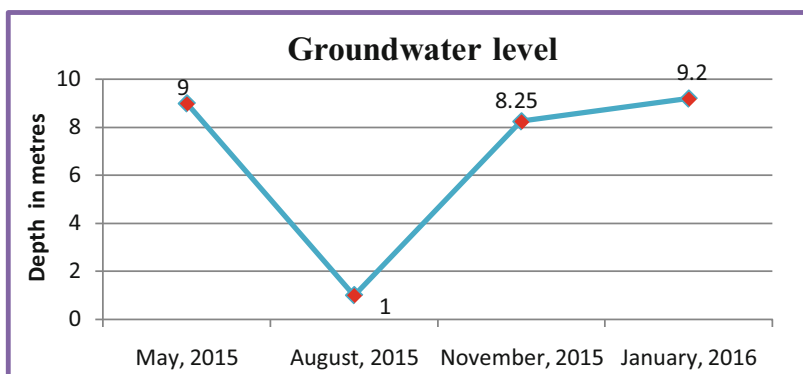


Fig. 13.3 Groundwater level of the study area in dry and wet seasons

filling, mine waste and heavy metals is mainly responsible for deteriorating the groundwater quality. The groundwater of this colliery area is also characterized by near-neutral to alkaline conditions, represented by predominance of calcium bicarbonate and sometimes calcium sulphate water types. Besides, groundwater scarcity is also the main problem here. So, quality and quantity both become a serious issue in this area which will be environmental threats unless all necessary measures are taken to reduce the impact:

- It is recommended to have further studies on the study area in order to shed more light on this area.
- Some parameters are required to add to cover as possible as the current status of the mining area.
- Create a strategic plan to aware the local people about pollution and how it can be prevented and save our environment from this important issue.
- Launch an environmental programme starting from primary school to the decision maker in the prevention and mitigation of water pollution.

References

- Abhishek, R.K. Tiwary and S.K. Sinha, (2006) "Status of Surface and Groundwater Quality in Coalmining and Industrial Areas of Jharia Coalfield", *International Journal of Environmental Protection (IJEP)*, Vol.26 (10): pp.905–910.
- Allen, S.K., Allen, J.M., Lucas, S. 1996, "Concentration of contaminants in surface water samples collected in west-central Indiana impacted by acid mine drainage," *Environ. Geol.* XXVII, pp. 34–37.
- Bernd, L. 2007. "Mine Waste; Characterization, Treatment and Environmental impacts". *Journal of Springer*, ISBN: 3642446094
- BIS., Indian standard drinking water specifications IS10500:2012, Bureau of Indian Standards, New Delhi, (2003).
- Choubey, V.D. 1991, "Hydrological and environmental impact of coal mining, Jharia coalfield, India", XVII, pp.185–194.
- Edet, A.E and Offiong, O.E (2002), Evaluation of water quality pollution indices for Heavy Metal Contamination Monitoring, A study case from Akpabuyo-Odukpani Area, Lower cross River Basin (South eastern Nigeria), *Geomicrobiology journal*, 57, 295–304.
- Horton, R.K (1965), "An Index Number System for Rating Water Quality". *Journal of the Water Pollution Control Federation*, 37, 300–306.
- Marcovecchio, JE., Botte, SE., Freije, RH. 2007. Heavy Metals, Major Metals, Trace Elements. In: *Handbook of Water Analysis*. L.M. Nollet, (Ed). 2nd Edn. London: CRC Press, pp:275–311
- Mohan, D., Gupta, VK., Shrivastav, SK. 1996. 'Kinetic parameters for the removal of lead and chromium from wastewater using activated carbon developed from fertilizer waste material'. *Environmental Modelling & Assessment* 1(4), 281–290.
- Momudu, M.A, Anyakora, C.A., 2010. Heavy Metal Contamination of Ground water: The surulere Case study. *Research journal Environmental and Earth Sciences* 2(1), 39–43.
- Prasad, B. and Mondal, K. Kr. (2008) The Impact of Filling an Abandoned Open Cast Mine with Fly Ash on Ground Water Quality: A Case Study. *Mine Water and the Environment* 27 (1):40–45

- Prasad, B. and Sangita, K. (2008) Heavy Metal Pollution Index of Ground Water of an Abandoned Open Cast Mine Filled with Fly Ash: a Case Study. *Mine Water and the Environment* 27 (4):265–267
- Ramakrishnaiah, C. R. et al., 2009, “Assessment of water quality index for the groundwater in Tumkur Taluk, Karnataka State, India”, *Journal of Chemistry*, 6(2): 523–530.
- Singh, A.K., Mahato, M.K., Neogi, B., Mondal, G.C. And Singh, T.B., 2011, “Hydro Geochemistry, Elemental Flux And Quality Assessment Of Mine Water in the Pootkeebalihari Mining Area, Jharia Coalfield, India”, *Mine Water And The Environment*, 30(3), 197–207
- Singh, P., Tiwari, AK. Singh, PK. 2014a, “Assessment of Groundwater Quality of Ranchi Township Area, Jharkhand, India by Using Water Quality Index Method”. *International Journal of ChemTech Research* 7(01), 73–79.
- Singh, PK., Tiwari, AK., Mahato, MK. 2013, “Qualitative Assessment of Surface Water of West Bokaro Coalfield, Jharkhand by Using Water Quality Index Method”. *International Journal of ChemTech Research* 5(5), 2351–2356.
- Sponza, D. and Karaoğlu, N. (2002) Environmental geochemistry and pollution studies of Aliğa metal industry district. *Environment International* 27(7):541–553
- Tiwari, AK., Singh, AK. 2014. “Hydro geochemical investigation and groundwater quality assessment of Pratapgarh district, Uttar Pradesh”. *Journal of the Geological Society of India* 83(3), 329-343.
- Tiwari, AK., Singh, PK., Mahato, MK. 2013. “Chemistry of Groundwater and Their Adverse Effects on Human Health: A Review”. *Indian Journal of Health and Wellbeing* 4(4), 923-92.
- Tiwary, R.K and Abhishek, (2004) “Impact of coal mining and allied industries on the aquatic environment in Jharia coalfield. National Seminar on Pollution in urban industrial environment, Bhubaneswar, Proceedings, pp 41–49.
- Tiwary, R.K and Abhishek, (2005) “Impact of coal washeries on water pollution of river Damodar in Jharia coalfield, *Indian J. Env. Prot.*, 25(6): 518–522.
- Tiwary, R.K and Dhar, B.B. 1994, “Effect of coal mining and coal based industrial activities on water quality of the river Damodar with special reference to heavy metals”. *International Journal Surface Mining, Reclamation Env.*, 8:111–115.
- Tyagi, S., Sharma, B., Singh, P., Dobhal, R. (2013) Water Quality Assessment in Terms of Water Quality Index. *American Journal of Water Resources* 1 (3):34–38
- WHO, 1984, Guidelines for drinking water quality, World Health Organization, Washington DC, pp.333–335.
- WHO, 1997, Guidelines for drinking-water quality. vol 1, Recommendations. World Health Organisation, Geneva, pp 1–4.

Chapter 14

Assessment of Groundwater Quality Interaction Using One-Decade Data: A Case Study from a Hard Rock Area



S. Satheeshkumar , S. Venkateswaran, and R. Suresh

Abstract Water is the most important resource to sustain to progress life on the earth. Most of the communities obtain their water recovered from groundwater. Aquifer is the geologic material that is capable of holding fresh water. Nearly 80% of water resource is used for human purposes. The chemical composition of river water is mainly depending upon many interrelated factors including geology, soil, topography, and biological process. The continuous runoff of water may cause land use changes; therefore, hydrogeochemistry of groundwater is the sum of the total character. Water quality character in some part of area is one of pollution problem comes when the concentration of the ions exceeds the acceptable limit. In this study area, nowadays the problem of environmental pollution increases day-to-day, and anthropogenic influence plays a concerned role in groundwater. The aim of the present study is to explore the physicochemical characterization of groundwater and their major ion interaction in hard rock of this study area. In this case, that is quality character of water resource especially for drinking and domestic purposes it is depend on the constituent of water. Once the concentration exceeds the permissible limit, it causes health effects. Gibbs and mixing plots were used to identify the source of major ions. The contribution of water pollution scenario can be confirmed by field studies by focusing on land use change, agriculture, and settlement activities. The relationship between variables of ions was determined through correlation analysis. A better understanding of hard rock aquifer for water quality changes as development progress by geochemical studies of groundwater is necessary.

Keywords Bivariate plot · Cation-exchange reaction · Silicate weathering process · Water quality

S. Satheeshkumar (✉) · S. Venkateswaran · R. Suresh
Department of Geology, Periyar University, Salem, India

14.1 Introduction

Groundwater is the ultimate, most suitable fresh water, resource with around well-adjusted concentration of the salt for human depletion (Tewari et al. 2010). Temporary changes in water quality exceptional are because an interaction of rock–water and oxydo-discount reactions at some stage in the separation of water thru the aquifers. By these processes toxic, nontoxic pollution and waterborne pathogens are the main water fine constraints which might be transported from a recharge region to discharge place via aquifers through groundwater movement (Varol and Davraz 2013). This study on the composition of groundwater provides an insight of understating the relationship between chemical weathering, evaporation, and atmospheric deposition.

The polluted water has a considerable negative impact on humans also. The various factors have influence on subbasin. Drainage pattern of an area depends on the course of stream and its tributaries. Drainage pattern is to locate characterization of vulnerable area and soil conservation measures. In this area, the most influence factor is precipitation by seasonal distribution.

The present research work are aim to evaluate the physical and chemical characterization of the study area for identifying the source factor and finally explore the contribution of chemical weathering and anthropogenic influence activities. The hydrochemical study reveals the suitability of water, that is, drinking, agriculture, and domestic purposes. Further, there are possible changes during water–rock interaction. The chemical analysis in graphical form indicated to understand the complex system. Gibbs proposed a simple model constructed with TDS and ions to represent the interaction process of rock–water.

A number of researchers have attempted to identify the interaction of controlling water chemistry, and there is assessment on the continuation of surface water into groundwater. Fluoride are threaten on water quality which can produce an extensive kind of acute and continual consequences in human beings, such as dental fluorosis and bone ailment (Satheeshkumar et al. 2017). Fluoride absorbed with the aid of the human frame disturbs many methods and sometimes is harmful. The hazard quotient (HQ) is widely used to symbolize health effects of poisonous metals and fluoride by using a comparison of their revelation outcomes to a reference dose (Qu et al. 2012 and Sun and Li 2011). This becomes documented in numerous studies through contemplating exposure eventualities of metal intake via contaminated water (Muhammad et al. 2011; Dou and Li 2012; Shah et al. 2019). A reliable opportunity accordingly depends on the concentration of trace elements, which gets dissolved from the aquifer-bearing rocks thru a complex hydrogeochemical manner by usage of groundwater as a storage potential (Mukherjee et al. 2015). The hydrogeochemical facies are accountable for water resource pollution; their strategies and deciphering unique indices had been usually used by a variety of techniques (Coetsiers and Walraevens 2006; Srivastava and Ramanathan 2008; Das and Kumar 2015).

14.2 Materials and Method

14.2.1 Study Area

In this area, the source of water recharge from Vanniyar river basin receives the maximum rainfall from Yercaud region (Fig. 14.1). It is the maximum elevation of the study area. It is covered by Shevaroy hills. The lithology of the area mainly consists of granitic to biotite gneissic rock. Most of the red soil is covered by black soil. Some places have dike and lineament present in the study area. They are most useful for groundwater targeting for water development and management. The Vanniyar river basin is one hard rock aquifer, and it covers mainly in south India of flowing non-perennial stream. This area is a subtropical climate region.

14.2.2 Data Collection

GW samples were collected from different regions in this study area. The 2005–2014 data is collected from PWD. The water quality parameters have been analyzed into cations and anions. Generally, the groundwater samples show the specific charge balance of less than 10% by NICB test. The samples were analyzed for anions and cations. For the determination, water quality parameters like temperature, pH, electrical conductivity, total solids, total dissolved solids, cations (sodium, potassium, calcium, magnesium), anions (bicarbonate, nitrate, sulfate, chloride), and total

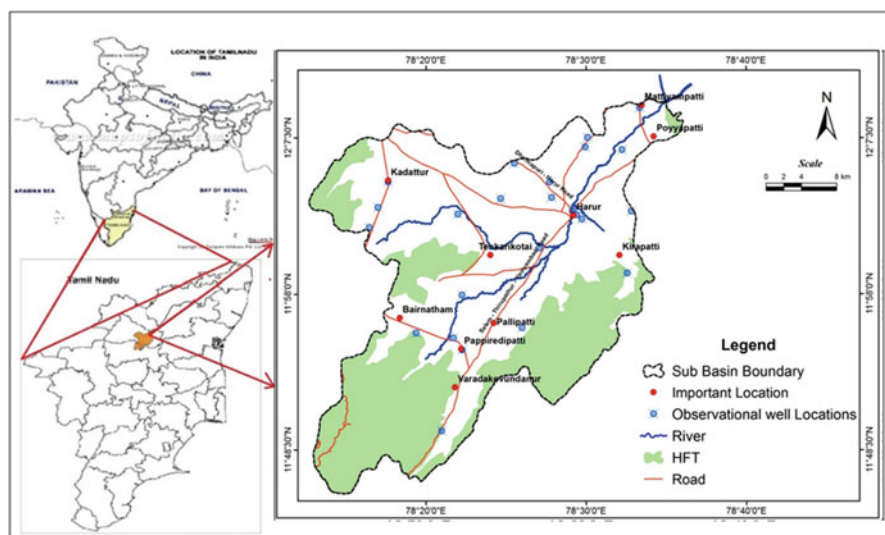


Fig. 14.1 Location of the water level observational well area

hardness in groundwater samples were subjected to a multivariate analysis. The evaluation of major cations are for most important ions to assess water quality index, analytical precision turned into checked by the NICB, normalized inorganic charge stability (Kumar et al. 2010, 2016a, b, c).

14.3 Result and Discussion

14.3.1 Assessment of Groundwater Quality

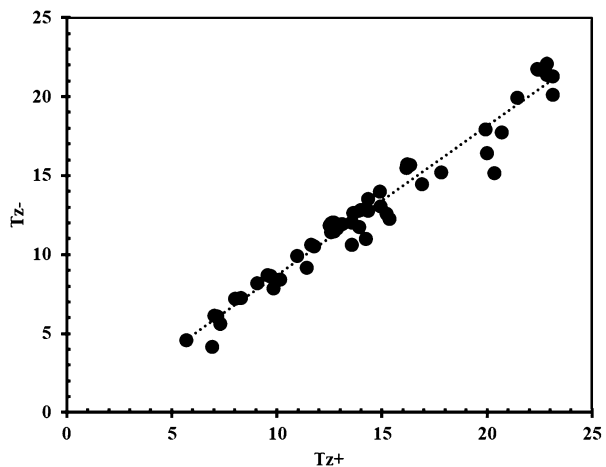
Water samples from this study area are generally less than 10% which is estimated (Fig. 14.2). The box plot is a simple visualization with respect to maxima and minima identified by the data variation (Fig. 14.3) of a diverse region of the study area for the drinking purposes of groundwater quality assessed.

14.3.2 Groundwater Quality for Drinking Usage

One of these techniques box plot is used to visually summarize and compare groups for drinking suitability at kompur and pappiredipatti in Figs. 14.4 and 14.5. Both have a good to moderate water quality in this region based on the BIS.

Major ion variations in different water types are shown in Fig. 14.6. The scatter diagram shows the relation between Na and Cl in Fig. 14.7. The geology of the study area is the primary factor for controlling the quality of natural water system. In the natural condition in the chemical composition, rainfall ranges between the temperatures of this region are shown in the process of evaporation.

Fig. 14.2 Sum of cation and anion (NICB<10%)



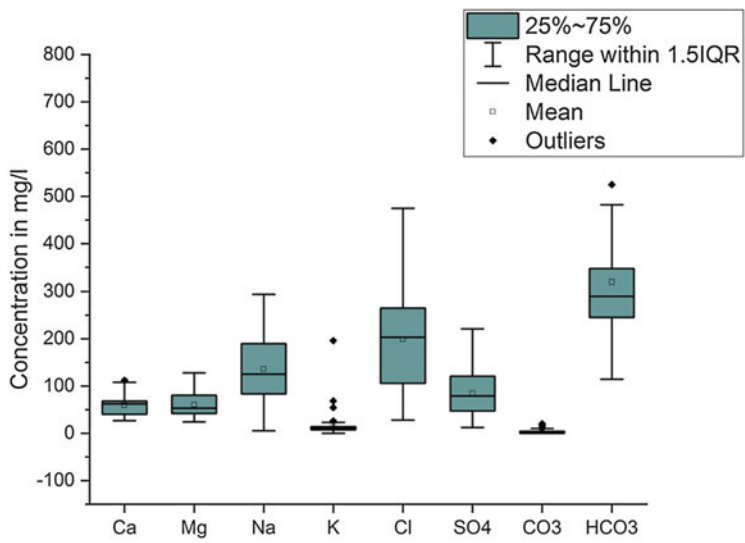


Fig. 14.3 Box plot showing the variation of ionic concentration

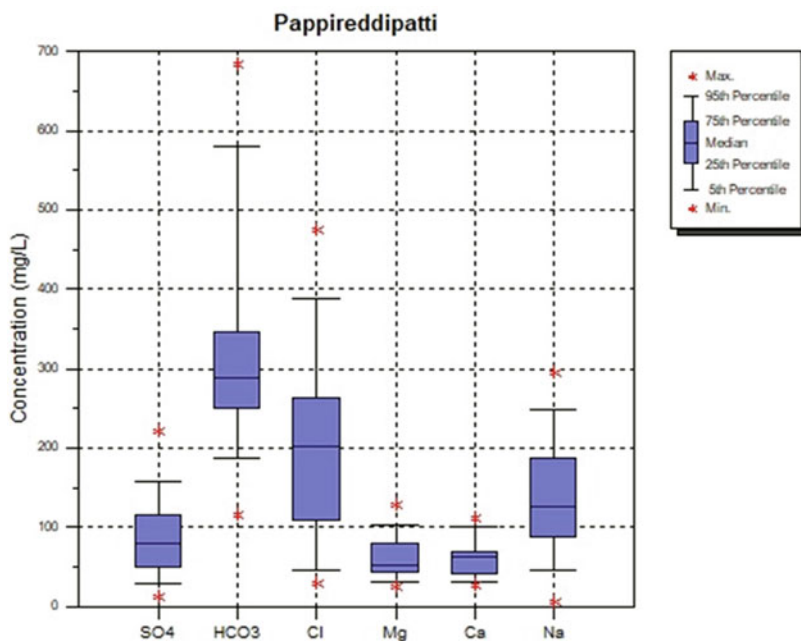


Fig. 14.4 Box plot showing the variation of ions at pappireddipatti

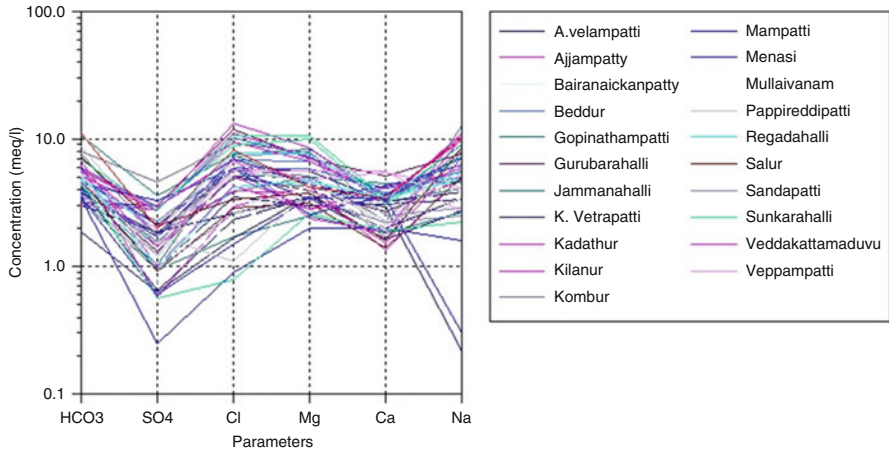


Fig. 14.5 Schoeller diagram showing the variation of major ions

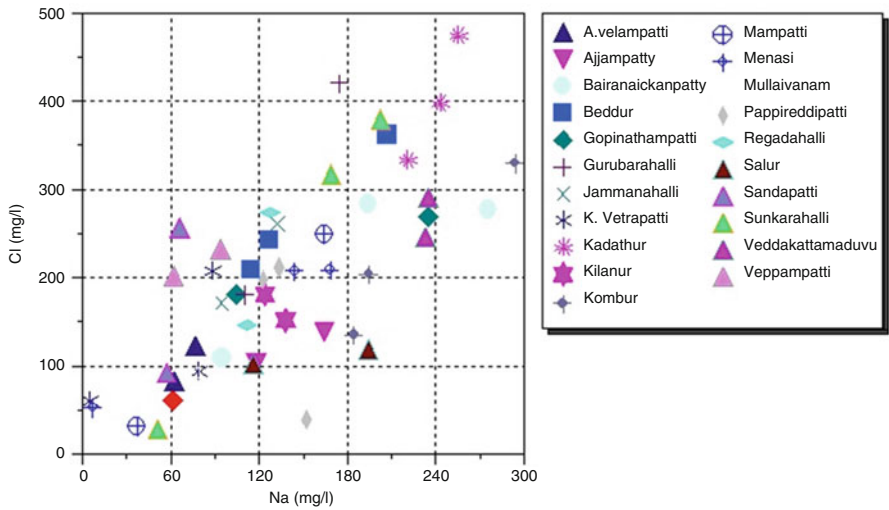


Fig. 14.6 Scatter diagram showing Na vs Cl

The Ludwig-Langelier plot is an appropriate grouping of cations and anions which have been plotted as percentages. Generally, this type of Ludwig-Langelier plot is used to plot the percentage of Na + K against percentage of $\text{HCO}_3 + \% \text{SO}_4$. In this plot, the percentage of Ca + Mg and Cl is also fixed. In Figure 14.7, the plot displays the relative ratios rather than absolute concentrations.

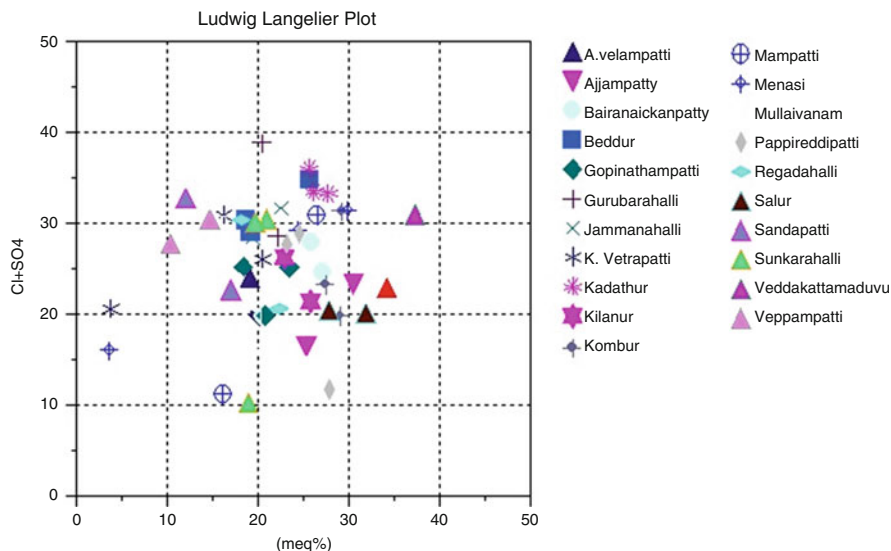


Fig. 14.7 Ludwig-Langelier plot of Cl + SO₄

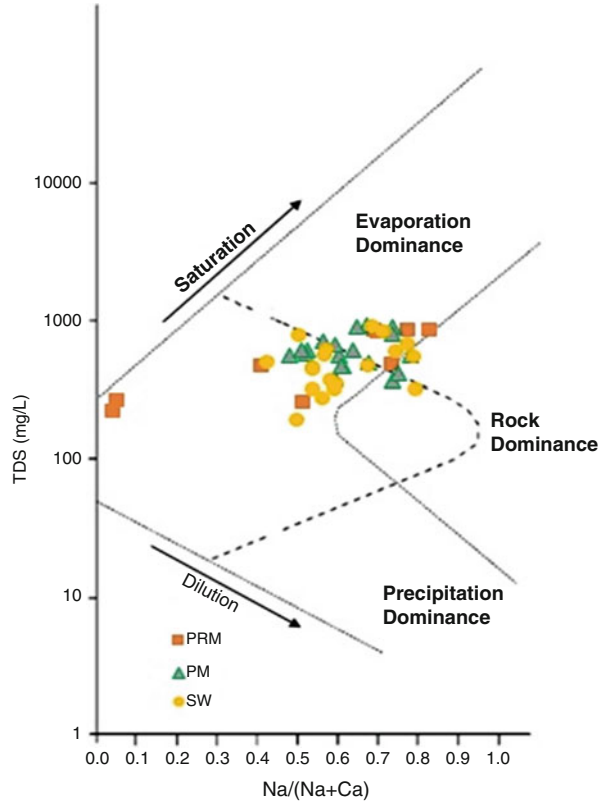
14.3.3 Mechanisms Controlling Hydrochemical Composition

The chemical components of water to their respective aquifers and their connection of between water chemistry of the rock types, chemistry of brought on water, and rate of evaporation have been recognized. Gibbs (1970) diagram has illustrated in which ratio between dominant of anions and cations have plotted in opposition to the fee of total dissolved solid. Anions $[Cl/(Cl + HCO_3)]$ and cations $[(Na + K)/(Na + K + Ca)]$ as functions of TDS are broadly employed to dissolved chemical parts inclusive of precipitation fall in upper region mostly rock and evaporation dominance in lower region (Gibbs 1970). Gibbs diagrams are representing the ratio. The chemical water data of groundwater samples are plotted inside the Gibbs diagram (Fig. 14.8). By Influencing water in weathering of rock-forming minerals of groundwater through dissolution of rock via which water is circulating through ions of the water.

14.3.4 Evaporation

Groundwater samples indicate the relation between Na (meq/l) and Cl (meq/l) in Fig. 14.9 and Na/Cl (meq/l) and EC in Fig. 14.10. Both are showing that evaporation is not a major part of the process. This process shows a slightly inclined relationship. The slightly elevated Na is indicating silicate weathering than evaporation. In this area Na is higher because of granite gneiss monitored by the evaporation process.

Fig. 14.8 Gibbs ratio for cations (Gibbs 1970)



14.3.5 Cation-Exchange Response

Cation-Exchange process which control occurrence and distribution of ions using this reaction it can be identified which is contamination sources. An excess of Cl over Na demarcates the ion exchange process (Fig. 14.11).

14.3.6 Silicate Weathering Process

Evidence of silicate weathering can be elucidated by the relation between Ca + Mg and HCO₃ in Fig. 14.12. This situation required CO₃ alkalinity to be balanced by alkalis. The relation between Ca + Mg and total cation is shown in Fig. 14.13, and relation between Na + K and total cation is shown in Fig. 14.14. The most of data points 1:1 equiline. The total cations are indicating silicate weathering when

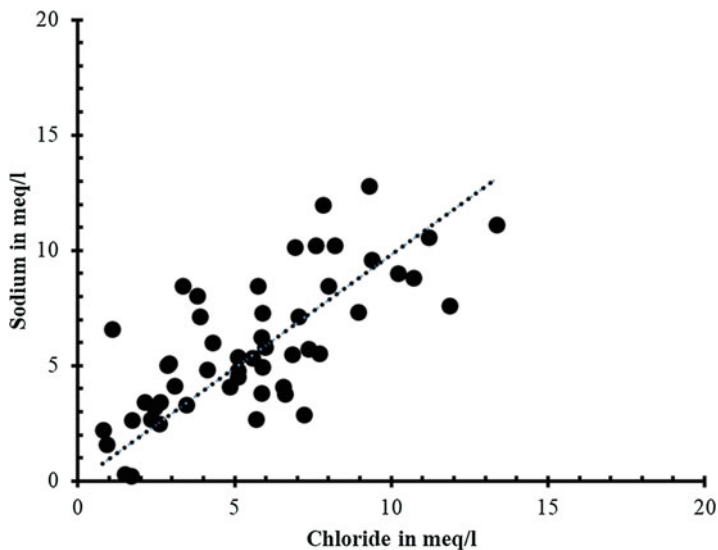


Fig. 14.9 Relation between Na (meq/l) and Cl (meq/l)

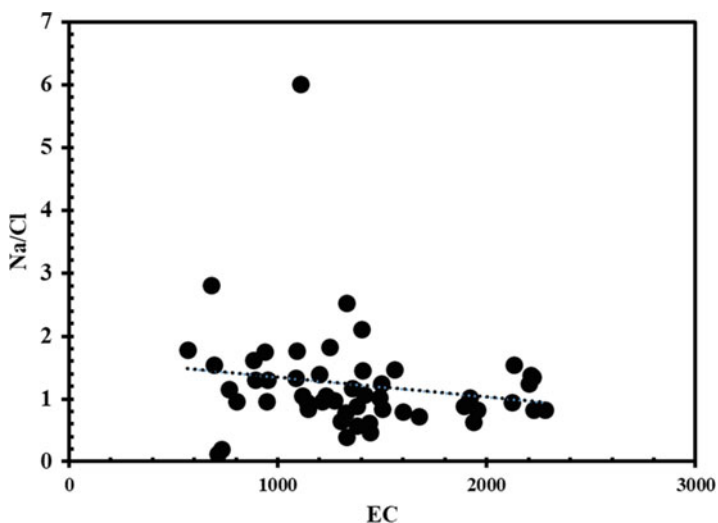


Fig. 14.10 Relation between Na/Cl (meq/l) and EC

contribution is higher in this case. Na-probable source is silicate dissolution because it is derived from silicate weathering. In this study the major source of cation and HCO_3 occurred by silicate process of weathering and also Ca and Mg by common minerals in granitic gneissic rock.

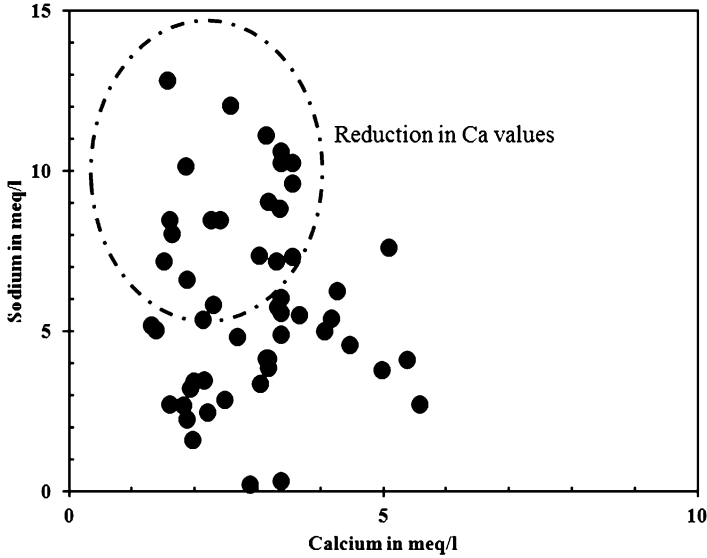


Fig. 14.11 Cation-exchange reaction between Ca and Na

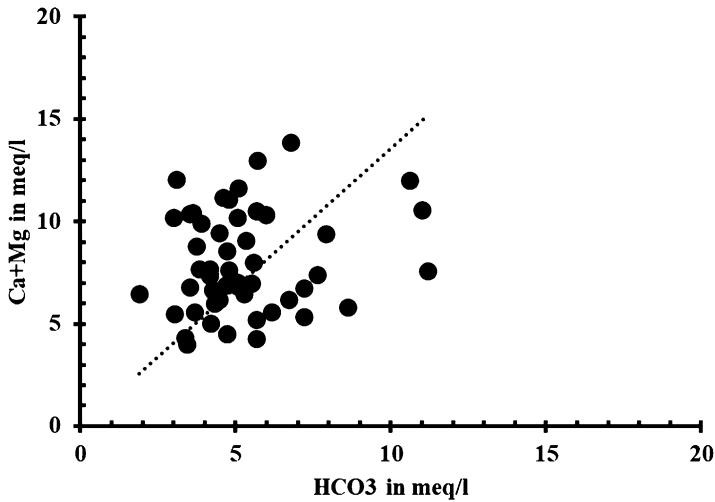


Fig. 14.12 Relation between Ca + Mg and HCO₃

Soil leaching is indicated in Fig. 14.15. The boxes represent in Fig. 14.16, without any mixing, the tiers of approximate compositions of the three important supply end individuals such as carbonate dissolution, silicate weathering, and evaporate dissolution.

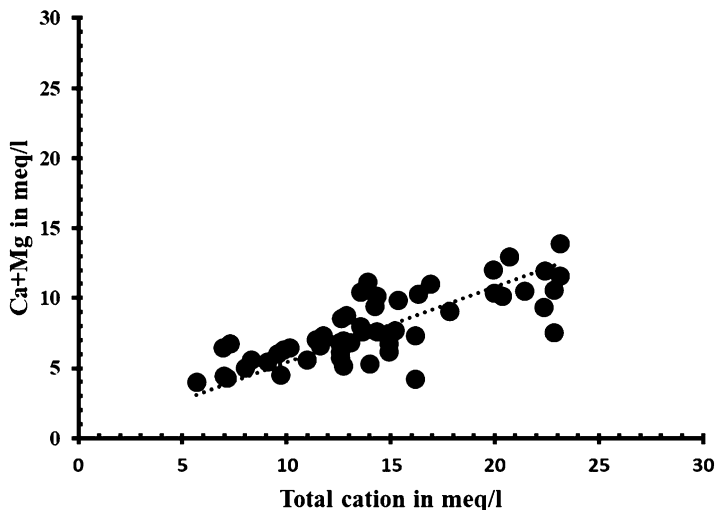


Fig. 14.13 Relation between Ca + Mg and total cation

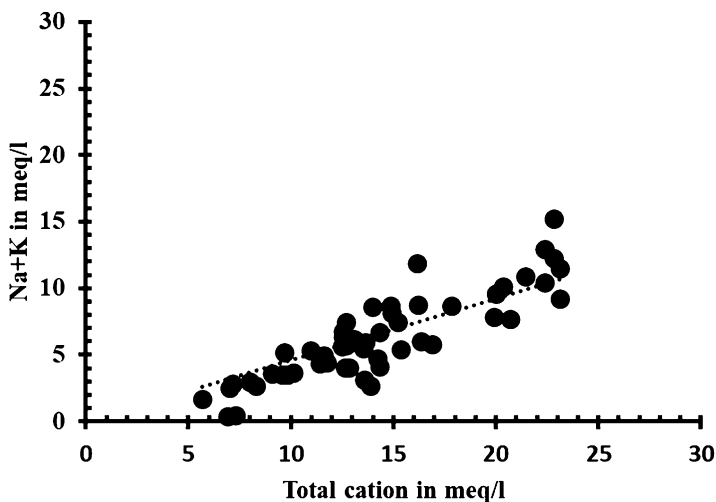


Fig. 14.14 Relation between Na + K and total cation

14.4 Conclusion

An examination presented the geochemical analysis of the subsurface water using statistical technique and estimated the ability rate of the groundwater sources in southern India. The groundwater qualities of the Vanniyar river basin sample were analyzed. Totally, all groundwater samples belong to rock dominance to evaporation

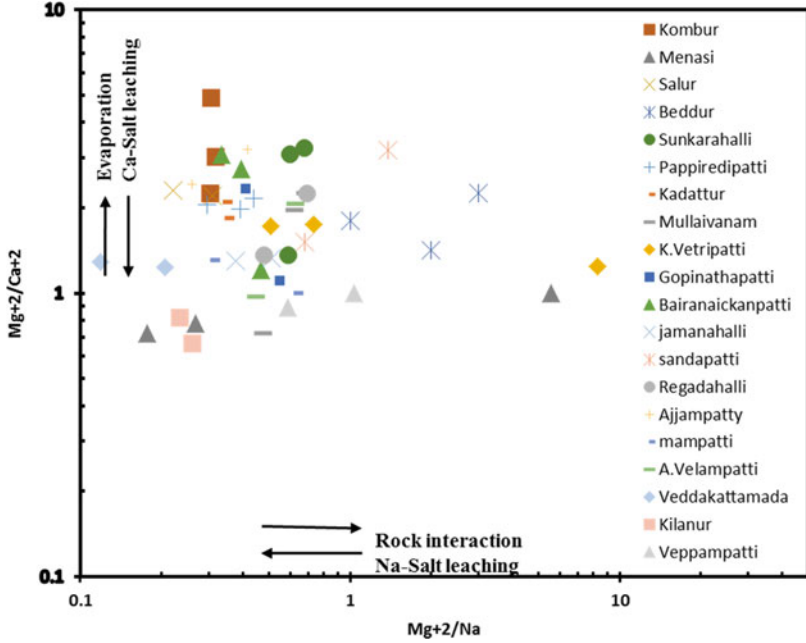


Fig. 14.15 Bivariate plot

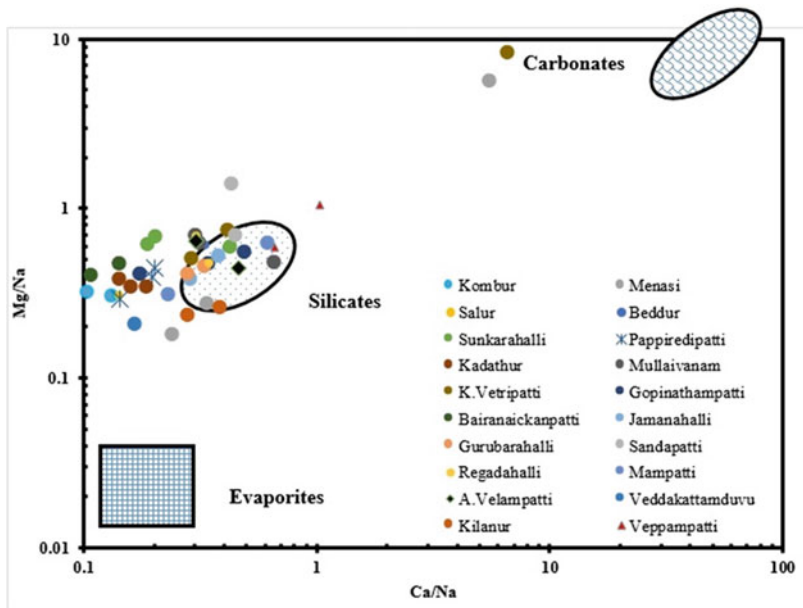


Fig. 14.16 Mixing plots of normalized Ca²⁺ and Mg²⁺

category and the results were confirmed with the Gibbs diagram show upper basin control by rock dominance and lower basin controlled by few samples show evaporation due to weathering. The results found that the arrangement of plenty of the major anions and cations is in the order $\text{Cl}^- > \text{HCO}_3^- > \text{Mg}^{2+} > \text{Na} > \text{Mg}^{2+} > \text{Ca}^{2+} > \text{SO}_4^{2-}$. The findings of this study will be of vital importance to the water management government to recognize the hydrochemistry of the groundwater components inside the location for viable control.

References

- Coetsiers, M., Walraevens, K. (2006). Chemical characterization of the neogene aquifer, Belgium. *Hydrogeol J* 14(8):1556–1568.
- Das A, Kumar M (2015). Arsenic enrichment in the groundwater of Diphu, Northeast India: coupled application of major ion chemistry, speciation modeling, and multivariate statistical techniques. *CLEAN Soil Air Water*, 43(11):1501–1513.
- Dou, M. and Li, C. (2012). Health risk assessment of Cadmium pollution emergency, *Energy Procedia*, 16, 290–295.
- Kumar P, Kumar A, Singh CK, Saraswat C, Avtar R, Ramanathan AL, Herath S (2016a). Hydrogeochemical evolution and appraisal of groundwater quality in Panna District, Central India. *Expo Health*, 8(1):19–30.
- Kumar P, Kumar M, Ramanathan AL, Tsujimura M (2010). Tracing the factors responsible for arsenic enrichment in groundwater of the middle Gangetic Plain, India: a source identification perspective. *Environ Geochem Health*, 32(2):129–146.
- Kumar P, Saraswat C, Mishra BK, Avtar R, Patel H, Patel A, Sharma T, Patel R (2016b). Batch technique to evaluate the efficiency of different natural adsorbents for defluoridation from groundwater. *Appl Water Sci*, 1–10.
- Kumar P, Tsujimura M, Saraswat C, Srivastava PK, Kumar M, Avtar R (2016c). Quantitative analysis of transient intertidal submarine groundwater discharge in coastal aquifer of Western Japan. *Proc. Natl Acad Sci India Sect A Phys Sci*, 87(3): 423–432.
- Muhammad, S., Shah, M. T., and Khan, S. (2011). Health risk assessment of heavy metals and their source apportionment in drinking water of Kohistan region, northern Pakistan, *Micro Chem J.*, 98, 334–343.
- Mukherjee A, Saha D, Harvey CF, Taylor RG, Ahmed KM, Bhanja SN (2015). Groundwater systems of the Indian sub-continent. *J Hydrol Reg Stud*, 4:1–14.
- Qu, C. S., Ma, Z. W., Yang, J., Liu, Y., Bi, J., and Huang, L. (2012). Human exposure pathways of heavy metals in a lead-zinc mining area, Jiangsu Province, China, *PLoS One*, 7, e46793, <https://doi.org/10.1371/journal.pone.0046793>.
- Satheeshkumar, S., Venkateswaran, S. & Kannan, R. (2017). Temporary fluoride concentration changes in groundwater in the context of impact assessment in the Vanniyar sub-basin, South India. *Acta Geochim* 36: 112. <https://doi.org/10.1007/s11631-016-0137-z>
- Shah, T., Ara, J., Muhammad, S., Khan, S., and Tariq, S. (2019). Health risk assessment via surface water and subsurface water consumptionwww.drink-water-eng-sci.net/12/23/2019/ *Drink. Water Eng. Sci.*, 12, 23–30,
- Simge Varol, Aysen Davraz (2013). Evaluation of the groundwater quality with WQI (Water Quality Index) and multivariate analysis: a case study of the Tefenni plain (Burdur/Turkey). *Environ Earth Sci*.
- Srivastava SK, Ramanathan AL (2008). Geochemical assessment of groundwater quality in vicinity of Bhalswa landfill, Delhi, India, using graphical and multivariate statistical methods. *Environ Geol*, 53(7):1509–1528.

- Sun, H. and Li, L. (2011). Investigation of distribution for trace Lead and Cadmium in Chinese herbal medicines and their decoctions by graphite furnace Atomic Absorption Spectrometry, *Am. J. Anal.Chem.*, 2, 217–222.
- Tewari, A., Dubey, A., and Trivedi, A. (2010). A study on physico-chemical characteristics of ground water quality. *J Chem Phar Res.*, 2(2): 510-518.

Chapter 15

Fluoride Dynamics in Precambrian Hard Rock Terrain of North Singhbhum Craton and Effect of Fluorosis on Human Health and Society



Biswajit Bera, Sumana Bhattacharjee, Meelan Chamling, Arijit Ghosh, Nairita Sengupta, and Supriya Ghosh

Abstract Today fluoride contamination in groundwater is a serious environmental concern of the world. An electronegative element with high chemical reactivity is profoundly a prerequisite for strong teeth and bones in human beings. But on contrary, the excessive consumption of fluoride causes various fluorosis-induced health hazards like dental, skeletal and non-skeletal diseases. At a glance, nearly 29 countries are affected with fluorosis-related health risk due to consumption of fluoride-rich drinking water. In 1984, the WHO prepared a standard range of fluoride in drinking water varying from 0.6 to 1.5 mg/L. The Bureau of Indian Standards (BIS, 1992) has also prescribed a normal class range between 0.6 and 1.2 mg/L in drinking water for healthy human consumption. In 1984, the WHO projected that more than 260 million people are consuming unhygienic fluoride-contaminated water where the fluoride level was above 1 mg/L. In India, roughly 90 million people together with 6 million children spread over 200 districts in 19 states are affected by different magnitudes of dental, skeletal/non-skeletal fluorosis where the fluoride infectivity ranges from 1 to 48 mg/L. In 2017, the fluoride-contaminated water with a range of 1–10 mg/L is found in around 43 community development (CD) blocks under 7 districts of West Bengal. The districts include Uttar Dinajpur, Dakshin Dinajpur, Malda, Birbhum, Bankura, Purulia and Dakshin 24 Parganas. In the district of Purulia alone, out of 20 blocks, 17 blocks divulge high fluoride adulteration in groundwater. The time period 2017–2018 exhibits around 400,000 people who have been exposed to various types of dental, skeletal and non-skeletal

B. Bera (✉) · M. Chamling · A. Ghosh · S. Ghosh
Department of Geography, Sidho-Kanho-Birsha University, Lagda, India

S. Bhattacharjee
Department of Geography, Jogesh Chandra Chaudhuri College, Calcutta University, Kolkata, India

N. Sengupta
Department of Geography, Sidho-Kanho-Birsha University, Lagda, India

Department of Geography, Diamond Harbour Women's University, Sarisha, WB, India

fluorosis in 185 villages of Purulia (India) due to long-term consumption of high fluoride in groundwater. High magnitude of fluorosis is not only associated with consumption of fluoride-contaminated drinking water but also depends on the kind of food habit along with human immunity system. A total of 619 water samples were collected from different sites of Purulia district with the aid of Global Positioning System (GPS) and tested in laboratory. Besides, huge archives of fluoride data for the year 2015–2016 are also compiled from the Public Health Engineering Department (PHED), Government of West Bengal. Around 1516 households were surveyed substantially, and relevant sampling techniques like stratified, random and quota sampling were applied. Moreover, focus group discussion (FGD) of some selected villages was scheduled. Remote sensing and geographic information system (GIS) are used to prepare some digital thematic maps. Subsequently, quantitative measures like regression and correlation are applied to find out the scientific correlation among the variables. This empirical study also advocates a few in situ and ex situ approaches to resolve fluoride-related problems in the region and attempts to explore specific hydrogeological sites for the construction of dams.

Keywords Dental and skeletal fluorosis · Fluoride contamination · Focus group discussion · In situ and ex situ methods · Sampling techniques

15.1 Introduction

Water is perhaps the most important requirement for physiological and biological activities of plants and animals including human beings. It is predominantly the vital parameter for achieving the main objectives of sustainable development for human civilization (Gleick 1996). Today in most of the parts of the world, surface water is greatly polluted by multivarious agents and sources. About 75% of population of the world depends on groundwater for drinking purposes. Most of the countries of the world extract groundwater through deep tube well, shallow tube well and dug well by hand pump or mechanical pumping technique. Beyond the permissible limit, the concentration of certain ions is the primary issue as they create the groundwater unfeasible for diverse uses. As a result, threats to groundwater have become fatal due to unprecedented urban and rural growth and their enormous needs. Fluoride, arsenic, iron, nitrate, boron, manganese and heavy metals are a big concern if they cross the permissible limit.

Fluoride (F^-) ions belong in halogen family whose atomic number and atomic weight are 9 and 18.998, respectively. Within the periodic table, fluoride has electronegative and reactive capacity compared with other chemical elements (Greenwood and Earnshaw 1984; Gillespie et al. 1989). It has no colour, smell and taste in soluble stage. Therefore, chemical experiment is highly essential to detect fluoride ion in the water. It manages dental caries and gives an antimicrobial action. Similarly, it assists to build strong teeth and bones of humans. Reputed organizations like the World Health Organization (WHO, 1984), Bureau of Indian

Standards (BIS, 1992) and Indian Council of Medical Research (ICMR) have given the prescribed range of fluoride in drinking water as 0.6–1.5 mg/L, 0.6–1.2 mg/L and 0.5–1.5 mg/L, respectively. Beyond the authorized range of fluoride in drinking water is detrimental to human health. The World Health Organization (WHO) has reported that more than 260 million people are drinking contaminated groundwater with fluoride which is beyond the permissible limit. Today, 29 nations are found to be suffering due to fluorosis-related health hazard. Many studies have been reported that worldwide groundwater is contaminated by fluoride ions, and these countries include China, India, Ethiopia, Canada, Norway, Ghana, Kenya, North Jordan, Japan, Iran, Sri Lanka, Pakistan, Turkey, Korea, Southern Algeria, Italy, Mexico, Brazil, etc. (Phan et al. 2010; Young et al. 2011; Brindha and Elango 2011; Adhikary et al. 2014). Tropical countries are more vulnerable to fluorosis-related health hazard because people are consuming higher quantity of water for prevailing weather and climate.

In India, around 90 million people along with 60 million children are affected (mild to severe) with dental, skeletal and non-skeletal fluorosis. These cases are found in over 19 states with 200 districts. In 2015, the National Programme for Prevention and Control of Fluorosis (NPPCF), Govt. of India, has notified that the highest concentration of fluoride is found in Narnaul district of Haryana (nearly 22 times higher than the permissible limit). The neighbouring country like China is also equally affected due to severe fluorosis-allied health hazard (Ayooob and Gupta 2006). In India the range of fluoride in groundwater usually varies within 1–48 mg/L. In the recent years, the high to very high fluoride-affected states are Andhra Pradesh, Bihar, Delhi, Gujarat, Haryana, Jammu and Kashmir, Karnataka, Kerala, Madhya Pradesh, Maharashtra, Odisha, Rajasthan, Uttar Pradesh, Tamil Nadu and West Bengal.

In case of West Bengal (2018), around 43 community development blocks in 7 districts are found to be affected with fluoride contamination where the range varies from 1 to 10 mg/L. The fluoride-affected districts are Birbhum, Purulia, Bankura, Uttar Dinajpur, Dakshin Dinajpur, Malda and Dakshin 24 Parganas. Out of 20 blocks in Purulia, 17 blocks are found to be affected with high fluoride contamination in groundwater (Bera and Ghosh 2019).

According to the Public Health Engineering Department, Purulia, Government of West Bengal, and Ministry of Drinking Water and Sanitation, Govt. of India's programme on National Rural Drinking Water report (of 2016–2017 and 2017–2018) along with the survey conducted in the time period 2017–2018 show that approximately 400,000 people have been exposed to moderate to severe fluorosis-related health disorders. In most of the fluoride-affected villages of Purulia district, people are still not getting fresh drinking water. Sometimes knowing the poor quality of tube well water, they are consuming such filthy polluted water. Potash and superphosphate fertilizers contain a significant amount of fluoride which is extensively applied during rabi or kharif seasons in this area. This anthropogenic source is also partially responsible for high fluoride content in the soils as well as groundwater in Rarh Bengal region (Bera 2018). In the last few decades, population growth (both rural and urban) is tremendously increasing, and during the winter

season, excess population (tourist population) creates unprecedented pressure on the vulnerable landscape. Most of the reservoirs or dams and rivers are being dried up, and lake or channel bottoms also are exposed on the surface. People have no alternate source of drinking water during lean season from March to June. Medical facilities and social awareness are very much weak and insufficient in different blocks of Purulia.

In case of Jhalda II, Manbazar I and Puncha blocks of Purulia, there are no primary health centres or medical treatment facilities within the 10 km buffer area. Due to physical and mental disability linked with fluorosis, the people have permanently lost their working ability. Job loss, social rejection, school dropout, witchcraft, morbidity, malnutrition and starvation are very common socio-economic phenomena in different villages under 20 blocks of the district. Due to dental and skeletal/non-skeletal fluorosis, many people have been isolated from the main stream of economy and culture. Therefore, the main objectives of the present study are to (i) highlight the interrelationship between food habit of local people and degree of fluorosis in one hand and amount of fluoride-rich water intake and magnitude of health hazards on other hand and (ii) to assess and typify the different health hazards and socio-economic consequences of their livelihood pattern.

15.2 Area of Study

According to the Human Development Report (HDR), Purulia is one of the most undeveloped districts of West Bengal. The region contains rich biological diversity with valuable rocks and minerals. It is the fifth largest district in West Bengal having 6259 sq.km geographical area. The district shares its border line with three other districts of West Bengal, i.e. Paschim Bardhaman in north-east, Bankura in east and Jhargram in south-east. Similarly, south-western and western sides of the district are linked with the state boundary of Jharkhand. Geographically, the district is bounded by $22^{\circ}42'35''\text{N}$ to $23^{\circ}42'00''\text{N}$ and from $85^{\circ}49'25''\text{E}$ to $86^{\circ}54'37''\text{E}$, respectively. The average elevation of the plateau (extended part of Chota Nagpur plateau) is 255 metres above mean sea level (Fig. 15.1). The district consists of 20 community development blocks with 170 gram panchayats and 2667 villages. The highest number of villages ($N = 219$) is found in Manbazar I block while the lowest in Raghunathpur ($N = 79$). With only one population, Premsinghdih village in Bandwan block is the most remarkable and least populated village.

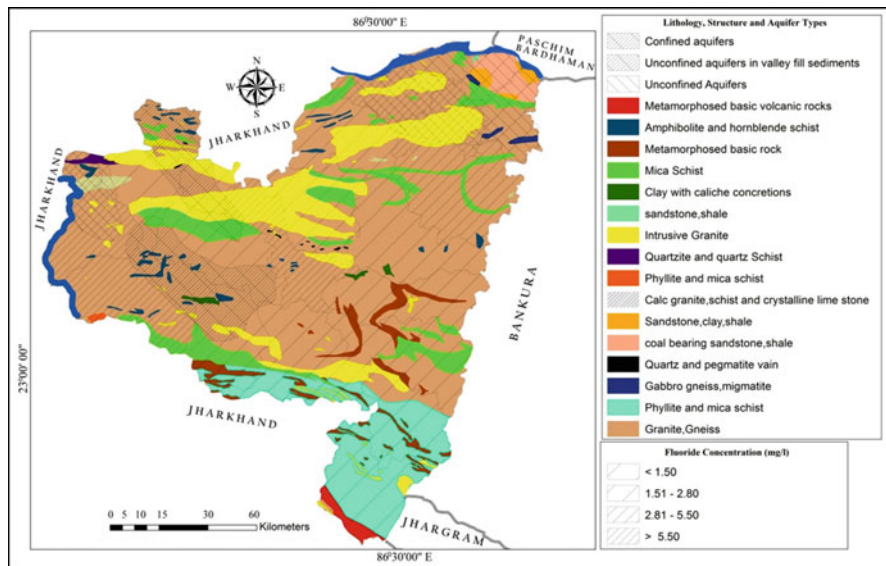


Fig. 15.1 Study area along with fluoride concentration in lithology and structural diversity of Purulia district

15.2.1 Geological Background of the North Singhbhum Craton

Geologically, Purulia district is the part of North Singhbhum Craton which is situated in the eastern Indian Peninsular Shield. This Singhbhum Craton is the comprehensive part of Chota Nagpur gneissic complex (CGC) (Dunn 1942). Precambrian rocks such as granite gneiss and pegmatite act as dominating rocks in this Peninsular Shield region. North-eastern pockets mainly Santuri and Neturia blocks of Purulia district exhibit Gondwana sediments with coal seams. Phyllite and mica schist are also found in the southern parts of the district. Phyllite, mica schists and china clay are also the host rocks in the southern parts like Bandwan, Barabazar, Balarampur, Manbazar II and Baghmundi blocks. The Archaean metamorphic rocks are also formed in different parts of the district. These metamorphic rocks are meta-basic rocks, metavolcanics, phyllite and mica schist, granite gneiss (Chota Nagpur) and calc granulites.

Pegmatite granite formation rocks (under Precambrian era) are mainly massive granite, pegmatite and quartzite. This North Singhbhum Peninsular Shield also hosts a few meta-sedimentary rocks like calc granulite, gametiferrous sillimanite schist (graphite and kyanite bearing) and crystalline limestone which are scattered over the district. Similarly, the meta-basic rocks are traced out on diverse in nature which include amphibolite, metanorite and hornblende schist. Permo-carboniferous ages of Gondwana rock formation like shale, sandstone and coal are confined in the north-eastern parts of the district. These rocks are also extended part of Gondwana, Panchet and Raniganj formation. Semi-consolidated sediments are composed of gravel and conglomerate under Sijua formation. Natural river beds and valley margins show the existence of quaternary sediments. The various types of unconsolidated sediments are coarse to fine sand, clay, silt, yellow clay, calcareous nodules and laterite. It has an excellent capacity to hold subsurface and groundwater. These Holocene alluviums are not only confined on the river valley and valley margins but also traced out along the foothill zone.

Fluoride ions are mainly identified within the Precambrian rocks like granite gneiss and pegmatite in this particular region. Generally, higher fluoride content is found in these host rocks ranging from 500 to 12,400 mg kg⁻¹ (Koritnig 1978; Krauskopf and Bird 1995). On an average the granite rock contains 810 mg kg⁻¹ fluoride (Wedepohl 1969).

These Precambrian rocks like granite gneiss, calc granulites, biotite granite gneiss, meta-basic rocks, meta-sediments including biotite gneiss, crystalline limestone, pegmatite, hornblende schist, etc. have a higher amount of fluoride ion-bearing minerals. The fluoride-bearing minerals are apatite [Ca₅(PO₄)₃(OH,F,Cl)], fluorite or fluorspar [CaF₂], biotite [K(Mg,Fe)₃AlSi₃O₁₀(F,OH)₂], hornblende [Ca₂(Mg,Fe,Al)₅(Al,Si)₈O₂₂(OH)₂], sellaite [MgF₂], cryolite [Na₃AlF₆], fluormica (phlogopite) [KMg₃(Si₃Al)O₁₀(F,OH)₂], tremolite [Ca₂Mg₅Si₈O₂₂(OH)₂], epidote [Ca₂Al₂(Fe₃₊;Al)(SiO₄)(Si₂O₇)O(OH)], fluorapatite [3Ca₃(PO₄)₂Ca(F,Cl₂)], amphibole such as mica, villuanite, phosphorite and clays (Matthess 1982; Pickering 1985; Hem 1986; Handa 1988; Haidouti 1991; Gaumat et al. 1992; Gaciri and Davies 1993; Datta et al. 1996; Apambire et al. 1997; Kundu et al. 2001; Mohapatra et al. 2009). The principal Precambrian host rocks are being weathered, and the fluoride minerals as well as ions are exposed on the surface. These fluoride ions are automatically released by various natural agents. Subsequently, these minerals and ions are mixed with the soils and groundwater. The marine environmental condition also helps to deposit the adequate amount of fluoride ions in the sediments on the ocean floor and along the foothills (WHO 2001; Fawell et al. 2006).

15.3 Materials and Methods

15.3.1 Water Sample Collection

Around 619 water samples have been collected from different dug wells and tube wells (during the years 2017 and 2018) of various villages under 17 blocks of Purulia district and tested in the laboratory. Three significant parameters like fluoride (F^-), pH and iron (Fe) have been tested to understand the correlation of fluoride concentration with other key elements. The 2015–2016 concentration data of fluoride in different blocks has been obtained from the department of public health engineering under Govt. of West Bengal. Fluoride meter (atomic absorption spectrophotometer with furnace) is used to determine the amount of the fluoride content considering proper analytical procedure. Following the Bureau of Indian Standards (BIS) guidelines, the water samples are collected using a 100 ml plastic container, and these samples have been tested within 24 hours in the laboratory. The random sampling technique has been chosen to collect the samples from affected and non-affected villages.

15.3.2 Sampling Methods of Fluorosis-Related Health Hazard

To evaluate fluorosis-related health hazard and its direct and indirect impacts on society, a total of 320 villages with 1513 households have been selected for a detailed study. Out of 1513 households, 4348 male and 3456 female populations have been thoroughly surveyed. Based on public health engineering data, the affected villages (17 blocks out of 20) and non-affected villages have been thoroughly surveyed applying stratified random, systematic and quota sampling techniques. To understand the magnitude of dental, skeletal and non-skeletal fluorosis of the affected people along with its impact on their livelihood pattern, the survey is also conducted in different local and regional health centres (consulted with dental clinics and clinics of orthopaedic surgeon).

15.3.3 Focus Group Discussion (FGD) Study

Focus group discussion (FGD) is a qualitative research method which aims to explore the perception of people's attitude such as belief, superstition, traditional ideas and practices in a mass scale from gathered people who belong to a

homogeneous background. Such study has been organized for a few selective villages under 17 blocks of Purulia to get the general perception of fluorosis-affected and fluorosis-non-affected people. About 17 times FGD study had been conducted along with gram panchayat member, panchayat pradhan and willing male and female people from different sectors of the villages. A few but important questions (single, double and multiple options) have been framed regarding water quality, availability throughout the year, government role, medical assistance and social and environmental awareness. FGD study reflects very good results within a short time frame. It is very difficult to acquire big data bank where a huge number of villages and people have been suffering due to fluorosis disease. Individual interaction and group interaction helped to get the general trend of the people from such interviewed techniques. This traditional method is highly rational and effective for acquiring the overall ground reality of the villages within a short span of time.

15.3.4 Application of RS and GIS Techniques

When applying ArcGIS and PCI Geomatica V 9.1.0 software, different thematic maps have been prepared. High-resolution multispectral satellite imagery like Enhanced Thematic Mapper (ETM) image and Advanced Spaceborne Thermal Emission and Reflection Radiometer (ASTER) Digital Elevation Model (DEM) are downloaded from <https://earthexplorer.usgs.gov/>. Enhanced Thematic Mapper (ETM) image consists of six visible-near infrared (VNIR), shortwave infrared (SWIR) band (30 m spatial resolution) and eight panchromatic band (15 m spatial resolution). On the other hand, Advanced Spaceborne Thermal Emission and Reflection Radiometer (ASTER) image comprises three visible-near infrared (VNIR) band with a 15 m spatial resolution and shortwave infrared (SWIR) band of a 30 m spatial resolution. Both images are fused to extract the lineaments and prepare the lineament density map on the lithological attributes (Bera et al. 2019b). Besides, the images are also reprojected following geographical coordinate system for a precise geometrical assessment (Bera et al. 2019b). Garmin GPS Etrex30x is used to collect the coordinates of different locations of water samples and source points of the fluoride ions. The principal host rocks (granite, gneiss and pegmatite) are also brought from different sites, and the amount of fluoride ions are measured in the geophysical laboratory of the Geological Survey of India, Eastern Region (Kolkata).

15.3.5 Application of Quantitative Techniques

An empirical quantitative analysis is performed to find out the relationship between the parameters. Significant statistical techniques are applied to deduce the consistency and actual correlation among the variables (Bera et al. 2019a). IBM SPSS

Statistics 22.0.0.0 (Statistical Packages for Social Science) software is used to calculate the Pearson correlation coefficient or Pearson 'r' and similarly to quantify how strong the relationship exists between the variables. The most commonly used sample formula is represented by the alphabet 'r' which can be acquired by computing the variance and covariance on a sample. By this way if one dataset of (x_1, \dots, x_n) containing 'n' value and another dataset (y_1, \dots, y_n) containing 'n' value is available, then the formula for 'r' is as follows:

$$r = \frac{\sum_{i=1}^n (x_i - \bar{x})(y_i - \bar{y})}{\sqrt{\sum_{i=1}^n (x_i - \bar{x})^2} \sqrt{\sum_{i=1}^n (y_i - \bar{y})^2}}$$

where n is the sample and x_i and y_i are the single samples indexed with i , $\bar{x} = \frac{1}{n} \sum_{i=1}^n x_i$ (sample mean) and analogously for \bar{y} .

The 'r' value varies within the range between +1 and -1 where +1 represents the total positive linear correlation whereas -1 shows the total negative correlation. 0 means no correlation. Positive correlation means y increases conducts to increase in x variable, while negative correlation indicates an increase in y variable which results in the decrease in x variables. Further, scatter plot or graph has been designed to explain the visual illustration of correlation between (i) food habits and degree of fluorosis and (ii) water intake and magnitude of fluorosis.

15.4 Results and Discussions

15.4.1 Fluoride Concentration of Different Blocks of Purulia (2017–2018)

Out of 20 blocks, 18 blocks have crossed the permissible limit of fluoride content (0–1.5 mg l^{-1}). The study was conducted in the time span of 2017–2018. The data shows that the highest concentration of fluoride in groundwater is 6.77 mg l^{-1} in the Daha village under Manbazar I block. Similarly Purulia II [(Bhangra, 5.56 mg l^{-1} , 4.65 mg l^{-1}), Belman (4.35 mg l^{-1}), Makraber (4.21 mg l^{-1})] and Manbazar I (Khayerbani, 5.26 mg l^{-1}) blocks have crossed the critical limit (Fig. 15.2).

In case of Santuri block, fluoride concentration in groundwater is found beyond the permissible limit in the villages of Nimitkuri (1.62 mg l^{-1}) and Talberya (1.81 mg l^{-1}). In case of Raghunathpur I block, water samples are collected from five villages, and the result shows that Shanka (2.18 mg l^{-1} , 1.51 mg l^{-1}), Mahinda Alias Babudergan (1.62 mg l^{-1}) and Shyamsundarpur (1.453 mg l^{-1}) have higher fluoride concentration (above permissible limit). Two villages, namely, Barrah (1.98 mg l^{-1}) and Citarma (1.85 mg l^{-1} , 1.54 mg l^{-1}), under Raghunathpur II block reveal fluoride contamination more than permissible limit. Around 6 villages, viz. Bhul (1.96 mg l^{-1}), Manguria (1.86 mg l^{-1}), Dimdiha (1.58 mg l^{-1} , 1.87 mg l^{-1} and 1.96

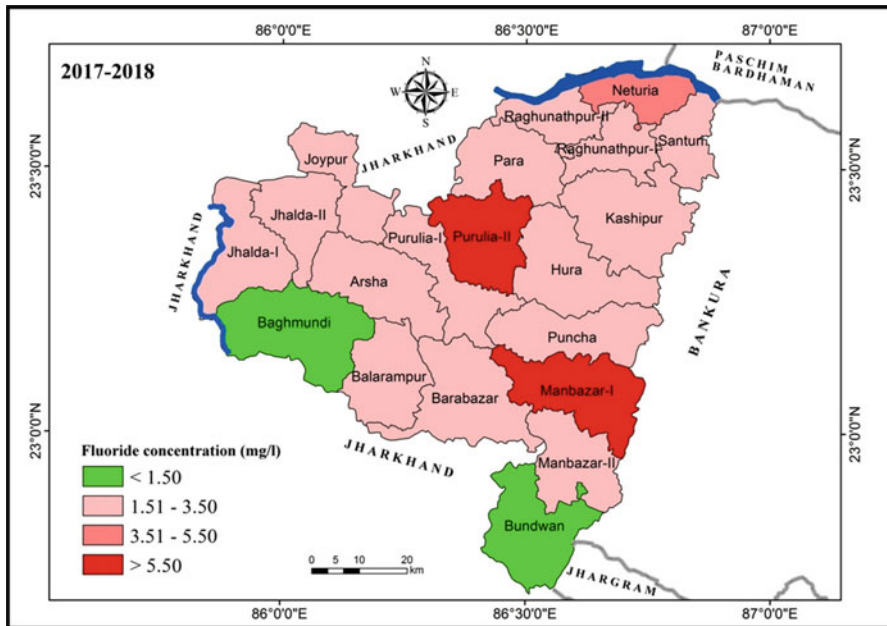


Fig. 15.2 Blockwise fluoride variation in different affected villages (surveyed 2017–2018)

mg l^{-1}), Satar (1.76 mg l^{-1}), Petadi (1.88 mg l^{-1}) and Hulka (1.85 mg l^{-1} , 1.69 mg l^{-1}), in Purulia I block groundwater are also contaminated by fluoride. The data of Purulia II block shows very high concentration of fluoride in groundwater. The affected villages are Belma (1.85 mg l^{-1} , 2.26 mg l^{-1} , 2.53 mg l^{-1} and 4.36 mg l^{-1}), Hirbahal (1.90 mg l^{-1}), Bhangra (2.69 mg l^{-1} , 4.65 mg l^{-1} , and 5.56 mg l^{-1}), Pankidi Alias Bheladi (2.65 mg l^{-1}), Chanchra (1.62 mg l^{-1} , 1.96 mg l^{-1} , 1.65 mg l^{-1} , 2.66 mg l^{-1}), Bhagwanpur (1.96 mg l^{-1}), Chirumacha (2.36 mg l^{-1}), Hutmuru (1.65 mg l^{-1} , 1.69 mg l^{-1} , 1.96 mg l^{-1} , 2.36 mg l^{-1} , 2.65 mg l^{-1} , 2.63 mg l^{-1}), Mahara (1.96 mg l^{-1} , 2.65 mg l^{-1}), Makraberba (4.21 mg l^{-1}), Shitalpur (1.67 mg l^{-1} , 1.68 mg l^{-1} , 1.85 mg l^{-1} , 1.86 mg l^{-1} , $1. \text{mg l}^{-1}$, 2.09 mg l^{-1} , 3.28 mg l^{-1}), Singhbazar (2.30 mg l^{-1}) and Chharra (1.56 mg l^{-1} , 1.68 mg l^{-1}).

Around 07 villages under Pancha block have crossed the permissible limit in groundwater. The name of the villages are as follows – Badra (1.66 mg l^{-1} , 1.98 mg l^{-1}), Bagda (2.14 mg l^{-1}), Chandra (1.65 mg l^{-1} , 1.69 mg l^{-1} , 2.26 mg l^{-1}), Deorang (1.86 mg l^{-1} , 2.32 mg l^{-1}), Gopalpur (1.789 mg l^{-1} , 2.26 mg l^{-1}), Kanchannagar (1.62 mg l^{-1}) and Kenda (1.79 mg l^{-1} , 1.99 mg l^{-1} , 2.92 mg l^{-1}). In the year 2017–2018, water samples were collected from 17 villages under Balarampur block, but only 1 village Biramdih has crossed the permissible limit (1.63 mg l^{-1}). Out of 17 villages under Hura block, 4 villages are found to be fluoride contaminated surpassing the permissible limit. The villages are Arjunjora (1.56 mg l^{-1}), Kundrudi (1.51 mg l^{-1}), Palgan (1.85 mg l^{-1}) and Sinara (1.68 mg l^{-1}). Jhalda I block has three villages having the fluoride concentration out of eight

surveyed villages. They are Ichag (2.58 mg l^{-1}), Panrri (1.55 mg l^{-1}) and Tulin (1.86 mg l^{-1}). In Jhalda II block, two villages have fluoride concentration higher than the permissible limit. The villages include Guridi (1.58 mg l^{-1}) and Sarjumatu (1.29 mg l^{-1} , 1.88 mg l^{-1}).

The highest fluoride concentration is found in Manbazar I block that is in Daha village (6.77 mg l^{-1}), and 13 villages are affected with fluoride contamination beyond permissible limit. In case of Neturia block, only three villages, namely, Gunyara (3.65 mg l^{-1}), Tantloi (1.85 mg l^{-1}) and Mahishnadi (2.24 mg l^{-1}), show fluoride contamination above permissible limit. Para block also shows only three villages with high fluoride contamination in groundwater. These villages are Churni (1.53 mg l^{-1}), Kaluhar (1.83 mg l^{-1}) and Rautara (1.67 mg l^{-1}). In Arsha block, two villages, namely, Nagra (1.58 mg l^{-1}) and Kishanpur (1.59 mg l^{-1}), show fluoride concentration beyond permissible limit. Sankura village has 1.52 mg l^{-1} fluoride under Manbazar II block that is beyond the desirable limit. Fluoride limit is higher than permissible limit that is detected in two villages of Barabazar block in Dhandanga (1.52 mg l^{-1}) and Ladiha (1.87 mg l^{-1}). Three villages, namely, Jaypur (1.62 mg l^{-1}), Karkara (1.96 mg l^{-1}) and Damru (1.87 mg l^{-1}), reveal fluoride beyond permissible limit in the block of Joypur. Kashipur block also shows fluoride incidence of beyond permissible limit in the village of Shalaya (1.53 mg l^{-1}).

15.4.2 Fluoride Variation with Affected Villages of Purulia for the Year 2016–2017 (NRDWP)

According to the National Rural Drinking Water Programme (NRDWP) report under the Ministry of Drinking Water and Sanitation, Govt. of India, in 2016–2017 for Purulia district, a total of 185 villages were affected with fluoride contamination spread over 15 blocks (Table 15.1). Balarampur block had the highest number of villages ($N = 34$) with fluoride concentration beyond the permissible limit followed by Santuri ($N = 26$), Puncha ($N = 26$) and Manbazar I ($N = 24$). On the other hand, Joypur ($N = 2$) and Jhalda I ($N = 2$) blocks have recorded the lowest number of villages with fluoride contamination. The report shows that Rambani village (8.01 mg l^{-1}) under Kashipur block was highly affected out of 15 affected blocks of Purulia district. Out of the 15 blocks, groundwater of 7 blocks is adversely affected by high content of fluoride (above 4 mg l^{-1}). The villages are Hansdima, 4.50 mg/L (Santuri block); Balakdi, 6.45 mg l^{-1} (Puncha); Khagerbani, 5.14 mg l^{-1} (Manbazar I); Khajura, 4.51 mg l^{-1} (Raghunathpur I), Rambani, 8.01 mg l^{-1} (Kashipur block); Kewabathan, 5.43 mg l^{-1} (Raghunathpur II); and lastly Jargo, 7.41 mg l^{-1} (Jhalda I).

Table 15.1 Blockwise highest fluoride concentration with the total number of affected villages (2016–2017)

Sl. no.	Block	Total no. of affected villages	Village with the highest fluoride concentration	Highest concentration of fluoride (mg l^{-1})
1.	Balarampur	34	Biramdir	1.94
2.	Santuri	26	Hansdima	4.50
3.	Puncha	26	Balakdi	6.45
4.	Manbazar I	24	Khagerbani	5.14
5.	Purulia I	12	Patamputra	2.32
6.	Arsha	10	Jaratanr	1.94
7.	Jhalda II	10	Chitarpur Alias Kokarkhap	3.20
8.	Raghunathpur I	10	Khajura	4.51
9.	Kashipur	09	Rambani	8.01
10.	Para	08	Jabarra	2.20
11.	Purulia II	05	Hirbahal	1.97
12.	Raghunathpur II	04	Kewabathan	5.43
13.	Hura	03	Tilabani	2.21
14.	Joypur	02	Kalyanpur	1.92
15.	Jhalda I	02	Jargo	7.41

Source: National Rural Drinking Water Programme (NRDWP) report under the Ministry of Drinking Water and Sanitation, Govt. of India

15.4.3 Fluoride Variation with Affected Villages of Purulia for the Period Between 2017 and 2018 (NRDWP)

The report of 2017–2018 period for fluoride contamination data of the National Rural Drinking Water Programme (NRDWP) published by the Ministry of Drinking Water and Sanitation, Govt. of India, reveals that around 118 villages under 14 blocks were affected with high fluoride content above permissible limit (Table 15.2). The maximum number of villages ($N = 29$) contaminated with fluoride was found in the Puncha block. It was followed by Manbazar I ($N = 27$) and Balarampur ($N = 12$). On the other hand, Jhalda I with one village has the lowest fluoride content. It was followed by Hura block ($N = 3$) and Kashipur ($N = 03$). Village wise, the highest fluoride contamination was found in the Puncha village (4.24 mg l^{-1}) under Puncha block. Other affected villages in descending order include Juhidi, 3.810 mg l^{-1} (Raghunathpur I); Mamurjor, 2.77 mg l^{-1} (Purulia II); Chaupad, 2.65 mg l^{-1} (Jhalda I); Baliguma, 2.37 mg l^{-1} (Manbazar I); and Patpur, 2.34 mg l^{-1} (Barabazar).

Table 15.2 Blockwise highest fluoride concentration with the total number of affected villages (2017–2018)

Sl. no.	Block	Total no. of affected villages	Village with the highest fluoride concentration	Highest concentration of fluoride (mg/L)
1.	Puncha	29	Puncha	4.24
2.	Manbazar I	27	Baliguma	2.37
3.	Balarampur	12	Chakulia	1.76
4.	Purulia II	07	Mamurjor	2.77
5.	Arsha	06	Haranama	1.20
6.	Barabazar	06	Patpur	2.34
7.	Purulia I	06	Ghaghajuri	2.10
8.	Santuri	06	Kalipahari	2.14
9.	Raghunathpur I	04	Juhidi	3.80
10.	Raghunathpur	04	Ichhar	2.10
11.	Jhalda II	04	Belyadi	1.70
12.	Kashipur	03	Gourangdih	1.74
13.	Hura	03	Sijumakahna	2.09
14.	Jhalda I	01	Chaupad	2.65

Source: National Rural Drinking Water Programme (NRDWP) report under the Ministry of Drinking Water and Sanitation, Govt. of India

15.5 Impact of Fluorosis on Human Health

15.5.1 Food Habits and Degree of Fluorosis

Rice and wheat are the staple food of the people who are residing in the different blocks of the Purulia district. Out of 7806 surveyed populations, 4674 people have been affected by fluorosis due to intake of fluoride-contaminated groundwater. The survey is conducted for both affected and non-affected people, and a few selective questions have been prepared to know the food habits of the local residents. The collected data reveals that most of the people (20 blocks) are vegetarian (Table 15.3). Egg is the second most preferred food item in the food habits followed by fish and meat both in weekly and monthly food charts. Food items like fish and meat with high protein content are found to be missing from the main dietary food chart. Barabazar block (5%) has the highest fish consumption followed by Hura (3.18%), Manbazar II (2.33%) and Jhalda I (2.07%) on a weekly basis. On the other hand, on monthly routine, Baghmundi (14.29%), Balarampur (12.77%), Kashipur (8.89%) and Barabazar (8.75%) have fish frequently on their menu chart. In case of meat, the blocks show a very poor status. Subsequently, meat is consumed by the people in the block of Barabazar (1.25%), Hura (1.06%), Balarampur (1.06%) and Arsha (1.01%). Overall, there is a high deficit of intake of protein and fat in their dietary chart. But there is a relationship between food habits and degree of fluorosis of the affected people. The survey shows that those people who are consuming sufficient protein

Table 15.3 Food habits and water intake capacity of the fluoride-affected people of Purulia district

Sl. no.	Block	Food habits												Intake of water (litre per day)					
		Weekly						Monthly						Male	Female				
		Egg	Fish	Meat	Veg	Egg	Fish	Meat	Veg	Egg	Fish	Meat	Veg						
No.	%	No.	%	No.	%	No.	%	No.	%	No.	%	No.	%	No.	%	No.	%		
1.	Arsha	18	9.09	3	1.51	2	1.01	175	88.38	33	16.67	9	4.54	4	2.02	152	76.77	3.0	2.0
2.	Balarampur	17	18.09	2	2.12	1	1.06	74	78.72	14	14.89	12	12.77	7	7.44	61	64.89	2.5	1.5
3.	Barabazar	12	15.00	4	5.00	1	1.25	63	78.75	18	22.50	7	8.75	4	5.00	51	63.75	2.5	2
4.	Hura	35	12.37	9	3.18	3	1.06	236	83.39	49	17.31	13	4.59	5	1.77	216	76.33	3.5	2.5
5.	Jhalda I	17	7.02	5	2.07	1	0.41	219	90.50	43	17.77	9	3.72	8	3.31	182	75.21	3.5	2
6.	Jhalda II	27	12.50	3	1.39	0	0.00	186	86.11	39	18.06	11	5.09	4	1.85	162	75.00	3.0	2.5
7.	Joypur	25	9.03	3	1.08	0	0.00	249	89.89	47	16.97	8	0.30	3	1.08	219	79.06	4.0	3
8.	Kashipur	18	13.33	2	1.48	1	0.74	114	84.44	29	21.48	12	8.89	5	3.70	89	65.93	2.5	1.2
9.	Manbazar I	24	5.78	0	0.00	0	0.00	391	94.22	36	8.67	4	0.96	1	0.24	374	90.12	4.2	3.3
10.	Baghmundi	3	21.43	0	0.00	0	0.00	11	78.57	4	28.57	2	14.29	1	7.14	7	50.00	2.1	1.3
11.	Bandwan	1	11.11	0	0.00	0	0.00	8	88.89	3	33.33	0	0.00	0	0.00	6	66.67	2.4	1.5
12.	Manbazar II	8	4.65	4	2.33	1	0.58	159	92.44	17	9.88	5	2.91	3	1.74	147	85.47	2.5	1.3
13.	Neturia	9	2.61	2	0.58	0	0.00	334	96.81	22	6.38	4	1.16	2	0.58	317	91.88	4.2	3.5
14.	Para	12	5.85	3	1.46	1	0.49	189	92.20	24	11.71	3	1.46	3	1.46	175	85.37	2.8	1.5
15.	Puncha	23	6.42	4	1.12	0	0.00	331	92.46	39	10.89	5	1.40	2	0.56	312	87.15	4.5	3.7
16.	Purulia I	13	3.04	1	0.23	1	0.23	413	96.50	26	6.07	4	0.93	2	0.47	396	92.52	4.0	3.5
17.	Purulia II	11	2.36	2	0.43	0	0.00	453	97.21	28	6.01	3	0.64	1	0.21	434	93.13	4.6	3.9
18.	Raghumathpur I	17	8.21	3	1.45	0	0.00	187	90.34	28	13.53	6	2.90	2	0.97	171	82.61	3.1	2.4
19.	Raghumathpur II	14	4.86	2	0.69	1	0.35	271	94.10	29	10.07	3	1.04	2	0.69	254	88.19	2.9	2.1
20.	Santuri	12	4.88	1	0.41	0	0.00	233	94.72	17	6.91	4	1.63	1	0.41	224	91.06	2.5	1.4

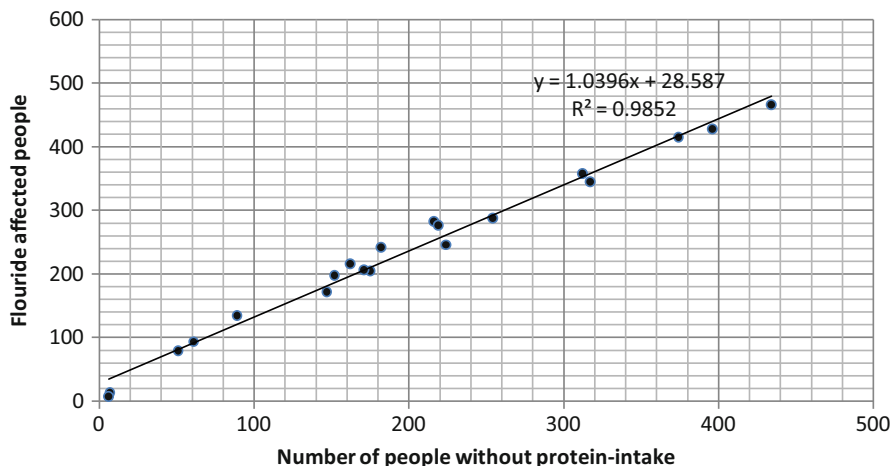


Fig. 15.3 Relationship between food habit (without protein) and degree of fluorosis

and fat regularly in their dietary chart have relatively low symptoms of skeletal and non-skeletal fluorosis. The survey was also specifically conducted for the low-income grouped tribal people in the different blocks of Purulia district. As the few tribal villages are contaminated by fluoride in groundwater, most of the tribal people are subsequently severely affected with dental caries, knee joint and hip joint pain, kidney stone, etc. They have lost their protective power (low immunity power) due to the deficiency of protein- and fat-rich diet in their daily dietary routine (most of the people belong to below poverty line). The statistical analysis reveals that there is a positive correlation between the food habit and degree of fluorosis. The people who are not able to consume protein are mainly affected due to fluorosis. Protein-rich food can help people to resist this fatal disease. But in maximum cases, vegetables hold the predominant position in the regular diet chart of local villagers because of extreme poverty. Actually economic distress bounds the poor villagers to depend on nonprotein foods.

The correlation coefficient (r) indicates a strong positive correlation between the two variables, i.e. no. of people without protein intake (food habit) and fluoride-affected people (Fig. 15.3). The statistical computation shows $df = n-2$ ($20-2 = 18$) at 90 degrees of freedom, and the calculated coefficient (r) is more than 0.2050. Therefore, it is said to be statistically significant at 5% significance level. In this study, the coefficient of determination (R^2) value is 0.985, indicating that 98% variation of one variable can be explained by another variable.

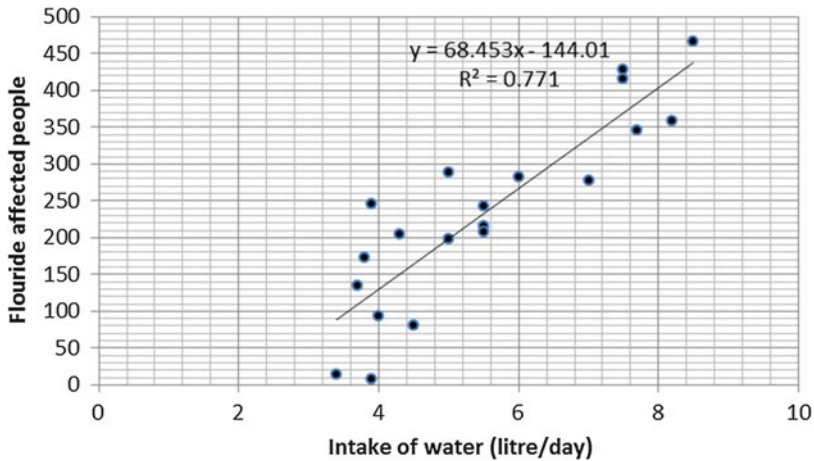


Fig. 15.4 Relationship between water intake and magnitude of fluorosis

15.5.2 Water Intake and Magnitude of Fluorosis

On average 3–5 litres of water is required on a daily basis for proper biological as well as physiological functioning of the human body. In case of tropical regions, normal human body requires a high amount of water for microbiological activities of a body. In general, people who are living in tropical region drink on an average 4 litres of water daily except in winter season. In case of sub-tropical, temperate and subpolar regions, the normal intake capacity of water is 2–3 litres on a daily basis. Sometimes people drink less than 1.5 litres per day. There is a positive correlation between water intake (in case of fluoride-contaminated water) and magnitude of fluorosis. If a person consumes fluoride-contaminated water above 4 litres per day along with fluoride ion-contaminated green vegetables, food grains, etc., the person will be consuming more amount of fluoride ions. As a result, after a certain period of time, he or she will be exposed to fluoride-related health hazards. In Purulia district, the average intake of water is 3.5 litres per day for male and 3 litres per day for female (Table 15.3). But in a few cases, people consume more than 4.5 litres per day (Purulia II – 4.6 litres per day). As Purulia district is the part of semi-desert area, it has long summer months, and the average temperature stands 30.5°C. From March to September, due to very hot weather conditions (both day and night), people prefer to drink more amount of water to survive in an unfavourable climatic situation.

It is evident from the study that high rate of water intake intensifies the magnitude of fluorosis (Fig. 15.4). The strong relationship ($r = 0.8780$) between the above-said two variables specifies that the people who consume more water are mainly vulnerable in the context of fluorosis. The statistical inference found that the $df = n-2$ ($20-2 = 18$) at 90 degrees of freedom, and the calculated coefficient (r) is more than 0.2050. Hence, it is statistically significant at 5% significance level. Here, the

Table 15.4 Fluoride impact magnitude ranges on human health

Sl. no.	Fluoride concentration (mg l ⁻¹)	Impact on human health
1.	0.0	Limited growth and fertility
2.	<0.5	Dental caries
3.	0.5–1.5	Promote dental health and prevent tooth decay
4.	1.5–4.0	Dental fluorosis
5.	4.0–10.0	Skeletal fluorosis
6.	>10	Crippling fluorosis

coefficient of determination (R^2) value is 0.771 which reveals that 77% variation of one variable has been explained by another variable.

15.5.3 Blockwise Scenario of Fluorosis

Around 4674 people (out of 7806) have been severely affected by dental, skeletal and non-skeletal fluorosis, whereas 2694 males (61.96%) and 1980 females (57.29%) are suffering due to intake of fluoride-contaminated drinking water from the tube wells and dug wells that are installed by the Govt. agency.

In case of Arsha block, 113 males (61.08%) and 85 females (54.00%) are highly affected, while 71% of male and 45% of female populations are being seriously affected by dental fluorosis. Similarly, 22% of male and 27% of female suffer from chronic pain in knee joints followed by 20% of male and 13% of female with pain in hip joints. In case of Arsha block, the average intake of water by male is 3 litres per day, whereas female consume 2 litres on average per day. The average income of the people (80.03%) of Arsha block (surveyed household) is below Rs 5000/– while only 1% of people earn Rs 10,000–15,000 per month.

In case of Balarampur block, 24.45% of male and 20.00% of female are affected by both dental and skeletal fluorosis (Table 15.4). But most of the 53.35% of male (<15 year age group) and 55% of female are severely affected by dental fluorosis followed by pain in knee joints and hip joints. Meanwhile, the average intake of water is 2.5 litres per day (male), and the striking feature is that the average water intake of the female population is 1.5 litres per day. 68.09% of the people earn less than Rs 5000/– per month. Basically, the Balarampur block is unproductive from agricultural perspective.

In Barabazar block, 26.74% of male and 25.00% of female are exposed to both dental and skeletal fluorosis. Around 60.87% of male and 53.00% of female population are suffering due to serious dental caries. Children (with age group <15 years) are widely exposed to dental fluorosis. Around 19.57% of male and 21% of female show knee joint pains, and 15.22% of male and 24.00% of female suffer due to severe hip joint pain. In case of Barabazar, most of the skeletal fluorosis patients are under the age group of above 45 years (Fig. 15.5b). Out of the surveyed population,



Fig. 15.5 (a) Dental caries found on the teeth of Debraj Soren (Palgoan, Hura block), (b) dental crippling exposed on the teeth of Subash Mahato (Palgoan, Hura block), (c) discoloured teeth with dental crippling of Krishna Mandi (Khairabera, Jhalda block) and (d) severe skeletal fluorosis patient (Tulin, Jhalda I block)

88.75% of the population earn below Rs 5000/– per month. Poverty, malnutrition and morbidity are common socio-economic features of this block.

In case of Hura block, 76.50% of male and 68.00% of female population have been exposed to both dental and skeletal fluorosis, whereas 50.00% of male and female population with age group above 30 years are severely suffering due to knee and hip joint pain. Around 0.6% of male and 0.9% of female populations can't able to move their body including the hands and leg easily (Fig. 15.5c). Economically the people are very poor and living below poverty line.

In case of Jhalda I block, it is found that about 79.89% of male and 69.00% of female are severely affected due to dental, skeletal (Fig. 15.5c) and non-skeletal

fluorosis (Table 15.4). The similar features are also seen in case of the above-mentioned blocks. The Jhalda II block is following a similar trend, but almost 50% of male and female population are suffering from both dental and skeletal fluorosis, while above 60-year age groups (male and female) are also affected by non-skeletal fluorosis diseases like kidney stone and osteoporosis disease. In this block, many people above 50 years age group have been restricted to voluntary movement due to skeletal fluorosis (Fig. 15.5b).

Joypur and Kashipur blocks have a similar trend like Jhalda I and II.

In case of Manbazar I block, around 90.07% of male and 88.00% of female have both dental and non-skeletal fluorosis diseases. Most of the youth (male and female) have been suffering from dental crippling (Fig. 15.5a), whereas above 30-year age groups (male and female) are suffering due to muscle fibre degeneration, nervousness, depression, etc. In this block the survey shows that around 5.31% of male and female are being suffered due to chronic skeletal and non-skeletal fluorosis that is already mentioned above.

In case of Manbazar II block, around 65.13% of male and 59.00% of female are affected from dental and skeletal fluorosis diseases. Most of the male and female population (>30-year age group) have chronic knee and hip joint pain (Table 15.4).

In case of Baghmundi and Bandwan blocks, less than 3.00% of male and female have been suffering due to dental and knee joint pain, whereas there is no fluoride ion present in the groundwater (>1.5 mg/L). People have very low income due to water scarcity through the year with rocky exposure. Poverty, starvation and hunger are the common socio-economic phenomena in these blocks. In case of Neturia block, 33.51% of male and 33.00% of female population are suffering from dental fluorosis. Knee pain (28.87% in male and 28.00% in female) and hip pain (34.07% in male and 35.00% in female) are also found. Around 2.06% of male and 1.3% of female population show advance stage of fluorosis of can't do sit as they are not able to move their body muscles freely. The average intake of water in both male and female per day is around 4.2 litres. On the other hand, the blocks have low- to moderate-income level.

In the block of Para, almost 57.56% of male and 51.00% of female are suffering due to both dental and skeletal fluorosis. Out of 200 populations, most of the people (both male and female) above 30-year age group are severely affected by skeletal and non-skeletal fluorosis like reduced immunity, excessive thirst, urinary tract malfunctions, etc.

The Pancha block also shows reasonable case of fluorosis (Fig. 15.5d). Around 28.64% of male and 27% of female exhibit knee joint pain. On the other hand, hip joint pain in male and female is found to be 33.98% and 38.00%, respectively. About 34.00% of female and 33.5% of male are exposed to dental fluorosis over the year.

The Purulia II block has a maximum number of fluorosis patients. Almost 91.07% of male and 90.00% of female are being affected due to dental crippling, dental caries, knee joint pain and hip joint pain. Around 32.00% of male and 38.00% of female have high dental fluorosis, whereas 17.00% of male and female are also affected by skeletal and non-skeletal fluorosis such as deformities in RBCs, repeated abortions or stillbirths, abdominal pain, headache, etc.

Table 15.5 Various social impacts of fluorosis-affected people of the Purulia district

Sl. no.	Block	Social impacts									
		School dropout		Social isolation		Remarriage		Physical disabled		Attempt to suicide	
		No.	%	No.	%	No.	%	No.	%	No.	%
1.	Arsha	52	26.26	64	32.32	2	1.01	66	33.33	2	1.01
2.	Balarampur	39	41.49	34	36.17	3	3.19	15	15.96	0	0.00
3.	Barabazar	43	53.75	19	23.75	1	1.32	11	13.75	0	0.00
4.	Hura	68	24.03	76	26.86	0	0.00	87	30.74	2	0.71
5.	Jhalda I	74	30.58	68	28.10	0	0.00	78	32.23	3	1.24
6.	Jhalda II	76	35.19	43	19.91	4	1.85	82	37.96	2	0.93
7.	Joypur	75	27.08	56	20.22	2	0.72	115	41.52	1	0.36
8.	Kashipur	47	34.81	42	31.11	0	0.00	39	28.89	1	0.74
9.	Manbazar I	113	27.23	127	30.60	2	0.48	159	38.31	2	0.48
10.	Bagmundi	6	42.86	4	28.57	1	7.14	3	21.43	0	0.00
11.	Bandwan	2	22.22	5	55.56	0	0.00	2	22.22	0	0.00
12.	Manbazar II	54	31.40	42	24.42	0	0.00	61	35.47	1	0.58
13.	Neturia	114	33.04	91	26.38	1	0.29	121	35.07	2	0.58
14.	Para	61	29.76	67	32.68	1	0.49	71	34.63	1	0.49
15.	Puncha	105	29.33	97	27.09	0	0.00	142	39.66	3	0.84
16.	Purulia I	159	37.15	103	24.07	3	0.70	137	32.01	1	0.23
17.	Purulia II	132	28.33	138	29.61	2	0.43	146	31.33	3	0.64
18.	Raghunathpur I	87	42.03	46	22.22	1	0.48	60	28.99	0	0.00
19.	Raghunathpur II	114	39.58	61	21.18	2	0.70	93	32.29	2	0.70
20.	Santuri	114	46.34	45	18.29	1	0.41	68	27.64	1	0.41

The Purulia I block has almost similar fluorosis scenario followed by Raghunathpur I and II and Santuri block in the district.

15.6 Impact of Fluorosis on Society

15.6.1 School Dropouts

The maximum school dropout ($N = 159$) is found in the block of Purulia I followed by Neturia ($N = 114$), Purulia II ($N = 132$), Raghunathpur I ($N = 114$), Santuri ($N = 114$) and Manbazar I ($N = 113$) where the educational status of the parents and their family members is very poor (illiterate). Graduate and postgraduate qualified people are not satisfactory in all the blocks of the district (Table 15.5). In most of the cases, students stop their education after Madhyamik or higher secondary standard

due to poor and very poor economic background. The National Institute of Mental Health (NIMH) in 1984 warns that children are highly vulnerable or stand at a high risk of psychological problem due to severe dental fluorosis. A child has lost their self-esteem and confidence due to disfigured teeth for severe dental fluorosis.

In Purulia district, the survey result shows that dental fluorosis causes highly horizontal brown and yellow streak on the teeth which brings chronic embarrassment and social anxiety among friends and teachers in the school. The survey is undertaken in different villages of Purulia II, Manbazar I and Puncha blocks. It is found that school-going students (with severe dental fluorosis) are frequently teased for having dirty or filthy teeth and often least interest to smile or show their teeth. Children with severe dental fluorosis can face chronic psychological suffering not only in Purulia but also in different fluoride-contaminated regions of the world. Around 50–70% of respondents who are severely exposed to dental fluorosis are treated as great psychological distressed and simultaneously get unfavourable effects on an individual personality. Moreover, severely affected dental fluorosis people are suffering from hinder smiling, worry and psychological stress. During the field interaction, many severely affected dental fluorosis people were trying to avoid to talk with the survey team, and many young boys told that they are regularly avoiding social gathering and refused to go in the schools and colleges. The study also highlighted that due to severe fluorosis-related health disorders, people's behaviour has also been partially changed (Fig. 15.6).

The intensive study also reveals that when parents along with the family members suffer due to chronic skeletal and non-skeletal health disorders, elder family members do not send their children to school. In many cases, it is seen that these dropout students are engaged as a child labour in different mining areas of Jharkhand and Odisha to support their family financially. In the recent years in Barabazar and Manbazar blocks of Purulia district, school dropout students (<15 years) are now separated from the main stream of the society or economy, and most probably they are working as an active member of different anti-national regional organizations or socially unhealthy or unaccepted associations.

15.6.1.1 A Case Study on Fluorosis-Affected School Students

The menace of fluoride contamination highly hampers the flow of life of children in different blocks of Purulia. School-level survey in different blocks like Puncha, Raghunathpur I, Purulia II and Hura has revealed the ruthless truth of the miserable condition of poor students (Fig. 15.6). Students of different age and sex have been mainly suffered from dental and skeletal fluorosis because their immunity level is very low due to poor nutritional status (Table 15.5). Due to the deficiency of protein in their diet chart, vulnerability increases and it turns into high risk related to health. At Bhagabandh Primary School of Puncha block, a total of 11 students are affected due to dental and skeletal fluorosis. Among them ten students are suffering from dental fluorosis, and one student is suffering from skeletal fluorosis. Maximum students have been suffering from mild dental fluorosis (nine students), and only

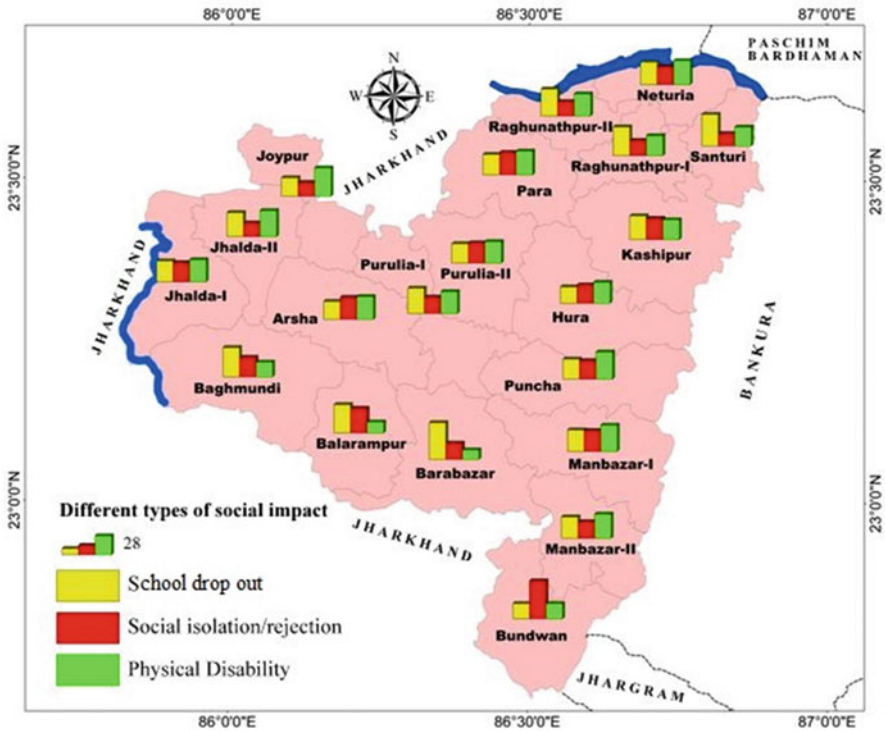


Fig. 15.6 Blockwise different types of social impacts related to fluorosis

one student is suffering from moderate dental fluorosis. The scenario is really devastating at Bansgram Primary School of Raghunathpur I block where 40 students are victimized due to fluorosis-related health hazards. These students have been mainly suffering from dental fluorosis. Among them, maximum students are suffering from moderate dental fluorosis (15 students), 14 students are highly victimized by severe dental fluorosis, and the rests of the students are affected by mild dental fluorosis. Besides this, 12 students at Sidpur Primary School of Purulia II block have been affected from dental fluorosis, and 2 students are suffering from skeletal fluorosis. At this school, nine students are victimized by moderate dental fluorosis. Another miserable condition has been identified at Layekdih Primary School in Hura block. Among 21 affected students, 20 students are affected by dental fluorosis, and 1 student is victimized by skeletal fluorosis. Here maximum students have been suffering from mild dental fluorosis (11 students), whereas the rest of the students are victimized by moderate (7 students) and severe (2 students) dental fluorosis (Table 15.5). The academic and social lives of these students are distressed due to the deadly impact of fluoride contamination. Some of the affected students are isolated from the main flow of society. So, effective strategies must be adopted to rescue this future generation from the fatal impact of fluoride contamination.

15.6.2 Social Rejection/Social Isolation and Job Loss

Many renowned social scientists have defined about the social isolation or rejection with considering social groups and social processes under a specific time frame. Many sociologists and anthropologists have also used social ostracism as synonym of social rejection or social isolation. The definition and paradigm of concept have been modified by individual or group of people through social evolution. Various societal factors have been directly or indirectly responsible for the social rejection or social isolation of people or a group from the rest of the association or groups. Social scientists argued that some internal and external agents are principal components that create rejection of people from the society. Meanwhile, there are some external hidden factors that play significant roles to reject an individual or groups from the others. Various studies are undertaken on different races, religions and castes in various socio-economic conditions of people. The results show that fear, threat, vandalism, conspiracy, etc. are also sometimes partially regulating factors that simulate the individual or groups. Subsequently, social pathology directly carries social isolation or rejection in a contemporary tribal-dominated economic society. There is no exception in case of Rarh region or most specifically the tribal-dominated food-gathering economy of Rarh Bengal.

The Purulia district of West Bengal is the home for many indigenous tribal people. They regularly practise various traditional tribal rituals and customs to preserve their age-old tribal culture. But now in Purulia, around 400,000 tribal and nontribal people are exposed to various degrees of dental, skeletal and non-skeletal fluorosis (Table 15.5). Principal project investigator has experienced the ground truth or reality during the interaction with the local people and got some distinct contemporary socio-environmental impressions. In Manbazar I, Purulia I and II and Barabazar blocks of Purulia district, many tribal people do not understand or believe about fluorosis-related health disorders. A shocking incidence happened when the principal project investigator interacted to a woman (fluorosis affected). The tribal woman told that there is no connection of fluoride ions with groundwater. She confidently replied that the dental- and skeletal-related health disorders are the gifts of God.

The highest number (N = 138) of social rejection or isolation is found in the blocks of Purulia II followed by Manbazar (N = 127) and Purulia I (N = 103). The district shows reasonable case of social rejection (Fig. 15.6). The people in almost all the blocks seem to follow such superstitious evil of social processes. The people of Khayerbani and Daha villages under Manbazar I block are socially rejected due to prominent symptoms of fluorosis. Many people who are not affected by fluorosis hazards are still residing in the same village; they thought that such diseases are untouchable. Many fluorosis-affected poor people have been rejected from the domestic activities due to prominent crippling dental fluorosis and dental caries. Another incidence took place in the village of Bhangra (Purulia II block) where a young girl Shampa Mahato (18 years of age) was rejected from her in-law's house after such severe dental fluorosis appeared on the teeth. Her father is basically a poor

farmer and has no property and bank balance, but he still bears extra burden on his shoulder, and during the interaction with the principal project investigator, he also replied that he sold his one bigha land during the marriage ceremony of his daughter and still he is not carrying the BPL card. He has three daughters and one son. Now he is unable to work due to knee and hip joint pain. Nobody in the society has extended their hands to help the poor family. Neighbours think that these diseases are untouchable and people are not interested to offer any domestic jobs.

In Purulia district many people in different villages are rejected from the neighbours, from neighbouring villages and sometimes from their family members. Social rejection or social ostracism is a common tribal ritual or punishment. The survey result also shows that the poor fluorosis-affected villages have yet not consulted with medical doctors like dentists or orthopaedic surgeons (Table 15.5).

A few cases have been reported from different pockets under Jhalda II, Raghunathpur I and Bagmundi blocks of Purulia district that fluorosis-affected people still believe and consult with *quack doctor/ojha/guinin*. Around 60–70% of respondents do not have any idea about fluorosis, and they have taken ayurvedic and homoeopathic treatment. In many areas, fluorosis-affected old people are treated by witch or *Diana*, and sometimes the family members with the help of local village leaders slap or bite the victims. In 2018, one such incidence took place in Raghunathpur I block where local people tied the woman by rope with the tree and tried to kill. At last with the help of police, the victim has been rescued from the angry superstitious and illiterate village mob.

15.6.3 Scenario of Physical Disability and Suicidal Tendency

Around 20% (N = 1000, out of the total affected population of 4674) of people are found to be physically disabled due to severe skeletal and non-skeletal fluorosis in 320 surveyed villages under 20 blocks in the district of Purulia. When people are not able to do their household and other activities, then it is termed as physical disability. Physical disability includes knee joint pain, hip joint pain, neck joint pain, shoulder joint pain, pelvic joint pain, inability to do sit-up, inability to bend forward easily, inability to work, bow legs, lumbar spines, etc. Mild to severely affected skeletal and non-skeletal fluorosis people are found in the different villages under Jhalda II, Raghunathpur I, Purulia I and II, Manbazar I and Puncha blocks. Above 30-year age group, male and female are also severely affected by skeletal fluorosis due to high consumption of fluoride content groundwater. Physical disability is also linked with mental disability. Many middle-aged people have lost their ability to do work due to severe knee, neck and hip joint pain. Therefore from their working incompetency, gradually the people reach the mental-disabled stage from the physical disability (Table 15.5). The highest number of disabled people of 159 is found in Manbazar I followed by 146 in Purulia II, 143 in Puncha, 137 in Purulia I, 121 in Neturia and finally 115 people in Joypur blocks.

In different blocks of Purulia, physically and mentally disabled persons are being treated as untouchable, and sometimes disabled people have been rejected by their family members. Disabled persons have lost their intelligence and knowledge and sometimes they behave like a child. There is no medical treatment that spreads for the fluorosis-affected people. Poverty, malnutrition, starvation, fasting, morbidity and even mortality are predominant contemporary social phenomena which are gripped in different parts of the district. The mentally and physically disabled persons often attempt to commit suicide. It is very difficult to investigate how many people have committed suicide for their disability. But from the direct door-to-door interaction with the people, a very realistic truth has surfaced out. The highest number of attempt to suicide ($N = 3$) appears in the blocks of Jhalda I, Purulia I and Purulia II, and in the same way five blocks, viz. Arsha, Hura, Jhalda II, Manbazar I, Neturia and Raghunathpur II, also have some suicidal case ($N = 2$) due to physical weakness, mental stress, depression and economic distress.

15.6.4 Divorce, Remarriage and Dowry System

In many cases, fluorosis-affected victim women are subjected to divorce due to crippling dental fluorosis and physical disability for skeletal fluorosis. The divorce women sometimes get remarriage with high dowry. Dowry system still persists in the rural society of India. In different parts of Purulia, suicidal deaths are the fate of remarried victim women. In almost all the blocks, many families have been socially boycotted due to unhealthy less attractive dental- and skeletal fluorosis-related health disorders. One such incident is found in the Jhalda II block that parents have failed to arrange social marriage for their three daughters. Even many fluorosis-affected people are socially detached to join any marriage or social festivals in the villages. During field survey, when the survey team wanted to talk with fluorosis-affected people, they were not willing to talk due to social ignorance. The principal investigator also forcefully talked with one of the remarried women. But she refused to talk at first; later she agreed. But during the conversation, she covered her face by cloth due to severe dental fluorosis. Many children hesitate to smile on open forum or any social gathering or occasion. They also try to hide their teeth while talking with the strangers. The highest remarriage ($N = 4$) is reported from Jhalda II block followed by Balarampur ($N = 3$) and Purulia I ($N = 3$). Other blocks have no such significant incidence of remarriage (based on survey report) (Table 15.5). The flow chart reflects the principal health-related dental, skeletal and non-skeletal fluorosis and its negative impacts on society due to consumption of fluoride-contaminated drinking water (Fig. 15.7).

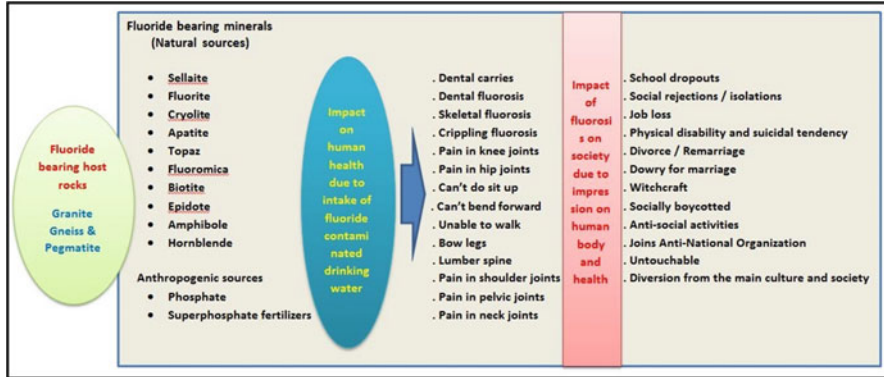


Fig. 15.7 Fluoride-contaminated drinking water and its direct and indirect impacts on human health and society

15.7 Conclusions

This scientific field-based study on fluoride dynamics and its impact on society has brought some model building and immediate management-oriented findings. These important findings are systematically outlined below:

1. Fluoride-bearing minerals like apatite, fluorite, hornblende and biotite are released from the host rocks granite, gneiss and pegmatite which cover almost 85% of geographical area of North Singhbhum Craton. These fluoride-bearing minerals are being released in moderate rate due to the presence of geological structures and higher rate of weathering. Moderate to high lineament density (0.30–0.66 km/km²) is found in the principal Precambrian rocks.
2. The (time period 2017–2018) study shows that 18 blocks have already crossed the permissible limit and the highest fluoride concentration (6.77 mg l⁻¹) is found in Daha village (Manbazar I block) followed by Purulia II, Manbazar I blocks, etc.
3. The NRDWP report of 2016–2017 reveals that 185 villages were affected (under 15 blocks), whereas the 2017–2018 report shows that 118 villages under 14 blocks were highly affected.
4. The various magnitudes of fluorosis on health include crippling dental fluorosis; dental caries; pain in the knee, hip, neck and pelvic joints; bow legs; etc. have been identified under different blocks of the area. Due to such health-related disorders, various social impacts have been found like school dropouts, social rejection or isolation, job loss, remarriage, divorce, dowry system, witchcraft, physical and mental disability, suicidal tendency, etc. Focus group discussion (FGD) also reflects that male and female above 30-year age group are severely

affected by skeletal fluorosis due to consumption of fluoride-contaminated groundwater. Today, more than 400,000 people in this region are affected with moderate to severe fluorosis-related diseases.

The suitable management techniques must be implemented to reduce the fluoride intensity and negative impacts of fluorosis hazards (Bhattacharya and Samal 2018). Generally, identification of substitute sources of purified drinking water, implementation of different defluoridation techniques and upliftment of nutritional scenario of vulnerable people are some basic preventive measures which can be adopted to check the devastating impacts of fluorosis in various parts of the region. The remedial methods are broadly classified into two categories – (i) in situ method and (ii) ex situ method. In situ method helps to reduce the intensity of fluoride in groundwater directly through artificial recharge system (Brindha and Elango 2011). Ex situ method can remove fluoride ions from water through applying different techniques of defluoridation (Brindha and Elango 2011). There are different types of defluoridation techniques like physical, chemical and biological technique (Annadurai et al. 2014). The defluoridation techniques include different processes like adsorption (Raichur and Basu 2001), precipitation-coagulation (Saha 1993; Wang and Reardon 2001), ion exchange (Singh et al. 1999), electrodialysis (Hichour et al. 1999a, b; Adhikari et al. 1989), electrolytic defluoridation (Mameri et al. 2001) and membrane separation (Amor et al. 2001; Dieye et al. 1998). The most effective processes of defluoridation are precipitation and adsorption process (Hussain et al. 2012). In addition with in situ and ex situ method, community involvement, development of nutritional status, development of awareness and expansion of health and effective education are highly crucial to avert the curse of fluoride contamination in Purulia (Hussain et al. 2012; Sreedevi et al. 2006; Bhattacharya and Chakrabarti 2011).

Despite the existing dams/reservoirs, new dams/reservoirs are required to be constructed to supply fluoride-free water to each and every household of fluorosis-affected blocks of Purulia district. In a few cases, across the tributary rivers of Subarnarekha, Kumari and Kangsabati, check dams should be constructed to improve irrigation facilities as well as to provide drinking water in different blocks of Pancha, Manbazar I, Manbazar II, Arsha and Joypur. Human resource development programmes like spread of medical facilities, human resource capabilities and skill profiles of firm, especially training programmes, need to be assessed. It is important to spread the education facilities and applied short-term courses and different training courses for the benefits of young generations of Rarh Bengal.

Acknowledgements The first author expresses his sincere gratitude to the Indian Council of Social Science Research (ICSSR), Ministry of HRD and Government of India for funding this research work. This work is part of the ICSSR Major Research Project.

References

- Adhikari, S. K., Tipnis, U. K., Harkare, W. P., & Govindan, K. P. (1989). Defluoridation during desalination of brackish water by electrodialysis. *Desalination*, 71(3), 301-312. [https://doi.org/10.1016/0011-9164\(89\)85031-3](https://doi.org/10.1016/0011-9164(89)85031-3)
- Adhikary, P.P., Dash, C.J., Sarangi, A., Singh, D.K. (2014). Hydrochemical characterization and spatial distribution of fluoride in groundwater of Delhi state, India. *Indian Journal of Soil Conservation*, 42 (2), 170-173
- Amor, Z., Bariou, B., Mameri, N., Taky, M., Nicolas, S., & Elmidaoui, A. (2001). Fluoride removal from brackish water by electrodialysis. *Desalination*, 133(3), 215-223. [https://doi.org/10.1016/S0011-9164\(01\)00102-3](https://doi.org/10.1016/S0011-9164(01)00102-3)
- Annadurai, S. T., Rengasamy, J. K., Sundaram, R., & Munusamy, A. P. (2014). Incidence and effects of fluoride in Indian natural ecosystem: a review. *AdvApplSci Res*, 5(2), 173-185. <http://www.imedpub.com/abstract/incidence-and-effects-of-fluoride-in-indian-natural-ecosystem-a-review-14097.html>
- Apambire, W. B., Boyle, D. R., & Michel, F. A. (1997). Geochemistry, genesis, and health implications of fluoriferous groundwaters in the upper regions of Ghana. *Environmental Geology*, 33(1), 13-24. <https://doi.org/10.1007/s002540050221>
- Ayoob, S., & Gupta, A. K. (2006). Fluoride in drinking water: a review on the status and stress effects. *Critical Reviews in Environmental Science and Technology*, 36(6), 433-487. <https://doi.org/10.1080/10643380600678112>
- Bera, B., (2018) Jelajure Fluoride Samosa Asustho Gramer Par Gramer Manush, Dainik Statesman, A daily newspaper
- Bera, B., Bhattacharjee, S., & Roy, C. (2019a). Estimating stream piracy in the lower Ganga Plain of a Quaternary geological site in West Bengal, India applying sedimentological bank facies, log and geospatial techniques. *Current science*. 117. 662–671. <https://doi.org/10.18520/cs/v117/i4/662-671>
- Bera, B., Bhattacharjee, S., Ghosh, A., Ghosh, S., & Chamling, M. (2019b). Dynamic of channel potholes on Precambrian geological sites of Chota Nagpur plateau, Indian peninsula: applying fluvio-hydrological and geospatial techniques. *SN Applied Sciences*, 1(5), 494. <https://doi.org/10.1007/s42452-019-0516-2>
- Bera, B., & Ghosh, A. (2019). Fluoride dynamics in hydrogeological diversity and Fluoride Contamination Index mapping: a correlation study of North Singhbhum Craton, India. *Arabian Journal of Geosciences*, 12(24), 802. <https://doi.org/10.1007/s12517-019-4994-8>
- Bhattacharya, H. N., & Chakrabarti, S. (2011). Incidence of fluoride in the groundwater of Purulia District, West Bengal: a geo-environmental appraisal. *Current Science*, 101(2), 152-155.
- Bhattacharya, P., & Samal, A.C. (2018). Fluoride contamination in groundwater, soil and cultivated foodstuffs of India and its associated health risks : A review. *Research Journal of Recent Sciences*, 7(4), 36-47.
- Brindha, K., & Elango, L. (2011). Fluoride in groundwater: causes, implications and mitigation measures. *Fluoride properties, applications and environmental management*, 1, 111-136. https://www.novapublishers.com/catalog/product_info.php?products_id=15895
- Datta, P. S., Deb, D. L., & Tyagi, S. K. (1996). Stable isotope (^{18}O) investigations on the processes controlling fluoride contamination of groundwater. *Journal of contaminant hydrology*, 24(1), 85-96. [https://doi.org/10.1016/0169-7722\(96\)00004-6](https://doi.org/10.1016/0169-7722(96)00004-6)
- Dieye, A., Larchet, C., Auclair, B., & Mar-Diop, C. (1998). Elimination des fluorures par la dialyse ionique croisée. *European Polymer Journal*, 34(1), 67-75. [https://doi.org/10.1016/S0014-3057\(97\)00079-7](https://doi.org/10.1016/S0014-3057(97)00079-7)
- Dunn, J. A. (1942). Geology and petrology of Eastern Singhbhum and surrounding areas. *Mem. Geol. Surv. India*, 69, 261-4.
- Fawell, J., Bailey, K., Chilton, J., Dahi, E., & Magara, Y. (2006). *Fluoride in drinking-water*. IWA publishing. <https://books.google.co.in/books?hl=en&lr=&id=7xu1yfOC8oC&oi=fnd&>

- pg=PR5&dq=Fluoride+in+drinking water.+IWA+publishing#v=onepage&q=Fluoride%20in%20drinking-water.%20IWA%20publishing&f=false
- Gaciri, S. J., & Davies, T. C. (1993). The occurrence and geochemistry of fluoride in some natural waters of Kenya. *Journal of Hydrology*, 143(3-4), 395-412. [https://doi.org/10.1016/0022-1694\(93\)90201-J](https://doi.org/10.1016/0022-1694(93)90201-J)
- Gamat, M. M., Rastogi, R., & Misra, M. M. (1992). Fluoride level in shallow groundwater in central part of Uttar Pradesh. *Bhu-Jal News*, 7(2), 17-19.
- Gillespie, R.J., Humphries, D.A., Baird, N.C., & Robinson, E.A., (1989). Chemistry, seconded. Allyn and Bacon, Boston.
- Gleick, P. H. (1996). Basic water requirements for human activities: Meeting basic needs. *Water international*, 21(2), 83-92. <https://doi.org/10.1080/02508069608686494>
- Greenwood, N. N., & Earnshaw, A. (1984). Chemistry of the Elements. [https://books.google.co.in/books?hl=en&lr=&id=EvTlouH3SsC&oi=fnd&pg=PP1&dq=Greenwood,+N.+N.,+%26+Earnshaw,+A.+\(1984\).+Chemistry+of+the+Elements](https://books.google.co.in/books?hl=en&lr=&id=EvTlouH3SsC&oi=fnd&pg=PP1&dq=Greenwood,+N.+N.,+%26+Earnshaw,+A.+(1984).+Chemistry+of+the+Elements)
- Haidouti, C. (1991). Fluoride distribution in soils in the vicinity of a point emission source in Greece. *Geoderma*, 49(1-2), 129-138. [https://doi.org/10.1016/0016-7061\(91\)90096-C](https://doi.org/10.1016/0016-7061(91)90096-C)
- Handa, B. K. (1988). Fluoride occurrence in natural waters in India and its significance. *Bhu-Jal News*, 3(2), 31-37.
- Hem, J.D. (1986). Study and interpretation of the chemical characteristics of natural water.
- Hichour, M., Persin, F., Sandeaux, J., & Gavach, C. (1999a). Fluoride removal from waters by Donnan dialysis. *Separation and Purification Technology*, 18(1), 1-11. [https://doi.org/10.1016/S1383-5866\(99\)00042-8](https://doi.org/10.1016/S1383-5866(99)00042-8)
- Hichour, M., Persin, F., Sandeaux, J., Molenat, J., & Gavach, C. (1999b). Water defluoridation by Donnan dialysis and electro dialysis. *Revue des Sciences de l'Eau/ Journal of Water Science*, 12(4), 671-686. <https://doi.org/10.7202/705372ar>
- Hussain, I., Arif, M., & Hussain, J. (2012). Fluoride contamination in drinking water in rural habitations of Central Rajasthan, India. *Environmental monitoring and assessment*, 184(8), 5151-5158. <https://doi.org/10.1007/s10661-011-2329-7>
- Koritnig, S. (1978) Fluorine. In: Wedepohl KH (ed) Handbook of geochemistry, vol II/1. Springer, Berlin, pp 9-C-1 to B-9-O-3.
- Krauskopf, K.B., & Bird, D.K. (1995) An introduction to geochemistry. McGraw-Hill Int, Singapore, p 647.
- Kundu, N., Panigrahi, M., Tripathy, S., Munshi, S., Powell, M. A., & Hart, B. (2001). Geochemical appraisal of fluoride contamination of groundwater in the Nayagarh District of Orissa, India. *Environmental Geology*, 41(3-4), 451-460. <https://doi.org/10.1007/s002540100414>
- Mameri, N., Lounici, H., Belhocine, D., Grib, H., Piron, D. L., & Yahiat, Y. (2001). Defluoridation of Sahara water by small plant electrocoagulation using bipolar aluminium electrodes. *Separation and Purification Technology*, 24(1-2), 113-119. [https://doi.org/10.1016/S1383-5866\(00\)00218-5](https://doi.org/10.1016/S1383-5866(00)00218-5)
- Matthess, G. (1982). *The properties of Ground-water* (No. 551.49 M38).
- Mohapatra, M., Anand, S., Mishra, B. K., Giles, D. E., & Singh, P. (2009). Review of fluoride removal from drinking water. *Journal of environmental management*, 91(1), 67-77. <https://doi.org/10.1016/j.jenvman.2009.08.015>
- Phan, K., Sthiannopkao, S., Kim, K. W., Wong, M. H., Sao, V., Hashim, J. H., & Aljunid, S. M. (2010). Health risk assessment of inorganic arsenic intake of Cambodia residents through groundwater drinking pathway. *Water Research*, 44(19), 5777-5788. <https://doi.org/10.1016/j.watres.2010.06.021>
- Pickering, W. F. (1985). The mobility of soluble fluoride in soils. *Environmental Pollution Series B, Chemical and Physical*, 9(4), 281-308. [https://doi.org/10.1016/0143-148X\(85\)90004-7](https://doi.org/10.1016/0143-148X(85)90004-7)
- Raichur, A. M., & Basu, M. J. (2001). Adsorption of fluoride onto mixed rare earth oxides. *Separation and Purification Technology*, 24(1-2), 121-127. [https://doi.org/10.1016/S1383-5866\(00\)00219-7](https://doi.org/10.1016/S1383-5866(00)00219-7)

- Saha, S. (1993). Treatment of aqueous effluent for fluoride removal. *Water Research*, 27(8), 1347-1350. [https://doi.org/10.1016/0043-1354\(93\)90222-4](https://doi.org/10.1016/0043-1354(93)90222-4)
- Singh, G., Kumar, B., Sen, P. K., & Majumdar, J. (1999). Removal of fluoride from spent pot liner leachate using ion exchange. *Water Environment Research*, 71(1), 36-42. <https://doi.org/10.2175/106143099X121571>
- Sreedevi, P. D., Ahmed, S., Madé, B., Ledoux, E., & Gandolfi, J. M. (2006). Association of hydrogeological factors in temporal variations of fluoride concentration in a crystalline aquifer in India. *Environmental Geology*, 50(1), 1-11. <https://doi.org/10.1007/s00254-005-0167-z>
- Wang, Y., & Reardon, E. J. (2001). Activation and regeneration of a soil sorbent for defluoridation of drinking water. *Applied Geochemistry*, 16(5), 531-539. [https://doi.org/10.1016/S0883-2927\(00\)00050-0](https://doi.org/10.1016/S0883-2927(00)00050-0)
- Wedepohl, K.H. (1969) Handbook of Geochemistry. Springer, Heidelberg. Softcover ISBN 978-3-642-46302-0, Series ISSN 0072-9817
- Who, U. (2001). UNU. *Iron deficiency anaemia: assessment, prevention and control, a guide for programme managers*. Geneva: World Health Organization.
- Young, S. M., Pitawala, A., & Ishiga, H. (2011). Factors controlling fluoride contents of ground-water in north-central and northwestern Sri Lanka. *Environmental Earth Sciences*, 63(6), 1333-1342. <https://doi.org/10.1007/s12665-010-0804-z>

Chapter 16

Coastal Aquifer Vulnerability for Saltwater Intrusion: A Case Study of Chennai Coast Using GALDIT Model and Geoinformatics



Debabrata Ghorai, Gouri Sankar Bhunia, and Pravat Kumar Shit

Abstract The saltwater ingress vulnerability map of Chennai coast, India, was prepared using GALDIT model in geospatial (GIS) environment by incorporating six factors toward saltwater intrusion vulnerability, namely, groundwater occurrence, depth of groundwater level, aquifer hydraulic conductivity, distance from shoreline, existing saltwater intrusion impact, and thickness of aquifer. The final seawater ingress vulnerability map was divided into five vulnerable zones, viz., very high, high, moderate, low, and very low vulnerability zones. The dominated saltwater ingress vulnerability zone along the coastal zone of Chennai comes under high to very high category. Coastal areas are coming under the very high saltwater ingress vulnerability zone. Hence, management strategies need to adopt for fresh groundwater sustainability by reducing the effect of saltwater.

Keywords Coastal aquifer · GALDIT model · GIS · Saltwater intrusion · Vulnerability

16.1 Introduction

Saltwater encroachment is the natural process of movement of seawater into the nearshore fresh groundwater due to density differences of saltwater and freshwater (Kayode et al. 2017). Saltwater has the higher density than the fresh groundwater. The groundwater becomes salty when seawater moves toward fresh groundwater (Johnson 2007). The interface or intersection zone of freshwater and saltwater is

D. Ghorai (✉)

Independent Researcher, Paschim Medinipur, West Bengal, India

G. S. Bhunia

RANDSTAD India Pvt Ltd., New Delhi, Delhi, India

P. K. Shit

PG Department of Geography, Raja N L Khan Women's College (Autonomous), Midnapore, West Bengal, India

called diffuse zone, and it is also referred to as dispersion zone (Barlow 2014) where freshwater and saltwater get mixing. Nowadays encroachment of saltwater is a rising concern for most of the coastal regions due to withdrawal of fresh groundwater through pumping in order to meet the demand of human needs for their livelihood (Mas-Pla et al. 2014). The freshwater recharge into the coastal aquifer is reducing due to excessive pumping of fresh groundwater, sea level rise, coastal flooding (associated with cyclone, tsunami, and storm surge), and canal system development for agriculture practices. Salinity encroachment happened in many ways, such as excessive pumping of freshwater from wells near the coast, sea level raise, flooding by natural catastrophes (like cyclone, tsunami, and storm surge), canal system development for agriculture, agricultural waste, etc. (Rahmstorf 2017).

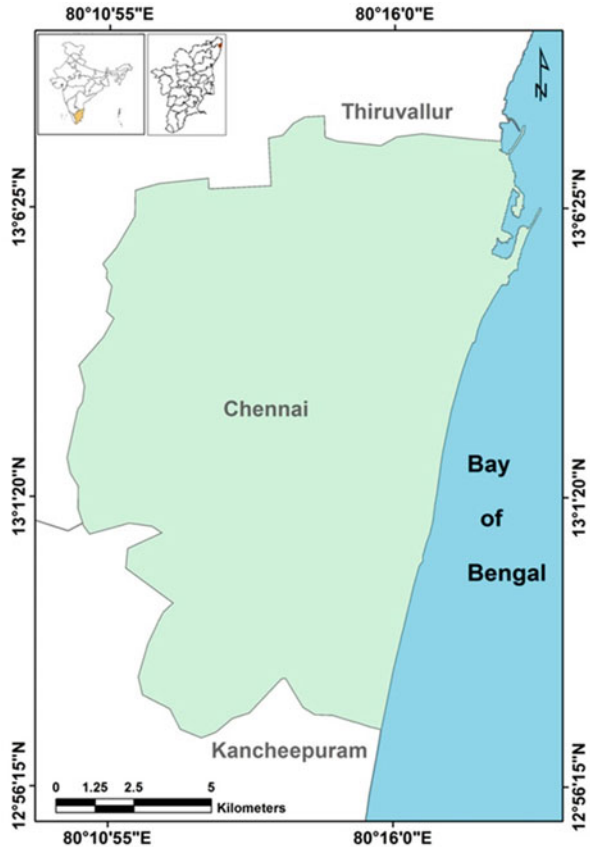
Freshwater, perhaps, is the most susceptible commodity of the twenty-first century in the world. About 40% increase of water use by human beings will be happening in the next two decades, which was assessed on a global scale, and it was also assessed that about 17% more water is required to grow more food for the growing population (Sharma 2008). Around the world all coastal aquifers are experiencing seawater interference to some extent because of density difference between saltwater and freshwater (Johnson 2007). Coastal zone has the dynamic nature where approximately 70% of the populations of the earth are inhabitants in the coastal region, and they are depending on coastal aquifers for freshwater resource (Satishkumar et al. 2016).

India is the second highest population country in the world, facing the saltwater pressure over freshwater along the coastal regions. The demand of water uses with the growing population for various purposes and supplying of water in eastern coast of India, such as Odisha, Andhra Pradesh, and Tamil Nadu coast causes a huge problem of groundwater salinization (Sharma 2008). The information of degree of salinity intrusion along the coastal region is very important to conserve freshwater for the population need as well as coastal ecosystem balance. To create such awareness, there is a need of salinity intrusion vulnerability mapping of the coastal region. The amount of salinity ingress or salinity encroachment estimation in the coastal zone due to natural or anthropogenic disasters is a complicated task. However, salinity ingress vulnerability zone can be measured using various physical parameters toward salinity encroachment in the GIS environment. Perhaps, it is very important to prepare saltwater intrusion vulnerability map to identify the highly susceptible area that can be used for better preparation and mitigate the effects of saltwater. Therefore, the present study derived a saltwater intrusion vulnerability map using GALDIT model which was developed by Chachadi and Lobo-Ferreira (2001).

16.2 Study Area

The geographical extent of Chennai district is between $80^{\circ}10'10.73''$ and $80^{\circ}18'21.49''$ E in longitude and $12^{\circ}57'6.33''$ and $13^{\circ}8'1.69''$ N in latitude (Fig. 16.1). The bordering districts and areas are Tiruvallur in north, Kancheepuram in south, and Bay of Bengal in east. This coastal area is very fertile due to the presence of two major rivers which are confluence at Bay of Bengal such as Cooum River and Adyar River. Most of the study area is characterized by sandy soils and clayey soils. The elevation of the study area ranges between 6 m and 60 m. As per 2011 census, the total population of the study area is recorded as 8,233,084 with an area of about 426 km^2 . Outside of the city periphery has an exceptional biodiversity hotspot, and a unique mangrove ecosystem is present in the east coastal area of the city (Ghorai et al. 2016).

Fig. 16.1 Location map of the study area



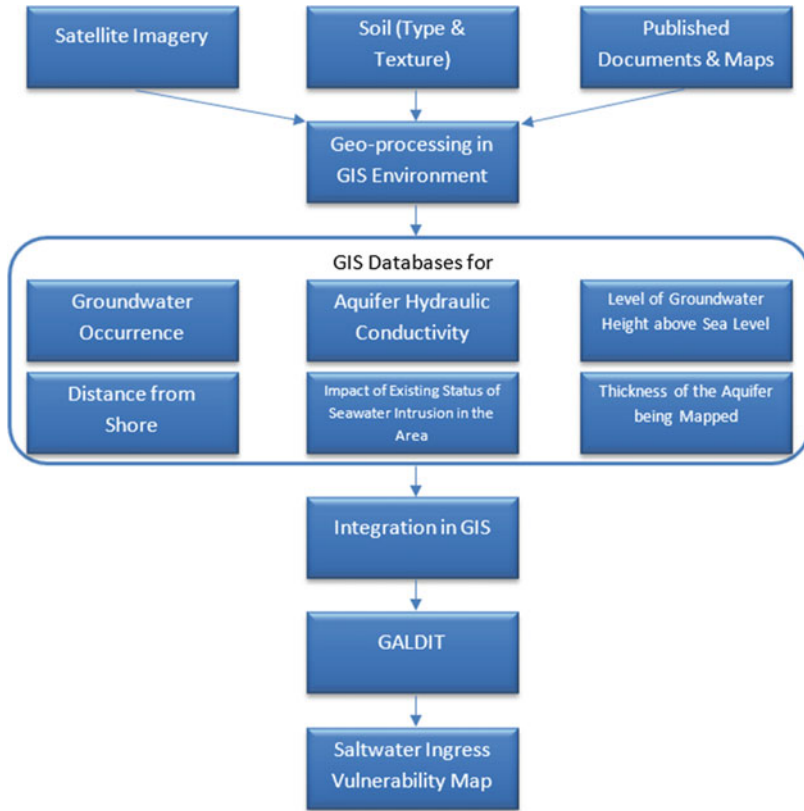


Fig. 16.3 Methodology adopted for saltwater ingress vulnerability mapping

16.3 GALDIT Model

In the last two decades, the quality of groundwater for coastal aquifers has dropped considerably because of seawater intrusion (Moghaddam et al. 2017). The mapping of the risk zone of saltwater in this coastal aquifer is very significant for monitoring and controlling groundwater. The GALDIT method was used in this study to draw up a saltwater susceptibility map of the Chennai coastal aquifer. This mechanism considers six hydrogeological parameters to mapping the coastal aquifer vulnerability in the case of substantial saltwater inflow (Satishkumar et al. 2016; Chachadi and Lobo-Ferreira 2001; Chang et al. 2019). The name of the model consists of a combination of letters with six parameters, and these are groundwater occurrence (G), hydraulic conductivity of aquifer (A), height of the groundwater level above average sea level (L), distance from coastline (D), impact of existing status of seawater intrusion (I) in the area, and aquifer thickness (T) (Chang et al. 2019; Chachadi and Lobo-Ferreira 2001).

The widely used GALDIT model is a numerical ranking and weightage-driven approach to assess coastal aquifer's saltwater ingress vulnerability using hydrogeological parameters. The broad methodology adopted in this study was presented in Fig. 16.3. The entire GALDIT model parameters are measurable from the available relative/data sources without detailed reconnaissance. The relative significance of the model factor is assessed in relation to the other model factor (Yogesh 2005). All model parameters are calculated by weights ranging from 1 to 4 based on their seawater intrusion, where 1 is the least important and 4 is the most significant. Each model has some variables that have a relative meaning for intrusion into seawater. All variables of all parameters have assigned ratings to a scale of 1–10, with 1 being least affected and 10 most affected, based on the relative importance to saltwater intrusion. A detailed discussion of the model parameters that have been selected based on their impact on seawater intrusion has been described in the following paragraph.

16.3.1 Aquifer Type or Groundwater Occurrence

The nature of the aquifer can influence the entry of seawater (Sundar and Yogesh 2014). Different aquifer types are allocated in this model, such as 8 for leaky confined, 9 for unconfined, and 10 for confined aquifer (Sundar and Yogesh 2014). The aquifer is given maximum rating when the region is a mixture of aquifers (Yogesh 2005).

16.3.2 Aquifer Hydraulic Conductivity

It refers to an aquifer's ability to transmit water based upon the number of interconnected pores in the sediments and the size of fractures in the accumulated rocks (Sundar and Yogesh 2014; Yogesh 2005). The seawater front moves quickly in a hydraulic conductivity, which means there is no impermeable layer between them, such as clay that prevents this movement (Sundar and Yogesh 2014). The higher the hydraulic conductivity, the greater the saltwater intruders.

16.3.3 Level of Groundwater Height Above the Mean Sea Level

Due to water column pressure, a hydraulic head forms if the groundwater table level is high in comparison with the mean sea level allowing seawater to reach the coastal area (Sundar and Yogesh 2014). The interface resides at a depth below the sea level

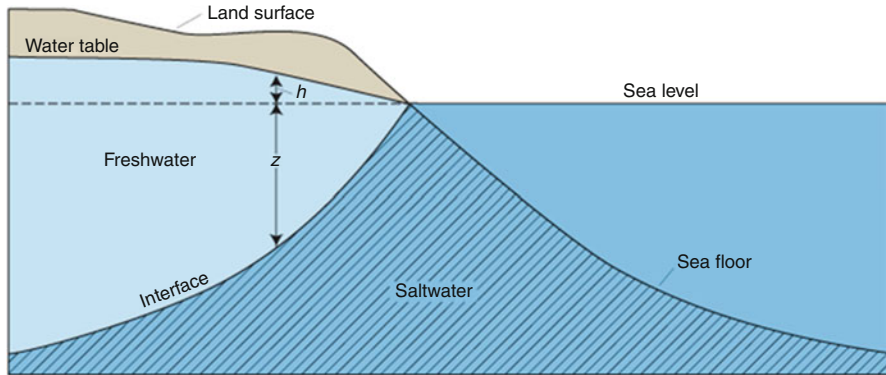


Fig. 16.2 The Ghyben-Herzberg relation. (Source: https://en.wikipedia.org/wiki/Saltwater_intrusion)

($h/2$), which is 40 times the freshwater over the sea level, according to the Ghyben-Herzberg relationship (Fig. 16.2).

So, each meter of fresh water deposited above the mean sea level in the coastal aquifers is held underneath the water to the interface (Sundar and Yogesh 2014; Yogesh 2005).

16.3.4 Distance from the Shore

According to Chachadi et al. (2007), seawater intrusion impact in the coastal zone is reduced when one moves forward toward inland at right angles from the shoreline. Near the coast, the impact of saltwater intrusion is high.

16.3.5 Impact of Existing Status of Seawater Intrusion

According to Chachadi and Lobo-Ferreira (2001), the ratio of Cl^- and $(\text{CO}_3^- + \text{HCO}_3^-)$ is a recommended alternative criterion to evaluate seawater intrusion in a coastal aquifer. It is found that seawater is dominated by chloride (Cl^-) ion whereas it has very less quantities in groundwater. Similarly, a good amount of bicarbonate (HCO_3^-)/carbonate (CO_3^-) is available in groundwater but very small quantities in seawater. Therefore, the ratio of these chemical properties of water can be used for the impact of seawater intrusion in the model.

16.3.6 Thickness of Aquifer Being Mapped

The area coverage and magnitude of saltwater ingress in the coastal zone are determined by thickness of aquifer or saturated thickness of an unconfined aquifer (Chachadi et al. 2007). Therefore, thickness of aquifer plays a significant role in saltwater ingress vulnerability study. It has been observed that when aquifer thickness is larger, the extent of seawater intrusion is also larger and vice versa.

16.4 Materials and Methods

16.4.1 Data Used

Digital soil data as well as various secondary information sources consisting of published maps and literatures have been used for GALDIT model in the current study along with Landsat 8 OLI/TIRS satellite image, dated 2014. The details of the data used in this study are presented in Table 16.1.

The following are the descriptions of the data that were used in GALDIT model to generate the saltwater intrusion vulnerability map of the study area.

16.4.1.1 Aquifer Type

Information for aquifer type was collected from CGWB atlas published in 2012. The present study area comes under unconfined and unconfined to confined aquifer types (CGWB 2012).

Table 16.1 Data used for the study

Sl. no.	Data	Source
1	Aquifer type	CGWB (2012)
2	Depth of groundwater level	CGWB (2012)
3	Aquifer hydraulic conductivity	CGWB (2012), NRCS (2016), FAO (2003)
4	Aquifer thickness	GSI (2006), CGWB (2012, 2014), Arulprakasam et al. (2013), Mondal et al. (2016)
5	Chloride distribution map	CGWB (2014)
6	Landsat 8 OLI/TIRS satellite image, 2014	Earth Explorer (USGS)
7	Digital soil map	FAO (2003)
8	Harmonized World Soil Database	FAO/IIASA/ISRIC/ISS-CAS/JRC 2009

16.4.1.2 Aquifer Thickness

CGWB (2012)-published aquifer data for the field of study from the atlas was used. All aquifer types were digitized in GIS environment (QGIS), and the aquifer name is written in the attribute table (created database) in a vector data format. The thickness data for the aquifer have been gathered from various source data, such as the GSI report (2006); published atlas by CGWB (2012); published report by CGWB (2014); literatures from Arulprakasam et al. (2013); and Mondal et al. (2016), and then assigned to the corresponding aquifer in the GIS database.

16.4.1.3 Soil Characteristics

Soil data have been collected from the released World Digital Soil Map (FAO 2003). The published Harmonized World Soil Database was used to obtain soil texture or texture class information (FAO/IIASA/ISRIC/ISS-CAS/JRC 2009). The hydraulic conductivity information was gathered from the different sources of information for the study area. The textural soil classification is specified in accordance with the proposed NRSC (2016) soil attribute table. The NRSC (2016) published soil attribute table assigns hydraulic conductivity values for each type of texture to be used.

16.4.1.4 Groundwater Level

The atlas published by CGWB (2012) was used to collect detailed information on depth of groundwater level for pre-monsoon (May 2011) season. A vector database was developed for this data in GIS environment.

16.4.1.5 Shoreline Demarcation

In order to prepare shoreline data, the Landsat 8 OLI/TIRS satellite image was used for the year 2014. Shoreline data considered the starting point for measuring the perpendicular distance to soil wells. A $0.09^\circ \times 0.09^\circ$ regular grid point was generated using Python programming language due to unavailability of well locations/points. After that perpendicular distances were calculated for each point from shoreline.

16.4.1.6 Chloride Concentration

Chloride (Cl) distribution map was obtained for the study area from the published report by CGWB (2014). The ratio of bicarbonate (HCO_3) and carbonate (CO_3) was not used for the present study as these data were not available for the area of interest;

instead, only chloride distribution data as existing saltwater intrusion status was used which was available for the study area. From the prescribed ratio for current saltwater effect conditions, it is known that more chloride has more saltwater intrusion into the area.

16.4.2 Methods

Saltwater intrusion vulnerability mapping of coastal aquifer has been done using GALDIT model in geoinformatics platform. A GIS database for groundwater occurrence (G), aquifer hydraulic conductivity (A), depth of groundwater level (L), distance from coastline (D), impact of existing status of seawater intrusion (I), and aquifer thickness (T) was developed to perform GALDIT model. These geospatial databases were integrated together by using weighted sum method in GIS environment. The overall methodology of the study was illustrated in Fig. 16.3.

16.4.2.1 Computing GALDIT Index

The relative weights of each of the GALDIT parameters (six parameters) have been predetermined which reflect the relative importance for saltwater intake. The vulnerability of water intrusion is derived by the following expression (Satishkumar et al. 2016; Chang et al. 2019):

$$\text{GALDIT} = 1 * G + 3 * A + 4 * L + 4 * D + 1 * I + 2 * T \quad (16.1)$$

Sensitive areas of seawater intrusion have been reported after the GALDIT index is determined. The high GALDIT index value is the high penetration region of the seawater, and the low GALDIT index value is the low saltwater entry zone.

16.5 Results and Discussions

It is found from the atlas that most of the aquifer types for the study area are multiple aquifer system. Therefore, the highest rating of 9.5 (Table 16.2) was assigned to the aquifer of the study area, and a surface raster at 30 m spatial resolution with the rating (Fig. 16.4) in the GIS environment was prepared. Similarly, to the above, a $0.09^\circ \times 0.09^\circ$ grid point was generated and assigned ratings to aquifer thickness (Table 16.2) based on the aquifer types, and then IDW interpolation method was adapted to prepare an aquifer thickness rating surface raster at 30 m resolution (Fig. 16.4) in the GIS environment. After successfully mapping the hydraulic conductivity values, rating was applied to all the soil types (Table 16.2). A $0.09^\circ \times 0.09^\circ$ grid point is created and then assigned saturated hydraulic

Table 16.2 Weights and ratings to the GALDIT parameters

Parameters/ Unit	G (groundwater occurrence)	A (aquifer hydraulic conductivity)	L (height of groundwater level above MSL)	D (distance from coast)	I (impact of existing status of seawater intrusion)	T (aquifer thickness)
Ratings/ weighting	Aquifer type	$\mu\text{m/s}$	m	m	mg/l	m
1	1	3	4	4	1	2
2		<7	>12	>50,000	<250	<2
3			10-12	20,000-50,000	250-500	2-3
4			8-10	10,000-20,000	500-750	3-4
5		7-14	7-8	5000-10,000	750-1000	4-5
6			6-7	3000-5000	1000-1250	5-7
7			5-6	2000-3000	1250-1500	7-10
8	Leaky confined	14-21	4-5	1500-2000	1500-2000	10-15
9	Unconfined		3-4	1000-1500	2000-3000	15-20
10	Confined	>21	2-3	500-1000	3000-5000	20-25
			<2	<500	>5000	>25

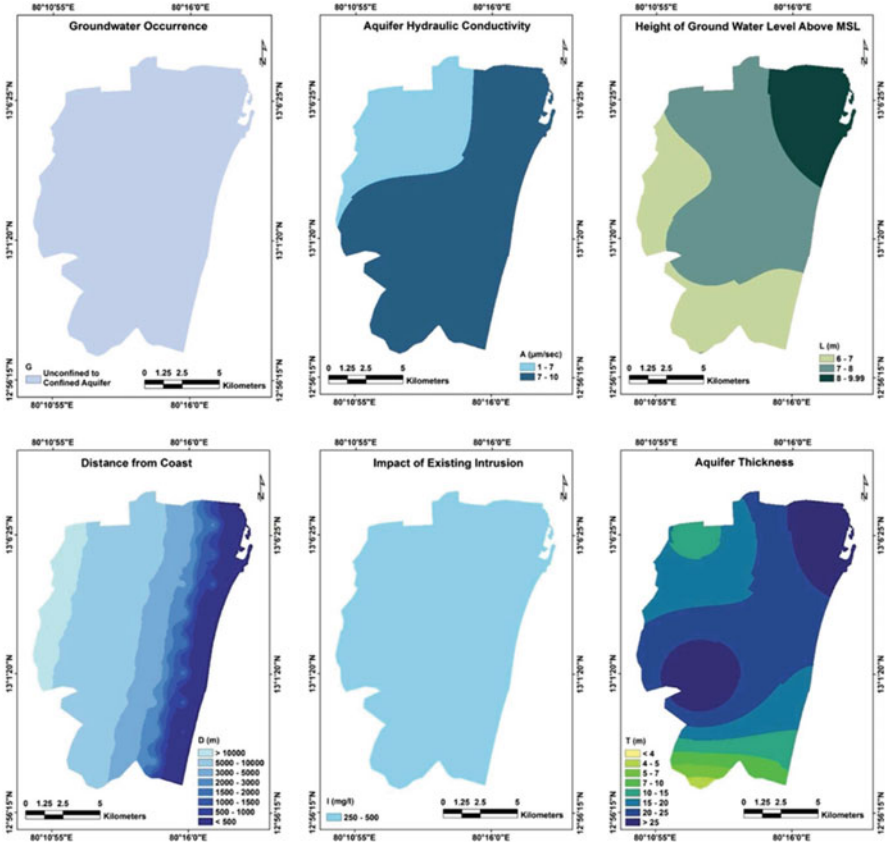


Fig. 16.4 Map showing the GALDIT parameters

conductivity rating from the soil type data. After that, inverse distance weighted (IDW) interpolation method was adapted to prepare a hydraulic conductivity rating raster surface at 30 m resolution (Fig. 16.4) in the GIS environment. A rating (Table 16.2) is assigned to each range of groundwater level in the vector data attribute table. A $0.09^\circ \times 0.09^\circ$ grid point was generated and assigned groundwater level rating in the attribute table from the vector data, and an IDW interpolation method was adapted to prepare a groundwater level rating surface raster at 30 m resolution (Fig. 16.4) in the GIS environment. The perpendicular distance from shoreline prepared a raster surface on the $0.09^\circ \times 0.09^\circ$ regular grid points by applying IDW interpolation at 30 m spatial resolution which was further reclassified according to the ratings (Table 16.2; Fig. 16.4) in the GIS environment. Chloride information was digitized in a vector data format and assigned rating (Table 16.2) to each chloride zone. A $0.09^\circ \times 0.09^\circ$ grid point was generated and assigned chloride zone rating and then IDW interpolation method applied to prepare a chloride zone rating surface raster at 30 m resolution (Fig. 16.4) in the GIS environment.

Fig. 16.5 Map showing the salinity ingress vulnerability zones of Tamil Nadu coast

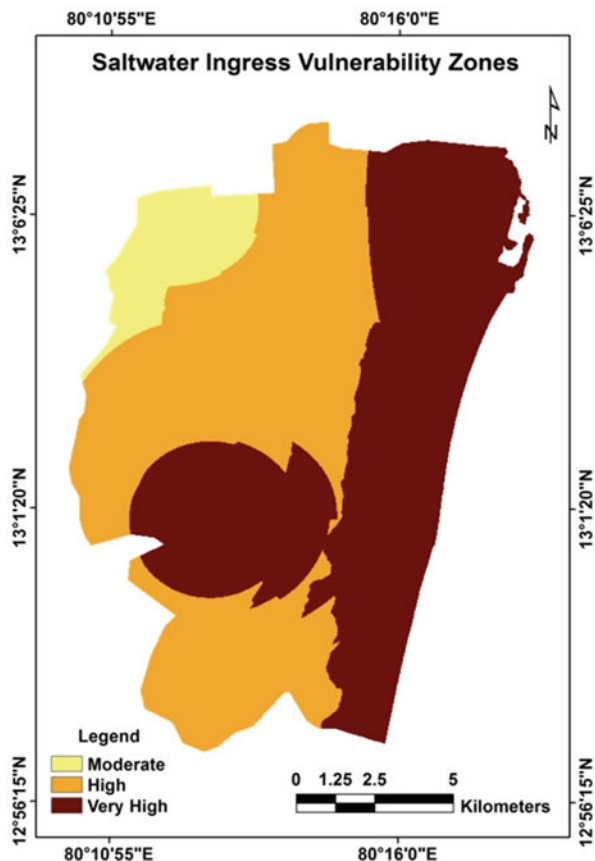


Table 16.3 Saltwater ingress vulnerability zone statistics of Chennai district

District/Taluk	Saltwater ingress (km ²)				
	Very low	Low	Moderate	High	Very high
Chennai	0	0	14.26	91.25	91.83

The result of the GALDIT index was divided into five categories, namely, very high (>95), high (80–95), moderate (65–80), low (50–65), and very low (<50) salinity ingress zone.

Saltwater ingress vulnerability zone has been divided into five vulnerable zones (Fig. 16.5) such as very high (95–127.5), high (80–95), moderate (65–80), low (50–65), and very low (24.5–50). Salinity intrusion is mainly observed along the coastal zone of the districts with a certain degree of extent toward the land from shoreline. The analysis of salinity ingress vulnerability zone shows that very high to very low salinity ingress vulnerability zones constitute 46.53%, 46.24%, 7.23%, 0%, and 0% of the area, respectively.

The area comes under high to very high saltwater intrusion vulnerability zones, and the reasons of high salinity ingress could be the following: low-lying topography, inundation by tsunami wave water, storm surge hazard, and overwithdrawal of nearshore groundwater.

The saltwater ingress vulnerability zone statistics are summarized in Table 16.3 for the entire coastal area of Chennai district. Across the coastal area, the dominated saltwater ingress vulnerability zone comes under very high to high category. The very high saltwater ingress vulnerability zone is found along the shoreline followed by high and moderate vulnerability zones toward landward side from the coastline.

16.6 Conclusion

The application of GALDIT model is to spot the areas that are extremely vulnerable to saltwater ingress through the integration of six parameters such as groundwater occurrence, aquifer hydraulic conductivity, depth of groundwater level, distance from coastline, impact of existing saltwater intrusion, and aquifer thickness in the GIS environment. The derived seawater intrusion vulnerability map using this model can be useful in mitigating the effect on fresh groundwater supplies. The map is also useful in understanding the future effect of seawater and setting up groundwater pumping wells in the appropriate location to fulfill the human needs. The analysis of the saltwater vulnerability map of Chennai coast, Tamil Nadu (India), shows that the dominated saltwater ingress vulnerability zone comes under high to very high category. The very high saltwater ingress vulnerability zone is found across the coastal zone of the study area. The saltwater ingress in the study area has to be controlled for the conservation of fresh groundwater and balance of the coastal ecosystem.

Acknowledgment The authors are thankful to Dr. Manik Mahapatra, National Centre for Sustainable Coastal Management (NCSCM), Chennai, India, for encouraging the research. The authors would like to thank the reviewers for their valuable feedback and various data sources for the free accessibility of the data.

References

- Arulprakasam, V., Sivakumar, R., and Gowtham, B. (2013) Determination of Hydraulic Characteristics Using Electrical Resistivity Methods – A Case Study from Vanur Watershed, Villupuram District, Tamil Nadu. *IOSR Journal of Applied Geology and Geophysics (IOSR-JAGG)*, e-ISSN: 2321–0990, p-ISSN: 2321–0982, 1(4), 10–14, www.iosrjournals.org.
- Barlow, P. (2014) Freshwater-Saltwater Interactions along the Atlantic Coast. USGS Groundwater Resources Program (GWRP).
- CGWB (2012) Aquifer System of Tamil Nadu & Puducherry (Atlas). Central Ground Water Board (CGWB), South Eastern Coastal Region, Chennai, Ministry of Water Resources, Government of India.

- CGWB (2014) Report on Status of Ground Water Quality in Coastal Aquifers of India. Central Ground Water Board (CGWB), Ministry of Water Resources, Government of India.
- Chachadi, A. G., Ferreira, J. P. L., and Vieira, J. M. P. (2007) Assessing aquifer vulnerability to seawater intrusion using GALDIT method: Part 2 – GALDIT indicators description.
- Chachadi, A.G., and Lobo-Ferreira, J. P. (2001) Assessing aquifer vulnerability to sea-water intrusion using GALDIT method: Part 2 – GALDIT Indicators Description.
- Chang, S. W., Chung, I. M., Kim, M. G., Tolera, M., & Koh, G. W. (2019). Application of GALDIT in Assessing the Seawater Intrusion Vulnerability of Jeju Island, South Korea. *Water*, 11(9), 1824.
- FAO (2003) The Digitized Soil Map of the World, Food and Agriculture Organization of The United Nations, Version 3.6, Completed January 2003, Land and Water Development Division, FAO, Rome (FAO/UNESCO, 1995).
- FAO/IIASA/ISRIC/ISS-CAS/JRC (2009) Harmonized World Soil Database (version 1.1). FAO, Rome, Italy and IIASA, Laxenburg, Austria.
- Ghorai, D., Mahapatra, M., & Paul, A. K. (2016). Application of remote sensing and GIS techniques for decadal change detection of mangroves along Tamil Nadu Coast, India. *Journal of Remote Sensing & GIS*, 7(1), 42-53.
- GSI (2006) Geology and Mineral Resources of The States of India. Miscellaneous Publication No. 30, Part VI – Tamil Nadu and Pondicherry, Geological Survey of India, Government of India.
- Johnson, T. (2007) Battling Seawater Intrusion in the Central & West Coast Basins. Water Replenishment District of Southern California. https://www.wrd.org/sites/pr/files/TB13_Fall07_Seawater_Barriers.pdf, Retrieved 23rd May 2017.
- Kayode, O. T., Odukoya, A. M., & Adagunodo, T. A. (2017). Saline water intrusion: its management and control. *Journal of Informatics and Mathematical Sciences*, 9(2), 493-499.
- Mas-Pla, J., Ghiglieri, G., & Uras, G. (2014). Seawater intrusion and coastal groundwater resources management. Examples from two Mediterranean regions: Catalonia and Sardinia, *Contrib. Sci.*, 10, 171–184. doi. org/10.2436/20.7010, 1.
- Moghaddam, K.H., Jafari, F., & Javadi, S. (2017). Vulnerability evaluation of a coastal aquifer via GALDIT model and comparison with DRASTIC index using quality parameters. *Hydrological Sciences Journal*, 62(1), 137-146.
- Mondal, N. C., Devi, A. B., Raj, P. A., Ahmed, S., & Jayakumar, K. V. (2016) Estimation of aquifer parameters from surfacial resistivity measurement in a granitic area in Tamil Nadu. *CURRENT SCIENCE*, 111(3), 524.
- NRCS (2016) United States Department of Agriculture, Saturated Hydraulic Conductivity, Natural Resources Conservation Service Soils, http://www.nrcs.usda.gov/wps/portal/nrcs/detail/soils/survey/office/ssr10/tr/?cid=nrcs144p2_074846, accessed on August 2016.
- Rahmstorf S. Rising hazard of storm-surge flooding. *Proc Natl Acad Sci U S A*. 2017;114(45):11806–11808. doi:<https://doi.org/10.1073/pnas.1715895114>
- Satishkumar, V., Sankaran, S., Amarender, B., & Dhakate, R. (2016). Mapping of salinity ingress using Galdit model for Sirkali coastal region: a case study. *Journal of Geographic Information System*, 8(4), 526-536.
- Sharma, S. K. (2008) 20th Salt Water Intrusion Meeting. Department of Environment Education, Carman School, Dehradun, India. <http://swim-site.nl/pdf/swim20/file269-272.pdf>, Retrieved 23rd May 2017.
- Sundar, S. S. and Yogesh, R. E. (2014). Assessing Aquifer Vulnerability to Seawater Intrusion in the Poombuhar Coast. *International Journal of Innovative Research in Science, Engineering and Technology*. Vol. 3, Issue 11, DOI: <https://doi.org/10.15680/IJIRSCCE.2015.0311104>, http://www.ijirset.com/upload/2014/november/104_Assessing.pdf.
- Yogesh, A. (2005) Salinity Mapping In Coastal Area Using GIS and Remote Sensing. Master of Science Thesis, IIRS, Dehradun, India.

Part III
Sustainable Groundwater Resources
Management

Chapter 17

Watershed Development Impact on Natural Resources: Groundwater and Surface Water Utilization



Partha Pratim Adhikary , M. Madhu, P. Jakhar, B. S. Naik, H. C. Hombegowda, D. Barman, G. B. Naik, and Ch. J. Dash

Abstract The dwindling situation of groundwater resources in the Eastern Ghats Highland region of East India has hampered the livelihood security of the rural peoples living in this area. In this context, the impact of watershed development activities, especially water resource management activities on the livelihood security of the peoples residing in this area, was assessed. Lacchaputraghati watershed of Koraput district of Odisha was chosen as the representative watershed for this study. The study area is dominated by agriculture land use with predominantly monocropping, covering 43% of the watershed area. Forest and scrublands are also dominant and shifting cultivation is rampant. Before the start of the project, the average runoff in the watershed was 24.4%, which was decreased to 14.6% after the successful implementation of the project. Finger millet and upland paddy cultivation are the highly runoff-prone land uses where watershed management treatments reduced the runoff from 29.92% to 15.4%. Even in forested areas, the runoff was decreased from 14.68% to 7.3%. Rainwater harvesting and storing capacity was increased by 93.91 ha-cm within the watershed. The average annual water storage depth in the water bodies was increased from 1.01 to 1.17 m during the project period. A positive change to the tune of 15.04% was observed in terms of water storage capacity within the watershed. The annual average depth to water table from the land surface was decreased from 7.95 to 7.80 m within a span of 5 years because of watershed management activities. The crop yield also responded posi-

P. P. Adhikary

ICAR Indian Institute of Water Management, Bhubaneswar, Odisha, India

e-mail: partha.adhikary@icar.gov.in

M. Madhu (✉) · P. Jakhar · B. S. Naik · H. C. Hombegowda · D. Barman · G. B. Naik · Ch. J. Dash

ICAR Indian Institute of Soil and Water Conservation, Research Centre, Koraput, Odisha, India

tively to the watershed management activities and increased by 9.14% with the range of 3–15% for different crops. Therefore, the watershed development activities have shown a positive impact on the conservation of natural resources, especially water resources, and need to be replicated in other areas for sustainable management of natural resources.

Keywords Eastern Ghats · Groundwater · Natural resources · Sustainability · Watershed development

17.1 Introduction

In the present century, the main challenge to the people of India will be to maintain the livelihood security without degrading the natural resources to such extent that it will become unsustainable (Madhu et al. 2016). The livelihood of rural people is mainly coming from agriculture where most of the agricultures are *rainfed*. *Rainfed* agriculture is the predominant agriculture in the world (80%) and produces 60% of the world's food. India is also not the exception, where 60% of arable lands (142 M ha) are *rainfed*. Overexploitation of these lands is converting them to degraded lands, slowly. In India more than 120 M ha of lands are facing one or other form of degradation (Maji 2007). Not only is the physical and chemical degradation of these lands but also the decline of water table a concern today. These lands can be managed properly through watershed development activities to get higher crop yield and higher income of the people residing there and to conserve the natural resources including soil and water (Madhu et al. 2016).

Watershed development is a time-tested, proven, and eco-friendly approach to conserve the natural resources and utilize them in a sustainable manner, with the active participation of the stakeholders residing within the watershed area. This approach has shown a tremendous potentiality in the *rainfed* areas and has the capacity to address various issues related to ecology, economy, and society (Wani et al. 2003). Comprehensive benefits of watershed management approach can be visualized from higher food production, better livelihood of the stakeholders, higher plant and animal diversity, greener environment, increased gender sensitiveness, and improved social fabric and equity (Joshi et al. 2005). Watershed management can also be considered as the best option to meet the global hunger through proper nurturing of *rainfed* agriculture (Rockström et al. 2007). It can also stabilize ravine and gullied lands and bring these land to their full potential (Kumar et al. 2020). Continuous use of new and tested natural resource management technologies under various watershed development activities has the ability to raise the level of crop yield and thus can narrow down the yield gap (Madhu et al. 2016). The importance of rainwater harvesting and management through watershed development activities to improve the livelihood of the rural people has been highlighted in various works conducted in India (Wani et al. 2003; Madhu et al. 2016; Kumar et al. 2020).

The success of watershed management to secure the livelihood of the stakeholders is dependent on many factors and issues. Among those various factors, augmentation of groundwater resources and their judicious use for different purposes is the foremost. In the watershed groundwater has been used for many purposes like drinking, domestic, water for livestock and poultry, irrigation of off-season vegetable crops for more income etc. In all the experiments it has been found that the efficiency of groundwater to all types of use is more than that of surface water. Groundwater is available at the point of application, it is relatively safe to use and it can be available on demand. These advantages of groundwater are making the groundwater vulnerable and resulted in the decline of water table in all parts of the world (Adhikary et al. 2012).

In the alluvial zone of India, the recharge of groundwater is relatively high. But in the hard rock areas, the availability as well as recharge of groundwater is very low. The Eastern Ghats Region of East India is coming under hard rock area where groundwater resources are of dwindling in nature. Overexploitation of groundwater has been reported from many parts of this region (Adhikary et al. 2019). If not taken care in a scientific way with the blend of people's participation, the day will be not so far when there will be no water even to drink. To augment the groundwater resources and to use this resource for securing the livelihood of the rural people, watershed management with people's participation can be a viable option (Madhu et al. 2016). Therefore, in a tribal area of Eastern Ghats Highland of Odisha, watershed management approach was evaluated through participatory resource conservation with special emphasis on groundwater resource augmentation. The immediate objective of this study was to assess the impact of watershed management activities on crop productivity and natural resource use especially water resource use.

17.2 Materials and Methods

17.2.1 Study Area

Lacchaputraghati watershed is located at Pottangi Tehsil of Koraput District in Odisha state, within the Eastern Ghats Highlands of East India (Fig. 17.1). The area of the watershed is 601.24 ha, and the topography is undulating where the slope goes more than 50%. The elevation varies between 900 and 1258 m above msl. Stream order of the watershed is fourth with a drainage density of 7.14 km km^{-2} . The physiographic detail of the watershed is presented in Table 17.1.

17.2.2 Climate and Water Balance

The climate is warm and humid with an average annual maximum and minimum temperature of 35.8°C and 7.6°C , respectively. The long-term average annual

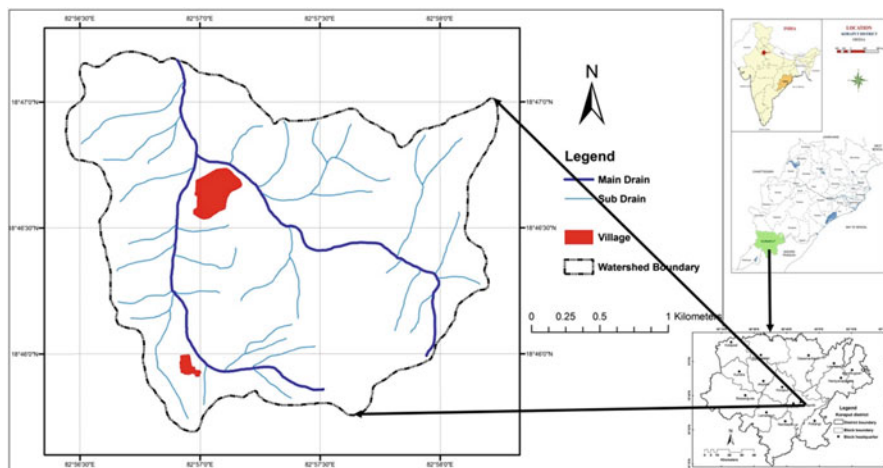


Fig. 17.1 Location map of the study area (Lacchaputraghati watershed)

Table 17.1 Physiographic details of Lacchaputraghati watershed

S. no.	Physiographic detail	
1	Agroecological region	12
2	Area (ha)	601.24
3	Elevation range (m amsl)	900–1258
4	Average slope (%)	12
5	Order of the watershed	Fourth
6	Drainage density (km km^{-1})	7.14
7	Form factor	0.67
8	Length of main channel (km)	3.75
9	Perimeter (km)	10.6

rainfall is 1452.2 mm with 77 rainy days (Fig. 17.2). Southwest monsoon season (June–September) is the main rainy season when about 81% of the total rainfall is received (Adhikary et al. 2015). The maximum (6.2 mm day^{-1}) and minimum (2.1 mm day^{-1}) evaporation was observed during May and August months with an annual average rate of 3.7 mm day^{-1} . Six months (May–October) are the water surplus months, and the length of growing period is about 170 days (Fig. 17.3).

17.2.3 Soil and Geology

The soils of the watershed vary spatially. The dominant texture in hillslopes is loamy sand, whereas *jhola* beds are showing clay loam soil texture. The soils are acidic in nature with pH (1:2 soil/water suspension) varying between 4.2 and 5.4. Average soil organic carbon, available nitrogen, phosphorus, and potassium content are

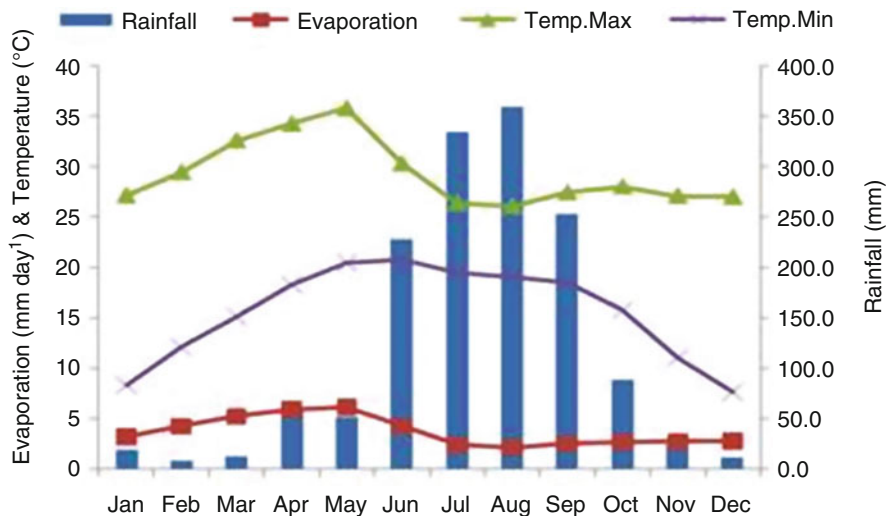


Fig. 17.2 Weather parameters at Lacchaputraghati watershed

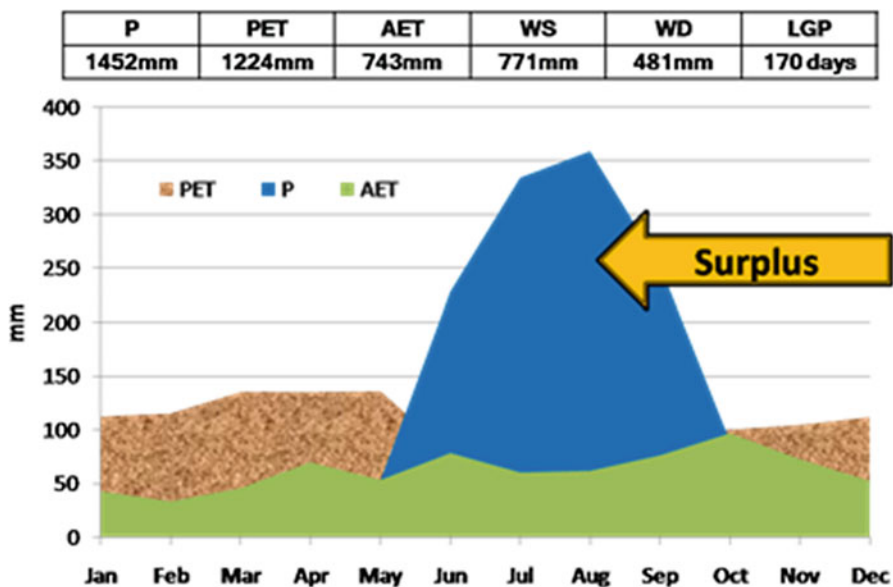


Fig. 17.3 Water balance diagram of the Lacchaputraghati watershed

0.69%, 288 kg ha⁻¹, 11.1 kg ha⁻¹, and 313 kg ha⁻¹, respectively. According to the USDA land capability classification, 43.1% watershed area is under class III, 22.6% under class VI, and 20% under class VII. 6.6% and 7.7% of the area have been covered by class II and IV lands, respectively.

Shale, slate, and sandstones are the main lithological compositions where faults and fissures are also present. The weathered and fractured granite/granitoid gneiss constitutes the major repository of groundwater. Besides these aquifers, weathered and fractured khondalites, shale, etc. also form aquifers about the small areal extent of low to moderate yield. Groundwater occurs in unconfined to confined conditions. Groundwater from shallow and deeper aquifers is suitable for irrigation, drinking, and other purposes.

17.2.4 Land Use and Water Resources

Degraded forest is the dominant land use covering 61% of the watershed area followed by the agriculture (20.2%), current fallow (11.5%), barren land (6.0%), and pastureland (1.4%). The presence of springs in upper hills, small perennial streams, and downstream flow in *jhola* beds are the major sources of water resources available in the watershed. Though the watershed receives high rainfall during monsoon season but acute water scarcity during postmonsoon, drying of springs and decreased downstream flow are the common features.

17.2.5 Resource Conservation Activities

In the watershed various developmental activities were undertaken. They were (i) soil conservation measures in arable lands, (ii) water resource development measures, and (iii) crop productivity enhancement activities. Specialized activities include field bunding, stone bunding, hedge planting, and vegetative filter strips in arable lands and trenching in nonarable lands. For gully stabilization brushwood check dams, loose boulder check dams, gabions, and stream bank riveting were done. Construction of farm ponds, desiltation and providing spillway of the existing water harvesting structures, construction of waterways, and digging of *jhola kundies* were the major water resource development activities. Agri-horticulture systems, bamboo plantation, energy plantation, fodder tree plantation, silvi-pasture system, green manuring, etc. were undertaken to improve the watershed land productivity.

17.2.6 Estimation of Runoff

The runoff was estimated using hydrologic soil cover complex method. This method is also called curve number method, based on the recharge capacity of the watershed.

The recharge capacity is determined by antecedent moisture conditions and physical characteristics of the watershed. Based on hydrologic soil group and land use cover, curve number (CN) value was determined and used to find out the potential maximum retention (S) (USDS-SCS 1972). The CN values for AMC II condition were taken using the correction factor for AMC I and AMC II conditions. Then runoff was estimated using the rainfall-runoff relationship.

17.2.7 Data Collection and Impact Assessment

Data on biophysical parameters were collected as described by Madhu et al. (2016). Participatory Rural Appraisal technique was used to get firsthand information. Field visit, household survey, meeting, interview, focus group discussion, and detailed resource survey were done during pre- and post-project implementation of the watershed project. The water table depths in the existing wells were monitored fortnightly till the project was ended. For impact analysis study, the baseline data was collected during 2008 (pre-project period), and all the biophysical parameters were monitored during the project implementation period till 2013. The effect of various activities to manage the watershed was quantified through various impact indicators.

17.3 Results and Discussion

17.3.1 Land Use of Lacchaputraghati Watershed

The watershed is mainly dominated by agricultural land use covering 43% of the watershed area. People take generally one crop, but in the jhola lands and the lands adjoining to the streams, double cropping has also been practiced (Fig. 17.4). After agriculture, the second most dominating land uses are the forest land use and then scrubland use. Forests are mainly devoid of vegetation due to massive deforestation. In the higher elevated areas, shifting cultivation is the predominant land use. People do slash and burn cultivation in the high elevated areas where the slope is moderate to high. This practice causes a huge amount of soil erosion and fastens the runoff rate. Therefore this practice reduces the recharge potential of rainwater and hinders the augmentation of groundwater resources. In a study by Adhikary et al. (2019), it was observed that shifting cultivation of Koraput district has come to a stabilized condition with the population and culture. The abandoned shifting cultivation is increasing, whereas the current shifting cultivation is decreasing in the district. The total amount of shifting cultivated area in the district is around 186.4 km², which is 2.2% of the total geographic area of the district.

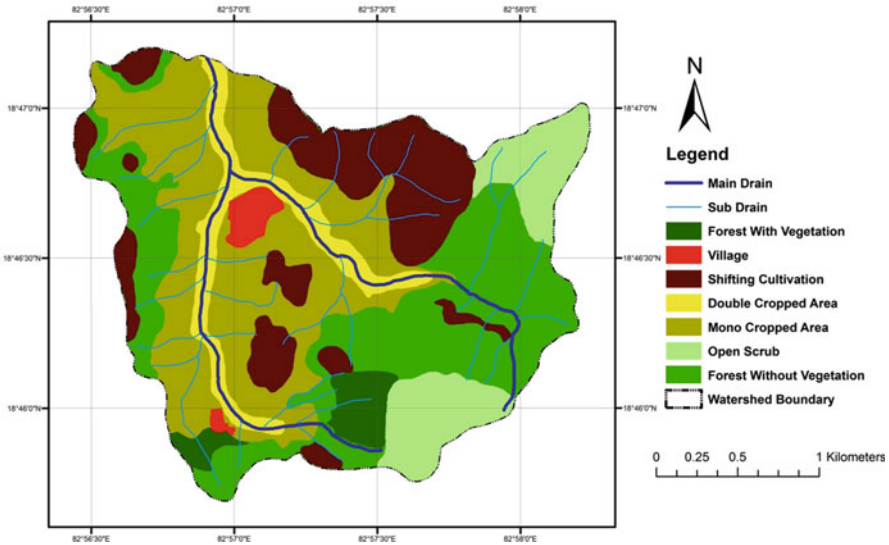


Fig. 17.4 Land use map of Lacchaputraghati watershed

17.3.2 *Runoff*

The runoff coming out from different land uses within the watershed varies greatly to the tune of 14.68–29.92% during pre-project period and 7.3–15.4% during post-project period (Fig. 17.5). Finger millet and upland paddy field generated the maximum runoff. During pre-project period, these land uses generated 29.92% runoff, and that was reduced to 15.4% during post-project period. Extensive field bunding in these lands has reduced the runoff (Fig. 17.6). The least runoff was observed in the well-vegetated forests where, during pre-project period, the runoff was 14.68% and during the post-project period, the runoff was reduced to a mere 7.3% due to the construction of staggered contour trenches in the inter-rill areas (Fig. 17.7), and loose boulder check dams in the streams within the forested areas. As a whole the overall runoff in the watershed was decreased from 24.4% during pre-project period to 14.6% during post-project period. This is because of the combined effect of all the physical interventions undertaken in the watershed area. Saving nearly 10% runoff means putting nearly 150 mm more water into the soil profile. This extra water will help the crops to cope up in dry rainfall spells and increase the base flow and also replenish the underground aquifer.

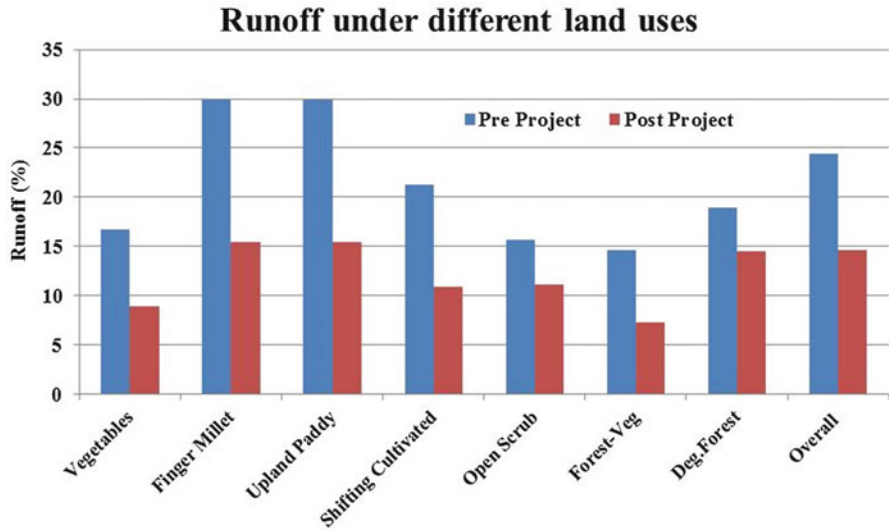


Fig. 17.5 Estimated runoff under different land use during pre- and post-project period in the watershed



Fig. 17.6 Field bunding in sloping degraded arable land: pigeon pea and marigold on the field bund



Fig. 17.7 Trenching in the slopping degraded nonarable land for conservation of soil moisture

17.3.3 Water Resource Development

The interventions such as dugout ponds, lined ponds, jhola kundi, check dams, and diversion channels (Fig. 17.8) were taken up in the watershed to increase the rainwater storage and availability. Thus, within the project period, the capacity of rainwater storage in the watershed was increased to the tune of 93.91 ha-cm (Fig. 17.9). During the year 2009, 36.06 ha-cm water harvesting capacity was created, and during the years 2011 and 2012, 27.37 and 30.48 ha-cm water harvesting capacities were created, respectively. Because of this increased capacity, 24.2 ha additional area was brought under protective irrigation for cultivation of paddy and vegetables. This has benefited nearly 177 peoples in the watershed (Table 17.2).



Fig. 17.8 Water convey channel to irrigate paddy and vegetable crops in the watershed

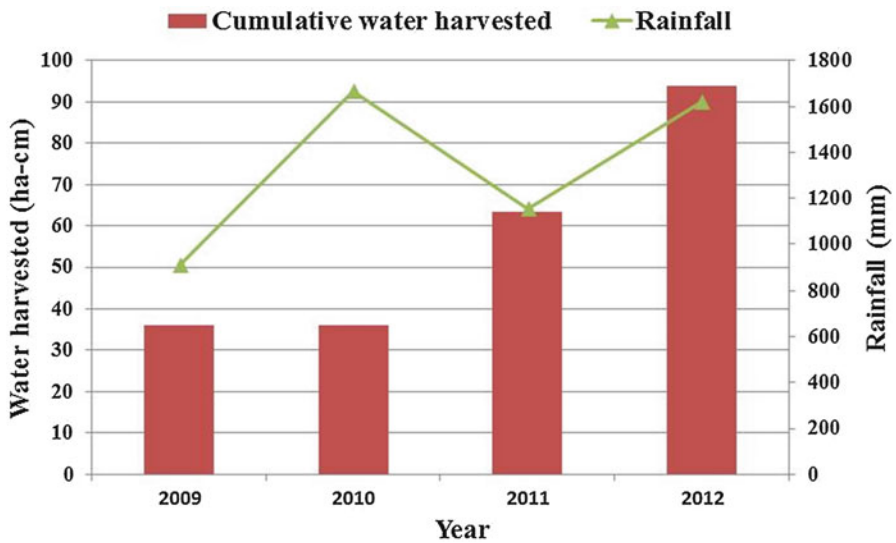


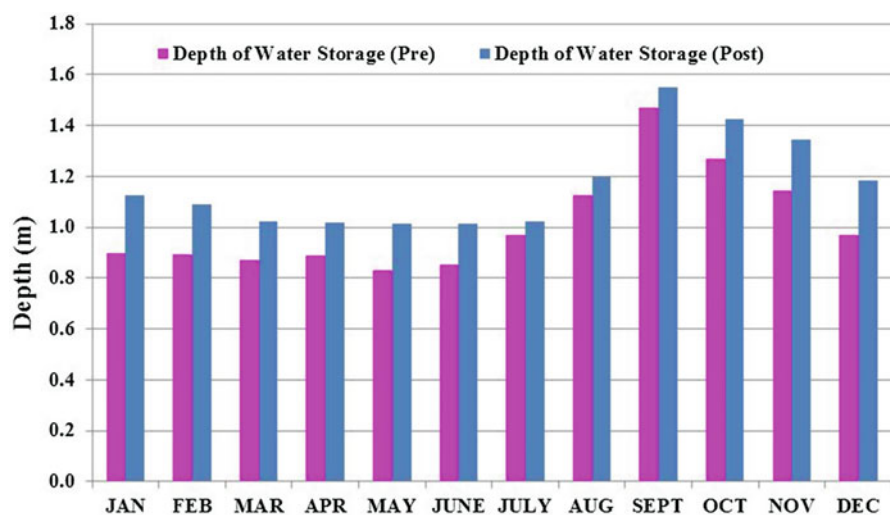
Fig. 17.9 Rainwater storage capacity created and harvested during the project period

17.3.4 Impact on Groundwater Resources

The depth of the water storage in a dugout pond was monitored, and the monthly variation of water storage depth is presented in Fig. 17.10. During the pre-project period, the depth of water storage varied between 0.831 m during the month of May

Table 17.2 Water resource development on irrigated areas and beneficiaries in the Lacchaputraghati watershed

S. no.	Water harvesting structure	Cost (Rs)	Irrigated area (ha)			Crops grown	Beneficiaries
			Before	After	Additional		
1	Convey channel (Ariputraghati)	2,19,476	2	6	4	Paddy and finger millet	30
2	Check dam I (Ariputraghati)	48,636	0	6	6	Paddy and vegetables	52
3	Check dam II (Ariputraghati)	78,034	0	1.6	1.6	Paddy	17
4	Check dam III (Ariputraghati)	1,24,878	0	2	2	Paddy and vegetables	12
5	New farm pond	99,641	0	3.2	3.2	Paddy Ginger	14
6	Convey channel	66,006	3.6	13	9.4	Paddy Vegetables	52
	Total	6,36,671	5.6	29.8	24.2		177

**Fig. 17.10** Depth of water storage in dugout pond during the pre- and post-project period in the watershed

and 1.27 m during the month of October. The impact of watershed development was found in the positive change of water storage depth in this dugout pond. After the project is over, the depth of water storage varied between 1.01 m during the month of May and 1.55 m during the month of September. On an average the annual water storage depth during pre-project period was 1.01 m, which has been increased to

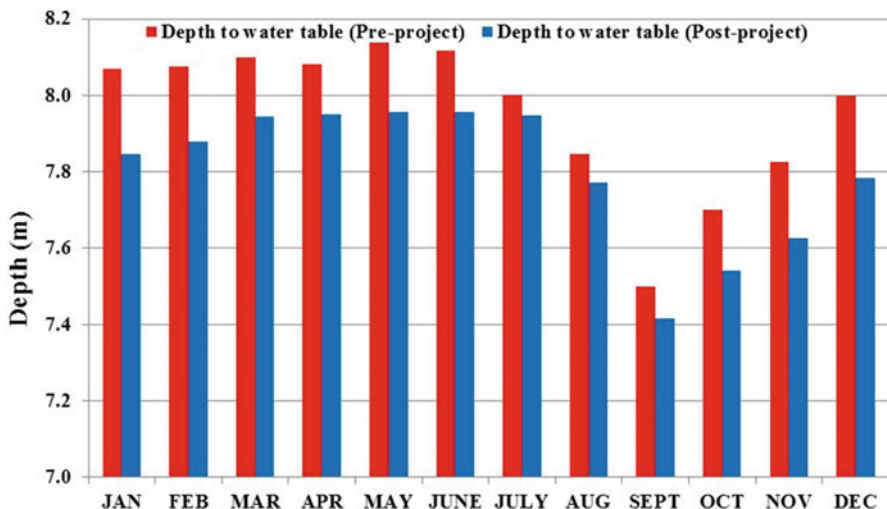


Fig. 17.11 Depth to water table during the pre- and post-project period in the Lacchaputraghati watershed

1.17 m during the post-project period. Because of the watershed development project, a positive change to the tune of 15.04% was observed in terms of water storage capacity within the watershed. The effect was most prominent during the postmonsoon season of the year.

The groundwater table depth was monitored in a dug well within the watershed. The result is very interesting and shown in Fig. 17.11. For all the months, there was a reduction of depth to water table within the watershed. During the pre-project period, the depth to water table varied between 8.16 m during the month of May and 7.50 m during the month of September. After the end of the watershed development project, the depth to water table was 7.96 m during the month of May and 7.41 m during the month of October. The annual average depth to water table during pre-project period was 7.95 m, which has been reduced to 7.80 m during the post-project period. Different watershed development interventions created a positive development of groundwater resources and increased it to the tune of 1.92% within a period of 5 years.

17.3.5 Crop Productivity and Diversification

Because of the positive development of the surface and groundwater resources, farmers have started cultivating more area than the pre-project period. Nearly 45.4 ha area has been added to field crops like cereals, pulses, and oilseeds, and 24 ha area has been added to horticultural crops (Fig. 17.12). The average yield of different crops was collected for pre- and post-project period from the watershed

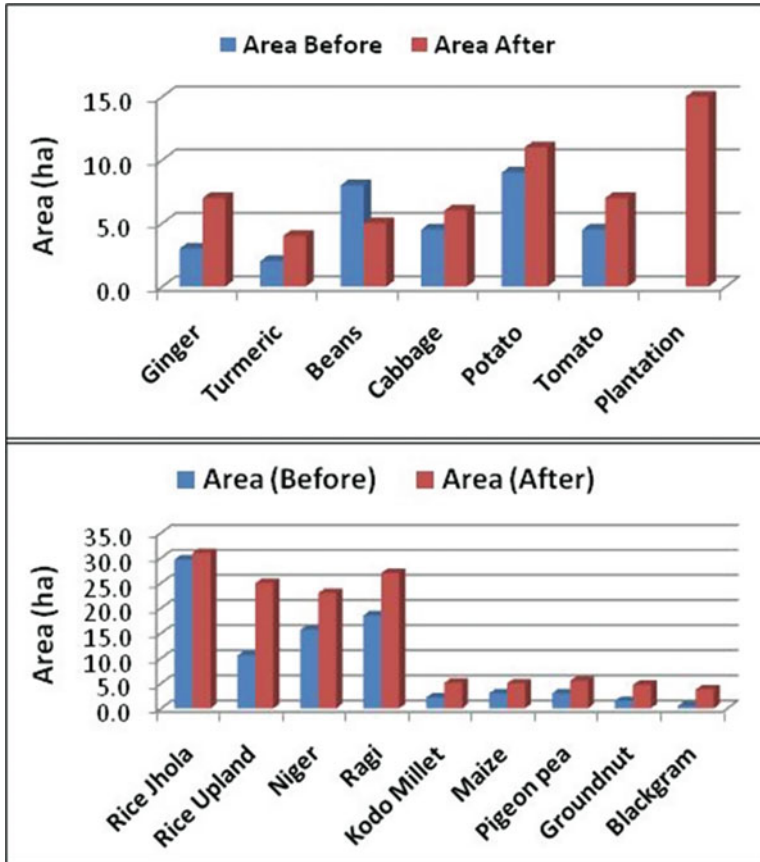


Fig. 17.12 Area under different crops during pre- and post-project period

areas and presented in Fig. 17.13. Crop yield was increased by 3–15% depending on the crop types and the overall average increase was 9.14%.

As the water availability in the watershed has been increased and there was high market demand for vegetable crops, efforts were made for popularizing cultivation of vegetables in the watershed area. The result was positive, and this effort has increased the vegetable-cultivated area from 31 ha during pre-project to 40 ha during post-project period. The increase of area was 30%. Crop diversification index (CDI) was worked out based on the area under each crop in different seasons for the period before and after the project. CDI values near to 1 indicate complete diversification. The overall pre-project CDI was 0.55 and it was increased to 0.71 during the post-project. Thus the increase of CDI was 30%. A similar degree of increase in productivity and CDI was also reported by Sikka et al. (2014) and Dass et al. (2009) under different watershed programs in India.

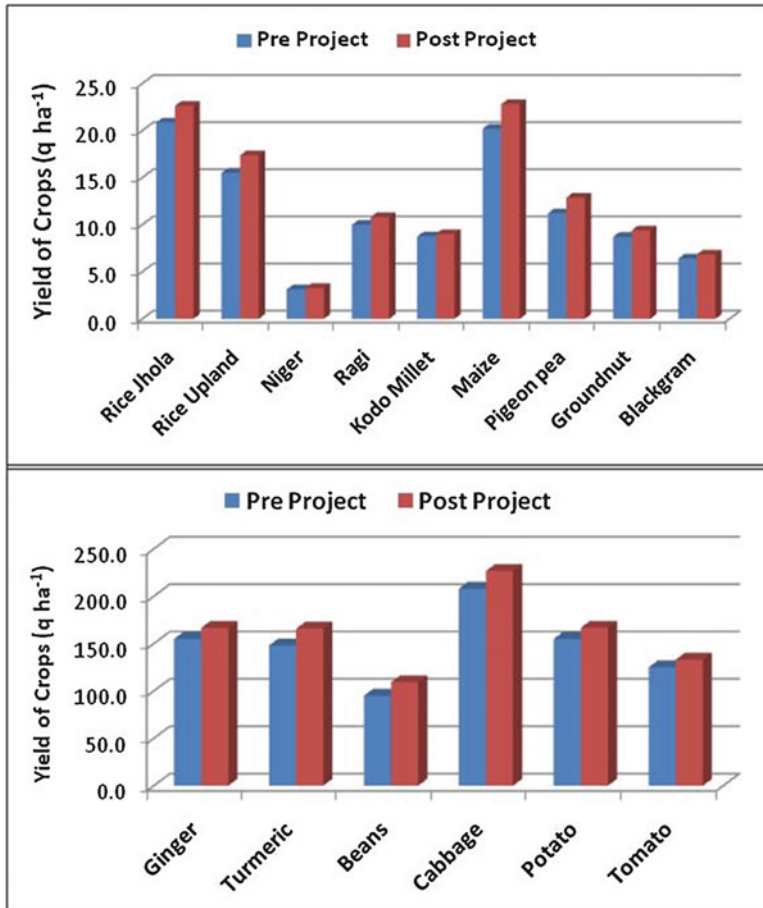


Fig. 17.13 Yield of crops during pre- and post-project period

17.4 Conclusions

The impact of participatory watershed development for resource conservation and securing livelihood of farmers residing in the *rainfed* area showed a big success. The positive impacts on ecology, economy, and society are well evidenced. The runoff was reduced from 24.4% to 14.6%. Water storage capacity was increase by 15.04%. Groundwater resource was increased by 1.92% within a period of 5 years. The crop yield was increased by 3–15%. In situ rainwater conservation and use of high-yielding varieties are responsible for higher water use efficiency and water productivity of the crops.. The knowledge of the local community is paramount in sustainable use of natural resources and delaying environmental degradation. Therefore, community-guided developmental activities will be more beneficial and sustainable.

Therefore, policy guidelines should focus on the requirement of skilled manpower per unit area for effective implementation and greater socio-environmental impacts of watershed development projects.

References

- Adhikary, P.P., Barman, D., Madhu, M., Dash, Ch.J., Jakhar, P., Hombegowda, H.C., Naik, B.S., Sahoo, D.C. and Karma Beer. (2019). Land use and land cover dynamics with special emphasis on shifting cultivation in Eastern Ghats Highlands of India using remote sensing data and GIS. *Environmental Monitoring and Assessment*, 191, 315
- Adhikary, P.P., Dash, Ch.J., Chandrasekharan, H., Rajput, T.B.S. and Dubey, S.K. (2012). Evaluation of groundwater quality for irrigation and drinking using GIS and geostatistics in a peri-urban area of Delhi, India. *Arabian Journal of Geosciences*, 5 (6), 1423–1434
- Adhikary, P.P., Madhu, M., Dash, Ch.J., Sahoo, D.C., Jakhar, P., Naik, B.S., Hombegowda, H.C., Naik, G.B. and Dash, B. (2015). Prioritization of traditional tribal field crops based on RWUE in Koraput district of Odisha. *Indian Journal of Traditional Knowledge*, 16(1), 88–95.
- Adhikary, P.P., Sena, D.R., Dash, Ch.J., Mandal, U., Nanda, S., Madhu, M., Sahoo, D.C. and Mishra, P.K. (2019). Effect of Calibration and Validation Decisions on Streamflow Modeling for a Heterogeneous and Low Runoff–Producing River Basin in India. *Journal of Hydrologic Engineering*, 24 (7), 05019015
- Dass, A., Sudhishri, S., Patnaik, U.S. and Lenka, N. (2009). Effect of agronomic management in watershed productivity, impact indices, crop diversification and soil fertility in Eastern Ghats of Odisha. *Journal of Soil and Water Conservation*, 8(3), 34–42.
- Joshi, P.K., Jha, A.K., Wani, S.P., Joshi Laxmi and Shiyani, R.L. (2005). Meta-analysis to assess impact of watershed program and people’s participation. Research Report 8, Comprehensive Assessment of watershed management in agriculture, International Crops Research Institute for the Semi-Arid Tropics and Asian Development Bank, 21 p.
- Kumar, G., Adhikary, P.P. and Dash, Ch.J. (2020). Spatial extent, formation process, reclaimability classification system and restoration strategies of gully and ravine lands in India. In: P.K. Shit et al. (eds.), *Gully Erosion Studies from India and Surrounding Regions, Advances in Science, Technology & Innovation*, pp. 1–20. doi:https://doi.org/10.1007/978-3-030-23243-6_1.
- Madhu, M., Naik, B.S., Jakhar, P., Hombegowda, H.C., Adhikary, P.P., Gore, K.P., Barman, D. and Naik, G.B. (2016). Comprehensive impact assessment of resource conservation measures in watershed of eastern region of India. *Journal of Environmental Biology*, 37(3), 391–398.
- Maji, A.K. (2007). Assessment of degradation and wastelands of Indian. *Journal of Indian Society of Soil Science*, 55(4), 427–435.
- Rockström, J., NuhuHatibu, Y., Theib, Oweis and Wani, S.P. (2007). Managing water in rain-fed agriculture. Pages 315–348 in *Water for Food, Water for Life: A Comprehensive Assessment of Water Management in Agriculture* (ed. David Molden). London, UK: Earthscan and Colombo, Sri-Lanka: International Water Management Institute.
- Sikka, A.K., Madhu, M., Subhash Chand, Singh, D.V., Selvi, V., Sundarambal, P., Jeevarathanam, K. and Murgaiyah, M. (2014). Impact analysis of participatory integrated watershed management programme in semi-arid region of Tamil Nadu, India. *Indian Journal of Soil Conservation*, 42 (1), 98–106.
- USDA-SCS. (1972). SCS National Engineering Handbook, Section 4, Hydrology. Chapter 10, Estimation of Direct Runoff from Storm Rainfall. U.S. Department of Agriculture, Soil Conservation Service, Washington, D.C., pp. 10.1–10.24.
- Wani, S.P., Pathak, P., Jangawad, L.S., Eswaran, H. and Singh, P. (2003). Improved management of Vertisols in the semi-arid tropics for increased productivity and soil carbon sequestration. *Soil Use and Management*, pp. 217–222.

Chapter 18

Long-Term Groundwater Behaviour Over an Agriculturally Developed State of North-West India: Trend and Impact on Agriculture



Omvir Singh, Amrita Kasana, and Pankaj Bhardwaj

Abstract The present study aims to examine the long-term groundwater behaviour in Haryana which is an agriculturally developed state of north-west India. For this study, groundwater level data has been acquired from the Groundwater Cell, Department of Agriculture, Haryana, for the period 1990–2013. By using this data, declining/rising groundwater level areas, groundwater balance, net groundwater balance and net rise/fall of groundwater level have been computed for the state as a whole and three climatic zones, i.e. sub-humid, semi-arid and arid. The analysis shows that approximately 77% area of the state has demonstrated a decline in groundwater levels during the study period. The state as a whole has experienced a fall of 0.7 cm/year in the average net annual groundwater levels with the highest decline in Fatehabad (5.1 cm/year) and Mahendergarh (4.1 cm/year) districts. Remarkably, northern and southern districts of the state are facing a problem of a sharp decline in groundwater levels, whereas central parts are experiencing a continuous increase leading to waterlogging problems. In sub-humid zone, about 95% area has witnessed a decline in groundwater levels followed by semi-arid (85%) and arid (77%) zones. Overall, the state has a negative groundwater balance, i.e. –1361.6 (00 ha-m). Therefore, urgent measures need to be taken up for sustainable utilisation and management of groundwater resources both at field and regional scale.

Keywords Groundwater · Haryana · Irrigation · Overexploitation · Tube well

O. Singh (✉) · A. Kasana
Department of Geography, Kurukshetra University, Kurukshetra, India
P. Bhardwaj
Department of Geography, Government College, Bahu, Jhajjar, India

18.1 Introduction

Groundwater is the principal source of water on the earth for sustainable human development (Kendy et al. 2003; Xue et al. 2014; Pande et al. 2019). It is a renewable resource and has the remarkable distinction of being a highly dependable source of water supply. Globally, it is subject to increasing abstraction pressure on account of increasing population and economic development (Ji et al. 2006). Furthermore, survival of greater than 50% of the total population of the world depends upon groundwater (Jha 2007). In several regions, people completely depend on groundwater (Howard 2015). It is considered as the highest extracted raw item on the earth (Jarvis 2012). On a global scale, about 38% (113 million hectares) of the total irrigated area (300 million hectares) is irrigated by groundwater (Siebert et al. 2010). Since 1960, agricultural sector has emerged as growingly reliant on groundwater, and its use has almost doubled during 1960–2000 (Siebert et al. 2010). The significance of groundwater is growing exponentially owing to the rising demand for irrigation and drinking water due to scarce surface water availability, thereby leading to overexploitation and lowering of groundwater levels in large parts of the world (Wada et al. 2010). Many aquifers in Bangkok, Beijing, Las Vegas, Manila and Yemen are facing serious water deficiencies due to overexploitation of groundwater (Chawla et al. 2010). Overexploitation of groundwater at alarming rates will adversely affect the ecosystem and social development (Gleeson et al. 2010).

In India, groundwater is a crucial component to support livelihood and reduce poverty (Chambers et al. 1989). About 60% of food productions have resulted in because of development of irrigation by groundwater (Shah et al. 2000; Bassi 2014). The area under irrigation using groundwater has increased sharply in India since the post-Green Revolution period (Dhawan 1989; Shah and Mukherjee 2001). Groundwater extraction has reached at unsustainable levels in the country owing to a rapid expansion of irrigation through groundwater (Shah 2009; Goyal et al. 2010a). The abstraction rate of groundwater has risen approximately tenfold in the last 50 years in India, and extracted the highest total groundwater in the year 2010, which is about two times of the USA's or China's annual abstraction (Margat and van der Gun 2013). In India, the private wells have crossed a number of 20 million and are rising at a rate of 1 million wells per year with the new one being dug at every 15 s (Mukherji and Shah 2005; Reddy et al. 2014). This alarming growth in groundwater extraction threatens the sustainability of this valuable resource, thereby causing serious socio-economic and environmental imbalances in the country (Goyal et al. 2010b; Kumar et al. 2018). Additionally, declining groundwater levels make its abstraction more difficult and expensive resulting in a reduction in India's harvest by 25% or more (Seckler et al. 1998).

Haryana is among the agriculturally developed states of India. The state accounts for about 2.5% of the total cultivated land, though it contributes approximately 7% to total food production of the country. After the creation of the state in 1966, agricultural sector has received priority; therefore, cropped area has increased from 4.6 to 6.5 Mha during 1966 and 2012 (Singh et al. 2020). However, this progression

of agriculture sector has also affected adversely the groundwater resources. In the last three decades, farmers have abandoned traditional crops and started to grow high-yielding crops which produce more profit, i.e. rice and wheat (Table 18.1). These two crops require a huge amount of water. To fulfil the water demand, the groundwater is being extracted rapidly by tube wells (both shallow and deep). Approximately 57% of the cultivated area is irrigated by tube wells (groundwater) followed by canals (surface water) (43%). A 30-time increase, i.e. from 0.02 to 0.77 million, has been witnessed during 1966–2013 (Singh and Amrita 2015a, b). Therefore, the net area irrigated by canals has decreased from 77% in 1966 to 43% in 2013 (Amrita 2017). The net groundwater availability in the state is about 9.79 billion cubic metres, while the net groundwater draft is about 13.06 billion cubic metres, thus leaving an annual deficit of 3.27 billion cubic metres (Amrita 2017). This overexploitation has put a tremendous pressure on groundwater resources, which may cause a major water crisis in the state in the near future. Therefore, a detailed knowledge of groundwater's long-term trends, pattern and behaviour is essential to develop effective and sustainable water management practices.

In the light of the above facts, the main objectives of the present study are (i) to identify the areas of declining and rising groundwater level in different climatic zones of Haryana during 1990–2013, (ii) to assess the average annual rise/fall of groundwater level, (iii) to identify the factors responsible for rise/fall in the groundwater level and (iv) to calculate the groundwater balance in response to the changes in rise/fall of groundwater level in different climatic zones.

18.2 Materials and Methods

18.2.1 Study Area

The state of Haryana is situated in the north-western parts of the country. It spreads from 27°39' to 30°55' N latitudes to 74°28' to 77°36' E longitudes (Fig. 18.1). It covers an area about 44,212 km², which is approximately 1.4% of the country's total geographical area. The state represents diversity in landscapes ranging from hills in north to alluvial plains in centre and sand dunes in south. The general direction of slope is north-east to south-west and west, whereas it is northwards in south (Srivastava et al. 2006). This pattern of slope makes a bowl-shaped landscape in central parts (Thussu 2006). Soils are generally good and suitable for cultivation for a variety of crops. Apart from this, soils are light to medium textured with 55% sandy loam, 30% loamy sand, 10% loamy and 5% sandy (Singh et al. 2010). The state exhibits dry sub-humid to arid climatic conditions (Pandey et al. 2004). The maximum temperature reaches up to 48 °C in June, whereas the minimum falls up to 1 °C during January.

Dust storms are common during summer season months (April–June) (Singh and Bhardwaj 2019). The mean annual rainfall is approximately 600 mm, which fluctuates between 300 and 1200 mm in the south-west and north-east, respectively

Table 18.1 Area and yield of crops for different time intervals in the state of Haryana during 1990–2013

Crops	Area (000 hectares)										Yield (kg/ha)									
	1990	1995	2000	2005	2010	2013	1990	1995	2000	2005	2010	2013	1990	1995	2000	2005	2010	2013		
Rice	642	796	1054	1030	1245	1215	2775	2225	2557	3051	3472	3976								
Jowar	103	110	109	100	72	56	497	238	208	272	28	36								
Bajra	627	569	608	576	661	411	864	711	1079	1117	785	1185								
Maize	41	29	15	17	10	9	1414	1824	2267	2118	23	19								
Wheat	1857	1985	2355	2323	2515	2497	3479	3697	4106	3844	11,117	11,163								
Banley	58	50	44	24	37	48	2092	2507	2682	2821	167	129								
Total	3328	3538	4186	4089	4540	4236	11,121	11,202	12,899	13,223	16,096	16,471								

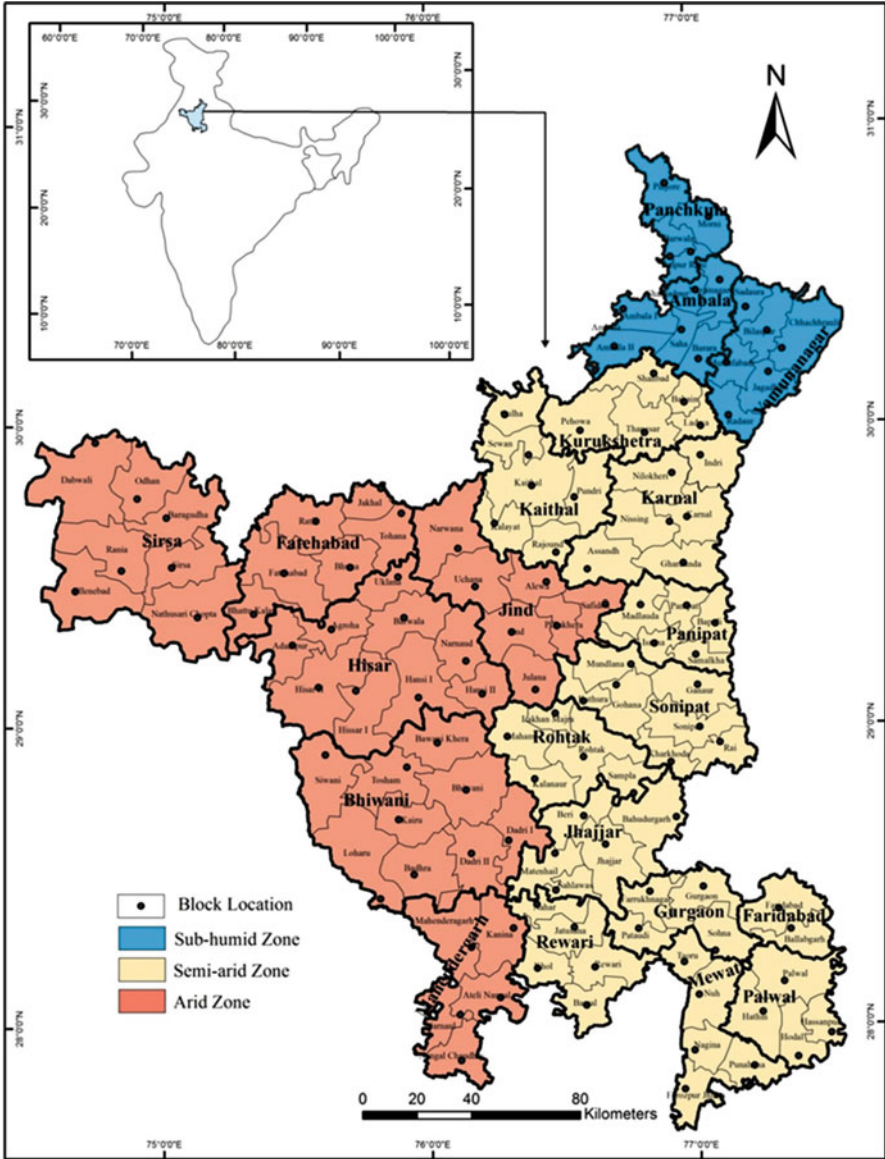


Fig. 18.1 Map showing the location of Haryana state in India along with its community development blocks, districts and climatic zones

(Bhardwaj and Singh 2018). More than 80% rainfall occurs during July, August and September months from south-west monsoon (Fig. 18.2). The coefficient of variation of rainfall is >45% over western parts, while it fluctuates amid 25–45% over eastern parts. The relative humidity is usually more in monsoon and winter months

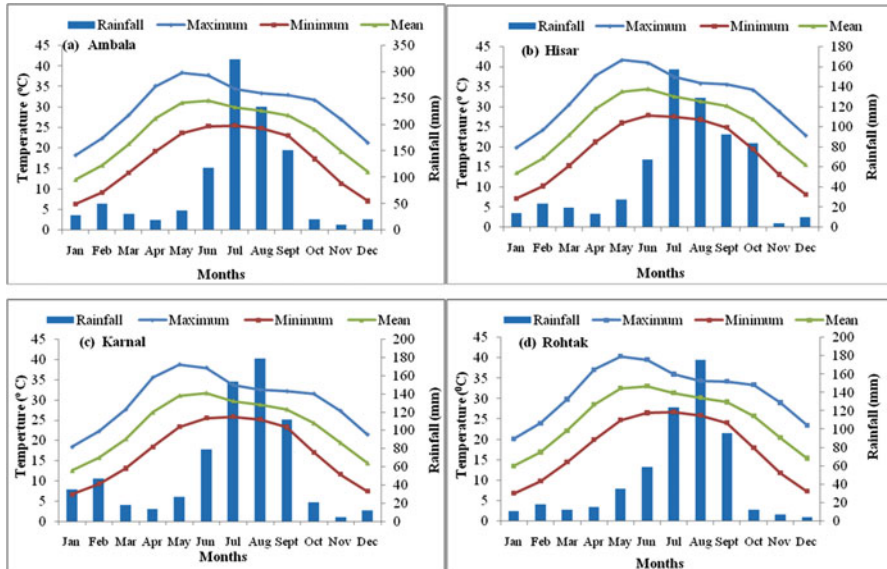


Fig. 18.2 Mean monthly temperature and rainfall in the state of Haryana during 1990–2013

ranging from 70% to 80% (Das et al. 2017). The aridity index is greater than 0.66, and potential evapotranspiration fluctuates between 1250 and 1650 mm (Murthy et al. 2015).

18.2.2 Data

The present study has been accomplished by secondary means of data. Therefore, groundwater level data of 118 community development blocks of the state has been acquired from unpublished records of Groundwater Cell, Department of Agriculture, Haryana, for the period 1990–2013. This is the only consistent and authorised source of data related to groundwater levels of the state. The obtained data has been carefully examined for consistency, continuity, analysis and interpretations to understand the behaviour and long-term patterns of groundwater levels. In addition, ancillary data pertaining to growth of tube wells, area under different crops and their yield, rainfall and temperature have been acquired from Statistical Abstract issued by the Department of Economic and Statistical Analysis, Haryana, and India Meteorological Department, Chandigarh, to assess their influence on groundwater level.

18.2.3 Methods

18.2.3.1 Calculation of Declining Groundwater Level Areas

To examine the various ranges of fall during a given period, the groundwater balance and fall in groundwater level from the declining groundwater level areas have been computed as:

Groundwater balance

$$\Delta v_f = S \left[\sum_{i=1}^n A_{fi} \bar{f}_i \right] \quad (18.1)$$

Δv_f = groundwater balance (ha-m) in falling groundwater level areas during a specific period

S = specific yield

A_{fi} = area of i^{th} falling groundwater level unit (ha)

\bar{f}_i = average fall in groundwater level in i^{th} unit (m)

n = number of falling groundwater level units

Fall in groundwater level

$$f_{wt} = \Delta v_f \div A_f T S \quad (18.2)$$

f_{wt} = fall in groundwater level per year (m)

A_f = area under falling groundwater level (ha)

T = period (years)

18.2.3.2 Calculation of Rising Groundwater Level Areas

Likewise, the water balance and rise in groundwater level for the rising groundwater level areas have been computed as:

Groundwater balance

$$\Delta v_r = S \left[\sum_{i=1}^n A_{ri} \bar{r}_i \right] \quad (18.3)$$

Δv_r = groundwater balance (ha-m) in rising groundwater level area

A_{ri} = area of i^{th} rising groundwater level unit (ha)

\bar{r}_i = average rise in groundwater level in the i^{th} unit (m)

Rise in groundwater level areas

$$R_{wt} = \Delta v_r \div A_r TS \quad (18.4)$$

R_{wt} = rise of groundwater level (m/year)

A_r = area under rising groundwater level (ha)

18.2.3.3 Calculation of Declining/Rising Groundwater Level Areas

Similarly, the net groundwater balance and net rise/fall of the groundwater level for areas having both rise and fall have also been computed as:

Net groundwater balance

$$\Delta v = \Delta v_r - \Delta v_f \quad (18.5)$$

Δv = net groundwater balance (+/−) (ha-m)

Net rise/fall of groundwater level

$$WT = \Delta v \div A \times T \times S \quad (18.6)$$

WT = rise/fall of groundwater level (m/year)

A = area in ha

Moreover, for district-wise analysis, groundwater level data for all blocks of a district has been averaged. The 24-year time has been divided into five periods, viz. 1990–1995, 1995–2000, 2000–2005, 2005–2010 and 2010–2013. To elucidate the changing behaviour of groundwater level and to identify the specific areas of rising and declining groundwater level, spatial interpolation maps have been prepared by using 118 community development blocks data for different time periods separately. The areas related with different ranges of rise and fall of groundwater level have been computed with the help of these interpolated maps. Apart from this, study area has been divided into three climatic zones as demonstrated in Fig. 18.1. The zonation scheme for the study area is based on average annual rainfall and potential evapotranspiration (Raju et al. 2013). Major characteristics of these climatic zones with respect to topography, soils, rainfall, major crops grown and specific yield have been highlighted in Table 18.2.

Table 18.2 Major characteristics of different climatic zones in the state of Haryana

Zone	Area (%)	Districts	Topography	Soil types	Annual rainfall (mm)	Major crops	Specific yield (%)
Sub-humid	9	Ambala, Panchkula, Yamunanagar	Sub-mountainous to plain	Alluvium loam to clay loam and silty loam	1000–1250	Wheat, rice, sugarcane, maize, mustard	10
Semi-arid	45	Faridabad, Gurgaon, Jhajjar, Kaithal, Karnal, Kurukshetra, Mewat, Palwal, Panipat, Rewari, Rohtak, Sonapat	Plain area	Loam to coarse loam	500–750	Wheat, rice, mustard, maize, bajra	6
Arid	46	Bhiwani, Fatehabad, Hisar, Jind, Mahendergath, Sirsa	Plain area and sub-mountainous	Silty clay to sandy and loam sand	<500	Wheat, cotton, moong, barley, cluster bean	15

18.3 Results and Discussion

18.3.1 Rise/Fall of Groundwater Level

The annual average and net rise/fall of groundwater level through the districts, climatic zones and state have been presented in Table 18.3. The state has experienced a fall of 0.7 cm/year in the average net annual groundwater level with the highest decline in Fatehabad (5.1 cm/year) and Mahendergarh (4.1 cm/year) districts. The groundwater level has decreased continuously with large fluctuations, except 1995–2000 when it has increased about 3.6 cm/year due to occurrence of floods over large parts of the state in the year 1995. Besides, Fig. 18.3a–f shows the systematic spatial pattern of rise/fall of the groundwater level for the periods 1990–1995, 1995–2000, 2000–2005, 2005–2010, 2010–2013 and 1990–2013. Remarkably, the state has exhibited a sharp fall (more than 6 m) in the groundwater level over large parts except central and central-western and two small pockets in extreme north and north-west (Fig. 18.3f). However, central parts have shown a continuous rise (about 4–6 m) in groundwater level, whereas a continuous fall has been witnessed over northern and southern parts (more than 6 m). This decline in groundwater level may be accredited to huge extraction of groundwater through installation of tube wells in large number (Table 18.4). The groundwater development over most of these parts has crossed the safe limits of groundwater exploitation and has been categorised as overexploited (Singh and Amrita 2015a, b; Singh and Kasana 2017). Besides, groundwater level in central parts is relatively high due to bowl-shaped topography, less extraction on account of poor quality of groundwater and intensive canal irrigation (Singh et al. 2020). The zone-wise description of rise/fall in groundwater level has been described in the following paragraphs.

18.3.1.1 Sub-humid Zone

In sub-humid zone, an average net annual fall of about 0.1 cm in groundwater level has been witnessed during 1990–2013 (Table 18.3). In this zone, a consistent fall has been observed in average net annual groundwater level except 1995–2000. During 1995–2000, a rise of 5.1 cm/year and a fall of approximately 15.0 and 13.2 cm/year have been observed during 2005–2010 and 2010–2013, respectively, in an average net groundwater level. Within this zone, Yamunanagar district has witnessed a fall of 0.8 cm/year, whereas Ambala and Panchkula districts have witnessed a slight rise of 0.2 and 0.4 cm/year, respectively, during 1990–2013. This decline in average net annual groundwater level in this zone is directly attributed to an increase in the number of tube wells (Table 18.4). Likewise, the area under wheat and rice cultivation has increased substantially (Table 18.5), and these crops need a huge amount of water. Therefore, to fulfil the need of irrigation, farmers have started to extract the groundwater through tube wells in this zone.

Table 18.3 District-wise fall, rise and net rise/fall (cm) in groundwater level for different time intervals in the state of Haryana during 1990–2013

Districts	1990–1995		1995–2000		2000–2005		2005–2010		2010–2013		1990–2013							
	Fall	Rise	Net rise/fall	Fall	Rise	Net rise/fall	Fall	Rise	Net rise/fall	Fall	Rise	Net rise/fall						
Sub-humid zone																		
Ambala	-16.6	15.9	-0.7	-4.0	10.9	6.9	-15.0	9.4	-5.6	-9.8	4.0	-5.8	-17.8	32.7	14.8	-2.7	2.8	0.2
Panchkula	-21.8	20.8	-1.0	-12.8	20.6	7.8	-14.9	31.0	16.1	-23.6	4.9	-18.7	-68.7	26.0	-42.7	-4.4	4.8	0.4
Yamunanagar	-13.7	6.9	-6.8	-14.3	14.8	0.5	-13.2	1.6	-11.6	-20.4	0.0	-20.4	-45.0	33.3	-11.7	-3.6	2.8	-0.8
Sub-total	-17.4	14.5	-2.8	-10.4	15.4	5.1	-14.4	14.0	-0.4	-17.9	3.0	-15.0	-43.8	30.7	-13.2	-3.6	3.5	-0.1
Semi-arid zone																		
Faridabad	-8.1	13.4	5.3	-19.2	11.5	-7.7	-15.4	5.4	-10.0	-10.4	57.6	47.2	-29.9	0.0	-29.9	-2.9	2.2	-0.7
Gurgaon	-6.4	0.0	-6.4	-14.1	18.7	4.6	-18.7	26.2	7.5	-27.2	5.9	-21.4	-28.7	25.3	-3.3	-4.3	3.9	-0.4
Jhajjar	-2.7	2.7	0.0	-4.3	15.3	11.0	-6.4	8.2	1.9	-3.2	0.0	-3.2	-13.0	21.8	8.8	-1.1	1.6	0.4
Kaithal	-18.4	7.1	-11.3	-9.9	8.2	-1.7	-18.4	0.0	-18.4	-27.0	0.0	-27.0	-31.4	0.0	-31.4	-4.5	1.4	-3.1
Karnal	-14	9.9	-4.1	-19.6	12.2	-7.5	-14.7	0.0	-14.7	-18.9	11.4	-7.5	-24.2	27.0	2.8	-3.5	2.6	-0.9
Kurukshetra	-13.4	1.8	-11.6	-3.6	9.0	5.4	-30.6	0.0	-30.6	-21.4	0.0	-21.4	-67.7	21.7	-46.0	-4.7	1.3	-3.4
Mewat	-3.8	3.3	-0.5	-9.5	26.6	17.1	-16.0	5.6	-10.4	-7.8	0.6	-7.2	-1.8	16.0	14.2	-2.2	1.6	-0.5
Palwal	-6.4	3.4	-3.0	-5.2	8.6	3.3	-11.3	15.4	4.2	-7.7	0.0	-7.7	-11.7	9.7	-2.0	-1.6	1.7	0.2
Panipat	-7.4	3.8	-3.6	-9.2	16.8	7.6	-14.1	0.0	-14.1	-11.7	38	-26.3	-28.0	24.3	-3.7	-2.2	2.7	0.5
Rewari	-10.2	9.3	-0.9	-15.2	22.4	7.2	-27.1	0.0	-27.1	-9.1	2.8	-6.3	-32.2	68.3	36.2	-3.1	3.3	0.2
Rohtak	-14.9	13.4	-1.5	-6.6	19.2	12.6	-7.9	7.9	0.0	-2.0	0.0	-2.0	-12.7	17.0	4.3	-1.4	2.1	0.7
Sonipat	-9.1	9.2	0.1	-7.5	12.2	4.7	-11.5	3.3	-8.2	-5.3	1.4	-3.9	-11.2	16.3	5.2	-2.0	1.3	-0.6
Sub-total	-9.6	6.4	-3.1	-10.3	15.1	4.7	-16.0	6.0	-10.0	-12.6	9.8	-7.2	-24.4	20.6	-3.7	-2.8	2.1	-0.6
Arid zone																		
Bhiwani	-4.2	9.2	5.0	-7.9	12.2	4.3	-15.1	23.5	8.4	-28.8	0.0	-28.8	-32.7	39.3	6.7	-4.0	3.1	-0.9
Fatehabad	-12.4	3.6	-8.8	-31.2	13.6	-17.7	-37.5	8.1	-29.4	-64.8	0.0	-64.8	-27.3	0.0	-27.3	-8.0	2.9	-5.1
Hisar	-6.4	8.2	1.8	-10.0	13.4	3.3	-9.0	14.6	5.7	-16.7	0.0	-16.7	-3.7	16.3	12.7	-3.1	2.9	-0.3

(continued)

Table 18.3 (continued)

Districts	1990-1995		1995-2000		2000-2005		2005-2010		2010-2013		1990-2013							
	Fall	Rise	Net rise/fall	Fall	Rise	Net rise/fall	Fall	Rise	Net rise/fall	Fall	Rise	Net rise/fall						
Jind	-11.6	6.0	-5.6	-11.5	21.3	9.8	-12.4	5.2	-7.2	-13.7	4.4	-9.3	-31.2	-36.3	-67.5	-2.1	2.2	0.1
Mahendragarh	-17.3	10.3	-7.0	-36.3	28.7	-7.6	-92.4	20.3	-72.1	-38.4	0.0	-38.4	-33.3	100.7	67.3	-9.1	5.0	-4.1
Sirsa	-7.2	9.8	2.7	-4.1	7.0	2.9	-7.1	0.0	-7.1	-29.4	16.6	-12.8	-9.3	16.7	7.3	-2.8	1.7	-1.1
Sub-total	-9.9	7.9	-2.0	-16.8	16.0	-0.8	-28.9	12.0	-17.0	-32.0	3.5	-28.5	-22.9	22.8	-0.1	-4.9	3.0	-1.9
State	-12.2	9.5	-2.8	-11.8	15.4	3.6	-18.3	10.0	-8.3	-18.7	6.1	-12.4	-30.5	24.5	-6.1	-3.5	2.8	-0.7

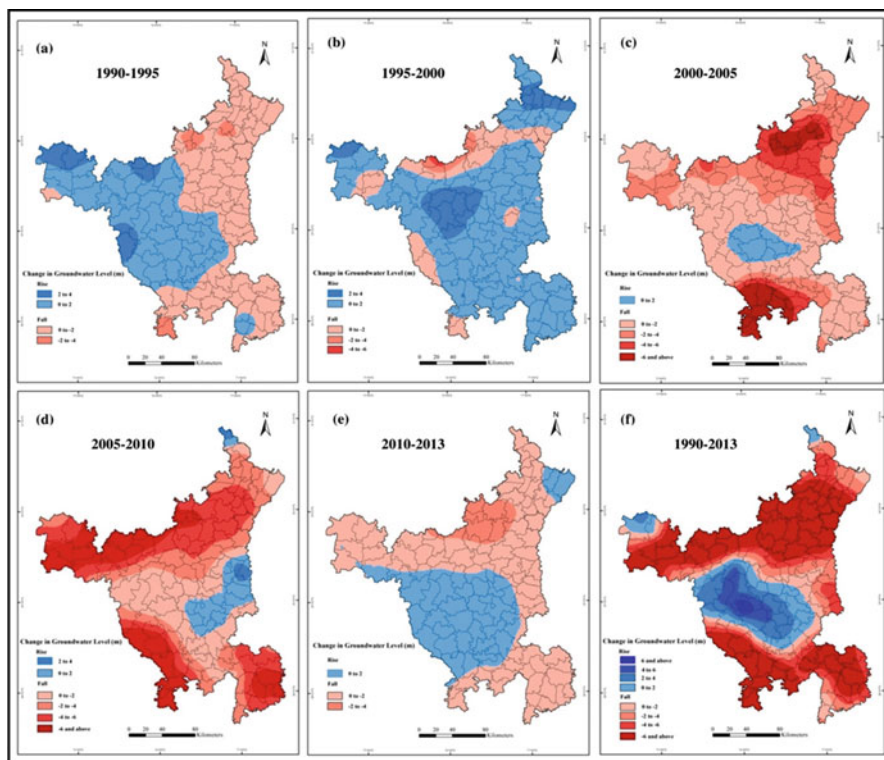


Fig. 18.3 Pattern of groundwater level for different time intervals in the state of Haryana during 1990–2013

18.3.1.2 Semi-arid Zone

Like sub-humid zone, semi-arid zone has revealed a fall of about 0.6 cm/year in net groundwater level (Table 18.3). A consistent fall has been witnessed in average net annual groundwater level in the zone except 1995–2000. During 1995–2000, the groundwater level has witnessed an average net rise of 4.7 cm/year. However, a fall of approximately 10.0 cm/year has been observed during 2000–2005. Within this zone, out of 12 districts, 7 districts, namely, Kurukshetra, Kaithal, Karnal, Faridabad, Sonapat, Mewat and Gurgaon, have recorded a fall, whereas Rohtak, Panipat, Jhajjar, Palwal and Rewari districts have recorded an average net annual rise in groundwater level during the study period. Apart from this, the northern districts of this zone, namely, Kaithal, Karnal and Kurukshetra, have the highest acreage under rice and wheat cultivation; therefore groundwater extraction through tube wells is very high (Fig. 18.3f; Table 18.5). Conversely, central parts have witnessed a rising groundwater level, whereas very low groundwater level in the southern parts of this zone can be accredited to enhanced processes of industrial development and

Table 18.4 District-wise growth of tube wells for different time intervals in the state of Haryana during 1990–2013

Districts	1990	1995	2000	2005	2010	2013
Sub-humid zone						
Ambala	24,300 (50.4)	19,789 (43.6)	20,136 (40.0)	22,240 (40.0)	26,316 (42.6)	28,127 (42.3)
Panchkula	0 (0.0)	0 (0.0)	4958 (10.0)	4537 (8.0)	4652 (7.5)	5091 (7.7)
Yamunanagar	23,820 (49.6)	25,588 (56.4)	26,632 (50.0)	28,561 (52.0)	30,865 (49.9)	33,254 (50.0)
Sub-total	48,120 (9.7)	45,377 (8.3)	51,726 (8.8)	55,338 (9.07)	61,833 (8.6)	66,472 (8.6)
Semi-arid zone						
Faridabad	26,339 (8.2)	27,976 (8.3)	24,849 (6.9)	28,251 (7.8)	10,061 (2.5)	10,678 (2.5)
Gurgaon	39,351 (12.2)	32,845 (9.8)	31,888 (8.8)	22,764 (6.3)	24,576 (6.0)	26,319 (6.1)
Jhajjar	0 (0.0)	0 (0.0)	32,974 (9.1)	33,624 (9.3)	29,312 (7.2)	29,394 (6.9)
Kaithal	57,454 (7.8)	36,448 (10.8)	50,470 (14.0)	53,539 (14.8)	60,772 (14.9)	64,244 (15.0)
Karnal	59,476 (18.4)	59,072 (17.5)	65,412 (18.1)	68,057 (18.8)	40,347 (9.9)	44,204 (10.3)
Kurukshetra	32,474 (10.1)	33,877 (10.1)	36,218 (10.0)	37,251 (10.3)	71,910 (17.6)	74,944 (17.5)
Mewat	0 (0.0)	0 (0.0)	0 (0.0)	0 (0.0)	15,657 (3.8)	16,334 (3.8)
Palwal	0 (0.0)	0 (0.0)	0 (0.0)	0 (0.0)	25,150 (6.2)	25,529 (6.0)
Panipat	36,459 (11.3)	27,136 (8.1)	29,411 (8.1)	32,244 (8.9)	31,929 (7.8)	34,313 (8.0)
Rewari	23,075 (7.1)	27,433 (8.1)	27,955 (7.7)	30,600 (8.5)	33,531 (8.2)	35,884 (8.4)
Rohtak	21,676 (6.7)	51,399 (15.3)	19,869 (5.5)	16,896 (4.7)	19,989 (4.9)	19,785 (4.6)
Sonapat	26,722 (8.3)	40,488 (12.0)	41,959 (11.6)	38,177 (10.6)	44,265 (10.9)	46,041 (10.8)
Sub-total	323,026 (64.9)	336,674 (61.4)	361,005 (61.2)	361,403 (58.5)	407,499 (56.9)	427,669 (55.4)
Arid zone						
Bhiwani	18,151 (14.4)	27,134 (16.4)	28,726 (16.3)	30,551 (16.4)	51,174 (20.8)	57,891 (20.8)
Fatehabad	0 (0.0)	0 (0.0)	27,411 (15.5)	30,464 (16.3)	30,102 (12.2)	40,736 (14.6)
Hisar	33,069 (26.1)	50,942 (30.7)	26,480 (15.0)	23,153 (12.4)	31,101 (12.6)	32,713 (11.8)
Jind	29,648 (23.4)	35,158 (21.2)	40,645 (23.0)	39,589 (21.2)	50,201 (20.4)	53,485 (19.2)
Mahendgarh	22,943 (18.1)	24,410 (14.7)	20,929 (11.8)	23,586 (12.6)	27,408 (11.1)	30,442 (10.9)
Sirsa	22,664 (17.9)	28,283 (17.0)	32,551 (18.4)	39,233 (21.0)	56,229 (22.8)	62,902 (22.6)
Sub-total	126,475 (25.4)	165,927 (30.3)	176,742 (30.0)	186,576 (30.2)	246,215 (34.0)	278,169 (36.0)
State	497,621 (100.0)	547,978 (100.0)	589,473 (100.0)	617,835 (100.0)	715,547 (100.0)	772,310 (100.0)

Figures in parentheses are percentages

Table 18.5 District-wise area under rice-wheat crops (000 ha) for different time intervals in the state of Haryana during 1990–2013

Districts	1990		1995		2000		2005		2010		2013	
	Rice	Wheat	Rice	Wheat	Rice	Wheat	Rice	Wheat	Rice	Wheat	Rice	Wheat
Sub-humid zone												
Ambala	64	90	67	84	72	79	74	83	82	87	83	87
Panchkula	0	0	0	0	6	17	7	18	9	16	10	16
Yamunanagar	44	62	44	61	56	62	59	73	75	83	73	85
Sub-total	108	152	111	145	134	158	140	174	166	186	166	188
Semi-arid zone												
Faridabad	9	120	14	122	29	134	29	136	10	32	12	31
Gurgaon	1	89	5	102	8	137	7	116	5	51	5	52
Jhajjar	0	0	0	0	17	105	15	88	31	101	31	99
Kaithal	109	176	128	168	164	153	153	175	159	178	159	173
Karnal	121	132	159	165	158	167	168	171	173	171	165	172
Kurukshetra	92	107	112	102	112	109	122	114	120	114	121	112
Mewat	0	0	0	0	0	0	0	0	6	73	6	71
Palwal	0	0	0	0	0	0	0	0	33	98	33	97
Panipat	75	111	63	80	77	83	73	84	77	87	76	87
Rewari	0	42	0	44	1	55	0	45	2	51	3	48
Rohatak	7	196	9	147	24	92	14	84	39	102	34	103
Sonapat	22	83	46	130	77	140	66	133	94	144	95	162
Sub-total	436	1056	536	1060	667	1175	647	1146	749	1202	740	1207
Arid zone												
Bhiwani	0	65	0	73	8	144	12	127	21	159	18	151
Fatehabad	0	0	0	0	61	174	66	178	88	187	87	189
Hisar	31	251	55	297	33	207	29	203	45	222	43	237
Jind	45	151	64	175	112	207	91	206	114	216	115	217
Mahendgarh	0	34	0	36	0	49	0	41	0	46	0	41
Sirsa	22	149	31	200	40	244	45	248	61	290	63	299
Sub-total	98	650	150	781	254	1025	243	1003	329	1120	326	1134
State	642	1858	797	1986	1055	2358	1030	2323	1244	2508	1232	2529

resultant urbanisation. Also, groundwater has been exploited sharply due to inadequate surface water facilities in southern parts of this zone.

18.3.1.3 Arid Zone

This zone has witnessed the highest fall of about 1.9 cm/year in net groundwater level during 1990–2013 (Table 18.3). However, the highest fall of approximately 28.5 cm/year has been observed during 2005–2010. Within arid zone, all the districts have witnessed a fall in average net annual groundwater level except Jind district, which has recorded a slight rise of 0.1 cm/year during the study period. Similarly, parts of Bhiwani, Hisar and Fatehabad districts have also witnessed a rise in groundwater level (Fig. 18.2f). This rise in groundwater level can be ascribed to poor quality, growing of non-paddy crops and availability of canal water (Ambast et al. 2006). Apart from this, a fall in groundwater levels in south-western parts of this zone is anomalously attributed to hard rock topography as well as less availability of canal water.

18.3.2 Groundwater Balance

The state has witnessed a negative groundwater balance, i.e. -1361.6 (00 ha-m), during 1990–2013 (Table 18.6). However, during 2005–2010, the highest negative net groundwater balance (-5271.5) has been recorded, while it has been found highest positive during 1995–2000 (651.0). The net rise/fall in groundwater balance has ranged from -442.7 (Fatehabad district) to 27.8 (Rohtak district) in Haryana. The zone-wise status of groundwater balance is as follows.

18.3.2.1 Sub-humid Zone

In sub-humid zone, a negative groundwater balance, i.e. -17.6 (00 ha-m), has been witnessed during 1990–2013 (Table 18.6). This zone has continuously recorded a negative groundwater balance except 1995–2000. During 1995–2000, the net groundwater balance has been found to the tune of 93.7, whereas it has been found about -309.8 (00 ha-m) during 2005–2010. The positive groundwater balance during 1995–2000 is chiefly attributed to the good quantity of rainfall and commencement of watershed management projects in this zone. Within the sub-humid zone, Yamunanagar district has recorded a negative groundwater balance (-31.7), whereas Ambala and Panchkula districts have recorded a positive groundwater balance to the tune of 6.3 and 7.8 (00 ha-m), respectively. Overall, quantity of groundwater balance and measures implemented previously are relatively suitable, so necessity to be continued for sustaining favourable groundwater regime. Also, presence of perennial (Yamuna) and seasonal rivulets (Ghaggar, Tangri, Bengana,

Table 18.6 District-wise groundwater balance per year (00 ha-m) in declining and rising groundwater level areas and net groundwater balance for different time intervals in the state of Haryana during 1990–2013

Districts	1990–1995			1995–2000			2000–2005			2005–2010			2010–2013			1990–2013		
	Fall	Rise	Net rise/fall	Fall	Rise	Net rise/fall	Fall	Rise	Net rise/fall	Fall	Rise	Net rise/fall	Fall	Rise	Net rise/fall	Fall	Rise	Net rise/fall
Sub-humid zone																		
Ambala	-130.6	125.1	-5.5	-31.5	85.8	54.3	-117.7	74.0	-43.7	-76.8	31.5	-45.3	-84.2	154.3	70.0	-96.4	102.7	6.3
Panchkula	-97.9	93.4	-4.5	-57.5	92.5	35.0	-66.9	139.2	72.3	-106.0	21.9	-84.1	-185.0	70.0	-114.9	-91.8	99.6	7.8
Yamunanagar	-121.4	61.0	-60.4	-126.4	130.8	4.4	-116.7	14.1	-102.5	-180.3	0.0	-180.3	-238.7	176.8	-61.9	-146.0	114.3	-31.7
Sub-total	-349.9	279.5	-70.4	-215.4	309.1	93.7	-301.2	227.3	-73.9	-363.1	53.3	-309.8	-507.9	401.1	-106.8	-334.2	316.6	-17.6
Semi-arid zone																		
Faridabad	-31.8	52.5	20.6	-75.2	45.2	-30.0	-60.3	21.1	-39.2	-40.6	225.5	184.9	-70.2	0.0	-70.2	-52.5	40.4	-12.1
Gurgaon	-38.8	0.0	-38.8	-86.2	114.1	27.9	-113.8	159.8	46.1	-166.2	35.8	-130.4	-104.9	92.7	-12.2	-122	109.8	-12.2
Jhajjar	-37.1	37.6	0.5	-59.6	210.5	150.8	-87.3	112.8	25.4	-44.0	0.0	-44.0	-107.3	180.2	72.9	-71.8	98.3	26.6
Kaithal	-213.2	81.9	-131.3	-115.1	95.0	-20.1	-212.7	0.0	-212.7	-313.3	0.0	-313.3	-218.6	0.0	-218.6	-238.5	72.2	-166.3
Karnal	-176.4	124.7	-51.7	-247.0	153.1	-93.9	-185.5	0.0	-185.5	-238.4	143.6	-94.8	-182.7	204.1	21.4	-203.8	152.3	-51.5
Kurukshetra	-102.5	13.8	-88.7	-27.9	68.8	40.9	-233.8	0.0	-233.8	-164.0	0.0	-164	-310.6	99.4	-211.1	-164.6	44.4	-120.2
Mewat	-28.4	24.9	-3.5	-70.7	198.7	128.0	-119.5	41.8	-77.7	-58.0	4.5	-53.5	-8.2	71.7	63.5	-75.1	56.6	-18.4
Palwal	-43.8	23.3	-20.5	-35.6	58.5	22.9	-77.0	105.3	28.4	-52.7	0.0	-52.7	-47.9	39.7	-8.2	-49.4	54.7	5.3
Panipat	-46.6	24.1	-22.5	-58.3	106.5	48.2	-89.3	0.0	-89.3	-74.1	-240.9	-315	-106.5	92.6	-13.9	-64.9	79.0	14.1
Rewari	-121.9	111.2	-10.8	-181.7	267.8	86.1	-323.7	0.0	-323.7	-109.0	33.5	-75.6	-230.7	490.2	259.4	-172.7	182.9	10.2
Rohtak	-130.0	116.9	-13.1	-57.6	167.5	109.9	-68.6	68.9	0.3	-17.4	0.0	-17.4	-66.3	89.0	22.7	-55.2	83.0	27.8
Sonapat	-96.9	97.6	0.7	-79.2	129.4	50.2	-121.7	35.0	-86.6	-55.7	14.9	-40.8	-71.1	104.0	32.9	-96.3	65.1	-31.2
Sub-total	-1067.4	708.5	-359.1	-1094.1	1615.1	520.9	-1693.2	544.7	-1148.3	-1333.4	216.9	-1116.6	-1525	1463.6	-61.4	-1366.8	1038.7	-327.9
Arid zone																		
Bhiwani	-150.5	329.7	179.2	-283.1	437.2	154.1	-542.3	842.1	299.8	-1032.0	0.0	-1032	-702.4	845.7	143.3	-652.2	508.3	-143.9
Fatehabad	-236	68.5	-167.5	-593.9	257.9	-336.0	-713.8	153.5	-560.3	-1232.5	0.0	-1232.5	-312.2	0.0	-312.2	-696.7	254.0	-442.7
Hisar	-191.2	243.5	52.3	-298.7	398.8	100.1	-267.4	436.1	168.8	-498.9	0.0	-498.9	-65.7	292.8	227.0	-291.4	298.7	7.3
Jind	-156.7	81.1	-75.7	-155.4	288.2	132.8	-167.5	70.3	-97.3	-185.4	59.4	-125.9	-252.6	-294.5	-547.2	-193.8	178.0	-15.7
Mahendgarh	-246.9	146.7	-100.2	-517.0	409.2	-107.8	-1316	289.1	-1026.9	-546.9	0.0	-546.9	-284.9	860.2	575.4	-593.9	328.5	-265.4
Sirsa	-231.0	316.0	85.0	-131.5	224.5	93.0	-228.4	0.0	-228.4	-941.5	532.5	-409	-179.6	320.8	141.1	-411.5	255.9	-155.6
Sub-total	-1212.3	1185.5	-26.9	-1979.6	2015.8	36.2	-3235.4	1791.1	-1444.3	-4437.2	591.9	-3845.2	-1797.4	2025.0	227.4	-2839.5	1823.4	-1016
State	-2629.7	2173.3	-456.4	-3289.0	3940.1	651.0	-5229.8	2563.4	-2666.4	-6133.6	862.1	-5271.5	-3830.3	3889.6	59.3	-4540.6	3179.0	-1361.6

Markanda, Somb, Pathrala, etc.) in this zone has helped in maintaining balanced quantities of groundwater.

18.3.2.2 Semi-arid Zone

In semi-arid zone, a negative groundwater balance to the tune of -327.9 (00 ha-m) has been witnessed during the study period (Table 18.6). Like sub-humid zone, this zone has also continuously recorded a negative groundwater balance except 1995–2000. During 1995–2000, net groundwater balance has been found to be 520.9, whereas it has been recorded to the tune of -1148.3 during 2000–2005. The major cause behind a negative groundwater balance particularly in northern districts (Kurukshetra, Karnal and Kaithal) of this zone is attributed to installation of tube wells in large numbers and rapid increase in area under rice and wheat cultivation (Tables 18.4 and 18.5). An increase in area under these crops has led to more pressure on groundwater resources as surface water supply for irrigation is restricted. Farmers have adopted rice and wheat crops eagerly without considering the falling groundwater level on account of state government's purchasing policy of all rice and wheat at a minimum support price, which is unavailable for other crops (Chawla et al. 2010). Besides, the state government charge subsidized electricity rates (flat rates) for running tube wells which results in more decline of groundwater level. Interestingly, collective impact of these policies has resulted in mass level exploitation of groundwater, which caused very high negative groundwater balance in this zone. Also, lack of strict legislations regarding groundwater withdrawals has played havoc with groundwater resources. The central districts of this zone, namely, Panipat, Rohtak and Jhajjar, have witnessed a positive groundwater balance, whereas southern districts of this zone have witnessed both positive and negative groundwater balances.

18.3.2.3 Arid Zone

In arid zone, net groundwater balance is highly negative (-1016.0) (00 ha-m) than other two climatic zones, and a wide variation has been noticed in it over the study period (Table 18.6). The net groundwater balance has been found to be -3845.2 ha-m in 2005–2010, whereas it has been observed to the tune of 227.4 ha-m in 2010–2013. Among the climatic zones, this zone receives the least amount of rainfall (Table 18.7); therefore, replenishment of groundwater is at its minimum level. Conversely, the area under rice and wheat crops has increased almost consistently in all districts of this zone except Mahendergarh over the study period. An increase in area under these crops needs more water to fulfil the irrigation demand, which can only be met with extraction of groundwater through tube wells. Consequently, a consistent increase in installation of number of tube wells has been witnessed (Table 18.4). Prevalence of fresh water availability in Ghaggar flood plain along with recharge through canal seepage promotes the farmers for installation of tube

Table 18.7 District-wise average annual rainfall (mm) for different time intervals in the state of Haryana during 1990–2013

Districts	1990–1995	1995–2000	2000–2005	2005–2010	2010–2013	1990–2013
Sub-humid zone						
Ambala	1039	1031	1028	986	938	1004
Panchkula	1039	1135	1015	829	846	972
Yamunanagar	1093	761	880	951	930	923
Sub-total	1057	976	974	922	905	967
Semi-arid zone						
Faridabad	544	453	624	512	488	524
Gurgaon	519	464	549	616	487	527
Jhajjar	596	256	454	496	236	408
Kaithal	592	622	526	566	539	569
Karnal	589	949	546	466	329	576
Kurukshetra	615	610	591	481	278	515
Mewat	519	464	549	560	411	501
Palwal	544	453	624	556	486	533
Panipat	497	412	398	502	500	462
Rewari	564	457	566	591	437	523
Rohtak	596	292	535	446	226	419
Sonipat	609	442	534	584	659	566
Sub-total	565	490	541	531	423	510
Arid zone						
Bhiwani	371	305	387	451	335	370
Fatehabad	318	238	292	362	258	294
Hisar	318	251	380	320	248	303
Jind	448	357	531	536	521	479
Mahendergarh	482	394	293	514	529	442
Sirsa	288	197	243	318	311	271
Sub-total	371	290	354	417	367	360
State	664	585	623	623	565	612

wells in this zone, thereby resulting in the largest negative groundwater balance among the different climatic zones of the state.

18.3.3 Areas of Declining and Rising Groundwater Level

Table 18.8 shows the average declining and rising groundwater level areas for different time intervals across the districts. Approximately 77% area of the state has been found under declining groundwater level during 1990–2013, whereas only 23% area has witnessed a rise in groundwater level. The declining groundwater level area has ranged from 17% in 1995–2000 to 94% in 2000–2005, while rising

Table 18.8 District-wise average declining and rising groundwater level areas for different time intervals in the state of during 1990–2013

Districts	Total area (00 ha)										
	Declining groundwater level area (00 ha-m)					Rising groundwater level area (00 ha-m)					
	1990–1995	1995–2000	2000–2005	2005–2010	2010–2013	1990–2013	1995–2000	2000–2005	2005–2010	2010–2013	1990–2013
Sub-humid zone											
Ambala	1574 (100.0)	0 (0.0)	1574 (100.0)	1574 (100.0)	1574 (100.0)	1574 (100.0)	1574 (100.0)	0 (0.0)	0 (0.0)	0 (0.0)	0 (0.0)
Panchkula	898 (100.0)	0 (0.0)	898 (1000)	626 (70.0)	898 (1000)	689 (77.0)	898 (100.0)	0 (0.0)	0 (0.0)	272 (30.0)	209 (23.0)
Yamunanagar	1768 (100.0)	324 (18.0)	1768 (100.0)	1768 (100.0)	1768 (100.0)	1768 (100.0)	1444 (82.0)	0 (0.0)	0 (0.0)	0 (0.0)	1052 (60.0)
Sub-total	4240 (100.0)	324 (8.0)	4240 (100.0)	3968 (93.6)	3188 (75.0)	4031 (95.1)	3916 (92.0)	0 (0.0)	0 (0.0)	272 (6.4)	209 (4.9)
Semi-arid zone											
Faridabad	783 (100.0)	0 (0.0)	783 (1000)	783 (100.0)	783 (100.0)	783 (100.0)	783 (100.0)	0 (0.0)	0 (0.0)	0 (0.0)	0 (0.0)
Gurgaon	1220 (100.0)	22 (2.0)	1220 (100.0)	1220 (100.0)	1220 (100.0)	1220 (100.0)	1198 (98.0)	0 (0.0)	0 (0.0)	0 (0.0)	0 (0.0)
Jhajjar	1834 (100.0)	729 (40.0)	1698 (93.0)	1470 (80.0)	249 (14.0)	912 (50.0)	1834 (100.0)	1105 (60.0)	0 (0.0)	364 (20.0)	922 (50.0)
Kaithal	2317 (91.0)	1306 (56.0)	2317 (100.0)	2317 (100.0)	2317 (100.0)	2317 (100.0)	1011 (44.0)	197 (9.0)	0 (0.0)	0 (0.0)	0 (0.0)
Karnal	2520 (100.0)	150 (6.0)	2520 (100.0)	2439 (100.0)	2520 (100.0)	2520 (100.0)	2370 (94.0)	0 (0.0)	0 (0.0)	81 (3.0)	0 (0.0)
Kurukshetra	1530 (100.0)	1159 (76.0)	1530 (100.0)	1530 (100.0)	1530 (100.0)	1530 (100.0)	371 (24.0)	0 (0.0)	0 (0.0)	0 (0.0)	0 (0.0)
Mewat	1494 (69.0)	0 (0.0)	1494 (100.0)	1494 (100.0)	1494 (100.0)	1494 (100.0)	1494 (100.0)	470 (31.0)	0 (0.0)	0 (0.0)	0 (0.0)
Palwal	1368 (100.0)	0 (0.0)	1368 (100.0)	1368 (100.0)	1368 (100.0)	1368 (100.0)	1368 (100.0)	0 (0.0)	0 (0.0)	0 (0.0)	0 (0.0)
Panipat	1268 (100.0)	84 (7.0)	1268 (100.0)	351 (28.0)	1268 (100.0)	1268 (100.0)	1184 (93.0)	0 (0.0)	0 (0.0)	917 (72.0)	0 (0.0)

Rewari	1594	1450 (91.0)	0 (0.0)	1594 (100.0)	1594 (100.0)	1129 (71.0)	1594 (100.0)	144 (9.0)	1594 (100.0)	0 (0.0)	0 (0.0)	0 (0.0)	465 (29.0)	0 (0.0)
Rohtak	1745	1745 (100.0)	0 (0.0)	1034 (59.0)	499 (29.0)	0 (0.0)	81 (5.0)	0 (0.0)	1745 (100.0)	711 (41.0)	1246 (71.0)	1745 (100.0)	1664 (95.0)	
Sonipat	2122	2122 (100.0)	366 (1.7)	2122 (100.0)	964 (45.0)	1277 (60.0)	1748 (82.0)	0 (0.0)	1756 (83.0)	0 (0.0)	1158 (55.0)	845 (40.0)	374 (18.0)	
Sub-total	19,795	17,879 (90.0)	3087 (16.0)	18,948 (96.0)	16,029 (81.0)	15,155 (77.0)	16,835 (85.0)	1916 (10.0)	16,708 (84.0)	847 (4.0)	3766 (19.0)	4640 (23.0)	2960 (15.0)	
Arid zone														
Bhiwani	4778	0 (0.0)	1170 (24.0)	3046 (64.0)	4778 (100.0)	0 (0.0)	2425 (51.0)	4778 (100.0)	3608 (76.0)	1732 (36.0)	0 (0.0)	4778 (100.0)	2353 (49.0)	
Fatehabad	2538	0 (0.0)	964 (38.0)	2538 (100.0)	2538 (100.0)	2430 (96.0)	2538 (100.0)	2538 (100.0)	1574 (62.0)	0 (0.0)	0 (0.0)	108 (4.0)	0 (0.0)	
Hisar	3983	0 (0.0)	0 (0.0)	3848 (97.0)	3983 (100.0)	662 (17.0)	497 (12.0)	3983 (100.0)	3983 (100.0)	135 (3.0)	0 (0.0)	3321 (83.0)	3486 (88.0)	
Jind	2702	1278 (47.0)	465 (17.0)	2702 (100.0)	2702 (100.0)	1942 (72.0)	2441 (90.0)	1424 (53.0)	2237 (83.0)	0 (0.0)	0 (0.0)	760 (28.0)	261 (100)	
Mahendgarh	1899	1620 (85.0)	460 (24.0)	1899 (100.0)	1899 (100.0)	1041 (55.0)	1899 (100.0)	279 (15.0)	1439 (76.0)	0 (0.0)	0 (0.0)	858 (45.0)	0 (0.0)	
Sirsa	4277	278 (6.0)	947 (22.0)	4277 (100.0)	4277 (100.0)	3784 (88.0)	3568 (83.0)	3999 (94.0)	3330 (78.0)	0 (0.0)	0 (0.0)	493 (12.0)	709 (17.0)	
Sub-total	20,177	3176 (16.0)	4006 (20.0)	18,310 (91.0)	20,177 (100.0)	9859 (49.0)	13,368 (66.0)	17,001 (84.0)	16,171 (80.0)	1867 (9.0)	0 (0.0)	10,318 (51.0)	6809 (34.0)	
State	44,212	25,295 (57.0)	7417 (17.0)	41,498 (94.0)	40,174 (91.0)	28,202 (64.0)	34,234 (77.0)	18,917 (43.0)	36,795 (83.0)	2714 (6.0)	4038 (9.0)	16,010 (36.0)	9978 (23.0)	

Figures in parentheses are percentages of the total area

groundwater level area has varied from 6% in 2000–2005 to 83% in 1995–2000. The zone-wise status of declining and rising of groundwater level areas has been presented in the following subsections.

18.3.3.1 Sub-humid Zone

In sub-humid climatic zone, about 95% of the total area has witnessed a decline in groundwater levels during 1990–2013 (Table 18.8). Out of three districts of this zone, two districts, namely, Ambala and Yamunanagar, have noticed a decline in groundwater level areas in all parts. Exceptionally, about 23% area of Panchkula district has witnessed a rise in groundwater level due to increase in water storage in several water harvesting and other soil conservation structures in hilly parts, which finally enhanced groundwater recharge.

18.3.3.2 Semi-arid Zone

In this zone, about 85% of the total area has recorded a decline, while 15% area has witnessed a rise in groundwater level during 1990–2013 (Table 18.8). Out of 12 districts, 9 districts have witnessed a decline in groundwater level in all the parts, whereas in the remaining 3 districts, namely, Rohtak, Jhajjar and Sonipat, a decline of about 5%, 50% and 82% area, respectively, has been witnessed. These findings reveal that large parts of Rohtak and Jhajjar districts suffer from the problem of waterlogging. This problem in these districts can be attributed to the nature of topography and recharge through seepage of canal water in this zone.

18.3.3.3 Arid Zone

In arid climatic zone of the state, about 77% of the total area has witnessed a decline, whereas about 23% area has recorded a rise in groundwater level during 1990–2013 (Table 18.8). All parts of Mahendergarh and Fatehabad districts have experienced a decline in groundwater level area due to absence of surface water resources. Conversely, large parts of Hisar and Bhiwani districts have witnessed a rise in groundwater level on account of round-the-clock canal water supply and growing of non-paddy crops. In the same way, minuscule parts of Sirsa and Jind districts have been suffering from rising groundwater level areas (Fig. 18.3f).

Finally, Table 18.9 presents the overall scenario of groundwater balance and rise/fall in groundwater level during the study period. The net groundwater balance has been found negative (−1361.6) in the state. However, the net groundwater balance has been found positive to the tune of 651 and 59.3 (00 ha-m) during the periods 1995–2000 and 2010–2013, respectively. The groundwater balance in declining groundwater level areas has been found negative to the tune of −4540.6 (00 ha-m), whereas it has been witnessed in positive direction to the tune of 3179.0 (00 ha-

Table 18.9 Groundwater balance and rise/fall of groundwater level for different time intervals in the state of Haryana during 1990–2013

Particulars	1990–1995	1995–2000	2000–2005	2005–2010	2010–2013	1990–2013
Groundwater balance in declining groundwater level area (ha-m)	-2629.7	-3289.0	-5229.8	-6133.6	-3830.3	-4540.6
Groundwater balance in rising groundwater level area (ha-m)	2173.3	3940.1	2563.4	862.1	3889.6	3179.0
Net groundwater balance (ha-m)	-456.4	651.0	-2666.4	-5271.5	59.3	-1361.6
Rise/fall of groundwater level in declining groundwater level areas (cm/year)	-12.2	-11.8	-18.3	-18.1	-30.5	-3.5
Rise/fall of groundwater level in rising groundwater level areas (cm/year)	9.5	15.4	10.0	3.3	24.5	2.8

m) in rising groundwater level areas. The groundwater level in declining groundwater level areas has been found declining at the rate of 3.5 cm/years, whereas it has been rising at the marginal rate of 2.8 cm/year in rising groundwater level areas through the study period.

18.4 Conclusions

This study has been attempted to examine the long-term groundwater behaviour in Haryana state under rice-wheat ecosystem, which is regarded as an agriculturally developed state in north-west India. The findings from the study reveal a sharp fall (more than 6 m) in groundwater level over large parts of the state except central and central-western parts and two small pockets in extreme north and north-west. Exceptionally, the state has witnessed a marginal rise in groundwater level during

the period 1995–2000 due to occurrence of floods over large parts in the year 1995. Likewise, central parts of the state have witnessed a continuous rise (about 4–6 m) in groundwater level during the study period, whereas a continuous fall has been witnessed over northern and southern parts (more than 6 m). Groundwater level in central parts is relatively high due to the bowl-shaped topography of this region. Both of these situations are harmful for the sustainability of agriculture as well as groundwater resources in the state. The state as a whole has a negative groundwater balance to the tune of -1361.6 (00 ha-m) with high temporal variations. During the period 2005–2010, net groundwater balance has been observed to be -5271.5 (00 ha-m), whereas it has been found about 651 (00 ha-m) during the period 1995–2000. Moreover, approximately 77% of the total area of the state has witnessed a decline in groundwater level, whereas only 23% area has witnessed a rise in groundwater level area. Similarly, groundwater levels in declining groundwater level areas have been marginally declining at the rate of 3.5 cm/years, whereas it is also rising at the marginal rate of 2.8 cm/year in rising groundwater level areas. Finally, from the point of view of future use of groundwater resources in the state, central parts are relatively safe, while the northern and southern parts are worst-hit. Therefore, immediate remedial measures are required to be taken up to control the fast-receding groundwater levels in this agriculturally developed state on behalf of the water resource managers for sustainability of the resource as well as for food production.

References

- Ambast, S.K., Tyagi, N.K., & Raul, S.K. (2006). Management of declining groundwater in the Trans Indo-Gangetic Plain (India): Some options. *Agricultural Water Management*, 82, 279–296.
- Amrita. (2017). Dynamics and economy of groundwater resources in Haryana. Ph.D. thesis. Department of Geography, Kurukshetra University, Kurukshetra.
- Bassi, N. (2014). Assessing potential of water rights and energy pricing in making groundwater use for irrigation sustainable in India. *Water Policy*, 16, 442–453.
- Bhardwaj, P., & Singh, O. (2018) Spatial and temporal analysis of thunderstorm and rainfall activity over India. *Atmosfera*, 31(3), 255–284.
- Chambers, R., Saxena, N.C., & Shah, T. (1989). *To the hands of the poor, water and trees*. New Delhi, Oxford and IBH Publishing Company.
- Chawla, J. K., Khepar, S. D., Sondhi, S.K., & Yadav, A. K. (2010). Assessment of long-term groundwater behaviour in Punjab, India. *Water International*, 35, 63–77.
- Das, P. K., Sahay, B., Seshasai M. V. R., & Dutta, D. (2017) Generation of improved surface moisture information using angle-based drought index derived from Resourcesat-2 AWiFS for Haryana state, India. *Geomatics, Natural Hazards and Risk*, 8(2), 271–281.
- Dhawan, B. D. (1989). *Studies in Irrigation and Water Management*. New Delhi: Commonwealth Publishers.
- Gleeson, T., Vander Steen, J., Sophocleous, A. A., Taniguchi, M., Alley, W. M., Allen, D. M., & Zhou, Y. (2010) Commentary: Groundwater sustainability strategies. *Nature Geoscience*, 3, 378–379.
- Goyal, S.K., Chaudhary, B. S., Singh, O., Sethi, G. K., & Thakur, P. K. (2010a). Variability analysis of groundwater levels: A GIS based case study. *Journal of the Indian Society of Remote Sensing*, 38, 355–364.

- Goyal, S.K., Chaudhary, B. S., Singh, O., Sethi, G. K., & Thakur, P. K. (2010b). GIS based spatial distribution mapping and suitability evaluation of groundwater quality for domestic and agricultural purpose in Kaithal district, Haryana. *Environmental Earth Sciences*, 61, 1587–1597.
- Howard, K. W. F. (2015). Sustainable cities and the groundwater governance challenge. *Environmental Earth Sciences*, 73(6), 2543–2554.
- Jarvis, W.T. (2012). Integrating Groundwater Boundary Matters into Catchment Management. In Taniguchi, M. & Shiraiwa, T. (eds) *The Dilemma of Boundaries*. Springer, Japan. pp. 161–176.
- Jha, B. M. (2007). Groundwater development and management strategies in India. *Bhu-Jal News*, 22, 1–15.
- Ji, X.B., Kang, E.S., Chen, R.S., Zhao, W.Z., & Jin, B.W. (2006). The impact of the development of water resources on environment in arid inland river basins of Hexi region, north-western China. *Environmental Geology*, 50, 793–801.
- Kendy, E., Gerard-Merchant, P., Walter, M.T., Zhang, Y., Liu, C., & Steenhuis, T.S. (2003). A soil water balance approach to quantify groundwater recharge from irrigated cropland in the North China Plain. *Hydrological Processes*, 17, 2011–2031.
- Kumar, P., Thakur, P. K., Bansod, B. K. S., & Debnath, S. K. (2018). Groundwater: A regional resource and a regional governance. *Environment, Development and Sustainability*, 20, 1133–1151.
- Margat, J., & J. van der Gun (2013). Groundwater around the world: A geographic synopsis. CRC Press, London, UK.
- Mukherji, A., & Shah, T. (2005). Groundwater socio-ecology and governance: A review of institutions and policies in selected countries. *Hydrogeology Journal*, 13, 328–345.
- Murthy, C. S., Yadav, M., Mohammed Ahamed, J., Laxman, B., Prawasi, R., Sessa Sai, M. V. R., & Hooda, R. S. (2015). A study on agricultural drought vulnerability at disaggregated level in a highly irrigated and intensely cropped state of India. *Environmental Monitoring and Assessment*, 187(3), 140.
- Pande, C. B., Moharir, K. N., Singh, S. K., & Varade, A. (2019). An integrated approach to delineate the groundwater potential zones in Devdari watershed area of Akola district, Maharashtra, Central India. *Environment, Development and Sustainability*. doi:<https://doi.org/10.1007/s10668-019-00409-1>.
- Pandey, A. C., Hooda, R. S., Nathawat, M. S., & Rao, T. B. V. M. (2004). *Resource Atlas of Haryana*. Chandigarh: Haryana State Council for Science and Technology.
- Raju, B. M. K., Rao, K. V., Venkateswarlu, B., Rao, A. V. M. S., Rama Rao, C. A., Rao, V. U. M., Bapuji Rao, B., Ravi Kumar, N., Dhakar, R., Swapna, N., & Latha, P. (2013). Revisiting climatic classification in India: A district-level analysis. *Current Science*, 105, 492–495.
- Reddy, V. R., Reddy, M. S., & Rout, S. K. (2014). Groundwater governance: A tale of three participatory models in Andhra Pradesh, India. *Water Alternatives*, 7(2), 275–297.
- Seckler, D., Molden, D., Baker, R. (1998). *Water scarcity in the 21st century*. Colombo: International Water Management Institute.
- Shah, T. (2009). *Taming the anarchy: Groundwater governance in South Asia*. Colombo: International Water Management Institute.
- Shah, T., & Mukherjee, A. (2001). *The socio ecology of groundwater in Asia*. Anand: International Water Management Institute.
- Shah, T., Molden, D., Saktivadivel, R., & Seckler, D. (2000). *The global groundwater: Overview of opportunity and challenges*. Colombo: International Water Management Institute.
- Siebert, S., Burke, J., Faures, J. M., Frenken, K., Hoogeveen, J., Doll, P., & Portmann, F. T. (2010). Groundwater use for irrigation: A global inventory. *Hydrology and Earth System Sciences Discussions*, 14, 1863–1880.
- Singh, A., Krause, P., Panda, S. N., & Flugel, W. A. (2010). Rising water table: A threat to sustainable agriculture in an irrigated semi-arid region of Haryana, India. *Agricultural Water Management*, 97(10), 1443–1451.
- Singh, O., & Amrita. (2015a). Groundwater availability and utilization in Haryana: A geographical study. *Bharatiya Vaiganik evam Udyogik Anusandhan Patrika*, 23, 36–41.

- Singh, O., & Amrita. (2015b). Groundwater variability in Haryana: A spatio-temporal analysis. *Punjab Geographer*, 11(1), 13–36.
- Singh, O., & Bhardwaj, P. (2019). Spatial and temporal variations in the frequency of thunderstorm days over India. *Weather*, 74(4), 138–144.
- Singh, O., & Kasana, A. (2017). GIS-based spatial and temporal investigation of groundwater level fluctuations under rice-wheat ecosystem over Haryana. *Journal of the Geological Society of India*, 89, 554–562.
- Singh, O., Kasana, A., Singh, K. P., & Sarangi, A. (2020). Analysis of drivers of trends in groundwater levels under rice-wheat ecosystem in Haryana, India. *Natural Resources Research*, 29 (2), 1101–1126.
- Srivastava, G. S., Singh, I. B., & Kulshrestha, A. K. (2006). Late quaternary geomorphic evolution of Yamuna-Sutlej interfluvium: Significance of terminal fan. *Journal of the Indian Society of Remote Sensing*, 34, 123.
- Thussu, J. L. (2006). *Geology of Haryana and Delhi*. Bangalore: Geological Society of India.
- Wada, Y., van Beek, L. P. H., van Kempen, C. M., Reckman, J. W. T. M., Vasak, S., & Bierkens, M. F. P. (2010). Global depletion of groundwater resources. *Geophysical Research Letters*, 37, L20402.
- Xue, L., Guomin, L., & Yuan, Z. (2014). Identifying major factors affecting groundwater change in the north China plain with grey relational analysis. *Water*, 6, 1581–1600.

Chapter 19

Spatial Appraisals of Groundwater Recharge Potential Zone Identification Using Remote Sensing and GIS



Gouri Sankar Bhunia, Pranab Kumar Maity, and Pravat Kumar Shit

Abstract Freshwater demand is increasing rapidly in India, and the southwest of West Bengal State in India is undergoing sporadic water stress due to monsoon irregularity and dearth of surface water supplies. Most of the surface water in the field under study is used for agricultural purposes. The present research used an innovative approach to offer an effective forum for concurrent investigation of multidisciplinary evidence and decision building in the project region for possible groundwater recharge. Leading thematic layers such as geology, geomorphology, soil, aridity index, drainage density, annual average water level, slope, linear length distance, and land use/land cover have been incorporated into the geographic information system (GIS) framework. The suggested recharge potential region was delineated using weighted linear combination approach. Landsat 8 satellite data are used to determine land use features, irrigation features and lineaments. Results revealed that approximately 2.73% and 34.76% of the Shilabati river drainage are classified as excellent and high potential groundwater recharge, respectively. The subsequent map and methods suggested in this study would provide a framework for a prospective approach to water management.

Keywords Geographic information system (GIS) · Groundwater recharge · Landsat data · Water resource management · Weighted index overlay

G. S. Bhunia
RANDSTAD India Pvt Ltd., New Delhi, Delhi, India

P. K. Maity
Ceinsys Tech Ltd, Nagpur, Maharashtra, India

P. K. Shit (✉)
PG Department of Geography, Raja N L Khan Women's College (Autonomous), Phulpahari,
West Bengal, India

19.1 Introduction

Artificial regeneration is a method of refilling groundwater to the depletion zone by means other than normal (Hashemi et al. 2013). Demand for freshwater supplies on the globe is significantly growing with raising water demands in India for domestic and agricultural purposes (Dhawan 2017). Thereafter, overuse of groundwater sources and the consequent decrease in water levels are causes of serious concern in many areas of India. Groundwater depletion has resulted in a significant decrease in the groundwater reservoir, particularly in dry uplands. Episodically, the dry zone faces drought due to disparities in temperature, high evaporation levels and special groundwater circumstances (Hashemi et al. 2013; Alam et al. 2014; Karmakar et al. 2016). Consequently, the scarcity and seclusion of water supplies from the surface force people to cultivate groundwater for their residential, agrarian and manufacturing uses. Groundwater table drains as the injection levels reach the replenishment limit. Artificial land recovery appears to be the only solution for overexploitation (Yeh et al. 2014).

Artificial groundwater refuelling' begins rising freshwater recharging, conserving and monitoring groundwater levels and enhancing water quality through the removal of adjourned contaminants (Bouwer 2002). At artificial recharge, surface water is used for absorption and eventual transport to the aquifer to improve groundwater supplies (Datta 2019). Therefore, the option of artificial recharge sites is very challenging and depends on several factors such as runoff, drainage rate, plant characteristics, soil permeability, slope, geology, lineage rate, geomorphology, land use/land cover, etc. Duration and rainfall level assist with groundwater recovery and recharge. Natural drainage network efficiency is a circuitous indication of high permeability and porosity of the ground due to its association with the soil runoff. Geological discontinuities, such as fault and crack processes, serve as conduits for the flow and preservation of groundwater (Senthil Kumar et al. 2019). In a particular area, the lineament density can also be used to conjecture high secondary porosity. Krishnamurthy et al. (2000) stated that a 300 m buffer zone along each line is called a groundwater recharge free zone. Because of substantial accumulation of rain water, flat fields promote groundwater depletion, creating mild evaporation conditions. Coefficient of soil permeability plays a significant role in building artificial recharge systems (Elbeih 2007). Crop size, structural structure of crop and ratio of voids are directly proportional to soil permeability. In addition, land use and land cover characteristics affect the rate of surface runoff, drainage and use of groundwater, regarded as a factor of site selection for artificial groundwater recharge (Leduc et al. 2001). Geomorphological factors and lithology supervise groundwater frequency, flow and consistency.

Artificial recharge site identification has been of considerable significance in India for the last few decades. A variety of research studies were carried out to delineate the future groundwater recharge region using remote sensing and GIS (Jaiswal et al. 2003; Jha et al. 2007; Rahman 2008). Most of the inquiries concerned the knowledge-driven factor analysis and the incorporation of numerous thematic

maps, and the satellite data were used in the preparation of factor layers. Choudhary and Saraf (2001) reported that high spatial resolution satellite data is very useful when locating artificial recharging sites. Jasrotia et al. (2007) evaluated remote sensing and GIS techniques as an important platform for converging multidisciplinary data and artificial groundwater recharge determination. Senanayake et al. (2016) analysed artificial groundwater recharge sites using multiple thematic layers in the GIS framework. Nevertheless, because of their capacity to produce spatio-temporal knowledge and usefulness in spatial data examination and prophecy, geospatial technology is a valuable tool for defining the groundwater recharge potential region. Depending on the above criterion, we have used the weighted linear combination approach based on specific sub-surface parameters to classify groundwater recharge sites in West Bengal’s Shilabati river basin, India.

19.2 Study Area

The catchment area (Fig. 19.1) is characterized by the tropical monsoon type of climate with an average rainfall of 1320 mm. Annual temperature ranges from 6 °C (December–January) to 50 °C (May–June). The average annual rainfall within the

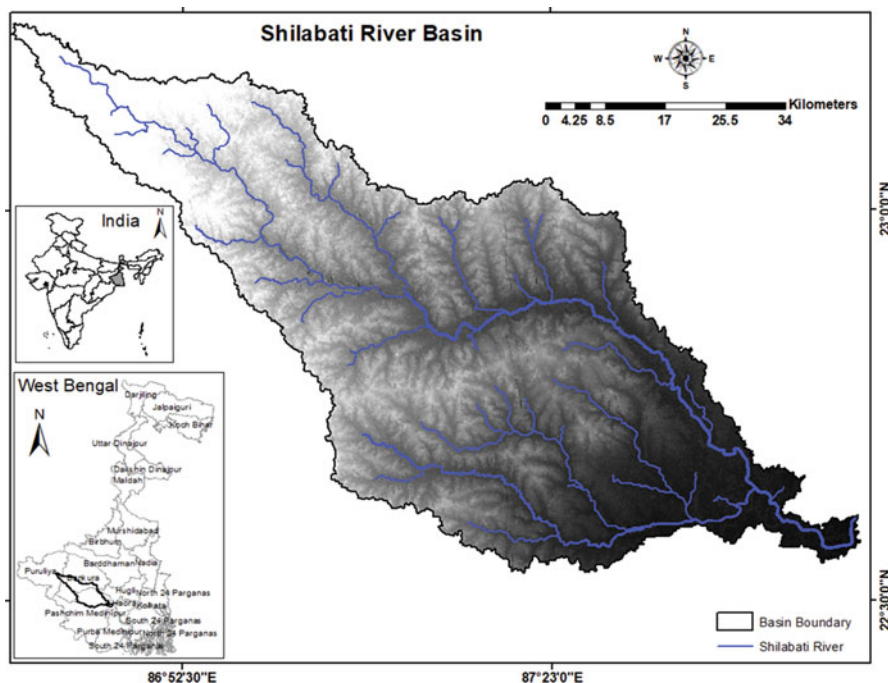


Fig. 19.1 Location map of the Shilabati river basin in West Bengal (India)

basin is 150 cm, with a relative average humidity of 60–65%. The region is distinguished, topographically, by isolated hills at the higher basin and gentle slope in the lower catchment area. The angle of junction of Shilabati river with respect to the Rupnarayan river is 230 degrees, and the gradient of Shilabati is $0011'55.03''$ (Das and Bandyopadhyay 2015). The basin's general slope is towards the southeast. The soil in the upper catchment area of the river does not allow agriculture to flourish. With rising population demand and urbanization, the use of sub-surface water in the study area is growing.

19.3 Materials and Methods

Groundwater drainage says water flows from unsaturated area to saturated area. Certain aspects, such as geological, hydrogeological, geophysical and geospatial techniques, may be used to monitor the potential recharge zone of groundwater (Yeh et al. 2016). Throughout this research, remote sensing and GIS technologies were used to demarcate future groundwater recharge region based on cost-effectiveness and time-effectiveness. Appropriate groundwater recharge sites have been delineated by knowledge-based factor analysis using geology, geomorphology, soil, water depth, land use/land cover, drainage area, aridity index, slope and line density. In the flow map in Fig. 19.2, the technique used in this analysis was seen. In ERDAS Imagine program v8.5, the survey of India image was georeferenced by single-pixel rectification technique. The Universal Transverse Mercator (UTM) projection with World Geodetic Survey (WGS) data with zone 84 and 45 north regions was considered as rectifying a root-mean-square error (RMSE) of less than 0.5 m per pixel.

19.3.1 Geology

Local geographical structures play a critical function in groundwater occurrence and distribution. Shaban et al. (2006) reported that recharging groundwater depends on rock exposure and also affects water percolation (El-Baz and Himida 1995). The accessible 1:50,000 river basin geology map, obtained from the Kolkata Geological Survey (West Bengal, India), depicts the river basin's lithological features. Polygon layer was created in ArcGIS program v9.0 after georeferencing of the geological map via a map-to-map rectification method. The river system geological features were demarcated according to the geological chart suggested. Different units of lithological characteristics have been digitized. Less compaction environment with higher weathering and fracking enables greater drainage with reduced runoff and has played a critical role in groundwater regeneration. After each lithology class, weights based on their textured properties and weathered zone-forming ability were assigned.

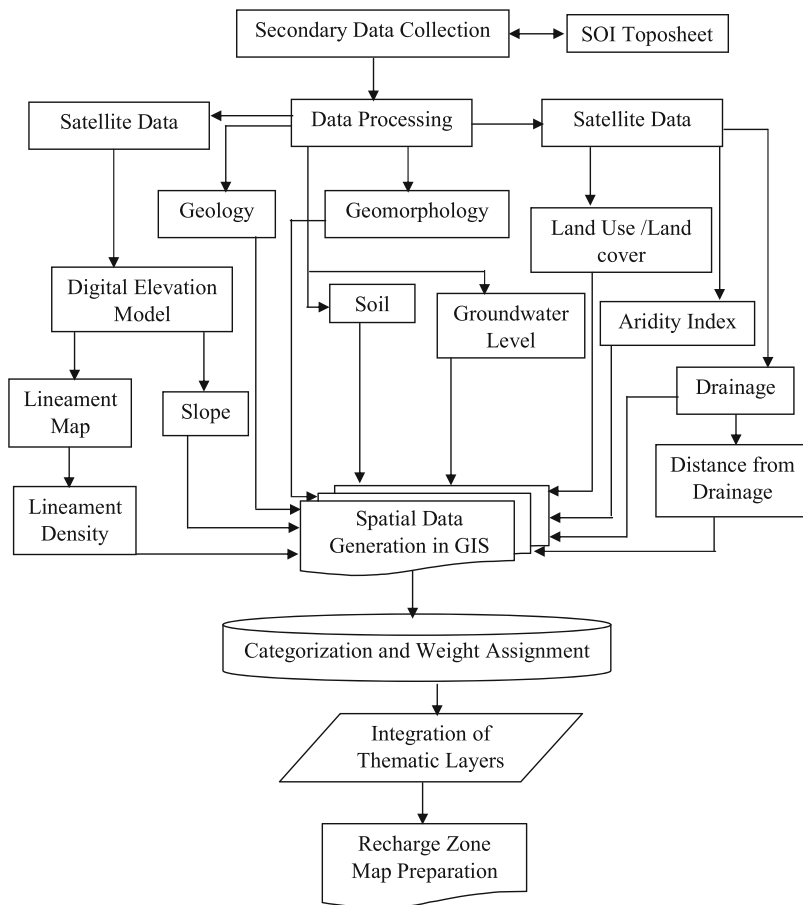


Fig. 19.2 Flow chart map of the overall methodology

19.3.2 Geomorphology

The valley of the Shilabati river is located in the south-west portion of the province of Bengal with an isolated hillock in the upper part of the valley. Previous study suggested landforms in the search for artificial recharge sites are significant surface markers. The geomorphological map was extracted from the literature presented here. The polygon layer was generated in GIS setting after georeferencing of the geomorphological map, and the attribute of geomorphological characteristics was incorporated into the polygon layer.

19.3.3 Soil

Information derived from the National Bureau of Soil Survey and Land Use Planning (NBSSLUP), Nagpur, and assigned codes were used to prepare the soil texture chart. The soil map was georeferenced with respect to toposheet Indian Survey (SOI). Area soil is lateritic. The latest alluvial sediment that is deposited by the main river system and its tributaries is found in the lower portion of the basin. The polygon layer was developed in GIS setting based on soil characteristics. After that, each of the sections of soil characteristics is defined.

19.3.4 Aridity Index

The aridity index (AI) is a numerical measure, since the ratio of annual mean precipitation (P) to the annual mean potential evapotranspiration (PET) measures the degree of climate dryness at a given location (Feng and Fu 2013; Fu and Feng 2014). The AI can be calculated as

$$AI = P/PET$$

where P is the precipitation and PET is the potential evapotranspiration. The value of $AI < 0.2$ is considered as arid, and the value of $AI > 0.65$ is considered as humid. There, the precipitation is P , and potential evapotranspiration is PET. The $AI < 0.2$ value is called arid, and the $AI > 0.65$ value is called humid.

19.3.5 Water Level

For the study of groundwater recharging levels, data from drilled sources across the river basin were collected pre- and post-monsoon depth of water levels. A total of 50 points were randomly identified, spread throughout the basin regions. Pre- and post-monsoon water table depth values were combined, and annual water level was measured for each point position. These points were employed to intercalate the grids in GIS setting and eventually configure the thematic layers of the river basin's annual water volume.

19.3.6 Land Use/Land Covers (LULC)

In the current study, Landsat 8-Operational Land Imager (OLI) satellite data (path/row, 139/44; date of pass, 07/09/2015) was used. Land use/land cover (LULC)

provides essential measures of the degree of groundwater needs and use of groundwater, as well as artificial groundwater recharge sites by specifying the location of housing areas, vegetation cover, etc. LULC is also expected to help measure the evapotranspiration (Das et al. 2018), runoff (Garg et al. 2019), water allocation (Patidar and Behera 2019) and groundwater system recharge (Leduc et al. 2001). Specific land use groups have been established (e.g. thick agricultural forest land, built-up areas, surface water sources, lateral upland) by controlled classification with maximum likelihood algorithm in ERDAS Imagine software v8.6. In the artificial colour composite image, the river beds look like cyan and light blue. Dense areas of woodland have been marked with reddish colour. Built-up areas have been known as blocky looks. Agricultural fields in the false colour composite image were defined step by step as patterns in a dull red colour.

19.3.7 Drainage Density

The research area drainage network layer was delineated from Landsat 8 satellite data by heads-up digitizing system. The quality of the lithology-based drainage network determines the percolation rate. The technical features of the drainage network therefore help to determine the groundwater recharge zone. The drainage length density (D_d) [L^{-1}] as defined by Greenbaum (1985) indicates and defines the total drainage distance in a single unit area, calculated as

$$D_d = \frac{\sum_{i=1}^{i=n} L_i}{A}$$

where $\sum_{i=1}^{i=n} L_i$ defines the total length of drainage (L). The D_d correlates greatly with the groundwater recharging, e.g. a greater D_d value with a high groundwater recharge point.

19.3.8 Slope

The slope promotes moisture accumulation right away. Steeper slope creates less recharge as water drifts down a steep slope rapidly during rainfall (Al Saud 2010). Therefore the polluted region does not have enough time to enter and refresh. The slope chart was prepared using digital elevation model (DEM) data from the Advanced Spaceborne Thermal Emission and Reflection Radiometer (ASTER). There was a better risk of erosion and rebound in the region where the slope is lowest, and alluvial soil appeared to hold water for longer.

19.3.9 Lineament

Lineament is an image of a geological underlying structure formed in a straight line or gentle curve as observed by the high-pass filtering of remote sensing data (O'Leary et al. 1976). This method has been followed by numerous scholars to study groundwater in a complicated geological area (Lattman and Parizek 1964; Solomon and Quiel 2006). The lineament in this analysis was derived from Landsat 8 satellite data by using ERDAS Imagine program v8.6 spectral enhancement technique. Finally, the lineament length density (L_d) (Al Saud 2010) was calculated which denotes the overall extent of lineaments in a unit area as

$$L_d = \frac{\sum_{i=1}^{i=n} L_i}{A}$$

where $\sum_{i=1}^{i=n} L_i$ represents the entire length of lineament (L) and A signifies the unit area (L^2). A high value deduces high secondary porosity; thus, it represents a region of high values of possible groundwater recharge.

19.3.10 Weighted Overlay Analysis

All factors do not have the same effect during the development of groundwater regeneration, and not every component was independent (Shaban et al. 2006). Such thematic maps have all been incorporated into the GIS database. Eventually, the weighted linear combination approach was taken using the following equation to determine the possible indices for each pixel in the river basin for groundwater recharge:

$$GW_{rp} = G_w G_r + GG_w GG_r + LD_w LD_r + SL_w SL_r + AI_w AI_r + S_w S_r + DD_w DD_r + WL_w WL_r + LULC_w LULC_r$$

where GW_{rp} is the groundwater recharge probable index, 'G' is the geological index, 'GG' is the geomorphological index, 'LD' is the lineament density index, 'SL' is the slope index, 'AI' is the aridity index, 'S' is the soil cover index, 'DD' is the distance from drainage index, 'WL' is the groundwater level index and 'LULC' is the land use/land cover index. The subscripts 'w' and 'r' refer to the weight of a theme and the rank of individual theme identifiers, respectively. Table 19.1 lists the ranks assigned to each groundwater potential parameter.

Bearing in mind the relative importance, the actual ground condition is better represented (Choudhury 1999). Determining the weight of each class is the most critical aspect of a unified investigation, because the data relies entirely on the

Table 19.1 Categorization of the factor influencing groundwater recharge potential of Shilabati river basin

Factors	Classes	Area (km ²)	Percent of area	Weight assigned	
Geology	Alluvium(sand/silt/clay)	841.2	24.37	6	
	Older alluvium	73.84	2.14	5	
	Younger alluvium	378.14	10.96	6	
	Fluviodeltaic overlaid by secondary laterite	1489.06	43.14	5	
	Unclassified crystalline gneiss	466.47	13.52	3	
	Gneiss and gneiss	60.77	1.76	2	
	Sijua formation	6.15	0.18	1	
	Gneiss and schist	135.85	3.94	1	
Geomorphology	Dissected plateau	878.75	25.46	7	
	Crests of undulating plateau	59.13	1.71	5	
	Flood plain	323.2	9.36	8	
	Residual hillocks and mountains	137.39	3.98	1	
	Gently sloping upland	414.14	12.00	2	
	Upper undulating alluvial plain	1078.99	31.26	3	
	Lower alluvial plain	428.76	12.42	4	
	Dissected highland	25.46	0.74	1	
	Lowland	15.61	0.45	5	
	Badland	90.05	2.61	3	
	Soil	Coarse loamy typic haplustalfs	380.58	11.03	7
		Fine loamy aeris ochraqualfs	276.9	8.02	6
Fine loamy typic ustifluvents		178.91	5.18	6	
Fine loamy ultic paleustalfs		619.52	17.95	5	
Fine vertic haplaquepts		193.34	5.60	1	
Fine vertic ochraqualfs		269.08	7.80	1	
Lithic ustrothents		445.74	12.91	3	
Loamy sand		112.44	3.26	7	
Sandy clay loam		31.92	0.92	5	
Typic haplaquepts		1.83	0.05	2	
Typic ustrothents		197.43	5.72	3	
Udic haplustalfs		686.15	19.88	4	
Very fine vertic haplaquepts		57.64	1.67	1	
Aridity index	Arid (<0.06)	21.01	0.61	1	
	Semi-arid (0.061–0.20)	740.06	21.44	2	
	Dry sub-humid (0.21–0.45)	568.92	16.48	3	
	Humid (0.45–0.65)	2116.44	61.32	5	
	Very humid (>0.65)	5.05	0.15	6	
Drainage density (km/km ²)	<0.50	1829.95	53.02	9	
	0.51–1.00	904.157	26.20	8	
	1.01–1.50	381.65	11.06	7	

(continued)

Table 19.1 (continued)

Factors	Classes	Area (km ²)	Percent of area	Weight assigned
	1.51–2.00	161.702	4.69	5
	>2.01	174.02	5.04	4
Annual average water level (mbgl)	Very shallow (<5.7)	124.38	3.60	6
	Shallow (5.7–6.1)	567.7	16.45	5
	Medium (6.1–6.5)	1650.17	47.81	4
	Deep (>6.5)	1109.23	32.14	3
Slope (degree)	< 2 (nearly levelled/very gentle)	1579.37	45.76	8
	2–4 (gently sloping)	965.01	27.96	6
	4–6 (moderate)	511.54	14.82	5
	6–8 (moderate to steep)	220.91	6.40	3
	>8 (very steep)	174.65	5.06	2
Lineament length density (km/km ²)	<0.50	348.69	10.10	2
	0.51–1.00	457.71	13.26	3
	1.01–1.50	468.04	13.56	4
	1.51–2.00	440.1	12.75	5
	>2.01	1736.94	50.32	6
Land use/land cover	Dense forest	720.28	20.87	7
	Agricultural fallow land	138.91	4.02	6
	Water bodies (ponds/lake/river/reservoir, etc.)	320.69	9.29	8
	Lateritic belt	35.48	1.03	3
	Built-up area	98.85	2.86	2
	Agriculture land	2137.25	61.92	4

assignment of the correct weight. Each parameter considered in this study has been given weight based on its impact on storage and transmission; for example, water depth plays an important part in groundwater charging, and higher weights are assigned. Highest weighting is provided to deepwater level to provide room for recharge. The effect of land usage on recharge is given less weight. Hydrological soil structure is assigned a lower weight, as the soil form compensated for the permeability and water retaining capacity. Table 19.2 details the weight allocated by various aspects and weights to dissimilar clusters for each theme (1–100).

Technical testing was conducted to test the quality of the raw data. Additionally, artificial recharge probable zone has been checked to verify if the defined zones are in compliance with the conditions of area.

Table 19.2 Groundwater recharge potential factor weight of Shilabati river basin

Factors	Assigned weight
Geology	13
Geomorphology	12
Soil	10
Aridity index	9
Drainage density (km/km ²)	12
Annual average water level (mbgl)	10
Slope (degree)	11.5
Lineament length density (km/km ²)	12.5
Land use/land cover	10

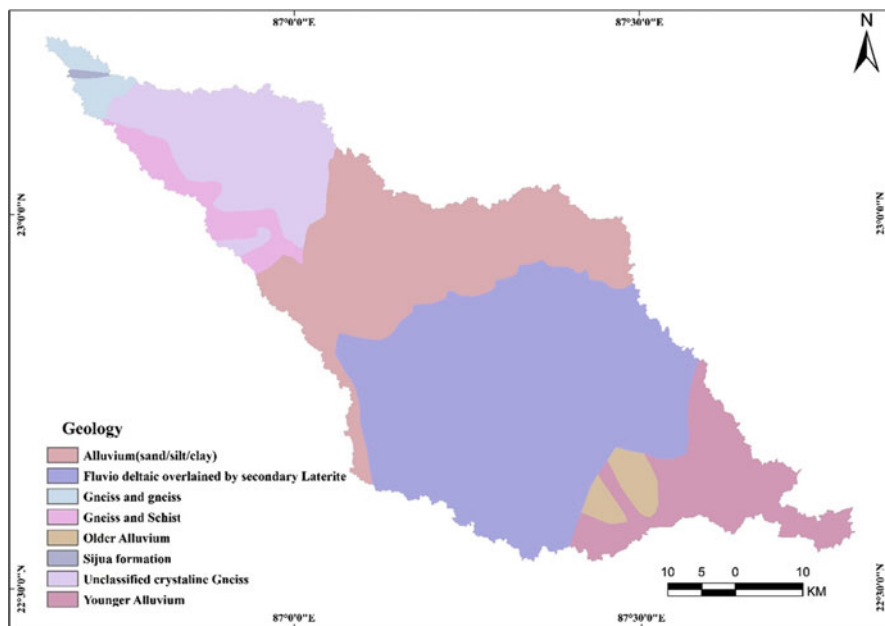


Fig. 19.3 Geological characteristics of the study area

19.4 Results and Discussion

Geologically, the drainage of the Shilabati river is distinguished by tertiary soil covered beneath the canopy of alluvium Ganga Brahmaputra. It falls within the Bengal plateau area. The field of research was distinguished by alluvium, older alluvium, younger alluvium, secondary laterite fluvial deltaic, unclassified crystal gneiss, gneiss and gneiss, sijua formation and gneiss and schist (Fig. 19.3). The lower portion of the basin is of sedimentary origin, while the upper part of the basin is formed by metamorphic rocks. Therefore, the maximum rock foliation is observed

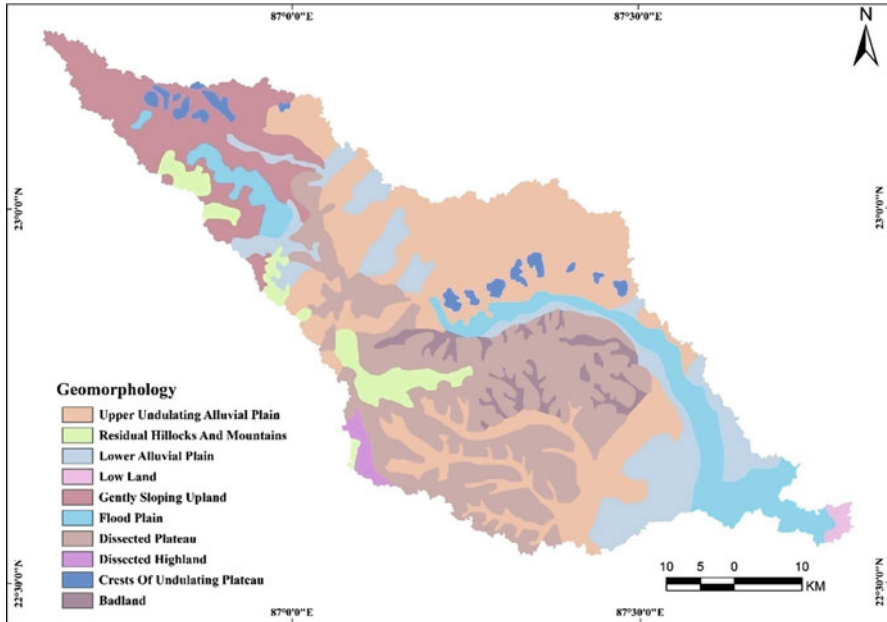


Fig. 19.4 Geomorphological characteristics of the Shilabati river basin

in the southern and south-eastern directions. More compact regions with a higher degree of weather and fracture allow runoff to be permeated and thus are more suitable for groundwater recharge (Krishnamurthy et al. 2000). In this analysis, alluvium was given maximum weight, and the lowest weight was allocated for sijua formation and gneiss and schist.

Geomorphologically, the research region is characterized by dissected plateau, undulating plateau crests, flood plains, residual hills and valleys, gently sloping uplands, upper undulating alluvial plains, lower alluvial plains, dissected highlands and lowland badlands (Fig. 19.4). Flood plain and alluvial plateau define the very lower portion of the basin. In the north-central portion of the basin, the upper undulating alluvial plain is found. The upper catchment area is dominated by residual mountains and hills and strongly sloping uplands. In the central and southwestern part of the basin, the lowland badland is observed. The ranks were assigned to the individual geomorphological dimension according to its effect on the rebound, maintaining and occurrence of groundwater (Table 19.1).

In the Shilabati river basin, the soil is categorized as coarse loamy typic haplustalfs, fine loamy aerichraqualfs, fine loamy typic ustifluvents, fine loamy ultic paleustalfs, fine vertic haplaquepts, fine vertic ochraqualfs, lithic ustrothents, loamy sand, sandy clay loam, typic haplaquepts, typic ustrothents, udic haplustalfs and very fine vertic haplaquepts (Fig. 19.5). The coarse loamy typic haplustalfs and

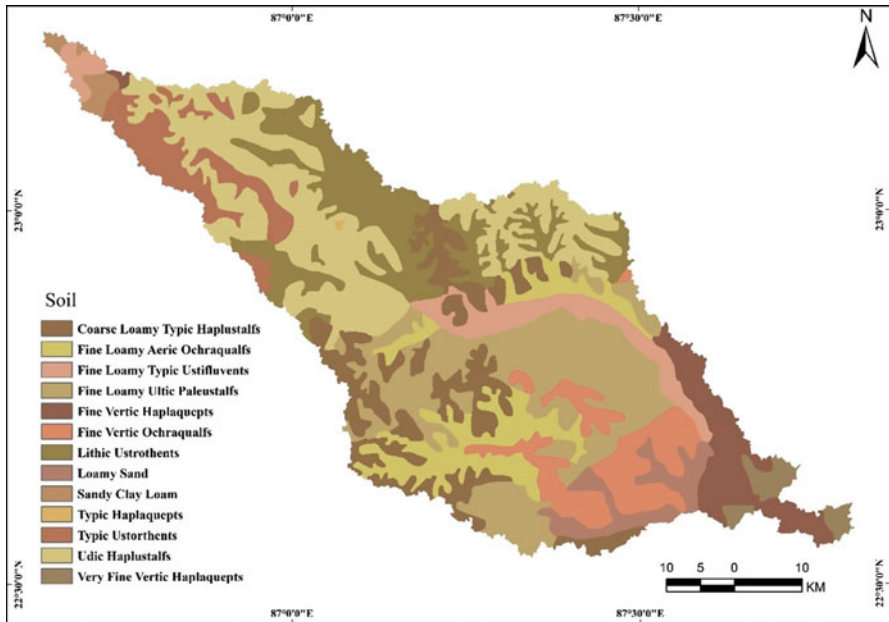


Fig. 19.5 Soil characteristics of the study area

loamy sand are given the maximum weightage due to their respective influence on the groundwater recharge and its occurrence. Moreover, the lower weightage is assigned for very fine vertic haplaquepts, fine vertic haplaquepts and fine vertic ochraqualfs soil types.

The aridity index map of the Shilabati river basin is represented in Fig. 19.6. Based on the value derived from AI, the study area is divided into (i) arid (<0.06), (ii) semi-arid (0.061–0.20), (iii) dry sub-humid (0.21–0.45), (iv) humid (0.45–0.65) and (v) very humid (>0.65). The lower and middle portion of the basin reflects the wet climate, while the higher catchment area portrays the arid zone. Based on the aridity index, weightage has been given in order to groundwater potential recharge (Table 19.1).

The spreading of drainage in the basin area was delineated from the Landsat 8 satellite data. The main stream of Shilabati river exists from the Chota Nagpur plateau and moves in south-easterly direction through Bankura district and meets with the Dwarkeswar river at Bandar, and after combined flow as a Rupnarayan river and finally joins the Hooghly river. Figure 19.7 portrayed the D_d map of Shilabati river basin. The D_d was more than 2.0 sq. km, creating the region an admirable filtration recharge zone. Based on the drainage density, the study area is categorized into (i) <0.50 km², (ii) 0.51–1.00km², (iii) 1.01–1.50km², (iv) 1.51–2.00km² and (v) >2.01km². The higher drainage density is assigned as maximum weightage value and vice versa.

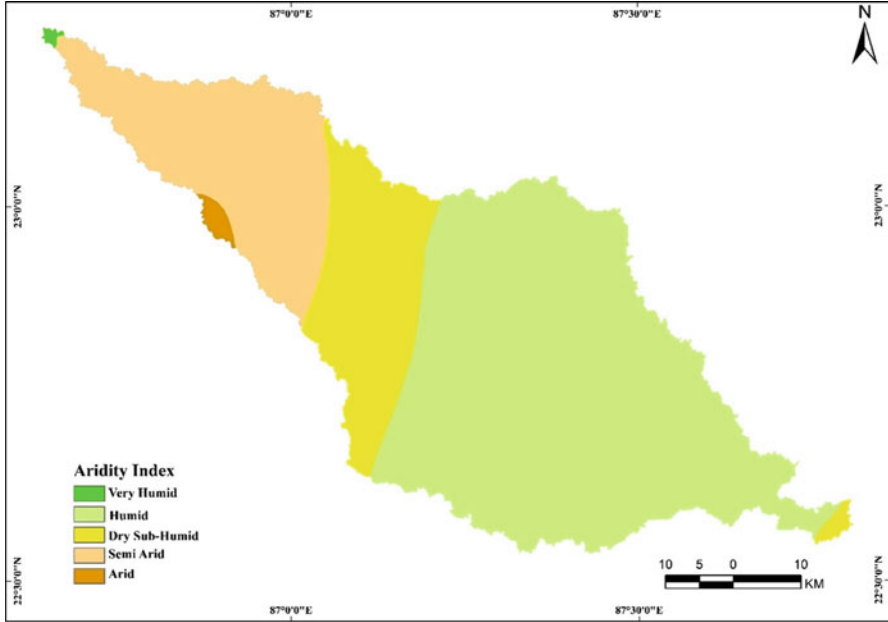


Fig. 19.6 Aridity index of the Shilabati river basin

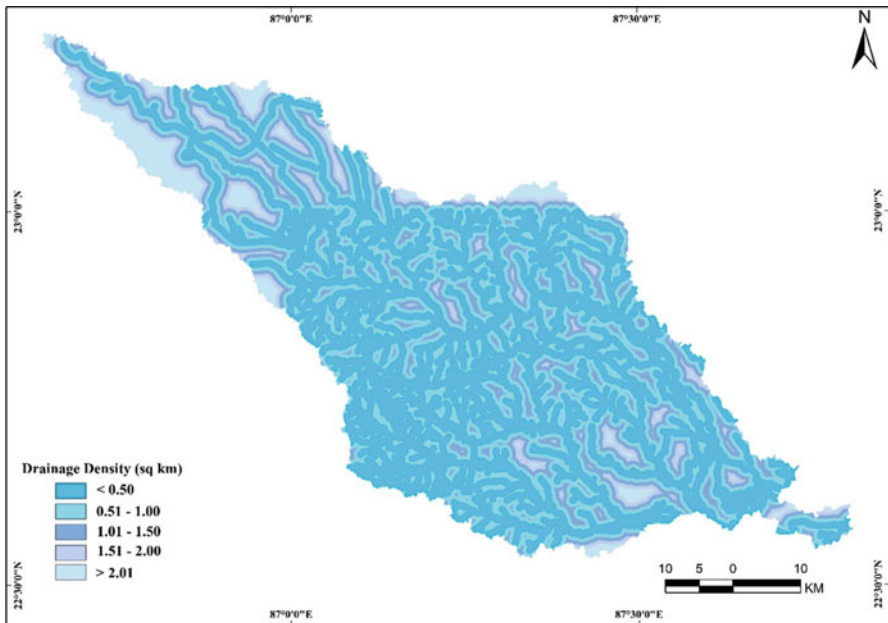


Fig. 19.7 Drainage density in the Shilabati river basin

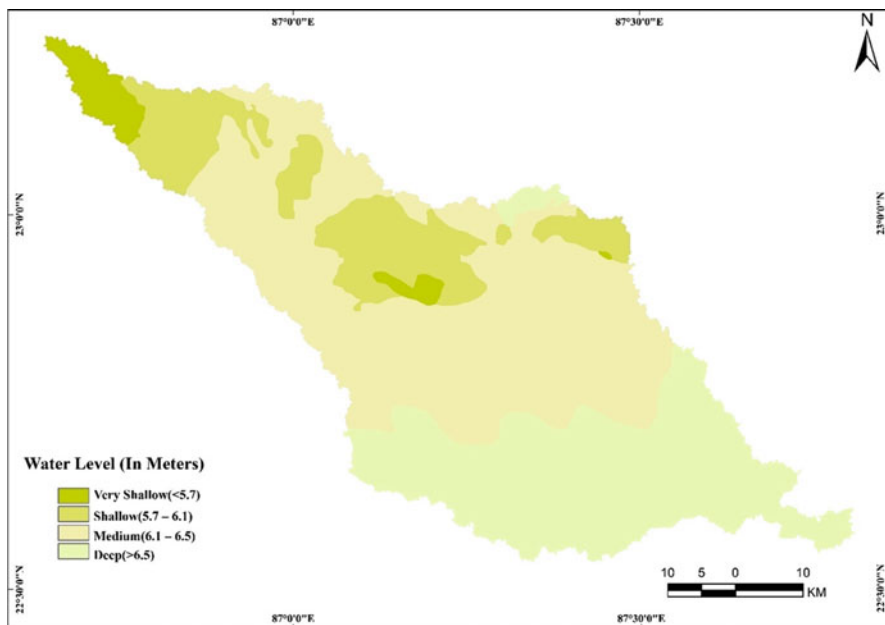


Fig. 19.8 Annual water level in the Shilabati river basin

The present water levels in the aquifer system varies from 4.7 to 19.7 m below ground level (bgl) during pre-monsoon (May) and from 2.8 to 10.9 mbgl during the post-monsoon (November). To identify the average differences in groundwater levels, decadal mean of groundwater level was created for periods before and after monsoon. Before the onset of monsoon, most of the regions are less than 7.5 mbgl, whereas groundwater level after the monsoon is less than 4 mbgl in most of the river basin. Figure 19.8 illustrates the annual average water level of the Shilabati river basin. The water level depth of >6.01 mbgl is covered by 79.95% of the river basin. The deeper level is mainly observed in the central and southern part of the basin.

The slope map of the river basin area was generated from the ASTER DEM data of 30 m spatial resolution. The river basin was a part of the lateritic upland areas. In the north and north-east of the river basin, the highest slope was recorded, and therefore unsuitable for groundwater recharge. The slope becomes less and smoother towards the south and southwest, thereby increasing the percolation period in this area. Based on the slope, the river basin was divided into five categories such as (i) <2°, (ii) 2°–4°, (iii) 4°–6°, (iv) 6°–8° and (v) >8° (Fig. 19.9). The lower slope is assigned maximum weightage based on the water holding capacity.

Figure 19.10 shows the lineament density of the Shilabati river basin, derived through Landsat 8 satellite data. Results revealed that most of the lineaments are distributed in the central part of the basin. Based on the density, the basin area is alienated into five categories as follows: (i) <0.50 km/km², (ii) 0.51–1.00 km/km², (iii) 1.01–1.50 km/km², (iv) 1.51–2.00 km/km² and (v) >2.01 km/km². The

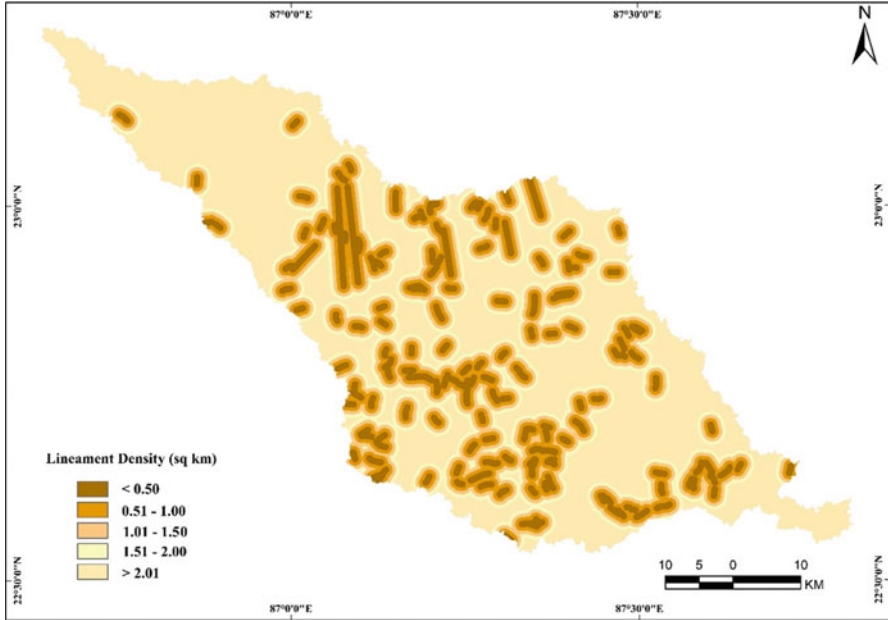


Fig. 19.9 Lineament density in the Shilabati river basin

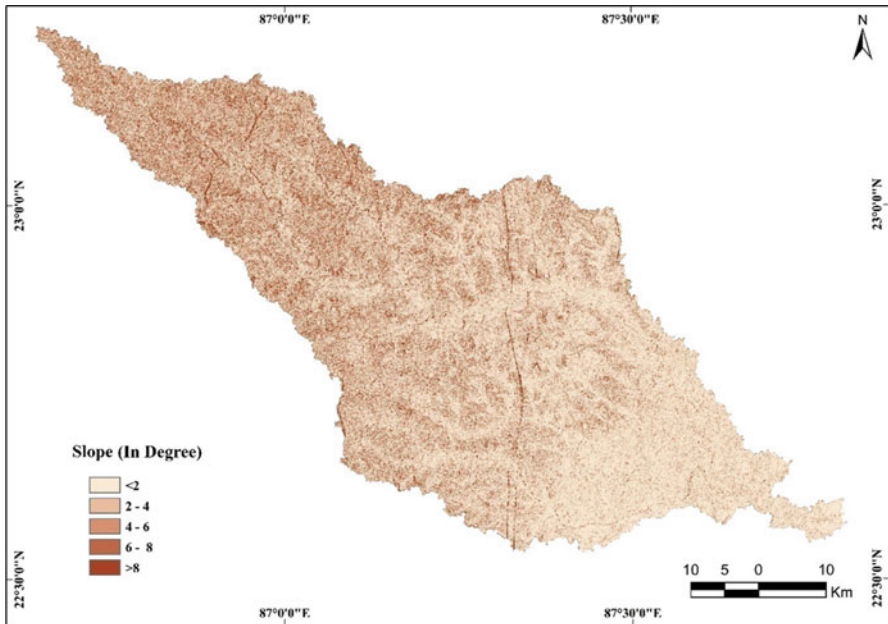


Fig. 19.10 Spatial variation of slope in the Shilabati river basin

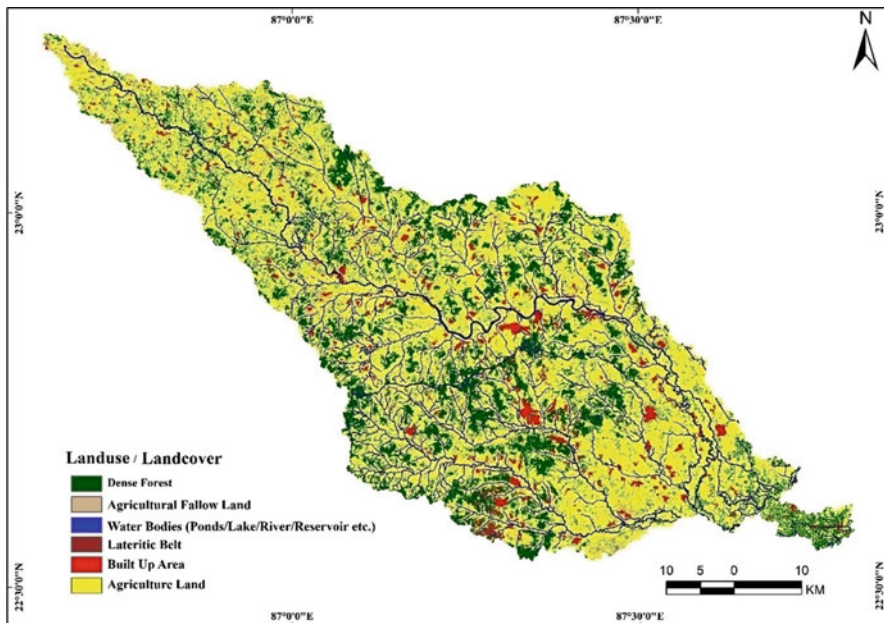


Fig. 19.11 Land use/land cover characteristics of the study area

weightage given to each category in association with groundwater recharge potential is represented in Table 19.1.

The land use/land cover characteristic of the Shilabati river area was assessed based on the Landsat 8-OLI data (Fig. 19.11). The basin area has been divided into six thematic classes as follows: dense forest, agricultural fallow land, water bodies, lateritic belt, built-up area and agriculture land. More than 60% of the study area is characterized by agricultural land, followed by dense forest (20.87%). The estimated surface water bodies in the basin area are recorded as 320.69 sq km (9.29%). The lateritic upland is mainly observed in central and north-west part of the basin area. The weightage factor is assigned for the LULC for groundwater recharge given in Table 19.1. The maximum weightage is assigned for the surface water bodies, followed by dense and agricultural fallow land.

In the future recharge scale, the weight factor reflects the proportion of its value and is subjectively calculated as stated by the significance of individual factor during the recharge cycle. Therefore, the higher recharge weight was determined as the maximum effect (Table 19.2). In terms of groundwater regeneration, each contribution has a positive influence and adverse effect.

Centred on the incorporation of thematic layers into GIS platform, the prospect map for the groundwater recharge region was planned. Based on Boolean logic and conditional methods, the groundwater recharge sites were selected. In accordance with the particular logical conditions obtained, the last map of output was ranked as

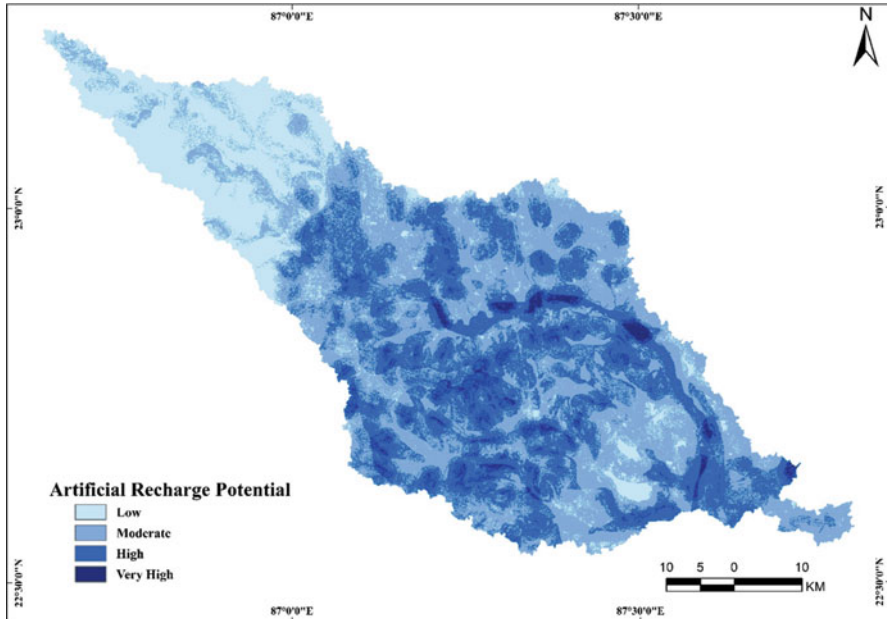


Fig. 19.12 Potential artificial recharge sites of the Shilabati river basin

‘excellent’, ‘good’, ‘fair’ and ‘low’. The weighted index overlay result class most appropriate was paired with other binary weight maps using the subsequent location selection principles:

- The field is loamy in nature and alluvial.
- Geologically, stone, pebble, sand silt and clay may be protected in the regions.
- Geomorphologically the region would be plain flood and dissected plateau.
- The water depth will be high.
- Further inclination should be provided to the surface in and around dam, reservoirs and reservoir.
- The site should be characterized by maximum rainfall.
- The location will have high drainage capacity and lineament capacity.
- The site should be less than 0–2% slope.

This region was ranked as ‘excellent’ for a high storativity artificial charge zone, a very deepwater table, water holding potential in the alluvial plain in piedmont. The resultant values are reclassified into four categories of equal interval (Fig. 19.12). This is attributed as (i) low (<45.0), (ii) moderate (45.01–55.00), (iii) high (55.01–65.00) and (iv) very high (>65.01). Table 19.3 showed the areal distribution of groundwater recharge potential zone of Shilabati river basin. Moderate groundwater recharge potential area is covered by 42.83%. The high groundwater recharge potential area is estimated as 1199.72 km² (34.76%). The findings also revealed that a very strong possible recharge zone in the lower part of the basin was identified.

Table 19.3 Areal distribution of groundwater recharge potential zone of Shilabati river basin

Groundwater recharge potential	Area (km ²)	%
Low (<45.0)	679.34	19.68
Moderate (45.01–55.00)	1478.10	42.83
High (55.01–65.00)	1199.72	34.76
Very high (>65.01)	94.32	2.73

Additionally, the runoff volume also helps restore the groundwater supply through the streamflow. The upstream region was less important, and the steep slope with hard rock terrains was affected. However, the current reservoirs and tanks reduced their holding capacity and the normal drainage of groundwater into the study area. The wetlands and the low-lying field in the drainage areas are in a dilapidated state and occupied for agricultural purposes by farmers. It is necessary to restore or change these current structures and low-lying areas to give out as recharge. In addition, percolation ponds, test dams, refuelling wells, ridges and furrows are some of the artificial recharging approaches that can be applied to enhance groundwater reservoir replenishment.

Numerous investigations have been conducted worldwide to delineate potential groundwater areas and potential artificial recharge areas using geospatial technology (Sarup et al. 2011; Riad et al. 2011; Manap et al. 2013; Manikandan et al. 2014). The present investigation is focused on rational conditioning and justification for the assimilation of various thematic levels to discriminate against groundwater recharge. The number of different thematic layers, their consistency and the weight allocated for weight analyses may have a substantial impact on the accuracy of the results of groundwater research. Thus, the quality of the thematic data, their degree of accuracy and local climate play an important role in the management of this groundwater.

19.5 Conclusion

In the present research, an optimized solution using remote sensing and GIS techniques was established to a groundwater recharge zone. This research is critical for the efficient use of groundwater resources and thus enhances groundwater recharge. This study also examines the links between possible factors of groundwater recharge. Our findings showed that the most important possible recharge region is reserved in the lower part of the Shilabati river basin. Approximately 43% of the sample area has low regions for the location of groundwater recharge systems, and 35% comes under the high category. Only 2.73% of the basin areas are demarcated as very high recharge potential zone. This increases the precision of the analysis and the spatial resolution of the results. In addition, this approach can be applied into other arid and semi-arid areas to delineate the future groundwater recovery zone for safe use of groundwater.

Acknowledgement We thank the reviewers for their positive comments to improve the manuscript. We are also thankful to the USGS Earth Explorer Community for freely obtaining satellite data.

References


- Al Saud M. (2010). Mapping potential areas for groundwater storage in Wadi Aurnah Basin, western Arabian Peninsula, using remote sensing and geographic information system techniques. *Hydrogeol J*, 18:1481–1495.
- Alam NM, Mishra PK, Jana C, Adhikary PP (2014). Stochastic model for drought forecasting for Bundelkhand region in Central India. *Indian Journal of Agricultural Sciences*, 84 (2): 255–260.
- Bouwer H. (2002). Artificial Recharge of Groundwater: Hydrogeology and Engineering. *Hydrogeology Journal*, 10(1):121–142.
- Choudhary PS, and Saraf AK. (2001). Artificial recharge site selection using GIS and remote sensing. In *Proceedings of the 2nd ICORG on Spatial Information Technology, Remote Sensing and Geographical Information Systems, Hyderabad Vol. 2*, pp. 519–524
- Choudhury PR. (1999). Integrated remote sensing and GIS techniques for groundwater studies in part of Betwa basin, Ph.D. Thesis (unpublished), Department of Earth Sciences, University of Roorkee, INDIA
- Das B, Bandyopadhyay A. (2015). Flood Risk Reduction of Rupnarayana River, towards Disaster Management—A Case Study at Bandar of Ghatal Block in Gangetic Delta. *Journal of Geography & Natural Disasters*, 5:1, DOI: <https://doi.org/10.4172/2167-0587.1000135>
- Das P, Behera MD, Patidar N, Sahoo B, Tripathi P, Behera PR, Srivastava SK, Roy PS, Thakur P, Agrawal SP, Krishnamurthy YVN. (2018). Impact of LULC change on the runoff, base flow and evapotranspiration dynamics in eastern Indian river basins during 1985–2005 using variable infiltration capacity approach. *Journal of Earth System Science*, 127:19
- Datta PS. (2019). *Water Harvesting for Groundwater Management: Issues, Perspectives, Scope, and Challenges*. John Wiley & Sons, 29-Jan-2019.
- Dhawan, V. (2017). *Water and Agriculture in India*. Background paper for the South Asia expert panel during the Global Forum for Food and Agriculture (GFFA). Available at: https://www.oav.de/fileadmin/user_upload/5_Publikationen/5_Studien/170118_Study_Water_Agriculture_India.pdf
- El-Baz F, Himida I. (1995). *Groundwater Potential of the Sinai Peninsula, Egypt*. Cairo, Egypt: US Agency for International Development.
- Elbeih, S.F. (2007). *Impact of Groundwater Recharge on the Surrounding Environment*. Ph.D. thesis. Faculty of Engineering, Ain Shams University, Egypt.
- Feng S, Fu Q. (2013). Expansion of global drylands in a warming world. *Atmospheric Chemistry and Physics*, 13:10,081–10,094
- Fu Q, Feng S. (2014). Responses of terrestrial aridity to global warming. *Journal of Geophysical Research: Atmospheres*, 119: 7863–7875. doi:<https://doi.org/10.1002/2014JD021608>
- Garg V, Nikam BR, Thakur PK, Aggarwal SP, Gupta PK, Srivastav SK. (2019). Human-induced land use land cover change and its impact on hydrology. *Hydro Research*, 1: 48–56.
- Greenbaum D. (1985). *Review of remote sensing applications to groundwater exploration in basement and regolith*. Nottingham, UK: British Geological Survey.
- Hashemi H, Berndtsson R, Kompani-Zare M, Persson M. (2013). Natural vs. artificial groundwater recharge, quantification through inverse modelling. *Hydrology and Earth System Sciences*, 17, 637–650.
- Jaiswal RK, Mukherjee S, Krishnamurthy J, Saxena R. (2003). Role of remote sensing and GIS techniques for generation of groundwater prospect zones towards rural development e an approach. *International Journal of Remote Sensing*, 24:993–1008.

- Jasrotia AS, Kumar R and Saraf AK (2007) Delineation of groundwater recharge sites using integrated remote sensing and GIS in Jammu district, India, *International Journal of Remote Sensing*, 28:22, 5019 - 5036
- Jha MK, Chowdhury A, Chowdary VM, Peiffer S. (2007). Groundwater management and development by integrated remote sensing and geographic information systems: prospects and constraints. *Water Resource Management*, 21:427–467.
- Karmakar R, Das I, Dutta D, Rakshit A. (2016). Potential Effects of Climate Change on Soil Properties: A Review. *Science International*, 4: 51–73.
- Krishnamurthy, J., Mani, A., Jayaraman, V., Manivel, M., (2000). Groundwater resources development in hard rock terrain- An approach using remote sensing and GIS techniques. *International Journal of Applied Earth Observation and Geoinformation* 2 (3e4), 204–215
- Lattman LH, Parizek RR. (1964). Relationship between fracture traces and the occurrence of ground water in carbonate rocks. *Journal of Hydrology*, 2:73–91.
- Leduc C, Favreau G, Schroeter P. (2001). Long-term rise in a Sahelian water-table: The Continental Terminal in south-west Niger. *Journal of Hydrology*, 243:43–54.
- Manap MA, Sulaiman WNA, Ramli MF, Pradhan, B, Surip N. (2013). A knowledge-driven GIS modeling technique for groundwater potential mapping at the Upper Langat Basin, Malaysia. *Arabian Journal of Geosciences* 6 (5),1621–1637.
- Manikandan J, Kiruthika AM, Sureshbabu S. (2014). Evaluation of groundwater potential zones in Krishnagiri District, Tamil Nadu using MIF Technique. *International Journal of Innovative Research in Science, Engineering and Technology*, 3(3): 10524–10534.
- O’Leary DW, Friedman JD, Pohn HA. (1976). Lineament, linear, lineation: some proposed new standards for old terms. *Geological Society of America Bulletin*, 87:1463–1469.
- Patidar N, Behera MD. (2019). How Significantly do Land Use and Land Cover (LULC) Changes Influence the Water Balance of a River Basin? A Study in Ganga River Basin, India. *Proceedings of the National Academy of Sciences, India Section A: Physical Sciences*, 89(2): 353–36
- Rahman A. (2008). A GIS based DRASTIC model for assessing groundwater vulnerability in shallow aquifer in Aligarh, India. *Applied Geography*, 28:32–53.
- Riad, P.H., Billib, M.H., Hassan, A.A., Omar, M.A. (2011). Water scarcity management in a semi-arid area in Egypt: overlay weighted model and Fuzzy logic to determine the best locations for artificial recharge of groundwater Nile Basin. *Water Science & Engineering Journal* 4 (1), 24–35.
- Sarup, J., Tiwari, M.K., Khatediya, V. (2011). Delineate groundwater prospect zones and identification of artificial recharge sites using geospatial technique. *International Journal of Advance Technology & Engineering Research* 1, 6–20.
- Senanayake IP, Dissanayake DMDOK, Mayadunna BB, Weerasekera WL (2016) An approach to delineate groundwater recharge potential sites in Ambalantota, Sri Lanka using GIS techniques. *Geoscience Frontiers*, 7: 115e124
- Senthilkumar M, Gnanasundar D, Arumugam R. (2019). Identifying groundwater recharge zones using remote sensing & GIS techniques in Amaravathi aquifer system, Tamil Nadu, South India. *Sustainable Environment Research*, 29:15, doi:<https://doi.org/10.1186/s42834-019-0014-7>
- Shaban A, Khawlie M, Abdallah C. (2006). Use of remote sensing and GIS to determine recharge potential zones: the case of Occidental Lebanon. *Hydrogeology Journal*, 14:433–443.
- Solomon S, Quiel F. (2006). Groundwater study using remote sensing and geographic information systems (GIS) in the central highlands of Eritrea. *Hydrogeology Journal*, 14:1029–1041
- Yeh HF, Lin HI, Lee ST, Chang MH, Hsu KC, Lee CH (2014) GIS and SBF for estimating groundwater recharge of a mountainous basin in the Wu river watershed, Taiwan. *J Earth Syst Sci* 123(3):503–516
- Yeh HF, Cheng YS, Lin HI, Lee CH (2016). Mapping groundwater recharge potential zone using a GIS approach in Hualian River, Taiwan. *Sustainable Environment Research* 26, 33–43.

Chapter 20

Spatial Mapping of Groundwater Depth to Prioritize the Areas Under Water Stress in Rayalaseema Region of Andhra Pradesh, India



Ch. Jyotiprava Dash, Partha Pratim Adhikary , and Uday Mandal

Abstract India stands first in the world in terms of groundwater use followed by China and the USA. However day by day, the groundwater level is depleting in an alarming rate all over the country. The Rayalaseema region of Andhra Pradesh is one of such regions, where groundwater depletion is a major problem and attributed to both natural and anthropogenic causes. In this study the spatial variation of groundwater was mapped for the year 2018 in Anantapur district, Andhra Pradesh, India, which is located in the Rayalaseema region. The groundwater level varied from 2.0 to 69.96 m with a mean value of 18.52 m during pre-monsoon, and during post-monsoon the depth of groundwater ranged between 1.15 m and 68.37 m with a mean value of 17.63 m. With respect to groundwater development, one-third of the *mandals* has reached the critical or overexploited stage. The overall stage of groundwater development was observed to be more than 80% in the study area, indicating heavy withdrawal of water from the aquifer. *Mandals* like Agali, Peddapappur, Rolla, Tadimarri, and Yellanur showed the level of groundwater development even more than 150%. In the study area, the *mandals* in which groundwater is at critical stage are Madakasira, Parigi, Penukonda, Raptadu, and Roddam. Therefore water conservation and groundwater recharge techniques may be executed, and awareness about judicious use of water may be created to avoid further depletion of aquifer in the district.

Keywords GIS · Groundwater development · IDW · Rayalaseema region · Water table fluctuation

Ch. J. Dash

ICAR-Indian Institute of Soil and Water Conservation, Research Centre, Koraput, Odisha, India
e-mail: jyoti.dash@icar.gov.in

P. P. Adhikary

ICAR-Indian Institute of Water Management, Chandrasekharpur, Bhubaneswar, Odisha, India
e-mail: partha.adhikary@icar.gov.in

U. Mandal (✉)

ICAR-Indian Institute of Soil and Water Conservation, Dehradun, Uttarakhand, India

20.1 Introduction

India stands first in terms of groundwater use in the world followed by China and the USA (Margat and van der Gun 2013) using an estimated 250 cubic kilometers of groundwater per annum. The dependency of India on groundwater can be realized from the fact that about two-thirds of its agriculture and nearly 85% of rural water supply for drinking and other household works are obtained from this precious source of water (World Bank 2010). The reasons for inclination of people toward groundwater instead of surface water include (a) erratic and uncertain nature of southwest monsoon, (b) unreliable and inadequate municipal water supplies, and (c) most importantly availability of water at the point of use. The massive dependency on groundwater use leads to both depletion of water table and deterioration of groundwater quality across India. The overexploitation of groundwater resources can be evidenced from the fact that in India, about 36% of groundwater assessment units (known as blocks) are either semi-critical, critical, or overexploited (CGWB 2019). During the last decade (2011–2019), the numbers of overexploited blocks have increased from 1071 to 1186, whereas the number of safe blocks decreased to the tune of 4310, indicating groundwater extraction exceeding the annually replenishable groundwater recharge. It is reported that the trend of aquifer depletion is directly related to population, industrial, and agricultural development of the area. Not only groundwater depletion but also its quality is also deteriorating in an alarming rate throughout India (Dash et al. 2016). Intensive use of groundwater has caused widespread and serious water table decline (in order of 1–2 m per year) in parts of north Gujarat, Saurashtra region, southern Rajasthan, part of Tamil Nadu and Karnataka, entire Rayalaseema region of Andhra Pradesh, Punjab, Haryana, and parts of western Uttar Pradesh (Singh and Singh 2002; Aggarwal et al. 2009a, b; Chatterjee et al. 2009; Chatterjee and Purohit 2009; Chawla et al. 2010; Dash et al. 2010; Singh et al. 2015; Singh et al. 2019). The major social, economic, and environmental implications of depletion of water table include (a) possible reduction in total food grain production, (b) difficulty in abstraction of water, (c) increase in cost of pumping, (d) biodiversity reduction, (e) interruption in the natural water cycle putting disproportionately more water into the sea, and (f) land subsidence. Therefore it is high time to conserve water and implement groundwater recharge techniques.

Groundwater monitoring gives an idea about the water table depth in an area. However as the cost of installation and maintenance of groundwater monitoring network is high, it is not easy task to establish monitoring station everywhere. In this context, spatial interpolation analysis can be considered as a good option for knowing the spatial distribution of water table depth in any area (Yang et al. 2008; Dash et al. 2010). Inverse distance weighting (IDW) method is one of the most widely applicable spatial interpolation methods used for the interpolation and mapping of both groundwater table and pollution level across the world (Rabah et al. 2011; Rani and Chaudhary 2016; Adhikary and Dash 2017). The operational simplicity of the IDW method made this approach to be preferred over other spatial

interpolation techniques (Sarangi et al. 2006; Dash et al. 2019). IDW is a deterministic interpolation method, and in this method estimation of values at unknown points is carried out using values at known points using some mathematical functions that work on extent of similarity.

Anantapur district of Andhra Pradesh in Rayalaseema region, India, falls under rain shadow region and has been faced with severe water problem (Seckler et al. 1998). In this area, groundwater is the main source of agricultural and municipal water supply. Naidu et al. (2014) reported that in Kalyandurg, Anantapur district, there was more than 2 m drawdown in the aquifer during the last 10 years due to excessive pumping. Another recent report revealed that deep depletion of groundwater in the district had adversely affected more than 75,000 bore wells which dried up in the summer season during 2019 (Deccan Chronicle 2019). The reason behind this attributed to both natural and anthropogenic causes. The first cause is that the region receives very little water from monsoon. Second there is a change in agricultural pattern in Rayalaseema region. Farmers are preferring to grow more remunerative crops such as sugarcane, tomato, and groundnut which are water demanding instead of going for low-water-demanding crops such as millets (foxtail, small millet, pearl millet) and pulses (green gram, black gram). This practice, along with recurring droughts in this region, has led to overexploitation of the aquifers. Meinzen-Dick et al. (2016) reported that there was an annual depletion of water level by 0.15–0.65 m in Anantapur district and more than half (55%) of the existing wells had a trend of falling water level. The Central Ground Water Board (2013) also reported there was fall in pre-monsoon water level in 87% of the wells in Anantapur district during 2000–2012. These concerns underlie the importance of investigating spatial variability of groundwater in the Anantapur district. Therefore, the present study has been undertaken with the aim to understand the spatial distribution of groundwater depth in Anantapur district, Andhra Pradesh, India, during the year 2018 and to know the pattern of water table fluctuation during pre-monsoon and post-monsoon seasons.

20.2 Material and Methods

20.2.1 Description of Study Area

The Anantapur district is the largest district of the state Andhra Pradesh and falls under Rayalaseema region which is a drought-prone area. The total area of the district is 19,197 km². The study area is bounded by 13°41'19" to 15°14'58" N latitudes and 76°47'23" to 78°26'00" E longitudes (Fig. 20.1). The surrounding districts are YSR district on the east, Chittoor district on the southeast, and Kurnool district on the north. The Karnataka state makes the southwest boundary of the study area. The study area has 63 administrative *mandals* (also known as blocks). The population of the district is 4.08 million with a density of 213 persons per km² (Census 2011), which is below the state average. The study area comes under

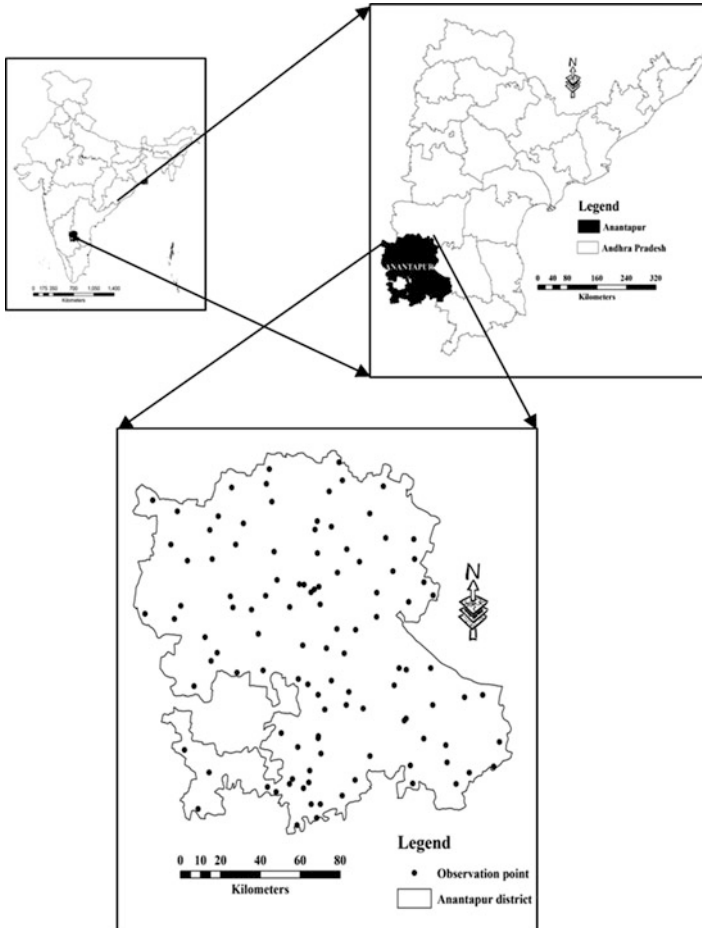


Fig. 20.1 Map of the study area showing locations of observation well

semiarid region with hot and dry summer and mild winter (Rukmani and Manjula 2010). The average annual rainfall is 560 mm. Southwest monsoon reaches the study area by September and lasts for only 2 months and sometimes up to early November. The average annual temperature is 27.6 °C. The major soil types found in the study area are red (82%) and black (18%) soils. It has been reported that sandy loam, rocky land, and clay soil occupies 63%, 14%, and 19% of the total area of the district, respectively (Rukmani and Manjula 2010). As majority of the district is having coarse-textured soil, therefore it is poor in both soil moisture and nutrient retention capacity, which makes the district prone to water and wind erosion. Both high mountainous and plain areas prevail in the study area. In the district, gently sloping lands and very gently sloping plains occupy about 54% of the total study area, followed by undulating hills and ridges, which cover 27% and 14% of the study area,

respectively (Rukmani and Manjula 2010). Valleys occupy only 5% of the district (Rukmani and Manjula 2010). Similarly forests occupy 10%, barren and uncultivable land use covers 9%, and land put to nonagricultural use is 8% in the study area. The net sown area is 8.25 lakh ha. The major crops cultivated in the district are rice (*Oryza sativa*), sorghum (*Sorghum bicolor*), finger millet (*Eleusine coracana*), chilly (*Capsicum frutescens*), sugarcane (*Saccharum officinarum*), onions (*Allium cepa*), and groundnut (*Arachis hypogaea*). Rice and groundnut are the predominant crops accounting for 65,550 and 36,500 ha, respectively. Though agriculture is considered as the main livelihood for most of the people of the district, however it is prone to high levels of instability and uncertainty due to recurring drought. As the study area is situated in the rain shadow region, drought is a regular phenomenon, which prompts farmers to go for construction of medium to deep bore well to assure irrigation for their crops. It has been reported that construction of a large number of bore wells in the study area was the main cause of depletion of aquifers (Govt. of Andhra Pradesh 2008).

20.2.2 Data and Methodology Used

The data used in this study were collected from the Central Ground Water Board (CGWB). The groundwater depth data of 110 wells for the year 2018 were used for this study. Both pre-monsoon (Month to May) and post-monsoon (Month to November) water level data were used to know the seasonal variation of groundwater in the district. The location of the 110 observation wells is shown in Fig. 20.1. The spatial and temporal variation of groundwater depth and groundwater fluctuation over the study area were mapped using the IDW spatial interpolation technique in ArcGIS software 10.0 (ESRI 2010), and the methodology used for mapping is presented in Fig. 20.2.

20.2.3 Inverse Distance Weighting Method

All interpolation methods are based on the assumption that the similarities and correlations between points are inversely proportional to the spatial distance between them. Inverse distance weighting is one of the deterministic spatial interpolation methods in which a continuous surface of values is estimated through weighted average considering values at known locations. The operational simplicity of IDW method makes its wider application in interpolating groundwater level (Reed et al. 2000; Rani and Chaudhary 2016; Adhikary and Dash 2017). A weight is given to data points in such a manner that their influence on prediction is reduced as the

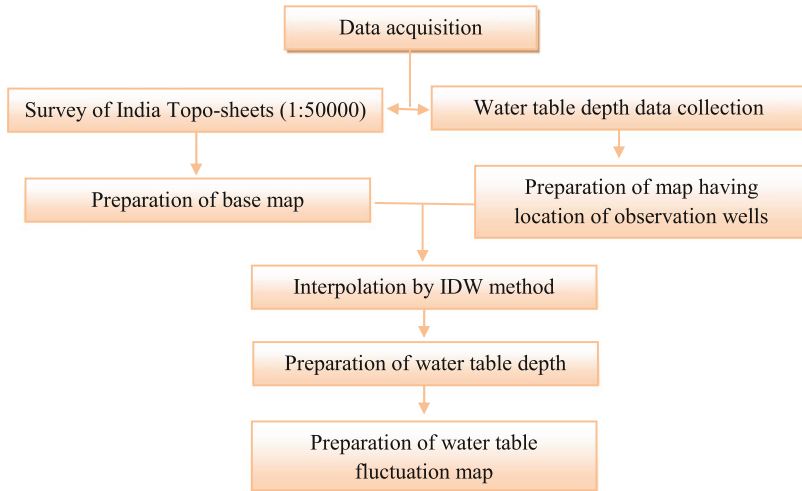


Fig. 20.2 Methodology used for mapping of groundwater depth

distance from the point increases (Adhikary and Dash 2017). Mathematically, IDW method can be described by Eq. 20.1:

$$z(s_0) = \frac{\sum_{i=1}^n \frac{s_i}{h_{ij}^\beta}}{\sum_{i=1}^n \frac{1}{h_{ij}^\beta}} \tag{20.1}$$

where $z(s_0)$ = spatially interpolated value

s_i = i^{th} data value

n = total number of sample data values

h_{ij} = separation distance between interpolated and the sample data value

β = the weighting power

The prediction accuracy of IDW method mainly depends on the value of the weighting power parameter β (Burrough and McDonnell, 1998). In addition, the size of the neighborhood and the number of adjacent points are also influenced by the accuracy of the results (Adhikary and Dash 2017).

20.2.3.1 Selection of Weighting Power Function for IDW

In IDW method, weighting power plays an important role for accurate prediction of groundwater level at the unknown location. Various researchers reported that the value of optimal weighting power function ranged between 1.0 and 4.0 (Kravchenko and Bullock 1999; Adhikary and Dash 2017, Dash et al. 2019). The optimal value of weighting power was obtained by evaluating a series of values ranging from 1.0 to 4.0, and the value for which minimum mean error (ME) and root mean square error (RMSE) are observed was considered as the optimal weighting power function.

20.2.3.2 Validation of Performance of IDW

Prediction performances of IDW method were evaluated by cross-validation. In this all the observed groundwater depth data were divided into two parts randomly. Two-thirds of the observed data were used to develop a model for prediction, and the rest of the one-third data was used for validation of the model. The effectiveness of IDW method for prediction of groundwater level was evaluated based on three commonly used statistics such as root-mean-square error, mean error, and mean relative error (MRE) (Nash and Sutcliffe 1970). The accuracy of the prediction is evaluated by RMSE, and RMSE value close to 0 indicates accurate prediction. Similarly the bias of prediction is represented by ME, and ME value close to 0 indicates unbiased results. These measures can be determined using the following formulas:

$$MAE = \sum_{i=1}^n |(O_i - P_i)| / n \quad (20.2)$$

$$RMSE = \sqrt{\sum_{i=1}^n (O_i - P_i)^2 / n} \quad (20.3)$$

$$MRE = \frac{RMSE}{\Delta} \quad (20.4)$$

where O_i and P_i are the observed and predicted groundwater table depth at i th location and n is the number of observations. Δ is the range and can be calculated by subtracting the minimum observed water table depth from the maximum.

20.3 Results and Discussion

20.3.1 Distribution of Data Set

The normal distribution of observed groundwater level data of the study area was verified using the Kolmogorov and Smirnov test, and it was noticed from the Kolmogorov and Smirnov test that the data are not normally distributed, which can be verified from the descriptive statistics of the data sets (Table 20.1). The skewness values were found to be 1.63 and 1.57 for pre-monsoon and post-monsoon data sets, respectively, which implied that the data sets were not normally distributed, as these were not close to 0. Therefore log transformation was carried to make the data sets normal distribution. After completion of log transformation, the weighting power function was optimized, and the cross-validation data set was analyzed using IDW method. The optimized weighting power function was taken as 1.8. The depth of water table from the ground level varied from 2.0 m to 69.96 m with a mean value of 18.52 m during pre-monsoon of 2018 (Table 20.1). Similarly

Table 20.1 Descriptive statistics of observed groundwater depth in the study area

Season	Minimum depth (m)	Maximum depth (m)	Mean depth (m)	SD (m)	CV (%)	SEM (m)	Kurtosis	Skewness	
								Without transfer	With transfer
Pre-monsoon	2.0	69.96	18.52	12.34	66.6	1.18	3.49	1.63	0.38
Post-monsoon	1.15	68.37	17.63	12.03	68.3	1.15	3.37	1.57	0.21

Note: *SD* Standard deviation, *CV* Coefficient of variation, *SEM* Standard error of mean

during post-monsoon, the depth of groundwater ranged from 1.15 m to 68.37 m with an average value of 17.63 m.

20.3.2 Performance Analysis of IDW Method

Both RMSE and MAE values obtained by IDW method were observed to be low, which indicated that the applicability of IDW to predict water table depth is acceptable (Table 20.2), which was also confirmed by the result reported by Rani and Chaudhary (2016). The MRE values, which indicate relative errors of the predicted data in comparison with the observed data, were also found to be very low (Table 20.2).

20.3.3 Spatial Variability of Groundwater Depth

The spatial variability maps of water table depth during pre-monsoon and post-monsoon seasons of 2018 are shown in Fig. 20.3a, b, respectively, with five classes, indicating areas having a water table within 5 m, between 5 and 10 m, between 10 and 20 m, between 20 and 40 m, and greater than 40 m from the ground surface. The groundwater level during pre-monsoon ranged from 2.0 to 69.96 m. In the northern part of the study area, shallow water levels up to of 5 m were observed (Fig. 20.3a) during both pre-monsoon and post-monsoon seasons. The depth to water levels between 10 and 20 m was observed in majority of the study area. Deeper water levels of greater than 40 m below the ground surface were observed in southeastern parts of the area (Fig. 20.3a).

The area-wise distribution of various water table depths within the study area was also calculated and presented in Table 20.3. Both from the groundwater depth variability map and Table 20.3, it showed that during pre-monsoon season, only 0.82% of the study area had a water table depth occurring within 5 m, 53.42% area had a water table depth varied between 10 and 20 m, and 1.68% area had a water table depth greater than 40 m from the ground surface. During post-monsoon season, there was a very little increase in water level with respect to groundwater depth below 5 m. The groundwater fluctuation map of the study area is presented in Fig. 20.4. Majority areas of the district showed 0–2 m rise in water level between pre- and post-monsoon period of 2018. The rise of water level of 2–4 m and greater

Table 20.2 Performance of IDW method to predict groundwater table depth in the study area

Season	R ²	ME (m)	RMSE (m)	MRE
Pre-monsoon	0.84	0.25	10.81	0.15
Post-monsoon	0.87	0.35	10.91	0.16

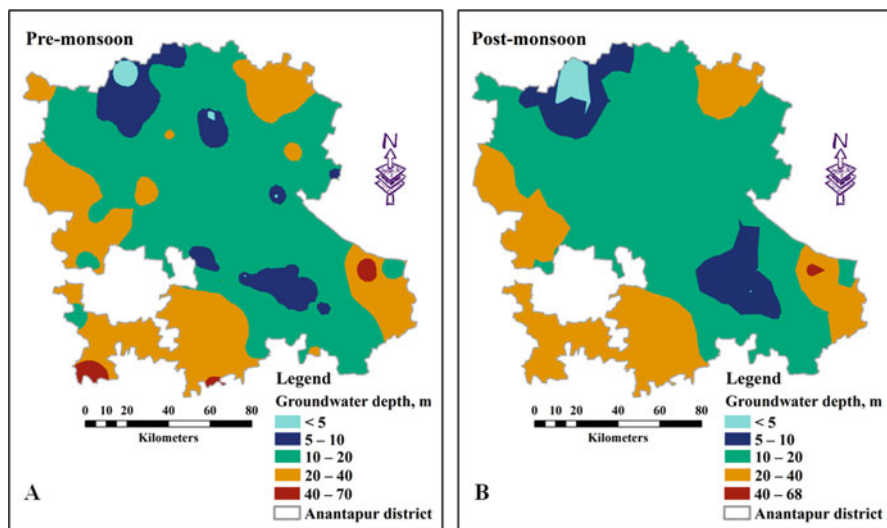


Fig. 20.3 Predicted groundwater table depth map of Anantapur district, Andhra Pradesh, interpolated through inverse distance weighting for (a) pre-monsoon and (b) post-monsoon seasons

Table 20.3 Delineated areas interpolated through IDW under different water table depths

Groundwater depth (m)	Area (km ²)		Area (%)	
	Pre-monsoon	Post-monsoon	Pre-monsoon	Post-monsoon
<5	156.6	208.5	0.82	1.09
5–10	1229.8	1015.6	6.41	5.29
10–20	10255.8	10755.6	53.42	56.03
20–40	7232.1	7149.1	37.67	37.24
>40	322.8	68.2	1.68	0.36

than 4 m was observed in northwest and northwestern part of the district as isolated pockets, respectively. It was also observed that fall of water levels of 0–2 m occurred in isolated patches in north, south, and west part of the district. Fall of water level of more than 2 m was observed in the southern part of the study area.

20.3.4 Stage of Groundwater Development

The stage of groundwater development in the study area was adopted from the Central Ground Water Board (CGWB, 2013) and is presented in Table 20.4 and Fig. 20.5.

In Anantapur district, out of 63 *mandals*, 19, 20, 15, and 19 *mandals* fall under safe, semi-critical, critical, and overexploited category, respectively (Fig. 20.5). It was observed that in one-third of the *mandals*, the pumping of water from aquifer

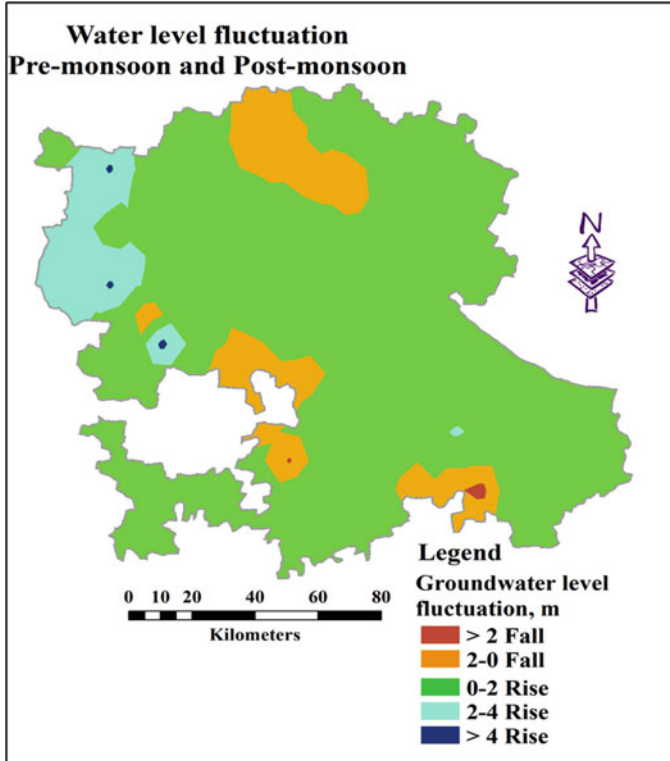


Fig. 20.4 Water table fluctuation map of Anantapur district, during pre- and post-monsoon seasons of 2018

was so high that they reached at either critical or overexploited stage. Almost all *mandals* in the study area belong to very high groundwater usage having an overall stage of groundwater development more than 80% (Table 20.4). *Mandals* like Agali, Peddapappur, Rolla, Tadimarri, and Yellanur have the level of groundwater development even more than 150%. Critical groundwater stage *mandals* are Madakasira, Parigi, Penukonda, Raptadu, and Roddam in the study area.

20.3.5 Prioritization of Mandals

Mandals are classified into high, medium, and low priority based on the stage of groundwater development in the *mandal* and presented in the Table 20.5. Where the groundwater utilization is more than 100%, it is considered as high priority area, where water utilization is in between 50 and 100%, it falls under medium priority, and the rest of the *mandals* fall under low priority area. Out of 63 *mandals*,

Table 20.4 Stage of groundwater development in different *mandals* in the study area

Sl. no.	<i>Mandal</i> name	Stage of development (%)	Sl. no.	<i>Mandal</i> name	Stage of development (%)
1	Agali	161	33	Madakasira	93
2	Amadagur	136	34	Mudigubba	54
3	Amarapuram	120	35	NP Kunta	66
4	Anantapur	74	36	Nallacheruvu	60
5	Atmakur	77	37	Nallamada	37
6	Bukkarayasamudram	81	38	Narpala	84
7	Bathalapalli	116	39	Obuladevaracheruvu	84
8	Beluguppa	109	40	Pamidi	31
9	Bommanahal	41	41	Parigi	91
10	Brahmasamudram	108	42	Peddapappur	203
11	Bukkapatnam	79	43	Peddvaduguru	36
12	Chennekotha Palli	67	44	Penukonda	93
13	Chilamathur	65	45	Putlur	173
14	D. Hirehal	61	46	Puttaparathi	53
15	Dharmavaram	45	47	Ramagiri	74
16	Gandlapenta	119	48	Raptadu	90
17	Garladinne	73	49	Rayadurg	77
18	Gooty	74	50	Roddam	94
19	Gorantla	85	51	Rolla	162
20	Gudibanda	118	52	Settur	81
21	Gummagatta	78	53	Singanamala	45
22	Guntakal	63	54	Somandepalli	83
23	Hindupur	106	55	Tadimarri	166
24	Kadiri	76	56	Tadipatri	123
25	Kalyandurga	84	57	Talupula	77
26	Kambadur	84	57	Tanakallu	61
27	Kanaganapalli	75	59	Uravakonda	27
27	Kanekal	53	60	Vajrakarur	44
29	Kothacheruvu	110	61	Vidapanakal	19
30	Kudair	83	62	Yadiki	148
31	Kundurpi	104	63	Yellanur	170
32	Lepakshi	115			

19 *mandals* come under high priority area whereas 37 *mandals* are under medium category and the rest 7 *mandals* under low priority category (Table 20.5).

Therefore precaution should be taken in those high priority *mandals* for future groundwater development. Construction of rainwater harvesting structures like farm ponds, percolation tanks, contour bunding, and check dams should be advocated widely at appropriate places to conserve water and facilitate groundwater recharge. Rooftop rainwater harvesting should be taken up in a wider scale so as to avoid building pressure on the groundwater, and to some extent the harvested water can be

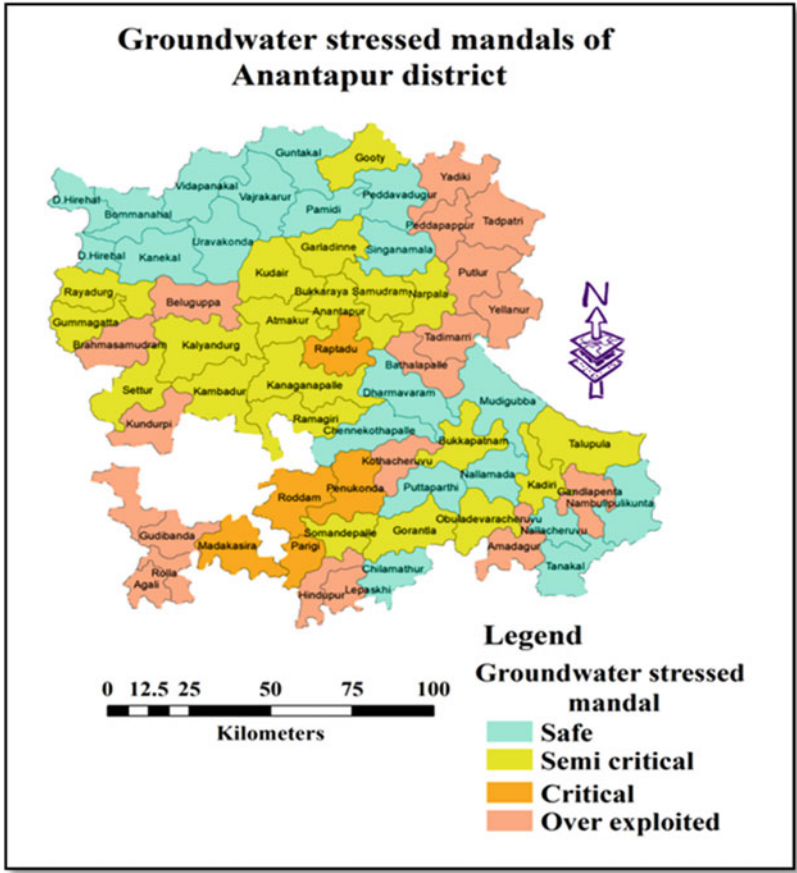


Fig. 20.5 Mandal-wise categorization of groundwater-stressed area in Anantapur district, Andhra Pradesh

helpful in irrigating kitchen garden. Most importantly, awareness should be created among the people regarding optimum utilization of water both for household and irrigation purposes. Similarly, farmers should be encouraged to practice contour farming, strip cropping, cover cropping, etc. for in situ conservation of moisture in the field. Apart from this, low water-demanding crops like sorghum, pulses, and finger millet should be encouraged to adopt. Wherever there is a demand of high water-requiring crops, those crops should be raised using water-saving irrigation techniques like sprinkler and drip irrigation. Further community-based sprinkler and drip irrigation system must be practiced. Broad bed and furrow (BBF) system of cultivation should be encouraged instead of flat cultivation, which is beneficial in terms of moisture conservation.

Table 20.5 Prioritization of *mandals* based on water stress in Anantapur district

High priority	Medium priority	Low priority
Agali, Amadagur, Amarapuram, Bathalapalli, Beluguppa, Brahasamudram, Gandlapenta, Gudibanda, Hindupur, Kothacheruvu, Kundurpi, Lepakshi, Peddapappur, Putlur, Rolla, Tadimarri, Tadipatri Yellanur, Yadiki	Anantapur, Atmakur, Bukkarayasamudram, Bukkapatnam, Chennekotha Palli, Chilamathur, D. Hirehal, Garladinne, Gooty, Gorantla, Gummagatta, Guntakal, Kadiri, Kalyandurga, Kambadur, Kanaganapalli, Kanekal, Kudair, Madakasira, Mudigubba, NP Kunta, Nallacheruvu, Narpala, Obuladevaracheruvu, Parigi, Peddvaduguru, Penukonda, Puttaparthi, Ramagiri, Raptadu, Rayadurg, Roddam, Settur, Somandepalli, Talupula, Tanakallu, Vidapanakal	Bommanahal, Dharmavaram, Nallamada, Pamidi, Singanamala, Uravakonda, Vajrakarur

20.4 Conclusions

The present study has been conducted to know the spatial and temporal variation of groundwater depth in the Anantapur district, Andhra Pradesh, India. The study area comes under rain shadow region and receives only 560 mm of rainfall annually. The area is prone to recurring drought, and majority of the people depend on groundwater for both irrigation and domestic uses. It was observed that all the *mandals* of the district are very high uses of groundwater and average groundwater development of the district is more than 80%. In some of the *mandals*, the groundwater development even reached 200%. Therefore, water conservation and groundwater recharge techniques may be executed, and awareness about judicious use of water may be created to avoid further depletion of aquifer in the district.

References

- Adhikary, P.P. & Dash, Ch. J. (2017). Comparison of deterministic and stochastic methods to predict spatial variation of groundwater depth. *Applied Water Sciences*, 7(1), 339–348.
- Aggarwal, R., Kaur, S. & Miglani, P. (2009a) Block wise assessment of water resources in Jalandhar district of Indian Punjab. *Journal of Soil and Water Conservation*, 8, 69–73.
- Aggarwal, R., Kaur, S. & Miglani, P. (2009b). Assessment of block wise availability and demand of water resources in Hoshiarpur district of Punjab. *Indian Journal of Soil Conservation*, 37, 106–111.
- Burrough, P.A. & McDonnell, R.A. (1998). *Creating continuous surfaces from point data*. In: Burrough PA, Goodchild, MF, McDonnell, RA, Switzer P, Worboys, M (Eds), *Principles of Geographic Information Systems*. Oxford University Press, Oxford, UK.
- Census (2011). *Census of India*. New Delhi: Government of India.

- CGWB (2013) *Groundwater Brochure, Anantapur district, Andhra Pradesh*, Central Ground Water Board, Ministry of Water Resources, Government of India, pp. 23.
- CGWB (2019) *National compilation on dynamic ground water resources of India, 2017*, Central Ground Water Board, Ministry of Jal Shakti, Faridabad, India.
- Chatterjee, R. & Purohit, R. (2009). Estimation of replenishable groundwater resources of India and their status of utilization. *Current Science*, 96, 1581–1591.
- Chatterjee, R., Gupta, B.K., Mohiddin, S.K., Singh, P.N., Shekhar, S. & Purohit, R. (2009). Dynamic groundwater resources of National Capital Territory, Delhi: assessment, development and management options. *Environmental Earth Sciences*, 59, 669–686.
- Chawla, J.K. Khepar, S.D., Sondhi, S.K. & Yadav, A.K. (2010). Assessment of long term groundwater behaviour in Punjab, India. *Water International*, 35, 63–77.
- Dash, Ch. J., Das, N.K. & Adhikary, P.P. (2019). Rainfall erosivity and erosivity density in Eastern Ghats Highland of east India. *Natural Hazards*, 97(2), 727–746.
- Dash, Ch. J., Sarangi, A., Adhikary, P.P. & Singh, D.K. (2016). Simulation of nitrate leaching under maize-wheat cropping system in a semiarid irrigated area of the Indo-Gangetic Plain, India. *Journal of Irrigation and Drainage Engineering*, 142(2), 04015053. [https://doi.org/10.1061/\(ASCE\)IR.1943-4774.0000965](https://doi.org/10.1061/(ASCE)IR.1943-4774.0000965).
- Dash, J.P., Sarangi, A. & Singh, D.K. (2010). Spatial variability of groundwater depth and quality parameters in the National Capital Territory of Delhi. *Environmental Management*, 45(3), 640–650.
- Deccan Chronicle (2019). Anantapur: Borewells dry up as groundwater levels go down. <https://www.deccanchronicle.com/nation/current-affairs/070519/anantapur-borewells-dry-up-as-groundwater-levels-go-down.html>. Accessed on 10th October 2019.
- Environmental System Research Institute (ESRI) (2010). Software help documentation.
- Government of Andhra Pradesh (2008). *Groundwater conditions in Anantapur district*. Groundwater Department. Anantapur, Andhra Pradesh.
- Kravchenko, A. & Bullock, D.G. (1999). A comparative study of interpolation methods for mapping soil properties. *Agronomy Journal*, 91, 393–400.
- Margat, J. & van der Gun, J. (2013). *Groundwater around the world: a geographical synopsis*. CRC Press, London
- Meinzen-Dick, R., Chaturvedi, R., Domènech, L., Ghate, R., Janssen, M. A., Rollins, N. D. & Sandeep, K. (2016). Games for groundwater governance: field experiments in Andhra Pradesh, India. *Ecology and Society*, 21(3), 38. <https://doi.org/10.5751/ES-08416-210338>.
- Naidu, R., Nagaraja, R.K. & Ramanaiah, Y.V. (2014). Assessment of depth to groundwater levels (DTW) in Kalyandurg area of Anantapur district, Andhra Pradesh, India using geospatial techniques, *International Journal of Current Research*, 6 (8), 7816–7821.
- Nash, J.E. & Sutcliffe, L.V. (1970). River flow forecasting through conceptual models part I-a discussion of principles. *Journal of Hydrology*, 10(3), 282–290.
- Rabah, F.K.J., Ghabayen, S.M. & Salha, A.A. (2011). Effect of GIS interpolation techniques on the accuracy of the spatial representation of groundwater monitoring data in Gaza Strip. *Journal of Environmental Science and Technology*, 4, 579–589.
- Rani, Reeta. & Chaudhary, B.S. (2016). GIS Based Spatio-temporal mapping of groundwater depth in Hisar district, Haryana state, India. *International Journal of Advanced Remote Sensing and GIS*, 5 (11), 1971–1980.
- Reed, P., Minsker, B. & Valocchi, A.J. (2000). Cost-effective long-term groundwater monitoring design using a genetic algorithm and global mass interpolation. *Water Resources Research*, 36(12), 3731–3741.
- Rukmani, R. & Manjula, M. (2010). *Designing rural technology delivery systems for mitigating agricultural distress: A study of Anantapur district*. M.S. Swaminathan Research Foundation, Chennai.
- Sarangi, A., Madramootoo, C.A. & Enright, P. (2006). Comparison of spatial variability techniques for runoff estimation from a Canadian watershed. *Biosystem Engineering*, 95(2), 295–308.

- Seckler, D., Amarasinghe, U., David, M., deSilva, R. & Barker, R. (1998). *World water demand and supply 1990 to 2025: Scenarios and issues*. Research Report-19. International Water Management Institute, Colombo, Sri Lanka.
- Singh, A., Sharma, C.S., Jeyaseelan, A.T. & Chowdary, V.M. (2015). Spatiotemporal analysis of groundwater resources in Jalandhar district of Punjab state, India. *Sustainable Water Resources Management*, 1, 293–304.
- Singh, D.K. & Singh, A.K. (2002). Groundwater situation in India: problems and perspective. *International Journal of Water Resources Development*, 18, 563–580.
- Singh, O., Kasana, A., Singh, K.P. & Sarangi, A. (2019). Spatial and temporal trends of groundwater level under rice-wheat ecosystem in north-west India. *Natural Resources Research* DOI: <https://doi.org/10.1007/s11053-019-09477-6>.
- World Bank (2010). India Groundwater: a valuable but diminishing resource. <https://www.worldbank.org/en/news/feature/2012/03/06/india-groundwater-critical-diminishing> (Accessed on November 2019)
- Yang, F.G., Cao, S.Y., Liu, X.N. & Yang, K.J. (2008) Design of groundwater level monitoring network with ordinary Kriging. *Journal of Hydrology*, 20(3), 339–346.

Chapter 21

Exploring Vulnerability of Groundwater Using AHP and GIS Techniques: A Study in Cooch Behar District, West Bengal, India



Dipankar Saha, Debasish Talukdar, Ujjal Senapati, and Tapan Kumar Das

Abstract Sustainable groundwater balance is dropping off day by day throughout the world. Owing to random withdrawal of groundwater to meet the demand of tremendous population pressure, extensive irrigation and inefficient use of surface water in the different territories of the world, groundwater storage becomes prone to depletion. Cooch Behar district in the northern part of West Bengal is dominated by loamy types of soil which are very conducive for groundwater recharge, but overexploitation of groundwater in this district has created stress on groundwater reserve. In this study, a newly developed PCP_L method is used for predicting groundwater vulnerability. It is a GIS-based method used for mapping projected groundwater vulnerability giving priority on the basis of AHP technique considering three interlinked and interdependent variables such as (i) groundwater potentiality, (ii) groundwater consumption and (iii) long-term groundwater fluctuation. It is evident from the result that areas under the category of very low, low and moderate groundwater vulnerability are decreasing, whereas areas under high and very high category of groundwater vulnerability are increasing in all three projected cases of 2028, 2034 and 2040. The projected areas under very low, low, moderate, high and very high groundwater vulnerability zone in 2040 are 8%, 16%, 23%, 23% and 30%, respectively. This stress on groundwater can definitely be reduced through wide use of surface water, reuse and recycling of water, extensive rainwater harvesting, modernized irrigation system and nature-friendly afforestation with community involvement.

D. Saha

Department of Geoinformatics, Cooch Behar College, Cooch Behar, West Bengal, India

D. Talukdar · U. Senapati

Department of Geography, Cooch Behar Panchanan Barma University, Cooch Behar, West Bengal, India

T. K. Das (✉)

Department of Geography, Cooch Behar College, Cooch Behar, West Bengal, India

Keywords AHP technique · Groundwater balance · PCP_L method · Projected groundwater level

21.1 Introduction

Sustainable groundwater balance is dropping off day by day throughout the world. The main three reasons for suitable groundwater shrinking are depletion for withdrawal, salinization and pollution. In the different world territories, tremendous population pressure, extensive tube well irrigation and inefficient use of surface water are creating stress to groundwater storage (Saha et al. 2001). Currently 69% of groundwater is being utilized for the purpose of agriculture, 23% for industry and rest 8% for domestic use. The overuse of groundwater per unit of population in 1950 has decreased to 60% in developed countries and 30% in the developing countries in 2000.

India is one of the countries which are rapidly proceeding towards the acute scarcity of groundwater due to the growing population. The national per capita annual availability of water in India has shortened from 1816 cubic metre in 2001 to 1544 cubic metre in 2011. The rate of negative change is 15%. In India 89% of groundwater is extracted for use in the irrigation sector, and its extraction for the purpose of domestic use and industrial use is, respectively, 9% and 2%. 50% of urban domestic water demands and 85% of rural domestic water demands are met by groundwater. The whole West Bengal except the northern hilly terrain comes under the alluvial aquifers of the Indo-Gangetic plains (Saha et al. 2001).

The main type of soil found in West Bengal is the younger alluvial soil (Ray and Shekhar. 2009) which has the great potential for development of groundwater, but incessant extraction of groundwater for the purpose of agriculture and domestic use is causing the rapid reduction of groundwater storage. High population density, fast development and extensive irrigation have created stress in groundwater storage of West Bengal. The annual per capita availability of fresh water in 1961 was 5177 cubic metres, which has decreased to 1869 cubic metres in 2001 (Bhuin 2014). The present water crisis in West Bengal is due to misuse and abuse of water (Rudra 2005). Cooch Behar district in the northern part of the West Bengal is dominated by loamy types of soil which is very conducive for groundwater recharge, but overexploitation of groundwater in this district has created stress on groundwater reserve. The present study deals with groundwater potentiality, groundwater consumption and projection of groundwater vulnerability in Cooch Behar district, West Bengal.

21.2 Study Area

The study area, Cooch Behar district, is situated in the north-eastern part of West Bengal (Fig. 21.1) covering an area of 3387 sq. km (District Census Handbook 1961). The latitudinal and longitudinal extension of the study area is from 25°57'47"

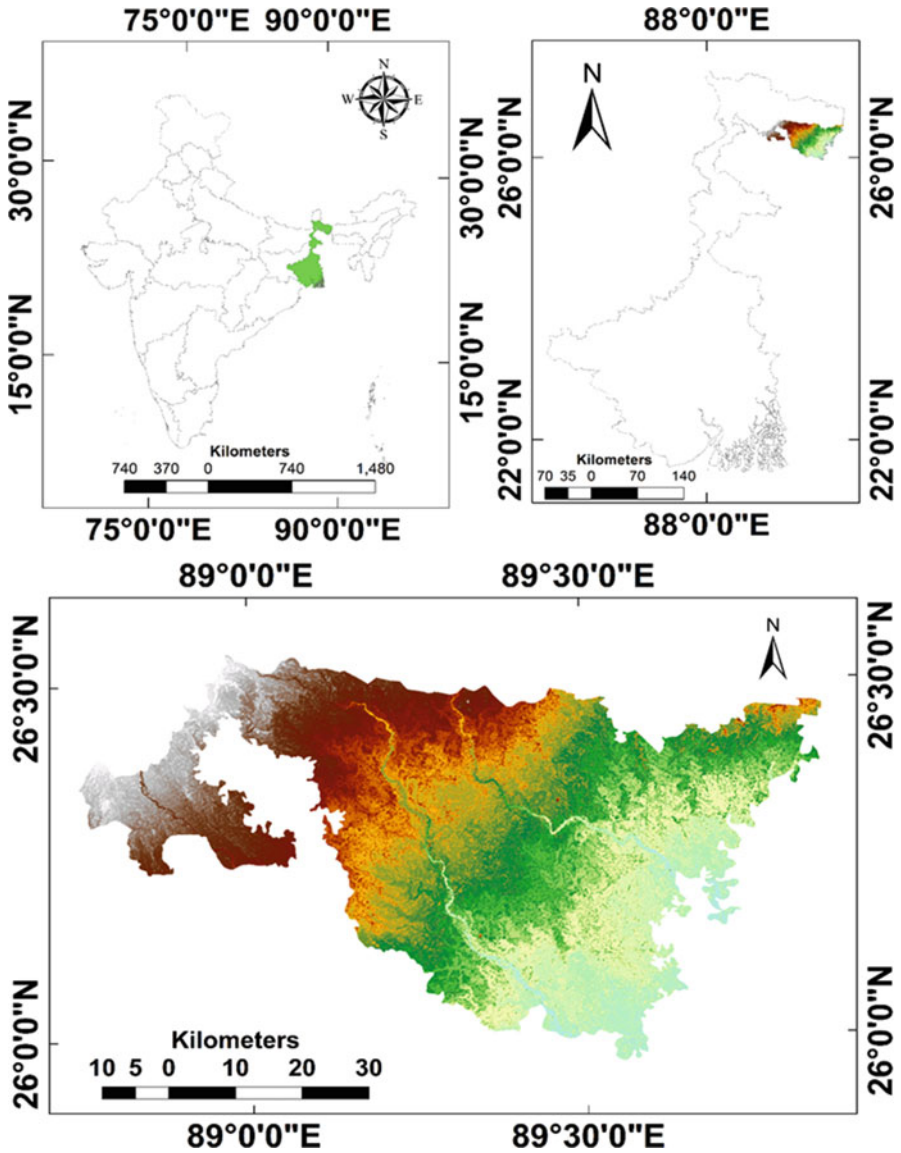


Fig. 21.1 Location map of study area

N to 26°36'20" N and from 88°47'44" E to 89°54'35" E, respectively. The total amount of rainfall received in a year is 3021 mm, and the temperature varies from 20 to 37°C in summer and 10 to 22°C in winter. The atmosphere is highly humid throughout the year. The district holds a total population of 28,19,086 in 12 numbers of blocks (Census 2011). The physiography of the district comes under the active and old floodplain dominated by loamy types of soil. That's why most of the peoples are engaged in agricultural activity. The source of the district's entire groundwater is alluvial aquifers.

21.3 Materials and Methods

21.3.1 Materials

To prepare the maps of groundwater potential zones, groundwater level zone and groundwater consumption zone, data collection was done from different sources (Table 21.1).

21.3.2 Methods

Assessment of groundwater vulnerability has been done using different methods in respect to different views of area, such as groundwater pollution sensitive area,

Table 21.1 Details of data and sources

Attribute	Sources
Landsat 8 (spatial resolution 30 m) (LC08_L1TP_138042_20181229_20190130_01)	USGS EarthExplorer
SRTM DEM (spatial resolution 30 m) (n25_e088, n25_e089, n26_e088, n26_e089)	USGS EarthExplorer
Soil texture map	NBSS & LUP
Rainfall data	Indian Meteorological Department (IMD)
Geomorphology	BHUVAN
Lithology	Geological Survey of India (GOI)
Population	Census of India, 2011
Irrigation	Assistant engineer (agri-irrigation), Assistant engineer (agri-mech), Dy. Director of agri- culture, Cooch Behar, West Bengal
Agriculture data	Dy. Director of agriculture, Cooch Behar, Govt. of West Bengal
Livestock	Dy. Director, Animal Resources Develop- ment Parishad Office, Cooch Behar
Groundwater data	Central Groundwater Board (CGWB), India

groundwater shortage area and hydro-geological area various method namely, “GOD” method (Foster 1987; Huang et al. 2013; Ghazavi and Ebrahimi 2015), “AVI” method (Stempvoort et al. 1993), “DRASTIC” (Aller 1985; Rahman 2008; Neshat et al. 2014), SINTACS (Civita 1994; Busico et al. 2017), EPIK (Doerfliger and Zwahlen 1997; Doerfliger et al. 1999), Hydro-geological complex method (Albinet and Margat 1970), ISIS method (Civita and De regibus 1995). GIS, modeling (Nobre et al. 2007; Gogu and Dassargues 2000; Shirazi et al. 2012; Joshi and Gupta 2018), are used to grow water assessment, but a single holistic model assessing potentiality as well as withdrawal of groundwater projecting vulnerability of groundwater has not level been yet introduced.

In this study a newly developed PCP_L method is used for forecasting and predicting groundwater vulnerability. It is a GIS-based weight overlay method using priority and weight on the basis of AHP technique considering three interlinked variables such as (i) groundwater recharge or potentiality (*P*), (ii) groundwater discharge or withdrawal for different purposes of consumption (*C*) and (iii) projected groundwater level (*P_L*) (Fig. 21.2).

Weighting parameters are assigned to consider their importance for vulnerability and the vulnerability index is calculated with the help of following equation:

$$VI_{pcp} = (P \times \alpha) + (C \times \beta) + (P_L \times \gamma)$$

where:

VI_{pcp} = vulnerability index of the PCP_L method.

P = the rating value of “potential groundwater zone” (*P*).

C = the rating value of “groundwater consumption zone” (*C*).

P_L = the rating value of “projected groundwater level” (*P_L*).

α, β, γ = relative weight factors for PCP_L method assigned based on AHP technique.

Weights are as follows: $\alpha = 0.539, \beta = 0.296, \gamma = 0.163$.

21.3.2.1 AHP Weighted Overlay Method Using GIS Technique

Delineation of Groundwater Potential Zones

In this study groundwater potential zones of the study area are identified and mapped using knowledge-based factor analysis of a total of eight layers of information such as land use/land cover (LULC), soil, rainfall, drainage density, geomorphology, lithology, normalized difference vegetation index (NDVI) and topographic wetness index (TWI)

The weights of each parameter were given Satty’s scale of relative importance value (Saaty 1990; Arulbalaji et al. 2019). Further, the weights are allotted to the thematic layer on the basis of their importance to the potentiality of groundwater recharge considering review of the literature, field observation and experience. Accordingly, eight thematic layers have been linked with each other in a pairwise

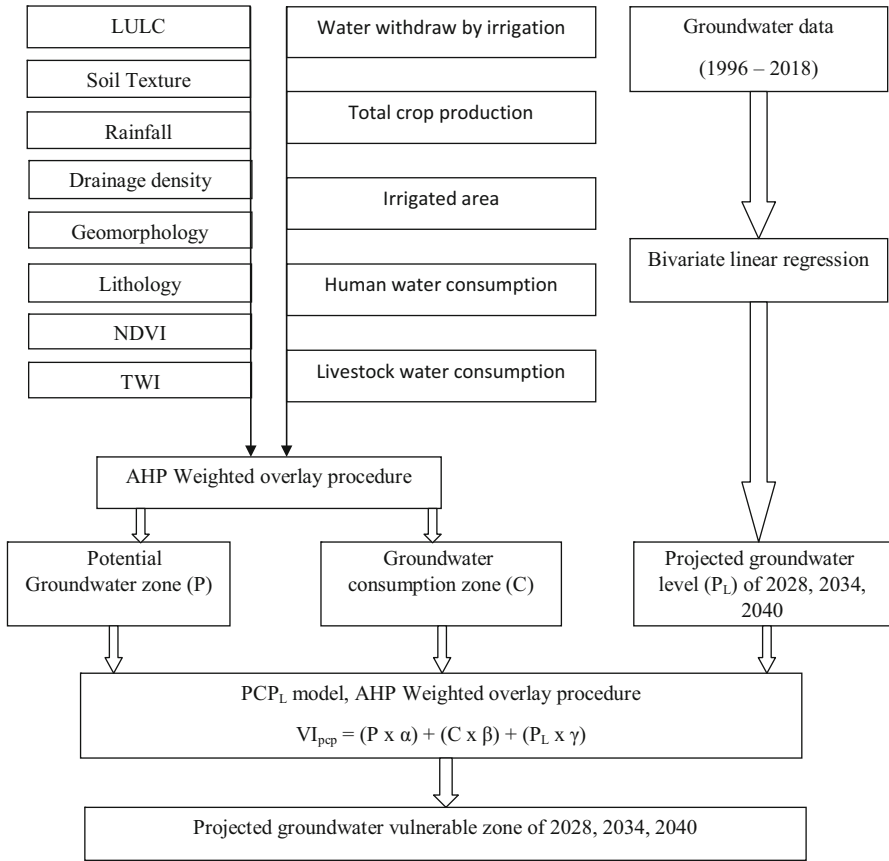


Fig. 21.2 Flow chart of methodology used for deriving projected groundwater vulnerable zone

comparison matrix (Table 21.2). The sub-classes of thematic layers were re-categorized using a GIS platform for assigning weight. For computation of the consistency ratio (CR), the subsequent steps are used: Principal eigenvalue (λ) was computed by eigenvector technique (Tables 21.2 and 21.3), consistency index (CI) was calculated from the equation given below (Saaty 1990; Arulbalaji et al. 2019).

Calculation for groundwater potential zones (GWPZ)

$$\lambda_{max} = 64/8 = 8$$

$$C.I = (\lambda_{max} \cdot n)/(n - 1)$$

n = Number of parameters used in the analysis.

$$\text{So, } C.I = (8 - 8)/(8 - 1) = 0$$

Table 21.2 Pairwise comparison matrix of GWPZ

Themes	Assigned weight	LULC	Soil	Rainfall	D. D	Geomorphology	Lithology	NDVI	TWI	Geometric mean	Normalized weight
LULC	7	7/7	7/6	7/5	7/5	7/4	7/3	7/2	7/1	1.972	0.212
Soil	6	6/7	6/6	6/5	6/5	6/4	6/3	6/2	6/1	1.690	0.182
Rainfall	5	5/7	5/6	5/5	5/5	5/4	5/3	5/2	5/1	1.409	0.152
D.D	5	5/7	5/6	5/5	5/5	5/4	5/3	5/2	5/1	1.409	0.152
Geomorphology	4	4/7	4/6	4/5	4/5	4/4	4/3	4/2	4/1	1.127	0.121
Lithology	3	3/7	3/6	3/5	3/5	3/4	3/3	3/2	3/1	0.845	0.091
NDVI	2	2/7	2/6	2/5	2/5	2/4	2/3	2/2	2/1	0.563	0.061
TWI	1	1/7	1/6	1/5	1/5	1/4	1/3	1/2	1/1	0.282	0.030

Table 21.3 Normalized matrix of GWPZ

Themes	LULC	Soil	Rainfall	D.D	Geomorphology	Lithology	NDVI	TWI	Weighted sum	Row average	λ
LULC	0.212	0.212	0.212	0.212	0.212	0.212	0.212	0.212	1.697	0.212	8.000
Soil	0.182	0.182	0.182	0.182	0.182	0.182	0.182	0.182	1.455	0.182	8.000
Rainfall	0.152	0.152	0.152	0.152	0.152	0.152	0.152	0.152	1.212	0.152	8.000
D.D	0.152	0.152	0.152	0.152	0.152	0.152	0.152	0.152	1.212	0.152	8.000
Geomorphology	0.121	0.121	0.121	0.121	0.121	0.121	0.121	0.121	0.970	0.121	8.000
Lithology	0.091	0.091	0.091	0.091	0.091	0.091	0.091	0.091	0.727	0.091	8.000
NDVI	0.061	0.061	0.061	0.061	0.061	0.061	0.061	0.061	0.485	0.061	8.000
TWI	0.030	0.030	0.030	0.030	0.030	0.030	0.030	0.030	0.242	0.030	8.000

Table 21.4 Saaty’s ratio index for different values of N

Order of matrix										
N	1	2	3	4	5	6	7	8	9	10
RCI value	0	0	0.58	0.9	1.12	1.24	1.32	1.41	1.45	149

Consistency ratio (CR) is determined as the ratio between CI and RCI (where CI = consistency index, RCI = random consistency index) whose value is taken from Saaty’s standard values (Saaty 1990) (Table 21.4).

$$\text{Hence, CR} = \text{CI}/\text{RCI}$$

$$\text{CR} = 0/1.41 = 0$$

The groundwater potential zone (GWPZ) of the study area was generated through the integration of the concerned eight thematic layers (Table 21.5) into one layer on the basis of groundwater potential index which is calculated using the following equation (Shekhar and Pandey 2015; Das et al. 2018):

$$\text{GWPI} = \text{LU}_w\text{LU}_r + \text{S}_w\text{S}_r + \text{R}_w\text{R}_r + \text{DD}_w\text{DD}_r + \text{G}_w\text{G}_r + \text{L}_w\text{L}_r + \text{N}_w\text{N}_r + \text{TWI}_w\text{TWI}_r$$

where LU denotes land use/land cover, S denotes soil, R denotes rainfall, and DD denotes drainage density. G denotes geomorphology, L denotes lithology, N denotes normalized difference vegetation index, and TWI denotes topographic wetness index. w denotes the parameter weight, and r is the sub-factor weight of corresponding parameter.

Delineation of Groundwater Consumption Zones (GWCZ)

Although recycled by nature, fresh water is a limited resource. High water-consuming activities such as agriculture, industry and domestic use of the growing population are responsible for the declining per capita water availability (Shaban and Sharma 2007). To prepare groundwater consumption zones, block-wise data of five parameters have been incorporated on the basis of AHP using knowledge-based factors analysis. The parameters are (i) average groundwater withdrawal of water by different irrigation techniques (such as dug well, deep tube well, shallow tube well, high-capacity deep tube well, low-capacity tube well, river lifting irrigation), (ii) total crop production, (ii) irrigated area, (iv) human water consumption and (v) livestock water consumption (Table 21.6).

Calculation of groundwater consumption zones (GWCZ)

Table 21.5 Normalized weight of sub-factors of GWPZ

Factor	Domain of effect	Normalized weight	Area (sq. km.)	% of area
LULC	Settlement	0.035	1253	37
	Sand Bar	0.051	373	11
	Agricultural fallow	0.078	440	13
	Cultivation land	0.123	948	28
	Water bodies	0.198	68	2
	Sparsed vegetation	0.198	135	4
	Dense vegetation	0.316	169	5
Soil texture	Fine-coarse loamy	0.061	677	20
	Fine loamy-coarse loamy	0.097	1084	32
	Fine loamy	0.159	373	11
	Coarse loamy	0.262	813	24
	Coarse loamy-fine loamy	0.148	440	13
Rainfall	2545–2684 mm (very poor)	0.061	271	8
	2684–2845 mm (poor)	0.097	203	6
	2845–2969 mm (moderate)	0.159	1084	32
	2969–3043 mm (good)	0.262	1016	30
	3043–3178 mm (very good)	0.061	813	24
Drainage density	< 0.5 (very poor)	0.061	474	14
	0.5–1.00 (poor)	0.097	1118	33
	1.00–1.50 (moderate)	0.149	1253	37
	1.51–2.00 (good)	0.329	474	14
	>2.00 (very good)	0.361	68	2
Geomorphology	Fluvial origin younger alluvial plain	0.277	1727	51
	Fluvial origin active floodplains	0.467	542	16
	Fluvial origin older floodplain	0.160	948	28
	Fluvial origin Piedmont alluvial plain	0.095	169	5
Lithology	Light grey silty loams underlain by unaltered multiple sequence of fine sand, silt and clay with bog clay	0.160	837	25
	Alternate layers of sand silt and clay	0.095	10	0
	Gravel, coarse to fine sand, silt and clay	0.277	1558	46
	Very fine sand, silt and clay	0.467	982	29
NDVI	No vegetation	0.097	1152	34
	Shrubs and grassland	0.163	1456	43
	Moderately healthy vegetation	0.337	677	20
	Water bodies	0.408	102	3
TWI	2.43–7.78 (very poor)	0.033	237	7
	7.78–10.33 (poor)	0.063	677	20
	10.33–12.27 (moderate)	0.128	779	23
	12.27–14.67 (good)	0.261	711	21
	14.67–22.19 (very good)	0.512	982	29

Table 21.6 Pairwise comparison matrix of GWCZ

Themes	Assigned weight	Daily average groundwater withdrawal for irrigation	Total crop production	Irrigated area	Human water consumption	Livestock water consumption	Geometric mean	Normalized weight
Daily average groundwater withdrawal for irrigation	5	5/5	5/4	5/3	5/2	5/1	1.919	0.333
Total crop production	4	4/5	4/4	4/3	4/2	4/1	1.535	0.267
Irrigated area	3	3/5	3/4	3/3	3/2	3/1	1.152	0.200
Human water consumption	2	2/5	2/4	2/3	2/2	2/1	0.768	0.133
Livestock water consumption	1	1/5	1/4	1/3	1/2	1/1	0.384	0.067

Table 21.7 Normalized matrix of GWCZ

Daily average groundwater withdrawal for irrigation	0.333	0.333	0.333	0.333	0.333	1.667	0.333	5.000
Total crop production	0.267	0.267	0.267	0.267	0.267	1.333	0.267	5.000
Irrigated area	0.200	0.200	0.200	0.200	0.200	1.000	0.200	5.000
Human water consumption	0.133	0.133	0.133	0.133	0.133	0.667	0.133	5.000
Livestock water consumption	0.067	0.067	0.067	0.067	0.067	0.333	0.067	5.000

$$\lambda_{\max} = 25/5 = 5$$

$$C.I = (\lambda_{\max} - n)/(n - 1)$$

n = Number of parameters used in the analysis

$$C.I = (5 - 5)/(5 - 1) = 0$$

Consistency ratio (CR) is defined as the ratio between CI and RCI, where CI = consistency index and RCI = random consistency index value, whose value is taken from Saaty's standard values (Saaty 1990) (Table 21.4).

$$CR = 0/1.12 = 0$$

According to Saaty, if the value of CR is 0.10 or less, it is satisfactory to continue the analysis. If the CR value is 0, it means that there is a perfect level of consistency (Saaty 1990; (Arulbalaji et al. 2019). The values of CR in both cases of groundwater potential zones (GWPZ) and groundwater consumption zones (GWCZ) are 0. It implies perfect consistency and acceptance in both cases (Table 21.7).

The *groundwater consumption zones* (GWCZ) of the study area were created through the combination of the concerned five thematic layers into one layer on the basis of groundwater consumption index (GWCI) which is calculated using the following equation (Shekhar and Pandey 2015; Das et al. 2018):

$$GWCI = IT_wIT_r + TCP_wTCP_r + IA_wIA_r + HC_wHC_r + LC_wLC_r$$

where IT denotes irrigation techniques, TCP denotes total crop production, IA denotes irrigated area, HC denotes human water consumption, LC denotes human water consumption, w denotes the parameter weight and r is the sub-factor weight of the corresponding parameter (Table 21.8).

21.3.2.2 Projection of Groundwater Level Using Bivariate Linear Regression Method

On the basis of the groundwater data for the period of 1996–2018, the projected ground level data are calculated using bivariate linear regression technique for all

Table 21.8 Normalized weight of sub-factors of GWCZ

Factor	Domain of effect	Normalized weight
Daily average groundwater withdrawal for irrigation	55.398–60.663	0.079
	60.663–68.562	0.120
	68.562–117.270	0.189
	117.270–234.431	0.251
	234.431–391.085	0.385
Total crop production	0.318–0.363	0.080
	0.363–0.475	0.136
	0.475–0.731	0.226
	0.731–0.843	0.256
	0.843–0.965	0.300
Irrigated area	8.403–11.489	0.106
	11.489–15.280	0.184
	15.280–23.919	0.292
	23.919–30.884	0.415
Human water consumption	95.1–120	0.106
	120.1–143	0.184
	143.1–155	0.292
	155.1–200	0.415
Livestock water consumption	5.1–6	0.106
	6.1–33	0.184
	33.1–36	0.292
	36.1–53	0.415

blocks of the Cooch Behar district, and the interpolation technique on ArcGIS platform has been used for delineation of projected groundwater zonation map.

21.4 Results and Discussion

21.4.1 Groundwater Potential Zones (GWPZ)

21.4.1.1 Land Use/Land Cover (LULC)

LULC is the most leading aspect in terms of defining groundwater availability in alluvial aquifers because various types of LULC act differently in the runoff and infiltration of water. Dense vegetation cover is ideal for groundwater recharge, whereas urbanized area promotes the rate of runoff restricting groundwater recharge by man made concrete coverage of earth surface. Land use/land cover map has been prepared by a mosaic of Landsat 8 satellite images of the study area. Unsupervised image classification technique was applied to obtain major LULC features. A total of 168 sample points were taken to check the correctness of the categorization. The overall accuracy and kappa coefficient values are 96.43 and 95.62, respectively.

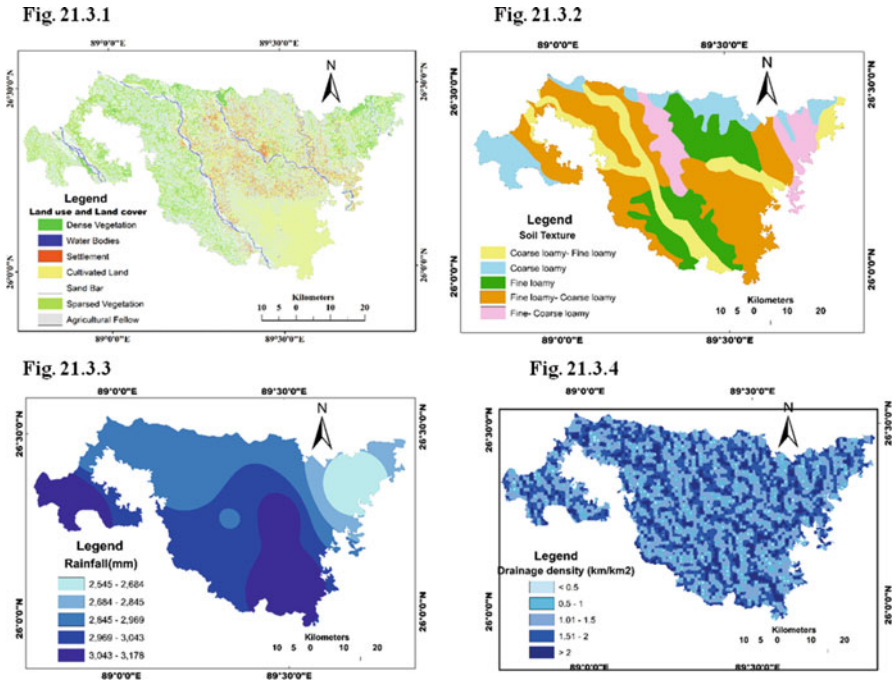


Fig. 21.3 Groundwater potential factors: (a) land use/land cover (LULC), (b) soil, (c) rainfall, (d) drainage density, (e) geomorphology, (f) lithology, (g) normalized vegetation index (NDVI), (h) topographical wetted index (TWI)

The result shows that dense vegetation, water bodies, sparse vegetation, cultivated land, agricultural fallow, sand bar and settlement cover 5%, 2%, 4%, 28%, 13%, 11% and 37% of the study area, respectively (Fig. 21.3a). High weight is assigned to dense vegetation because it is suitable for infiltration, and low weight is assigned to settlement because of its least contribution to groundwater recharge supporting runoff.

21.4.1.2 Soil

Soil type is one of the most leading constituents in terms of groundwater potential as type of soil texture directly accelerates or decelerates the process of infiltration. The coarse texture of soil is suitable for infiltration of water, whereas fine texture of soil favours surface runoff (Das et al. 2017). The soil in the study area is categorized by five main soil types, namely, (i) coarse loamy-fine loamy soil (440 sq. km.), (ii) coarse loamy soil (813 sq. km.), (iii) fine loamy soil (373 sq. km.), (iv) fine loamy-coarse loamy soil (1084 sq. km.) and (v) fine-coarse loamy soil (677 sq. km.)

(Fig. 21.3b). Ranks of the soil have been allotted on the basis of their infiltration rate. As coarse-textured soil has the greatest infiltration rate, it has been given a higher weight, whereas fine soil has been given a lesser weight for its low rate of infiltration (Shekhar and Pandey 2015).

21.4.1.3 Rainfall

Rainfall is the solitary principal source of groundwater. So areas under high rainfall account to maximum groundwater potentiality (Arulbalaji et al. 2019). The study area, as it is located in the foothill zone of the Himalayas, receives maximum orographic rainfall. The mean annual rainfall is about 2850 mm. The thematic of rainfall has been prepared on the basis of (NDCQ-2019-07-089) data collected from IDM Pune of seven weather stations namely Cooch Behar AEROBAY, Dinhata, Halibari, Mekhliganj, Mathabhanga, Pundibari and Tufanganj by using Inverse distance weighted (IDW) method of spatial interpolation in ArcGIS platform. The study area is classified into five rainfall zones on the basis of the amount of rainfall receives by the area: (i) 8% of the area falls under the class of 2545–2684 mm denoted as very poor; (ii) 6% of the total area falls under the class of 2684–2845 mm. denoted as poor; (iii) 32% of the total area comes under the class of 2845–2969 mm. denoted as moderate; (iv) 30% of the total area comes under the class of 2969–3043 mm. denoted as good; and (v) 24% of the total area falls under the class of 3043–3178 mm. marked as a very good rainfall zone (Fig. 21.3c). High rainfall was found in the south-eastern and north-western parts of the study area; the central part was characterized by moderate rainfall, while the north-eastern portion was characterized by poor rainfall. For sensing groundwater potential zonation, a higher weight is assigned to the higher rainfall zone and vice versa.

21.4.1.4 Drainage Density

Drainage density is one of the dynamic parameters to assessing groundwater potentiality (Shekhar and Pandey 2015). Drainage density is inversely related to penetrability of water. The higher the drainage density, the lower the groundwater recharge and vice versa. Drainage density can be calculated by dividing the total length of the drainage by the total area (Arulbalaji et al. 2019). The drainage density (km/km^2) of the study area has been grouped into five classes on the basis of their drainage density values (Fig. 21.3d). Areas under very poor (< 0.5), poor (0.5–1.00), moderate (1.01–1.5), good (1.51–2.00) and very good (> 2.00) occupy 14%, 33%, 37%, 14% and 2% of the total study area, respectively. To detect groundwater potential zonation, high weight was allotted to low drainage density, and low weight was allotted for high drainage density (Shekhar and Pandey 2015).

21.4.1.5 Geomorphology

Geomorphology denotes the study of land forms in a given area, and it is one of the key elements widely used for delineating groundwater potential zone. Geomorphology of the study area is mainly controlled by fluvial activity, that's why it has the great potentiality for groundwater recharge. Geomorphic landforms observed in the study area and their coverage in percentage are:

- (i) Fluvial origin younger alluvial plain found in almost all parts, 51%, of the study area apart from the southern part
- (ii) Fluvial origin active floodplains which are 16% of the study area detected along the river channel
- (iii) Fluvial origin older floodplain which is 28% mainly found in the southern part
- (iv) Fluvial origin Piedmont alluvial plain which is only 5% situated in the northern part of the study area (Fig. 21.3e)

The weight is assigned as per their role in groundwater recharge. High weight is allotted to fluvial origin active floodplains because they are adjacent to the river and so have great potentiality of recharge (Shekhar and Pandey 2015), while low weight was allotted to piedmont alluvial plain because of high runoff.

21.4.1.6 Lithology

Four types of lithological units have been detected in the study area, namely, (i) very fine sand, silt and clay which are found along the river channel and covered 24% of the total area; (ii) gravel, coarse to fine sand, silt and clay which covered 0.3% of the total area; (iii) alternate layers of sand silt and clay which covered 46.7% of the total area; and (iv) light grey silty loams underlain by unaltered multiple sequences of fine sand, silt and clay with bog clay covering 29% of the total area (Fig. 21.3f). Very fine sand, silt and clay are assigned high weight because they are situated along the river channel in our study area, and gravel, coarse to fine sand, silt and clay were also given high weight compared to light grey silty loams underlain by unaltered multiple sequences of fine sand, silt and clay with bog clay because they have low infiltration rate (Shekhar and Pandey 2015).

21.4.1.7 Normalized Difference Vegetation Index (NDVI)

It is an important parameter which is often used to detect groundwater potential zone. Different types of vegetation cover act dissimilarly in the infiltration. The importance of normalized difference vegetation index (NDVI) is observed as rough approximation of vegetation amount present and groundwater prospect over the space. The NDVI always ranges from -1 to $+1$ (Sar et al. 2015). The thematic map of NDVI of the study area has been divided into four categories. These are as

follows: (i) water bodies which covered 3% of the total area, (ii) no vegetation zone covering 34% of the total area, (iii) shrubs and grasslands covering 43% of the total area and (iv) moderately healthy vegetation covering 20% of the total area (Fig. 21.3g). High weight is given to water bodies and lower weight assigned to the no vegetation zone.

21.4.1.8 Topographic Wetness Index (TWI)

Topographic wetness index (TWI) is a parameter used to delineate groundwater potential zone because it is used to calculate topographic control on hydrological processes and reproduces the potential groundwater infiltration caused by the effects of topography (Arulbalaji et al. 2019). The value of TWI in our study area varied from 2.43 to 22.19. The values were classified into five categories. These are:

- (i) 2.43–7.78: covered 7% of the total area and denoted as very poor
- (ii) 7.78–10.33: covered 20% of the area, denoted as poor
- (iii) 10.33–12.27: covered 23% of the total area, denoted as moderate
- (iv) 12.27–14.67: covered 20% of the total area, denoted as good
- (v) 14.67–22.19: covered 29% of the total area, denoted as very good (Fig. 21.3h)

The high weight has been allocated for high TWI value and vice versa.

21.4.1.9 Discussion on Groundwater Potential Zones

The final groundwater potential map has been prepared by summing up the weights of eight thematic layers (Fig. 21.4). The groundwater potential map of the study area has been classified into five classes, i.e. “very poor”, “poor”, “moderate”, “good” and “excellent”. 1795 km² (55%) area comes under “Good” and “Excellent” classes, indicating high potentiality of groundwater in Cooch Behar district for favourable condition of upper-mentioned factors, whereas hindrance of these factors is responsible for the low potentiality zone amounting 779 km² (23%) of the total area. Detailed areal extent of groundwater potential zones is shown in Table 21.9.

21.4.2 Groundwater Consumption Zones (GWCZ)

21.4.2.1 Daily Average Groundwater Withdrawal for Irrigation

Being an agrarian district, Cooch Behar spends most of its groundwater for irrigation purposes. So, daily average groundwater withdrawal for irrigation is major factor indicating the consumption (Baker et al. 2002; Van der gulik et al. 2010). The types of irrigations in different blocks of Cooch Behar are dug well (dw), deep tube well (dtw), shallow tube well (stw) and river lifting (rl). Block wise daily average

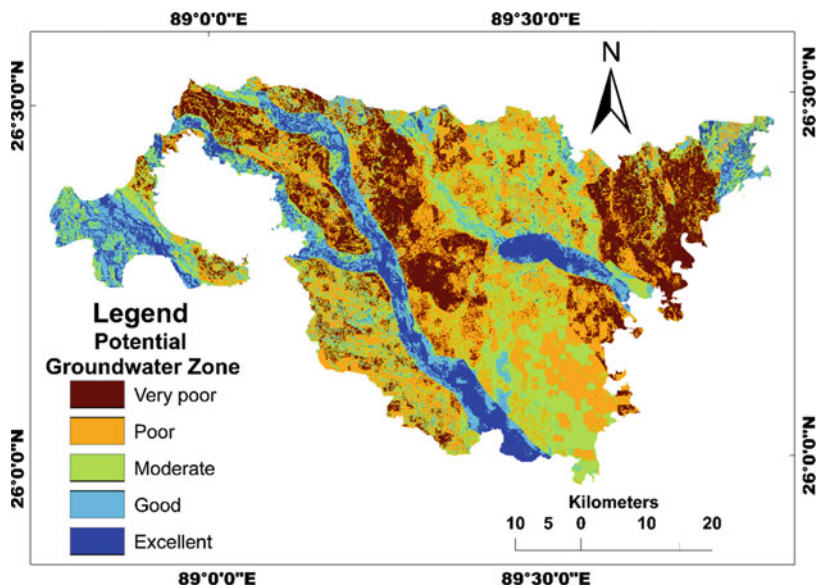


Fig. 21.4 Groundwater potential zones

Table 21.9 Classification of groundwater potential zones (after integration of all thematic maps)

Groundwater potential index	Percentage of the area	Area (sq.km)
Very poor (74.75–143.84)	8	271
Poor (143.84–177.39)	15	508
Moderate (177.39–212.92)	24	813
Good (212.92–258.32)	33	1118
Excellent (258.32–578.08)	20	677

groundwater withdrawal for irrigation have been computed in $\text{m}^3/\text{day}/\text{km}^2$ from the data of groundwater withdrawal by different irrigation technique.

Based on the results, the study area has been classified into five daily average groundwater withdrawal zones for irrigation on the basis of the amount of withdrawal ($\text{m}^3/\text{day}/\text{km}^2$): (i) 55.398–60.66, (ii) 60.663–68.562, (iii) 68.562–117.270, (iv) 117.270–234.431 and (v) 234.431–391.085 (Fig. 21.5a). For mapping groundwater consumption zone, high weight is allotted to high amount of withdrawal for irrigation and low weight for low amount of withdrawal by irrigation (Howell, T. A. 2003).

21.4.2.2 Total Crop Production

Total crop production is considered as another criterion for groundwater consumption because where the total crop production is more, the withdrawal of groundwater

Fig. 21.5.1

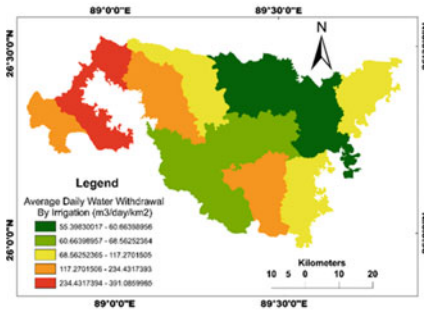


Fig. 21.5.2

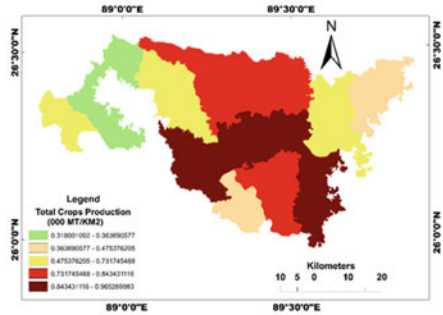


Fig. 21.5.3

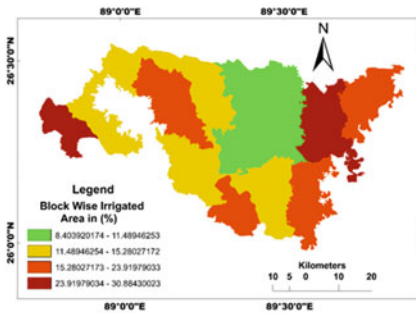


Fig. 21.5.4

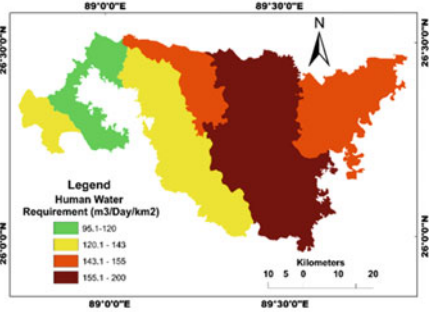


Fig. 21.5.5

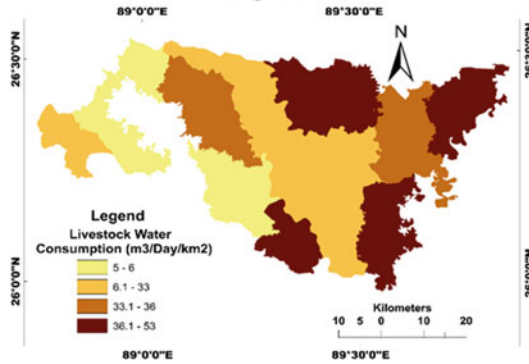


Fig. 21.5 Groundwater consumption factors: (a) daily average groundwater withdrawal for irrigation, (b) total crop production, (c) block-wise irrigated area, (d) human water consumption, (e) livestock water consumption

is also more (Bennett and Harms 2011). People from different blocks of Cooch Behar cultivated different types of crops as per their need such as paddy (aus, aman, boro), wheat, maize, maskalai, khesari, mustard, til, potato, sugarcane, jute and masur. Different crops also have different requirements of water (Rost et al. 2008).

Total crop production calculated by the formula: *Block-wise total crop production/block area*. Based on the result, the study area has been categorized into five total crop production zones on the basis of the amount of production (000 mt/km²): (i) 0.318–0.363, (ii) 0.363–0.475, (iii) 0.475–0.731, (iv) 0.731–0.843 and (iv) 0.843–0.965 (Fig. 21.5b). High weight is allotted to high total crop production and vice versa (Bennett and Harms 2011).

21.4.2.3 Irrigated Area

Irrigated area is another leading factor to identify the groundwater consumption zone because the area of irrigated land is directly proportional to the withdrawal of groundwater (Baker et al. 2002). The formula which has been used to calculate the block-wise irrigated land (%) is: *(Irrigated area/total area) x 100*. Based on the result, the study area has been categorized into four zones on the basis of the percentage of irrigated area: (i) 8.403–11.489, (ii) 11.489–15.280, (iii) 15.280–23.919 and (iv) 23.919–30.884 (Fig. 21.5c). For delineating groundwater consumption zone, high weight is allotted to high percentage of irrigated land, and low weight is allotted to low percentage of irrigated land (Jiménez and Asano 2008).

21.4.2.4 Human Water Consumption

Water is a primary need of human survival, so human water consumption is another parameter for identifying groundwater consumption zones. People use groundwater for different purposes like drinking, bathing, cooking of foods, washing clothes, cleaning and removing of waste and lavatory uses (Gleick 1996). The consumption of water varies with culture, diet, climatic condition and lifestyle. According to the Bureau of Indian Standards, IS: 1172-1993, a minimum of 200 litres of water supply is required per capita per day for domestic use with full flushing system (Shaban 2008).

Human water consumption is calculated through the following formula: *(Total population x per capita water used per day)/area*. On the basis of results, the study area has been classified into four human consumption zones in m³/day/km²: (i) 95.1–120, (ii) 120.1–143, (iii) 143.1–155 and (iv) 155.1–200 (Fig. 21.5d). For delineating groundwater consumption zone, high weight is allotted to high water consumption zones and vice versa.

21.4.2.5 Livestock Water Consumption

Livestock water consumption is one of the determinant factors for delineating groundwater consumption zones because water is a very essential factor for their living. Livestock water consumption is proportional to the number of livestock (Ward and McKague 2007). Horse, ponies, pigs, cows, buffaloes, goats, sheep,

poultry birds, fowls and ducks are the livestock animals normally nurtured in different blocks of Cooch Behar. Livestock water consumption has been calculated by the following formula: $(Total\ Livestock \times per\ capita\ water\ consumption\ per\ day) / area$.

Based on the result, the study area’s livestock water consumption has been categorized into four groups ($m^3/day/km^2$): (i) 5.1–6, (ii) 6.1–33, (iii) 33.1–36 and (iv) 36.1–53 (Fig. 21.5e). For preparation of groundwater consumption zone, high weight is allotted to high consumption and vice versa (Adams 1995).

21.4.2.6 Discussion on Groundwater Consumption Zones (GWCZ)

The study area is mainly dominated by primary economic activity mainly agriculture and livestock rearing; that’s why the consumption rate of ground is quite high. The final groundwater consumption map (Fig. 21.6) has been prepared by summing up the weights of the upper-mentioned five-thematic layer. The groundwater consumption map of Cooch Behar has been classified into five classes, i.e. “very low”, “low”, “moderate”, “high” and “very high”. A real extent of groundwater consumption zones is shown in Table 21.10.

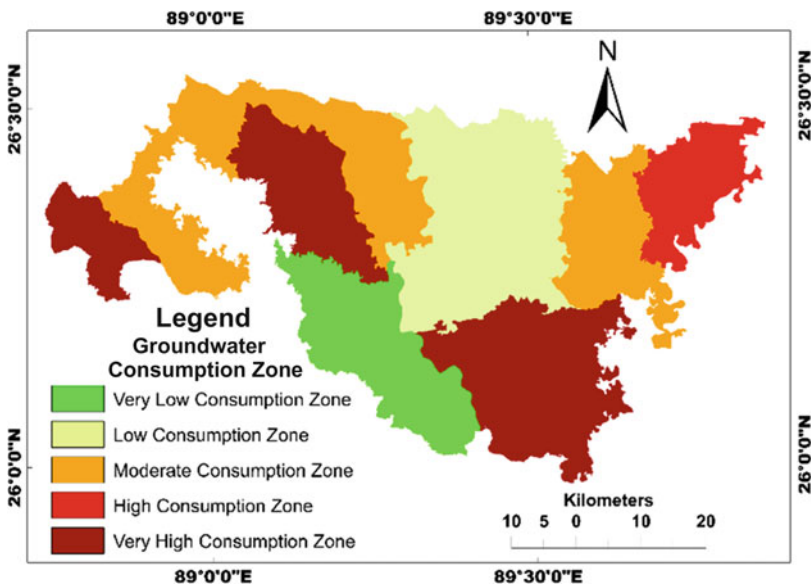


Fig. 21.6 Groundwater consumption zone

Table 21.10 Classification of groundwater consumption zones (after integration of all thematic maps)

Groundwater consumption index	Percentage of the area	Area (sq.km)
Very low(183.33–195.66)	13	440
Low (195.66–208.47)	22	745
Moderate (208.47–225.24)	28	948
High (225.24–250.94)	7	237
Very high (250.94–309.04)	30	1010

Table 21.11 Linear regression of groundwater data by blocks

Block Name	“y” value	r^2 value	RMSE
Sitalkuchi	$-0.004x + 2.967$	0.007	0.065534519
Sitai	$0.081x + 2.579$	0.231	0.111061658
Dinhata I and II	$-0.012x + 3.678$	0.026	0.090439130
Mekhliganj	$0.019x + 3.511$	0.067	0.132098462
Cooch Behar I and II	$0.002x + 2.609$	0.003	0.063324874
Haldibari	$-0.013x + 3.034$	0.067	0.067303042
Tufanganj I	$0.002x + 4.198$	0.000	0.147132696
Tufanganj II	$0.024x + 2.292$	0.041	0.067295359
Mathabhanga I	$0.041x + 2.986$	0.236	0.031750000
Mathabhanga II	$0.047x + 3.225$	0.107	0.084457761
Average of RMSE			0.086039750

21.4.3 Projected Groundwater Level Zone (PGWLZ)

Groundwater is a refill resource of nature, but the natural process of groundwater replenishment has been decreased ominously due to human activities in last four to five decades (Arulbalaji et al. 2019). The equation for calculating values of y (groundwater level) in relation to x (year) as well as r^2 (Table 21.11, Fig. 21.7) value is computed. Then the maps showing spatial distribution of projected of groundwater level have been prepared for the years 2028 (Fig. 21.8a), 2034 (Fig. 21.8b) and 2040 (Fig. 21.8c) using interpolation GIS technique.

21.4.4 Projected Groundwater Vulnerable Zone

The result of the study shows that areas under the category of very low, low and moderate groundwater vulnerably are decreasing, whereas areas under high and very high groundwater vulnerability are increasing in all three years, 2028, 2034 and 2040. The projected areas under very low, low, moderate, high and very high groundwater vulnerability zone in 2040 are 8%, 16%, 23%, 23% and 30%, respectively (Fig. 21.9; Table 21.12).

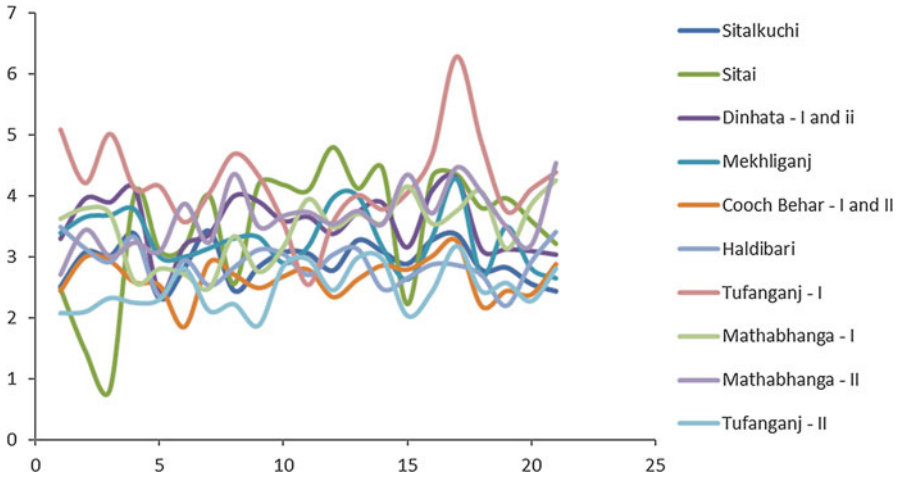


Fig. 21.7 Line graph of groundwater data of 12 blocks (Sitalkuchi, Sitai, Dinhata I and II, Mekhliganj, Cooch Behar I and II, Haldibari, Tufanganj I and II, Mathabhanga I and II)

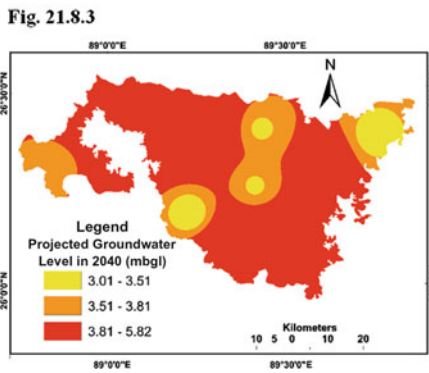
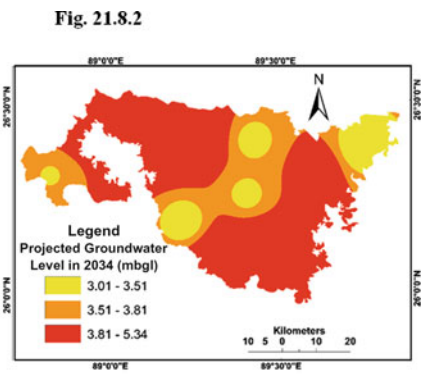
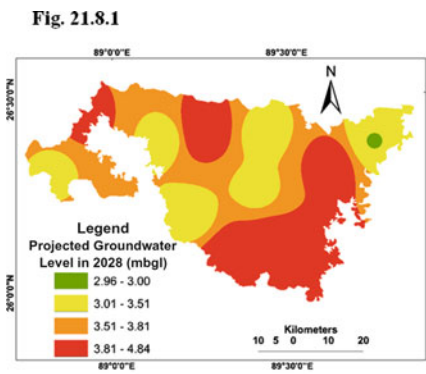


Fig. 21.8 Projected groundwater level: (a) projected groundwater level of 2028, (b) projected groundwater level of 2034, (c) projected groundwater level of 2040

Fig. 21.9.1

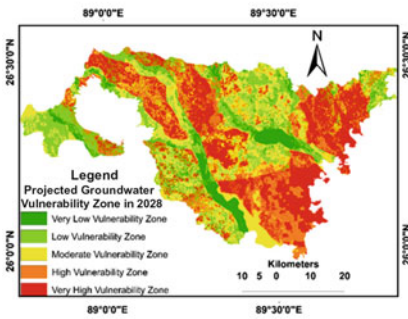


Fig. 21.9.2

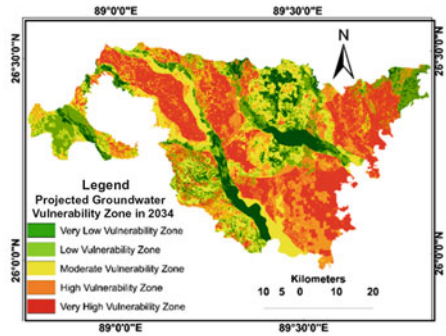


Fig. 21.9.3

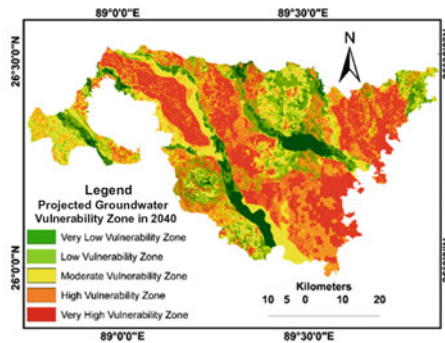


Fig. 21.9 Projected groundwater vulnerable zone: (a) projected groundwater vulnerable zone in 2028, (b) projected groundwater vulnerable zone in 2034, (c) projected groundwater vulnerable zone in 2040

Table 21.12 Projected groundwater vulnerability for 2028, 2034 and 2040

Groundwater vulnerable index	Area (sq.km)			Percentage of area		
	2028	2034	2040	2028	2034	2040
Very low (100.680–147.163)	305	305	271	9	9	8
Low (147.163–187.195)	711	576	542	21	17	16
Moderate (187.195–228.520)	847	813	779	25	24	23
High (228.520–284.044)	644	711	779	19	21	23
Very high (284.040–429.960)	881	982	1016	26	29	30

21.4.5 Validation

The complete analysis of particular parameters through AHP techniques generated a suitable groundwater potential zone map (GWPZ) in ArcGIS after the integration of all maps (Shekhar and Pandey 2015). Validation of groundwater potential zone (GWPZ) has been done with the help of 45 actual groundwater data samples collected from Central Groundwater Board (CGWB), and the receiver operating

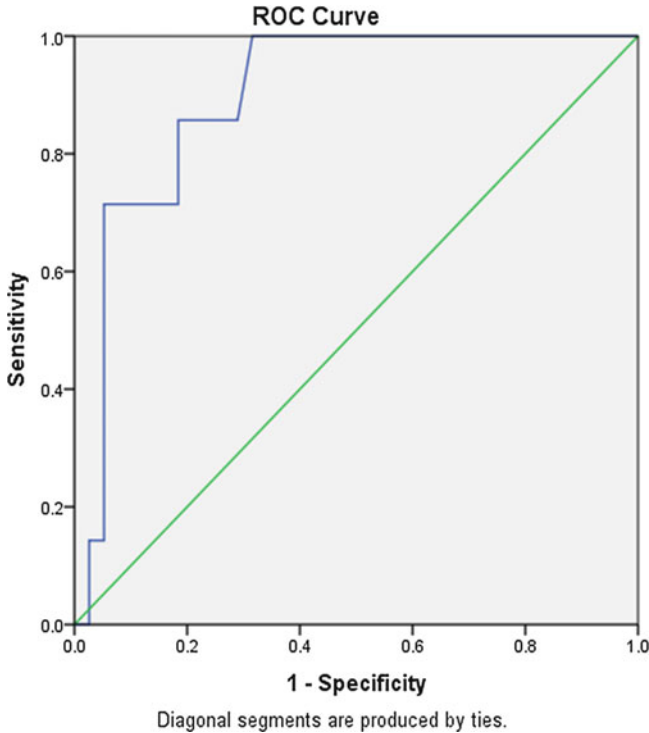


Fig. 21.10 ROC curve

characteristic (ROC) curve is deployed to validate the technique (Senapati and Das 2020; Hajian-Tilaki 2013). The prediction rate has been shown through pictorial representation with the blue line (Fig. 21.10).

The forecasting rate has been examined on the basis of the area under curve (AUC) ranging from 0.5 to 1.0. The classification of the AUC values can be shown through the following order: poor, average, good, very good and excellent with ranges from “0.5 to 0.6”, “0.6 to 0.7”, “0.7 to 0.8”, “0.8 to 0.9” and “0.9 to 1”, respectively (Senapati and Das 2020; Arabameri et al. 2019; Rahmati and Melesse 2016). The results of AUC (0.897) and STD.error (0.052) under non-parametric assumption denote that it is a good predictor model having an accuracy of 89.7% which means the accuracy of the model to delineate the groundwater potential zone (GWPZ) is very good.

The RMSE (root mean square error) is used to compute the average error of the differences between the values predicted and known observed value. Linear regression model is used for projected groundwater level (PGWL) and the actual values of groundwater level data (Table 21.11). The 100% accurately fitted model shows the RMSE value of 0 (Akhondi et al. 2011). The calculated average value of RMSE being 0.08 is very near to 0. Hence, it indicates that the used model is fairly fit and valid.

21.5 Conclusion

The entire study aims to identify the future vulnerability of groundwater in Cooch Behar district in the context of groundwater potentiality, existing groundwater level and sector-wise consumption of groundwater with an analytical look regarding spatial vulnerability in temporal span.

Very high projected groundwater vulnerability is found in five blocks, namely, Mathabhanga-I, Cooch Behar I, Dinhata I and II and Tufanganj I, whereas the remaining seven blocks are not that much vulnerable. So, wide use of surface water, reuse and recycling of water, extensive rainwater harvesting, modernized irrigation system and nature-friendly afforestation should be followed to reduce groundwater stress. But sustainable groundwater management will only be fruitful if community involvement is effective.

References

- Adams, R. S. (1995). Calculating drinking water intake for lactating cows. *Dairy reference manual*, Ithaca, NY: Northeast Regional Agricultural Engineering Service.
- Akhondi, E., Kazemi, A., & Maghsoodi, V. (2011). Determination of a suitable thin layer drying curve model for saffron (*Crocus sativus* L) stigmas in an infrared dryer. *Scientia Iranica*, 18(6), 1397–1401.
- Albinet, M. and Margat, J., 1970. Cartographie de la vulnérabilité à la pollution des nappes d'eau souterraine. *Bull. BRGM, 2ème série*, 3(4), pp.13–22.
- Aller, L., 1985. *DRASTIC: a standardized system for evaluating groundwater pollution potential using hydrogeologic settings*. Robert S. Kerr Environmental Research Laboratory, Office of Research and Development, US Environmental Protection Agency.
- Arabameri, A., Pradhan, B., & Rezaei, K. (2019). Gully erosion zonation mapping using integrated geographically weighted regression with certainty factor and random forest models in GIS. *Journal of Environmental Management*, 232, 928–942.
- Arulbalaji, P., Padmalal, D., & Sreelash, K. (2019). GIS and AHP techniques based delineation of groundwater potential zones: a case study from southern Western Ghats, India. *Scientific Reports*, 9(1), 2082.
- Baker, D., Ryan, L., & Kroker, K. (2002). Deriving irrigation water demands through the Irrigation District Model (IDM). *Irrigation in the 21st Century. Volume 4: Modeling Irrigation Water Management*, 1–103.
- Bennett, D. R., & Harms, T. E. (2011). Crop yield and water requirement relationships for major irrigated crops in southern Alberta. *Canadian Water Resources Journal*, 36(2), 159–170
- Bhuni, P. K. (2014). Sustainable Water Resource Management in West Bengal: A Review. *Bhatter College Journal of Multidisciplinary Studies, Vol. IV*, 94–104.
- Busico, G., Kazakis, N., Colombani, N., Mastrocicco, M., Voudouris, K. and Tedesco, D. (2017). A modified SINTACS method for groundwater vulnerability and pollution risk assessment in highly anthropized regions based on NO₃– and SO₄²⁻ concentrations. *Science of the Total Environment*, 609, 1512–1523.
- Civita, M. (1994). Le carte della vulnerabilità degli acquiferi all'inquinamento. *Teoria e pratica [Aquifer vulnerability map to pollution. Theory and application]*. Pitagora, Bologna, 13.
- Civita, M. and De Regibus, C. (1995). Sperimentazione di alcune metodologie per la valutazione della vulnerabilità degli acquiferi. *Q Geol Appl Pitagora Bologna*, 3, 63–71.

- Das, B., Pal, S. C., Malik, S., & Chakraborty, R. (2018). Modeling groundwater potential zones of Puruliya district, West Bengal, India using remote sensing and GIS techniques. *Geology, Ecology, and Landscapes*, 1–15.
- Das, S., Gupta, A., & Ghosh, S. (2017). Exploring groundwater potential zones using MIF technique in semi-arid region: a case study of Hingoli district, Maharashtra. *Spatial Information Research*, 25(6), 749–756.
- Doerfliger, N. and Zwahlen, F. (1997). EPIK: a new method for outlining of protection areas in karstic environment. In *International symposium and field seminar on "karst waters and environmental impacts"*, edited by: Günay, G. and Jonshon, AI, Antalya, Turkey, Balkema, Rotterdam (pp. 117–123).
- Doerfliger, N., Jeannin, P.Y. and Zwahlen, F. (1999). Water vulnerability assessment in karst environments: a new method of defining protection areas using a multi-attribute approach and GIS tools (EPIK method). *Environmental Geology*, 39(2), 165–176.
- Foster, S.S.D. (1987). *Fundamental Concepts in Aquifer Vulnerability, Pollution Risk and Protection Strategy: International Conference, 1987, Noordwijk Aan Zee, the Netherlands Vulnerability of Soil and Ground water to Pollutants The Hague, Netherlands Organization for Applied Scientific Research*. Netherlands Organization for Applied Scientific Research.
- Ghazavi, R. and Ebrahimi, Z. (2015). Assessing groundwater vulnerability to contamination in an arid environment using DRASTIC and GOD models. *International Journal of Environmental Science and Technology*, 12(9), 2909–2918.
- Gleick, P. H. (1996). Basic water requirements for human activities: meeting basic needs. *Water International*, 21(2), 83–92.
- Gogu, R.C. and Dassargues, A. (2000). Current trends and future challenges in groundwater vulnerability assessment using overlay and index methods. *Environmental geology*, 39(6), pp.549–559.
- Hajian-Tilaki, K. (2013). Receiver operating characteristic (ROC) curve analysis for medical diagnostic test evaluation. *Caspian journal of internal medicine*, 4(2), 627.
- Howell, T. A. (2003). Irrigation efficiency. *Encyclopedia of water science*, 467–472.
- Huang, C.C., Yeh, H.F., Lin, H.I., Lee, S.T., Hsu, K.C. and Lee, C.H. (2013). Ground water recharge and exploitative potential zone mapping using GIS and GOD techniques. *Environmental Earth Sciences*, 68(1), 267–280.
- Jiménez, B., & Asano, T. (Eds.). (2008). *Water reuse: An international survey of current practice, issues and needs*. London: IWA.
- Joshi, P. and Gupta, P.K. (2018). Assessing Ground water Resource Vulnerability by Coupling GIS-Based DRASTIC and Solute Transport Model in Ajmer District, Rajasthan. *Journal of the Geological Society of India*, 92(1), 101–106.
- Neshat, A., Pradhan, B. and Dadras, M. (2014). Ground water vulnerability assessment using an improved DRASTIC method in GIS. *Resources, Conservation and Recycling*, 86, pp.74–86.
- Nobre, R.C.M., Rotunno Filho, O.C., Mansur, W.J., Nobre, M.M.M. and Cosenza, C.A.N. (2007). Ground water vulnerability and risk mapping using GIS, modeling and a fuzzy logic tool. *Journal of Contaminant Hydrology*, 94(3–4), 277–292.
- Rahman, A. (2008). A GIS based DRASTIC model for assessing groundwater vulnerability in shallow aquifer in Aligarh, India. *Applied Geography*, 28(1), 32–53.
- Rahmati, O., & Melesse, A. M. (2016). Application of Dempster–Shafer theory, spatial analysis and remote sensing for groundwater potentiality and nitrate pollution analysis in the semi-arid region of Khuzestan, Iran. *Science of the Total Environment*, 568, 1110–1123.
- Ray, A., & Shekhar, S. (2009). Ground water issues and development strategies in West Bengal. *Bhu-Jal News*, 24(1), 1–17.
- Rost, S., Gerten, D., Bondeau, A., Lucht, W., Rohwer, J., & Schaphoff, S. (2008). Agricultural green and blue water consumption and its influence on the global water system. *Water Resources Research*, 44(9).
- Rudra, K. (2005). *The Status of Water Resources in West Bengal (A Brief Report)*

- Saaty, T. L. (1990). *Decision making for leaders: the analytic hierarchy process for decisions in a complex world*. RWS publications.
- Sar, N., Khan, A., Chatterjee, S., & Das, A. (2015). Hydrologic delineation of groundwater potential zones using geospatial technique for Keleghai river basin, India. *Modeling Earth Systems and Environment*, 1(3), 25.
- Senapati & Das, (2020). *Assessment of Potential Land Degradation in Akarsha Watershed, Using GIS and Multi-influencing technique*. Edit. Gully erosion studies from Indian surrounding regions, advances in Science, Technology & Innovation. doi:https://doi.org/10.1007/978-3-030-23243-6_11, pp.187–205
- Shaban, A. (2008). Water poverty in urban India: a study of major cities. In *Seminar Paper UGC Summer Programme June–July*.
- Shaban, A., & Sharma, R. N. (2007). Water consumption patterns in domestic households in major cities. *Economic and Political Weekly*, 2190–2197.
- Shah, T., Molden, D., Sakthivadivel, R., & Seckler, D. (2001). Global groundwater situation: Opportunities and challenges. *Economic and Political Weekly*, 4142–4150.
- Shekhar, S., & Pandey, A. C. (2015). Delineation of groundwater potential zone in hard rock terrain of India using remote sensing, geographical information system (GIS) and analytic hierarchy process (AHP) techniques. *Geocarto International*, 30(4), 402–421.
- Shirazi, S.M., Imran, H.M. and Akib, S. (2012). GIS-based DRASTIC method for groundwater vulnerability assessment: a review. *Journal of Risk Research*, 15(8), 991–1011.
- Stempvoort, D.V., Ewert, L. and Wassenaar, L. (1993). Aquifer vulnerability index: a GIS-compatible method for groundwater vulnerability mapping. *Canadian Water Resources Journal*, 18(1), 25–37.
- Van der Gulik, T. W., Neilsen, D., & Fretwell, R. (2010). Agriculture water demand model: report for the Okanagan Basin. Ministry of Agriculture and Lands, Sustainable Agriculture Management Branch.
- Ward, D., & McKague, K. (2007). Water requirements of livestock. <http://citeseerx.ist.psu.edu/viewdoc/summary?doi=10.1.1.557.5795>

Chapter 22

Applicability of Geospatial Technology, Weight of Evidence, and Multilayer Perceptron Methods for Groundwater Management: A Geoscientific Study on Birbhum District, West Bengal, India



Niladri Das, Subhasish Sutradhar, Ranajit Ghosh, and Prolay Mondal

Abstract Groundwater resource is one of the prime essential but rapidly declining resources in the present era of so-called development. Rapid industrialization, massive irrigation in agriculture, and other economic and domestic activities accelerate its declining rates. So, most of the researchers and planners keep their concentration for the development of groundwater resources. In geoscience, a large number of methods and techniques are used for the sustainable development of these resources. The aim of the study is to determine groundwater potential zones in one hand, but on the other hand, this study is used to compare two methods, viz., statistical method and machine learning method, and test which one is more reliable in present methodological revolution. Weight of evidence or WoE method is applied here as statistical method, and multilayer perceptron or MLP method is applied here as machine learning method. The result of both methods is to some extent similar, where both methods depict that the eastern part of the study area is more potential than the western part. To run both methods, nine thematic layers have been used as inputs, viz., slope, geology, rainfall, soil texture, pond frequency, drainage density, aquifer thickness, lineament density, and land use/land cover. Two methods have been validated using receiver operating characteristic curve or ROC curve, where ROC curve of WoE method shows the accuracy of 76% and ROC curve of MLP method shows the accuracy of 89%. Therefore, this ROC curves make a conclusion that machine learning method is more reliable and acceptable than the statistical method.

N. Das (✉)

Department of Geography, Hiralal Bhakat College, Birbhum, West Bengal, India

S. Sutradhar · P. Mondal

Department of Geography, Raiganj University, Uttar Dinajpur, West Bengal, India

R. Ghosh

Department of Geography, Suri Vidyasagar College, Birbhum, West Bengal, India

Keywords Groundwater potential zones · Multilayer perceptron · ROC curve · Weight of evidence

22.1 Introduction

Groundwater is not only an essential but also a most valuable resource for the sustenance of the biotic world. But population explosion, rapid industrialization, and development of irrigation system for agricultural betterment push the groundwater level at the threshold of depletion (Chezgi et al. 2016; Venkatesan et al. 2019; D. Abijith et al. 2020). Therefore, in this present era, groundwater depletion and water scarcity are the best challenges for all citizens). During the past few decades, constantly increasing demand for groundwater in different economic sectors has created long time crisis, which results in failure to meet the demand of rapidly growing population (Das and Mukhopadhyay 2020). So, the time has come to rethink about our most precious hydrological resource, and we must plan for its sustainable development.

All states of our nation have been suffering from acute groundwater crisis problems, and the MLPual replenishable rate of groundwater in our country is about 433 billion m³, out of which above 90% water has been used for different economic purposes. Irrigation is one of the major sectors in India which is mostly responsible for the groundwater depletion (Arulbalaji et al. 2019). For the development of sustainable groundwater resource management, various researchers are engaged to identify potential groundwater recharge zones not only for India but also for all the regions of the world, and for this holy work, they take the help of remote sensing and GIS technology (Ali et al. 2015; Pande et al. 2018; Ramu and Vinay 2014).

Remote sensing and GIS technology are the widely used modern computer-based technologies, which make the work of geoscientist more easy (Panigrahi et al. 1995; Krishnamurthy et al. 1996; Sander et al. 1996; Jha et al. 2007; Manap et al. 2014; Rahmati et al. 2015). GIS technology is the most advanced map-making tool where one platform can handle voluminous data and give one reliable output (Magesh et al. 2012). On the other hand, remote sensing technology provides us the most reliable multispectral and multispatial database which have been used to identify the most preferable groundwater recharge zones (Das and Mukhopadhyay 2020). In this connection, it has been noticed that remote sensing technology can not directly collect the data of groundwater; rather it helps to provide many spatial and temporal data, e.g., land use/land cover data, lineament data, surface storage data, etc.

Apart from the technological tools, many statistical tools are used to detect potential zones of groundwater resource for its sustainable development. There are so many statistical tools that have been applied to extract artificial recharge zones in different parts of the world (Prasad et al. 2008) like logistic regression model (Pourtaghi and Pourghasemi 2014), frequency ratio model (Oh et al. 2011; Razandi et al. 2015), multi-influencing factor model (Magesh et al. 2012), analytic hierarchy

process or AHP model (Das and Mukhopadhyay 2020), etc. Along with the statistical models, various machine learning models have been implied to delineate groundwater, and machine learning models give a highly accurate forecast about the database (Olden et al. 2008; Marjanović et al. 2011). Among the most machine learning models, multilayer perceptron model has been used in this study to identify the potential groundwater recharge zone (Pourghasemi et al. 2020; Sokeng et al. 2016; Lee and Talib 2005). A multilayer perceptron (MLP) model has been inspired by the nervous system of the human body, and this model is eligible to work with multivariate data and convert into a forecasted data (Lee and Pradhan 2006). The main aim of this model is to generate database which help to generalize and predict the probable output of groundwater potential zones. On the other hand, one of the statistical methods weight of evidence (WoE) has also been used to predict probable groundwater potential zones. This method was developed to be used in medical science for medical diagnosis process (Aspinall 1983). Later this method has been applied in mineralogy to identify mineral potentiality (Sun et al. 2020). However, in recent time WoE method has also been applied to extract groundwater potential zones (Lee et al. 2012). In this method spatial association has been done through the calculation of weight of each influencing factor and by the overlay analysis and gives an output of groundwater potential zones.

Birbhum district is one of the geologically diversified districts; therefore, quality and quantity of groundwater also varied. Qualitatively western part of the district is more vulnerable than the eastern part (Das et al. 2019). So, to identify the quantitative nature of groundwater and its sustainability, groundwater potential zones have been identified in this district using statistical and machine learning method.

The main goal of this study is to find out which method is more reliable to delineate groundwater potential zone, i.e., statistical method or machine learning method. So, this study is a kind of comparative analysis of the said methods.

22.2 Materials and Method

22.2.1 Description of Examination Area

Birbhum district is located between the latitude of 23°32'30"N–24°35'00"N and longitude of 87°05'04"E–88°01' 04" E, covering an area of 4545 sq. km, and it contains 19 community development (CD) blocks (Fig. 22.1).

Administratively, the study area is surrounded by the Jharkhand state in the west and the north and Murshidabad in the east and Burdwan district in the south. All the maps, viz., India, West Bengal, and Birbhum districts, have been downloaded from <http://www.diva-gis.org/> website, and the digital elevation data of Birbhum district has been downloaded from the USGS EarthExplorer. All maps are in a pre-georeferenced and digitized form (Fig. 22.1).

In geomorphological point of view, this region is under “Rarh Banga” area, where lateritic soil is predominant. A large drainage system is running from the western

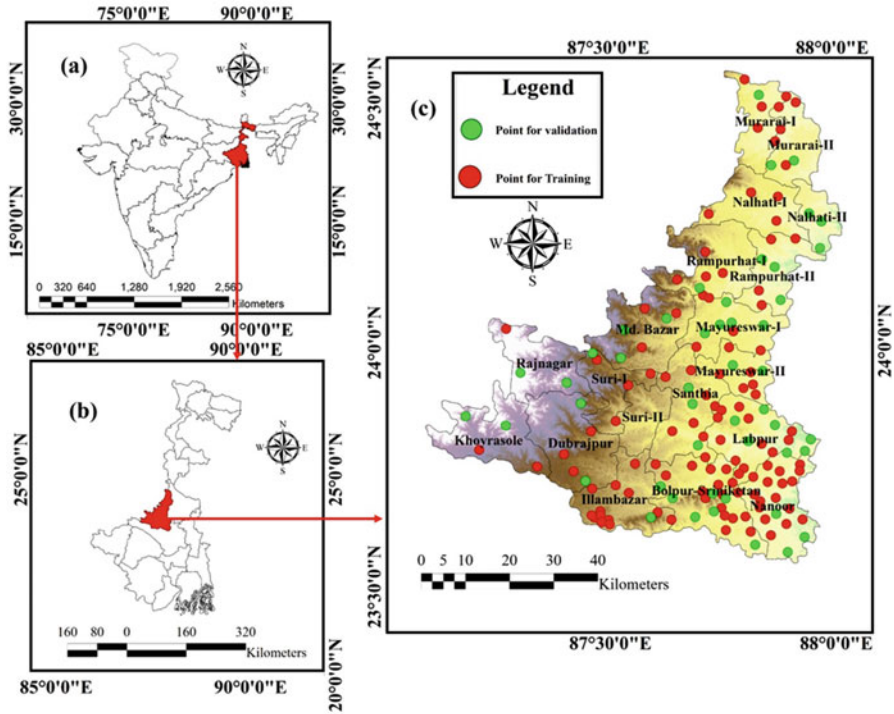


Fig. 22.1 Location of examination area: (a) India, (b) West Bengal, and (c) Birbhum

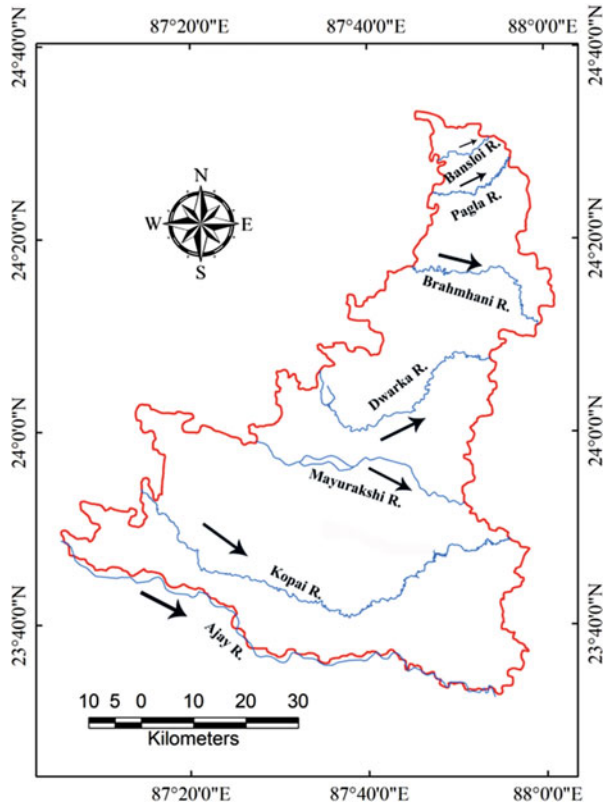
part where Chota Nagpur plateau is present to the east with a little bit southeasterly inclination in the Suri subdivision (Das and Mukhopadhyay 2020). The river widths vary according to the configuration of the country, from 200 yards to half a mile (Majumdar 1975). The major rivers of this district are Mayurakshi, Ajay, Kopai, Bakreswar, Brahmani, Dwarka, Bansloi, etc. (Fig. 22.2).

This district typically is under the tropical monsoon climate where 80% of rainfall is received between June and September with a rainfall of 14,305 mm and the summer temperature rises to 40 °C and winter temperature falls around 10 °C.

22.2.2 Database and Method

For the delineation of groundwater potentiality, different influential spatial data have been taken into consideration like topographical sheet (1:50,000) of the Survey of India, the geological map of the Geological Survey of India (1:2,50,000), rainfall distribution map of the NATMO (1:10,00000), soil texture map from Birbhum district portal, and aquifer thickness map of India-WRIS portal, slope map has been proceed using ArcMap 10.5 software from USGS EarthExplorer SRTM

Fig. 22.2 River network of examination area



DEM, and land use map has been made with ArcMap 10.5 software using Landsat 8 OLI satellite image. All the thematic layers have been prepared with the aid of RS and GIS techniques. The present work has been conducted in different phases, and the entire methodological overview depicts in Fig. 22.3.

22.2.2.1 Phase I

It includes preparation of inventory map and thematic layers of groundwater potentiality like geological setup, rainfall distribution, lineament density, pond frequency, drainage density, soil texture, and aquifer thickness (Table 22.1).

22.2.2.2 Phase II

Two different models have been run for the spatial mapping of groundwater potentiality – the weight of evidence and the multilayer perceptron – and categorized into five different classes.

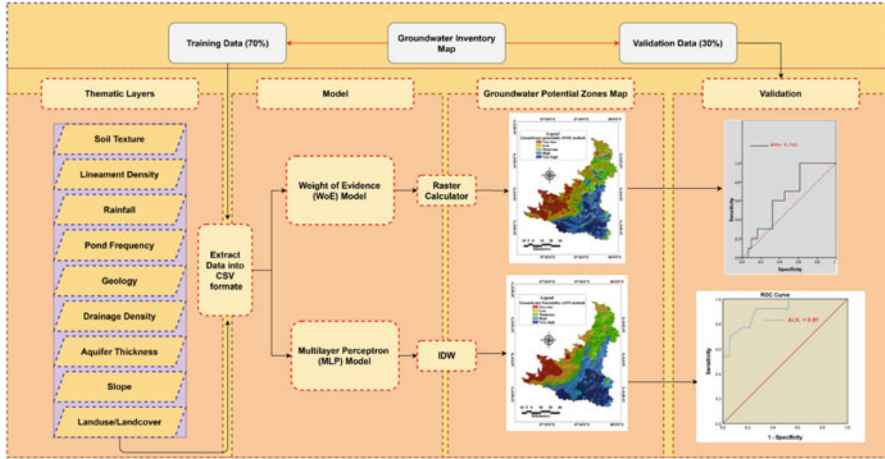


Fig. 22.3 Methodological framework of the entire study

22.2.2.3 Phase III

Validation of the result with the ROC curve and comparison have been made between the two models.

22.2.3 Groundwater Inventory Map Preparation

As inventory data is one of the significant inputs of groundwater potentiality mapping, an inventory map should be made very carefully, and while preparing the inventory map, researchers should keep in mind the different physical aspects of the study area. In this study, an inventory map has been developed with the help of groundwater yield data provided by the National Remote Sensing Centre of ISRO, Department of Space, Government of India. A total of 160 groundwater wells have been taken into consideration for the preparation of the inventory map. Out of 160 groundwater wells, 70% of wells have been randomly selected as training points, and the rest of 30% of wells have been treated for validation purposes (Fig. 22.1c).

22.2.4 Models

22.2.4.1 Weights of Evidence Model

One of the widely used quantitative “data-driven” models is the weights of evidence (WoE) model used to detect the probability of an event based on Bayes’ rule

Table 22.1 Datasets and their characteristics

Layer	Class	Source	Scale
Soil texture	Sandy	http://birbhum.gov.in/	1:300000
	Clay loam		
	Sandy loam		
	Clay		
	Loam		
Lineament density (km/sq. km)	<0.0512	https://bhuvan.nrsc.gov.in/	1:300000
	0.0512–0.139		
	0.139–0.244		
	0.244–0.392		
	0.392–0.722		
Rainfall (mm)	>1400	DPMS map of NATMO, Kolkata	1:300000
	1300–1400		
	1200–1300		
	1100–1200		
	<1100		
Pond frequency (pond/sq. km)	<2.39	Topographical sheet, SOI	1:300000
	2.39–4.79		
	4.79–7.19		
	7.19–9.59		
	>9.59		
Geology	Laterite	Geological Survey of India	1:300000
	Hard clay impregnated with caliche nodules		
	Alternating layer of sand, silt, and clay		
	Rajmahal trap		
	Sandstone, siltstone, and shale with coal seam		
	Granitic gneiss with enclaves of metamorphites		
Drainage density (km/sq. km)	<0.5	Topographical sheet, SOI	1:300000
	0.5–1		
	1–1.5		
	1.5–2		
	>2		
Aquifer thickness (meter)	1.00021565–20	https://indiawris.gov.in/	1:300000
	20.00000001–35		
	35.00000001–65		
	65.00000001–185.9817657		
Slope (%)	<2	Digital elevation model	1:300000
	2–4	https://earthexplorer.usgs.gov/	
	>4		

(continued)

Table 22.1 (continued)

Layer	Class	Source	Scale
Land use/land cover	Water bodies	Landsat OLI	1:300000
	Agricultural land	https://earthexplorer.usgs.gov/	
	Scattered vegetation		
	Forest		
	Built-up area		
	Sand		
	Current fellow		

(Arabameri et al. 2019; Gayen and Saha 2017; Ghorbani Nejad et al. 2017; Tahmassebi-poor et al. 2016). To prepare this model, positive weight (W^+) and negative weight (W^-) must be calculated. The method measures the weight for each conditioning factor (B) depending on the presence or absence of the disaster (A) within the area (Bonham-Carter 1994) as in the following Eqs. (22.1), (22.2), and (22.3):

$$W^+ = \ln \left\{ \frac{P(B/A)}{P(\bar{B}/\bar{A})} \right\} \tag{22.1}$$

$$W^- = \ln \left\{ \frac{P(\bar{B}/A)}{P(B/\bar{A})} \right\} \tag{22.2}$$

$$W_f = W^+ - W^- \tag{22.3}$$

where P is the probability and \ln is the natural log. B represents the presence of the groundwater potentiality influencing factor, and \bar{B} means the absence of that factor. A is the presence of a well and \bar{A} means the absence of a well. Weight contrast (W_f) represents a spatial relationship based on weight (Table 22.2). A positive contrast value means a positive correlation among the variables, negative contrast value means a negative correlation, and zero means there is no significant correlation (Table 22.2) (Corsini et al. 2009; Tahmassebi-poor et al. 2016).

22.2.4.2 Multilayer Perceptron

Multilayer perceptron (MLP) neural network is one of the widely used neural network algorithms in the field of geosciences (Salarian et al. 2014). This model is composed of three segments input, hidden layer, and output. Just like the biological neural system, this model works. All the variables of each segment are connected by an independent processing unit called neurons (Moayedi et al. 2019; Salarian et al. 2014). Two different datasets, i.e., training and validation, are required for the processing of the model like the other machine learning algorithms. With the help

Table 22.2 Spatial relation of each groundwater potentiality influencing factors and groundwater potentiality by WoE method

Sl. no.	Parameters	Type/class	No. of class pixels	No. of sample points	npix1	npix2	npix3	npix4	W+	W-	W _f
1	Soil texture	Sandy	36,566	10	10	150	36,556	405,641	-0.27967	0.021748	-0.30142
		Clay loam	141,957	55	55	105	141,902	300,295	0.068779	-0.03422	0.103003
		Sandy loam	132,436	38	38	122	132,398	309,799	-0.23165	0.08468	-0.31633
		Clay	98,958	40	40	120	98,918	343,279	0.111169	-0.03447	0.145639
		Loam	32,440	17	17	143	32,423	409,774	0.370928	-0.03618	0.407107
	Total		442,357	160							
2	Aquifer thickness (meter)	1.00021565-20	257,044	51	51	109	256,993	185,204	-0.60064	0.486472	-1.08711
		20.00000001-35	96,994	46	46	114	96,948	345,249	0.271048	-0.09149	0.362534
		35.00000001-65	67,213	34	34	126	67,179	375,018	0.335581	-0.07411	0.409692
		65.00000001-185.9817657	21,106	29	29	131	21,077	421,120	1.335695	-0.15114	1.486834
			Total		442,357	160					
3	Drainage density (km/sq. km)	<0.5	258,344	111	111	49	258,233	183,964	0.172251	-0.30634	0.478592
		0.5-1	153,595	44	44	116	153,551	288,646	-0.23326	0.104971	-0.33823
		1-1.5	28,167	4	4	156	28,163	414,034	-0.93512	0.040488	-0.9756
		1.5-2	2124	1	1	159	2123	440,074	0	-0.00146	0.001458
		>2	128	0	0	160	128	442,069	0	0.000289	-0.00029
	Total		442,357	160							
4	Geology	Laterite	107,310	41	41	119	107,269	334,928	0.054812	-0.01821	0.073022
		Hard clay impregnated with caliche nodules	170,226	82	82	78	170,144	272,053	0.286659	-0.23271	0.519367
		Alternating layer of sand, silt, and clay	78,985	25	25	135	78,960	363,237	-0.13348	0.0268	-0.16028
		Rajmahal trap	14,363	4	4	156	14,359	427,838	-0.26153	0.007694	-0.26923
		Sandstone, siltstone, and shale with coal seam	2537	0	0	160	2537	439,660	0	0.005754	-0.00575
	Total		68,936	8	8	68,928	373,269	-1.13704	0.118163	-1.2552	
	Total		442,357	160							

(continued)

Table 22.2 (continued)

Sl. no.	Parameters	Type/class	No. of class pixels	No. of sample points	npix1	npix2	npix3	npix4	W+	W-	W _f
5	Lineament density (km/sq. km)	<0.0512	181,366	80	80	181,286	260,911	0.19853	-0.16557	0.3641	
		0.0512-0.139	110,589	41	119	110,548	331,649	0.024702	-0.00837	0.033073	
		0.139-0.244	75,201	21	139	75,180	367,017	-0.25878	0.045647	-0.30442	
		0.244-0.392	44,236	13	147	44,223	397,974	-0.20771	0.020627	-0.22833	
		0.392-0.722	30,965	5	155	30,960	411,237	-0.80668	0.040837	-0.84751	
	Total		442,357	160							
6	Pond frequency (pond/sq. km)	<2.39	82,445	19	141	82,426	359,771	-0.45088	0.079874	-0.53076	
		2.39-4.79	155,953	51	109	155,902	286,295	-0.10082	0.050909	-0.15173	
		4.79-7.19	133,035	51	109	132,984	309,213	0.058178	-0.0261	0.084278	
		7.19-9.59	66,253	39	121	66,214	375,983	0.487244	-0.11717	0.604415	
		>9.59	4670	0	160	4670	437,527	0	0.010617	-0.01062	
	Total		442,357	160							
7	Rainfall	>1400 mm	93,034	26	134	93,008	349,189	-0.25801	0.058808	-0.31681	
		1300-1400 mm	115,988	18	142	115,970	326,227	-0.84638	0.184814	-1.03119	
		1200-1300 mm	175,965	97	63	175,868	266,329	0.421558	-0.42502	0.846574	
		1100-1200 mm	34,629	13	147	34,616	407,581	0.037212	-0.00323	0.040437	
		<1100 mm	22,741	6	154	22,735	419,462	-0.31558	0.014562	-0.33014	
	Total		442,357	160							

8	LULC	Water bodies	3155	8	8	152	3147	439,050	1,949,708	-0.04415	1.99386	
		Agricultural land	290,181	67	67	93	290,114	152,083	-0.449	0.524754	-0.97375	
		Scatter vegetation	61,338	23	23	137	61,315	380,882	0.036051	-0.00593	0.041978	
		Forest	5806	11	11	149	5795	436,402	1.657527	-0.05804	1.715563	
		Built-up area	34,605	17	17	143	34,588	407,609	0.306296	-0.03088	0.337179	
		Sand	13,791	15	15	145	13,776	428,421	1.101717	-0.06679	1.168508	
		Current fellow	33,482	19	19	141	33,463	408,734	0.450572	-0.04772	0.498294	
		Total	442,357	160								
		9	Slope (%)	154,825	87	87	73	154,738	287,459	0.440757	-0.35404	0.794796
			2-4	88,471	27	27	133	88,444	353,753	-0.16996	0.038333	-0.20829
	>4	199,061	46	46	114	199,015	243,182	-0.44816	0.258969	-0.70712		
	Total	442,357	160									

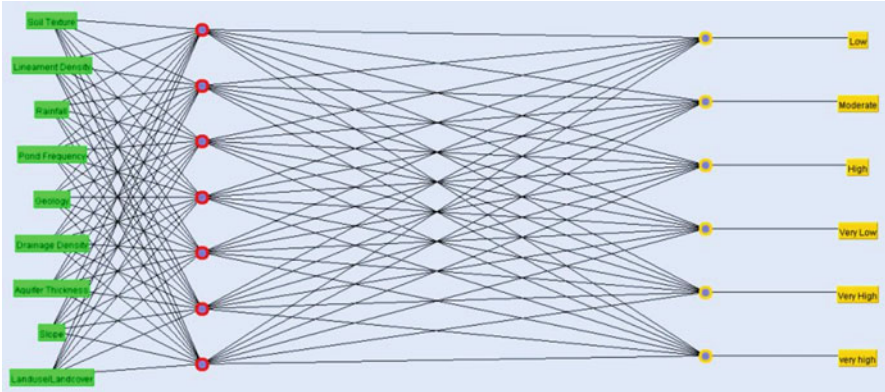


Fig. 22.4 Structure of the multilayer perceptron model

of training data as the input variable, this MLP model will run through the hidden layer (red dots in Fig. 22.4) and ultimately produce the output. Figure 22.4 depicts the typical structure of the MLP model for the study.

In MLP model input data which receive a single neuron to the hidden layer ($x_1, x_2, x_3 \dots x_n$) and from the hidden layer, neurons produce the output layer (n_0, n_1, n_2, n_3, n_4) (Li et al. 2019); therefore, model operation among the input layer, hidden layer, and output layer can be expressed using the following Eq. (22.4):

$$z_i = \sum_{i=1}^{n_0} w_{ij}x_i + b_j \tag{22.4}$$

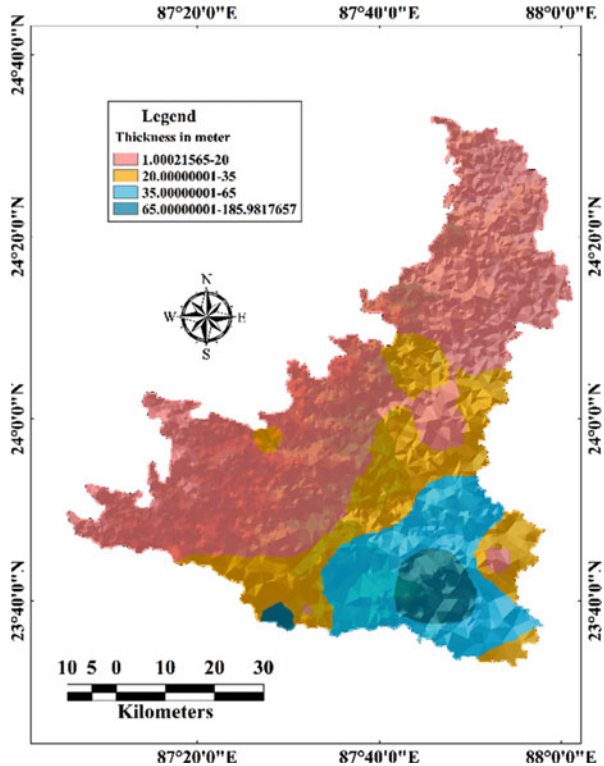
$$y_i = f(z_j) = (1 + e^{-z_j})^{-1} \tag{22.5}$$

where z_i denotes the input, b_j represents the threshold, y_i denotes the output of the j^{th} neuron in the hidden layer of the model, and $f(z_j)$ represents the activation function. The function is a nonlinear sigmoid function applied before the entry to the next level.

22.2.4.3 Application of the Models

Integration of weight contrast (W_f) has been done using raster calculator of ArcMap 10.5 software to delineate groundwater potential zone using the following Eq. (22.6):

Fig. 22.5 Aquifer thickness



$$\begin{aligned}
 \text{GWPZ}_{WoE} = & \text{Soil Texture}_{wf} + \text{Lineament Density}_{Wf} + \text{Rainfall}_{Wf} \\
 & + \text{Pond Frequency}_{WoE} + \text{Geology}_{Wf} + \text{Drainage Density}_{Wf} \\
 & + \text{Aquifer Thickness}_{Wf} + \text{Slope}_{Wf} \\
 & + \text{Landuse/Landcover}_{Wf}
 \end{aligned}
 \tag{22.6}$$

The integrated layers produced groundwater potential zone map that is categorized into five different classes – very low, low, moderate, high, and very high (Fig. 22.4).

To execute the MLP model, Weka 3.8.4 software has been used. With the help of training data in CSV format, the entire model has been carried out, and validation has been done with the validation points. After the classification of the data with MLP, result has been obtained. With that result, the groundwater potential zone map has been generated in the ArcGIS environment categorized into five different classes – very low, low, moderate, high, and very high (Fig. 22.5).

22.3 Result and Discussion

22.3.1 *Generation of Thematic Layers*

Collecting and constructing spatial data is one of the most critical factors in any research work. In geohydrological studies, a spatial database is considered as conditioning factors, which influence the groundwater occurrence. To carry out this study, a spatial database of aquifer thickness, drainage density, geology, lineament density, pond frequency, rainfall, and soil texture has been taken into consideration (Table 22.1). After collecting these parameters, ArcGIS 10.5 and RStudio-1.1.463 software have been used for constructing weight of evidence (WoE) and analytical neural network (MLP) model, respectively.

22.3.2 *Hydrogeological Factors*

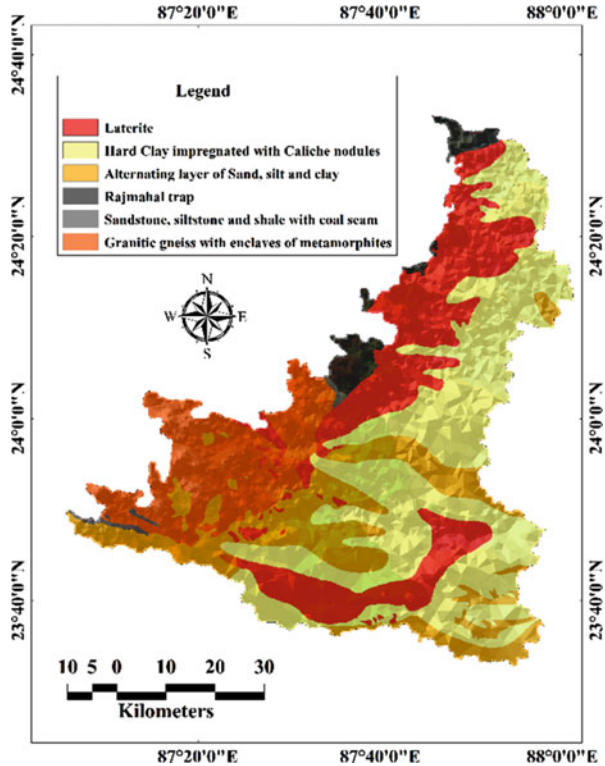
Aquifer thickness or aquifer material is one of the most significant parameters, which governed the groundwater potentiality (Das and Mukhopadhyay 2020). The storage capacity of groundwater is determined by porosity and permeability, which is directly related to the lithology of aquifer material (Ahmed and Sajjad 2018). The excellent storage capacity of groundwater is usually occurring when the aquifer is more thickness. On the other hand, if the aquifer thickness is low, then the storage capacity of groundwater is also low (Thomas et al. 2016). The spatial data of aquifer thickness have been assembled from WRIS WebGIS Portal, National Remote Sensing Centre, Government of India. The spatial variation of the aquifer thickness of this study is shown in Fig. 22.5.

22.3.3 *Geological Factors*

Lithology is also one of the most critical factors which determine the porosity and movement of groundwater, both vertical and horizontal (Chowdhury et al. 2010; Al Saud 2010). The lithological data of this study area has been extracted from the Geological Survey of India. The study area comprised six major lithological formations, viz., granitic gneiss with enclaves of metamorphites; siltstone and shale with coal seam; Rajmahal trap; alternative layer of sand, silt, and clay; hard clay impregnated with caliche nodules; and laterite (Fig. 22.6).

Lineament density plays a critical role in the determination of the groundwater regime of any terrain because it controls the movement of water between the surface and subsurface through faults and dikes (Ahmed and Sajjad 2018). So, there is a

Fig. 22.6 Geological facies

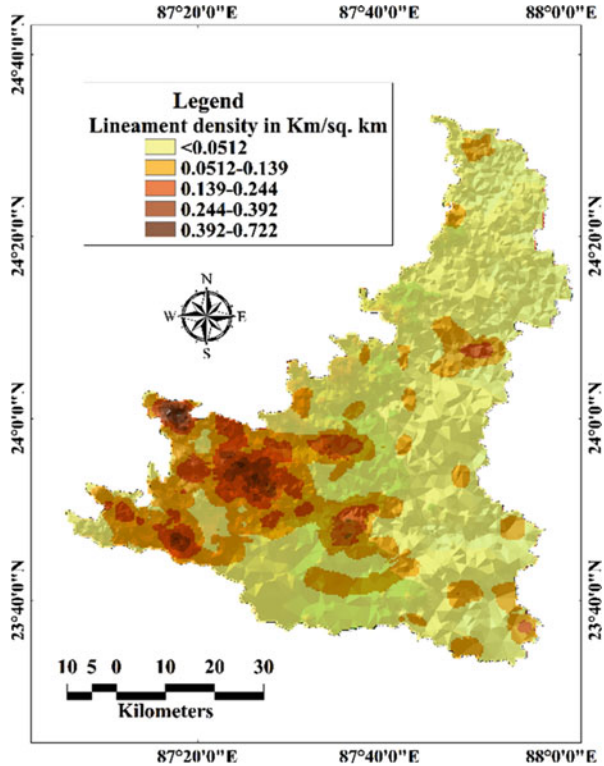


positive relationship between groundwater recharge and lineament density. For example, the higher the lineament density, the higher will be the groundwater potentiality because of a more significant recharge and vice versa. Figure 22.7 illustrates the lineament density of this study area. Maximum lineament density has been observed on the western side of this study region, and minimum lineament density has been observed on the eastern side.

22.3.4 Hydrological Factors

Drainage density is defined as the total length of streams per unit area (Horton 1932). Drainage density is a necessary parameter for assessing the potential site of groundwater because it plays a critical role in the process of permeability (Ajay Kumar et al. 2020). Areas with higher drainage density values favor for a good runoff. So, there may not be much time for surface water infiltration. Therefore

Fig. 22.7 Lineament density



higher drainage density values indicate low groundwater potentiality and vice versa (Pinto et al. 2017). Figure 22.8 illustrates the spatial variation of the drainage density of this study region.

Pond frequency is another important parameter for the delineation of the groundwater potential zone. It plays a critical role in the process of infiltration because it acts as an artificial groundwater recharge station (Kumar et al. 2011). So, there is a direct relationship between pond frequency and groundwater potentiality. Areas with higher pond frequency values indicate high groundwater potentiality and vice versa. Figure 22.9 illustrates the spatial variation of pond frequency of this test region. The higher pond frequency can be observed in the eastern part of the examination area than in the western part.

Fig. 22.8 Drainage density

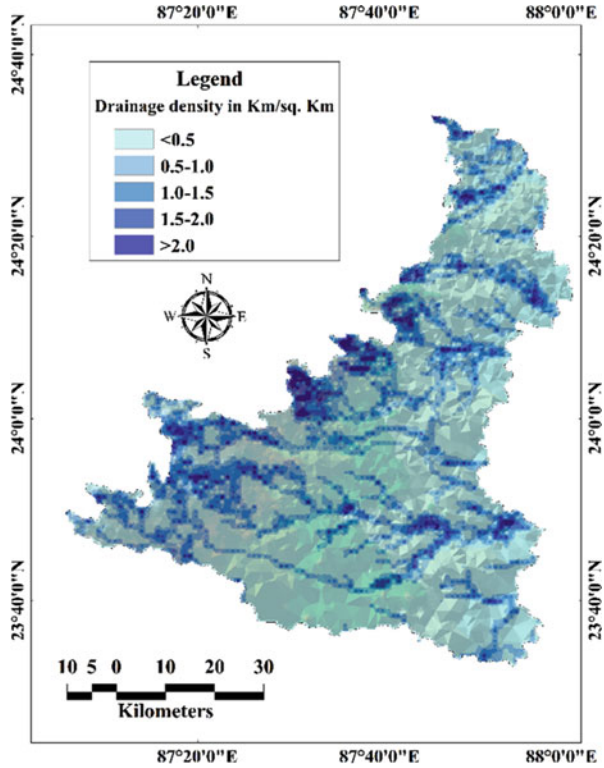
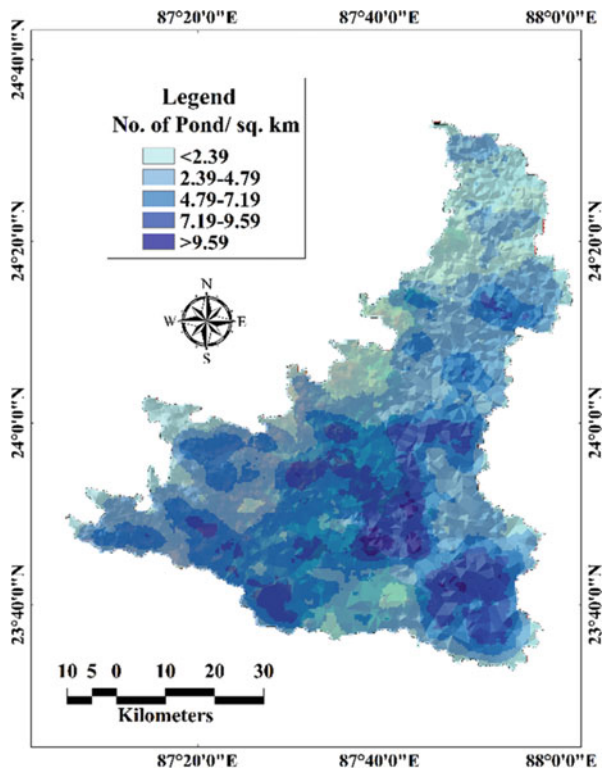


Fig. 22.9 Pond frequency



22.3.5 Pedological Factors

Soil texture plays an essential role in the movement of water, both horizontal and vertical. Different textural compositions of soils have a percolation rate (Nolan et al. 2003). That’s why this parameter has been selected as a significant pedological parameter for the extraction of the groundwater potential zone. The spatial database of soil texture has been collected from Birbhum district e-portal. In general, the refined textural class has low infiltration capacity and vice versa. In this study region, five significant soil textural groups have been identified, viz., sandy, clay loam, sandy loam, clay, and loam (Fig. 22.10).

22.3.6 Climatic Factors

The intensity of **rainfall** is the most influencing climatic factor to determine groundwater recharge. It plays a crucial role in the surface as well as subsurface water resource distribution (Wu et al. 1996). Though different topographical factors are

Fig. 22.10 Soil texture

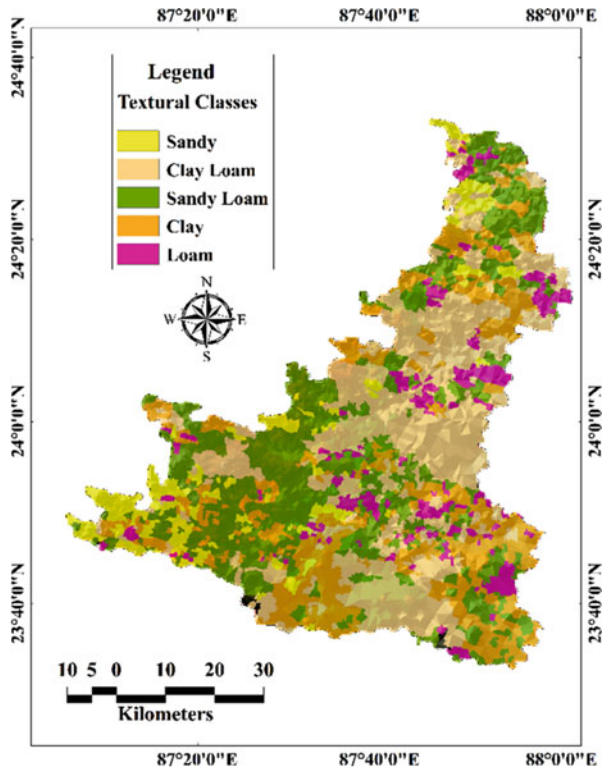
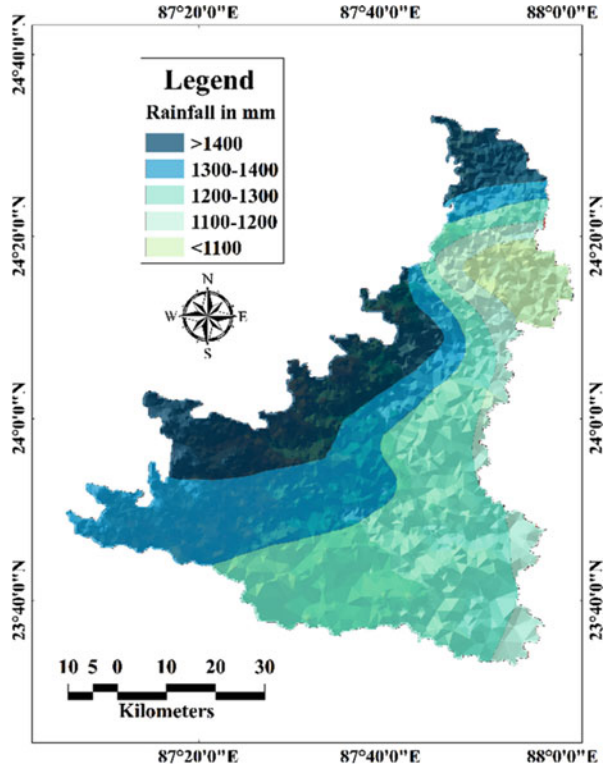


Fig. 22.11 Spatial pattern of rainfall

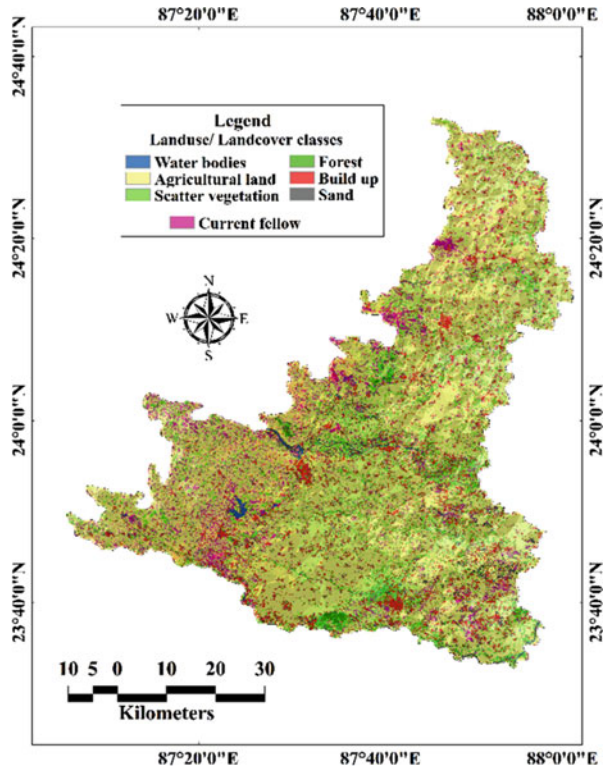


also essential, there is a chance of more rainfall region which has more possibility of groundwater recharge and vice versa. This region received 80% of MLPual rainfall from southwest monsoon wind. Based on the distribution of rainfall, the entire area has been divided into five rainfall zones, viz., very high (>1400 mm), high (1300–1400 mm), moderate (1200–1300 mm), low (1100–1200 mm), and very low (1100 mm) rainfall zone (Fig. 22.11).

22.3.7 *Physiocultural Factors*

Land use and land cover (LULC) plays a significant role in determining the horizontal as well as vertical movement of water in any region (Duan et al. 2016). It is the outcome of a complex physiocultural process in any area. The land use and land cover map of this region has been prepared from the Landsat 8 satellite image, which has been collected from USGS EarthExplorer, and classified with the help of supervised classification using maximum likelihood classification in ArcGIS 10.5 software. Seven land use and land cover classes have been identified within the entire region, viz., water bodies, agricultural land, scattered vegetation, forest, built-up area, sandy surface, and current fellow (Fig. 22.12).

Fig. 22.12 Land use and land cover map



22.3.8 Topographical Factors

The **slope** is an essential topographical factor for the delineation of the groundwater potential zone in any region. The slope map of this study area has been compiled from SRTM Digital Elevation Model (DEM) data. In general, flat or gentle slopy land is more suitable in the process of infiltration than the steep slopy land because in steep slopy, land runoff process is more active (Rahmati and Samani 2014). The maximum slope has been observed on the western side of this region. On the other portion of this study area, moderate to gentle slope has been observed (Fig. 22.13).

22.3.9 Comparative Analysis of Potential Zones

Figures 22.14 and 22.15 explain the groundwater potential zones on the basis of two methods; one is statistical method and another is machine learning method, viz., weight of evidence and multilayer perceptron method. The result of two methods is to some extent similar. If we focus on the map based on WoE method, it can be observed that in this map, potential zones are in scattered mMLPer, and several small

Fig. 22.13 Slope map

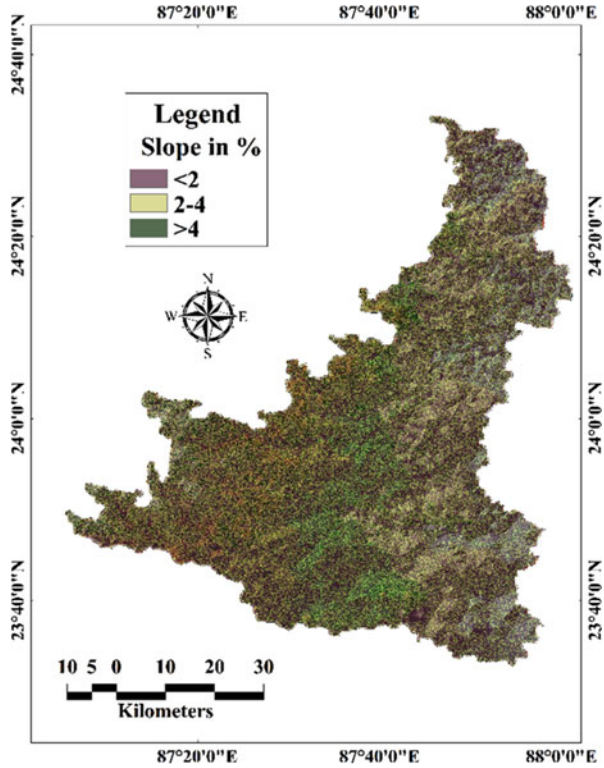


Fig. 22.14 Groundwater potential zones based on WoE method

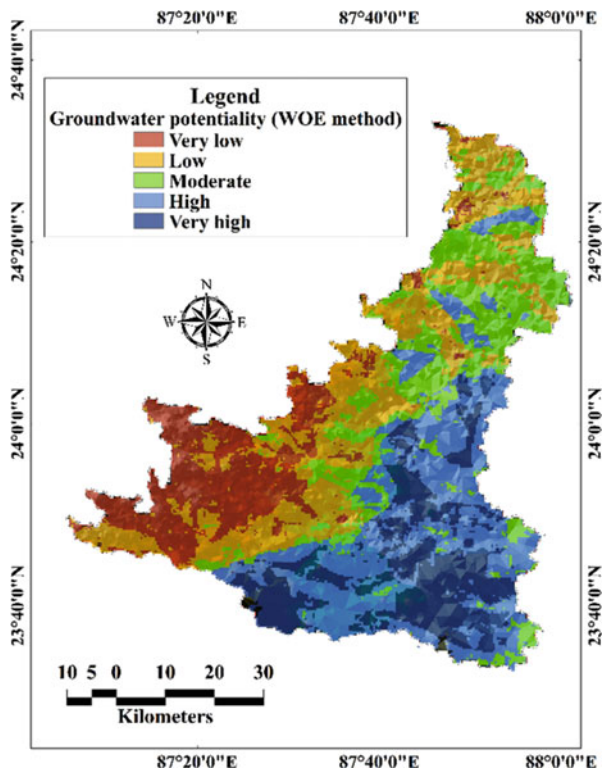
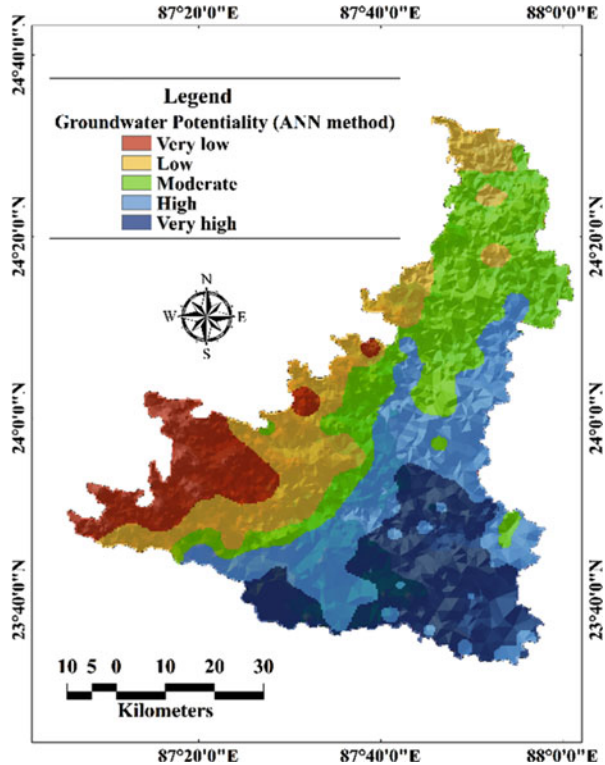


Fig. 22.15 Groundwater potential zones based on MLP method



pockets have been developed all around the district (Fig. 22.14). But if we want to generalize the map of groundwater potential, we can say that eastern part of the district is more potential than the western part. On the other hand, groundwater potential map based on multilayer perceptron method also shows the same characteristics, i.e., eastern part is more potential than western part. Moreover, in Fig. 22.15 the zones are continuous and regular.

Now which method is more acceptable and reliable to us? This is a big question. So, to validate and to test the reliability of the model, receiver operating characteristic curve or ROC curve has been taken into consideration. To operate ROC curve, we have considered 30% data of groundwater yield for validation purpose (vide Fig. 22.1). On the basis of validation point, it has been estimated that WoE statistical method has 76% accuracy as the area under curve (AUC) is 0.761 (Fig. 22.16). On the other hand, MLP machine learning method has 89% accuracy as AUC value of this curve is 0.89 (Fig. 22.17). So, it is obvious from both ROC curves (Figs. 22.16 and 22.17) that machine learning method is more powerful than the statistical method. As WoE method is based on the weight giving to each layer, MLP method is based on three segments, viz., input, hidden layer, and output. Moreover, complex algorithm has been used to get an output in MLP model. Therefore, statistical method depends on the skill of researcher who prepared the weight of each layer,

Fig. 22.16 ROC curve to validate WoE method

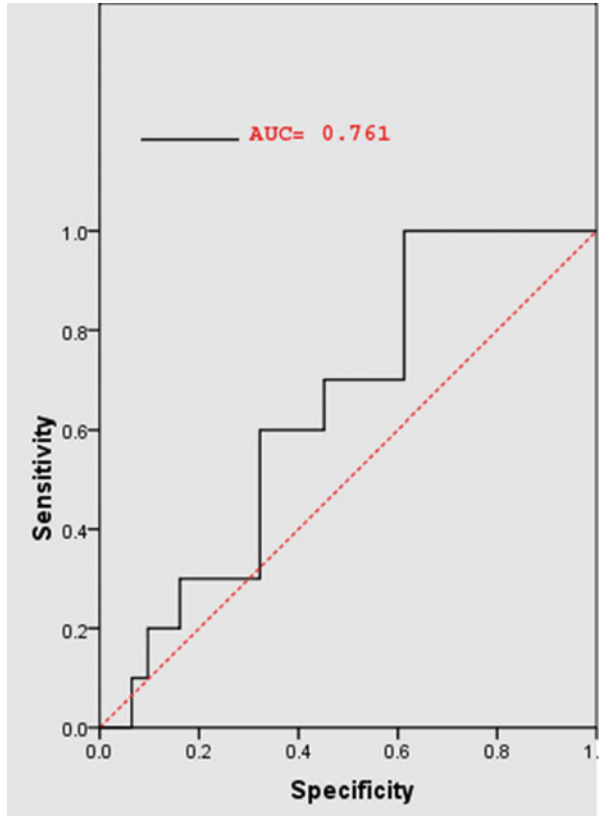
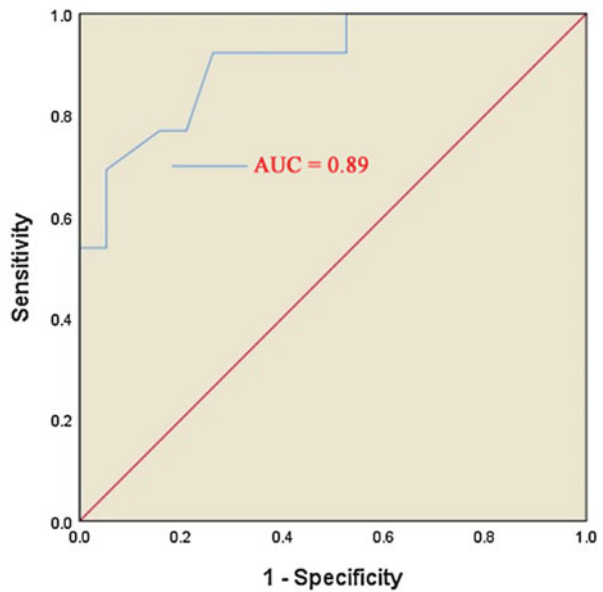


Fig. 22.17 ROC curve to validate MLP method



and one should be more knowledgeable during the time of weight manipulation of each layer. But in the machine learning process, computer technology plays an important role for the combination of all layers, which does not mean that human knowledge is not necessary but here computer programming is more valuable than human skill. Therefore, ultimately machine learning method gives a more satisfactory result than statistical method in this study.

22.4 Conclusion

In this study statistical and machine learning methods along with remote sensing and GIS computer-based technology have successfully been applied to extract groundwater potential zones in the concerned district. This study is basically a comparative study between two methods. As we know, in the present day, machine learning methods are widely applied for the integration of various thematic layers and extract a reliable output. Both statistical and machine learning methods give a similar result, i.e., eastern part of the district is more potential than the western part, but the result from the machine learning method is more appropriate and reliable. For the identification of reliability of the model, ROC curve has been used where the ROC curve of WoE method shows 76% accuracy and ROC curve of MLP method shows 89% accuracy. In this point of view, we can easily justify that machine learning method is more reliable than the statistical method. Whatever methods are used here is not the prime objective of the study, but another part of the study is sustainability of groundwater resource because the final output will be helpful for the higher authorities who basically belong to the field of water resource management. Therefore, this kind of systematic study will enrich the society and save the society from the future groundwater resource crisis problems.

References

- Abijith D, Saravanan S, Singh L, et al (2020) GIS-based multi-criteria analysis for identification of potential groundwater recharge zones – a case study from Ponnaniyaru watershed, Tamil Nadu, India. *HydroResearch* 3:1–14. <https://doi.org/10.1016/j.hydres.2020.02.002>
- Ahmed R, Sajjad H (2018) Analyzing Factors of Groundwater Potential and Its Relation with Population in the Lower Barpani Watershed, Assam, India. *Nat Resour Res* 27:503–515. <https://doi.org/10.1007/s11053-017-9367-y>
- Ajay Kumar V, Mondal NC, Ahmed S (2020) Identification of Groundwater Potential Zones Using RS, GIS and AHP Techniques: A Case Study in a Part of Deccan Volcanic Province (DVP), Maharashtra, India. *J Indian Soc Remote Sens* 3. <https://doi.org/10.1007/s12524-019-01086-3>
- Ali QSW, Lal D, & Ahsan J (2015) Assessment of groundwater potential zones in Allahabad district by using remote sensing & GIS techniques. *International Journal of Applied Research*, 1(13), 586–591

- Arabameri A, Roy J, Saha S, et al (2019) Application of probabilistic and machine learning models for groundwater potentiality mapping in Damghan sedimentary plain, Iran. *Remote Sens* 11: <https://doi.org/10.3390/rs11243015>
- Arulbalaji P, Sreelash K, Maya K, Padmalal D (2019) Hydrological assessment of groundwater potential zones of Cauvery River Basin, India: a geospatial approach. *Environ Earth Sci* 78:1–21. <https://doi.org/10.1007/s12665-019-8673-6>
- Aspinall P (1983) Clinical inferences and decisions—I. Diagnosis and Bayes' theorem. *Ophthalmic Physiol Opt* 3:295–304. [https://doi.org/10.1016/0275-5408\(83\)90011-x](https://doi.org/10.1016/0275-5408(83)90011-x)
- Bonham-Carter GF (1994) *C O M P U T E R M E T H O D S I N T H E G E O S C I E N C E S* Geographic Information Systems for Geoscientists : Modelling with GIS. 402
- Chezgi J, Pourghasemi HR, Naghibi SA, et al (2016) Assessment of a spatial multi-criteria evaluation to site selection underground dams in the Alborz Province, Iran. *Geocarto Int* 31:628–646. <https://doi.org/10.1080/10106049.2015.1073366>
- Chowdhury A, Jha MK, Chowdary VM (2010) Delineation of groundwater recharge zones and identification of artificial recharge sites in West Medinipur district, West Bengal, using RS, GIS and MCDM techniques. *Environ Earth Sci* 59:1209–1222. <https://doi.org/10.1007/s12665-009-0110-9>
- Corsini A, Cervi F, Ronchetti F (2009) Weight of evidence and artificial neural networks for potential groundwater spring mapping: an application to the Mt. Modino area (Northern Apennines, Italy). *Geomorphology* 111:79–87. <https://doi.org/10.1016/j.geomorph.2008.03.015>
- Das N, Mondal P, Ghosh R, Sutradhar S (2019) Groundwater quality assessment using multivariate statistical technique and hydro-chemical facies in Birbhum District, West Bengal, India. *SN Appl Sci* 1:1–21. <https://doi.org/10.1007/s42452-019-0841-5>
- Das N, Mukhopadhyay S (2020) Application of multi-criteria decision making technique for the assessment of groundwater potential zones: a study on Birbhum district, West Bengal, India. *Environ Dev Sustain* 22:931–955. <https://doi.org/10.1007/s10668-018-0227-7>
- Duan H, Deng Z, Deng F, Wang D (2016) Assessment of groundwater potential based on multicriteria decision making model and decision tree algorithms. *Math Probl Eng* 2016:1–12. <https://doi.org/10.1155/2016/2064575>
- Gayen A, Saha S (2017) Application of weights-of-evidence (WoE) and evidential belief function (EBF) models for the delineation of soil erosion vulnerable zones: a study on Pathro river basin, Jharkhand, India. *Model Earth Syst Environ* 3:1123–1139. <https://doi.org/10.1007/s40808-017-0362-4>
- Ghorbani Nejad S, Falah F, Daneshfar M, et al (2017) Delineation of groundwater potential zones using remote sensing and GIS-based data-driven models. *Geocarto Int* 32:167–187. <https://doi.org/10.1080/10106049.2015.1132481>
- Horton RE (1932) Drainage-basin characteristics. *Eos, Trans Am Geophys Union* 13:350–361. <https://doi.org/10.1029/TR013i001p00350>
- Jha MK, Chowdhury A, Chowdary VM, Peiffer S (2007) Groundwater management and development by integrated remote sensing and geographic information systems: Prospects and constraints. *Water Resour Manag* 21:427–467. <https://doi.org/10.1007/s11269-006-9024-4>
- Krishnamurthy J, Venkatesa Kumar N, Jayaraman V, Manivel M (1996) An approach to demarcate ground water potential zones through remote sensing and a geographical information system. *Int J Remote Sens* 17:1867–1884. <https://doi.org/10.1080/01431169608948744>
- Kumar R, Thaman S, Agrawal G, Poonam S (2011) Rain Water Harvesting and Ground Water Recharging in North Western Himalayan Region for Sustainable Agricultural Productivity. *Univers J Environ Res Technol* 1:539–544
- Lee S, Kim YS, Oh HJ (2012) Application of a weights-of-evidence method and GIS to regional groundwater productivity potential mapping. *J Environ Manage* 96:91–105. <https://doi.org/10.1016/j.jenvman.2011.09.016>
- Lee S, Pradhan B (2006) Probabilistic landslide hazards and risk mapping on Penang Island, Malaysia. *J Earth Syst Sci* 115:661–672. <https://doi.org/10.1007/s12040-006-0004-0>

- Lee S, Talib JA (2005) Probabilistic landslide susceptibility and factor effect analysis. *Environ Geol* 47:982–990. <https://doi.org/10.1007/s00254-005-1228-z>
- Li D, Huang F, Yan L, et al (2019) Landslide susceptibility prediction using particle-swarm-optimized multilayer perceptron: Comparisons with multilayer-perceptron-only, BP neural network, and information value models. *Appl Sci* 9. <https://doi.org/10.3390/app9183664>
- Magesh NS, Chandrasekar N, Soundranayagam JP (2012) Delineation of groundwater potential zones in Theni district, Tamil Nadu, using remote sensing, GIS and MIF techniques. *Geosci Front* 3:189–196. <https://doi.org/10.1016/j.gsf.2011.10.007>
- Majumdar D (1975) Bengal District Gazetteer, Birbhum. State editor, Government of West Bengal
- Manap MA, Nampak H, Pradhan B, et al (2014) Application of probabilistic-based frequency ratio model in groundwater potential mapping using remote sensing data and GIS. *Arab J Geosci* 7:711–724. <https://doi.org/10.1007/s12517-012-0795-z>
- Marjanović M, Kovačević M, Bajat B, Voženilek V (2011) Landslide susceptibility assessment using SVM machine learning algorithm. *Eng Geol* 123:225–234. <https://doi.org/10.1016/j.enggeo.2011.09.006>
- Moayedi H, Osouli A, Bui DT, Foong LK (2019) Spatial landslide susceptibility assessment based on novel neural-metaheuristic geographic information system based ensembles. *Sensors (Switzerland)* 19:. <https://doi.org/10.3390/s19214698>
- Nolan BT, Baehr AL, Kauffman LJ (2003) Groundwater Quality in Southern New Jersey. *Vadose Zo J* 691:677–691
- Oh HJ, Kim YS, Choi JK, et al (2011) GIS mapping of regional probabilistic groundwater potential in the area of Pohang City, Korea. *J Hydrol* 399:158–172. <https://doi.org/10.1016/j.jhydrol.2010.12.027>
- Olden JD, Lawler JJ, Poff NL (2008) Machine learning methods without tears: A primer for ecologists. *Q Rev Biol* 83:171–193. <https://doi.org/10.1086/587826>
- Pande CB, Khadri SFR, Moharir KN, Patode RS (2018) Assessment of groundwater potential zonation of Mahesh River basin Akola and Buldhana districts, Maharashtra, India using remote sensing and GIS techniques. *Sustain Water Resour Manag* 4:965–979. <https://doi.org/10.1007/s40899-017-0193-5>
- Panigrahi B, Nayak AK, Sharma SD (1995) Application of remote sensing technology for groundwater potential evaluation. *Water Resour Manag* 9:161–173. <https://doi.org/10.1007/BF00872127>
- Pinto D, Shrestha S, Babel MS, Ninsawat S (2017) Delineation of groundwater potential zones in the Comoro watershed, Timor Leste using GIS, remote sensing and analytic hierarchy process (AHP) technique. *Appl Water Sci* 7:503–519. <https://doi.org/10.1007/s13201-015-0270-6>
- Pourghasemi HR, Sadhasivam N, Yousefi S, et al (2020) Using machine learning algorithms to map the groundwater recharge potential zones. *J Environ Manage* 265:110525. <https://doi.org/10.1016/j.jenvman.2020.110525>
- Pourtaghi ZS, Pourghasemi HR (2014) Evaluation de la potentialité des sources d'eau souterraine à partir d'un SIG et cartographie dans le district de Birjand, Sud de la province de Khorasan, Iran. *Hydrogeol J* 22:643–662. <https://doi.org/10.1007/s10040-013-1089-6>
- Prasad RK, Mondal NC, Banerjee P, et al (2008) Deciphering potential groundwater zone in hard rock through the application of GIS. *Environ Geol* 55:467–475. <https://doi.org/10.1007/s00254-007-0992-3>
- Rahmati O, Samani AN (2014) Groundwater potential mapping at Kurdistan region of Iran using analytic hierarchy process and GIS. <https://doi.org/10.1007/s12517-014-1668-4>
- Rahmati O, Nazari Samani A, Mahdavi M, Pourghasemi HR, Zeinivand H (2015) Groundwater potential mapping at Kurdistan region of Iran using analytic hierarchy process and GIS. *Arabian Journal of Geosciences*, 8(9), 7059–7071. <https://doi.org/10.1007/s12517-014-1668-4>
- Ramu MB, Vinay M (2014) Identification of ground water potential zones using GIS and Remote Sensing Techniques: A case study of Mysore taluk -Karnataka. *Int J Geomatics Geosci* 5:393–403

- Razandi Y, Pourghasemi HR, Neisani NS, Rahmati O (2015) Application of analytical hierarchy process, frequency ratio, and certainty factor models for groundwater potential mapping using GIS. *Earth Sci Informatics* 8:867–883. <https://doi.org/10.1007/s12145-015-0220-8>
- Salarian T, Zare M, Jouri MH, Miarrostami S (2014) Evaluation of shallow landslides hazard using artificial neural network of Multi-Layer Perceptron method in Subalpine Grassland (Case study: Glandrood watershed – Mazandaran). 795–804
- Sander, Per; Chesley, Matthew M.; Minor TB (1996) Groundwater Assessment Using Remote Sensing And GIS In A Rural Groundwater Project In Ghana: Lessons Learned. 40–49
- Al Saud M (2010) Mapping potential areas for groundwater storage in Wadi Aurnah Basin , western Arabian Peninsula , using remote sensing and geographic information system techniques. 1481–1495. <https://doi.org/10.1007/s10040-010-0598-9>
- Sokeng V-CJ, Kouame F., Nagatcha N, et al (2016) Delineating groundwater potential zones in Western Cameroon Highlands using GIS based Artificial Neural Networks model and remote sensing data. *Int J Innov Appl Stud* 15:747–759
- Sun T, Li H, Wu K, et al (2020) Data-driven predictive modelling of mineral prospectivity using machine learning and deep learning methods: A case study from Southern Jiangxi Province, China. *Minerals* 10:.. <https://doi.org/10.3390/min10020102>
- Tahmassebipoor N, Rahmati O, Noormohamadi F, Lee S (2016) Spatial analysis of groundwater potential using weights-of-evidence and evidential belief function models and remote sensing. *Arab J Geosci* 9:1–18. <https://doi.org/10.1007/s12517-015-2166-z>
- Thomas BF, Behrangi A, Famiglietti JS (2016) Precipitation intensity effects on groundwater recharge in the southwestern United States. *Water (Switzerland)* 8:12–17. <https://doi.org/10.3390/w8030090>
- Venkatesan G, Pitchaikani S, Saravanan S (2019) Assessment of Groundwater Vulnerability Using GIS and DRASTIC for Upper Palar River Basin, Tamil Nadu. *J Geol Soc India* 94:387–394. <https://doi.org/10.1007/s12594-019-1326-2>
- Wu J, Zhang R, Yang J (1996) Analysis of rainfall-recharge relationships. 177:143–160

Chapter 23

Water Resource Management in Semi-arid Purulia District of West Bengal, in the Context of Sustainable Development Goals



Amit Bera and Shubhamita Das

Abstract Water, being one of the most significant resources, is of paramount importance for development of all kinds. At present factors like limited water reservoirs, water supply, global water demand, regional disparities and climate change make water resource management a great challenge in semi-arid hard rock regions like Purulia. Even after 72 years of independence, inhabitants of this region remain devoid of basic needs like food and drinking water and need to struggle for meeting these fundamental requirements of their daily lives. Thus management of water resources in Purulia needs proper planning and participation of everyone in order to conserve this asset. Groundwater is utilised in Purulia for drinking and agricultural purposes with increasing demand. Rivers are one of the most important surface water resources used by local people for their different purposes. Adequate check dams to hold a considerable amount of water in the reservoirs during the monsoon would help them during dry seasons. Rainwater harvesting at all possible scales would be very helpful to mitigate water crisis of Purulia. The present chapter has been designed to discuss the groundwater and surface water management and various ways to alleviate suffering of people during water shortage and enhance their socio-economic development.

Keywords Water resource management · Surface water · Groundwater management · Irrigation · Human participation · Development · Purulia

A. Bera (✉) · S. Das

Department of Earth Sciences, Indian Institute of Engineering Science and Technology, Shibpur, Howrah, West Bengal, India

e-mail: amit.rs2017@geology.iiests.ac.in

© The Author(s), under exclusive license to Springer Nature Switzerland AG 2021

P. K. Shit et al. (eds.), *Groundwater and Society*,

https://doi.org/10.1007/978-3-030-64136-8_23

501

23.1 Introduction

Maintaining stability between supply and consumption of water by incorporating all possible measures of water conservation is the main motto of water resource management. Water is an integral part of social, health and economic development. Integrating all kinds of developmental thoughts, a judicious planning of management is essential in the present scenario when demand for water is increasing day by day. Optimal implementation and, for conservation, distinguishing groundwater potential zones are very important (Hutti and Nijagunappa 2011). Both surface water and groundwater are equally important and need well-thought-out schemes for management. Hydrometeorological factors govern the availability of ground and surface water of any region. Hydrometeorological factors have a great impact on water paucity of Purulia. Factors include runoff, air temperature, evapotranspiration, precipitation and soil moisture (Haldar and Saha 2015). The district has been suffering from critical water crisis for a long time, and this water shortage is a significant issue affecting the socio-economic development of Purulia (Das 2018). Thus, for a successful strategy, climatic, topographic, geological, socio-economic and various other vital conditions including the pivotal causes of water scarcity of a region need to be considered by decision makers (Bera et al. 2020; Biswas et al. 2020). Purulia, a hard rock terrain, is known to be a drought-prone district of West Bengal where economically backward sections dominate the population. Purulia, which is one of the most backward districts of West Bengal, in terms of both economy and development, is having the second highest concentration of schedule tribe population and agro-based economy according to the 2011 census. Previous researchers have studied water resource management in various semi-arid regions of the world (Ragab and Prudhomme 2002; Shangguan et al. 2002; Ortega et al. 2004; Branco et al. 2005; Tonkaz et al. 2007; Cirilo 2008; Shen and Chen 2010; Singh 2010; Feng et al. 2011; Mahmoud et al. 2011; Hu et al. 2014; Niazi et al. 2014; Hussain et al. 2019). But in Purulia not many researches emphasizing mainly on water resource management have been undertaken before. So, water management is an indispensable step towards overall development of Purulia. Purulia shows a long history of water crisis. In Purulia, physical as well as economic water shortages have been noted (Haldar and Saha 2015). In a study, in Purulia, conducted by the Central Ground Water Board (CGWB), it has been shown that occurrence of groundwater in the district is within four distinct zones, i.e. (i) weathered mantle, (ii) saprolitic zone, (iii) fractured zone of hard rock and (iv) zone of unconsolidated sediments (Haldar and Saha 2015). Social awareness regarding scientific and wise use of water and effects of deforestation on water scarcity leading to mass participation along with government assistance can be the best method for water resource management. Practices mainly at household scale leading to economic profit, keeping in mind hygienic conditions of the family and not requiring unaffordable investment, can be practised by local people. For village scale, water management government intervention is essential (Kyessi 2005). A thorough analysis of the district's water conditions and requirements and identification of potential zones of water resource

management and regions under maximum threat of water scarcity need to be done for an advantageous planning and decisionmaking. Groundwater is the most dynamic and replenishable resource which has both direct and indirect influences on the water availability and utilisation of water in agriculture. The fundamental principle of watershed management is to preserve and develop water resources for development. So, in areas which are drought prone, micro-watershed-based development may be deemed as the best practice for the overall progress of a region (Deshpande and Narayanmoorthy 2000). Construction of check dams has proved to be an important step towards the progress of water resource management in Purulia. Construction of check dams within Bankura and Purulia has been undertaken under Rashtriya Krishi Vikas Yojana (RKVY) with an objective to support 24,800 rural farmers by ensuring water resources as the basic need for agriculture activities as well as daily life. The project as approved by the State Level Sanctioning Committee (SLSC) consists of construction of 30 check dams at Purulia and 05 check dams at Bankura in a period of 5 years with an outlay of rupees 4138 lakhs. So far 35 projects have been executed. Schemes of water management can be applied through different ways which include water conservation, expansion of irrigation facilities, effectual dealing of drought seasons, recharging underground aquifers and spreading public awareness on methods of mitigation (Halder and Sadhukhan 2012). This study will provide a general idea on water resource management in the context of socio-economic development of local inhabitants of Purulia.

23.2 Study Area

Purulia is the westernmost district of West Bengal and is the fourth largest district of Bengal with latitudinal and longitudinal extensions of 22°43'N to 23°42'N and 85°89'E to 86°54'E, respectively, having a total area of 6259 sq. km (Fig. 23.1). The district has 3 subdivisions (Purulia Sadar, Jhalda and Raghunathpur) and 20 development blocks. Based on 2011 census report, this district is having less population density (468/sq. km) with a total of 2,927,965 inhabitants. Structurally Purulia is the eastern part of Chota Nagpur plateau and happens to be a part of Ranchi penepain. The district is characterised by the presence of undulating topography, steep hills and low-lying valleys. Lying to the west of this district is the Ajodhya hills, to the south there is the Dalma hills, and to the north-east, there is the Panchet hills. The Gorgaburu peak (677 m) of Ajodhya hills is the highest peak in the western part of West Bengal. Most of the part of this district shows flat terrain topographic features. The notable rivers of the district include Kangsabati, Damodar, Subarnarekha and Kumari. As a consequence of the overall land slope of the district, most of the rivers flow towards east or north-east. As the rivers originate from a plateau, they generally have water shortage during the summer and winter seasons, but there is a considerable increase in the amount of water during the monsoon season. Purulia shows semi-arid type of climate. The maximum and minimum temperatures of Purulia in the summer season are 45 °C and 26 °C, respectively.

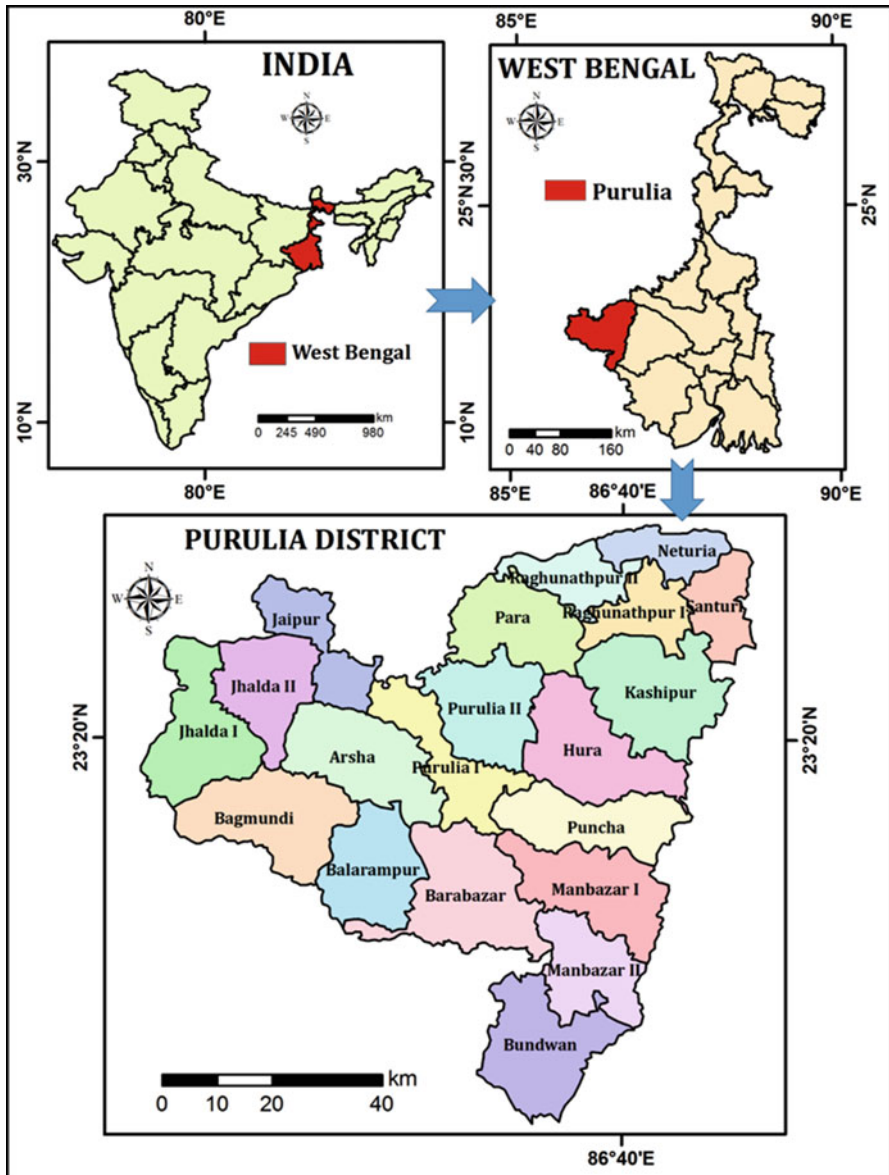


Fig. 23.1 Location map of the study area

Here, the winter season sees a maximum temperature of 28 °C and minimum temperature of 8 °C. The mean annual rainfall of the district ranges from 1050 to 1420 mm. The soil type of this region is coarse and rough and includes sandy skeletal and gravelly loam types. Apart from this, some regions also have the presence of iron-rich red laterite soil. The high amount of potash and calcium

carbonate makes the soil unsuitable for agriculture. As the district is drought prone, farmers depend on rainfall during the monsoon for their agricultural activities.

23.3 Materials and Method

The present study has been done, based mainly on secondary data which have been collected from central and state government offices and their websites. The drainage map has been digitised from Survey of India Toposheet on ArcGIS 10.0 platform. Depth to water level data, which is mainly of lean season of 2015, has been collected from the Central Ground Water Board (CGWB). Also, groundwater development status and groundwater resource availability data have been taken from a published report booklet of CGWB on Purulia district. Source of irrigation and data of total irrigated area have been taken from the District Statistical Handbook (2004, 2008, 2010, 2012 and 2015) of Purulia district, which has been collected from the Ministry of Statistics and Programme Implementation office of West Bengal. In case of depth to water level map, using an inverse distance weighted interpolation technique in ArcGIS environment, spatial distribution map has been prepared. Necessary data related to irrigation have been collected from Irrigation and Waterways Department, Government of West Bengal. Here, statistical tools and techniques have been used to represent the collected and calculated data.

23.4 Impact of Geo-environmental Factors on Availability of Water Resources

Distribution and availability of groundwater and surface water are determined by some geo-environmental factors which are soil texture and type, nature of aquifer media, lithological factor, evapotranspiration rate, vegetation cover, drainage density, agricultural pattern, urbanisation, etc. Geologically, Purulia is a hard rock terrain and, as a consequence of this, has low primary porosity and permeability. The layer of soil overlying the hard rock terrain shows a maximum depth of 25 m, and the retaining capacity of soil ranges from medium to low. Water retained in these zones is extracted through tube wells. The water yielding capacity of these zones is markedly less. The water bodies of the northern blocks of Purulia district show relatively more water retaining capacity. A large part of the district is covered by hills and is an essential portion of Chota Nagpur plateau. The Ajodhya hills of Purulia rise to a height of 2200 ft, the Panchakot hill shows a height of 2110 ft, and Jaichandi hills have a height of about 1045 ft. The slope of these western hills gradually flattens and joins the flat terrains of the eastern and south eastern side. So, the surface runoff due to precipitation follows the slope that is from the western to

the eastern side. Thus, the infiltration rate in the western and the north western regions is relatively low.

The district mainly shows semi-arid climatic conditions. Here the difference between the changes in diurnal temperature is remarkable. Temperature during the summer season reaches a maximum of 50 C, and as a result air becomes dry and soil humidity also decreases. Here the rate of evapotranspiration is higher, because the water bodies dry up during the summer seasons. This gives rise to many water-related problems. Purulia is an economically backward district of West Bengal, and the lower-class population which constitutes a major part of the population of the district lacks modern technologies and required economy for tube well construction for themselves or for the benefit of the whole village. So, the inhabitants have to depend on surface water bodies or dams for their water requirements. The usage of groundwater in the blocks of Arsha, Manbazar, Bundwan, Raghunathpur, Baghmundi and Balarampur is significantly less. In Purulia, the main mode of livelihood is agriculture. The rivers of these regions are rainfed, and hence the water flow is seasonal and confined mainly to the monsoon season. During the dry seasons, people thus need to depend on canal water for irrigation purposes. So, a considerable part of this water gets utilised only for irrigation. Previously, crops were grown once during a year, but with the changing scenario, now, there are various crop-growing schemes in a year giving rise to an augmentation in the demand of water for irrigation.

23.5 Surface Water Resource Management

One of the main sources of surface water is rivers. There are seven main rivers in Purulia, which are Damodar, Kangsabati, Dwarakeswar, Shilabati, Subarnarekha, Kumari and Totko (Fig. 23.2). Apart from this there are some small tributaries – Hanumata, Nangasai, Chaka, Beko, Rupai, Paltoi, Jam, Kutlung, Bandu, etc. For the development of agricultural activities, many river dams have been constructed, depending on which different irrigation schemes or projects have been planned and carried out. Aside from the construction of dam on big rivers, check dams have been built on small jhoras (a type of small and narrow tributaries which have water only during the monsoon) and tributaries. Though rainfall, here, is adequate, farmers are unable to use this rainwater during the advent of monsoon. Thus, farmers, after struggling hard, construct dams made of soil to restrict water flow of small jhoras and other important small surface source of water. Though this helps them to store water for agricultural activities, with the advancement of monsoon, during heavy rainfall, these dams get carried away like straw by the strong flow of water. Therefore, construction of concrete dams can help farmers in their agricultural activities without any hurdle. Acute water shortage has been observed in this

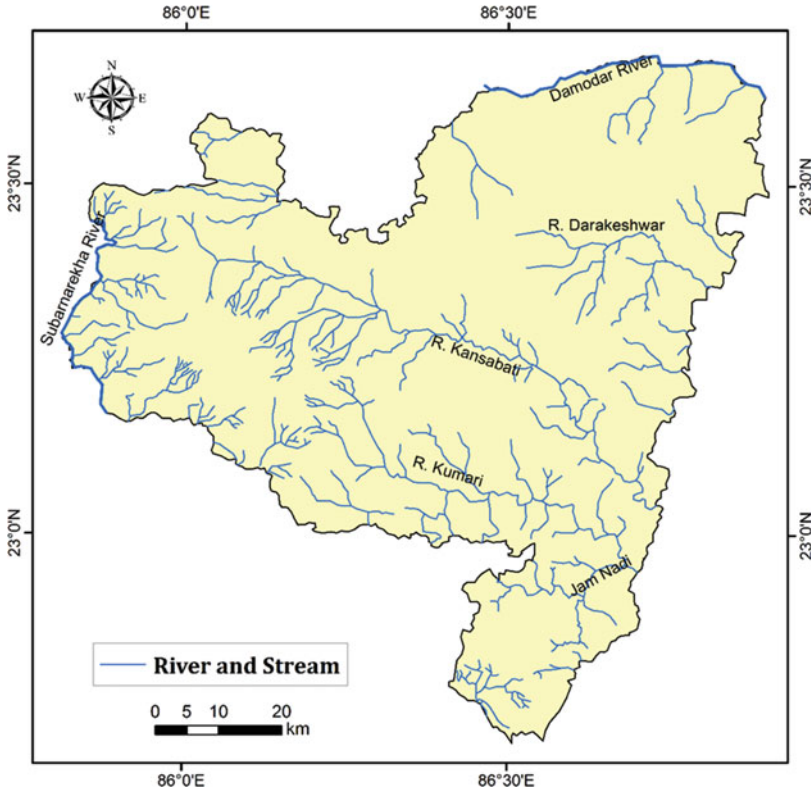


Fig. 23.2 Drainage map of the Purulia district

drought-prone district mainly during the summer season. Animal husbandry, which is another source of livelihood for the people living in Purulia, requires a good amount of water for maintenance of animals. During the summer season, almost all the rivers and tributaries of Purulia also dry up or have a narrow flow of water in them. During this crisis the reservoirs of 32 irrigations ran by irrigation department provide water. The check dams during the scarcity supply water not only for agriculture but also for drinking, animal husbandry and daily domestic uses. Some important reservoirs are lower dam and upper dam (Ajodhya), Khairabera (Bagmundi), Tara dam (Kenda), Kumari dam (Urma), Murguma dam (Jhalda), Bandu dam (Arsha), Lipania dam (Lipania), Murardi dam (Santuri), etc. (Fig. 23.3). Aside from these, a few other notable ways of water conservation in Purulia include big bandh or lakes, which are Saheb Bandh (Purulia), Ranibandh (Joypur), Jamdar bandh (Balarampur), Beror bandh (Raghunathpur), Sunri bandh (Hura), Sayer (Maheshpur) and Supsagar (Jhalda). Also, there are large- and small-scale ponds. Many ponds are also being dug under different schemes or projects going on in Purulia presently (Fig. 23.4).



Fig. 23.3 Some typical dams of the Purulia district: (a) Bandu dam, (b) Hanumata dam, (c) Kumari dam, (d) Barabhum dam



Fig. 23.4 Excavation of a pond in Kashipur gram panchayat in Purulia district

23.6 Groundwater Resource Management

Groundwater is a dynamic and replenishable resource which directly or indirectly influences water availability and its utilisation in domestic agricultural and industrial activities. During the lean period in Purulia, the groundwater table varies from 0.80 mbgl to 10.1 mbgl (Fig. 23.5). Higher groundwater depth ranging from 6.39 mbgl to 10.01 mbgl is observed in certain blocks of Purulia, which are Jhalda-I and Jhalda-II in the west, Banduan and Manbazar-II in the south, Kashipur and Hura in the east. On the other hand, shallow groundwater depth can be observed mainly in Neturia, Raghunathpur I and II, Purulia I, Bagmundi and Manbazar I blocks. Other than being a source of drinking water, groundwater is being highly used in agricultural activities as well. As the basic rules of groundwater extraction are not being followed, therefore, in many places, maintaining groundwater equilibrium is getting hampered. Hence, Purulia is suffering from water crisis. The nature of topography

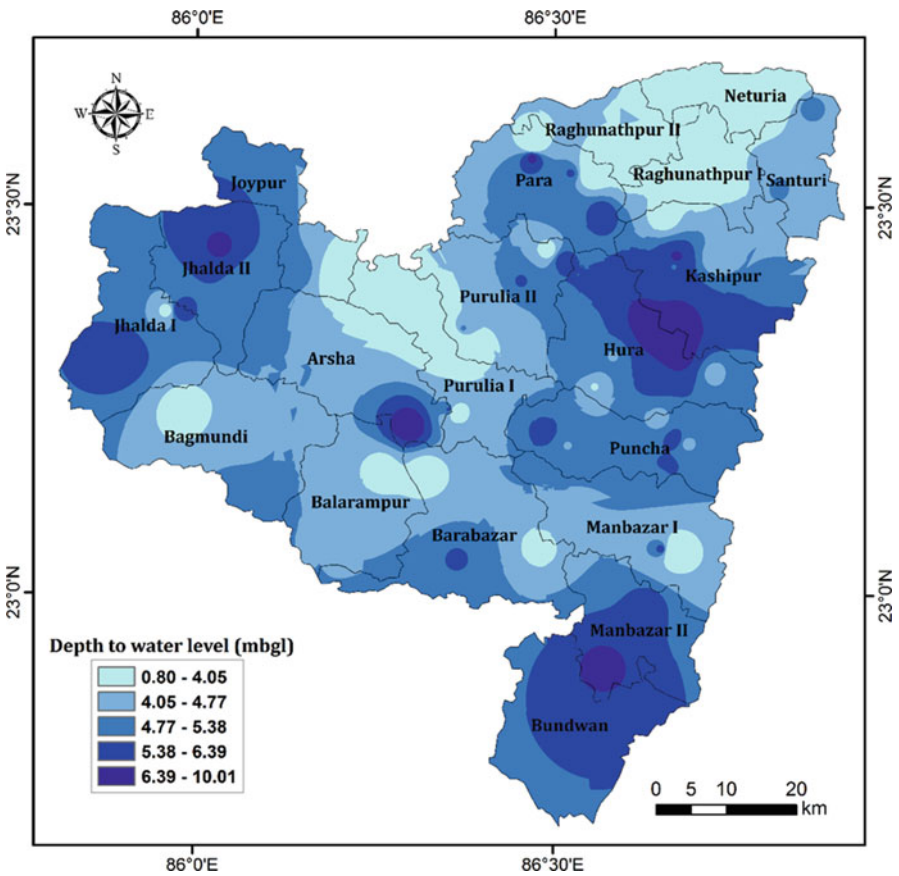


Fig. 23.5 Spatial distribution of groundwater depth of Purulia district during lean season in 2018

and amount of precipitation determine the quantity of groundwater. As the soil type of Purulia is coarse and skeletal, therefore, there is limited availability of groundwater. Soil type and texture determine the depth of groundwater aquifer which differs from one place to another. While digging a well, water-saturated layers of soil need to be considered as these layers are always in a state of flow. At times these layers remain under pressure, and on digging the underground, water finds its way to the surface at a great speed. Rainwater percolates through the fractures in hard rocks and reaches underground and flows along the slope of the land and accumulates in the weathered residuum layers below the fractured layer. Groundwater flow in hard rock terrain is much lesser than in the soft rock terrain. Because of this same reason, groundwater flow in Purulia is less. Because of less availability of groundwater in the hard rock terrain of Purulia, mainly in summer season, the district faces water crisis, and collection of minimum amount of required water becomes tough. Because of uneven topography of this district, flat terrain is much less than hard and rocky land. Also because of difference in demand of underground water in different regions of this district, extraction of water is also not uniform everywhere in Purulia. A major percentage of this underground water serves as a source of drinking water, and the rest amount is utilised for irrigation facilities. Recent appearance of new technologies of agriculture has led to a rise in demand of groundwater. For extraction, deep and shallow wells have been dug (Fig. 23.6), and in many places, therefore, wastage of this valuable asset has also been observed. From Fig. 23.7, we can get an overall idea about block-wise groundwater development of Purulia. It can be seen that in the blocks of Jhalda I, Joypur and Baghmundi groundwater development is considerably high (24.49–46.49%) as compared to groundwater development status of Arsha, Banduan, Santuri and Manbazar I and II. Taking all these factors into consideration, it can be said that water resource of Purulia is under



Fig. 23.6 A typical dug well in Purulia district

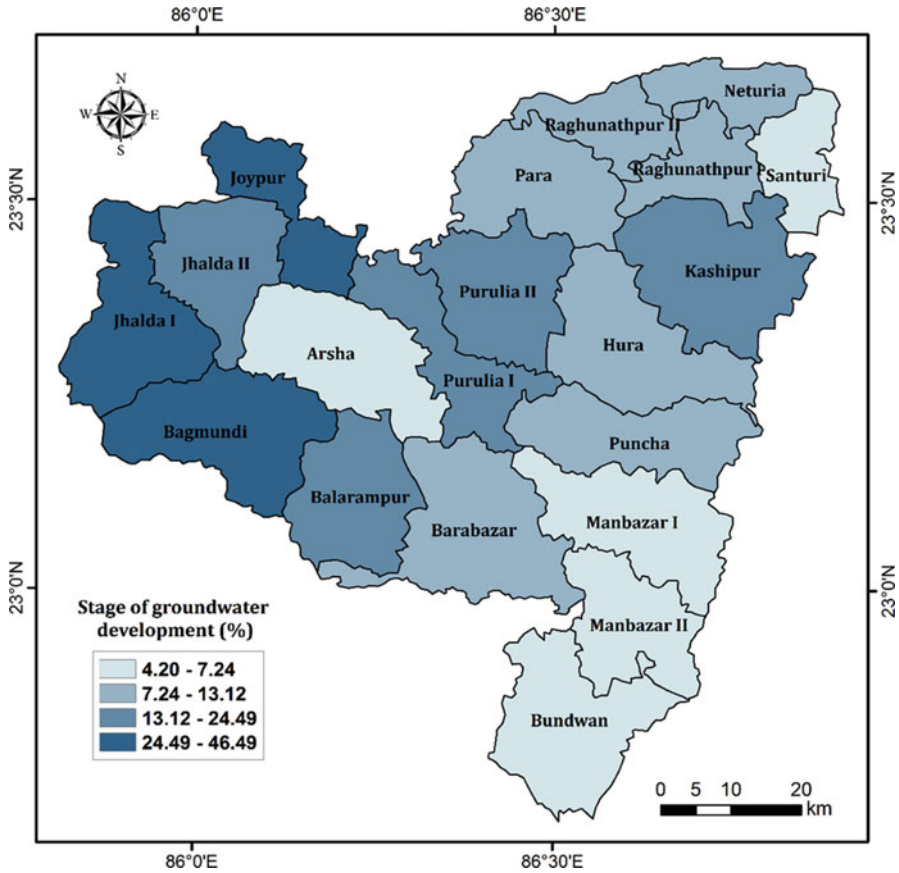


Fig. 23.7 Block-wise groundwater development status of Purulia district

threat. To recover Purulia from this crisis, necessary and proper steps must be taken. Different artificial structures can be constructed for the purpose of increasing groundwater recharge. The NRWDP is working in different regions to manage the groundwater recharge by building various artificial structures. Some engineering structures for artificial groundwater recharge are recharge pit, recharge trench, recharge dug well, recharge shaft and lateral shaft with bore well. Table 23.1 provides the basic knowledge on groundwater resource in Purulia.

23.7 Expansion of Irrigation Facilities

Irrigation has always played a significant role in ensuring food security and reducing poverty. But in a district lying in Purulia, the opportunities available for attaining a better quality of livelihood through utilisation of irrigation facilities have not been

Table 23.1 The summarised groundwater resources in the Purulia district (block-wise)

Block	Net groundwater availability (in ha m)	Existing gross groundwater draft for irrigation (in ha m)	Existing gross groundwater draft for domestic and industrial water supply (in ha m)	Existing gross groundwater draft for all uses (in ha m)	Net groundwater availability for future irrigation development (in ha m)	Stage of groundwater development (%)
Arsha	3704	48	204	251	3382	6.79
Baghmundi	2172	417	180	597	1513	27.47
Balarampur	2988	263	153	416	2518	13.93
Barabazar	6275	248	235	483	5711	7.70
Bandwan	2947	77	133	210	2691	7.11
Hura	3417	132	207	338	3007	9.90
Jhalda I	2144	816	180	996	1086	46.44
Jhalda II	2707	369	191	560	2081	20.68
Joypur	2090	799	172	972	1058	46.49
Kashipur	6073	764	264	1028	4953	16.93
Manbazar I	5258	157	214	371	4812	7.06
Manbazar II	3992	24	144	168	3775	4.20
Neturia	2942	138	139	277	2617	9.41
Para	3178	146	256	401	2688	12.62
Puncha	4970	257	175	433	4476	8.71
Purulia I	3602	586	199	785	2748	21.80
Purulia II	3781	381	223	604	3100	15.97
Raghunathpur I	2496	168	135	303	2147	12.12
Raghunathpur II	2267	100	146	246	1970	10.86
Santuri	3143	112	116	228	2875	7.24
Total	70,147	6000	3666	9666	59,207	13.78

adequately used everywhere. Now through different government projects in different regions, development of irrigation facilities is being carried out by the government. In Purulia, there are mainly four sources of irrigation, which are canal, tank, river-lifting irrigation and groundwater irrigation. Among these, tank and river-lifting irrigation are used for maximum activities. Open dug well irrigation is the main source in case of groundwater irrigation. Though following the trend of temporal changes of Purulia as total irrigated area, it can be seen that in the blocks of Hura, Manbazar I, Kashipur, Santuri, Neturia, Purulia I and Purulia II, there has been an increase in total irrigated area (Fig. 23.8). The total irrigated area of 2015 is more than of 2004, but irrigation has not seen much development in the blocks of Jhalda II, Para and Barabazar (Fig. 23.9). Among other food crops, Paddy forms the staple food crop in this locality. Apart from this, corn, mustard, pulses and various vegetables are also grown. For agricultural benefits, different irrigation projects have been carried out in Purulia like Kansai irrigation scheme, Kumari irrigation scheme, Bandu irrigation scheme, Barabhum irrigation scheme, Hanumata irrigation scheme, etc. Also, check dams have been constructed through various government projects for use in irrigation activities. From check dams water is generally extracted

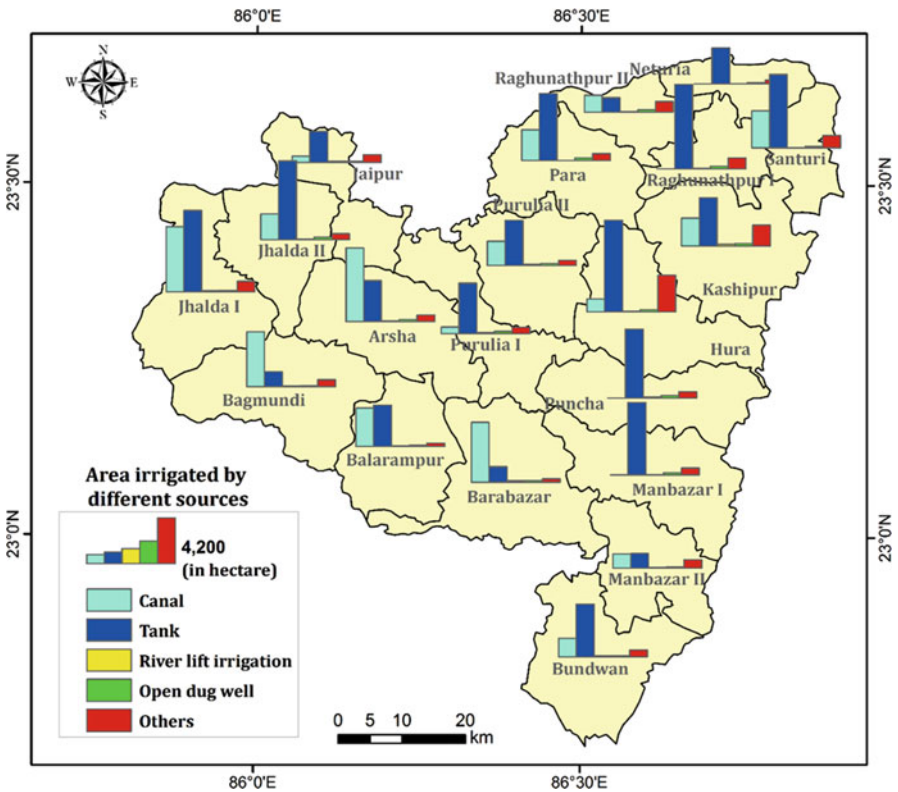


Fig. 23.8 Area irrigated by different sources in the blocks of Purulia district

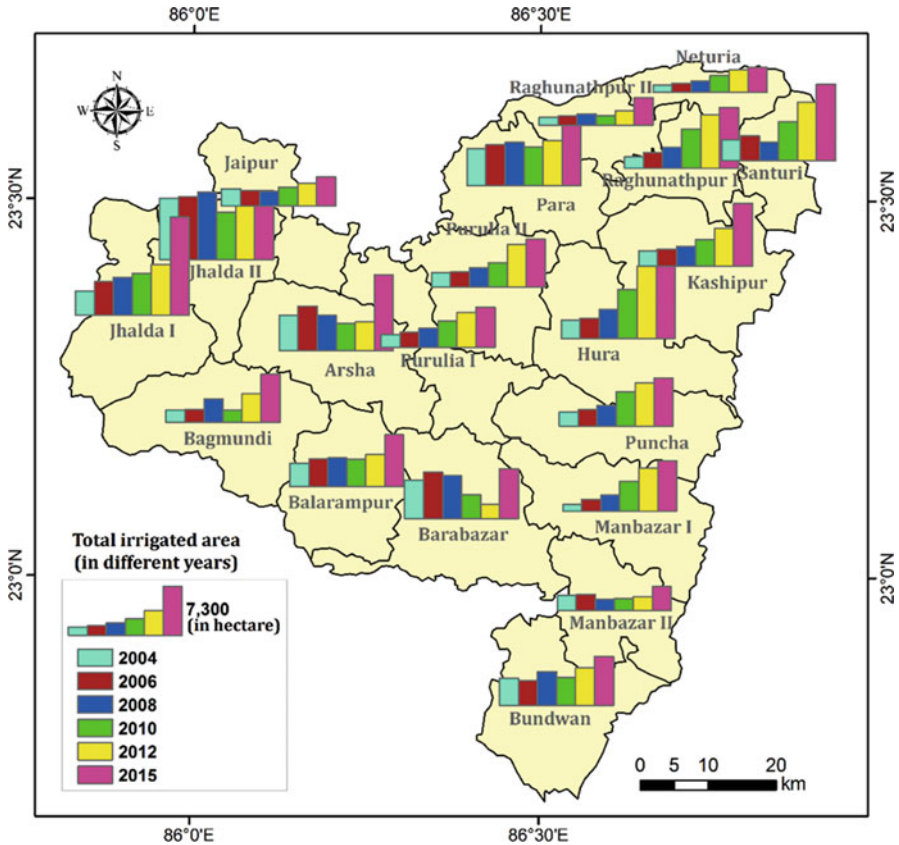


Fig. 23.9 Temporal changes of total irrigated area in the blocks of Purulia district

through pumps, and then it is sent for use in agricultural lands. Agricultural lands adjacent to or near the check dams have a good opportunity of irrigation, but through multistage pumping, water can be used for irrigating distant agricultural lands. At first, water from check dam is transferred to a nearby water body through pumps. Then from this water body, water is transferred to another water body through a second set of pumps. Therefore, in this way, with the help of multistage pumping, supplying water to distant agricultural lands is made possible. Because of this progress in irrigation techniques, farmers are able to cultivate their lands in dry seasons leading to improvement in agriculture and strengthening of their overall economic condition.

23.8 Schemes of Socio-Economic Development Through Sustainable Water Resource Management

23.8.1 'USHARMUKTI' Micro-Watershed Scheme

The name 'USHARMUKTI' itself explains the objective of this scheme. In addition to Purulia, six other drought-prone districts of West Bengal are under this scheme to eradicate dryness and convert them into lush green terrain with rich growth of crop and vegetation. The pivotal point of this project is the Mahatma Gandhi National Rural Employment Guarantee Scheme. Apart from this, organisations like Bharat Rural Livelihoods Foundation (BRLF) and other different voluntary service organisations have also joined the scheme. This is mainly a water divide development project. For the conservation of water and soil, different constructions like contour trench, contour embankment, 30 × 40 model, plantation, check dam, etc. are done. The main goal of USHARMUKTI project is socio-economic development of people by maintaining unity and balance among water, soil and plant kingdom. Though the amount of rainfall in the monsoon season of Purulia is considerably high, this region of West Bengal suffers from acute water shortage. Through this project, people will not only get wages for their hard work but will also lead a self-dependent livelihood through development of land and water resources. Besides, this will also lead to an increase in groundwater level. During the monsoon season, heavy rainfall causes water to flow down the slope carrying the topsoil with it and ultimately results in loss of water and fertile topsoil and sedimentation in the lower region water bodies leading to the decrease in their depths. Through this project, application of a 30 × 40 model in the upper tar lands will help to reduce water runoff speed, and planting trees along with this will lead to ultimate decrease in loss of soil. Also, the runoff water can be made to reach underground through small pockets of holes, and as a consequence of this, there will be an increase in level of groundwater. Apart from this, the land can be made useful as forest lands or can be utilised for mixed fruit farming which will become a permanent source of income for the regional people. When water gets restricted in tar land (high and dry land), and if hapa (a type of deep well dug in an agricultural land) is dug in Baid land (low-lying agricultural lands) for the purpose of containing water, then the retained water can be utilised for agricultural and fishery activities. Baid and Kanali lands which are mainly used for monoculture can also be converted into multiple crop-growing land through increment of humidity and proper irrigation. This will not only result in augmentation of family income but will also provide them with food security. Thus, increase in crop supply and crop variety will help regional people to change and upgrade their food habits for a better health. The socio-economic development therefore will aid people to spend more money on their health and education. Besides, the water bodies or the artificial water reservoirs or tanks can be used for fishery to provide non-veg nutrients to the families and can also be a source of a small-scale income for them.

23.8.2 ‘Jal Dharo-Jal Bharo’ Scheme

The Jal Dharo-Jal Bharo (JDJB) scheme was inaugurated during 2011–2012 financial year in West Bengal. The main objective of this campaign is to appropriately conserve water and to construct check dams, tanks, ponds, reservoirs and canals for the fulfilment of the purpose. Through this project, in different blocks of Purulia, construction of small check dams and redigging and reclamation of various other small- and large-scale structures like ponds, deep tanks and nayanjuli have been carried out. This has led to their increased water holding capacity. Also, fishery activities are simultaneously going on in these water bodies, and as a result there is an upsurge in fish production which is boosting up the quality of livelihood and income of the village people through different fishing activities. Apart from this with the aid of Panchayat and village development authority, stored water from the roof of houses is getting utilised for domestic purposes. This scheme is not only providing opportunity for water conservation but also helping day labourers who dig ponds and other manmade water bodies by giving them wages for their hard work. The state government has decided to construct 251 check dams in 17 blocks out of 20 blocks of Purulia during the dry season. Check dams have been built in blocks like Banduan, Balarampur, Purulia II, Raghunathpur, etc. This provides water for irrigation during the Rabi season.

23.8.3 ‘Jalathirtha’ Scheme

The Jalathirtha scheme in drought-prone Purulia region has not only provided proper irrigation facilities but also helped innumerable poor families with source of income for better livelihood. In 2013–2014 the irrigation department, under the Rashtriya Krishi Vikas Yojana (RKVY), constructed seven check dams in Purulia with the total expenditure of five crores. During the period of construction, this project received immense support and unimaginable encouragement from almost all regions of Purulia. After this, through the Jalathirtha scheme, construction of 500 check dams in the district was announced by the irrigation department. A huge amount of 65 crores have been spent by the irrigation department for the construction of 89 check dams. In Balarampur block, 8 check dams have been built with an extra expenditure of 6 crores, and as a result of this, 274 more hectares of land were brought under irrigation facility (Pal 2017). A total area of 3462 hectares of land were irrigated by 97 check dams. Blocks which got this facility include Arsha (3 check dams); Balarampur (9); Barabazar (5); Hura (6); Joypur (1); Kashipur (1); Manbazar I (6); Para (1); Pancha (19); Purulia I (15); Purulia II (17); Raghunathpur (13); and Santuri (1). The reservoirs of these check dams provide water for irrigation in the Rabi season. Apart from this, water from the reservoirs can be utilised for supplying water to the cattle, fishery activities and various domestic uses. Jalathirtha scheme has become a symbol of fulfilling hopes and desire of

poverty-stricken people of Purulia and has strengthened the economic foundation of Purulia's inhabitants.

23.9 Recommendation

The typical hydrogeological conditions of Purulia hinder the groundwater development in the district. Groundwater structures like dug well or bore well can be constructed depending on groundwater availability. Rainwater harvesting can be practised by local people. Both rooftop and land rainwater harvesting can be done based on suitability. Water from rooftop can be sand filtered and stored in tanks for use in dry season. Surface water (that flowing in rivers) can be conserved by check dam construction. Gully plug can be suitable on cultivated land. In feasible hydrogeological locations, artificial recharge like percolation tank structure for groundwater recharge can be constructed. Dry dug well can also be utilised for artificial recharge after cleaning. These measures to some extent can help to reduce the misery of village people during water shortage or drought.

23.10 Conclusion

Water is the most copious element on earth and one of the vital constituents of all living things. Water scarcity is a threat to nature and all its elements, and water resource management is therefore of paramount importance now. Dealing with one of the biggest threats, like water scarcity, claims the need of multidisciplinary approach to water resource management, especially in regions having a multitude of obstacles such as illiteracy, natural and topographic barriers, soil type and texture, inadequate economy, poor health condition of community and climate change. Besides maintaining an equilibrium of water resources available in nature, for an augmentation in financial development and improvement of public health, proper management of water is inevitably essential. For sustainable management of water resources, involvement of government, institutions, industries and local people is imperative. With change of climate and increase in demand of water in various sectors, mainly irrigation as in Purulia, continuous monitoring of the inducing needs and sustaining a balance among supply, demand and conservation of water can be crucial steps for sustainable water resource management. Water is indispensable for survival. So water crisis isn't just another environmental crisis but a cause of instability and endangerment for the whole civilisation. So, it is one of the fundamental rights of every human being to justifiably and judiciously use water.

Acknowledgements The authors are thankful to the Indian Space Research Organisation (ISRO), Central Ground Water Board (CGWB), State Water Investigation Directorate (SWID), India Meteorological Department (IMD) and Irrigation and Waterways Department (West Bengal) for

their support during the work. We are thankful to Mr. Bibek Mahato (journalist, Purulia Darpan) for providing some field photographs. We are thankful to Dr. Pravat Kumar Shit (editor of this book) for suggesting necessary modifications, which improved our manuscript. The authors also heartily extend their thanks to anonymous reviewers for their valuable constructive comments and suggestions.

References

- Bera, A., Mukhopadhyay, B.P. & Barua, S. (2020). Delineation of groundwater potential zones in Karha river basin, Maharashtra, India, using AHP and geospatial techniques. *Arabian Journal of Geosciences*, 13, 693 <https://doi.org/10.1007/s12517-020-05702-2>
- Biswas, S., Mukhopadhyay, B. P., & Bera, A. (2020). Delineating groundwater potential zones of agriculture dominated landscapes using GIS based AHP techniques: a case study from Uttar Dinajpur district, West Bengal. *Environmental Earth Sciences*, 79(12), 1–25.
- Branco, A. D. M., Suassuna, J., & Vainsencher, S. A. (2005). Improving access to water resources through rainwater harvesting as a mitigation measure: The case of the Brazilian semi-arid region. *Mitigation and Adaptation Strategies for Global Change*, 10(3), 393–409.
- Cirilo, J. A. (2008). Public water resources policy for the semi-arid region. *estudosavancados*, 22 (63), 61–82.
- Das, B. (2018) A Geo-spatial prelude of water prospect and their sustainable utilisation in drought prone region of West Bengal: A case study of Raghunathpur-I Block, Purulia District. *International Journal of Research and Analytical Reviews*, 5(3), 297–303
- Deshpande, R. S., & Narayanmoorthy, A. (2000). Appraisal of watershed development programme across regions in India. Gokhale Institute of Politics and Economics (GIPE), Pune (India).
- Feng, S., Huo, Z., Kang, S., Tang, Z., & Wang, F. (2011). Groundwater simulation using a numerical model under different water resources management scenarios in an arid region of China. *Environmental Earth Sciences*, 62(5), 961–971.
- Haldar, S., & Saha, P. (2015). Identifying the causes of water scarcity in Purulia, West Bengal, India—a geographical perspective. *IOSR Journal of Environmental Science, Toxicology and Food Technology*, 9(8), 41–51.
- Halder, S., & Sadhukhan, D. (2012) Adaptability of water management strategies in the context of Climate change for drought prone areas of West Bengal. Paper presented at the International Conference on Impact of Climate Change on Water Resources, At: Karunya University, Coimbatore, India
- Hu, X. J., Xiong, Y. C., Li, Y. J., Wang, J. X., Li, F. M., Wang, H. Y., & Li, L. L. (2014). Integrated water resources management and water users' associations in the arid region of northwest China: A case study of farmers' perceptions. *Journal of environmental management*, 145, 162–169.
- Hussain, M. I., Muscolo, A., Farooq, M., & Ahmad, W. (2019). Sustainable use and management of non-conventional water resources for rehabilitation of marginal lands in arid and semiarid environments. *Agricultural water management*, 221, 462–476.
- Hutti, B., & Nijagunappa, R. (2011). Applications of geoinformatics in water resources management of semiarid region, North Karnataka, India. *International Journal of Geomatics and Geosciences*, 2(2), 373–342.
- Kyessi, A. G. (2005). Community-based urban water management in fringe neighbourhoods: the case of Dar es Salaam, Tanzania. *Habitat International*, 29(1), 1–25.
- Mahmoud, M. I., Gupta, H. V., & Rajagopal, S. (2011). Scenario development for water resources planning and watershed management: Methodology and semi-arid region case study. *Environmental Modelling & Software*, 26(7), 873–885.

- Niazi, A., Prasher, S. O., Adamowski, J., & Gleeson, T. (2014). A system dynamics model to conserve arid region water resources through aquifer storage and recovery in conjunction with a dam. *Water*, 6(8), 2300–2321.
- Ortega, J. F., De Juan, J. A., & Tarjuelo, J. M. (2004). Evaluation of the water cost effect on water resource management: Application to typical crops in a semiarid region. *Agricultural water management*, 66(2), 125–144.
- Pal, K.J. (2017). Puruliamatite Jalatirtha. *SechPatra. Irrigation & Waterways Department of West Bengal*, pp. 10–13
- Ragab, R., & Prudhomme, C. (2002). Sw—soil and Water: climate change and water resources management in arid and semi-arid regions: prospective and challenges for the 21st century. *Biosystems engineering*, 81(1), 3–34.
- Shangguan, Z., Shao, M., Horton, R., Lei, T., Qin, L., & Ma, J. (2002). A model for regional optimal allocation of irrigation water resources under deficit irrigation and its applications. *Agricultural Water Management*, 52(2), 139–154.
- Shen, Y., & Chen, Y. (2010). Global perspective on hydrology, water balance, and water resources management in arid basins. *Hydrological Processes: An International Journal*, 24(2), 129–135.
- Singh, A. (2010). Decision support for on-farm water management and long-term agricultural sustainability in a semi-arid region of India. *Journal of Hydrology*, 391(1–2), 63–76.
- Tonkaz, T., Çetin, M., & Tülücü, K. (2007). The impact of water resources development projects on water vapor pressure trends in a semi-arid region, Turkey. *Climatic change*, 82(1–2), 195–209.

Index

A

- Abandoned coal mines, 290
- Abandoned Sangramgarh coal mines
 - alkalinity, 297
 - AMD, 297
 - BOD test, 298
 - COD test, 297
 - colliery, 291
 - drinking water specification, 292
 - groundwater level, 299
 - high TSS parameter, 297
 - HPI, 295, 298
 - seasonal change in water quality, 299
 - TDS, 297
 - total hardness of water, 298
 - turbidity, 297
 - water samples, 292
 - WQI, 292–295
- Accuracy assessment, 197
- Acid mine drainage (AMD), 290, 297
- Active/passive optical sensors, 90
- Acute groundwater crisis problems, 474
- Adaptive strategies, 13, 20, 24
- Advanced Spaceborne Thermal Emission and Reflection Radiometer (ASTER), 413
- Agricultural land, 14, 22
- Agricultural practices, 12
- Agriculture, 224
- Agro-forestry, 7
- AHP model, Joyponda river basin
 - accuracy assessment, GPZ map, 211, 212
 - classification factors, 199
 - CR, 195
 - curvature, 204, 205
 - drainage density, 205
 - geological setting, 198, 200
 - geomorphology, 202, 203
 - GPZ, 210
 - GPZI, 195, 197
 - groundwater recharge estimation, 198
 - infiltration number, 207, 208
 - land use land cover, 209
 - lineament density, 201, 202
 - methodology, 197
 - natural groundwater recharge, 213
 - nine-point scale, 195
 - pair-wise comparison matrix, 195, 196
 - rainfall, 206
 - slope, 203
 - soil, 207
 - thematic layers, 194
 - topographic wetness index, 208
- AHP model, Joyponda river basineigenvector technique, 195
- AHP weighted overlay method
 - GW CZ delineation (*see* Groundwater consumption zones (GWCZ))
 - GWPZ delineation (*see* Groundwater potential zones (GWPZ))
 - PGWLZ, 466
 - projected groundwater vulnerable zone, 466
 - validation, 468
- AkvaGIS application, 46
- Alluvial aquifers, 54
- Alluvium Ganga Brahmaputra, 417
- Altitude, 228, 230
- Analytical hierarchy process (AHP), 162, 474

- Analytical hierarchy process (AHP) (*cont.*)
 ANN, 143
 as data-driven model, 142
 fuzzy-based MCDA, 143
 fuzzy logic, 142
 GIS-based fuzzy-AHP approach, 157
 hydro-geological factors, 194
 knowledge-driven model-like SI, 142
 MCDM, 191
 multi-criteria decision-making technique,
 167, 194
 pairwise comparison matrix, 167, 177
 SVMs, 143
 thematic layers, 146
 WOA method, 146
 WoE, 143
 thematic layers, 167
- Analytical network process (ANP), 92
- Anantapur district
 annual rainfall, 432
 annual water depletion, 431
 coarse-textured soil, 432
 drought-prone area, 431
 groundwater spatial variability (*see* Spatial
 variability study, Anantapur district)
mandals, 431
 rain shadow region, 433
 Rayalaseema region, 431
 rice and groundnut, 433
 valleys, 433
- Ancient civilization, 13
- Anthropogenic source, 321
- Aquifer, 54, 222, 236–239
- Aquifer thickness, 485
- Aquifers, 36
- Arapahoe aquifer, 41
- ArcGIS environment, 485
- ArcGIS platform, 459
- ArcGIS software, 194, 195, 198, 211
- Arc-hydro tool, 251
- Area under curve (AUC), 469, 494
- Arid zones, 396
- Aridity index (AI), 412
- Arsenic content, 84
- Artificial groundwater refuelling, 408
- Artificial intelligence (AI), 95
- Artificial neural networks (ANN), 35, 143, 162
 aquifer, 248
 categorical variables, 253
 clean-up process, 253
 data, 249, 252
 digital elevation model, 249
 factors, 250
 geomorphological units, 251
 groundwater management, 248
 groundwater potential map, 255
 groundwater storage, 251
 groundwater table, 255
 Holocene age deposition, 255
 Hugli district, 248, 249
 hydro-geomorphic feature, 255
 methodology, 251, 252
 parameters, 254
 population density, study area, 256
 ROC curve, 254
 Spatial Analyst tool, 249
 SRTM DEM, 249
 training data, 254
- Artificial recharge site identification
 AI, 412
 conditional methods, 423
 drainage density, 413
 geology, 410
 geomorphology, 411
 geospatial technology, 425
 GIS framework (*see* Geographic
 information system (GIS))
 knowledge-based factor analysis, 410
 lineament, 414
 location selection principles, 424
 LULC, 412, 413
 remote sensing, 408, 410
 slope, 413
 soil, 412
 study area, 409, 417
 water level, 412
 weighted overlay analysis, 414, 416
- Artificial regeneration, 408
- B**
- Backpropagation neural networks
 (BP-NN), 35
- Banking (groundwater), 30
- Barren land, 210
- Biological oxygen demand (BOD) test, 298
- Birbhum district, 475
- Bivariate plot, 316
- Bowl-shaped topography, 390, 404
- Broad bed and furrow (BBF) system, 441
- Bureau of Indian Standards (BIS), 321
- C**
- Calcium carbonate, 58, 71, 72
- Cation-exchange reaction, 312, 314

- Central Ground Water Board (CGWB), 190, 206, 251, 433, 468
- Central Water Commission (CWC), 190
- Chemical experiment, 320
- Chemical oxygen demand (COD) test, 297
- Chemical weathering, 306
- Chota Nagpur plateau, 419
- Climate and ecosystem management, 40
- Climate change, 17, 84
 - and groundwater depletion, 16
 - global warming, 16
 - monsoon rainfall, 20
 - water stress, 17
- Climatic oscillations, 16
- Coarse loamy typic haplustalfs, 418
- Coastal aquifer, 353
 - Chennai, 352
 - freshwater recharge, 350
 - GALDIT method, 352–354, 357
- Community-based sprinkler and drip irrigation system, 441
- Community development (CD), 475
- Composite Water Management Index (CWMI), 84
- Computational models, 35, 38
- Computer Graphics Laboratory Technology, 93
- Consistency index (CI), 450
- Consistency ratio (CR), 195, 453, 456
- Consumption/vulnerability study, Cooch Behar district
 - AHP techniques (*see* AHP weighted overlay method)
 - data and sources, 448
 - groundwater pollution sensitive area, 448
 - latitudinal and longitudinal extension, 447
 - methods, 449
 - physiography, 448
 - weighting parameters, 449
- Cost-effectivity, 55
- Crop diversification index (CDI), 378
- Crop failure, 14, 18
- Curvature, 204, 205
- D**
- DEM data, 225
- Dental and skeletal fluorosis, 321, 322
- Dental and skeletal fluorosis in Purulia villages, 325
 - biological diversity, 322
 - blockwise fluoride variation, 327–329
 - FGD study, 325, 326
 - fluoride variation and NRDWP, 329–331
 - fluoride, lithology and structural diversity, 323
 - fluoride-affected villages, 321
 - on human health
 - Arsha block, 335
 - Baghmundi and Bandwan blocks, 337
 - Balarampur block, 335
 - Barabazar block, 335
 - block of Para, 337
 - food habits, 331, 333
 - Hura block, 336
 - Jhalda I block, 336
 - Manbazar I block, 337
 - Manbazar II block, 337
 - Puncha block, 337
 - Purulia I block, 338
 - Purulia II block, 337
 - water intake and magnitude of, fluorosis, 332, 334–335
 - on society
 - divorce, 343
 - dowry system, 343
 - fluorosis-affected school students, 338–340
 - physical disability, 342, 343
 - remarriage, 343
 - school dropout, 338, 339
 - school-level survey, 339
 - social isolation/rejection, 341–342
- Pegmatite granite formation rocks, 324
- Precambrian rocks, 324
- quantitative analysis, 326, 327
- RS and GIS techniques, 326
- sampling methods, fluorosis-related
 - health hazard, 325
 - Singhbhum Craton, 323–324
- Dependability, 55
- Digital elevation model (DEM), 33, 90, 91, 149, 413
- Digital surface model (DSM), 90
- Digital terrain model (DTM), 90
- Drainage density, 205, 206, 233, 237, 487
- Drainage length density (D_d), 413
- Drainage network layer, 413
- Drinking water quality index (DWQI), 42
- Dry-crop farming, 21
- Dust storms, 383
- Dwarkeswar river, 419
- E**
- Eastern Ghats Highlands of East India, 367
- Eastern Ghats Region of East India, 367
- Electrical conductivity (EC), 117, 265, 271
- Electromagnetic spectrum, 86
- ERDAS Imagine program v8.5, 410
- ERDAS Imagine program v8.6, 414

ERDAS Imagine software v8.6, 413
 Evaporation, 311
 Ex situ method, 345
 Ex situ weathering, 54

F

False-positive rate (FPR), 237, 243
 Fluoride, 306
 Fluoride contamination
 Balarampur block, 329
 community development blocks, 321
 correlation between water intake, 334
 (*see also* Dental and skeletal fluorosis in Purulia villages)
 fluoride concentration, 329
 fluorosis-affected school students, 339
 NRDWP, 330
 Fluoride ions, 324
 Fluoride-affected districts, 321
 Fluorosis-related health hazard, 321
 Focus group discussion (FGD), 325, 326, 344
 FR model, Jhargram and Paschim Medinipur
 altitude, 228
 aquifer, 236–238
 area statistics, potentiality map, 244
 calculation, 240
 data collection, 225, 226
 drainage density, 233, 237
 geology, 231
 geomorphology, 232, 235
 hydrogeology, 232, 235, 236
 lineament density, 234, 238
 location, 224, 225
 LULC, 227, 228
 methodology, 225–227
 rainfall, 230, 232
 slope, 229, 231
 soil, 230, 233
 sub-tropical climate zone, 224
 vegetation, 228, 229
 Frequency ratio (FR), 162
 calculation, 240
 definition, 226
 groundwater conditioning factor *vs.*
 distribution of groundwater well
 locations, 227
 groundwater potential zones, 224, 226
 Jhargram and Paschim Medinipur (*see* FR
 model, Jhargram and Paschim
 Medinipur)
 GPZ map, 243
 parameters, 242

Fresh water availability, 398
 Freshwater, 190
 Fuzzy-based mapping, 143
 Fuzzy-based MCDA, 143

G

GALDIT method, Chennai coastal aquifer
 aquifer type, 355
 aquifer type/groundwater occurrence, 353
 Cl distribution map, 356
 coastal area, 351
 computing GALDIT index, 357
 groundwater level, 356
 groundwater table level, 353
 IDW interpolation method, 357, 359
 perpendicular distance, 356
 quality of groundwater, 352
 saturated thickness, 355
 seawater intrusion, 354
 shoreline, 354
 soil data, 356
 thickness, aquifer, 356
 vulnerability, 353
 GALDIT model
 application, 361
 Genetic algorithm methods, 35
 Geo-electrical technique, 55
 Geographic information system (GIS), 5, 191, 248
 application in groundwater studies, 85, 86
 ArcGIS program, 410
 ES and SDSS, 95
 fluorosis-induced health hazards, 326
 GIS programme, 40
 grids, 412
 groundwater recharge zone, 425
 groundwater research, 34
 hydrological simulation, 95
 Kashipur block, 138
 knowledge-driven factor analysis, 408
 MCDA method, 142
 modern GIS techniques, 138
 multi-criteria-based GIS approach, 7
 polygon layer, 411, 412
 satellite imagery, 33
 thematic maps, 414, 423
 VES, 162
 village level PIG zonation, 134
 Geological discontinuities, 408
 Geological Survey of India, 486
 Geology, 231, 234
 Geomorphology, 202, 203, 232, 235

- Geophysical imaging technique, 55
- Geophysical imaging, Delhi
 - Bagargarh village, 68
 - Chawala village, 72
 - Daurala village, 69
 - Dhansa village, 73
 - Dichaon Kalan village, 63
 - Ghalibpur village, 70
 - Ghummanhera village, 72
 - Goela Khurd village, 68
 - Hasanpur village, 72
 - interpretation, geophysical data, 60
 - Jaffarpur Kalan village, 70
 - Jharoda Kalan village, 66
 - Kanganheri village, 73
 - land uses, 58
 - Lund imaging technique, 58
 - Mitraon village, 70
 - natural vegetation, 58
 - Pindwala Kalan village, 69
 - Qazipur village, 69
 - soils and geology, 58
 - spatial variability map, 61
 - study area
 - climatic condition, 57
 - location, 56
 - physiography, relief and drainage, 56–57
 - Surkhpur village, 71
 - Ujwah village, 71
 - village Kair, 68
- Geophysical technique, 55, 190
- Geophysics, 35
- Geoscientific study, Birbhum district
 - climatic factors, 490
 - comparative analysis, 492
 - dataset, 476, 479
 - geological factors, 486, 487
 - groundwater inventory map preparation, 478
 - hydrogeological factors, 486
 - hydrological factors, 487, 488
 - location, 475, 476
 - methodological framework
 - phase I, 477
 - phase II, 477
 - phase III, 478
 - MLP, 480, 484
 - models application, 484
 - pedological factors, 490
 - physiocultural factors, 491
 - thematic layers generation, 486
 - topographical factors, 492
 - WoE model, 478
- Geospatial interpolation approach, 55
- Geospatial technique, 162, 223
- Geospatial technologies, 85, 425
 - geochemical quality, 41, 42
 - groundwater exploration, 36, 37
 - groundwater modelling, 38, 40
 - groundwater potential mapping, 37, 38
 - implementations, 94
- Geostatistical techniques, 5
- Geostatistics, 35
- Gibbs ratio, 278
- GIS programming, 40
- Global Land Data Assimilation System (GLDAS), 46
- Global Positioning System (GPS), 5
- Global warming, 13
- GRACE data, 223
- GRACE TWS anomalies, 46
- Gravity Recovery and Climate Experiment (GRACE), 33, 35, 45, 46, 88
- Green revolution, 12
- Groundwater, 222, 248
 - agricultural sector, 382
 - categorical safety status, Indian groundwater, 17
 - collective self-regulation, 30
 - defensive role, 17
 - drinking water supply, 12
 - eastern Gangetic basin, 30
 - efficiency in water utilization, 21, 22
 - extraction, 382
 - geochemical quality, 41, 42
 - geospatial technology, applications (see Geospatial technology)
 - in India, 382
 - intensive groundwater use, 31
 - irrigated agriculture, 30
 - irrigation and food industry, 4
 - overexploitation, 382
 - rainwater storage, 22–23
 - recharge, 23
 - renewable resource, 382
- Groundwater administration, 31
- Groundwater assessment, 430
 - advanced method, 191
 - conventional method, 191
 - ground surveys, 223
- Groundwater consumption index (GWCI), 456
- Groundwater consumption zones (GWCZ)
 - classification, 465, 466
 - human water consumption, 464
 - irrigated area, 464

- Groundwater consumption zones (GWCZ)
(*cont.*)
livestock water consumption, 464, 465
total crop production, 462, 464
withdrawal for irrigation, 461, 462
- Groundwater consumption zones (GWPZ)
calculation, 453
CR, 456
knowledge-based factors analysis, 453
normalized matrix, 453, 456
Satty's ratio, 456
sub-factors normalized weight, 457
thematic layers, 456
- Groundwater contamination, 260
- Groundwater crisis, 4
- Groundwater depletion, 12, 408
climate change, 16, 17
and urbanization, 19–20
- Groundwater depth
GRB, 166, 168
and potential groundwater depth, 179
- Groundwater Estimation Committee (GEC),
198
- Groundwater exploitation, 190
- Groundwater exploration, 36, 37
- Groundwater extraction, 190
- Groundwater fluctuation map, 437
- Groundwater hydro-geochemistry, Paschim
Bardhaman district
bicarbonate (HCO_3), 272
Ca and Mg, 271
chloride (Cl), 273
co-relation analysis, 274–276
EC, 265, 271
factor analysis, 276, 277
fluoride (F), 273
geological succession, 263
Gibbs ratio, 278
HCA, 264, 277
IDW, 265
iron (Fe), 273
irrigation suitability, 260, 280
mining-based industrial, 260
Na and K, 272
PCA, 264
Pearson's correlation matrix, 264
pH value, 265
 SiO_2 , 274
 SO_4 and PO_4 , 274
TDS, 271
test area, 261–264
test parameters, 264
total hardness (TH), 271
WQI, 278, 280
- Groundwater inventory map preparation, 478
- Groundwater level, 299
- Groundwater Level Mapping Tool, 46
- Groundwater management, 30, 31, 35, 47, 84,
92, 94
Purulia district, 509–512
- Groundwater modelling, 38, 40, 84
- Groundwater modelling system (GMS), 40
- Groundwater monitoring, 430
- Groundwater pollution, 7
- Groundwater potential, 32, 33, 37
assessment, 60
potential electrodes, 59, 60
- Groundwater potential index (GPI), 223
GRB, 168
and groundwater depth, 183
validation points in the GRB, 179
- Groundwater potential map (GPM), 37, 38
GRB, 179
- Groundwater potential zone (GPZ), 197,
210–212
Bagargarh village, 63
calculation, 450
Chhawala village, 67
classification, 461, 462
climatic features, 142
CR, 453
Daurala village, 64
delineation, 146, 148
Dhansa village, 67
Dichaon Kalan village, 62
drainage density, 459
geomorphology, 460
Ghalibpur village, 65
Ghummanhera village, 66
GIS platform, 450
Goela Khurd village, 63
Hasanpur village, 67
Jaffarpur Kalan village, 65
Jharoda Kalan village, 62
Kair village, 63
Kanganheri village, 68
knowledge-based factor analysis, 449
lithology, 460
LULC, 457, 458
Mitraon village, 65
NDVI, 460
normalized matrix, 452
pairwise comparison matrix, 451, 455
Pindwala Kalan village, 64
Qazipur village, 64
rainfall, 459
RS and GIS, 142
Saaty's ratio index, 453

- Satty's scale, 449
 - soil, 458
 - sub-factors normalized weights, 454
 - Surkhpur village, 66
 - thematic layers, 453
 - TWI, 461
 - Ujwah village, 66
 - urban residential zone development, 142
 - validation, 156, 157
 - Groundwater Potential Zones Index (GPZI), 195, 197
 - Groundwater potentiality, 222, 223
 - Groundwater quality, 7
 - assessment, 106
 - Damodar river, 106
 - hydro-chemical characteristics, 106
 - village level assessment, 6
 - zonation map, 106
 - Groundwater quality assessment, 43, 260, 261
 - Groundwater quality deterioration, 54
 - Groundwater recharge, 42, 47, 198, 207, 222, 233
 - Groundwater recharge free zone, 408
 - Groundwater recharge probable index, 414, 416
 - Groundwater resource, 6, 162, 248
 - Groundwater storage, 222, 251
 - Groundwater vulnerability, 8
 - Gumani river basin (GRB)
 - AHP, 167
 - district-wise soil maps, 164
 - factors influencing groundwater potentiality
 - distance from the river, 174
 - drainage density, 174
 - geomorphology, 171–173
 - lineaments density, 170, 171
 - lithology, 169, 170
 - LULC, 174–176
 - rainfall, 174
 - relief, 173
 - slope, 173
 - soil texture, 171
 - GPI, 168
 - groundwater potential zone, 176, 178–180, 182
 - location, 163, 164
 - methodological design, 165
 - principal river, 163
 - processing, geospatial data, 166
 - rainfall, 163
 - random consistency index, 167
 - study area, 163
 - thematic parameters, 164
 - three-step research, 165
 - topographic elevation, 163
 - validation, 168, 179
- H**
- Hand pump/mechanical pumping technique, 320
 - Haryana
 - agriculturally developed state, 382
 - agriculture sector, 383
 - climatic zones, 388, 389
 - district-wise average annual rainfall, 398, 399
 - groundwater balance, 404
 - high-yielding crops, 383, 384
 - long-term pattern/behaviour (*see* Long-term groundwater behaviour, Haryana)
 - mean annual rainfall, 383
 - net groundwater availability, 383
 - overexploitation, 383
 - remedial measures, 404
 - Hazard quotient (HQ), 306
 - Heavy metal, 294
 - Heavy metal pollution index (HPI), 294, 295, 298, 299
 - Hierarchical cluster analysis (HCA), 264, 277
 - Human civilizations, 13, 16, 20, 23
 - Humid, 412
 - Hydro-chemical method, 55
 - Hydrochemistry, 278
 - Hydrogeological factors, 486
 - AHP model, 194, 195
 - curvature, 204
 - drainage density, 205
 - geomorphology, 202
 - GIS, 191
 - groundwater exploration, 191
 - infiltration number, 207
 - Joyponda river basin, 193
 - land use land cover, 209
 - lineament density, 201
 - rainfall, 206
 - RS, 191
 - slope, 203
 - soil, 207
 - topographic wetness index, 208
 - Hydrogeological science methods, 31
 - Hydrogeology, 232, 235, 236
 - Hydrological budgets, 31

Hydrological elements, 89
 Hydrological resource, 474
 Hydrological soil structure, 416
 Hydrometeorological factors, 502

I

In situ method, 345
 India, groundwater
 Anantapur district, 431, 442
 dependency, 430
 depletion, 430
 overexploitation, 430
 use, 430
 Indian Council of Medical Research (ICMR), 321
 Indian summer monsoon (ISM), 13
 Indo-Gangetic plains, 446
 Indus civilization, 13
 Industrial development, 4
 Industrial effluents, 15
 Industrial revolution, 14
 Industrialization, 12
 Infiltration number, 207, 209
 Integrated geospatial technology, 85
 Integrated GIS, 43
 Intensive canal irrigation, 390
 Inverse distance weighting (IDW), 146, 265, 357, 359
 cross-validation data set, 435
 method description, 434
 operational simplicity, 433
 performance validation, 435, 437
 prediction accuracy, 434
 spatial interpolation, 430, 433
 water table depths, 438
 weighing power function selection, 434
 Ion variations, 308, 309
 Irrigated area, 464
 Irrigation, 4, 222
 Barabhum irrigation scheme, 513
 demand, 382, 398
 farmers, 390
 food security and reducing poverty, 511
 groundwater, 382
 Hanumata irrigation scheme, 513
 Jalathirtha scheme, 516, 517
 Kumari irrigation scheme, 513
 surface water supply, 398
 techniques, 514
 Irrigation suitability, 265, 272, 280
 alkalinity, 282
 calcium and magnesium, 283

evaluation, 280
 irregular and seasonal, 280
 parameters, 280
 Paschim Barddhaman, 260
 permeability index (PI), 283
 salinity content, 281
 sodium percent of water, 281
 Irrigation water quality
 Kashipur block
 Kelly's ratio, 132, 133
 MAR, 130, 132
 in post-monsoon, 131
 in pre-monsoon season, 129
 SAR, 128
 SSP, 130
 standardized parameters, 134

J

Jal Dhoro-Jal Bhoro (JDJB) scheme, 516
 Jhargram and Paschim Medinipur
 agriculture, 224
 altitude, 228, 230
 aquifer, 236–239
 area statistics, potentiality map, 244
 data collection, 225
 drainage density, 233, 237
 geology, 231, 234
 geomorphology, 232, 235
 GPZ map, 243
 hydrogeology, 232, 235, 236
 lineament density, 234, 238
 location, 224, 225
 LULC, 227, 228
 rainfall, 230, 232
 slope, 229, 231
 soil, 230, 233
 sub-tropical climate zone, 224
 vegetation, 228
 Joyponda river basin, West Bengal (India)
 accuracy assessment, GPZ map, 211, 212
 AHP model (*see* AHP model, Joyponda river basin)
 CGGC, 191
 curvature, 204, 205
 data sources, 193
 drainage density, 205, 206
 field photographs, 201
 geological setting, 198, 200
 geomorphology, 202
 GPZ, 210–212
 GPZI, 195
 groundwater recharge estimation, 198

hydro-geological factors, 192
 infiltration number, 207, 209
 land use land cover, 209, 211
 lineament density, 201, 202
 location, 192, 193
 natural groundwater recharge estimation, 213
 rainfall, 206, 207
 slope, 203, 204
 soils, 207, 208
 study area, 192
 thematic layers, 194
 topographic wetness index, 208, 210

K

Kappa co-efficient, 197, 212
 Kashipur block (Purulia district of West Bengal)
 amphibolites, 108
 correlation analysis, groundwater quality parameters
 for post-monsoon season, 123, 127
 for pre-monsoon season, 123, 126
 groundwater quality and chemistry
 Ca and Mg, 119, 120
 Cl and CO₃, 121
 EC, 117–118
 HCO₃⁻, SO₄, and F⁻, 113, 122, 123
 Na and K, 120, 121
 pH, 112–116
 TA, 118
 TDS, 117
 total hardness (TH), 119
 irrigation water quality, 111, 138
 (*see also* Irrigation water quality)
 location, 107
 PIG method, assessment of groundwater quality, 135
 quality of groundwater, 110
 rainfall, 107
 rivers, 108
 samples collection and chemical analysis, 110
 semi-arid and drought-prone, 107
 spatial interpolation, 112
 statistical analysis, 112
 statistical analysis, physico-chemical parameters
 in post-monsoon seasons, 123, 125
 in pre-monsoon seasons, 123, 124
 study area and sapling sites, 108
 surface and sub-surface factors, 109

water quality by physico-chemical conditions, 135
 Kelly's ratio (KR), 132, 133
 Knowledge-based factor analysis, 410
 Kolkata Geological Survey, 410
 Kolmogorov and Smirnov test, 435
 Kriging interpolation model, 112

L

Land use and land cover (LULC), 209, 211, 227, 228, 412, 413, 423, 491
 GRB, 166, 174, 175
 SUA, 151, 153
 Land use map, 477
 Land utilization practice, 223
 Landsat 8 satellite data, 414
 Landsat 8-Operational Land Imager (OLI), 412
 Landsat Thematic Mapper (TM) images, 33
 Landsat-TM thermal infrared remote sensing data, 33
 Lateritic upland, 423
 Lineament, 414
 Lineament density, 201, 234, 238, 486, 488
 Lithology, 460, 486
 Livestock water consumption, 464, 465
 Logistic regression (LR), 162
 Longitudinal unit conductance (S value), 60, 77, 78
 Long-term groundwater behaviour, Haryana
 annual groundwater level rise/fall
 arid zone, 396
 bowl-shaped topography, 390
 climatic zones and state, 390, 391
 semi-arid zone, 393, 396
 sub-humid zone, 390
 systematic spatial pattern, 390
 tube wells growth, 390, 394
 data, 386
 declining groundwater level areas
 calculation, 387
 declining/rising groundwater level areas
 calculation, 388
 groundwater balance, 397
 arid zone, 398
 positive/negative, 396
 semi-arid zone, 398
 sub-humid zone, 396
 groundwater declining/rising climatic zones
 arid zone, 402
 district-wise, 399, 400
 semi-arid zone, 402
 sub-humid zone, 402

- Long-term groundwater behaviour (*cont.*)
 time intervals, 402, 403
 rice-wheat ecosystem, 403
 rising groundwater level areas calculation,
 387, 388
 study area, 383, 386, 388
- Lowland badland, 418
- Ludwig-Langelier plot, 310
- Lund imaging technique, 58
- M**
- Machine learning methods, 35
- Magnesium adsorption ratio (MAR), 130, 132
- Mandals*
 classification, 439
 groundwater development, 442
 groundwater utilization, 439
 prioritization, 440
- MCDM method, 92
- Mean relative error (MRE), 435, 437
- Microwaves, 34
- Minimum mean error (ME), 434
- Mining, 290
- MLPual rainfall, 491
- MLPual replenishable rate, 474
- Modelling, 38, 40
- Moderate Resolution Imaging
 Spectroradiometer (MODIS), 33, 44,
 45
- Modern computer-based technologies, 474
- Modified advance data-driven machine learning
 techniques, 143
- Modified normalised difference moisture index
 (MNDMI), 145
- Moisture index (MI), 153
- Monsoonal rainfall, 15, 17
- Monsoonal uncertainty, 54
- Multi-criteria decision analysis (MCDA)
 method, 142, 143, 191
- Multi-influencing factor (MIF), 92, 106
- Multi-influencing factor model, 474
- Multilayer perceptron (MLP)
 groundwater potential zones, 494
 input data, 484
 machine learning method, 494
 multivariate data, 475
 neural network, 480
 nonlinear sigmoid function, 484
 ROC curve, 495, 496
 structure, 484
 Weka 3.8.4 software, 485
- Multiple-criteria decision-making, 167
- N**
- National Bureau of Soil Survey and Land Use
 Planning (NBSSLUP), 412
- National Mission on Geomorphological and
 Lineament Mapping (NMGLM), 234
- National per capita annual availability, 446
- National Programme for Prevention and
 Control of Fluorosis (NPPCF), 321
- National Remote Sensing Centre (NRSC), 194,
 478, 486
- National Rural Drinking Water Programme
 (NRDWP), 329, 330
- Natural drainage network efficiency, 408
- Natural groundwater recharge, 213
- Natural resource management technologies,
 366
- Natural resources, 366, 367
- Non-acidic mines, 297
- Nonlinear sigmoid function, 484
- Normalized difference vegetation index
 (NDVI), 228, 449, 460
- Numerical modelling, 35
- O**
- Open source data, 44
- Optimal implementation, 502
- Ordinary kriging (OK), 55, 56, 61, 107,
 112–116, 138
- P**
- PCI Geomatica software, 194
- PCP_L method, 449
- Pearson's correlation matrix, 264
- Permeability index (PI), 283
- Physical disability, 342, 343
- Piper trilinear diagram, 42
- Pollution Index of Groundwater (PIG), 106,
 110, 111, 134–138
- Pond frequency, 488, 489
- Population explosion, 474
- Post-monsoon season, 437
- Potential evapotranspiration (PET), 412
- Potential groundwater zones, 77
- Precipitation, 151
- Precision accuracy assessment (PAA), 157, 158
- Principal component analysis (PCA), 194, 264,
 276, 283
- Projected coordinate system (PCS), 166
- Projected Groundwater Level Zone (PGWLZ),
 466
- Projected groundwater vulnerability, 470

- Projected groundwater vulnerable zone, 466, 468
- Purulia district
- block-wise groundwater development, 510, 511
 - CGWB, 505
 - Dalma hills, 503
 - distinct zones, 502
 - drainage map, 505
 - geo-environmental factors, on water resources, 505–506
 - groundwater and surface water, 505
 - groundwater resource management, 509–512
 - hard rock terrain, 502
 - hydrometeorological factors, 502
 - irrigation facilities, 511–514
 - Jalathirtha scheme, 516, 517
 - JDJB Scheme, 516
 - Panchet hills, 503
 - rainwater harvesting, 517
 - rivers, 503
 - seasons, 503
 - socio-economic development, 502, 503
 - surface runoff, 505
 - surface water resource management, 506–507
 - sustainable management, water resources, 517
 - USHARMUKTI Micro-Watershed Scheme, 515
 - water crisis, 502
 - watershed management, 503
- R**
- Radar images, 34
 - Radar satellites, 89
 - Rainfall, 206, 207, 223, 230, 232, 459
 - Rainfall intensity, 490
 - Rainwater harvesting, 23
 - Rarh Banga area, 475
 - Rashtriya Krishi Vikas Yojana (RKVY), 503, 516
 - Rayalaseema region, 430, 431
 - Receiver operating characteristic (ROC), 468, 469
 - Red-Green-Blue (RGB), 37
 - Remote sensing (RS), 5, 162, 191, 223, 248, 474
 - computer-based technologies, 474
 - GIS computer-based technology, 496
 - multispectral and multispatial database, 474
 - application in groundwater studies, 86
 - fluorosis-induced health hazards, 326
 - groundwater exploration, 36
 - groundwater potential mapping, 37, 38
 - remotely sensed data in groundwater studies, 88–90
 - satellite-based, 32
 - SUA, 142
 - Remote sensors in groundwater
 - GRACE, 88
 - optical and radar RS techniques, 88
 - satellite, 87
 - satellite platforms, 86
 - water indices, 88
 - Replenishable groundwater recharge, 430
 - RES2DINV software, 59
 - Reservoirs, 507
 - Resistivity meter, 58
 - Resistivity, geophysical layer
 - Chhawala and Surkhpur villages, 73
 - Ghummanhera and Ujjaon village, 74
 - Goela Khurd village, 75
 - River/water bodies, 255
 - Rooftop rainwater harvesting, 440
 - Root mean square error (RMSE), 410, 434, 469
- S**
- Saaty's AHP, 142
 - Salinity intrusion, 350, 360
 - Saltwater encroachment, 349, 350
 - Saltwater intrusion, 350, 353–355, 357, 361
 - Sampling technique, 325
 - Sand, 248
 - Satellite-based RS, 32
 - Satellite Hydrology Bits Analysis and Mapping (SHBAAM) software, 46
 - Satellite imagery DEMs, 91
 - Seasonal fluctuation, water parameter, 299, 301
 - Sewage treatment plants, 16
 - Shilabati river basin, 409, 410
 - AI, 419, 420
 - annual water level, 421
 - ASTER DEM data, 421
 - drainage, 417
 - drainage density, 419, 420
 - filtration recharge zone, 419
 - geomorphological characteristics, 418
 - groundwater recharge influencing factors, 415
 - groundwater recharge potential zone, , 424, 425
 - higher recharge weight, 417, 423

- Shilabati river basin (*cont.*)
 lineament density, 421, 422
 LULC, 423
 research fields, 417
 slope spatial variation, 422
 slope-based categories, 421
 soil characteristics, 418, 419
 storativity artificial charge zone, 424
 water levels, 421
 wetlands, 425
- Shortwave infrared (SWIR), 86
- Shuttle Radar Topography Mission (SRTM), 225
- Silicate weathering process, 311–314
- Siliguri urban agglomeration (SUA)
 data processing and creation, thematic layers, 145, 146
 delineation, GPZ, 146, 148
 GPZ map, 154, 155
 location, 143
 location map, 144
 multi-spectral satellite imagery, 144
 thematic layers (*see* Thematic layers, GPZ in SUA)
 urbanisation, 143
 validation, GPZ map, 156, 157
- Slope, 203, 204, 229, 231, 413, 492
- Social-ecological systems (SES), 30
- Societal development, 6
- Socio-economic development, 24
- Sodium adsorption ratio (SAR), 128
- Soils, 207, 208, 230
- Soil categories, 251
- Soil leaching, 314
- Soil moisture mapping, 37
- Soil moisture methods, 33
- Soil permeability coefficient, 408
- Soil texture, 223, 490
- Soluble sodium percentage (SSP), 130
- Space technology, 35
- Spatial distribution mapping, 107
- Spatial gravity surveys, 89
- Spatial modelling
 aggregation of data, 92
 EALCO model, 93
 GIS, 93
 groundwater machine training, 92
 groundwater modeling system, 93
 hydrological, 92
 MCDM, 92
 MIF techniques, 92
 probabilistic models, 92
 weights comparative and intrinsic, 92
- Spatial variability map, 61
- Spatial variability study, Anantapur district
 area description, 431, 433
 data and methodology, 433, 434
 data set distribution, 435–437
 groundwater depth, 437, 438
 groundwater development stages, 438, 440
 groundwater table depth, 437, 438
 IDW method (*see* Inverse distance weighting (IDW))
mandals, 441
mandals prioritization, 439, 442
 observation wells, 432, 433
 water table fluctuation, 437, 439
- Spectral indicators, 89
- Spectral indices, 90
- SRTM data, 225
- SRTM DEM data, 194, 225, 228
- SRTM Digital Elevation Model (DEM), 492
- Standard vegetation index deviation (SDVI), 44
- Statistical methods, 112
- Statistical tools, 474
- Statistics, 35
- Steeper slope, 413
- Stochastic exogenous seasonal autoregressive
 dynamic moving average
 (SARIMAX), 41
- Sub-humid zone, 390, 393
- Support Vector Machine (SVM), 35, 143
- Surface and subsurface water, 106
- Surface runoff, 44
- Sustainability, 13, 20, 24, 366, 379
- Sustainable development, 474
- Sustainable groundwater balance, 446
- Sustainable groundwater management, 32, 470
- Sustainable groundwater resource management, 474
- Sustainable management, 5
- SWOT (Surface Water and Ocean Topography)
 mission, 45, 46
- Systematic planning and management, 5
- T**
- Thematic layers, GPZ in SUA
 data processing and creation, 145–146
 DEM, 149
 fuzzy-AHP and assignments, 146–147
 geology, 154
 lineament density, 151, 153
 LULC, 151, 153
 MI, 153
 precipitation, 151

- slope, 149
 - soil component, 149, 151
 - Topographic Position Index (TPI), 91
 - Topographic wetness index, 91, 208, 210, 449, 461
 - Topography, 91
 - Total alkalinity (TA), 118
 - Total crop production, 462, 464
 - Total dissolved solid (TDS), 117, 271
 - Transverse unit resistance (T value), 60, 77–79
 - True-positive rate (TPR), 237, 243
- U**
- Universal Transverse Mercator (UTM), 410
 - Urban-industrial development, 14, 24
 - Urbanization, 19, 20
 - USGS EarthExplorer, 475, 491
 - USGS EarthExplorer SRTM DEM, 476
 - USHARMUKTI' Micro-Watershed Scheme, 515
- V**
- Vegetation, 223, 228
 - Vegetation index maps, 37
 - Vertical electrical sounding (VES), 162
 - Village level PIG zonation, 134
 - Visible-Near-infrared-Shortwave infrared (VIS-NIR-SWIR) imagery, 37
 - Vulnerability, saltwater intrusion, 350, 352, 353, 355, 357, 360, 361
- W**
- Water, 190
 - Water assessment, 90
 - Water demands, 12
 - Water management, 5, 45
 - Water pollution, 15
 - Water quality, 12, 13
 - and human health, 15
 - assessment, 308
 - cations and anions, 307
 - drinking usage, 308, 310
 - parameters, 307
 - temporal changes, 306
 - Vanniyar river basin, 315
 - water quality index, 15
 - Water quality assessment, 260
 - Water quality index (WQI), 107, 278, 280, 283
 - numerical value, 294
 - quality of water, 292
 - relative scale, 293
 - relative weight (Wi), 293
 - values, 294
 - water basin, 292
 - water quality types, 293, 294
 - WAWQI method, 292
 - Water recharge
 - from Vanniyar river basin, 307
 - Water resource management, 425
 - Water scarcity, 4, 474
 - fresh water resources, 24
 - industrialization effect, 12
 - ISM, 13
 - rainwater storage, 22
 - sustainability, 20
 - utilization of water, 21
 - water availability status in India, 21
 - Water source
 - and agricultural practices, 14
 - and establishment of settlements, 13, 14
 - groundwater quality, 14–15
 - sanitation facilities in India, 16
 - sewage treatment plants, 15, 16
 - water quality and human health, 15
 - Water stress, 8
 - Water supply scarcity and seclusion, 408
 - Water table fluctuation, 430
 - Water utilization, 21, 22
 - Waterbody extraction, 86
 - Watershed development
 - comprehensive benefits, 366
 - Eastern Ghats Highland of Odisha, 367
 - Eastern Ghats Region of East India, 367
 - eco-friendly approach, 366
 - factors, 367
 - Lacchapatraghati watershed
 - climate and water balance, 367, 369
 - crop productivity and diversification, 377, 378
 - data collection and impact assessment, 371
 - land use and water resources, 370–372
 - on groundwater resources, 375–377
 - physiographic, 368
 - resource conservation activities, 370
 - runoff estimation, 370, 372, 373
 - soil and geology, 368, 370
 - study area, 367, 368
 - water resource development, 374, 375
 - rainfed agriculture, 366
 - rainwater harvesting, 366
 - Watershed development models, 7
 - Watershed management, 7
 - Web map service (WMS), 164

- Weight of evidence (WoE)
 - AUC, 494
 - groundwater potential zones, 493
 - quantitative “data-driven” models, 478
 - ROC curve, 495, 496
 - RStudio-1.1.463 software, 486
 - scattered mMLPer, 492
 - spatial relations, 481
 - statistical method, 475
- Weighted linear combination (WLC), 168, 414
- Weighted overlay analysis, 414, 416
- Weighting power function, 434
- Weights of evidence (WoE), 143, 162
- Wellhead protection areas (WHPAs), 93
- World Geodetic Survey (WGS), 410
- World Health Organization (WHO), 320, 321
- WRIS WebGIS Portal, 486